Open Research Online

The hydrogeology of the Oman Mountains

Thesis

oro.open.ac.uk

THE HYDROGEOLOGY
OF THE
OMAN MOUNTAINS

A THESIS PRESENTED
FOR THE DEGREE OF
DOCTOR OF PHILOSOPHY
BY

GORDON STANGER

HIGHER DEGREES OFFICE

LIBRARY AUTHORISATION

STUDENT: ...GORDON STANGER...................   SERIAL NO: HDJ 0490

DEGREE: ...PhD.

TITLE OF THESIS: ...The Hydrogeology of the Oman Mountains......

....

....

I confirm that I am willing that my thesis be made available to readers
and may be photocopied, subject to the discretion of the Librarian.

Signed: .....G. Stanger...................   Date: ...11 Aug 1986...

ABSTRACT

Northern Oman is an arid area almost entirely dependent upon groundwater recharged by highly sporadic rainfall. Precipitation estimates are hampered by a lack of any reliable altitude-rainfall relationship. Below 700 m there is no statistically significant relationship. The isotopic composition of groundwater is strongly influenced by the rainfall amount (related to storm frequency), and not just by altitude/temperature. Storm events with long return periods are of disproportionate importance to recharge.

Despite the huge volume of carbonate formations, holokarstic development is generally immature, and groundwater storage is greatest in alluvial piedmont surrounding main limestone massifs. Isotopes, chemistry and hydrologic measurements show that post-storm evaporative losses are very large. The origin of limestone springs and their chemical and physical anomalies are described. Structure rather than petrology controls groundwater flow in the limestones, hence regional differences in structural style produce contrasting hydrologic régimes between the various massifs.

The Semail nappe mantle sequence is the only other hard-rock formation of groundwater significance. Though much less productive than the carbonates, these ultramafics display extraordinary chemical activity, yielding bicarbonate waters from the weathered zone, whilst more deeply circulating groundwaters produce hyperalkaline springs by low-temperature serpentinisation. Associated processes include solute reduction, hydrogen evolution, hydroxide and carbonate precipitation, hydroxide-basic rock reaction, salt enrichment and water-rock isotopic exchange.

Throughout the interior catchments, groundwater mostly flows into narrow buried alluvial channels which are often constricted at hard-rock nodal points, thus facilitating very efficient interception and recovery by the "falaj" system. Traditional agriculture has evolved to cope with fluctuating groundwater supply but is sensitive to increased abstraction. On the Batinah plain, greatly increased coastal abstraction has locally induced moderate to severe salinisation. Existing process studies are insufficiently quantified to provide the resolution necessary to manage groundwater resources, especially in high-risk coastal areas.

Contents

Volume 1 : Main Text

Volume 2 : Annotated Data Appendices, Plates and Supporting Literature

Enclosures   Map 1   The Geology of Jebel Akhdar
              Map 2   The Geology of the Capital Area
              Map 3   Successive Salinity Surveys of
                      the Seeb Fan Area

              Supporting Papers

LIST OF FIGURES

LIST OF TABLES

Physically, and to a large extent culturally and historically, the Oman mountains constitute a single well-defined region, although the Northern area is currently divided by a distribution of political boundaries between enclaves and outposts of Oman and the UAE. Data has been collected from both countries and hence political boundaries are ignored for the purpose of this thesis. Grid references are given in the main text in the form of (LL, e, n) where LL are grid block letters used for rapid map location, and where e and n are three-digit eastings and northings respectively. Grid references in the appendices are listed in the alternative wholly numerical form for ease of computerised retrieval. All the references were taken from the U.K. Ministry of Defence 1:100,000 series maps based upon UTM Grid Zone 40. A few place names, especially on older maps, were found to be either erroneous or poorly transliterated, eg. "Jebel Hawrah" = "mountain mountain" (Smith, 1985), and have been altered accordingly. Apparent errors in Appendix C3 sampling sites consist of such changes. Location errors are generally ± 100 m relative to the base maps but occasionally may be as much as ± 3 km where based upon resection in low relief featureless areas of the interior. Field mapping was based upon various sources of aerial photography from 1:10,000 scale to 1:60,000 scale and supplemented by contrast-stretched multispectral satellite imagery with a resolution of 100 x 120 m (pixel dimensions). Subsequently, geological and hydrogeological maps were compiled at 1:100,000 scale and expanded or reduced as required. They are thus consistent with existing topographic maps even where geographical errors in the latter are known to exist. The natural environment is described in full but a familiarity with the basic human geography of Oman is assumed on behalf of the reader.

Semantic differences sometimes arise between Arabic and English. For example, Arabic toponym descriptions are based more upon territorial propriety than upon physiographic unity. Thus wadis frequently have several names throughout their course eg.: Wadi Bani Ruwaha – Wadi Semail – Wadi Fanjah – Wadi Al Khod, or Wadis Mistal – Jafnayn – Ma'Awil. For simplicty single wadi names have been used throughout and may therefore be at variance with local terminology. Certain Arabic words have also acquired several connotations dependent upon the context of their transliteration. The most extreme case is "Semail", variously translated as Samail, Samayil and Suma'il, which may mean:

(1) The name of a group of villages east of Jebel Nakhl

(2) The name of the major catchment in which the villages occur

(3) The name of the main wadi in that catchment and

(4) The formation name of the ophiolite nappe of which the Semail
      catchment is the type area.

Furthermore several common hydrological features are also common Arabic
place names, such as "Falaj" = stream derived from groundwater, and "Ayn" or
"Al-Ayn" = spring or pool. Conflicting terminology also arises between
English geological and hydrogeological usage, eg. (1) "Recent" here refers to
geological processes operative from several millennia B.P. to the present and
to demonstrably relatively young, uncemented and superficial sediments of
uncertain age; but in the hydrological context, refers to water of non-zero
tritium concentration (cf. Appendix B2) which has been involved in meteoric
circulation since about 1960. (2) "Deep" with reference to groundwater
circulation generally means hundreds of metres but is equivalent to "shallow"
in many geological contexts.

The term "watershed" is used in the English sense of a "bounding
perimeter" rather than the American "catchment area" connotation. Rustaq and
Nakhl springs (eg. section 4.2) are "vauclusian" in the sense of being
ascending springs with substantial discharges (Trombe, 1952) but might not
justify the term in comparison to the river sized "vauclusion springs" of the
Jura and Jugoslavia (Bogli, 1980). The term "piedmont" is taken as literally
"at the foot of the mountain", eg. piedmont alluvium = the coarse boulder
gravel such as the wadis, often several km wide, which surround the Jebel
Akhdar, or the outwash fans which form the upper limit of the Batinah Plain.
No wider regional connotation is implied.

Mineral identification was mostly based upon X-ray diffraction
supplemented, in the case of the more common and readily identifiable
minerals, by optical microscopy. The large number of diffractograms produced
are of little intrinsic interest and have therefore not been included in the
appendices.

CHAPTER 1

INTRODUCTION

1.1 The Environment of Oman

The area examined in this study is the mountain arc and adjacent alluvial basins of Northern Oman which extend some 650 km from the Musandam peninsula in the north to Ras Al Hadd in the east, and which lie between the approximate limits: 55½ to 60° east and 22 to 26½° north. From the earliest accounts, travellers have commented upon the unusual geology, high relief and rugged terrain as being strangely out of keeping with the general nature of the Arabian topography (eg. Pilgrim, 1908; Lees, 1928a and b; Thesiger, 1959). This striking contrast is apparent throughout the 600 km long landward perimeter of the Oman mountains whether approaching overland from either the south or west. It is preceded by a change from aeolian sands and sabkhas, characteristic of the interior, to fluvial Neogene and Recent fine grained clastic sediments of low gradient, which themselves grade into incised fanglomerates as they rise towards, and are abruptly truncated against, the foothills of the mountain front. With few exceptions these foothills are steep sided, sharp-peaked and heavily dissected by narrow winding wadis in which most of the sparse vegetation is concentrated. In the northern massif of Musandam (ie. the "Ruus al Jibal", Figure 1.1), the mountains rise to a maximum height of 2087 m before terminating in steep sea cliffs on their western, northern and eastern sides. Adjacent to the Ruus al Jibal, the mountainous area is composed entirely of relatively low (up to 800 m) foothills in a belt as narrow as 25 km. Further south and east the foothills become higher (1500 m or more) and reach a maximum width of 120 km.

Scattered within, and rising above the foothills are limestone mountains which vary in form from dramatically steep knife-edged pinnacles such as Jebels Misht and Yanqul, to the larger massifs of Tertiary uplift; Jebels Akhdar-Nakhl, Tayyin, and Ash Sharqiyah. In the southern foothills, sedimentation has produced a basin and range morphology which has facilitated easier travel, yet throughout the mountain arc, only six motorable tracks cross the mountain axis to the north-east coast. Even these roads are

1

Summary of Geological and Physiographic Features

(Modified after Glennie 1970,1974 and Wilkinson 1977)

Strait of Hormus

Ruus al Jibal

Gulf of Oman

Batina

Muscat

Umm as Sammim

Wahiba sands

Masirah

N

0   Km   100
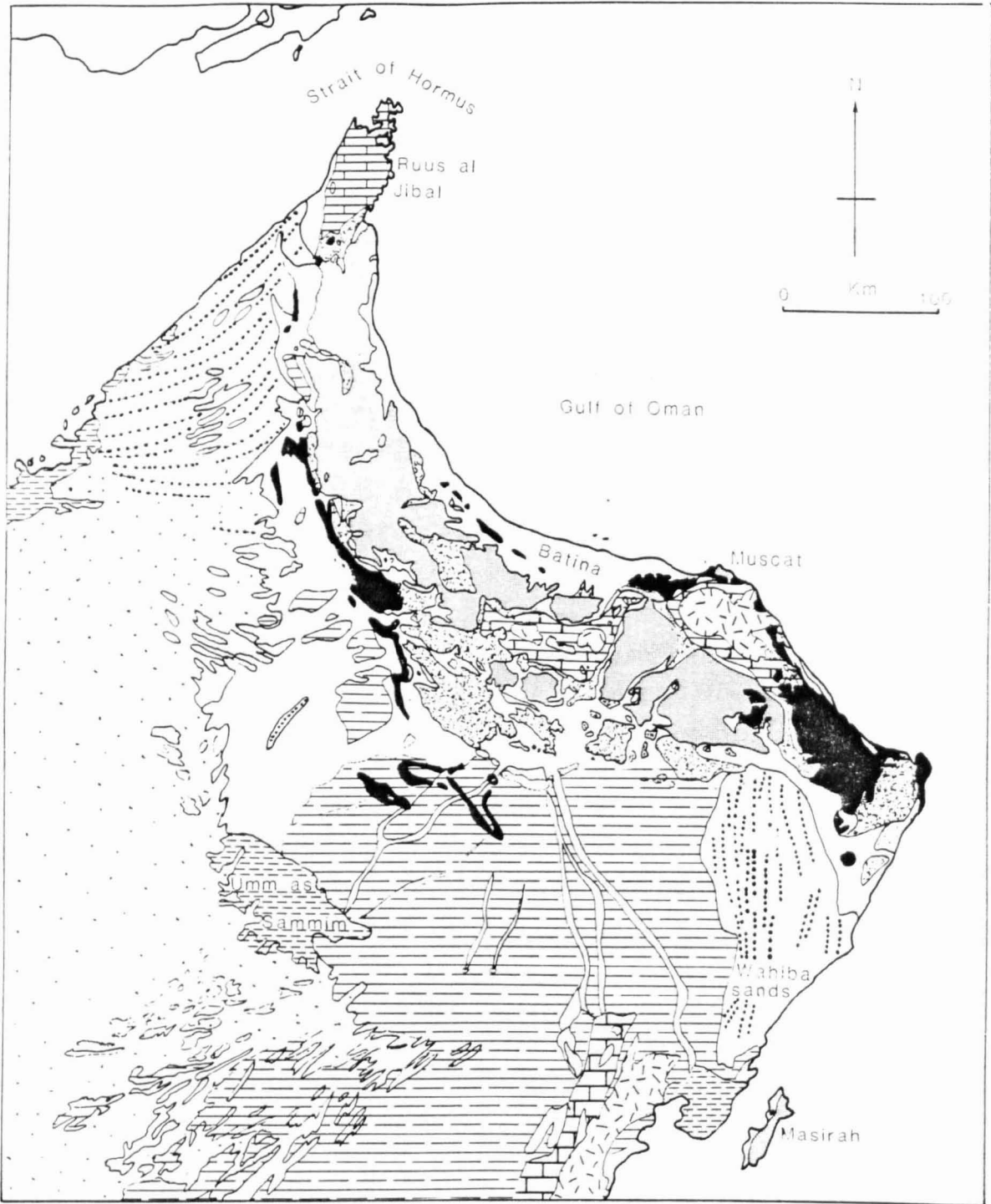
Coastal and inland Sabkha

Dune sand with seif lineations

Neogene and Quarternary Sediments

Oligo-Miocene desert platform

Palaeogene limestone

Semail nappe

Hawasina nappes

Permo-Cretaceous limestone

Pre-mid-Permian

confined to narrow passes where, until recently, communications were prone to disruption by occasional flash floods, but with the accession of Sultan Qaboos in 1970, a vigorous programme of road construction was implemented as part of an overall development plan. Consequently throughout the history of groundwater research (initiated in 1973) access to most populated areas (and hence areas of surface and groundwater occurrence) has steadily improved, although substantial mountain areas, especially at higher altitudes, are still accessible only by foot, and then only with extreme difficulty. Much of the mountain arc is bounded to the north-east by the "Batinah" coastal plain (cf. Figure 1.1), which takes the form of a low relief alluvial wedge which thickens to seaward. Vigorous drainage across this distinctive physiographic unit has, in several places, cut back across the mountain axis and now drains several "interior" basins in addition to a majority of the mountain and foothill areas. The Batinah is the most important of the alluvial aquifers and supports approximately half of Northern Oman's agriculture along a narrow strip of coastal cultivation.

The geology of the mountain arc is moderately complex but its analysis has also benefited from intensive research since 1970 with the result that all areas have been mapped at reconnaissance level, and many areas have been mapped in detail. Two outstanding projects have provided a particularly useful basis for further work. In 1974 Glennie et al. published the first comprehensive structural and stratigraphic summary of the Hajar mountain (Northern Oman) region. Although much of the original data and conclusions have since been superseded by more detailed studies, this was the most important "pioneering" project and remains the classic reference for most stratigraphic purposes. Secondly, the Oman ophiolite project is the largest of several subsequent projects to investigate the relatively unknown areas of Oman (eg. Gass, in press; Searle, 1980; Graham, 1980; Alabaster, 1982; Brown, 1982, Browning, 1982, Rothery, 1982; Bartholomew, 1983; Shelton, 1984; etc.) The latter references are mainly concerned with the structure and petrology of the ophiolites and other major nappe units which form a majority of the exposed hard-rock areas, and which were the focus of attention of most previous research (eg. Pilgrim, 1908; Lees, 1928; Morton, 1959; Tschopp, 1967).

Details of the hard-rock aquifers and aquicludes are fully discussed in the appropriate chapters, whilst their overall tectono-stratigraphic

Figure 1·2

Summary of the Tectono-Stratigraphic Relations in the Oman Mountains
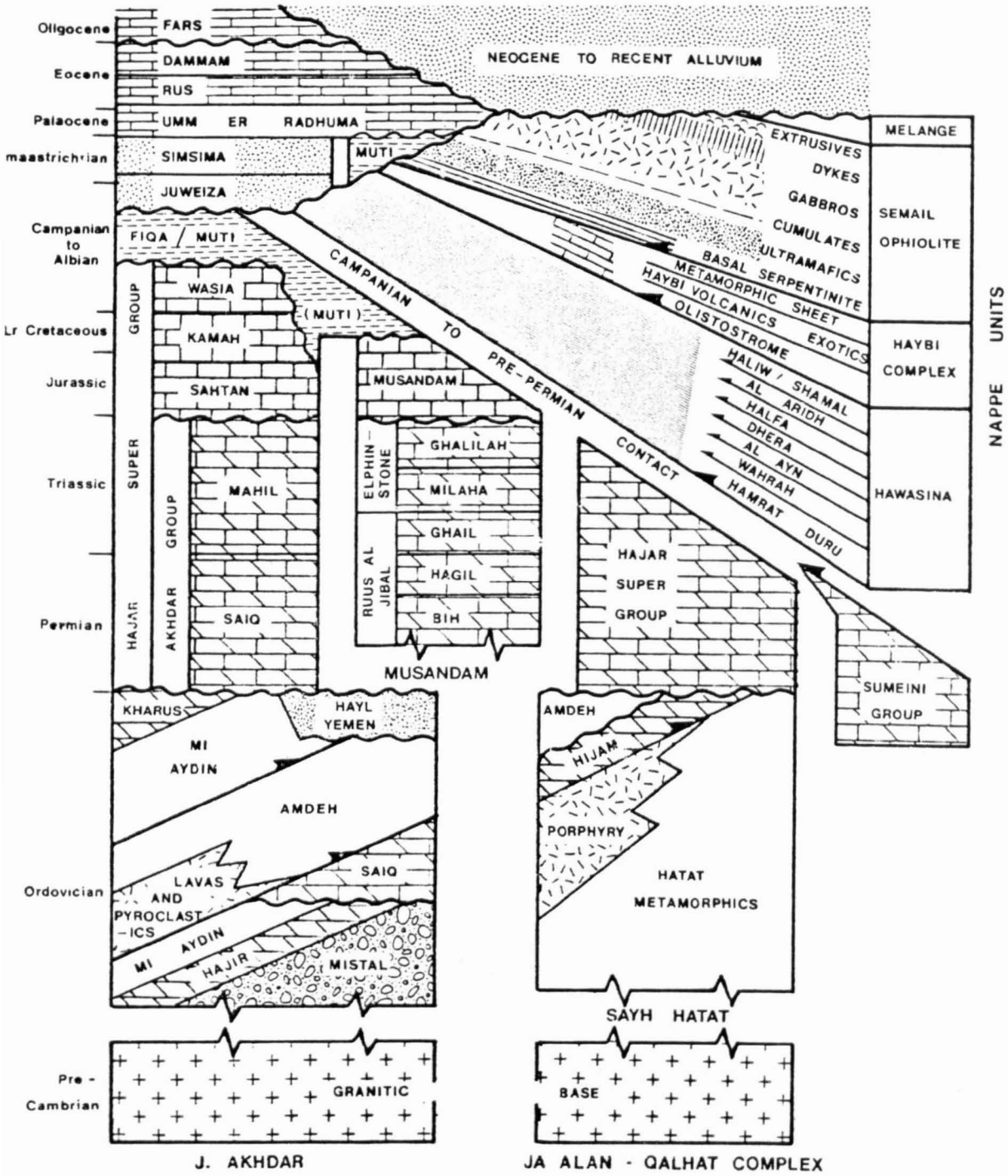
NB   Ages refer to the left hand part of the diagram

relationships are shown schematically in Figure 1.2. Initially however, it is sufficient to summarise the geology of the mountain areas in terms of five structurally coherent units:

5 Palaeogene Shelf Carbonates	=	Autochthonous
4 Semail Ophiolites	=	Allochthonous
3 Hawasina Oceanic Sediments	=	Allochthonous
2 Permo-Cretaceous Shelf Carbonates	=	Autochthonous/ Para-Autochthonous
1 Pre-Mid Permian Formations	=	Autochthonous.

1. With the minor exceptions of the Ja'Alan and Qalhat crystalline complexes and a few other granitic remnants discussed in section 4.7, crystalline basement is not exposed in the Oman mountains. Pre-Permian metasediments such as schists, conglomerates and quartzites are much more extensive and occur as inliers in the eroded cores of the Mesozoic massifs. Of these, neither the largest exposure (Sayh Hatat) nor the most complete section (Jebel Akhdar Inliers; cf composite section of Figure 1.2 and map 1) extends to the base of the sedimentary succession. An Ordovician fauna has been identified in the Amdeh formation of the southern Sayh Hatat (Lovelock et al., 1981) and in the Jebel Ramaq area of Musandam (Hudson et al., 1954), but elsewhere, despite differences in lateral facies variation and metamorphic grade, the stratigraphy has been estimated by correlation of lithofacies and is still inadequately known. Of the Pre-Permian carbonates, the Hajir and Hijam limestones have been both folded and eroded prior to subsequent carbonate sedimentation and are thus unconformably underplated against, and in hydraulic continuity with, the overlying Permo-Cretaceous carbonate succession in which case the former become locally important aquifers. Minor groundwater is also known from heavily fractured slates and shales in the Jebel Akhdar inliers which occasionally exhibit sufficient permeability to feed low yielding springs and water holes. In general however, the non-carbonate Pre-Permian formations are effectively aquicludes.

2. Permo-Cretaceous shelf sediments comprise a very thick sequence of limestones overlying dolomites, which together are known as the Hajar Super

Group (HSG). In addition to being the most productive and important of the hard-rock aquifers, the HSG massifs form most of the high relief areas (i.e. >1500 m), and hence are the highest rainfall areas of Oman, whilst its erosion products make a major contribution to the high yielding alluvial aquifers of the lower piedmont areas. The largest and highest of the HSG exposures is the entirely autochthonous Jebel Akhdar-Nakhl massif which emerges as a large reflexed anticline some half way along the axis of the mountain arc. This is the area considered in greatest detail in chapter four (the limestones) and Map 1, and is the source area of several alluvial basins discussed in chapter six. All the other major exposures of the HSG also occur as structural culminations at or close to the mountain axis, but vary greatly in tectonic style including an autochthonous/para-autochthonous anticline (Jebels Tayyin-Bosher), a para-autochthonous deeply faulted anticlinorium (Musandam), and an imbricate nappe zone south-east of Muscat. In these cases the tectonics involved in detachment have disrupted and overprinted the original structure with complex fracturing and folding in which the overall anticlinal mountain trend is less obvious. The hydrogeological properties of each area are sufficiently different to justify separate discussions in chapter four.

3.   During the Maastrichtian stage, the shelf sediments of Northern Oman were overthrust by a succession of nappes originating from "Neo-Tethys"; an oceanic environment to the north and north-east of the Arabian continental edge. These nappes are of two contrasting types; an upper ophiolite contrasting with a lower stack of thinner and much less competent sedimentary units collectively known as the "Hawasina nappe". These sediments are a very heterogeneous assemblage ranging from shallow-water oolites to abyssal radiolarites, and varying in thickness from a "pinched out" attenuated mélange only a few metres thick, to massive limestone Klippen (the "Oman Exotics") up to a kilometre thick, and the "Hamrat Duru limestone/chert group" which occurs as isoclinally repeated complexes some two kilometres or more thick. Recent authors have subdivided the Hawasina into two nappe sequences comprising an upper "Haybi Complex", of exotic limestone, metasediments and volcanics, and a lower sequence of oceanic sediments; the Hawasina sensuo-stricto, (cf. Searle, 1980). Of these sediments, only the "Exotics" are of any groundwater significance (cf. section 4.8).

4.   The Semail nappe is the largest and best exposed of all ophiolites, and covers more than half of the Oman mountain area. The upper part of the

Semail nappe, or "crustal sequence" is a highly competent predominantly basi
assemblage and essentially an aquiclude, whereas the lower nappe or "mantle
sequence" has undergone pervasive fracturing to permit minor groundwater flow
throughout the "hard-rock". Although the Semail nappe plays only a minor
role in the overall hydrological cycle, hydrochemical processes in the mantle
sequence result in extraordinarily alkaline conditions which is, in many
respects, the most interesting feature of the Oman environment. These
processes are discussed in chapter five.

5. Apart from uplift of the mountain arc during the Eocene period, most
tectonic activity and hence structural complexity is of Pre-Tertiary age.
Consequently, few publications and apparently little scientific interest has
been shown in the Palaeogene clastic and carbonate rocks. The latter form a
discontinuous folded and dissected drape around the flanks of the mountains,
and vary greatly in their aquifer potential, being aquicludes in most areas,
but occasionally constituting significant hard-rock aquifers where more
thickly developed (section 4.7).

It is impossible to consider the hydrology of the mountain catchments
without reference to groundwater in the associated alluvial basins of the
piedmont and outwash areas. These are mostly of late Neogene and Quaternary
age, and display considerable variation in facies and morphology, but do not
appear to have attracted significant geological investigation. Nevertheless,
since alluvium is the major source of groundwater storage and
abstraction/interception for agriculture, it is discussed in chapter six.

Apart from the distinctive physiographic and geological aspects, the
salient feature of the Oman environment is its aridity. There are obvious
dangers involved in comparing regional climates on the basis of a few highly
condensed statistics, but in the most general terms the data of Table 1.1,
for Oman (Rumais), Cyprus (Kyrenia) and England (Kew), serves to highlight
some of the major differences between the arid climate of Oman and more
temperate and Mediterranean climates. In particular the ratio of potential
evaporation to precipitation (E_T/pptn) is a measure of compatibility
between climate and vegetation growth. The gross departure from unity of
this value for Oman indicates potentially extreme transpiration stress which
can be overcome only by irrigation or by specialised adaptation of the
natural flora to xerophytic or phreatophytic forms. In addition, prolonged

7

Table 1.1

Comparison of typical near-coastal, low altitude climatic parameters.

Location Climate	Oman (Rumais)[1] Arid Subtropical	Cyprus (Kyrenia)[2] Mediterranean	U.K. (Kew)[3] Temperate Maritime
Altitude (m)	15	13	5.5
Temperature $^\circ$ C			
mean monthly minimum	19.2	15.2	7.1
mean annual	26.6	19.8	10.6
mean monthly maximum	34.0	24.5	14.1
annual range of monthly means	14.8	9.3	7.0
Wind Run : Mean daily km	185	109	334
Rainfall (mm) : Mean annual	70	534	594
Evaporation (mm) : Mean annual	2466	1800*	400
Evaporation/precipitation (E_T/pptn)	35.2	3.37	0.67

* Approximate

Sources: [1] Gibb, 1976 and Water Resources Dept. Data
[2] Takahashi and Arakawa, 1981
and Ismail, 1973
[3] Chandler and Gregory, 1976

droughts, the meagre soils, high exposure and overgrazing have generally reduced the natural vegetation still further to leave either sparse acacia or complete barrenness over most of the foothills and lowland plain. Despite the general aridity, however, Oman has a reputation throughout Arabia of being a land with relatively abundant flowing water and luxuriant vegetation, hence the name "Jebel Akhdar" (= Green Mountain). This expression is somewhat exaggerated, but greater rainfall in cooler high altitude areas results in both denser vegetation (plate 1.1), and in numerous springs and occasional surface water at lower altitudes, around which both natural and irrigated vegetation is locally profuse.

1.2 Rationale : Process Studies and Water Use

Ideally, the main objective of hydrological and hydrogeological research should be to quantify a wholly deterministic account of the water balance in such a way that available groundwater resources can be optimised and water management options clearly defined. This long term objective presupposes both a long hydrological data base (of the order of decades) and a comprehensive analysis of process studies in the environment concerned, both of which are currently inadequate. Indeed, although a few long rainfall records exist, from Muscat, Sharjah and Al Ayn, most of the hydrological data base covers a maximum of only 12 years, and even this record is incomplete due to discontinuity of measurement during the transfer of responsibility between consultants and other agencies, and to changes in emphasis of research. This difficulty is increased by both the lack of literature on comparable hot arid to semi-arid mountainous environments[1], and by the infrequency and extreme variability of rainfall-flood-recharge events (discussed in chapters two and three). In particular there were so few storm events in the study period 1979-81 that rainfall/runoff relationships were not adequately measured, and have had to be supplemented by estimates from indirect isotopic and chemical arguments. Further limitations were also imposed by the scale of the mountain environment, difficulty of access in the crucial high altitude areas, and other logistical problems. Consequently the high ideals of scientific rigour, for example with

---

[1] N.B. Previous consultants have made spurious comparisons with "similar" environments elsewhere such as Cyprus (Konteatis, 1980) and the southern U.S.A. (Water Resources Secretariat, 1978, pers.comm.), but significant differences in return periods, evaporation, rainfall and geology preclude the application of "conclusions" from such environments.

9

respect to raingauge network density, observation borehole density, statistically meaningful flood frequency analysis etc., are not achieved in reality. Rather, one is forced to the conclusion that hydrogeology in Oman, like politics, is the "art of the possible". This greatly affects the philosophy of approach. Instead of computing a fully deterministic analysis of any particular catchment, the present work is therefore a combination of deterministic, stochastic, empirical and inferential analyses which contribute towards a summary of the processes operative in Oman. A further objective is to draw attention to "weak links" in knowledge of the hydrological cycle with the hope that subsequent research will complete the picture.

It is assumed that readers will be familiar with the basic hydrological cycle but it should be noted at the outset that, in the environment of Oman, the relative importance of various components such as runoff, surface retention, interception, evaporation, infiltration etc., are grossly different from cooler environments, both in relative proportions, and in the time scale of the various processes. Of paramount importance is the immediate response to rainfall in the form of flash floods. Rainfall in Oman tends to be intense but of short duration, and since also, soil retention and interception by vegetation are both minimal, surface runoff typically occurs beyond a precipitation threshold of only 5 to 15 mm. Thus within a few minutes of the onset of rain, barren hillslopes are covered in innumerable rivulets which rapidly converge into streams and flash floods upon which most aquifer recharge is dependent. Although infrequent, these floods tend to cease flowing within a matter of a few hours, or at most only a few days and are crucial to the overall water balance of the region. Groundwater in the Oman mountains is therefore derived either from hard-rock springs or from alluvium in the active fluvial channels (wadis), which deeply dissect the mountains in all areas. This concentration of the groundwater into point or line sources has, historically, facilitated maximum exploitation by agriculture (mainly dates) in the form of falaj water supplies to hundreds of mountain oases and foothill villages. As discussed in chapter six, the "falaj" system has evolved as a varied and ingenious means of groundwater extraction and irrigation, and provides a simple but effective method of groundwater management during intermittent drought and flood conditions. Whether by trial and error or by design, the high efficiency of the falaj system has left very little unused groundwater in the mountains and therefore represents an approximate equilibrium between water use and natural baseflow. The origin of the system is obscure but extends at least as far back as the Sassanid period (Wilkinson, 1977), i.e. during

Persian influence between the third and seventh centuries A.D., and may well be much older. Biswas (1967) and English (1968) for example considered the spread of falaj-like structures from the eastern Mediterranean region to have occurred prior to 600 B.C., whilst traces of ancient, exceptionally long, open channel aquaducts may still be observed to cross the Batinah Plain in several places. Excavation of these undated but obviously early structures reveals smooth sided rectangular sections which, by measurement of roughness, cross-sectional area and slope, yield the following annual discharge estimates (using an estimated roughness coefficient of 0.02):

Ma-Awil channel	3 x 10^6 m^3.year^{-1}
Far "	6 " "
Sohar "	3 " "
Seeb "	3 " "

i.e. some 15 x 10^6 m^3 per year were transferred from the piedmont source area to areas of coastal cultivation. This is equivalent to about a tenth of the present-day irrigation consumptive use at the coast, and implies engineering expertise and a substantial quantity of groundwater use from antiquity. It is also interesting to note that such water transfer to the coastal strip obviated the danger of coastal salinization which in modern times is the principal threat to agriculture throughout the Middle East region in general, and to highly developed sections of the Batinah coastal strip in particular. Indeed the fragility of the groundwater system near the coast (i.e. the mobility of the "saline interface") is, from the human viewpoint, the most important aspect of hydrogeology in Oman, and must be considered within the context and limitations of the overall water-balance, discussed in chapter seven. The problems of coastal groundwater management become increasingly acute both with the escalating demands for municipal water supplies, and with increasingly conservative estimates of the available groundwater. The latter aspects are strikingly evident from comparisons of optimistic early water resources reports, with later reports (e.g. Gibb, 1976; Horn, 1979). This is largely due to a more realistic assessment of the complex partly-cemented alluvial sediments within the Batinah plain as opposed to the initial concept of a single homogeneous high yielding aquifer. Nevertheless groundwater processes within parts of the Batinah plain are still largely unresearched, and much work still remains to be done before a definitive account of hydrogeology in Northern Oman can be achieved.

CHAPTER 2

CLIMATE AND RAINFALL

2.1 The General Circulation

Overcast and unsettled weather is the exception in Oman. For more than 90% of the time the 'normal' climatic features are clear, bright skies, light winds, pleasantly warm dry winters and oppressively hot dry summers. These conditions may be related to simple processes of atmospheric circulation operating on a global scale and in particular to: heat exchange convection, the Coriolis Force, seasonal migration of maximum insolation, and the continent—ocean distribution.

About 40% of the Earth's surface lies within the tropics: an area which receives some 51% of the total insolation as opposed to less than 43% of the outgoing radiation. Consequently a thermal imbalance with latitude is set up, Figure 2.1a, which reaches equilibrium by means of the global convective system shown in Figure 2.1b. In this model, hot air rises in the equatorial zone and spreads polewards beneath the tropopause. In so doing, this creates a low pressure trough which is balanced by low level return circulation in the form of the trade winds. The latter are generated by the subsiding limbs of Hadley cells in which dry, dominantly cloudless air descends to form a high pressure zone in which subtropical anticyclones develop. Conservation of angular momentum dictates that with increasing latitude, winds will progressively deviate from the north—south circulation of Figure 2.1 and therefore become increasingly tangential to the isobars. These trade winds are symmetrically disposed around the equatorial trough, but due to the asymmetry of the continental distribution between the two geographical hemispheres, the mean position of the equatorial trough is itself displaced about 5° northwards, ie. the meteorological equator separates a larger southern meteorological "hemisphere" from a smaller northern one. Furthermore the equatorial trough meanders substantially with latitude, Figure 2.2a, due primarily to the annual cycle of the sun's zenithal position, and to modifying factors such as the seasonal contrast in land—sea thermal intertia, monsoonal influence and the stronger equatorial component of the southeast trades (which predominate over the northeast trades due to the absence of continental surface

12

Figure 2.1   Global Convection: Cause and Response
After Riley and Spolton, 1974
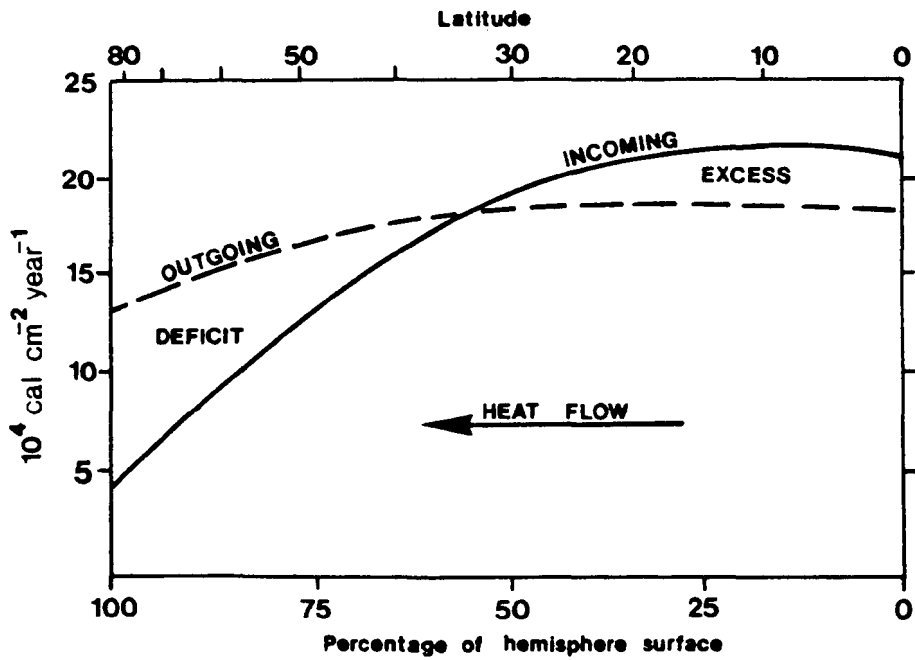
a) Mean zonal radiation balance
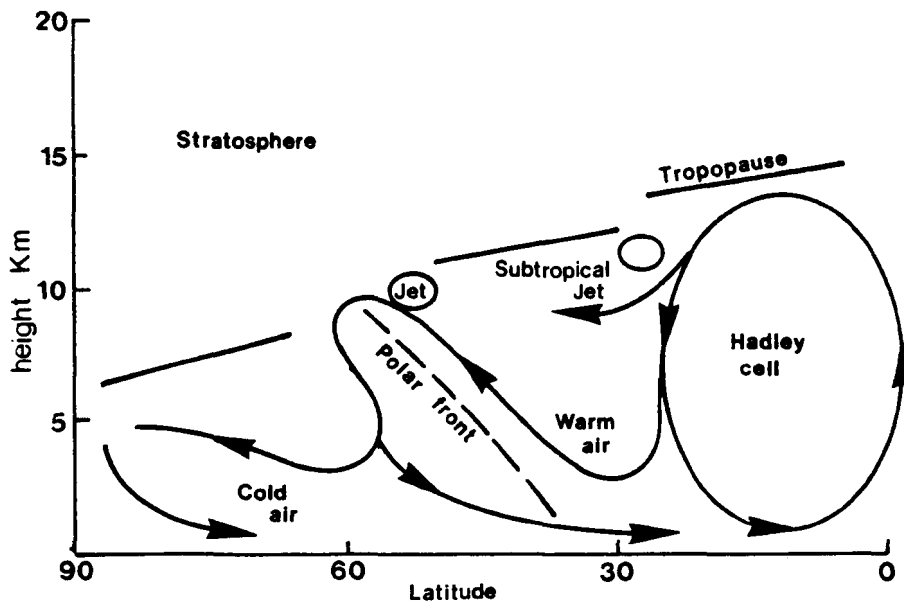
b) Predominant latitudinal heat flow mechanisms in the troposphere

friction in the southern oceans). Such latitudinal variation of the equatorial trough reaches a maximum in the longitude of Oman (Figure 2.2b). Thus the Oman mountains are bracketed between two zones; the main Equatorial Trough, and the Subtropical Anticyclonic belt, both of which may cross northern Oman in the course of seasonal periodicity.

The equatorial trough is more commonly known as the inter-tropical convergence zone (ITCZ), although convergence is only intermittent, and the zone is commonly branched and indistinct. At any one time it may be regarded as a locus of cloud clusters associated with a train of wave disturbances which reach their optimum northerly positions between June and September (cf. Gadgil et al, 1984). A good example is shown in a Tiros weather satellite image of the Northern Indian Ocean for 6 August 1980 (11.35 hrs, VIS band), Figure 2.3, in which waves of weakly developed cumulus clouds form a belt over the whole of Oman. The importance of the ITCZ lies in its separation of two contrasting climatic systems. It constitutes the easternmost limit of continental tropical air masses of westerly and northwesterly origin and consequently inhibits rainfall from that source during the summer months. On the other hand, the summer northwesterly migration of the ITCZ permits southeasterly trades which break away from the strong west Indian Ocean monsoonal airstream, Figure 2.4a. The normal and reliable consequence of this precipitation is the July to September Kharrif in Dhofar (the southern province of Oman). Further north infrequent disturbances in the ITCZ take the form of shallow near surface easterlies which penetrate the Sharqiyah and/or Gulf of Oman to provide occasional summer rainstorms.

The coincidence of a dry eastern continental coast with the subtropical anticyclonic belt tends to form one of the most geographically stable features of the global circulation. Unlike the ITCZ which migrates up to 35° southwards from Oman during the winter months, the anticyclonic belt north of Oman only broadens rather than migrates significantly southwards. Consequently Oman tends to lie just south of the high pressure belt, in the "horse latitudes" where warm continental air typically gives rise to light winds and dry cloudless weather. Between October and November, ie. the three driest months, westerly depressions mostly pass far to the north of Oman (eg. Figure 2.5), but with the build-up of a continental winter high pressure zone centered over the Caspian region, westerly winds veer to form the strong north-westerlies prevalent in north-west Oman and the Emirates.

Figure 2.2

a) Seasonal Variation of the ITCZ

—————— ITCZ in JULY
——·——·—— ITCZ in JANUARY
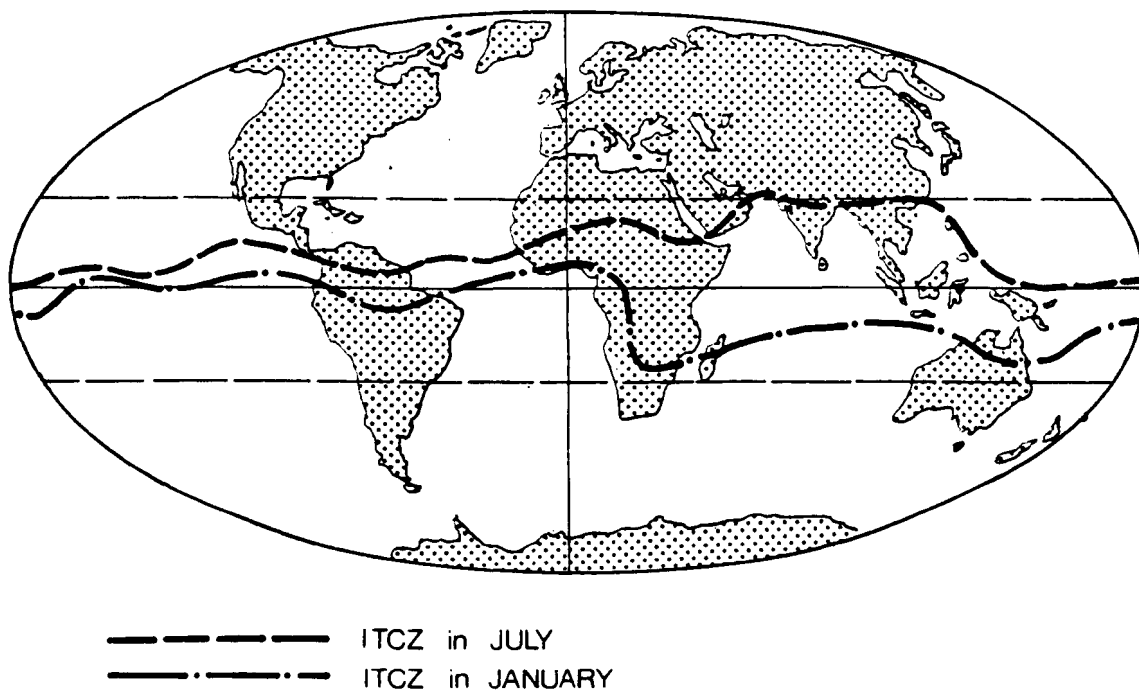
b) Lower Atmospheric Circulation in the longitude of Oman
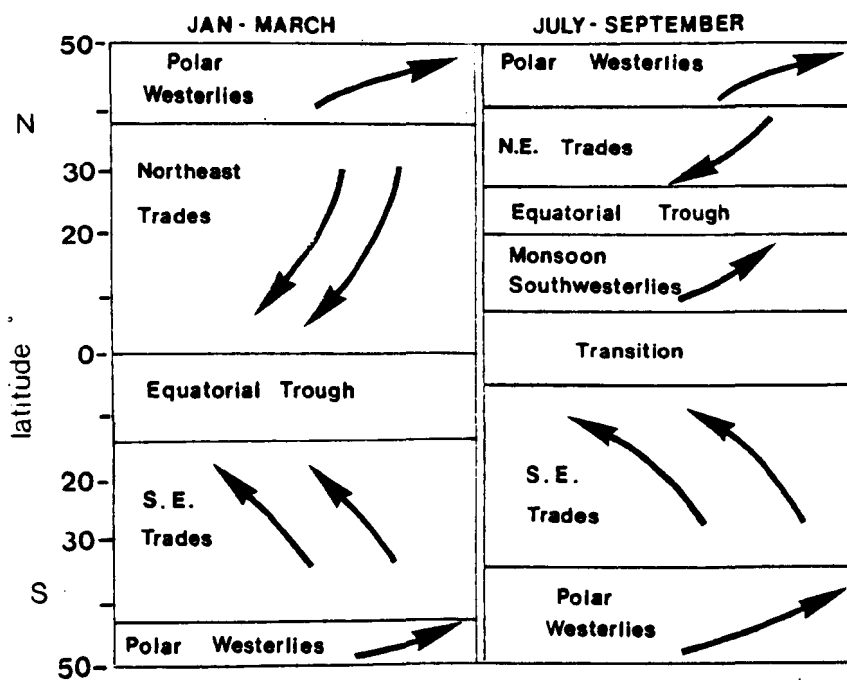
Figure 2.3   ITCZ Development Across Oman

Tiros-vis-6.8.80   0835 GMT
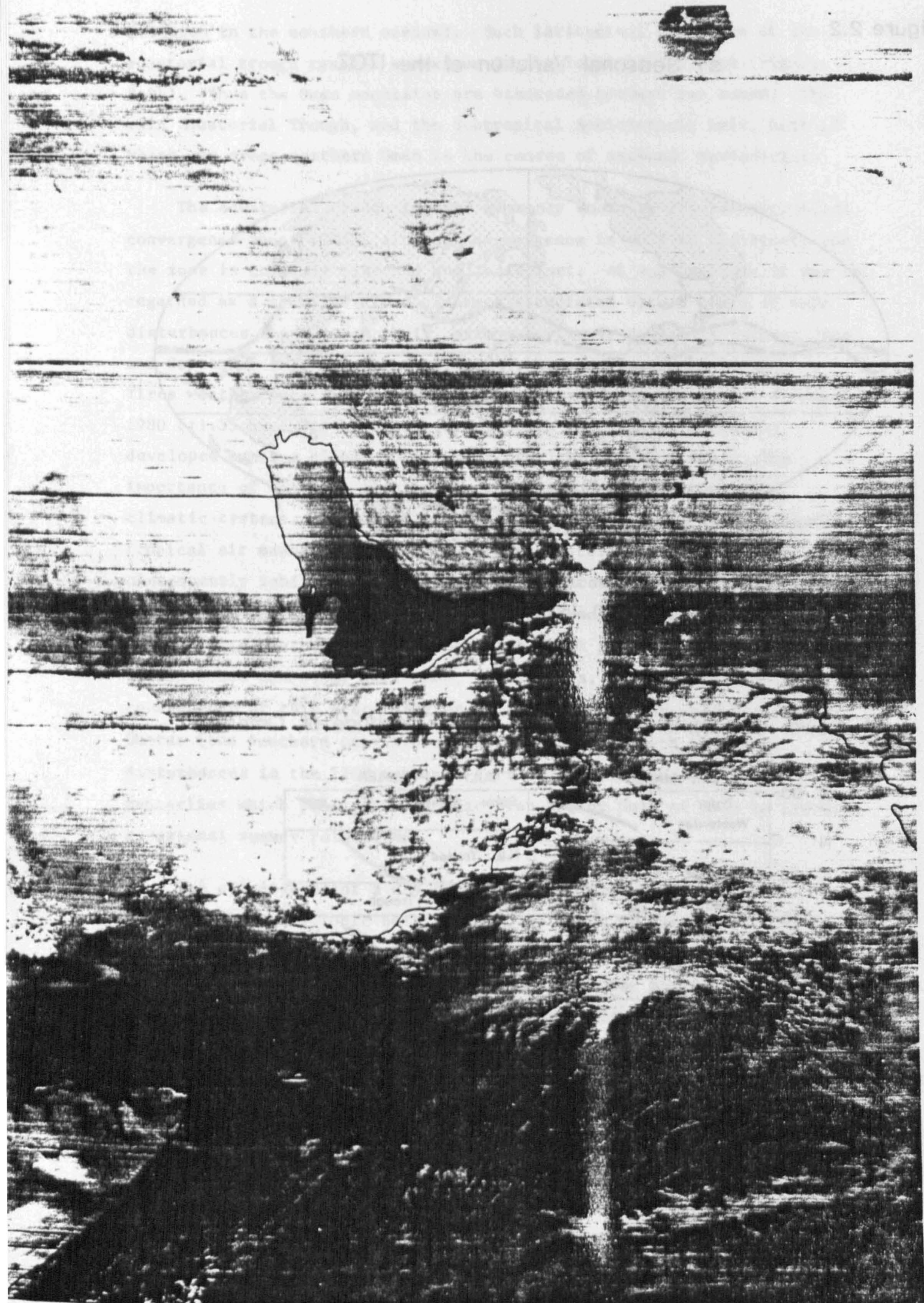
Figure 2.4　　　　　Schematic Surface to 850mb Air Circulation

Modified after Pedgeley,1970:Findlater,1977:Grant,1982:Membury,1983:and field observations

| January | April | July |
| mean pressure at Muscat 1016mb | Seif season: March to May | mean pressure at Muscat 997mb |
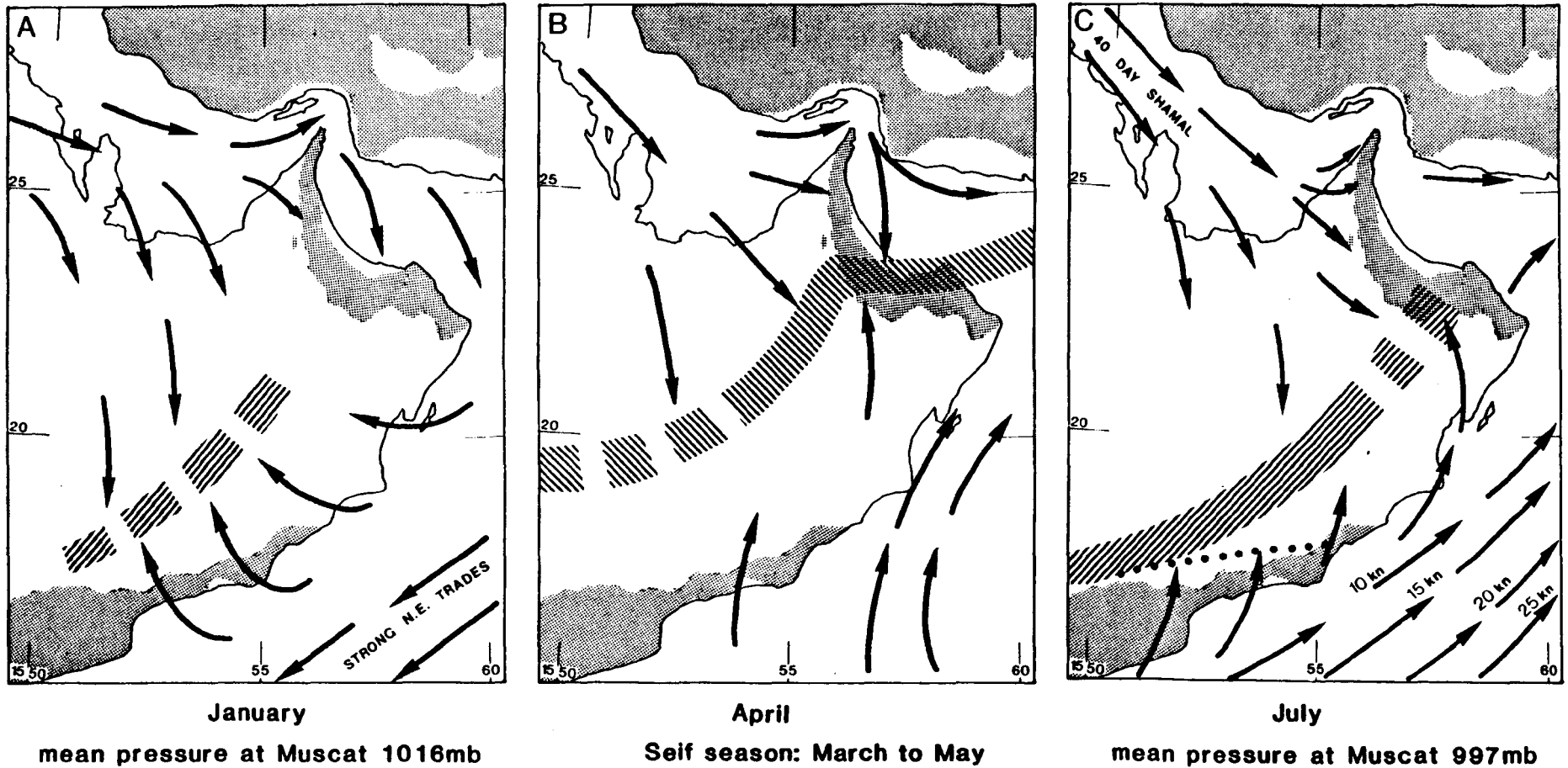
light stipple: land.　heavy stipple: mountains > about 500m.　　　•••• effective limit of the kharif (July to September)

hatched: Oman covergence zone or trade front,equivalent to the ITCZ during the summer months.

N.B. These are only average positions　ie.The locus of a broad succession of atmospheric eddies.

Figure 2.5   Dry Conditions in Oman with Decaying Monsoon Trades to the South

and Anticyclonic Westerlies far to the North

Tiros-Vis- 15.10.80   0835 GMT

Figure 2.5   Dry Conditions in Oman with Decaying Monsoon Trades to the South
and Anticyclonic Westerlies far to the North

Tiros-Vis- 15.10.80   0835 GMT

Throughout Oman these winds progressively weaken against a trade front derived from much stronger trades in the Arabian Sea (Figure 2.4c). This trade front; the "Oman Convergence Zone" of Pedgeley, 1970, is a shallow, weak, ill-defined and highly variable feature of the region but is probably responsible for many relatively localised low level storms in Northern Oman. Between January and March much larger storms result from deep westerly depressions but only the deepest of these are strong enough to give heavy precipitation and a large proportion of fronts probably miss the Oman mountains altogether, generally dissipating further north across Iran or Afghanistan. Indeed the main local influence upon the weather in northern Oman is the west to north-westerly airflow which dominates the lower troposphere throughout the winter, becoming more intense and localised in the Gulf between May and early July. These strong low level winds have mean speeds of up to 45 knots (Membury, 1983) and are deflected south westwards against the Zagros mountains of western Iran to form a persistent feature below 800 mb (Grant, 1982), locally known as the "forty day shamal". Following exhaustion of the shamal, dominance of the equatorial trough throughout the summer ensures relatively light winds. In the western mountains and Gulf littoral, these continue to be dominantly westerly, whilst in the central and eastern mountains, opposing monsoonal breezes predominate. The consistency of these contrasting prevailing wind directions is depicted in Figure 2.6 and results in the accumulation, parallel to the winds, of seif dunes whose lineations form the most prominent piedmont features of both the Western Emirates and the Wahiba sand seas (cf. Figure 1.1). In the latter case the present day north-south dunes are superimposed on a set of very much larger dunes with an intercrest spacing of up to a kilometre and a trend of 020°; a feature which may represent recent modification of a set of older dunes generated by very much stronger Pleistocene monsoonal winds (Glennie, 1970).

During the Gulf shamal, jet streams as low as 200 to 400 metres develop along the upper surface of strong nocturnal inversions (Membury 1983), thereby producing turbulent drag in the western piedmont areas which may take the form of low dust storms.

Figure 2·6   Frequency Percentage of Wind Direction
             April to August (shamal season)

A: Ibra 1974

DATA FROM RENARDET-SAUTI-ICE

at ground level,
means of 0600
and 1200 hrs

N

20 %

W

E

100 OBSERVATIONS

S

12 % CALM
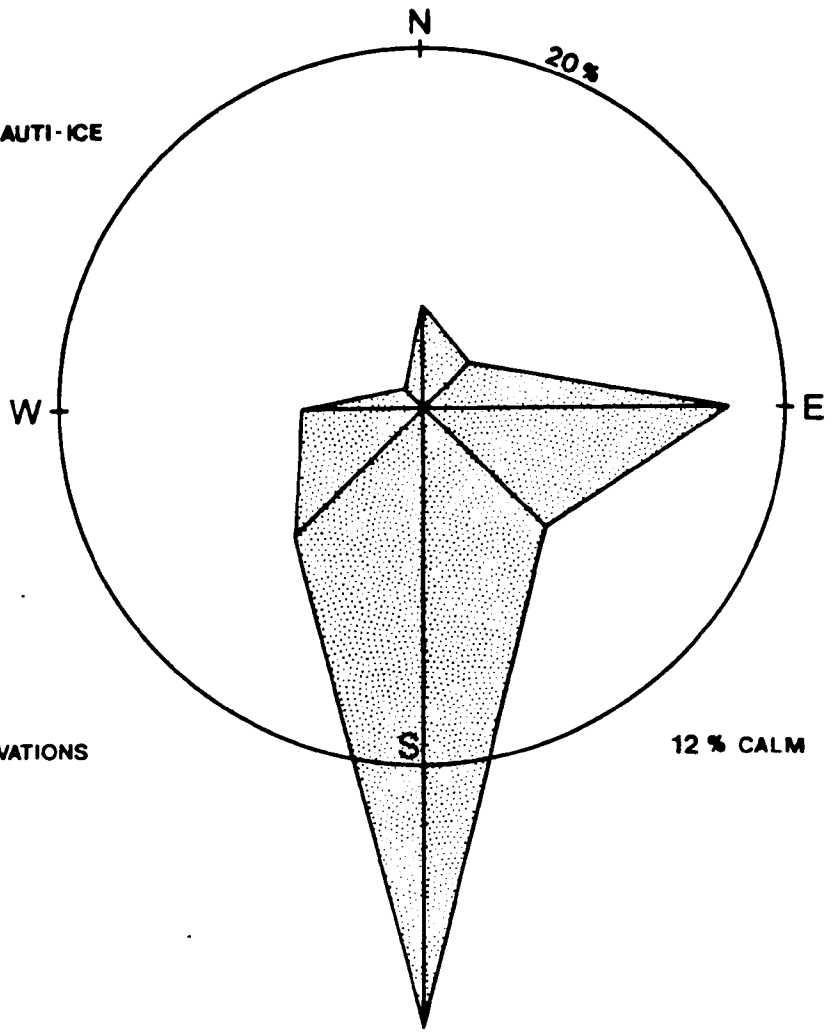
B: Sharjah 1961-65

DATA FROM PEDGELY 1970

1000 m at 1000 hr

N

10 %

W

E

723 OBSERVATIONS

22·2 % CALM

S

20
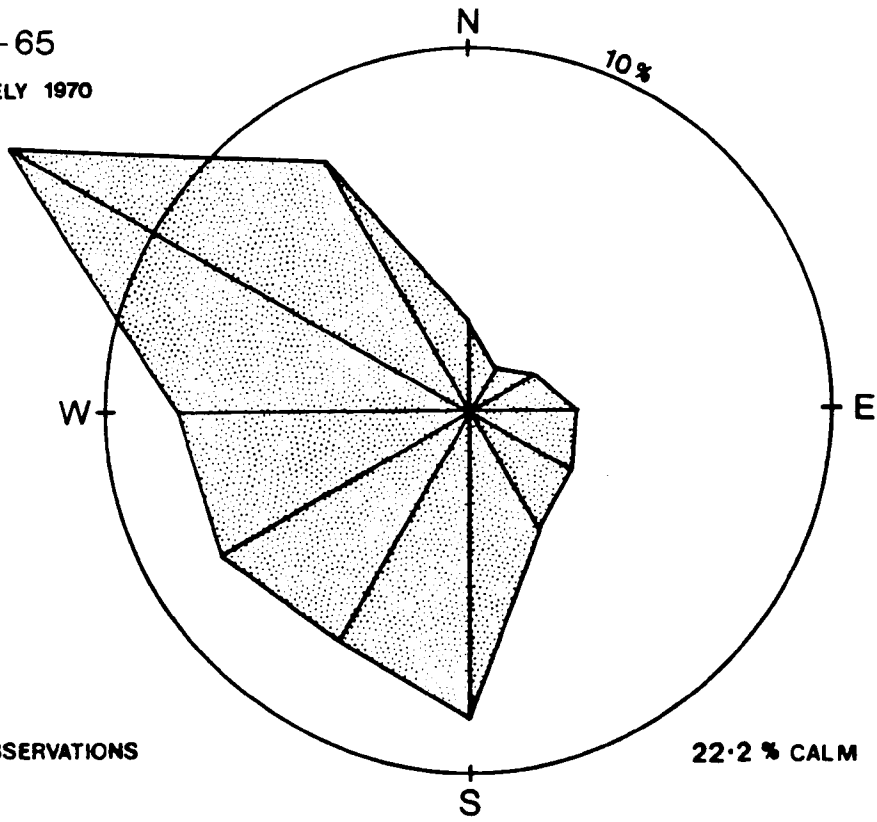
The resultant dust load sometimes persists in the foothill areas as a haze below about 1000 metres, ie. below the upper limit of the trade wind inversion regime. Large dense dust storms of the Saharan ("Haboob") type are rare and develop only during exceptional disturbances in the ITCZ.

2.2   The Climate of Northern Oman

Temperature

Northern Oman justifiably has a reputation for being an excessively hot area. This impression is heightened in many of the coastal centres of population due to high humidity, especially in the Arabian Gulf Littoral, and the close proximity of mountains whose shelter and thermal radiation maintains daytime temperatures well into the evenings. In general the mean annual air temperature of Northern Oman is about 4°C more than most other eastern seaboards of comparable latitude; eg. Taipei 25°N, 21.7°C;   Rockhampton 23 1/3°S, 22.9°C;   Dakhla UAR 23°N, 23°C;   Tampico 22°N, 24.3°C (Griffiths, 1972;   Arakama, 1969, Bryson and Hare, 1974, and Gentilli, 1971).

The locations of stations with reliable temperature data are shown in Figure 2.7, and the results are summarised in Tables 2.1 and 2.2, from which several trends and features are apparent. There is an obvious reduction of temperature with increasing altitude, shown at Saiq (2000 metres), but otherwise the mean annual air temperatures are consistently within a degree or two of 28°C, being slightly lower in broad alluvial areas and slightly higher in rocky coastal areas. The effect of "continentality" on the mean annual temperature range is tempered by the presence of sea on three sides of northern Oman although the Arabian Gulf is sufficiently shallow (generally less than 30 metres) to warm and cool rapidly, thus contributing relatively little to the thermal stability of the north-western coast. By contrast, the south-eastern seaboard is strongly influenced by the cold deep water upwelling off Dhofar during the Kharrif season. Although this thermal anomaly is attenuated further north, the summer sea temperature near the eastern mountains is often colder than in winter (Renardet et al. 1975), resulting in depressed mean annual air temperatures such as 26.1°C in Masirah Island, and 26.6°C at Ras Al Hadd. Consequently the annual range of monthly means is 17 to 18°C in the western Oman mountains ("continental side") compared to about 15°C in the eastern

Figure 2.7   Location of Meteorological Stations
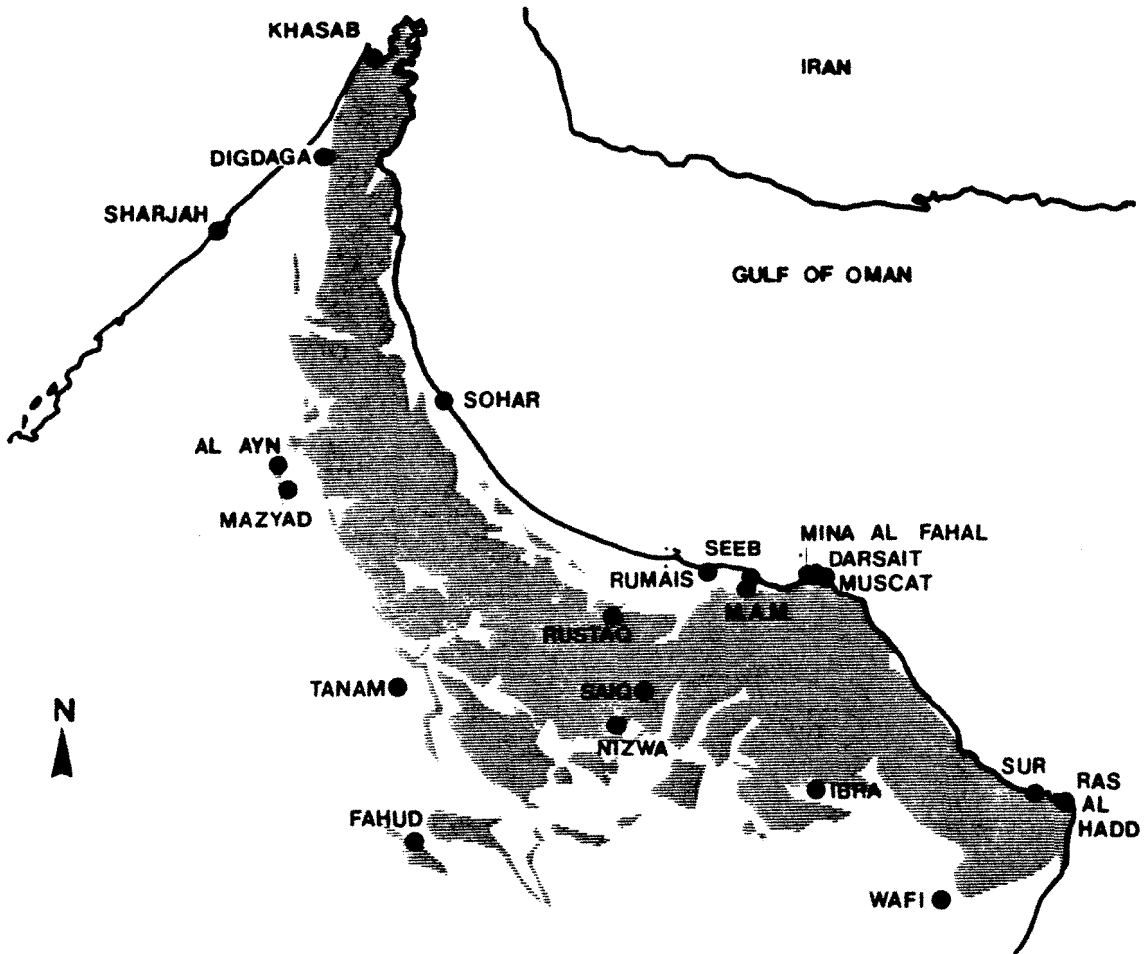
Table 2.1   Regional Annual Air Temperature Summary

Station*	Observation Period (yr)	Altitude (m)	Mean Annual Air Temperature °C	Annual Range of Monthly means, °C	Mean Diurnal Range °C
Al Ayn	12	295	26.1	19.0	16.3
Darsayt	3.5	25	28.3	14.8	7.8
Digdaga	2	15	24.4	17.8	14.8
Fahud	10	200	27.8	16.6	15.9
Ibra	1	400	26.8	15.0	–
Khasab	2	30	29.0	18.0	9.7
Mazyad	4	315	26.9	18.5	14.8
Mina Al Fahal	5	3	28.0	13.4	8.6
Muaskar Al Murtafa'a	2	30	29.7	15.2	10.1
Muscat	24	10	28.4	15.2	6.1
Nizwa	4	550	25.2	14.5	18.4
Ras Al Hadd	3	5	26.7	10.5	–
Rumais	2	15	26.6	14.8	12.1
Rustaq	4.5	350	26.8	16.9	15.6
Saiq	5	1897	17.1	15.1	11.9
Seeb	4	15	28.6	15.0	8.8
Sharjah	26	2	26.0	15.4	11.2
Sohar	7.5	15	25.7	15.7	13.2
Sur	3.5	6	28.6	13.7	9.4
Tan'am	1	300	28.3	17.8	16.5
Wafi	7	145	27.9	14.0	16.6

* cf. Figure 2.7

Table 2.2 Monthly Temperature Variation
(Mean Monthly Figures °C)

		J	F	M	A	M	J	J	A	S	O	N	D
	Max	23.0	24.2	29.6	34.0	39.5	42.8	43.4	43.0	40.5	35.8	29.7	24.9
Al Ayn	Min	9.2	10.5	14.6	17.5	20.0	23.1	26.2	27.2	25.8	17.7	12.8	10.0
	Mean	16.1	17.4	22.1	25.7	29.8	33.0	34.8	35.1	33.2	26.8	21.4	17.5
	Max	24.3	25.2	28.8	33.3	36.2	38.9	38.3	37.0	35.0	34.2	28.7	27.2
Darsait	Min	16.6	18.0	21.8	24.7	30.6	31.6	31.0	29.6	27.6	23.7	20.1	18.0
	Mean	20.4	21.6	25.3	29.0	33.4	35.2	34.6	33.3	31.3	29.0	24.4	22.6
	Max	25.5	25.0	27.0	29.8	33.5	38.8	40.0	39.2	36.7	32.0	27.7	26.1
Digdaga	Min	8.0	11.0	12.1	14.0	19.0	25.0	29.2	26.0	21.5	18.5	10.8	9.2
	Mean	16.8	18.0	19.5	21.9	26.2	31.9	34.6	32.6	29.1	25.3	19.3	17.6
	Max	15.3	17.9	22.9	26.2	35.0	40.3	42.1	41.6	38.6	32.7	24.3	18.2
Fahud	Min	4.3	5.2	8.4	12.5	17.6	21.1	24.3	23.5	19.2	14.1	9.0	5.3
	Mean	9.8	11.5	15.6	19.3	26.3	30.7	33.2	32.5	28.9	23.4	16.6	11.7
	Max	23.0	24.7	28.8	33.5	40.9	41.0	41.1	39.8	38.7	34.4	30.1	26.7
Khasab	Min	15.4	15.7	19.2	24.2	30.8	30.5	33.2	32.6	30.5	23.9	20.1	17.5
	Mean	19.2	20.2	24.0	28.8	35.9	35.8	37.2	36.2	34.6	29.1	25.1	22.1
	Max	22.7	25.0	31.5	35.5	39.2	42.0	42.2	42.5	40.6	35.6	30.0	24.3
Mazyad	Min	10.7	12.6	17.8	19.8	22.6	24.6	27.0	27.8	25.6	19.4	14.4	11.3
	Mean	16.7	18.8	24.7	27.6	30.9	33.3	34.6	35.2	33.1	27.4	22.0	18.0
	Max	25.1	25.4	29.5	33.2	38.7	39.1	36.8	35.4	34.9	33.4	29.4	26.6
Mina Al	Min	16.8	17.5	21.2	24.0	28.9	29.7	28.9	27.1	26.7	24.7	20.2	18.0
Fahal	Mean	21.0	21.5	25.3	28.6	33.8	34.4	32.8	31.2	30.8	29.0	24.8	22.3
	Max	26.2	27.1	31.3	38.5	40.8	42.1	41.3	37.7	36.6	37.0	31.2	27.3
Muaskar Al	Min	17.0	18.6	21.3	25.8	29.4	31.4	31.1	28.1	27.3	25.6	21.4	18.7
Murtafa'a	Mean	21.6	22.9	26.3	32.2	35.1	36.8	36.2	32.9	32.0	31.3	26.3	23.0
	Max	25.0	25.0	28.3	32.2	36.7	37.8	36.1	33.3	33.9	33.9	30.0	26.1
Muscat	Min	18.9	19.4	22.2	25.6	30.0	31.1	30.6	28.9	28.3	26.7	22.8	20.0
	Mean	21.7	22.2	25.0	28.9	33.4	34.5	33.4	31.1	31.1	30.6	26.1	22.8
	Max	25.7	26.3	32.2	35.3	39.3	41.4	40.2	40.5	38.6	34.3	31.1	28.0
Nizwa	Min	7.9	10.8	13.7	16.9	19.5	21.6	22.2	21.7	19.4	15.9	13.0	11.0
	Mean	16.8	18.5	22.2	26.1	29.4	31.5	31.2	31.1	29.0	25.1	22.0	19.5
	Max	24.7	24.5	29.3	33.1	38.2	40.0	39.7	36.6	35.8	33.1	29.5	26.4
Rumais	Min	13.4	14.4	17.5	20.4	24.4	26.6	28.0	26.3	24.4	19.6	16.3	15.0
	Mean	19.0	19.5	23.4	26.8	31.3	33.3	33.8	31.5	30.1	26.4	22.9	20.7
	Max	24.7	26.4	30.6	35.1	40.7	42.8	41.8	40.9	39.3	35.4	30.1	26.7
Rustaq	Min	10.9	11.9	15.1	17.4	22.5	25.3	27.6	24.8	23.6	20.0	14.9	13.9
	Mean	17.8	19.2	22.8	26.2	31.6	34.0	34.7	32.8	31.4	27.7	22.5	20.3

Table 2.2 cont. Monthly Temperature Variation
(Mean Monthly Figures °C)

		J	F	M	A	M	J	J	A	S	O	N	D
	Max	15.6	15.6	19.1	23.0	27.3	30.3	30.6	29.1	26.8	22.9	19.5	16.2
Saiq	Min	3.3	5.7	8.4	10.9	15.0	17.7	18.5	18.0	15.5	10.2	5.9	4.5
	Mean	9.5	10.6	13.7	17.0	21.1	24.0	24.6	23.6	21.1	16.5	12.7	10.4
	Max	24.3	25.7	28.0	34.0	39.7	40.8	39.0	36.5	36.6	34.4	29.9	26.4
Seeb	Min	17.3	17.7	20.3	24.0	29.2	30.8	30.2	28.6	27.5	25.7	20.5	18.0
	Mean	20.8	21.7	24.1	29.2	34.4	35.8	34.6	32.6	32.0	30.0	25.2	22.2
	Max	24.5	25.3	27.3	30.1	34.4	34.7	38.4	37.1	36.8	34.5	30.6	26.1
Sharjah	Min	12.0	15.0	17.2	18.5	21.3	23.6	28.6	27.9	25.2	23.1	18.8	14.5
	Mean	18.2	19.0	22.0	24.7	28.1	30.6	33.2	33.6	31.4	27.6	23.5	19.8
	Max	23.8	24.4	27.9	32.3	38.3	39.3	38.1	36.9	36.3	34.3	29.5	26.3
Sohar	Min	10.4	12.6	15.3	18.0	23.0	25.4	27.4	27.1	23.8	19.2	14.6	12.8
	Mean	17.1	18.5	21.6	25.1	30.6	32.4	32.8	32.0	30.1	26.7	22.0	19.6
	Max	25.6	26.7	29.7	34.0	39.0	41.0	38.0	37.0	36.7	35.1	29.8	27.2
Sur	Min	18.4	18.3	21.0	24.3	28.7	30.3	29.0	27.7	26.3	24.9	20.2	18.3
	Mean	22.0	22.5	25.4	29.1	33.9	35.7	33.5	32.3	31.5	30.0	25.0	22.7
	Max	25.8	26.2	34.2	37.2	41.4	45.9	45.5	44.6	41.7	37.5	31.7	26.9
Tan'am	Min	11.5	11.7	18.9	19.5	23.3	27.0	27.1	27.7	25.2	20.5	15.0	12.9
	Mean	18.6	19.0	26.6	28.3	32.3	36.4	36.3	36.1	33.5	29.0	23.3	19.9
	Max	29.3	29.2	35.6	37.8	42.3	43.1	47.1*	42.2	41.5	37.1	33.4	28.9
Wafi	Min	10.9	9.2	13.0	21.6	24.1	25.7	22.5	19.8	17.5	17.3	11.0	14.5
	Mean	20.1	19.2	24.3	29.7	33.2	34.4	34.8	31.0	29.5	27.2	22.2	21.7
Ibra	Mean	19.2	19.8	25.8	28.3	32.3	33.4	34.2	32.7	29.8	25.8	22.2	19.4
Ras Al Hadd	Mean	21.7	22.2	25.0	27.8	31.7	32.2	28.9	28.9	27.8	26.7	25.0	23.4

* July data at Wafi is suspect

25

mountains ("oceanic side"). More obvious moderating effects of sea temperatures are demonstrated by the mean diurnal range which is typically about 10°C at the coast as compared to about 16°C in the interior foothills. Contrary to the normal influence of oceanic proximity, the time lag between the maximum zenithal position of the sun, and the maximum air temperature, is about two months in the north and central mountains but only one month in southern and eastern mountains (i.e. peak air temperatures occurring during July/August, and June respectively). This varying phase difference is difficult to account for but may be related to the ITCZ, which also lags the sun's zenithal position by two months, as much as to anomalous sea temperatures.

Maximum air temperatures in the shade seldom exceed 45 or 46°C, the absolute highest reliable air temperature so far recorded being 47.8°C at Seeb (Horn, 1977). Unconfirmed reports of hot dry air gusts from the Interior in excess of 50°C (shade temperature) in the Semail gap and the southern desert edge (Smith G. pers. comm.) are improbable but not impossible. Nevertheless rock surface temperatures regularly exceed 50°C during the summer months.

At lower altitudes the two coldest months, December and January, are generally very pleasant with mean daily temperatures of around 20°C, whilst night time frosts are almost unknown. The single recorded exception is at Digdaga (altitude 15 metres) where katabatic winds from the Rus Al Jibal, laterally confined by Wadi Naqab, have been known to spill onto the western piedmont at − 0.6°C (Halcrow, 1967). At Saiq on the other hand, freezing or near freezing screen temperatures occur some 15 times during the winter period of late November to late February, which in the highly exposed terrain at such altitudes, results in widespread ground-frost.

Humidity

Daily spot measurements of relative humidity (R.H.), summarised in Table 2.3a, appear to show a misleadingly narrow and consistent range of values for any one site whereas the strong influence of air temperature results in large diurnal variations, eg. Table 2.3b, thereby making R.H. a highly variable climatic parameter. Few statistics report more than two humidity readings per day, and thus the range of humidity is generally underquoted. Of the few detailed records, that of Sharjah,

Table 2.3   Mean Relative Humidity (R.H.%)

Data mainly from the Oman Water Resources Dept. and Gibb, 1976

(a)   Spot Measurements at 9.00 a.m.

record length (yr)	J	F	M	A	M	J	J	A	S	O	N	D
Nizwa 8	68	63	51	44	45	47	55	52	57	53	53	60
Saiq 3	42	44	43	39	38	28	30	34	26	29	33	(23)
Wafi 7	72	72	56	58	60	62	55	61	67	61	64	64
Buraimi 2	68	63	51	44	45	47	55	52	57	53	53	60
Mazyad 4?	71	67	50	40	42	42	44	52	48	40	62	70
Muscat 8 a.m. 7	72	73	71	64	58	72	77	82	75	69	69	70
Rustaq 3	65	72	64	53	50	52	75	52	55	55	53	65
Rumais 2	66	67	60	51	45	51	65	68	58	57	67	70

(b)   R.H. Variation and Vapour Pressure at Rumais (after Horn, 1977)

Vp (mb)	15	17	18	20	22	26	30	32	30	25	20	17
mean max RH %	80	85	85	73	60	70	85	85	85	85	77	85
mean min RH %	45	45	40	35	25	40	55	50	45	40	40	50

Figure 2.8, shows the obvious temperature dependence in which highest R.H.s occur around dawn when temperatures are minimal, whereas maxima occur shortly after noon. The vapour pressure (specific moisture) increases substantially at the coast during the hottest months, especially in the north-west, thus contributing to the physiological discomfort of summer, but the high air temperatures suppress the R.H. so that, away from coastal areas, the highest values may occur during the winter months. High relief areas such as Saiq are well above the influence of moist inversion layers and offshore breezes, and therefore experience relatively dry airflow with low absolute vapour pressures (vp) in which typical seasonal ranges are 4 to 7 mb in winter, and from 9 to 14 mb in summer. Very dry air with a vp of less than 2 mb occurs about 20 times annually resulting in frequent R.H.s of less than 10% (at 9.00 a.m.) whilst high humidities of greater than 50% are rare (Horn, 1977). A marked tendency towards lower humidities also occurs in inland areas of lower relief such as Nizwa and Buraimi.

Wind Run

Peak airflow usually occurs in the "shamal" season of May to early July, with a second and sometimes stronger wind run maximum occurring earlier in some western and southern stations as shown in Table 2.4. The available wind observations are mostly confined to total wind run, so that information on wind direction and strength is somewhat sketchy and inadequate. However, the limited data, together with subjective assessment suggest that winds occur mostly during the day, and are steadiest during the winter months. During the summer, the almost complete absence of Coriolis force allows pressure differentials to equilibrate rapidly, thus producing short bursts of strong winds within a predominantly slow moving air mass. These typically take the form of thermal squalls from the interior or of weak convective vortices ("dust devils"), the latter probably accounting for the strongest gust so far recorded, of 57 knots (105 k.p.h.) at Seeb airport.

Comparison of wind run data is hampered by the non-standard height of most of the more recently installed anemometers. On the basis of the Rustaq data, in Table 2.4, an empirical correction factor of 1.57 should be applied to data from effective instrument heights of two metres, whereas the conventional correction from Hellmann's formula is 1.21

Table 2.4   Mean Wind Run (km/day)

Data mainly from the Oman Water Resources Dept. and Gibb 1976

	Record Length (yr)	Anemometer ht (m)	J	F	M	A	M	J	J	A	S	O	N	D
Nizwa	8	2	61	67	82	88	90	90	87	82	80	72	62	58
Saiq	3	10	278	330	331	302	323	356	296	311	336	282	252	224
Wafi	7	2	160	191	137	167	158	200	153	172	121	156	173	199
Al Ayn	12	2	202	209	243	224	217	216	214	218	211	173	138	164
Mazyad	4?	2	218	222	218	194	206	194	180	172	166	159	168	174
Muscat*	27	2	69	69	69	69	69	69	69	69	52	52	52	69
Rustaq	3	10	92	103	120	122	135	143	145	130	114	83	77	81
"		2	–	–	–	–	–	–	75	77	80	68	54	48
Rumais	2	10	229	253	240	241	249	251	273	253	229	223	205	205

*Suspect record

Table 2.5   Mean Wind Run Corrected to 10 m (km/day)

Station	Empricially corrected	Hellmann corrected
Nizwa	120	99
Saiq	275	275
Wafi	261	215
Al Ayn	317	261
Mazyad	297	244
Muscat	101	68
Rustaq	112	112
Rumais	238	238
Dar Sayt*	190	224

* instrument height – 4 metres

Figure 2.8   Sharjah; Mean Diurnal Variation in
Relative Humidity.   After Halcrow, 1967

Oct 1966 to Sept 1967
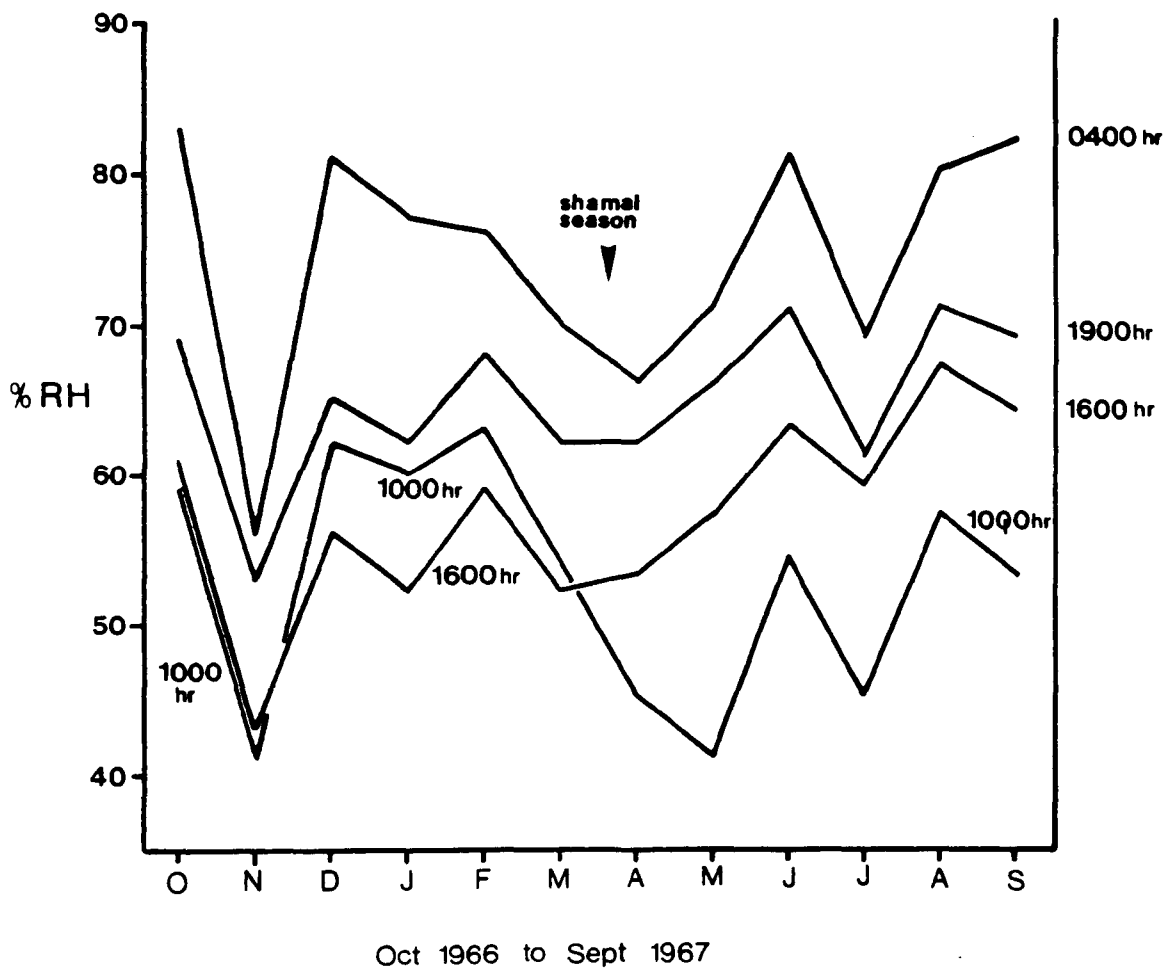
(Meteorological Office, 1969). The resulting corrected data, shown in Table 2.5, is rather inconsistent except to illustrate the substantial reduction in wind run that occurs in foothill positions. Two such values, occurring at Nizwa and Muscat, may therefore represent atypical microclimates. If so the unfortunate coincidence of Nizwa and Muscat in having the two longest rainfall records may have led to errors in some of the earlier regional rainfall estimates, cf. section 2.4.

Sunshine and Insolation

As with wind run, sun hours in the relative sheltered foothill sites of Nizwa and Rustaq experience lower than average values of 8.95 and 8.66 hours respectively. Morning mist and low cloud in winter also depresses the sun hours at some coastal stations, such a 8.67 hours at Sohar, but otherwise the values for most stations deviate little from the mean value of 9.2 hours. Consequently, the mean insolation is similarly consistent, ranging from a minimum of about 340 $cal.cm.^{-2}$/day in winter to a maximum of 600 $cal.cm.^{-2}$ d^{-1} in summer at low altitudes. The corresponding figures for high altitude at Saiq are about 400 and 600 $cal.cm.^{2}$ d^{-1}, (Gibb, 1976).

Rainfall Intensity

Rainfall amounts and distribution are fully considered in section 2.4, but any review of hydrometeorology must also take cognizance of short period storm intensities and frequencies in view of their controlling influence on flood runoff characteristics.

The five earliest autographic rainfall stations were established in 1974, a further seven being added in 1977, with an additional nine instruments being established by the author in 1979. Up to 1981 most of these had recorded so few rain events that little or no statistical conclusions could be derived from them. However, an important exception is at Saiq where an almost complete seven year record, including 125 rain events, has enabled the construction of the % frequency/intensity analysis shown in Figure 2.9. (As an example of interpretation, the second outer curve shows that 2% of rainstorms, equivalent to 0.36 events/yr, are likely to precipitate 27 mm within half an hour. The next curve indicates that 5% of rainstorms are likely to precipitate 27 mm within 1.5 hours, and so on. Conversely, 27 mm are likely to be precipitated with an intensity of 54 mm/hr once every 0.36 years, or with an intensity of 18 mm/hr once every 0.89 years .....etc.)

Figure 2.9   Maximum Rainfall Intensities at Saiq

The curves indicate the percentage of rain events attaining
the rainfall amounts shown.
The equivalent return periods (years)
are given in brackets

Based upon 125 rain events;
July 1973 to July 1980

0·71%
(8)

2%
(2·78)

5%
(1·12)

10%
(0·56)

25%
(0·22)

50%
(0·11)

mm

maximum precipitation

DURATION (Hours)
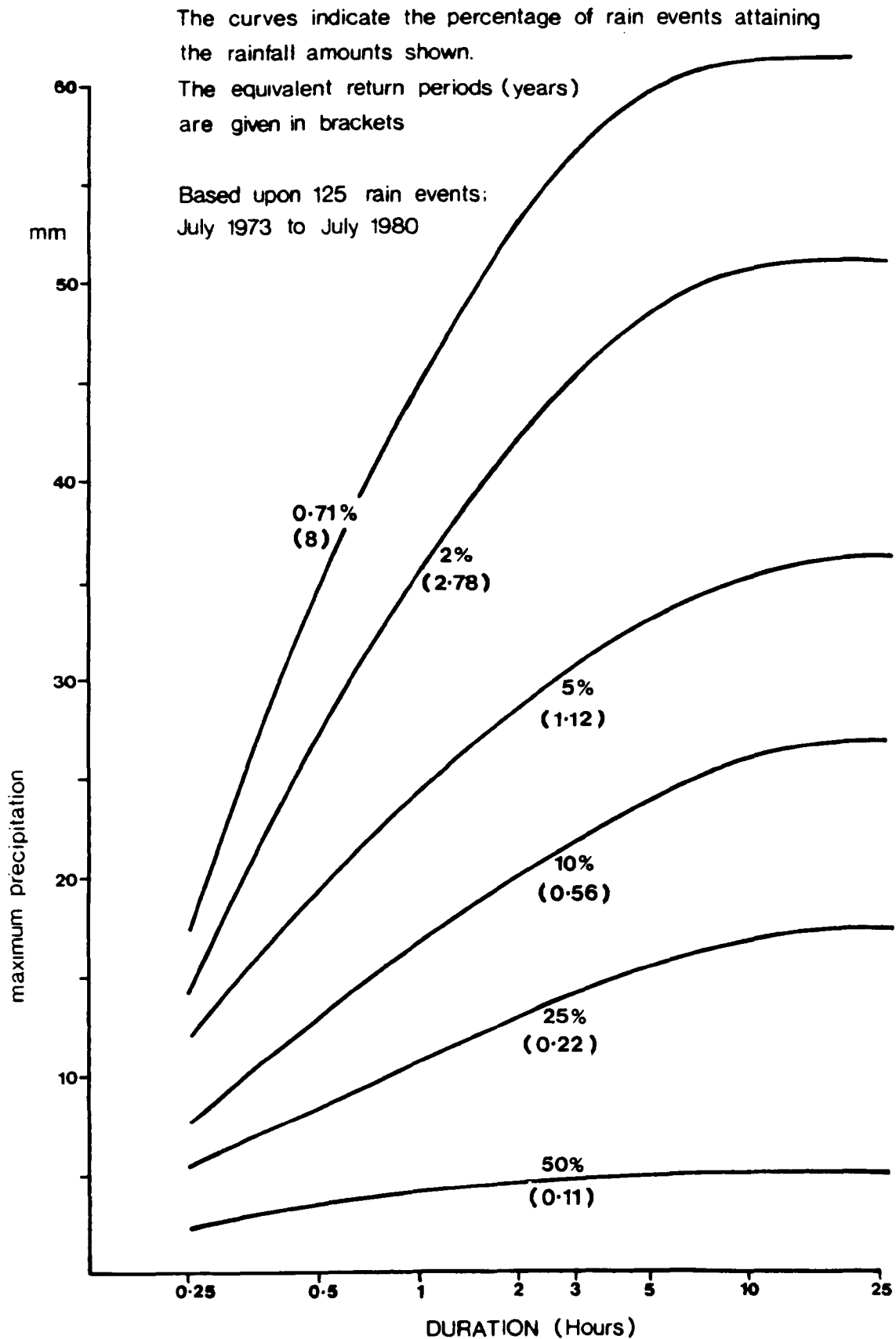
Notwithstanding the low R.H.^{s}, the high vapour pressure during the summer months coupled with vigorous convection in the mountain environment creates the potential for very short rainstorms of near tropical intensity. On the other hand most of the extremes of 24 hour rainfall occur during the winter months, (Horn 1978a). Despite these seasonal variations, the record provides an overall self-consistent pattern of rainfall intensities from which the return periods, at high altitudes, may be derived. Rainfall intensities and extreme values at lower altitudes appear to follow a broadly similar pattern but at lower frequencies. On this basis, Horn (1978a) further argued that since extreme events had a similar frequency at most stations, "but with Saiq having a noticeably higher frequency of moderate events", the five year record from both high and low sites, Table 2.6, could justifiably be combined using the station year method to give the return periods shown in Table 2.7. Return periods based on 24 hour data, derived both from the Muscat daily record, and interpolated graphically from the Saiq data are also included for comparison. All three estimates provide a good measure of agreement and hence may be regarded as a reliable indication of maximum rainfall frequency. However, as the frequency of lower rainfall maxima are largely derived from high altitude data, the shorter return periods are probably underestimates for such areas as the foothills and alluvial lowlands.

2.3 Factors Governing Rainfall Occurrence

Rainfall in Oman occurs as fronts, orographic and cyclonic effects, and minor processes which produce coastal and other more localised precipitation. In the absence of detailed synoptic analyses, it is difficult to establish the volumetric importance of these processes, but the isotopic evidence (section 2.5) suggests that deep frontal depressions of both Mediterranean and ITCZ origin are responsible for the great majority of groundwater recharge. Fronts of northerly to westerly origin, occur during the winter months and contrast with the summer rains by their more widespread distribution and longer duration although summer rains are generally more intense. Not all such "Mediterranean" fronts are significantly rain-bearing but the available record suggests that an average of 2.5 to 3.0 heavy rainfall storm events occur over a wide area each year, typically in January or

Table 2.6   Ranked Rainfall Maxima (mm) from a 5 year
record (after Horn, 1978a)

24 hour maxima				One hour maxima		
Rustaq	Saiq	Nizwa		Rustaq	Saiq	Nizwa
81	61	54		(50)	45	55
44	53	51		41	35	33
41	50	43		22	33	30
31	49	42		(20)	31	16
29	42	40		(15)	29	15

Table 2.7   Return Periods for 24 hour rainfall maxima

5 year record[1]		Saiq 7 year record[2]		Muscat record[1]	
mm	T(yr)	mm	T(yr)	mm	T(yr)
				110	54
81	16	79	26	79	27
		67	11	67	8
61	8	63	8		
56	5.3	56	4.6	57	5.3
53	4.0	53	3.7	54	4.0
51	3.2	51	3.1		
49	2.3	49	2.8	47	3.2
40	2.0	40	1.4		
		35	1.0		

[1] Derived $\dfrac{"n+1"}{m}$ where n = total station years and record
and m = ranked order of maxima.

[2] Derived graphically.

February or, less commonly, in December or March. Rarely, fronts occur in April, but outside these months the ITCZ is generally too far north for Mediterranean air masses to penetrate the eastern Gulf region. Comparison of rainfall records for the Northern, Central and Eastern Oman mountains reveals no significant difference in the "winter rain" frequency.

Summer rainfall is almost invariably more localised and tends to consist of either frontal rainfall associated with the "Oman Convergence zone", or of convective storm cells of typically 5 to 10 km (rarely up to about 25 km) width. The latter type, in common with most tropical rain, is typically cumuliform resulting in narrow storm track widths (Sharon, 1972; Letts, 1979) surrounded by warm or hot air which inhibits precipitation except where vigorous convection and cooling develops. Indeed, rainfall from small storms in July and August frequently evaporates as or even before it reaches the ground. Narrow storm cell widths and the high evaporation rates are such that summer rains seldom contribute significantly to groundwater storage despite their frequently high intensity, and in some years many stations receive no summer rain at all (cf. Appendix A).

During late winter and mid summer, northerly airflow and south-westerly airflow respectively crosses the Jebel Akhdar to produce slight to dense cumulus build up during the afternoons which, under favourable conditions of humidity and temperature, may produce heavy rainfall (up to 50 mm, mean of 44 measurements > 13 mm) over parts of the highland area. The cumulus nucleation is remarkably consistent both in time and place, i.e. late morning above the Eastern Jebel Akhdar (grid 558,2558 ± 10 km) and is clearly governed by preferred airflow pathways across the mountain barrier. The progressive build up of cumulus in the early afternoon is illustrated by the summer rainfall record at Saiq (grid 5658,25514) where 95% of the total rainfall occurs between 1300 and 2000 hours, the majority of which is between 1400 and 1800 hours (Horn et al., 1977). By comparison 70% of the winter (mainly frontal) rainfall falls at night. Notwithstanding the highly localised nucleation, optimum conditions sometimes result in more extensive cumulate build-up to cover the whole Jebel Akhdar-Nakhl-Tayyin range. However the height of the cumulus (and thus minimum air temperature) is

much more important than its extent in determining rainfall, and much of
the spring-early summer cumulus produces no rainfall at all. Both local
and widespread cumulus can be explained equally well by either normal
orographic effects, or by anabatic convection. In general the former
process is the more common cause of cumulus accretion and precipitation,
but the clear sky, calm air conditions, intense insolation over the high
albedo limestone of the Jebel Akhdar, and the timing of cloud formation
are all entirely consistent with the latter process. Furthermore,
anabatic airflow would be complementary to the undoubted katabatic
airflow at night described below.

Examination of the low altitude rainfall distribution (Appendix A
and Figure 2.10) shows a very wide scatter of mean annual rainfall
along the coast, ranging from 70 mm to 288 mm; i.e. covering nearly as
wide a rainfall range as the interior stations over the complete
altitude range. Since there is no consistent relationship between the
mountain proximity and rainfall, it is assumed that relief rainfall in
such mountainous coastlines as Muscat and Khasab makes only a trivial
contribution to the mean annual average, and that irregular coastal
showers are a locally important contribution to nett rainfall. The
averaged rainfall records, field observations and satellite imagery all
indicate that rainfall decreases markedly within a few kilometres of the
coast as moist low level offshore winds and attendant cloud and/or fog
warms rapidly on land. Coastal rain is largely restricted to winter and
almost always occurs soon after dawn before fog and cloud is dissipated
by the rapidly rising near-surface air temperature. When both air and
ground temperatures are sufficiently low, moist offshore winds sometimes
penetrate across the coastal plain until halted against the mountain
barrier. This is most evident when a sharp inversion, e.g. generated
overnight by cool katabatic breezes from the Jebel Akhdar, creates a
static stratocumulous cover over the entire Batinah plain, ranging in
height from about 1000 to 1500 m in the piedmont to near sea level at
the coast. A similar feature sometimes occurs between the Arabian Gulf
Littoral and the Musandam/Northern Oman mountains but in both cases the
low altitude inland precipitation is usually minimal. The coastal
rainfall tends to be frequent but relatively light and of short
duration.

Cyclones (Beaufort scale > 12) and cyclonic storms (Beaufort scale 8 to 12) have been held to account for a significant fraction of rainfall in the Sharqiyah region of Oman (Renardet, et al., 1975; Gibb, 1969). These extreme weather conditions originate either in the south-eastern Arabian Sea or in the Bay of Bengal, and do not normally approach the Arabian coast due to the very strong offshore monsoonal airstream (up to 30 knots at one km. in July, Findlater 1977) which parallels the south-eastern Arabian coast during the summer and winter, ie. southwesterlies and northeasterlies respectively (Figure 2.4 a and c). Cyclonic storm influence is therefore concentrated in the seasons May-June and October-November (Table 2.8), thus coinciding with the monsoon reversals when winds are relatively light and neither the ITCZ or the mediterranean air flows are well developed. In a detailed frequency analysis, Pedgely (1969) plotted the mean cyclonic storm loci across the North Arabian Sea for the period 1891 to 1967 from which he estimated the incidence of cyclonic rain (> 10 mm) to be:

Salalah (Dhofar); once every five years, contributing about 20% of the annual rainfall.

Masirah Island; once every 15 years, contributing about 4% of the annual rainfall, and

Muscat ; approximately once every 50 years, contribution unknown.

Table 2.8 Frequency of cyclones and Cyclonic Storms for the 75 year period 1890-1964 (after Chaudhuri et.al., 1959).

	J	F	M	A	M	J	J	A	S	O	N	D	Y
cyclones and cyclonic storms over the whole Arabian Sea	1	0	0	4	10	11	2	1	4	15	12	3	63
cyclones and cyclonic storms reaching the Arabian Coast	0	0	0	0	8	5	1	0	0	7	6	1	28
cyclones in the Arabian Coast	0	0	0	0	6	2	0	0	0	2	2	1	13

The most recent cyclone, of 12-13 June 1977, confirmed this pattern of northward rainfall attenuation by precipitating 430.6 mm in 24 hours at Masirah island whereas the corresponding rainfall in the Oman mountains was restricted to the eastern Sharqiyah only and averaged only 26 mm (data available only from low altitude stations). This event was insufficient to increase significantly the mean annual averages in the Sharqiyah. From the above data the occurrence of cyclonic rain clearly decreases northwards along a coastal belt estimated, on the basis of vegetation distribution (Denton, 1969; Roy et al., 1963) to be about 300 km wide. Thus although a freak cyclonic event in June 1880 is known to have produced 300 mm of rain at Muscat (Pedgeley op.cit.) there is some doubt as to whether cyclonic events contribute significantly to the mean annual rainfall. On the contrary, the detailed rainfall record since 1973 shows a consistent correlation between "cyclone season" and dry or nearly dry monthly rainfalls (Appendix A). Furthermore there is no significant total rainfall difference between the south-eastern and north-western Oman mountains as would be expected from the postulated storm track incidence.

2.4 Rainfall Measurement and Interpretation

Measurement of rainfall – the input to the hydrogeological system – is of crucial importance to the understanding of subsequent hydrological processes and to water resources estimation.

The primary aim, both here and in water resources research generally is the development of discrete event rainfall-runoff-infiltration models and their extrapolation to subdivide the mean annual rainfall into these components for various catchments. Although rainfall is in some respects the simplest of hydrological measurements its interpretation is, paradoxically, one of the most intractable problems in hydrology, especially in mountain environments and doubly so in the arid mountain conditions of Oman. Four important factors require detailed examination in order to assess realistically the available rainfall data: (i) the accuracy of point precipitation measurements, (ii) rainfall variation with time, (iii) the altitude/rainfall relationship and the (iv) spatial distribution of rainfall.

Rainfall Measurement

Numerous raingauge designs have been and still are operational in Oman, ranging from the simplest "daily" funnel collector to SIAP wide rim "armoured" autographic recorders; the latter predominating in the less accessible mountain areas. The logistics of daily inspection and cost have dictated that the great majority of gauges are of simple Snowdon or Meteorological Office "Mark II" design and are thus susceptible to three main sources of error: oblique (aerodynamic) catch, evaporation, and wetting. In Oman, only the gauges of Wadi Al Ayn in Musandam are installed with their rims close to ground level, and none are surrounded by anti-splash devices. Consequently aerodynamic losses ranging from 0.4% to over 17.5% in strong winds may be incurred (Rodda, 1970; Bruce and Clark, 1966). In practice this effect is probably subordinate to other errors since strong winds during rainfall mainly affect only the medium and higher altitude stations where wind speeds are grossly affected by the site relief and thus inherent errors are unavoidably large anyway.

The raingauges are most widely distributed in lowland areas where temperatures are highest, leading to potentially widespread evaporation losses. This error was investigated in the Saiq road experiment (section 2.5) where pairs of clean and "oil spiked" raingauges (to inhibit evaporation) were distributed over an altitude range of 1100 metres. Comparisons of rainfall in each pair after a mid-May rainstorm are shown in Table 2.9, from which it is concluded that errors of up to 0.1 mm are probable unless the gauge is checked within 12 hours of rainfall. In the less accessible raingauges where 24 hours may elapse between rainfall and measurement, the worst case of cumulative evaporation error is estimated to be about 16% per year, decreasing to less than 4% per year at high altitudes.

Table 2.9   48 Hour evaporative losses from standard
            raingauges;   May 1980

Altitude (m)	Estimated mean daily air temperature °C	Gauge	Evaporation mm
2216	20.4	Sr 1	1.5
1909	22.4	Sr 2	1.6
1668	23.9	Sr 3	0.8
1400	25.6	Sr 4	2.1
1113	27.4	Sr 5	3.4

N.B.   Evaporation in the highly exposed high altitude gauges is probably
       increased by high wind speeds and turbulence.

Raindrops evaporated from the surface of the raingauge or left on
the internal container surface after measurement is the "wetting loss"
and has been estimated to vary from 0.09 to 0.15 mm for most common
types of daily raingauges (Allerup and Madsen, 1980). At high altitudes
i.e. > 2000 m, minor snowfalls occur in some winters, but this is an
insignificant fraction of the annual precipitation. Larger "undercatch"
errors sometimes occur during hail which frequently accompanies severe
convective storms as late as March or April, but again, the likely
errors are small compared to the major variations in rainfall
encountered at high altitudes.

The armoured autographic recorders were all calibrated and
periodically checked in such a way as to compensate for systematic
errors. A few problems were encountered such as partial blockage of the
collector funnel by foreign matter (especially droppings from Neophron
Pecnopterus), chart drive malfunction and pen failure, but even in the
event of incomplete or garbled chart traces, measurement of the
reservoir contents usually enabled a complete record of monthly totals
to be maintained. Despite these drawbacks the rainfall records
condensed in appendix A are of a high standard, being reliable and, in
general, accurate to better than ± 5%. Where systematic errors have
occurred they are almost always negative, ie. low readings giving

conservative rainfall totals. The biggest sources of error are undoubtedly human and range, in extreme cases, from vandalism and theft (see Gibb, 1976) to delays in measurement (large evaporation errors), careless misreading of measuring cylinders, and transcription mistakes. A comprehensive evaluation of individual station reliabilities is given by Horn (1977, 1978). Gaps in the record, and obviously suspect data have been denoted in the listing of Appendix A.

Rainfall variation with time

The lengths of records, apparent from Appendix A, vary greatly. In Oman the only long records are for Masirah Island and Muscat. The former is an offshore station some 100 km south of the study area and is atypical as a result of both relatively high cyclonic rainfall and the almost complete lack of frontal rainfall. Muscat is in some respects a physically isolated coastal mountainous site with a sheltered microclimate characterised by high temperatures, high humidity and anomalous convective air turbulence. Surprisingly, however, its interstation rainfall correlation (0.623 relative to other stations with more than 10 years of record) is no lower than most other raingauge stations and may therefore be regarded as a reasonable "benchmark" for comparison of wet and dry years, though not for absolute rainfall amounts. A more typical station record is that of Nizwa (from 1963 but having an incomplete record) where 14 complete years of data provides a good representation of the foothill/interior rainfall from an environment typical of a large proportion of the Oman mountains. Otherwise, rainfall records exist only from the advent of water resources research in 1973/4, and commonly incorporate errors and/or broken records following the handover of raingauge maintenance from consultants to the Water Resources Department (W.R.D.) in 1975. Subsequently the W.R.D. has reinstated and built up the raingauge network to its present maximum extent, but reliable data only exists for about 7 to 11 years from a handful of key sites. Most other sites will require the accumulation of several more years of record before the data warrants rigorous analysis. In the United Arab Emirates hydrological research began earlier with a raingauge network established in 1965 and significantly expanded both in 1971 and 1975. The exception is Sharjah with an almost unbroken record since 1941 although this station lies on the Arabian Gulf Littoral some 50 km west of the piedmont area, and is

therefore unrepresentative of the area as a whole. In view of the
rather better overall record from the Northern mountain area,
altitude/rainfall and interstation correlation computations have been
made for both the whole of Oman and for the "Northern subarea".

Migration of the ITCZ in summer and the overall pressure systems
during the winter results in erratic and unreliable rainfall from year
to year. Isolated showers and local rainfall anomalies are sufficiently
common to cast doubt upon the typicality of any single station record so
the 19 best station records have been summarised in terms of annual
deviation from the mean, and combined to produce a graph of mean
regional variation with time for the most recent 7 to 10 year period;
Figure 2.11. This figure shows that there is a tendency for successions
of consecutive drought or rainy years rather than a completely random
variation. From the same figure it is also tempting to suggest a six
year periodicity of drought and excess although this pattern would have
to be repeated over a substantially longer period before it could be
regarded as a statistically valid feature. Previous attempts to
attribute periodicity to rainfall variation, eg. with triannual rates of
change of solar activity (Halcrow, 1967), have not been rigorously
argued and are unconvincing. The base line of Figure 2.11 implicitly
assumes that the mean regional rainfall between 1973 and 1983 inclusive
equals the long term mean. In fact the longer records for Muscat (25
years) suggests a slightly drier long term mean whereas the records for
both Nizwa (14 years) and Mina Al Fahal (15 years), suggest a wetter
long term average, ie., means for the longest record and for the station
most typical of the mountain environment (Nizwa), bracket the 11 year
regional mean, thereby giving a measure of confidence in the typicality
of the available record. The question of longer term climatic change is
considered in chapter 7.

The Altitude-Rainfall Relationship

An almost invariable feature of raingauge networks in any
environment is the preponderance of raingauges at low altitudes where
access and maintenance is easiest. In Oman this is a particularly
unfortunate tendency as it is almost entirely rainfall from the medium
to high altitude areas which generates maximum runoff and hence recharge

Figure 2.10 Altitude – Mean Annual Rainfall Relationships
A: Face Value Means 1973-83
B: Normalised Means
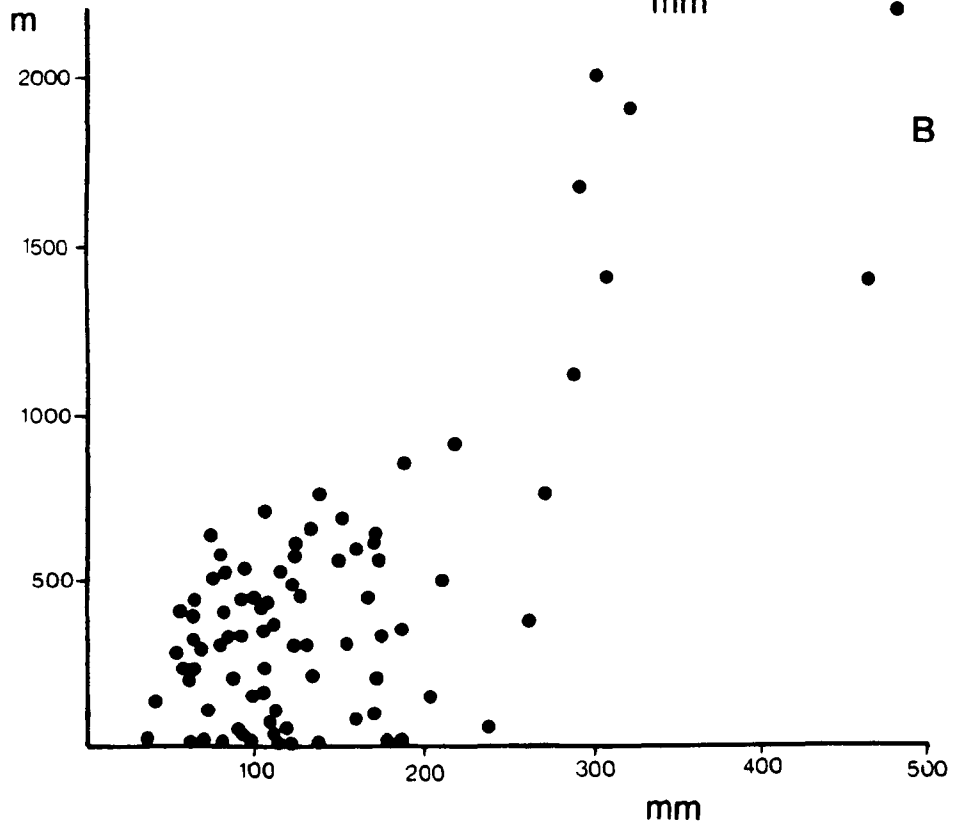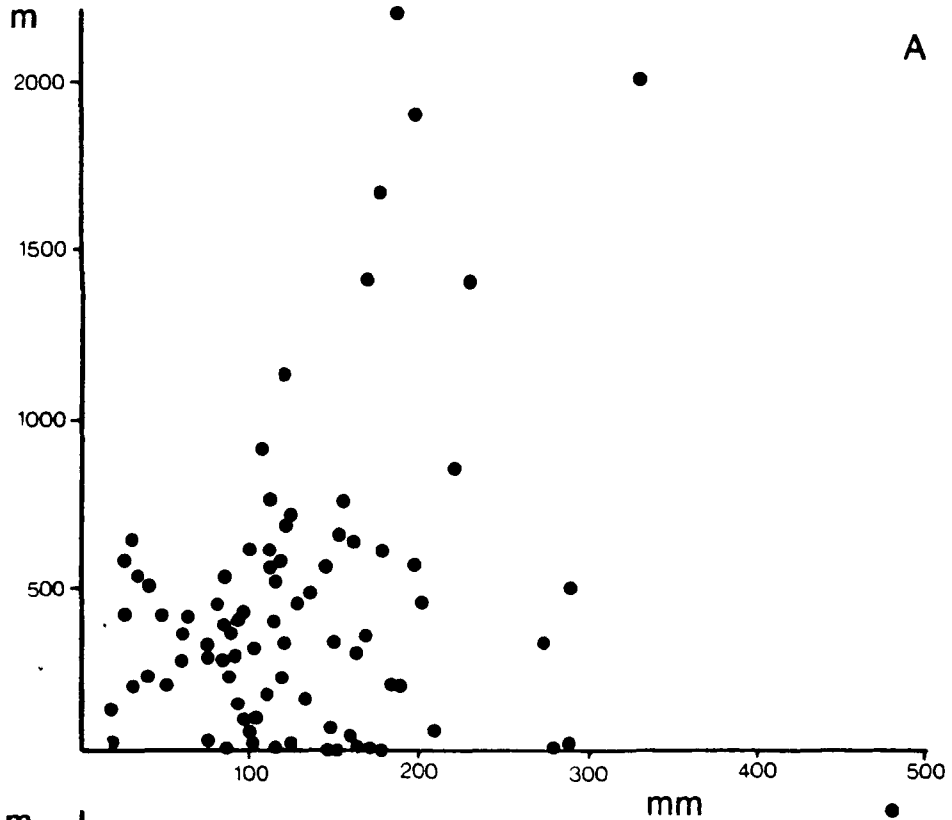
Figure 2.11   Regional Rainfall Variation With Time

(expressed as a proportion of the mean)
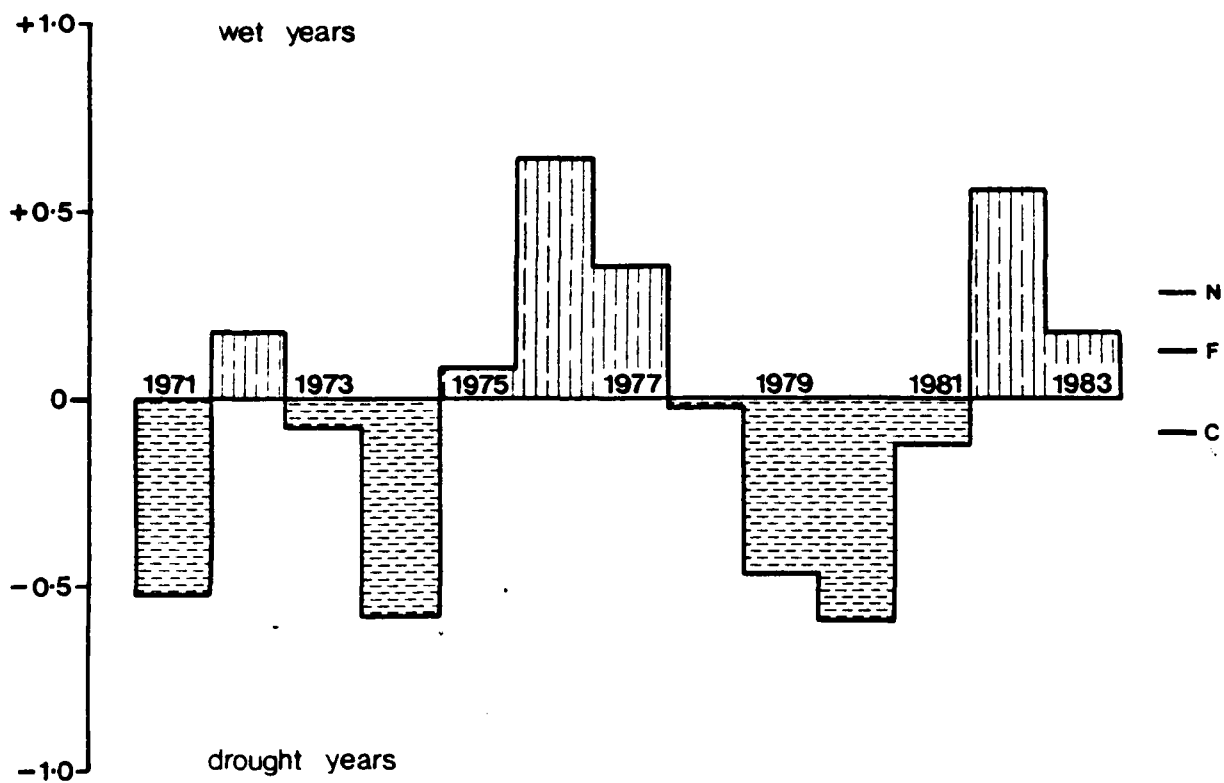
N = NIZWA   14 YEAR MEAN

F = MINA AL FAHAL 15 YEAR MEAN

C = MUSCAT 29 YEAR MEAN

to the alluvium at lower altitudes. The extreme difficulty of access in the limestone massifs requires a major effort of logistic support, including expensive helicopter transport, in order to maintain even the skeleton network of 3 medium altitude and 5 high altitude autographic recorders established by the author in 1979. Unfortunately, even this network was largely abandoned after responsibility was handed over to the Public Authority for Water Resources (PAWR) in 1981, with the result that Saiq, at 2000 metres, is the only high altitude station with a reliable record covering both drought and wet years. Additional short records are available from the 6 "daily" raingauges of Saiq road between the altitudes of 570 metres and 2216 metres, but these cover only the predominantly dry period from May 1979 to August 1981. Otherwise the rainfall data in the altitude range 900 metres to 2000 metres (ie. covering about 73% of the Jebel Akhdar-Nakhl mountain area) is totally absent.

The altitude-mean annual rainfall relationship is plotted both at "face value", Figure 2.10a, and "normalised", Figure 2.10b, using mean annual rainfall factors derived from Figure 2.11. The normalisation procedure has successfully eliminated some of the extreme values at lower altitudes, especially in the case of short record lengths, but has incurred the problem of greatly increasing the "Saiq road" values. In both Figures 2.10a and 2.10b, these are some of the most important data points but, unfortunately, are also amongst the least reliable.

The widely assumed approximation of linear rainfall increase with altitude appears to be applicable up to 700 metres in such climates as Britain (Bleasdale and Chan, 1972), and between 500 and 2000 metres in Sweden (Ryden, 1972). However, such well defined relationships only seem to hold good in less variable, more temperate environments. Several attempts to reduce the Oman data to linear form are summarised in Table 2.10 but these clearly fail to produce satisfactory correlation coefficients. Indeed, one is forced to the conclusion that, below 750 metres, there is no statistically significant altitude-rainfall relationship whatever. The higher correlation coefficients derived from the greater altitude ranges are caused by the small number of "extreme values" (themselves of relatively low confidence levels) and are

artifacts of the statistical method rather than intrinsically good regressions. Nevertheless, the single reliable rainfall record from Saiq and the normalised Saiq road rainfall values both indicate some form of altitudinal relationship, albeit of an unclear pattern.

Table 2.10   Altitude (H) - Rainfall Linear Regression Summaries

(a)   All of Oman excluding coastal stations;   Data from annual rainfall summaries at the end of Appendix A1

	Correlation	Slope	H intercept	n	Altitude range
Face value data	0.0895	0.286	353	65)	50-750 m
Normalised data	0.2039	0.704	298	66)	"
Face value data	0.458	3.140	143	75)	50-2200m
Normalised data	0.759	3.776	- 19	75)	"

(b)   The U.A.E. and Northern Oman (ie. stations with a longer average record), excluding coastal stations

	Correlation	Slope	H intercept	n	Altitude range
Face value data	0.248	0.61	0	58)	50-750 m
Normalised data	0.049	3.08	- 598	58)	"
Face value data	0.428	0.288	69	29)	50-1300 m
Normalised data	0.584	0.37	45	29)	"

Summation of the cumulative rainfall over a 30 month period for the Saiq road record, plotted against altitude in Figure 2.12a, suggests the development of two rainfall maxima, ie. at about 1400 metres and in excess of 2200 metres. In support of this distribution, synoptic reports from the MoD Saiq road construction camp (at 1700 metres) over an 18 month period (P.Walker, pers. comm.) frequently noted the concentration of narrow storm tracks with a cloud base well below the main watershed altitude of 2500 metres, ie. giving rise to intense summer storms at relatively low levels, whereas the more severe winter depressions appear to be generated at substantially higher altitudes.

Figure 2.12 Altitude - Rainfall Relationships

a) CUMULATIVE 30 MONTH TOTALS FROM SAIQ ROAD

b) 2-3rd MAY 1981 FRONTAL STORM TOTALS WITH LINEAR BEST ESTIMATE

c) WESTERN PAKISTAN MODEL AFTER KHURSHID ALAM, 1972

d) PRESENT AND PREVIOUS APPROXIMATIONS OF MEAN ANNUAL RAINFALL
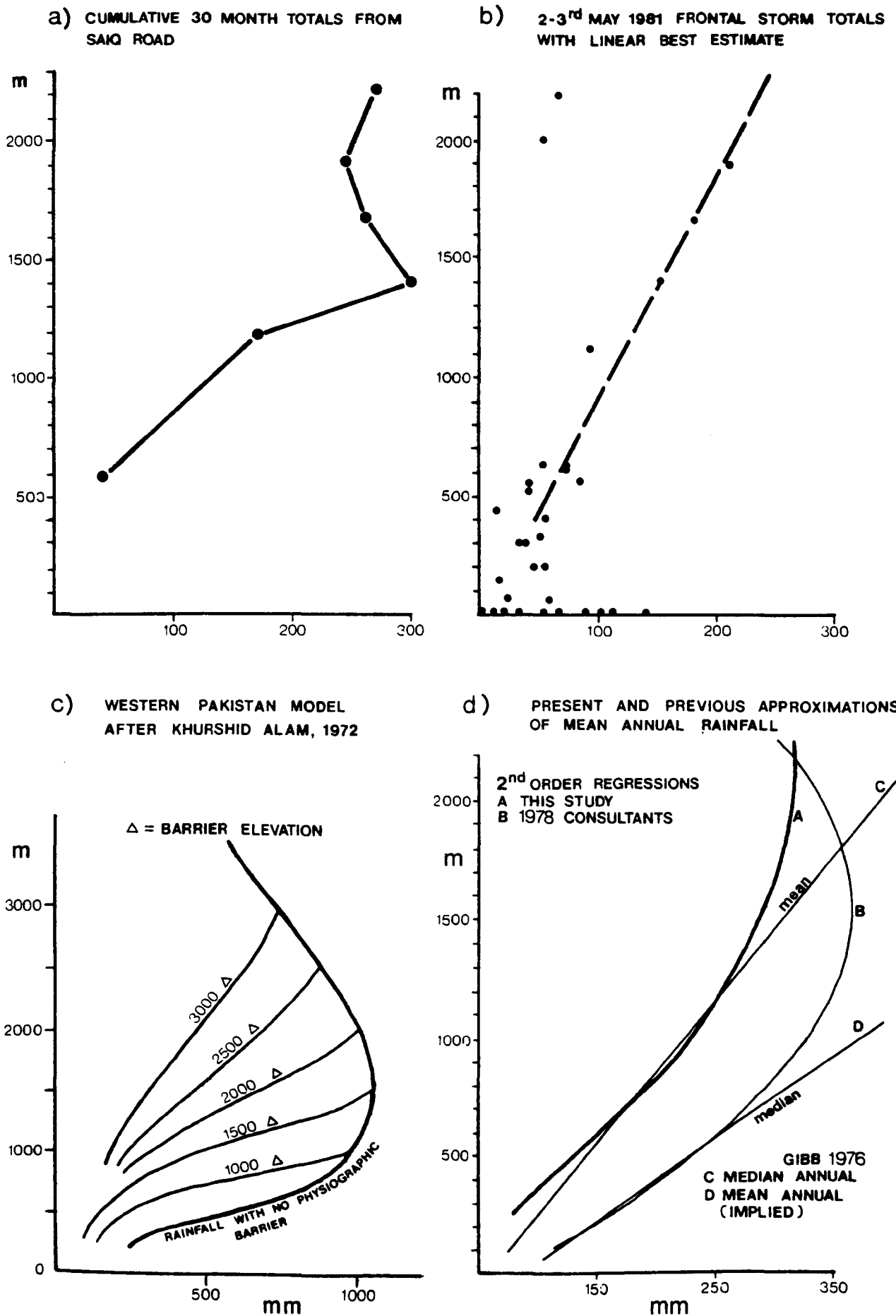
The best example of deep frontal (winter) rainfall, and also the
heaviest rainfall so far recorded in the Oman mountains, is the storm of
2-3 May 1981, Figure 2.12b, which gives an impression of linearity at
least as high as Saiq (2000 metres). Clearly, no linear increase of
rainfall with height can continue indefinitely but in this instance at
least, the maximum rainfall appears to occur at a very high
altitude, far higher than normal.

The dependence of the bimodal altitude-rainfall distribution upon
seasonality is consistent with the various past and present estimates of
optimum rainfall/altitude, eg:

	Altitude (m) at which rainfall
Maxima based on winter dominated rainfall data	maximum occurs
Second order regression of mean annual data intrinsically weighted towards the heavier winter rainfall (This study)	2217
May 1981: Frontal rainstorm	2000
Saiq road 30 month rainfall profile higher maximum	2216
Maxima based on summer dominated rainfall data	
1979 Consultants' rainfall model	1540
Saiq road 30 month rainfall profile lower maximum	1400
Western Pakistan model (derived from similar ITCZ controlled synoptic conditions, after Alam, 1972)	1500

Further support for a bimodal altitude-rainfall distribution is
demonstrated on isotopic grounds in section 2.5.

Whilst the above altitude-rainfall model may eventually be verified
quantitatively, the exigencies of generating rainfall volume estimates
from the present data requires a simple "compromise expression" such as

that given by a second order regression. Calculation of higher order relationships, though possibly a better fit in reality, would be inappropriate since the required sophistication of data analysis would far exceed the precision of the data available. Derivation of this expression is based upon the normalised rainfall (cf. appendix A1), but excludes both the wide spread of data from coastal and near coastal stations (less than 250 metres) and the two dubious extreme values of greater than 440 mm, the latter being based on short record lengths. To compensate for the preponderance of "foothills" data, the derived expression has also been weighted in favour of higher altitude values from the Jebel Akhdar. The resulting expression is;

mean annual rainfall (mm) $=$ $17.4 + 0.270$ $H(m) - 0.0000609H^2$

whose curve is shown together with previous consultants' estimates for approximately the same area, in Figure 2.12d.

Detailed multivariate analysis of rainfall in the western Canadian mountains (Storr and Fergusson, 1972) and subsequently verified in many other environments (eg. South Africa – Whitmore, 1976) shows that other physiographic factors are, taken together, of similar importance to altitude in determining rainfall. Of these, gradient, aspect and variations in exposure are significant but above all, the station position relative to upwind higher relief has the greatest control upon precipitation. This "barrier effect" may be represented either in terms of distance from the upwind physiographic barrier or as altitude of the upwind physiographic barrier, and should ideally be treated as a covariable in any attempt to improve the altitude – rainfall correlation. Although this cannot be achieved at present with the available Oman data, an analysis of a comparable subtropical airflow system from Western Pakistan shows the probable form of such a model (Figure 2.12c) and illustrates the severe rain shadow effects of high altitude ridges. The consistently low rainfall totals from such sites as Bidbid and Semail are good examples of such rain shadow anomalies and testify to the extreme spatial and altitudinal variation around the Jebel Akhdar.

Spatial distribution of rainfall stations

A major dichotomy exists between the raingauge network density required by experimental or theoretical considerations and the network density established in practice. To approach the network design from an analytical standpoint requires the prior knowledge of the rainfall distribution from experimental catchments or assumptions regarding the controlling processes. Since these are only available from research in other less arid and generally less mountainous terrains where rainfall is less variable, the conclusions regarding network density may not be directly transferable to Oman and must therefore be regarded as minimal guidelines. In the Japanese foothills for example, a study of an 840 km^2 experimental catchment (Kawabata, 1960) summarised the rainfall area to network density as:

Km^2/station	280	140	90	70	50	3
% error	25	18	13	10	6	3
	[17	12	9	7]		

The equivalent results from relatively flat terrain (% error shown in brackets) is derived from a U.S. Weather Bureau study (1947) and illustrates an apparent 30% gain in accuracy from low relief catchments. Similarly, a study of frequent summer storms in the relatively flat Muskingum basin of Ohio (Linsley et al., 1949) incurred low standard errors of 6% for a network density of 260 km^2/gauge, and 14% for a density of 1300 km^2/gauge. Results from the south-western U.S. however are much less encouraging. Although this region is relatively cool, the rainfall bears similarities to summer storms in Oman, being of intense convective origin and with short duration and limited areal extent. In such circumstances a simple correlation of 0.9 requires a gauge interstation separation of only 1.3 km (Osborne et al. 1979). An alternative analytical method using goodness of fit of the whole hydrological system (storage, runoff, baseflow etc.) was used by Richards (1975) to derive the "prediction efficiency" of raingauges in the 197 km^2 experimental Cam catchment of eastern England. The prediction efficiency "R^2" (= 100 for high confidence, = 0 for no confidence) was found to vary with raingauge density as follows:

prediction efficiency R^2	76	77	73	68	71	60
area/gauge km^2	19	25	32	49	98	197
mean interstation separation	4.4	5.0	5.7	7.0	9.9	14.0

Table 2.11 Raingauge performance in Western India, modified after Cole et al. 1972

Optimum raingauge density on the basis of maximum variability in seasonal

(monsoonal) rainfall. Figures give the area (km^2) per gauge

	desired error	confidence coefficient		
	%	90%	95%	99%
(a)	5	6.4	4.1	1.9
	10	26	16	7.5
	15	55	37	17
(b)	5	9.2	5.7	2.5
	10	36	23	10
	15	82	53	22

Catchment (a); 332 km^2, altitude range 342 m, 3 years data, E-W trending

Catchment (b); 900 km^2, altitude range 792 m, 7 years data, N-S trending

i.e. Errors introduced by reducing the number of gauges are trivial for small catchments but much more serious for larger catchments where the storm cell diameters are significantly less than the interstation separation. Amongst the few tropical experimental studies, an evaluation of ITCZ and orographic rainfall in high mountainous areas of Columbia (Stanescu and Lessmann, 1972) concluded that optimum rainfall evaluation requires a basic network density of about 200 km^2 / station with an interstation height interval of < 200 metres, supplemented by an high density catchment (of not more than 25 Km^2/station), devoted to parametric analysis. Finally, one of the nearest studies to Oman was based upon summer monsoonal rainfall in the Western Ghats (Gole et al., 1972) in which the raingauge density was computed in terms of both the desired error and the confidence limit, Table 2.11.

There are almost as many methods of raingauge assessment as there are catchment studies, yet there appears to be no objective method of inter-catchment comparison. Nevertheless, the conclusions from the above studies seem to be broadly consistent in suggesting that 100 km^2/gauge in a mountainous region, giving rise to approximately 15% error within about a 90% confidence level, would be the optimum density for operational hydrology. This is also consistent with the network density recommended by the World Meteorological Organisation (W.M.O.) i.e."100 to 250 km^2/gauge in temperate, mediterranean and tropical mountainous regions, subject to modification in the light of local conditions", (W.M.O. 1965).

The second approach to raingauge distribution, predominant in Oman, is essentially pragmatic, and consists of siting raingauges in towns and villages where adequate monitoring and maintenance can be ensured and where vandalism can be guarded against. In practise this has resulted in a mean interstation distance of 24 km (550 km^2/station), being more closely spaced along the coast and important alluvial basins, and more spread out (30 km or more) in the mountain areas. In view of the limitations of research this gives a less than ideal though still tolerable lateral spread of data, but gives rise to a seriously inadequate network in the mountain areas.

Figure 2.13   Interstation Rainfall Correlation
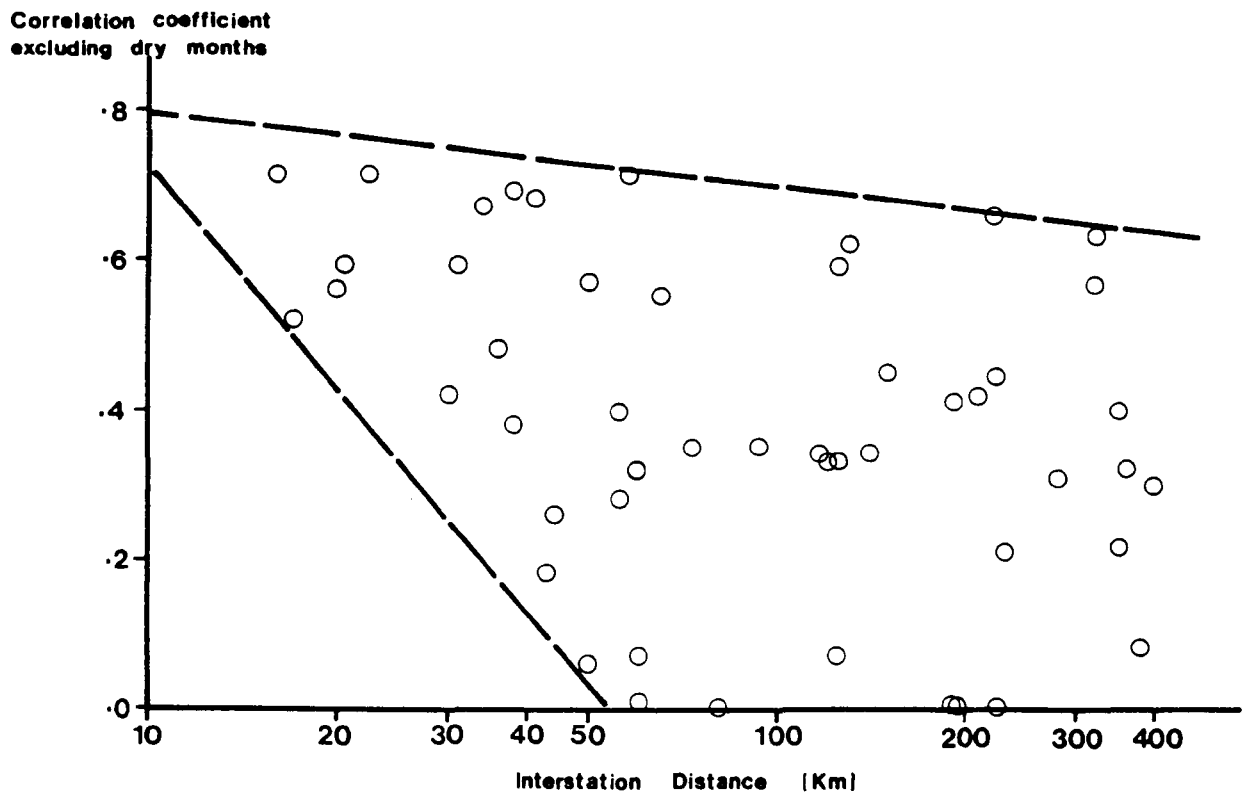
Given the scarcity of high altitude stations, the comparison of interstation correlation with interstation distance demonstrates the adequacy of the low altitude raingauge network. This relationship, summarised in Figure 2.13, was determined using non-zero monthly data, which gives slightly higher correlation coefficients than the annual rainfall data, though in both cases the interstation correlation at a distance of 50 km may vary between zero and about 0.7. Hence extrapolation or interpolation (eg. in order to generate isohyetal contours) is probably of dubious validity beyond 25 km from the reference station(s) and certainly cannot be justified with any degree of accuracy in the high relief areas. In view of the many uncertainties and anomalies involved in the rainfall distribution, attempts to construct a realistic isohyetal map of the mountain area are therefore considered to be premature. The provisional expression

$$"R = 17.4 + 0.270 \ H - 0.0000609 \ H^2"$$

is of necessity used in subsequent water balance estimates, but it is emphasised that significant negative deviations from this expression are likely to occur in leeward positions (predominantly south and east of Jebels Akhdar and Nakhl), whilst positive deviations may occur both in windward positions and as a result of extreme winter rainstorms. The almost total lack of data in the altitude range 1000 to 2000 and 2200 to 3000 metres may require substantial revision of the rainfall expression in the light of future research.

2.5 The Isotopic Composition of Rainfall

The rainfall isotopic composition is important in two respects. First, the uncertainties regarding high altitude rainfall necessitate further evaluation of the long term relative importance of seasonality, ie. summer vs. winter rainfall, though whether the resulting seasonal isotopic contrast is a function solely of temperature, or whether it is also influenced by differing climatic systems (Mediterranean or monsoonal air masses) has not been examined hitherto. Second, determination of the rainfall isotopic scheme in Oman provides a frame of reference against which to compare the much more abundant isotopic analyses of groundwater. In their assessment of water resources, the two isotopic studies previously published (Gibb, 1976; Renardet et al., 1975) have attempted to use the isotopes δ^2H and $\delta^{18}O$ to elucidate groundwater provenance but in both cases interpretation was hampered by the availability of only 5 analyses from 3 rainstorms; cf. 1974-75 data of Appendix B1.

In order to optimise sample collection from individual rainstorms over a high altitude range, about half of the 52 analysed rainwaters were obtained from an experimental catchment on the south-eastern slopes of Jebel Akhdar. Though normally of extremely difficult access, this was facilitated by the construction of a military road from Birkat Al Mawz (570 metres) to Saiq (2000 metres), across a ridge with a maximum elevation of 2216 metres, thereby permitting the deployment of six raingauges (Sr 1 to Sr 5 and Birkat Al Mawz, Figure 2.14) over a horizontal distance of 6 km, within a vertical range of 1646 metres. To avoid human and animal interference the standard copper raingauges were camouflaged to stop metallic reflection and placed in low stone cairns built into rock clefts and other natural features. Sites with deliberately difficult access were chosen some 100 metres from the road at approximately equal altitude intervals. A radio link was established between the road construction camp about half way up the mountain and an operational base some 85 km away, by means of which the occurrence of rainstorms and synoptic conditions were notified. Upon receipt of this information the raingauges were visited, the rainfall measured and the water collected, generally within 12 hours and always within 48 hours after the onset of rain. The gauges were paired, with and without an oil seal, to assess evaporation loss (cf. section 2.4), but evaporative fractionation was found to be within the limits of accuracy of the mass spectrometer, namely $\pm$ 0.1 for $\delta^{18}O$ and $\pm$ 1.0 for $\delta^{2}H$. Very light rainfall in which evaporative errors were potentially high, contaminated rainwater (eg. by dead lizards and insects) and rainfall over only a small part of the experimental area were not analysed. The remaining rainfall samples were obtained from recording or standard daily gauges wherever and whenever the opportunity arose and are thus widely distributed both spacially and chronologically (Figure 2.15, Appendix B1).

One of the most striking features of the isotopic results is the departure from linearity of both the absolute and amount weighted mean $\delta^{18}O$/temperature relationship (Figure 2.16) which is attributable to the non-equilibrium evaporation of raindrops as they descend through hot air (Stewart, 1974). This produces a non-linear trend associated with enriched isotopes in the $\delta^{2}H/\delta^{18}O$, shown in Figure 2.17, where an envelope around all the rainfall isotopes from Oman shows coincidence

Figure 2.14   Saiq Road Raingauge/Sampling Sites
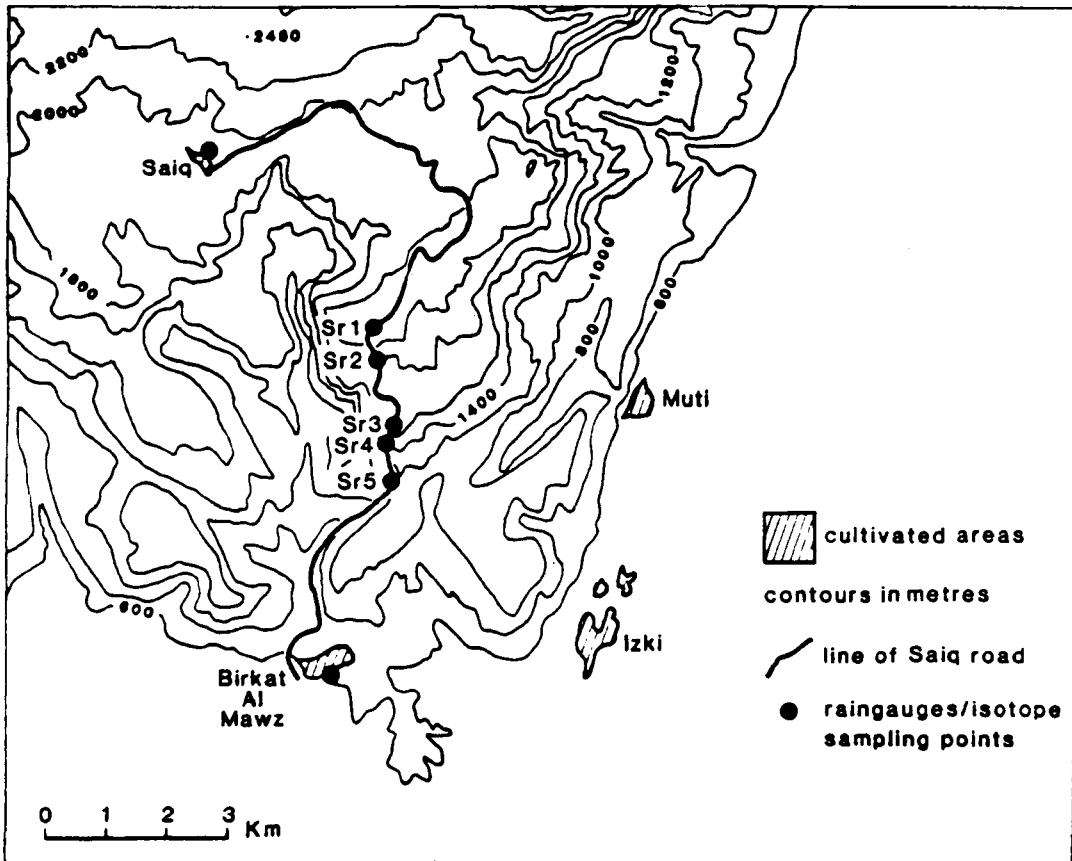
Figure 2.15   Rainfall Isotope Sampling Sites

Figure 2.16 δ^{18}O/ Air Temperature Relationship

1 Oman high altitude
   rainfall

2 Oman low altitude rainfall
   (unweighted)

3 Oman low altitude rainfall
   (amount weighted)

Mean annual air temperature.^{o}C
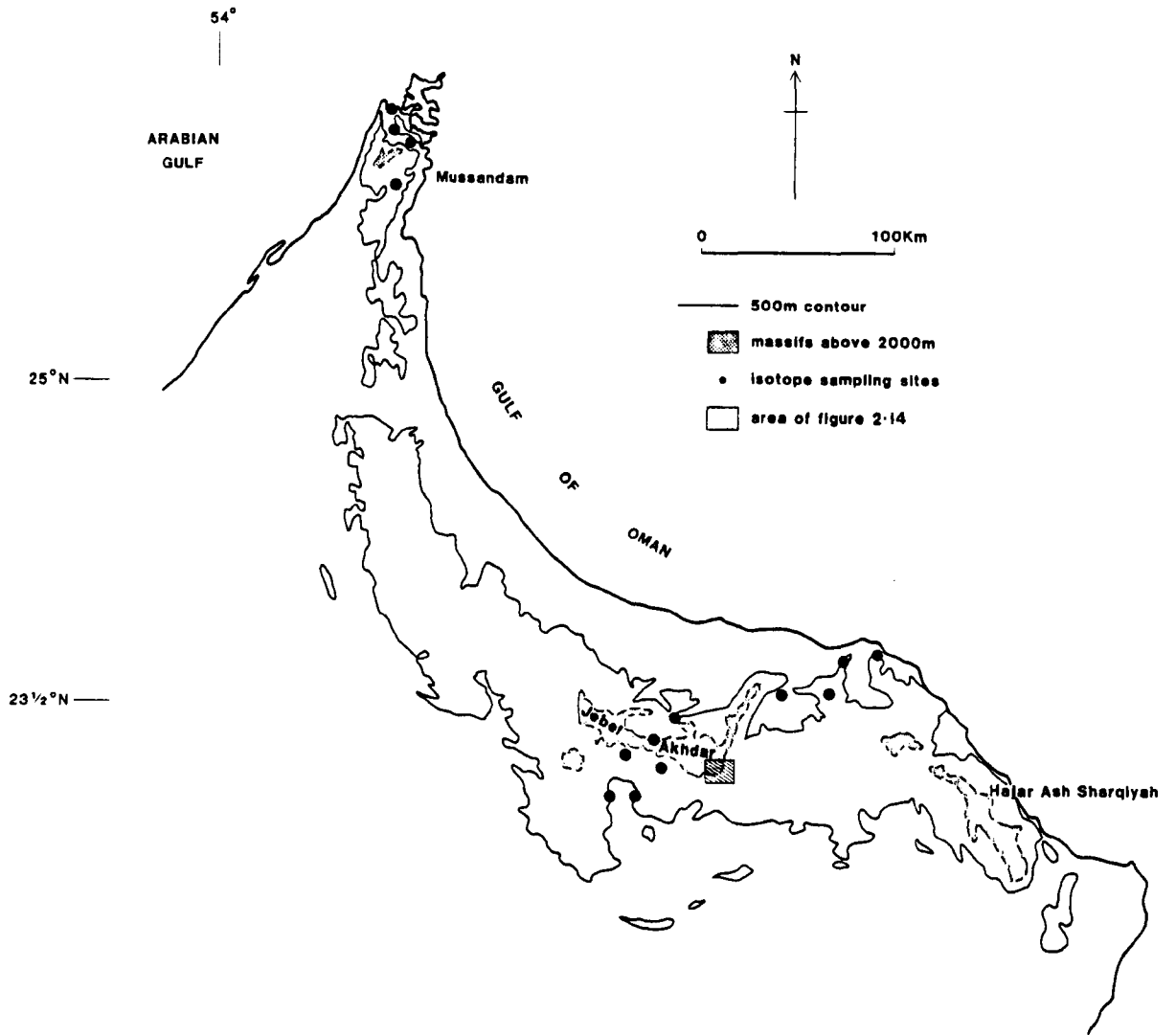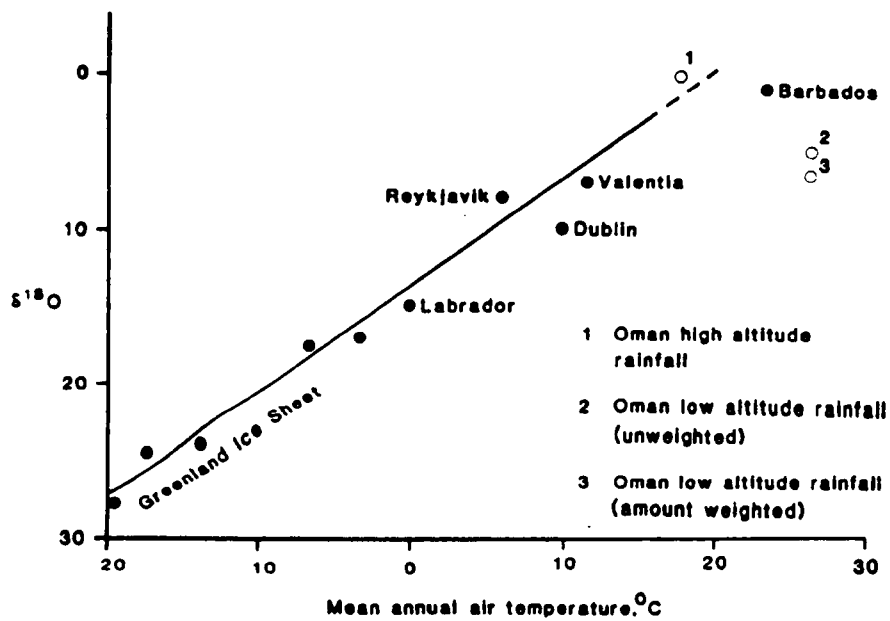
(non Oman data after Dansgaard 1964)

between the onset of curvature and heavy isotopes precipitated during the summer. In cooler climates, rainfall tends to cluster around the "world meteoric line"; $\delta^2H = 8 \, \delta^{18}O + 10$ but regional differences may alter the deuterium intercept as in the eastern Mediterranean line: $\delta^2H = \delta^{18} + 15$ (Levin et al., 1978). Various other local rainfall lines have been proposed including some arid zone lines with significantly lower slope such as the Bahrain line; $\delta^2H = 4.9 \, \delta^{18}O + 9.7$ (Gibb, 1976). There is however no reason to suppose that linearity is maintained at higher air temperatures. On the contrary, increasing air temperature would be expected to result in progressively non-equilibrium rainfall-water vapour conditions and hence to progressively falling gradients.

Temperature dependence within the isotope rainfall envelope of Figure 2.17 is demonstrated by a strongly seasonal trend from relatively cold isotopically light rainfall between January and April (lower left hand side) to warm, isotopically heavy rainfall between July and October (upper right hand side). Between the approximate limits

$$\delta^{18}O = -2 \text{ to } + 1^o/oo \text{ and } \delta^2H = -4 \text{ to } + 18^o/oo$$

there is considerable overlap of seasonal isotopic compositions. Apart from the seasonal (temperature) effect there is no apparent distinction between rainfall of monsoonal and Mediterranean origins. Within the isotopically heavier rainfall, where $\delta^{18}O$ is greater than $+1.5$, there is a slight correlation between rainfall amount and δ^2H depletion such that rainfall of 25 mm or more is biased towards the lower boundary of the rainfall envelope (cf. the "amount effect" of Dansgaard, 1964).

Results from within the Saiq road area (Tables 2.2 and 2.12, Figure 2.18) show that individual storms, whilst conforming to linear trends, precipitate under non-equilibrium conditions in which the δ^2H vs $\delta^{18}O$ gradients are about six. The altitude effect may be summarised as: -2.0 $^o/oo$ δ^2H per 100 metres and -0.33 $^o/oo$ $\delta^{18}O$ per 100 metres change in altitude. The assumption of a linear temperature gradient with altitude gives mean isotopic gradients of: 4.6 $^o/oo$ δ^2H per ^oC and 0.8 $^o/oo$ $\delta^{18}O$ per ^oC. In these calculations, only consistent linear relationships between at least three stations were used. The cluster of points derived from the higher sampling stations associated with storms I and H, both in March 1980, are spurious and caused by a low altitude layer analogous to the trade wind inversion, which

Contrasting Isotopic Trends of Rainfall and Groundwater

Mean Isotopic Trend of Rainfall

corr=0.876 cf. Appendix B

Groundwater Regression N=105

☆ Heaviest isotopic composition
.of rainfall consistent with
observed ground-water
isotopes

● Oman rainwater

δ D= -74.6

δ O= -11.1
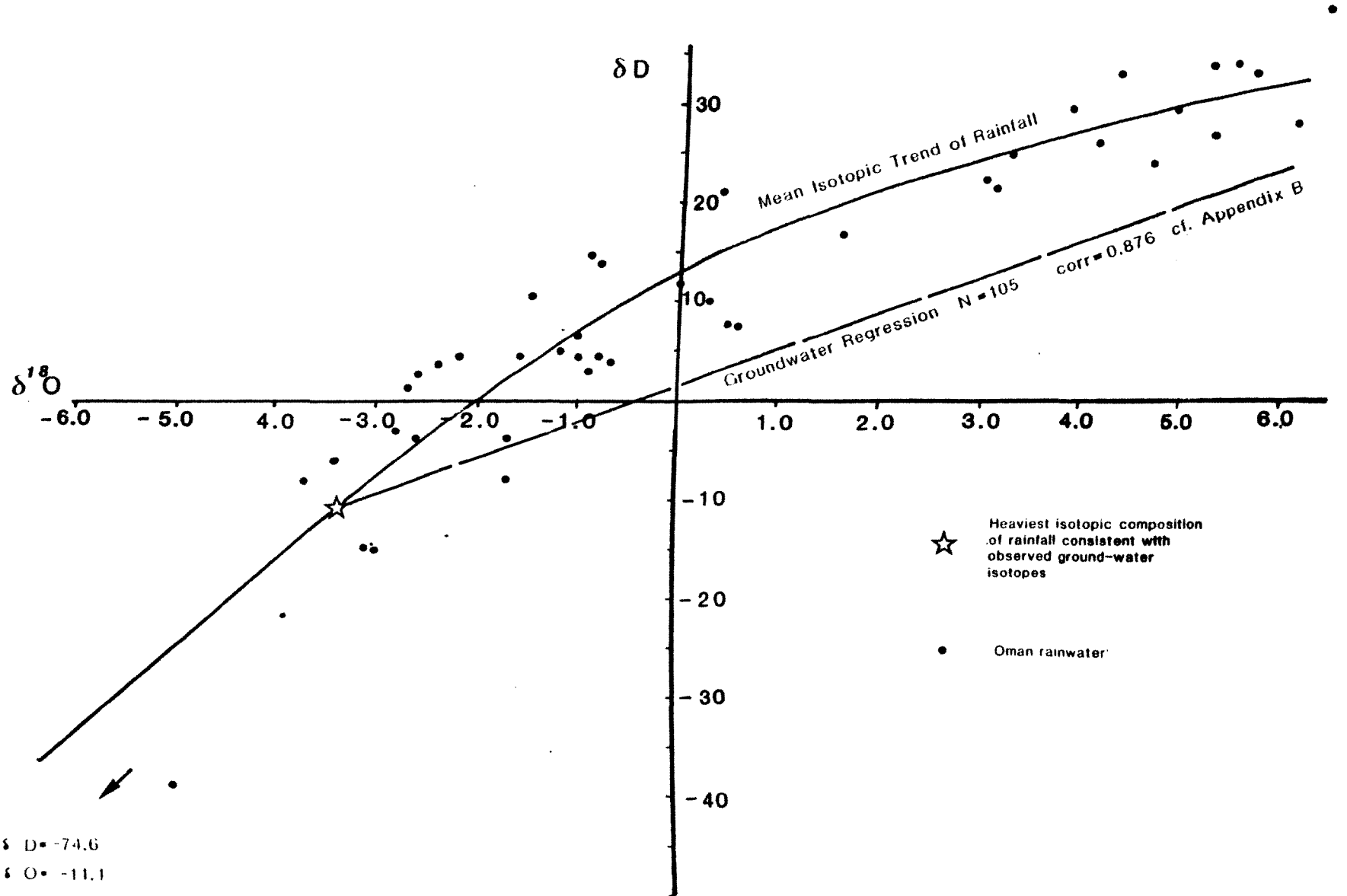
Figure 2.18   Individual Storm Rainfall Isotopic Trends from Saiq Road
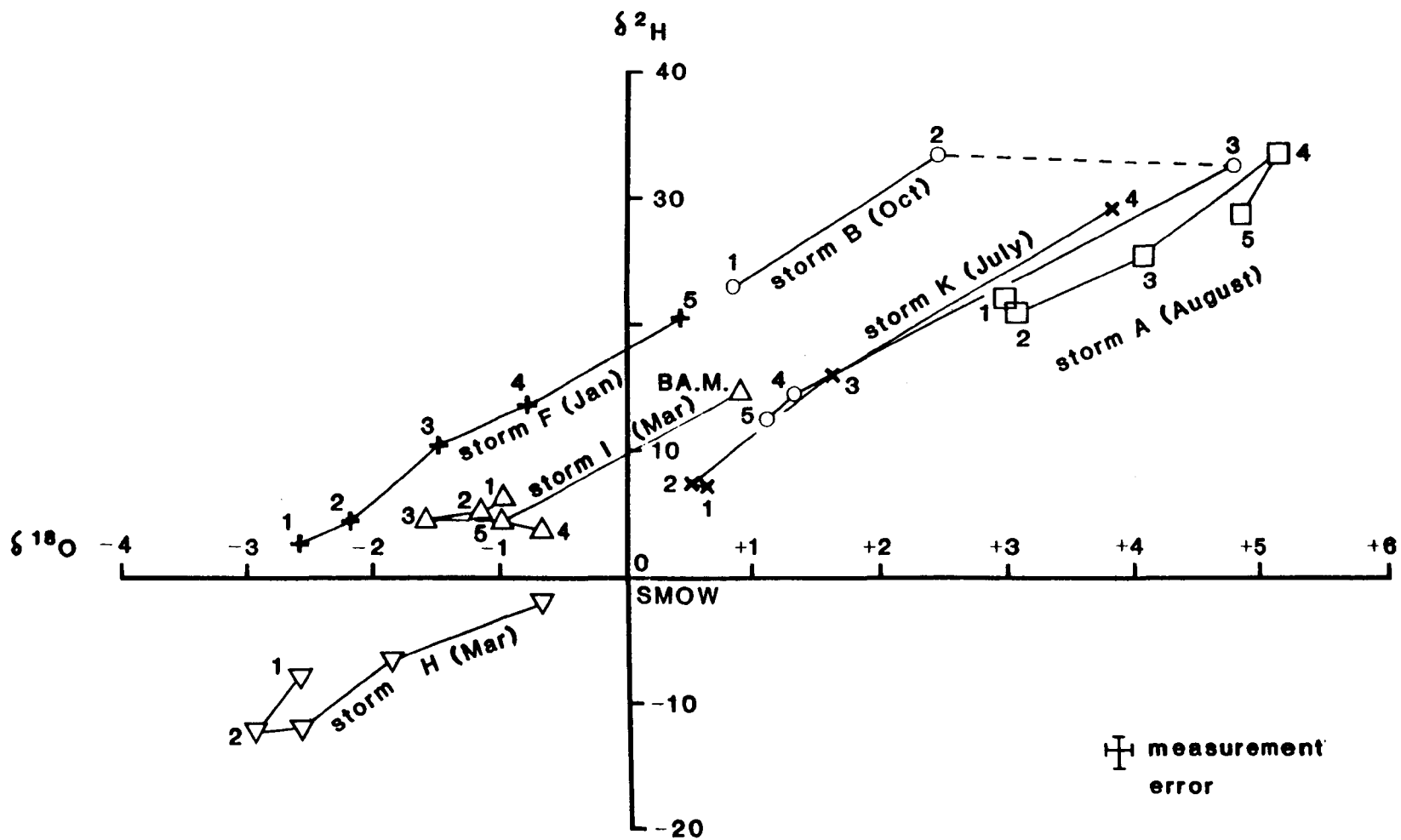
frequently forms in late winter and which disrupts the normal altitude/temperature correlation. The reason for the "isotopic reversal" of storm B (October 1980) is not known but may be due to the severe anabatic or kinetic atmospheric turbulence which often accompanies rainstorms in the mountain environment.

The mean isotopic composition of rainfall responsible for recharge may be estimated from the groundwater isotopes since the long residence times of many groundwaters in Oman, as indicated by the high incidence of low to zero tritium (Appendix B2), permit diffusion and mixing and tend to "damp" the isotopic extremes of recharge, thus providing a much smaller isotope field for groundwater than for rainwater. This field tends to fall around an "evaporative line" of lower gradient than the rainfall in which more intense evaporation results in heavy isotope enrichment; Figure 2.17. Conversely, extrapolation towards the intersection of the groundwater and rainfall fields, ie. the "zero evaporation" end of the groundwater field implies that the isotopic composition of the rainwater from which recharge was derived must have averaged about $\delta D = - 11$, $\delta^{18}O = - 3.4$. This conclusion is surprising in that almost all the observed rainfall is relatively enriched isotopically and therefore cannot be typical of recharge water. The two exceptions for which isotopic data is available are the rainstorms of 18 August 1975 and 2/3 May 1981. The former storm was a relatively localised product of instability within the ITCZ in which rainfall amounts were locally heavy, but not exceptional (cf. Appendix A). Furthermore the associated air temperatures, though depressed by some 6 to 7° C relative to normal (Gibb, 1976), were not particularly low and were substantially higher than normal winter temperatures. Nevertheless the rainfall was extremely depleted in heavy isotopes, Figure 2.17, suggesting very cold nucleation and hence a rainfall origin at high altitude. The second exception is the May 1981 storm in which one of the heaviest rainfalls so far recorded in the mountain area (110 mm at Medinat Qaboos - not an established raingauge station), had a composition almost identical to the deduced mean recharge, ie. $\delta D = - 14.9$, $\delta^{18}O = - 3.1$. This storm originated as a deep Mediterranean depression and, as shown in Figure 2.12b, also displayed relatively cold, high altitude characteristics. It therefore appears that high volumes of recharge are not restricted by either seasonality or climatic systems but result from cold air instability and rainstorm

Table 2.12 Rainfall amount and Isotopic content of Individual

Storms from Saiq Road

Station		Sr1	Sr2	Sr3	Sr4	Sr5	B.A.M.
Altitude (m)		2216	1909	1668	1400	1113	570
Storm A	δD	+22.3	+21.4	+26.1	+33.7	+29.4	–
18.8.80	$\delta^{18}O$	+ 2.94	+ 3.05	+ 4.05	+ 5.17	+ 4.85	–
	mm	27.8	51.6	60.5	49.4	24.4	0
Storm C	δD	+34.0	–	+24.0	+33.0	–	–
11.9.80	$\delta^{18}O$	+ 5.4	–	+ 4.6	+ 5.6	–	–
	mm	9.8	–	10.7	10.6	0	0
Storm F	δD	+ 2.6	+ 4.4	+10.4	+13.6	+20.8	–
22.1.80	$\delta^{18}O$	– 2.6	– 2.2	– 1.5	– 0.8	+ 0.4	–
	mm	28.9	24.8	16.2	15.6	15.5	0
Storm I	δD	+ 6.3	+ 5.1	+ 4.7	+ 3.9	+ 4.3	+ 14.8
22.3.80	$\delta^{18}O$	– 1.0	– 1.2	– 1.6	– 0.7	– 1.0	– 0.9
	mm	47.4	51.8	53.8	67.0	56.2	18.8
Storm K	δD	+ 7.4	+ 7.5	+16.3	+29.6	–	–
30.7.79	$\delta^{18}O$	+ 0.6	+ 0.5	+ 1.6	+ 3.8	–	–
	mm	2.2	12.6	29.9	44.8	11.8	11.6

generation at high altitude. By contrast, most of the isotopically
heavy rainfall, generated at intermediate altitudes of around 1500
metres, must be disregarded in view of its apparently minimal
contribution to the groundwater storage. It follows that considerable
caution is necessary in interpreting the rainfall record since the low
rainfall and low altitude showers, which are more likely to be recorded
with the existing raingauge network, are at least 10 times more frequent
than the heavier high rainfall storms and, cumulatively, give the
impression of constituting a large proportion of the mean annual
rainfall.

The apparent disparity between rainfall and groundwater
compositions seems to be a common feature of arid zone hydrology, since
a similar isotopic pattern has been reported both from Saudi Arabia
(unpublished data) and the Negev desert (Levin et al., 1978).

CHAPTER 3

SURFACE PROCESSES

        Quantitative division of rainfall into the subsequent components:
runoff, infiltration and "evapotranspiration" is a crucial element of any
deterministic model of the hydrological system. It is at this stage of the
analysis that the greatest implicit errors of the water balance are to be
found and yet, paradoxically, it is the transient surface or near-surface
processes which have received least attention from researchers in Oman.
Indeed, there has been no significant progress in this field since the
initial water resources surveys which reported in 1976. To some extent this
is inevitable since surface water processes are not amenable to short term
consultancy studies whilst the emphasis of research into surface processes,
within the relevant authorities, appears to have been directed at flood
events alone (i.e. magnitude and frequency). Experimental catchments set up
by the author have not, therefore, been maintained, and only a
semi-quantitative discussion on the basis of sparse data and by comparison
with other environments, is thus possible. Further difficulties arise from
the instrumentation itself. In particular, various types of flood gauges
have been subjected to vandalism, electro-mechanical component failure, and a
lack of adequate long term maintenance. Consequently flood records are at
best only intermittent and have not, as yet, been related satisfactorily
either to rainfall or aquifer response.

3.1 Runoff and Infiltration

        Narrow storm track widths and high rainfall variability in mountain
areas create particular difficulties in the estimation of valid
rainfall-runoff relationships. Either small experimental catchments may be
monitored, which raises the question of catchment typicality; or flood
gauges may be deployed in downstream exits from large catchments in which
case uneven precipitation across the catchment must be considered. As
discussed in chapter two, a sufficient raingauge network to determine mean
rainfall over a mountain catchment has not been realised in Oman and hence
the apparent rainfall-runoff data has a rather low covariance requiring a
larger number of records than is yet available to permit a rigorous
analysis. Nevertheless a provisional assessment is facilitated by the

existing results, which are shown in Figure 3.1, in terms of total rainfall (mm) and equivalent percentage runoff. These are obtained from four large and two small experimental catchments in predominantly hard-rock (limestone) environments on the southward draining slopes of the Jebel Akhdar massif and adjacent piedmont (Wadi Abyad); the exception being Wadi Aidan which is a small Eocene limestone catchment near Seeb. Wadis Nakhr and Misfah both drain exclusively Hajar Super Group limestones from the Wasia to Sahtan formations (cf. section 4.1), from high to low altitude, whilst the much smaller Saiq catchment drains only "Akhdar Group" mixed limestones and dolomites at a high altitude of 2000 to 2500 m. The Mu-Aydin catchment includes both Saiq area and parts of all other formations from pre-Permian slates to the Wasia limestones. However there is an overall similarity in geomorphology throughout the southern Akhdar area which permits comparison of the runoff results. The Saiq catchment drains over a free-fall, purpose-built, broad-crested weir (Plate 3.1) with an autographic stage recorder, and is therefore regarded as probably the more accurate of the various available flood records. Surface flows in wadis Misfah, Nakhr, Mu-Aydin and Abyad were estimated by stage recorder hydrographs with the use of Mannings velocity-area relationship: $Q = R^{2/3} . S^{\frac{1}{2}} . n^{-1} . A$

where Q is the discharge, R is the "hydraulic mean depth", S is the average channel gradient, A is the cross sectional area of flow and n is Mannings roughness coefficient.

The most critical factor, the "roughness coefficient", was taken by Gibb et al. (1976) to vary between 0.035 at high stages, and 0.058 at low stages. These values were regarded as "remarkably good" by subsequent F.A.O. observations (Horn, 1979, pers.comm.) and have since been verified by float measurements in Wadi Tanuf (19.2.1986, P.A.W.R. data) during which equivalent n values of 0.035 to 0.046 were obtained.

Data from Wadi Aidan was derived from an autographic recorder in conjunction with an 120° V notch weir (low flow conditions) built into a rectangular sharp crested weir (high stage conditions), designed in accordance with B.S.I. 1964; cf plate 3.2. This catchment is associated with an unusually dense raingauge coverage.

66

Figure 3·1

Rainfall / Runoff Relationships
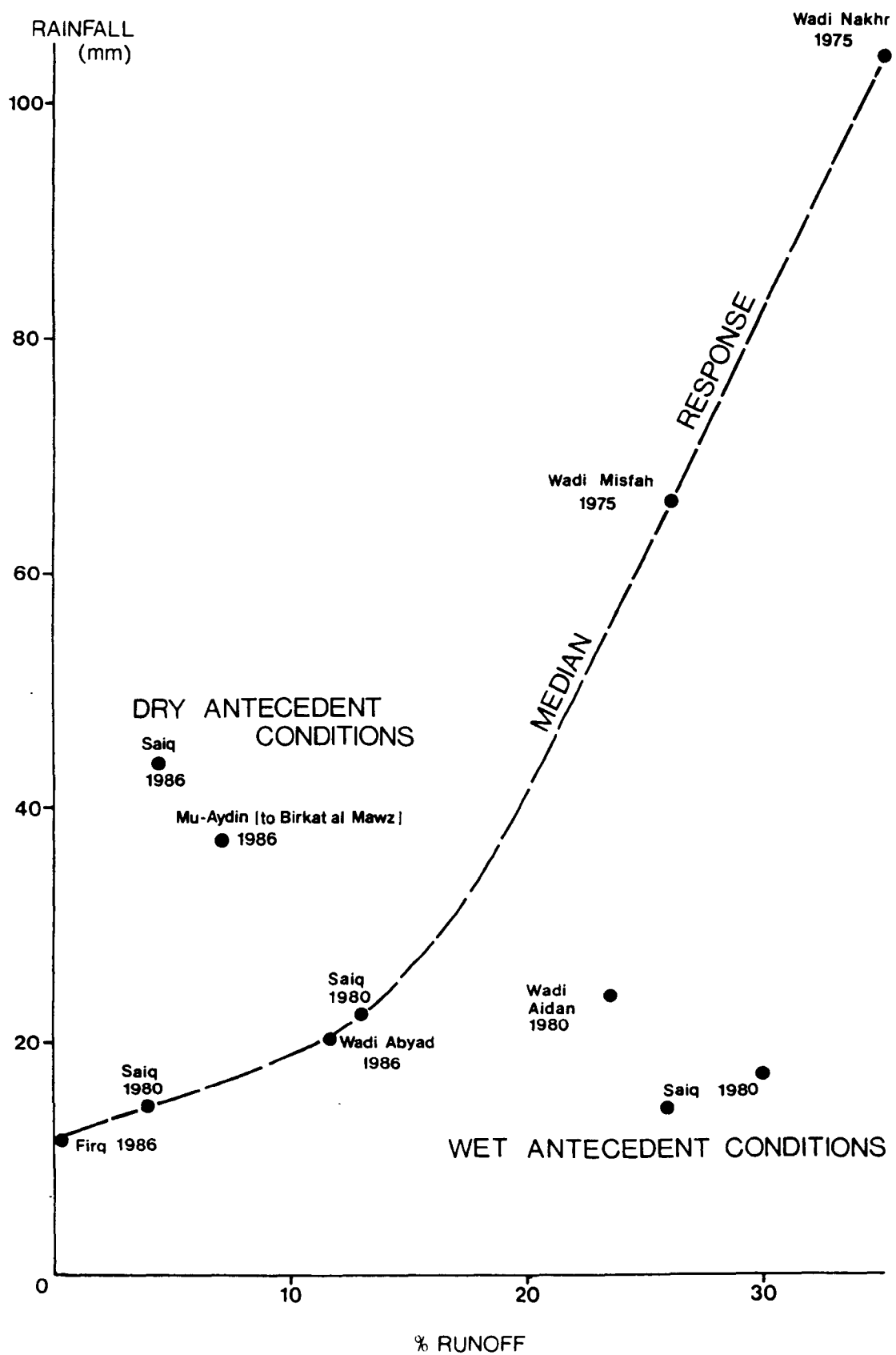
The results of Figure 3.1 show a very broad scatter of data from the small catchment of Saiq, compared to a more rational relationship for large catchments under higher rainfall conditions. This illustrates the overriding effect of antecedent conditions in controlling runoff from small rainstorms, since with increasing rainfall, the proportion of rainfall required to saturate the surface and near-surface zones is correspondingly reduced, leading to a more consistent rainfall-runoff relationship. Furthermore, the rainfall frequency is strongly skewed towards lower rainfall amounts whereas consistent relationships probably only occur during infrequent storms above about 50 mm; e.g. the Misfah and Nakhr results. Nevertheless Figure 3.1 implies two further points: firstly a threshold of about 15 mm appears to be required before any runoff occurs, which is consistent with casual observations of a 10 to 15 mm threshold from low angle limestone surfaces, mantle sequence foothills and low altitude terraces. In particular it was observed that rainfall of less than 18 mm at Saiq (i.e. about 75% of all rain events) consistently failed to produce runoff in the downstream piedmont area of Wadi Mu-Aydin. Secondly, the observed runoff is at most only about 35% and would probably exceed that amount only after heavy rains of > 100 mm.

Examination of the rainfall records in Appendix A indicates that several monthly totals of up to about 300 mm have been recorded over the decade 1973-83. Most of these were derived from single rainstorm events which would have produced runoff ratios substantially "off-scale" from Figure 3.1. In order to evaluate these flood events the following tentative estimates of hard-rock (limestone) runoff, in terms of return periods, have been suggested (Wheater R., 1981, pers.comm.):

return period (years)	10	25	50	100
runoff %	60	65	70	75

Although compiled from tenuous and indirect evidence, such high runoff fractions must be regarded as feasible for extreme rainfall events, but the heavy bed load and erosive power of large floods makes their measurement, and hence verification of the above estimates, inordinately difficult.

The gross infiltration capacity of limestones in Oman has not been determined. As with runoff, it cannot be assumed that infiltration can be expressed as a simple fraction of the rainfall. Rather, it is influenced by

hillslope, lithological homogeneity and structure, vegetation cover, rainfall duration and intensity and, most importantly in the case of the main carbonate aquifers, by karstic development. The most similar environments for which data are available are the Jurassic/Cretaceous limestones of Syria, and the mid-Cretaceous limestones of Palestine, both of which receive about double the rainfall of Oman, and hence have developed more mature karstic drainage. Consequently, comparisons with the results shown in Figure 3.2 probably lead to an overestimate of infiltration into Oman's limestones. It is therefore considered that average infiltration rates into the main Hajar Super Group aquifers are unlikely to exceed about 50% of the rainfall, and may be very much less as poorly developed vadose (or "subcutaneous") storage becomes saturated.

In alluvial infiltration, antecedent conditions are also important, but at least in the coarser sediments, are subordinate to the effects of particle size distribution. Rapid infiltration is most obvious in the boulder gravels of incised wadis and in the upper fanglomerates of the piedmont zone where extreme infiltration rates as high as 10 $m.s^{-1}$ have been cited (Kelly, 1985). A minor rainstorm of less than 20 mm has illustrated this in a small catchment near Tanuf on the southern Jebel Akhdar, where a five cumec flood peak was observed to completely infiltrate the boulder gravel within a channel length of only a few hundred metres (an inflow rate of greater than 10^{-3} $m.s^{-1}$), resulting in an overnight water table rise at the piedmont in excess of three metres. Throughout most of the fluvial systems however, the deposition of fine silt to clay grade layers during flood recession produces a highly variable but lower range of infiltration rates and, in many cases, effectively perches the last remnants of flood runoff. The high potential for fine-grained sedimentation during flood recession is illustrated in Figure 3.3; a typical example of flash-flood bed-load composition from a comparable arid area of Kenya (Reid and Frostick, 1984). Reduction of the infiltration rate in the middle section of wadis is partially compensated by flood attenuation and hence an increased duration of runoff, but in the lower wadi sections, especially towards the interior where wadi gradients are very low, the reduced duration and frequency of runoff combine with fine particle size and hence reduced infiltration capacity, to produce minimal recharge. This is reflected in the chemical composition of groundwater discussed in chapter six.

Figure 3·2   Mediterranean Karst Infiltration

after Burdon and Papakis, 1963
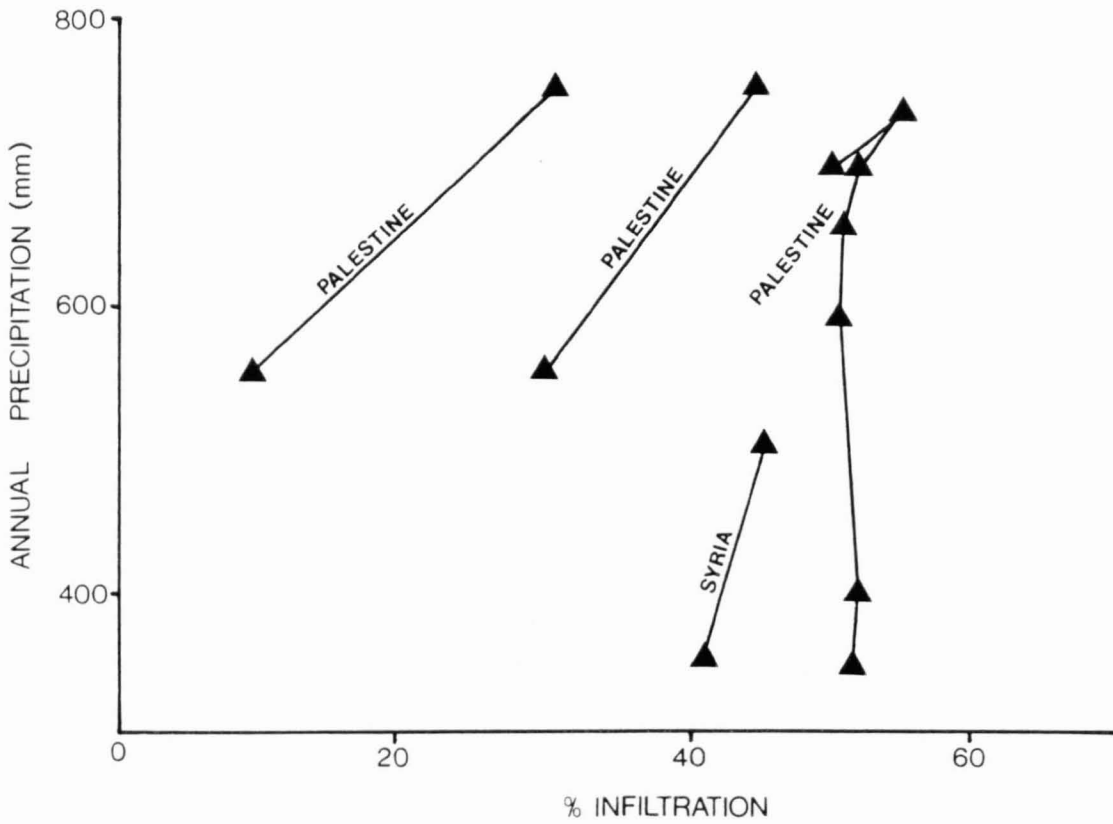
Figure 3·3   Flash-Flood Bedload Composition : An
Example from Kenya.

After Reid and Frostick, 1984
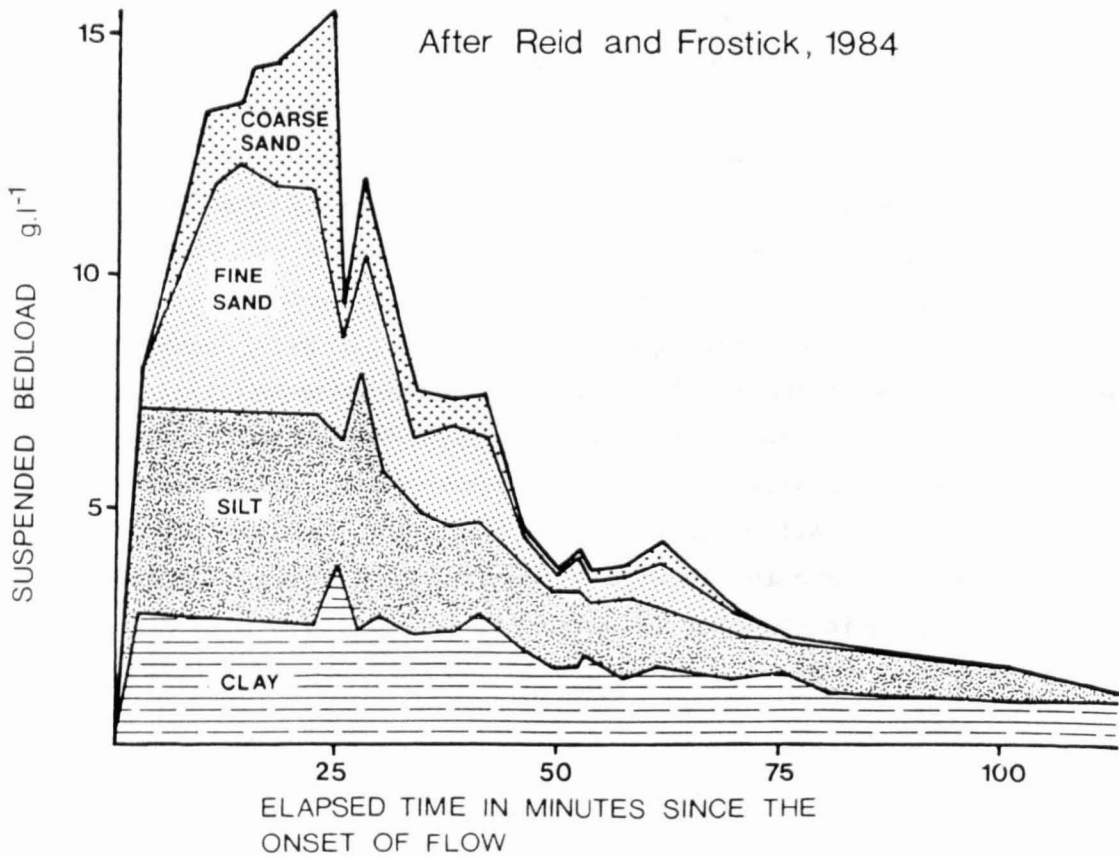
A qualitative assessment of variation due to antecedent conditions may be gained from two consecutive infiltration curves derived from an experimental catchment in Kenya, shown in Figure 3.4. Such a low steady state infiltration as 10^{-6} m.s^{-1} (the second curve) is typical of undisturbed clayey sediments, and may be compared with a study of irrigation losses from an unlined falaj reticulation system in the Dhahirah area of Oman (Letts, 1979). These results indicated an infiltration rate of 5 x 10^{-4} m.s^{-1} at the onset of irrigation, declining rapidly to a stable 1.5 x 10^{-4} m.s.$^{-1}$ after 20 minutes of surface saturation.

In low permeability interfluvial areas the extent of infiltration appears to be further influenced by the sedimentary thickness and hence the depth to water table. In the case of eastern Batinah mid-plain sediments, for example, significant water-table response to heavy rainfall has only been observed in association with lateral recharge close to wadis (e.g. Gibb, 1976), whereas the interfluvial water table was scarcely, if at all, affected by heavy rainfall. On the other hand, relatively shallow sedimentary interfluves in Interior areas have been observed to respond to rainfall within hours (Tibbitts C.G., 1985 pers.comm.). Thus it would appear that vertical infiltration can proceed only after some level of transient vadose storage (a function of the sedimentary thickness) has been reached. Although this storage is entirely unquantified, it seldom appears to be exceeded by lowland rainfall, and is subsequently lost by capillary action/evaporation, and by xerophytic transpiration.

3.2 Evapo-Transpiration Losses

Probably the biggest water loss within the hydrological system occurs by evaporation shortly after rainfall. That a substantial loss occurs is shown qualitatively by the bimodal distribution of isotope composition between rainfall and groundwater (Figure 2.17), since the implied "evaporitic shift", eg. by capillary rise and surface evaporation, cannot occur once recharge has penetrated the aquifer to a depth of more than a few metres. Two approaches to the determination of this loss are commonly employed. Firstly, highland catchment analysis expresses losses as the difference between rainfall and runoff. This has the advantage that piedmont outflow and its effect upon downstream aquifers can be modelled stoichastically, but implicitly assumes that infiltration into the hard-rock catchment is

Figure 3·4   Infiltration Response to Antecedent Conditions
From an alluvial wadi in Kenya
After Reid and Frostick, 1984

INITIAL STORM INFILTRATION

INFILTRATION FROM A SUBSEQUENT STORM OF
SIMILAR MAGNITUDE

5×10^{-5}

10^{-5}

INFILTRATION RATE : m.s^{-1}

0

30

60

TIME in MINUTES
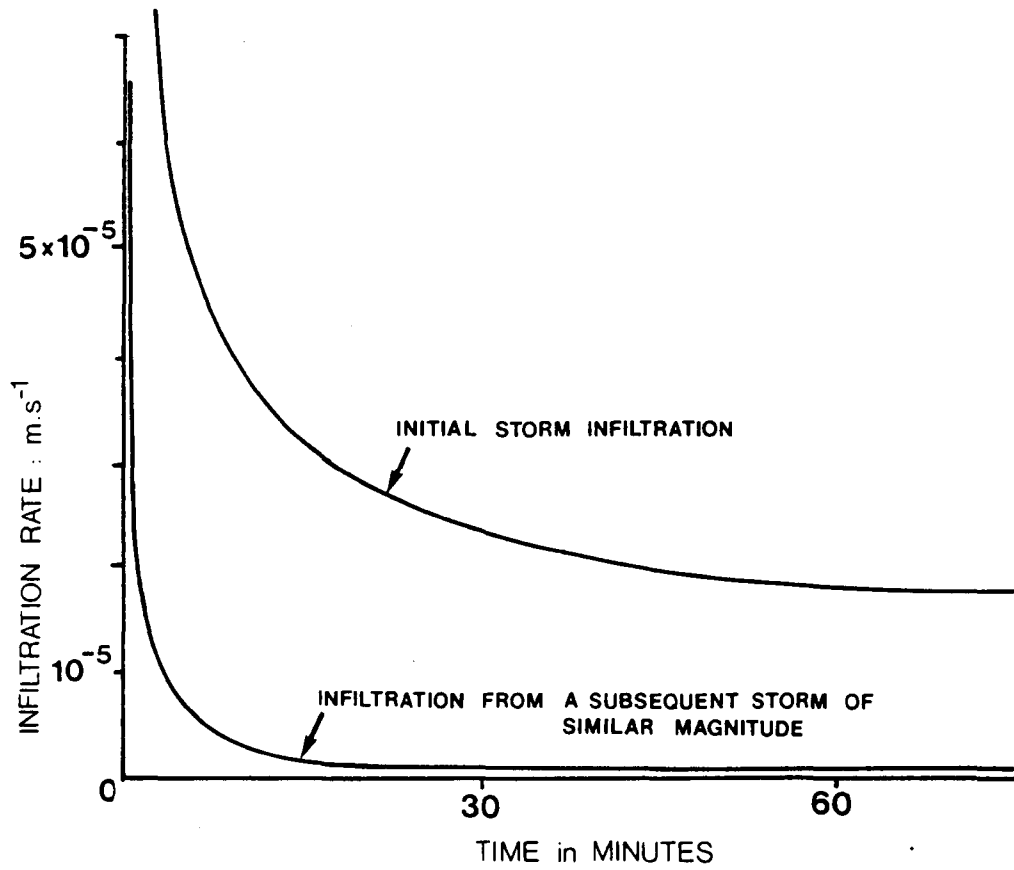
insignificant. This is a fair assumption in many arid geological environments but in the Oman mountains the presence of major carbonate aquifers, and hence of substantial hard-rock infiltration, demands a more deterministic approach to real evaporitic losses. The second approach is that of expressing the potential evaporation as a function of measured open-pan evaporation.

Prior to this study, "class A" pan evaporation had been monitored at only five sites in Oman (Figure 3.5) of which one, at Saiq meteorological station, was sited in an exposed limestone plateau environment. The other four were in lowland meteorological stations, primarily to supply information on transpiration rates, and hence were sited within agricultural microclimates under low exposure conditions. Initially, on the basis of these data, the effects of altitude appeared to be minimal, apparently due to a balance between the opposing effects of increased wind run vs lower air temperature at high altitude. In order to investigate evaporitic variation on a more general basis, i.e. over a wide range of environments, and in particular, over microclimates more typical of overall catchments, several class A pan evaporation experiments were set up. Initial problems of interference by goats, birds etc. were overcome by the liberal use of barbed wire fencing and translucent net screen (with a shade area of < 0.5%), but were sufficiently disruptive to reduce the valid observation period to just less than a year. In addition, logistic constraints prevented continuous daily measurements. The annual evaporation from these sites, shown as the last seven entries of Table 3.1 are therefore "best fit" estimates on the assumption that evaporation varies in proportion to a sinusoidal trend in monthly air temperatures, and may thus incorporate an estimated 15 to 20% error. Despite this high experimental error it was found that the degree of exposure far exceeds any other controlling parameter in determining open pan evaporation, and that the potential evaporation over large areas was up to double the values reported from agricultural microclimates. Furthermore, for a given degree of exposure, the evaporation at low altitude greatly exceeds that at Saiq, thereby signifying that air temperature is an important secondary control. The contrasts in apparent evaporation are summarised in Figure 3.5.

Figure 3·5

Comparative Open Pan Evaporation from Different Environments in Oman

A Ultramfic foothills and associated gravel outwash of the coastal and interior plains (high exposure conditions)

B Less exposed low altitude areas (mountain and coastal)

C Foothill cultivated areas of low exposure, and high altitude (2000m+) mountains

Evaporation rate mm/day

Month
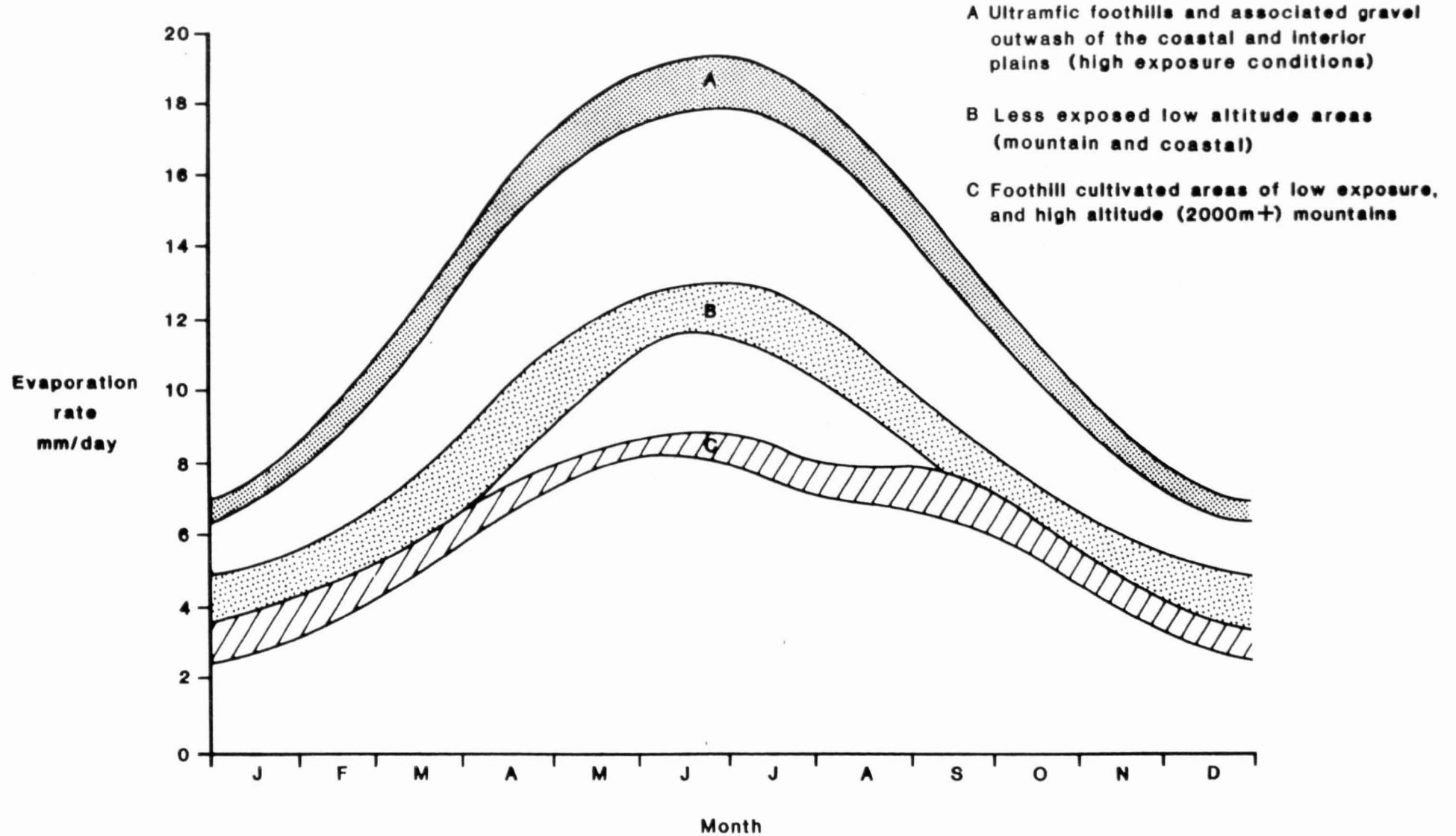
Table 3.1 Comparison of "Class A" Pan Evaporation with Environmental Conditions

Site	Environment	Altitude (m)	Degree of Exposure	Ann. Evaporatio (mm)
Saiq	Mountain Plateau	1897	high	2384
Rumais	Coastal Agricultural Belt	15	low	2466
Rustaq	Foothill Oasis	350	low	2173
Nizwa	Foothill Oasis	550	low	2052
Wafi	Interior Alluvial Plain	145	med	2982
Sharjah UAE	Western Coastal Belt	2	–	3414
Digdagah UAE	12 km inland. In lee of dunes	15	–	3029
Falaj Mu Allah UAE	38 km inland	–	–	3705
Milayha UAE	53 km inland. Foothills	–	–	4202
Kalba UAE	East Coast	10	–	3241
Khasab	Musandam in major wadi	30	med	(2993)
Karshah	Interior plain	440	very high	(4836)
Al Uqq	Ophiolite Hills	600	high	(4544)
Seeb (1)	Coastal Agricultural Belt	10	low	(2920)
Seeb (2)	Coastal Sand Dunes	5	med	(3296)
Seeb Fan	Gravel Terrace. Low albedo	40	high	(4361)
Muaskar	Limestone terrace. High albedo	60	very high	(5099)

NB (1) The first four figures are taken from the two year records of Gibb et al. 1976.

(2) The UAE records are taken from Halcrow et al. 1969.

(3) Figures in brackets are extrapolated from less than one year's records, assuming a sinusoidal distribution of mean monthly evaporation rates.

(4) For comparison, the mean annual evaporation rate for the southern part of the Arabian Gulf is 1240 mm, i.e. much lower than the above data due to the suppressing effect of very high humidity during the summer months.

Whilst the evaporation rates of Table 3.1 are self-consistent, they are based upon a very small sample area of 1.17 m^2, and clearly overestimate the surface water evaporation rate from either an open water body, or from a water-saturated surface (e.g. during and after rain), since any large scale evaporation would increase the humidity, and hence suppress further evaporation. Katsnelson (1963), suggested that in hot arid areas such as the Gulf of Aqaba, the commonly used pan evaporation coefficient of 0.7 was too high, although there appears to be no reference in the literature to the likely minimum pan coefficient for arid zone conditions. By assuming a minimum coefficient of, for example, 0.6, the maximum summer evaporation rate over a large area could still be in excess of 11 mm per day. This, however, raises the second major problem; the effective duration of evaporation. It is common for resource estimates to use expressions of the form: rainfall = runoff + infiltration + (potential daily evaporation x number of rain days in the period under study). Whilst convenient in their ease of computation, such expressions do not appear to have been supported by any verification of effective evaporation lasting for 24 hours, and must therefore be regarded as only a most general approximation.

Although reduced potential evaporation occurs at higher altitudes, the frequency of rainfall is also higher so that the variation of actual evaporation with altitude is less than one might expect from Figure 3.5. Indeed, studies in the Zagros mountains of western Iran show that, within the limits of experimental error, the variations in potential evaporation rate, and rainfall variation with altitude cancel out to leave an essentially uniform amount of actual evaporation over a wide altitude range (Sutcliffe and Carpenter, 1967). As the authors point out, this is a fortuitous relationship and should not be assumed for other environments, such as Oman. Nevertheless, even a general trend towards constant amounts of annual evaporation in a given environment reinforces the argument that low rainfall in lowland areas suffers disproportionate evaporative loss and is hence of minor significance to the alluvial recharge, relative to the mountain rainfall.

Subsequent to recharge, evaporative losses are only significant from shallow water tables where alluvium is poorly cemented and of fine grain size. Such conditions are almost entirely restricted to "far downstream" areas such as; sand flats or sabkhas in coastal interfluves, lagoons in wadis barred by storm beaches, and in silty playas in the interior desert

platform. All of these environments are downstream of principal water users, and hence the associated severe salinisation of residual groundwater is of little importance. Experimental shallow evaporation losses have been determined as co-functions of the depth to water table, and: (1) the percentage of surface evaporation (Figure 3.6; after Sleight, 1917; White, 1932; and Hellwig, 1973), and (2) the maximum capillary rise (Figure 3.7; after De Ridder, 1978; and Sleight, 1917). Both approaches show that the fine sandy alluvium incurs the greatest losses and that evaporation is trivial from water tables of greater than about three metres depth; i.e. the vast majority of the alluvial basins in Oman. In the interior basins it is probable that further near surface evaporation is retarded by widespread "subcutaneous" precipitation and cementation, arising from capillary action, in the form of caliche or gypsum/anhydritic crust. Much less commonly, high rates of groundwater evaporation are indicated by an additional surface efflorescence of halite as in eastern Bilad Bani Bu Ali (cf. Chapter 6) and most breaches of the Salakh Arch, south of the Jebel Akhdar.

Under conditions of adequate irrigation, the transpiration rate of the main crop (dates) assumes a consistently narrower range than that of evaporation. The best available estimates are: 1565 mm on the Batinah plain, estimated by the Blaney and Criddle method (Gibb et al., 1976) 1696 to 1802 mm in the Dhahirah also estimated by the Blaney and Criddle method (Letts, 1979), 1527 to 1838 mm in Semail, estimated empirically (Gibb et al., 1976), and 1511 to 1937* mm throughout Oman, estimated by the Penman method (MacDonald et al.). Of these, the lower values are most typical of large cultivated areas of average crop density, but higher values than those quoted locally arise due to intensive intercropping, high density plantations, and especially to fringe oasis effects (cf. section 6.3). Alternatively, Letts (1979) has cited consumptive water losses on an individual tree basis as: Eucalyptus, 120 m^3 per year; dates under ideal irrigation conditions, 150 m^3 per year; and dates under transpiration stress as little as 80 m^3 per year.

A more difficult problem concerns the transpiration loss from natural vegetation. Although the density of natural vegetation is generally low, (eg. Plate 3.1) it is more exposed to extreme desiccating conditions and is at least an order of magnitude more extensive than areas under cultivation,

* excluding a dubious value of 2351 mm per year from Sur.

77

Figure 3·6

SUBSURFACE EVAPORATION AS A FRACTION OF TOTAL
EVAPORATION

After Sleight 1917, White 1932, and Hellwig 1973

NB   Saturated surface evaporation = 92% of open-pan evaporation
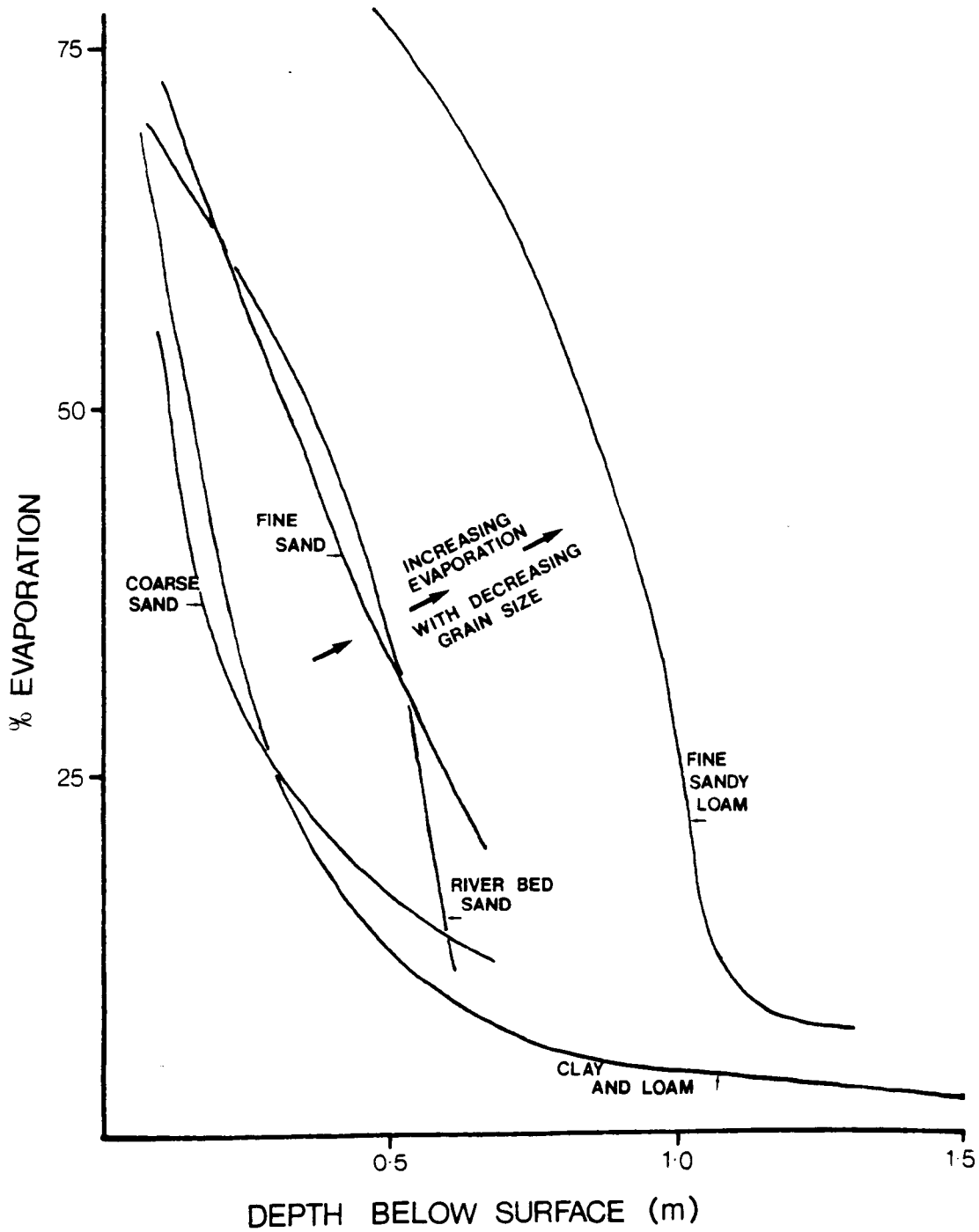
Figure 3·7

RELATION BETWEEN MAXIMUM CAPILLARY RISE, V,
FOR A SUCTION OF 15000 cm, AND THE DEPTH TO
WATER TABLE

After de Ridder, 1971 / Sleight 1917

Depth (m) to the
water table

FINE SANDY LOAM

SILTY CLAY-LOAM

FINE SILTY LOAM

V in mm/day
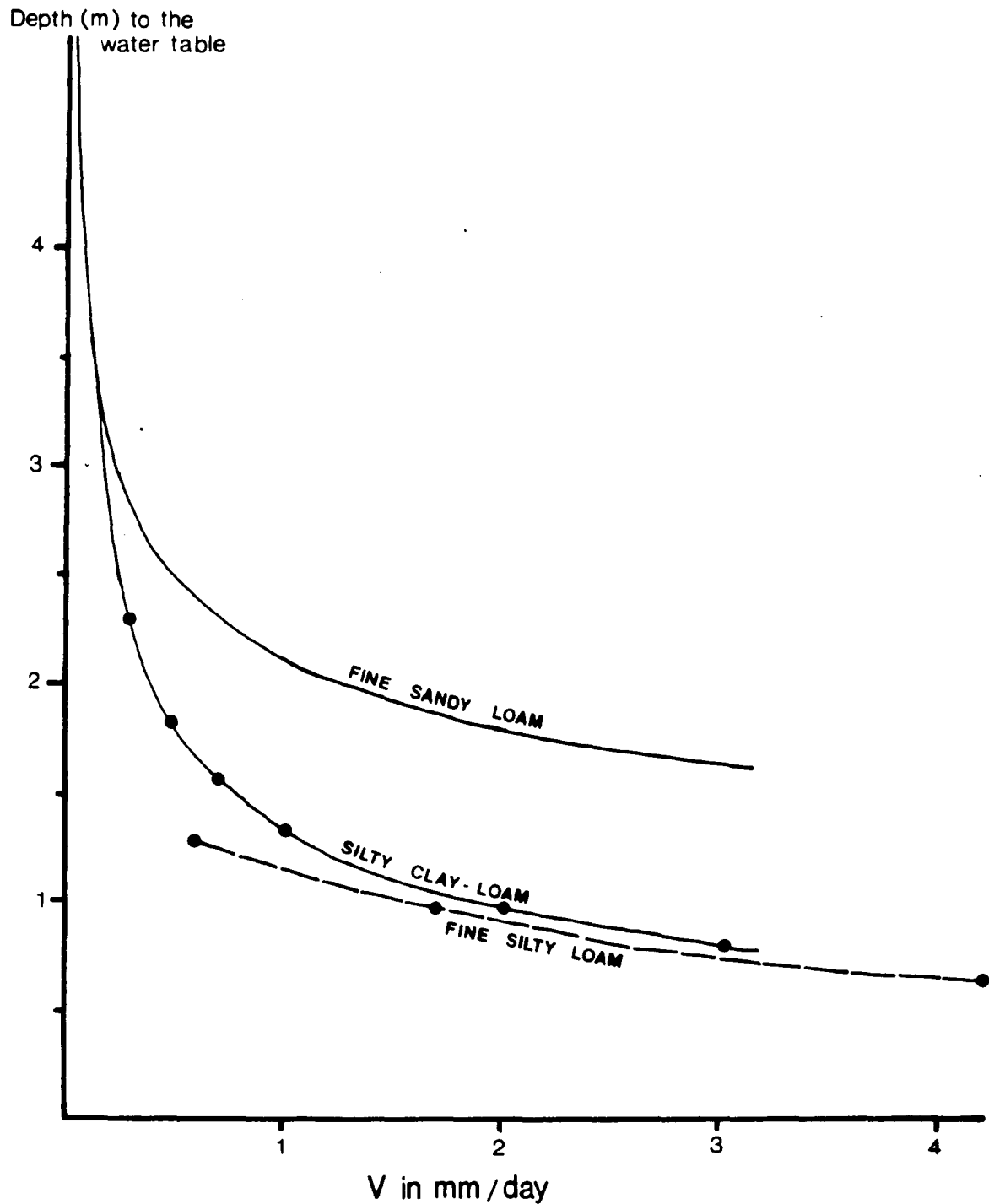
i.e. including much of the high mountainous area and approximately a third of the interior alluvium. Potentially therefore, the transpiration losses are an important component of the water balance. On the other hand, as only a proportion of this vegetation obviously taps the water table, the amount of actual evaporation is limited by the available water supply, including dew and ephemeral rainfall interception. The importance of the latter constraint has been demonstrated by a study of evapotranspiration of an arid plant community in the Arizona desert (Samms and Gay, 1979), in which remarkably close correspondence was found to exist between : rainfall 234 mm, soil evaporation 231 mm, weighing lysimeter evapotranspiration 259 mm, and a soil-water budget loss from a stand of creosote bush (Larrea tridentata) of 242 mm. By comparison it is therefore concluded that, at least in low lying alluvial areas, surface moisture/water losses are effectively total, whereas there is no evidence of widespread additional groundwater loss. On the contrary, rapid response to rainfall of the leaf area index in potential phreatophytes such as Acacia further suggests that such vegetation may not be in perennial contact with the water table, and hence may have only a minor effect upon the overall water balance. At higher altitudes the natural vegetation is substantially denser than elsewhere and also benefits from a greater rainfall frequency. In order to investigate the potentially higher water losses of this environment, a sample area comprising the Musandam peninsula was analysed by "Landsat" multispectral image enhancement in which: Date cultivation, Acacia scrub, and dispersed medium density vegetation – mainly xerophytic – was mapped by maximum likelihood classification using bands 4, 5 and 7. It was found that the medium density vegetation covered approximately 20% of the mountain area, or some 63 times the cultivated area. A greater figure of about 30% of the mountain area was found to correlate with the "Acacia scrub signature" but, subjectively, this figure seems too high and it is suspected that some "shadow areas" have also been misclassified as Acacia. Nevertheless, it is clear that even allowing for its dispersed nature, the total natural vegetation in mountainous areas is of comparable mass to that of the downstream cultivation, and may well result in significant transpiration loss from the overall water balance.

3.3 Hydrochemical Constraints

An alternative approach to quantifying evapotranspiration is to apply a mass balance calculation, utilising the most conservative ion(s), to assess

Figure 3·8

Rainfall / Halide Concentrations

Chloride – Rainfall + Dry fallout

Iodine – Rainfall + Dry fallout
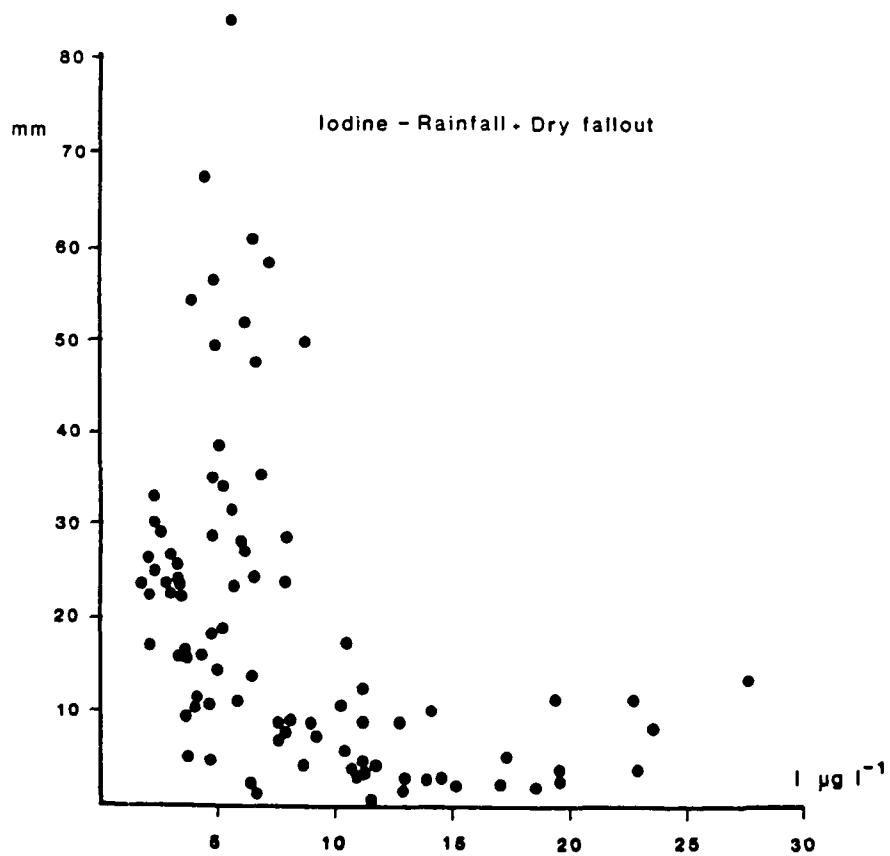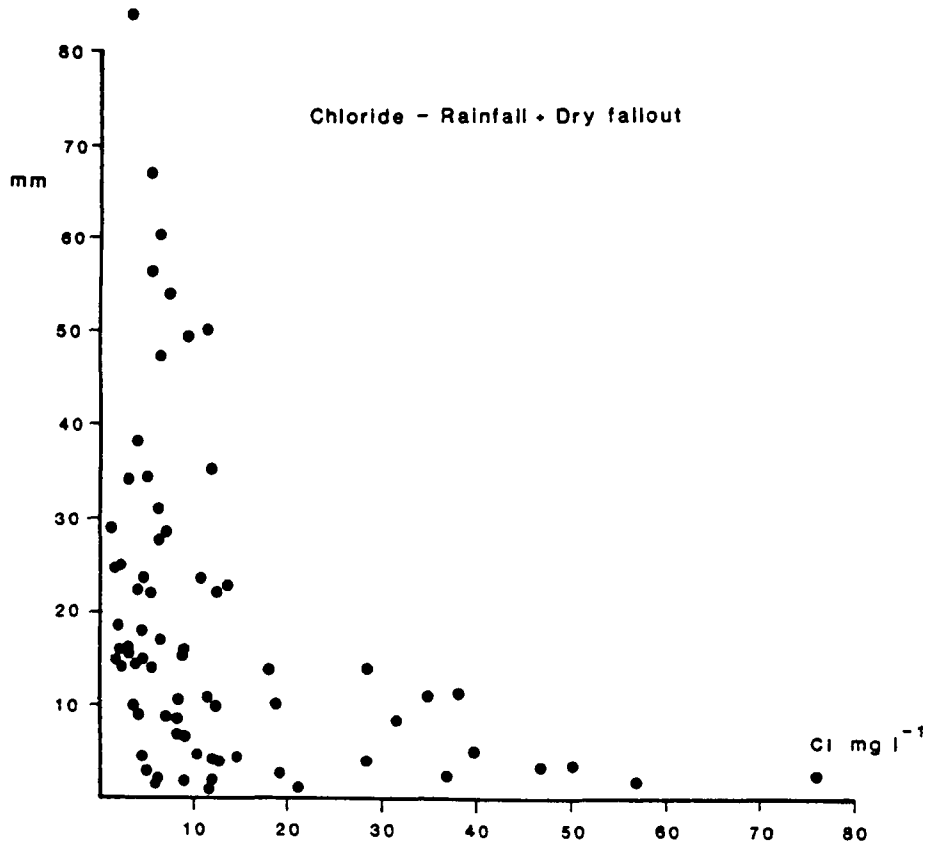
the concentration from rainfall to groundwater caused by evaporative loss. This requires a knowledge of all the ionic source concentrations throughout the environment, but is potentially more precise than pan-evaporation experiments since it involves neither extrapolation to a much larger scale, nor assumptions regarding loss mechanisms. The ion chosen was chloride (Cl^-) due to its stability in solution, lack of significant reactions within the aquifer, and the ease and precision of its measurement. In view of the natural variation of the Cl^- ion, a large number of samples were analysed to obtain statistically useful averages. This was most important for the rainfall or "chloride input" to the environment, where a strongly inverse relationship between rainfall and chloride concentration, shown in Figure 3.8, was determined. Such a relationship suggests that almost all the chloride in rainfall is precipitated during early raindrop nucleation and is efficiently scavenged from the atmosphere even by minor showers. Several authors have maintained that "dry fallout" of Cl^- is also important, especially in the near coastal arid environment; e.g. Yaalon, 1963. Irrespective of whether this is the case in the Oman mountains, the nett yield from undifferentiated gauge sites includes both "dry fallout" (if any) and "wet chloride", with an apparent amount weighted mean of 8 ppm. An attempt was also made to verify the Cl^- results by using total iodine as an alternative trace ion, from which a similar inverse rainfall-concentration relationship was determined (Figure 3.8). However, evaluation of the iodine enrichment between rainfall and groundwater showed a significant degree of volatile behaviour in which the evaporative concentration was indeterminate (Stanger and Neal, unpublished data).

During flood runoff several potential sources of chloride enrichment were envisaged, including: surface salt accumulation around roots, salts leached from animal droppings, halite dust etc. This was tested by analysing a time-series of flood waters at the edge of a small limestone catchment east of Tanuf; cf. Table 3.2. Although a small reduction in Cl^- was found during the flood recession, the leading edge, whilst heavily contaminated with organic pollutants, was not notably enriched in Cl^-. Indeed the observed Cl^- variation could have been due to fluctuations in the rainfall concentration rather than to subsequent surface solution. More significantly, the average Cl^- concentration for the whole flood was scarcely enriched above the mean rainfall Cl^-, thus indicating minimal surface chloride within the mountain environment.

Table 3.2 Flood Hydrochemical Variation with Time

parameter	Time (mins) since the leading edge of the flood.							Leading edge
	0	3	7	14	42	58	74	84
Cl^-	6.9	11.1	10.7	11.2	10.4	7.5	7.0	9.2
SO_4^{2-}	19	25	20	24	23	16	15.5	20
F^-	0.13	.08	.08	.08	.08	.07	.08	.08
NO_3^-	-	-	-	-	-	3.9	3.7	3.7
Na	7.0	6.0	6.0	6.0	5.0	4.0	3.0	5.0
Ca	33.3	28.1	40.0	36.0	33.3	32.0	39.3	34.0
Mg	1.7	1.2	2.4	1.2	4.4	10.4	1.9	3.4
Sr	.16	.13	.06	.27	.12	.16	.06	.12
pH	6.4	6.4	6.0	6.1	6.1	5.8	5.9	6.2
EC	210	210	220	220	210	178	158	200
approx flow (cumecs)	1	3	5	4	2	2	2	2

NB: The first five samples were too heavily polluted with organics to determine nitrate. All ions given in $mg.l^{-1}$.
The first seven samples were taken at grid ref EA515480
The "leading edge" sample was 2 km further downstream.

Table 3.3 Chloride Concentrations and Enrichment Factors

environment	n	$\bar{x}$**	*	σ
Chloride in rainfall (amount weighted)	71	8.0	-	-
Cl^- in piedmont runoff	15	7.6	2.8	0
Cl^- in coastal runoff	7	19.5	6.8	2.4
Cl^- in post-flood/recharge	4	28.2	12.0	3.5
Cl^- in piedmont groundwater during recession	9	23.7	10.4	3.0
Cl^- in downstream interior groundwater during recession	8	207	96	25.9

*   i.e. Apparent concentration factor with respect to mean rainfall
** mean $mg.l^{-1}$

NB. Large anomalous Cl^- values were obelised from the data.

The two most widespread lithologies were also analysed for Cl^-, with the results: (1) leachable Cl^- in serpentinite = 140 ppm (mean of five samples), as opposed to 29 ppm in fresh peridotite, and (2) mean total chloride in Hajar-Super-Group carbonates = 167 ppm (n = 51, σ = 88, cf. Appendix D). In view of the Ca and Mg concentrations in rainfall, surface waters and piedmont groundwaters, congruent dissolution of either silicates or carbonates would therefore produce corresponding Cl^- levels below the detection limits. It is therefore concluded that evaporative concentration upstream of major agricultural settlements, is the only significant mechanism of Cl^- enrichment. This apparent enrichment is shown for various hydrological regimes in Table 3.3, from which two main conclusions may be drawn. Firstly, in agreement with the above argument, there is no significant evaporative concentration between rainfall and runoff; and secondly up to two thirds of the total precipitation is lost before it reaches the water table. This is of course the result of processes averaged over a substantial period during which much of the chloride is probably in temporary residence within the unsaturated zone, i.e. precipitated during desiccation after floods, and leached down to the water table at the onset of recharge during subsequent floods.

More serious but localised Cl^- contamination could be envisaged downstream of village effluent, but substantially higher Cl^- concentrations in groundwater, e.g. due to irrigation return, are due more to water depletion than to new sources of chloride. Extreme Cl^- concentrations, i.e. approaching or locally exceeding saturation, are known from several inland areas immediately downstream of large villages and especially at "stagnation points" where shallow alluvium and low permeability preclude significant groundwater loss except by evaporation, eg. as in Bilad Bani Bu Ali (E.C. = 10^4 μmhos, grid GV 39-, 34-) and Southern Manah (E.C. = 10^5 μmhos, grid EA 61-, 17-). The only evidence for non-cyclic salt is around a few alkaline springs, discussed in section 5.5, but these do not appreciably contribute to the overall Cl^- budget. On the contrary, almost all natural evaporites in the Interior alluvial basins take the form of gypsum or anhydrite crust. Non cyclic salt uptake in groundwaters therefore results in an increasing SO_4^{2-}/Cl^- ratio, which is only characteristic of a few far downstream areas such as Adam, some 80 km south of the Akhdar source area. It therefore appears that, despite up to a hundred-fold concentration (cf.

Appendix C), Cl⁻ may still be a valid indication of total water losses throughout most of the hydrologic system, apart from the coastal and far inland areas. In fact despite possible dissolution of primary evaporites, first order estimates of the rainfall input, and groundwater flux out of the Nizwa basin at Adam (based upon average annual falaj and pumped well yields and salinities) are in close agreement at 3000 m^3 Cl⁻ as NaCl, thus implying a long-term basin-wide equilibrium in cyclic chloride.

CHAPTER 4

THE LIMESTONES

4.1 The Carbonate Aquifers

The massifs of Jebels Akhdar-Nakhl and Tayyin-Sharqiyah (cf.
Figure 1.1) are by far the most important hard-rock aquifers in Northern
Oman, and of these, Jebel Akhdar is pre-eminent by virtue of its great
extent, maximum depositional thickness and high altitude; i.e. 2250
km^2, greater than 2.5 km, and up to 3035 m respectively. In addition to
their intrinsic aquifer properties, erosion of these carbonate massifs
has produced the coarse grained piedmont wadi systems and alluvial
basins which are recharged from the high altitude areas, and which
constitute the most productive alluvial aquifers, discussed in chapter
six. Apart from the Sharqiyah, where Tertiary strata are well developed
(cf. section 4.7), the shelf carbonate massifs range in age from about
mid-Permian to the late Cretaceous. Conventionally the sequence is known as
the Hajar Super Group (HSG) and is divided into five major formations (after
Glennie et al., 1974) whose stratigraphic relationships are shown in Figure
4.1, and summarised below.

The lower Permo-Triassic sequence, comprising the Saiq and Mahil
or "Akhdar group", is well exposed in all the eroded anticlinal cores in
the form of thick, predominantly dolomitic cliffs, and differs markedly
from the overlying Jurassic to Cretaceous limestone sequence (i.e.
Sahtan to Wasia groups) which are mainly exposed upon the anticlinal
limbs. Both the limestones and dolomites are of similar thickness
throughout the Akhdar-Nakhl massif. Superficially, the limestones are a
monotonous series of hard thoroughly lithified and diagenetically mature
rocks of dark grey, rather impure appearance. Non-carbonate lithologies
form a relatively trivial fraction of the super-group, much less than 1%,
and even the more impure carbonates, typically described as "lime mudstones"
or "calciferous shales" seldom consist of less than 90% carbonate (cf.
Appendix D). The only exceptions are: (1) A sporadically developed
goethite cemented quartz sandstone, or limestone conglomerate in a

ferruginous oolitic matrix from the Wasia group of the southeast Akhdar area; (2) A more generally developed quartz sandstone which marks a short period of extreme regression near the base of the limestone (as opposed to the lower dolomitic sequence); (3) Thin black pyritic cherts in some of the deeper water limestone facies; and (4) Sporadic quartz siltstone/packstone horizons, scattered throughout the shallow water limestone facies but most noticeable in some of the lowermost "Saiq" horizons. Although these lithologies are relatively resistant to karstic dissolution, they have all been affected by pervasive fracturing and are thus unlikely to disrupt the overall hydraulic continuity of the carbonate sequence.

Formation descriptions of the HSG in the Akhdar-Nakhl massif, (partly based upon Glennie et al., 1974) may be summarised as:

The Saiq formation, which consists of a dark grey to black basal sequence of open marine grainstone to wackestone facies overlain by a thicker crystalline dolomitic sequence. The latter is dark grey to dark brown in colour, generally fine grained and comprises between 60% and 80% of the formation thickness. Both the limestone and dolomite vary from massive cliff-forming units up to several tens of metres thick, to the more common bedding thickness of between 10 and 50 cm. The limestone lithology is easily identified by its black colour and distinctive rich macro-fauna of Permian rugosa, abundant mounds of crinoidal, algal and bryozoan débris, and less common brachiopods including Permian spiriferidae. The overlying dolomite is characterised by more restricted shallow-water facies including tidal, subtidal and lagoonal deposition in which the relict fauna and oolites are mostly obscured by complete dolomitisation, except for sporadic megalodontid horizons. In the Saiq plateau area there is a locally conformable downward passage from the black limestones through an iron-stained quartz packstone to about 10 metres of orange-yellow siltstone over a basal haematite cemented conglomerate of unknown age (cf. Map 1). Elsewhere however the Saiq carbonates are separated from the underlying strata by an angular unconformity, typically of about 20°.

The Mahil formation is usually differentiable from the medium grey weathering Saiq formation by virtue of the former's pale brown

Figure 4.1 — Lithostratigraphic Summary of the Hajar–Super Group

AGE	STAGE	MICROFAUNAL ZONE after GLENNIE et al	Typical Thickness (& Range) in m. in Js Akhdar/Nakhl	FACIES emergent ↑ shallow deep ↓	Limestone ↑ Dolom ↓	FORMATION Group/Subgroup
Cretaceous	Cenomanian	8 Praealveolina	350 (0–400)			WASIA — Natih / Nahr Umr
	Albian Barremian	7 Orbitolina				
	Hauteverian	6 Tintinid	500 (0–750)			KAHMAH
	Portlandian					
Jurassic	Kimmeridgian Bathonian	5 Protoperopolis	300 (75–300)			SAHTAN
	Aulemian Sinemurian	4 Haurania				
Triassic	Hettangian Carnian	3 Involutina	>1000 (50–1500)			MAHIL — Dayqah
	Landinian	2 Multicoiled Trocholina				
	Scythian					
Permian	Tatarian	1 Fusulinid	450 (200–700)			SAIQ
	Kungurian					
			100 ?			(HAJIR / KHARUS)

EQUIVALENT FORMATION IN MUSANDAM

Ms1		Musandam Limestones
Ms 2		
Ms 3+4		
Ghalilah		
Milahah		
Ghail	Ruus al Jibal	
Hagil		
Bih	dolomite	

weathering and generally massive thicker bedded cliff-forming appearance. Otherwise it is a continuation of the restricted shallow marine conditions and consequently consists of a thick sequence of monotonous pale brown to light grey sucrosic dolomites. There is no macro-fauna other than occasional stromatolites, but a distinctive feature of the upper formation consists of more porcellanitic facies and frequent thin (decimetre) beds of pink dolomite interspersed between more numerous grey dolomites, all with rare relict non-linked porosity after evaporites. The coloured dolomites (apparently the "pink ferriginous cherts" of Glennie, 1974) are enriched in Fe_2O_3 and silica, and correlate with a slight Zr anomaly indicating an influx of more terriginous material. For example the silica content varies from 7% in Jebel Madar (south of the mountain axis) to 3.4% in the Jebel Akhdar, and 0.9% in Wadi Aday to the northeast; i.e. indicating more open marine sedimentary conditions to the north. The top of the Mahil is marked by the basal Jurassic unconformity.

Above the Mahil, the basal Sahtan formation consists of a thick ferruginous quartz-oolitic sandstone unit which was deposited during a brief period of maximum marine regression and which forms one of the few distinctive marker horizons of the HSG. Above this, the formation is almost entirely composed of shallow marine limestones which typically occur in cycles of mudstone to grainstone facies. Locally, minor pale brown dolomites are also developed.

The lower Kahmah formation is marked by a change to relatively deep water facies dominated by pale grey porcellanities and rare black cherts. These pass upwards into shallow water lime mudstone and wackestone, and then into a complex of bioclastic and pelletal lime wackestone and packstones, thin lime mudstones, oolites and grainstones. Some of the upper Kahmah beds may be recognised by distinctive packstone beds of large thick-shelled molluscan débris. Subsequently, a basal ostracod-rich calciferous shale indicates the basal Wasia group, above which the limestones are generally of wackestone to grainstone facies (as opposed to predominantly lime mudstone to wackestone facies in the Kahmah group). A further difference is the tendency of the Wasia to weather to a paler grey than the Kahmah limestones. Nevertheless, apart from the lower Kahmah porcellanites, there is an overall similarity of field appearance between the Sahtan and the top of the HSG.

Hydrologically, the detailed facies variation is only indirectly significant insofar as the macrofossiliferous beds tend to be thicker and more competent than the intervening "shaly" lime mudstones, and thus exhibit more widely spaced but better developed joint permeability.

The basal unconformity of the HSG normally overlies a wide range of siliclastic meta-sedimentary lithologies, typically quartzite, slate, siltstone and silty conglomerates, which together form an essentially impervious base to the carbonate aquifer. In the Saiq and Sahtan inliers, i.e. in the core of the Akhdar anticline, intense folding, conjugate shear and vertical rectangular fracturing has created low permeability within the slates, resulting in several water-holes and low discharge springs (less than 0.5 1 s^{-1}). The hydrochemistry of these sources (Nos. 253 and 341 in Appendix C) is indistinguisable from limestone spring waters but the low salinity, low temperature of 25 to 30°C, ephemeral nature of the springs and physical location suggests that recharge is derived by runoff from the local limestones rather than by groundwater seepage from the overlying limestone aquifer. More significant exceptions to the impervious base occur in parts of both the Sahtan and Bani Kharus inliers where the basal Saiq formation is also in contact with similar black, shallow, silty, partly crystalline, lime mudstones of pre-Permian age (cf Map 1). These limestones, the "Kharus" and "Hajir" formations are tightly interfolded with the siliclastic sediments and, where contact occurs, may be regarded as lower extensions of the HSG aquifer. A possible correlation exists between pre-Permian limestones of the Jebel Akhdar, and the Hijam dolomite of the Sayh Hatat inlier, but the latter is devoid of springs and does not appear to constitute an aquifer. Formations which overlie the HSG aquifer are of equally variable but consistently impervious lithology and consist of either a sedimentary contact with unconformable shales and limestone-conglomerates of the Muti formation, or a thrust contact with siliceous Hawasina sediments, Haybi volcanics or other nappe fragments.

Lithological comparison between the Jebel Akhdar (Figure 4.1), the Musandam peninsula (Figure 4.12), and more easterly sections reveals a broad similarity in which lower dolomites are separated from upper limestones by a thin terriginous sequence. In more detail however, important regional differences exist both in lithofacies and in the stratigraphic range of deposition. For example in Musandam the Wasia

formation is not represented, and the equivalent of the Lower Saiq formation (the lowermost Ruus Al Jibal group) is not exposed. North and east of the Jebel Akhdar, the uppermost limestones occur at increasingly lower horizons, such that the Wasia formation is totally absent east of Wadi Semail whilst the Kahmah, and locally even the Sahtan formations, are missing along the northern perimeter of Sayh Hatat. In the same area, the HSG also differs in several other important respects including severe structural dislocation (discussed in section 4.2) and more intense metamorphism. Indeed in Wadi Mijlas, south-east of the capital area, the Saiq formation has been totally dolomitised and altered to a micaceous foliated and faulted complex in which interfolded Permian and Pre-Permian carbonates are difficult to differentiate.

There are three important lateral variations in the HSG lithofacies. The first occurs in the Wadi Dayqah area of the western Sharqiyah massif, where the normally dolomitic Lower Mahil is represented by about 400 m porcellanous and crystalline limestones and calciferous shales and siltstones, which together form the "Dayqah" sub-group. The second difference lies in the extent of the terriginous influx at the base of the Sahtan unit. In the Jebel Akhdar, this event is often less than one metre thick whereas the equivalent facies in Musandam is up to 100 metres of the Ghalilah formation. Thirdly, more than 50 m of porcellanites which form a prominent feature of the Kahmah in the Jebel Akhdar, are poorly developed or absent in more north-easterly areas, in which case the Sahtan, Kahmah and Wasia groups may be undifferentiable in field appearance. Less obvious facies variations within the HSG are mostly associated with a trend from thick shallow-water deposition in the south west, to more distal fine grained and thinner deposition of deeper-water facies further to the north-east.

The overall volume of HSG carbonates substantially exceeds that of the Tertiary limestones, but in view of the latter's large surface exposure and local importance, they are discussed in detail in section 4.7. A strong contrast between the Tertiary and HSG carbonates is almost always immediately apparent. The most striking difference is in colour: Tertiary strata ranging from creamy-white crystalline limestones to yellow marls and dolomites, as opposed to shades of grey in most of the Mesozoic rocks. Exceptions are rare and occur only when unusually advanced diagenesis has imparted a grey colour to the Tertiary

91

formations as has happened in deeper sections of boreholes from the Seeb airport area, and in some deeply eroded cliff sections of the eastern Sharqiyah. Nevertheless in all cases the Tertiary age is readily identifiable on the basis of: nummulites and other Palaeogene macrofauna, common gypsum-marl alternations, or the characteristic rubbly or careous weathered appearance of the Palaeogene limestone surfaces. Whereas most of the Tertiary areas discussed in section 4.7 are thin, of varied lithology and form locally important aquifers, the eastern Sharqiyah massif, though of larger lateral extent (approaching that of the Jebel Akhdar) exhibits monotonous shelf limestone facies, contains only minor occurrences of groundwater, and has no alluvial recharge potential to seaward. Thus in view of the low priority and the extreme difficulty of access, this aquifer was only studied at reconnaissance level.

4.2   The Structural Control Upon Spring and Groundwater Distribution

Groundwater distribution in the limestone massifs is controlled both on a large scale by the overall structure and geometry of the aquifer, and on a smaller scale by the detailed disposition of fracture flowpaths. In the Jebel Akhdar, the gross structure consists of a relatively simple anticline with an eroded core in which the steeply dipping eastern (Jebel Nakhl) and western extremities are approximately symmetrical about the fold axis, as opposed to the major part of the Jebel Akhdar which has a prominent vergence to the north of about 10°. Consequently northward displacement of the fold axis and concomitant erosion of the anticlinal core, together with steeper and more vigorous northward drainage, has produced a dissected northern scarp (i.e. south facing), and a much larger relatively intact southern scarp from which most of the high altitude groundwater is derived. Despite local variations in lithology and structure, the scale of the massif is such that overall, approximately homogeneous groundwater flow may be assumed, thus giving rise to the spring line distributions summarised schematically in Figure 4.2. This figure illustrates two physiographically disposed spring environments. The first is that of piedmont springs which occur at relatively low altitude but at a high stratigraphic horizon. These are sparsely distributed around the piedmont, are often thermal (cf. section 4.5), and tend to have large

Figure 4.2　　　Schematic Section of the　Jebel Akhdar Anticline

Showing Spring Line Locations
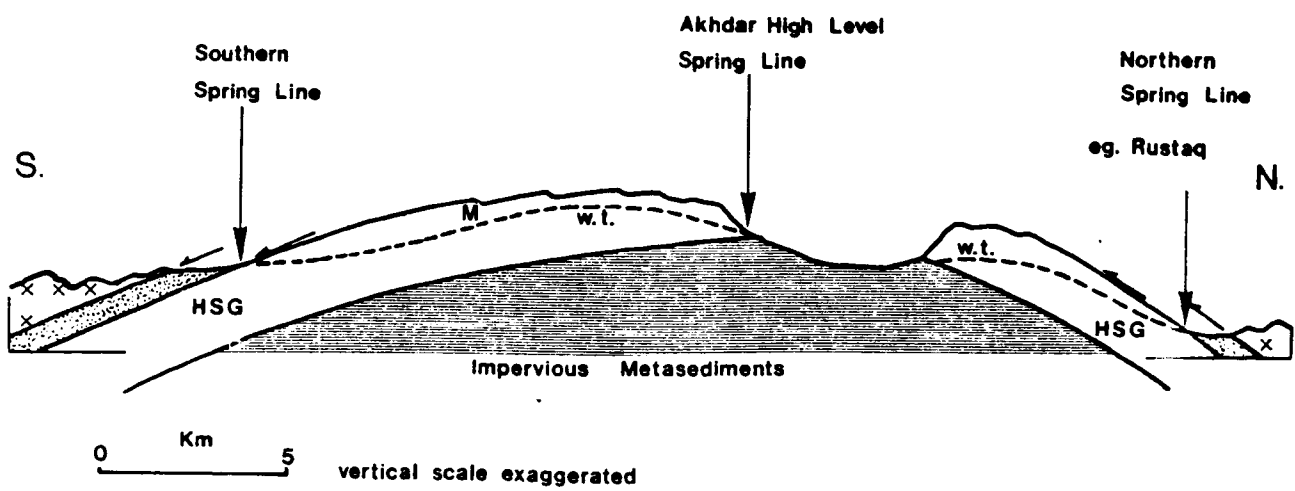
NB　The High Level Springs　at　Saiq　are　South Facing

stable discharges, as at: Rustaq Hammam 82 ±20 $1.s^{-1}$, Rustaq Sihre
42.6 $1.s^{-1}$, Nakhl Thowara 40 $1.s^{-1}$, and Tabaqah 36 ± 8 $1.s^{-1}$. The
second spring environment differs in each of these respects, ie.
occurring at high altitude but low stratigraphic level; having
invariably cold water temperatures of about 25°C, and low discharges
which exceed 10 $1.s^{-1}$ for only a short period after rainfall, if at
all. Numerous such "high level springs", both perennial and ephemeral,
occur along the foot of the main (north facing) scarp at or close to the
contact between Saiq limestones and the underlying impervious
siltstones, but occasionally larger springs also occur at higher
limestone horizons as at Saiq village and Wadi Bani Habib. Here the
recharge and groundwater storage areas can only be limestone hills to
the north of the Saiq plateau, but curiously, the groundwater flow is in
the opposite direction to the northerly dip (Figure 4.2 and Map 1) and
hence is presumably guided by complex and locally anomalous limestone
fracturing caused by intersection or realignment of the Akhdar and Nakhl
anticlinal axes. Elsewhere in the massif the fracture pattern is more
rational but far from homogeneous. A distinct contrast in tectonic
style occurs between the northern and southern limbs of the anticline.
In the northern part of Jebel Akhdar the relatively steeply dipping
carbonates (typically up to 40°N) mainly display compressive features,
resulting in ooid strain ratios of 3.5 or more, and widespread ductile
deformation of the thinner and less competent strata. A few
longitudinal faults are very prominent, and the Rustaq springs are
traceable to a large cross fault, but otherwise the fracturing does not
appear to be intense, and the few other springs in the area bear no
obvious relation to the limestone structure. In the southern limb of
the massif an entirely tensional régime exists. Here, the carbonates
have a lower but more consistent dip of about 20°S and display a
complete set of primary and secondary fractures. Most joints are
calcite-recemented and have undergone minimal solution opening.
However, continuing uplift along the Akhdar fold axis has reactivated at
least two of these intersecting fracture lineations in the form of
master joints and major faults. Of these, the primary longitudinal
fractures (i.e. trending approximately along strike) display the most
widespread evidence of groundwater flow, including; numerous east-west
solution pipes exposed in various gorge cliffs, the swallow-hole
drainage lineation east of Al-Qaryah, and the position along strike of
the Al Qaryah spring itself, (cf. Map 1). There is, however,
conflicting evidence concerning the controlling influence upon

interconnecting groundwater flow, i.e. downdip from the source area at the top of the scarp. Surface exposures show that north-west to south-east trending shears are the best developed lineations linking the longitudinal fractures, but speleological evidence from the only known large cave system of the Akhdar massif (Hoti, north-east of Al Hamra) suggests that 010° trending cross joints/faults are much more important and consistent conduits at depth (Waltham, 1985 pers.comm./in press) . In other parts of the massif piedmont springs are almost invariably aligned with fracture sets of varying origin: all the springs in the Khawr-Ghul exotic limestone are aligned with steep bounding faults which lie sub-parallel to the major fold axes, (cf. section 4.8). Similarly all limestone springs in the Fanjah area are derived from longitudinal tension faults which divide the plunging axial zone of the Northern Jebel Nakhl anticline (cf. Map 2). Only in the southern part of Jebel Nakhl do shear faults predominate as the main productive lineations, eg. the springs of Al Hubi, Minabak, and possibly the main spring of Nakhl village itself. In Jebel Nakhl, as in the southern Jebel Akhdar, development of, and groundwater flow, in the conjugate shear system appears to be asymmetrical, with left lateral shear predominating; i.e. skewed anticlockwise from the dip direction. No spring/right hand lateral shear association could be identified.

Although fractures, which occur in varying intensity throughout the HSG, are generally perpendicular to the bedding, many of the thicker, more competent and often dolomitic strata are relatively massive and thus behave occasionally as locally impervious horizons. This is most conspicuous in the low dipping anticlinorial area within and around the Saiq plateau, where about 20 perched and stagnant "water-holes" are scattered throughout various horizons of the Saiq and Mahil formations.

On the southern flank of the Jebel Akhdar the angle of dip only slightly exceeds that of the hillslope. In this situation, any groundwater flow restricted to bedding planes (as opposed to fractures) tends to leak laterally into boulder gravels within the deeply incised gorges, thereby exhibiting anomalous groundwater or spring occurrence at intermediate stratigraphic horizons and altitudes. The largest example is some 30 to 40 $l.s^{-1}$ at Misfah (north-east of Al Hamra), shown schematically as "M" in Figure 4.2, but several lesser sources are

scattered throughout the area. These intermediate level groundwater sources, and especially the implied locally impervious nature of some of the more massive beds, are uncharacteristic of a holokarstic environment, and testify to the widespread immature karstic development of the HSG.

The perimeter of the massif is in contact with the overlying impervious allochthonous units along a poorly exposed thrust fault. There are no surface indications of any groundwater flow along this thrust, but its low relief position around the massif determines the exit points of both spring and groundwater into the piedmont alluvium. Indeed many of the water sources from alluvium in the vicinity of the thrust contact are clearly too large to be maintained from local storage and must derive ultimately from concealed limestone sources whose structural origin is indeterminate (eg. Ghubrat Tanuf, Kahmah, Muti, Hamma, Kuri etc., located in appendix C, Nos. -, 128, 384, 100 and 335 respectively, and Map 1).

Whilst the above structural features influence groundwater occurrence in differing ways throughout the Jebel Akhdar, more important hydrogeological contrasts invest the HSG in other areas. For example, severe faulting and deformation together with unusual tectonic conditions render the Musandam peninsula a special case (discussed in section 4.6); also the sinuous extension of the HSG through Jebels Nakhl and Tayyin and its subsequent bifurcation towards Jebel Bosher and the Sharqiyah, Figure 4.3, has proved to be unexpectedly high yielding and hence of greater significance from the point of view of water supply to the capital area. Throughout the latter areas, more easterly positions correspond with an apparent increase in aquifer storage coefficient and yield caused by progressively more intense tectonic disruption. This contrast in aquifer characteristics first becomes apparent between Jebel Akhdar and Jebels Tayyin/Bosher, and is illustrated by a greater number of springs, albeit of mostly small individual discharges in the Bosher spring line. These together yield an almost constant 100 $l.s^{-1}$ derived from about 150 km^2 of hard-rock aquifer, as opposed to an estimated total spring discharge of about 800 $l.s^{-1}$ throughout the Jebel Akhdar, i.e. in terms of annual discharge per km^2, Jebels Tayyin/Bosher therefore yields 21,000 m^3 as opposed to

Figure 4·3

Carbonate Aquifers of the Capital Area

Structural details given in Map 2
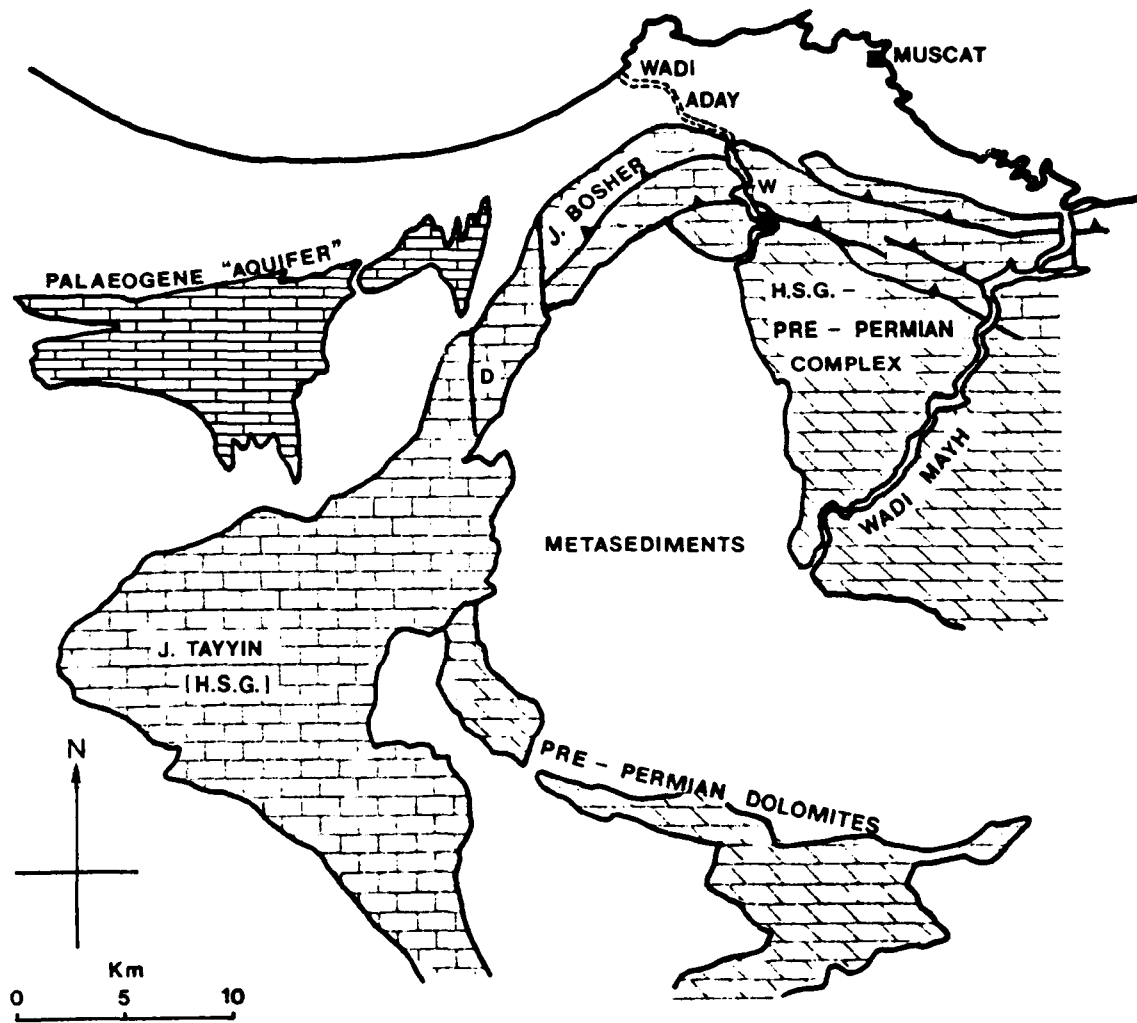
an equivalent figure of 11,200 m^3 for the Jebel Akhdar. Some error is
incurred in the latter estimate due to uncertainty regarding piedmont
alluvial vs hard-rock groundwater provenance, but the above gross
aquifer yields are regarded as a minimum contrast for two reasons.
First, the carbonate aquifer dimensions are substantially greater in the
Jebel Akhdar in terms of altitude range, absolute stratigraphic
thickness, and of mean thickness of exposed aquifer, and hence should
contain more storage potential. Second, other factors being equal, the
lesser dimensions of the Tayyin/Bosher aquifer would have logically
resulted in correspondingly smaller groundwater storage and shorter
flowpaths, whereas the tritium isotope data of Appendix B2 shows that
the reverse is true. Specifically, the Bosher spring line is entirely
of low to zero tritium concentration, indicating pre-1960 meteoric
origin, and hence a storage residence time of at least 25 years. By
contrast the low altitude Akhdar springs all have tritium concentrations
of 8 to 11 T.U.^{S}, indicating at least partial storage of relatively
recent origin which in turn implies lesser storage capacity. The
eastern termination of the Bosher spring line is effectively at Wadi
Aday (Figure 4.3): an area in which substantial groundwater development
has taken place since about 1979. Since then the Aday wellfield yields
have averaged about 3.0 x 10^{6}m^3.yr^{-1}, with a peak abstraction in 1982
of 5.4 x 10^{6}m^3.yr^{-1}. The main producing wells penetrate a compound
aquifer of alluvium and fractured dolomite of the Akhdar group in the
upper part of Wadi Aday gorge ("W" in Figure 4.3). Further upstream the
"aquifer" consists of shallow alluvium overlying impervious
non-carbonate metasediments of the Hatat inlier and are regarded as
having only trivial storage potential: first on the basis of
hydrochemistry in the lower wadi which indicates groundwater provenance
from a carbonate aquifer (cf. Appendix C, Nos. 98 with 403); and
secondly, villages which derive their irrigation water from the northern
Hatat inlier are frequently affected by severe drought. In the Aday
wellfield itself there is some debate (unpublished) as to whether
groundwater is derived from local storage or from interception of
underflow from the HSG to the wadi alluvium. The latter seems much more
probable since: (1) Pumped groundwater shows only a brief decrease in
groundwater salinity following storm recharge, (2) groundwaters from
boreholes which penetrate the hard-rock are of above average
temperatures, eg. 44°C from WD86 (Appendix C, No.98). This is similar

to all other groundwater temperatures from springs throughout the
eastern Bosher spring line, including the now defunct Wattayah spring
near the mouth of Wadi Aday gorge, whereas no groundwaters from alluvial
or short period hard-rock storage are known to exceed about 36° C.

(3) the hydrochemistry of borehole WD86 is virtually identical to that
of Wattayah spring (analysis given in Gibb, 1976, Appendix E3, p11).
Although both these sources are of higher than normal salinity, they
both share a high fluoride concentration of about 0.4 mg. 1^{-1} in common
with other spring waters from low tritium – long term storage in the
HSG; eg. Appendix C samples 53, 55 to 57, cf also the Fanjah area,
section 6.2(3). Thus the thermal and hydrochemical indications point to
a large proportion of the Wadi Aday groundwater, probably exceeding 2 x
10^6 m.^{3} yr^{-1}, being derived by lateral dewatering of the HSG aquifer.
Furthermore, since the aquifer volume of the more distant Jebel Tayyin
massif greatly exceeds that of the adjacent Jebel Bosher, it is probable
that groundwater storage lies predominantly within the former. Whether
this is the case or not, long term groundwater transfer along strike is
implied, and is intercepted in the incised intersection of the Saiq and
Lower Mahil formations of Upper Wadi Aday. These highly transmissive
horizons consist of a broad thrust fault zone of complex fractured and
folded Mahil, Saiq and Pre-Permian (possibly Carboniferous) dolomites,
above which the relatively undeformed HSG is detached as a
para-autochthonous homoclinal unit. The location of HSG transition from
autochthon to basal detachment is not known with certainty, but probably
occurs at about point "D" in Figure 4.3.

East of Wadi Aday, the Mahil formation is underplated by impervious
mica schist and is stacked in tectonic repetition over a more extensive
complex of marbles and other metasediments (Bailey, 1981; Lippard,
1984; Michard et al., 1984), all of which is orthogonally drained by
Wadi Mayh. As in Wadi Aday, Wadi Mayh terminates in brackish lagoonal
conditions indicative of fresh-water leakage to sea, and similarly
appears to derive most of its baseflow from storage in the fractured
basal thrust zone. So far these natural rates of storage depletion are
inadequately known but they have similar coastal outflows which probably
average about 100 l.s^{-1} each, thereby giving a total discharge from the
HSG of the capital area of about 9 x 10^6 m.^{3}yr^{-1}.

In the south-eastern limb of the Hatat inlier, the HSG is
structurally intact with respect to the underlying impervious base of
Amdeh quartzite, but folding and fracturing of the aquifer is locally
severe with a tectonic style more akin to the capital area than to the
Akhdar area. Downstream of the main HSG massif, unpublished IH-GDC
baseflow gauging from Mazara, indicates a minimum discharge and
recession constant of 200 $l.s^{-1}$ and 18.0×10^6s respectively. Together
these imply an annual upstream storage loss of 3.6×10^6 m^3. yr^{-1} of
which about one third or 1.2×10^6 $m.^3yr^{-1}$ is estimated to be from
hard-rock storage: cf the hydrochemical arguments of section 4.4

Despite some uncertainties regarding the proportion of groundwater
in alluvial as opposed to hard-rock storage, it is evident from the
above estimates that there is no consistent relationship between HSG
aquifer volume or area, and the groundwater yields. Rather, the storage
potential is primarily dependent upon the local development of varied
structural features and, presumably, upon the limitations of
infiltration in a given groundwater catchment area. As the southern
Akhdar, Bosher spring line and Wadi Aday areas imply, lateral
groundwater flow (ie. along strike) may occur over many kilometres and
hence the groundwater catchment boundaries cannot necessarily be deduced
from surface water divides. Few generalisations can therefore be
assigned to individual formations of the HSG, and the limited available
borehole data may thus be of only local validity.

4.3 Carbonate Dissolution and Karstic Development

Primary linked porosity is effectively absent from the carbonate
aquifers of Oman. Substantial matrix porosity caused by a theoretically
12% volume reduction during dolomitisation is occasionally encountered,
especially in near coastal exposures of immature Palaeogene rocks, and
rarely in the HSG (eg. dolomitised Kahmah limestone near Tul, Wadi
Dayqah), but these exceptions are not associated with enhanced solution
opening and appear to be of low overall permeability. Significant
permeability is thus entirely derived from solution opening of
secondary, ie. fracture, porosity. Despite the age of many of the
aquifers karstic development is, with a few local exceptions, poorly
developed. Cavernous development appears to exist only in the Sharqiyah
massif and north and east of Al Hamra. The latter area includes both

a cave system which has been traced northwards for over 5 kilometres and one of the few large surface karst features of Oman; a deep fault-guided doline containing an ephemeral swallow hole (Plate 4.1 and Map 1). Most endokarstic features have subsequently been exposed near the piedmont or in sporadic concentrations in the many precipitous gorges of the HSG, and take the form of pipes, exit holes and solution-widened fractures, as shown in Plate 4.2. These occur in only a small fraction of the exposed carbonates, and in many areas are completely absent. The endokarst is best developed and most widespread in the Wasia limestones of both the northern and southern flanks of the Jebel Akhdar, and has also been observed in all other formations of the HSG. As in all karst areas, exokarstic (surface dissolution) features are much more widespread and obvious and become increasingly so in higher rainfall areas and hence at higher altitude, eg. the Karren tables and rillenkarren of Plate 4.3 and 4.4. Rillenkarren are particularly well developed in steeply sloping pure limestones of which the best examples are the white exotic limestone described in section 4.8. In low dipping areas, the limestone pavements are sometimes strewn with thin careous weathered residuals and sharp edged pebbles, but are more commonly left bare as shown in Plate 4.5. In either case grikes or, where strata are more inclined, solution-widened bedding planes give the impression of high permeability and hence good aquifer potential. However, piedmont exploration drilling in superficially promising areas has usually encountered fewer widened fractures at depth. Consequently lower permeability and poor yields with high drawdowns have been reported from: (1) The Wasia limestones of the southern Adkhdar massif (Howsam pers.comm.), (2) Upper Kahmah limestones of the eastern Akhdar/Capital area (PAWR data – pers.comm.), (3) Faulted Eocene limestones east of Wadi Rusayl. Drilling experience in the Eocene limestones indicates a normally thin transition to impervious rock, whereas well developed exokarst in the HSG commonly overlies a "subcutaneous zone" some tens of metres thick, in which solution opening varies from slight to very extensive. A common feature of this zone is sub-surface red-calcareous clay infill which typically accumulates within the base of long dip slopes as in the Tanuf area, but whose presence is normally detectable only in borehole cuttings or in road cuttings.

Attenuation of the carbonate permeability with depth is a consistent feature of other environments, and conforms to a model of near surface dissolution in which the accumulation of soil in surface

depressions leads to vegetative growth, high soil pCO_2 concentrations and hence, initially, chemically aggressive water infiltration into transient near-surface storage. During lateral groundwater movement towards steeper groundwater flowpaths, the hydrochemistry approaches equilibrium and subsequently recharges the deeper phreatic zone with a reduced capacity for carbonate dissolution, e.g. Figure 4.4 after Williams, 1983. The zones of vertical flow are widely spaced and tend to be concealed beneath "dolines", i.e. silt-veneered brecciated or eroded depressions, and thus form difficult targets to intercept by drilling. The most prominent "doline fields" are found (1) between Wadi Aday and the Sharqiyah and especially in the Quryat-Wadi Dayqah area where a prominent wave-cut platform has planed the coastal carbonates, of both HSG and Palaeogene formations to form a dissected plateau at an average altitude of about 150 metres. In this area an initial cycle of minor Mesozoic karstic development has been followed by a second more intensive cycle in the Palaeogene limestones; both presumably being associated with a shallow water-table following the onset of marine regression. (2) Better developed but more localised doline fields are found in fractured Kamah limestones in the high plateau area above Upper Wadi Dayqah where they probably constitute a major recharge source to the upper gorge, discussed in section 4.4 These features take the form of silty clay depressions in an intersecting rectilinear fracture pattern. The dolines have occasionally coalesced into larger alluvial depressions but, in all cases, have obviously developed along longitudinal and cross faults in response to severe deformation during basal dislocation. Though less well developed, dolines are also relatively common in the Musandam limestones where, again, they occur in response to substantial structural disturbance of the area, discussed in section 4.6. In these areas, substantial vertical permeability appears to be maintained despite heavy cementation of the fault breccia and colluvial infill of the fracture zones.

The extent to which carbonate is dissolved is mainly determined by the total dissolved CO_2 in groundwater, which in the Jebel Akhdar is minimised by most of the influencing factors. Of these the sparse rainfall is the most obvious since, even at high altitudes, there is insufficient throughflow of groundwater to maintain hydrochemical aggression over long periods. Similarly the apparently short residence time at the surface may prevent the water in contact with carbonate and

Figure 4.4

Schematic Zone of Subcutaneous Storage
modified after Williams 1983

net water movement

zone
of
subcutaneous
storage

Net
Movement
Water

silt veneered doline

recharge to deep phreatic zone
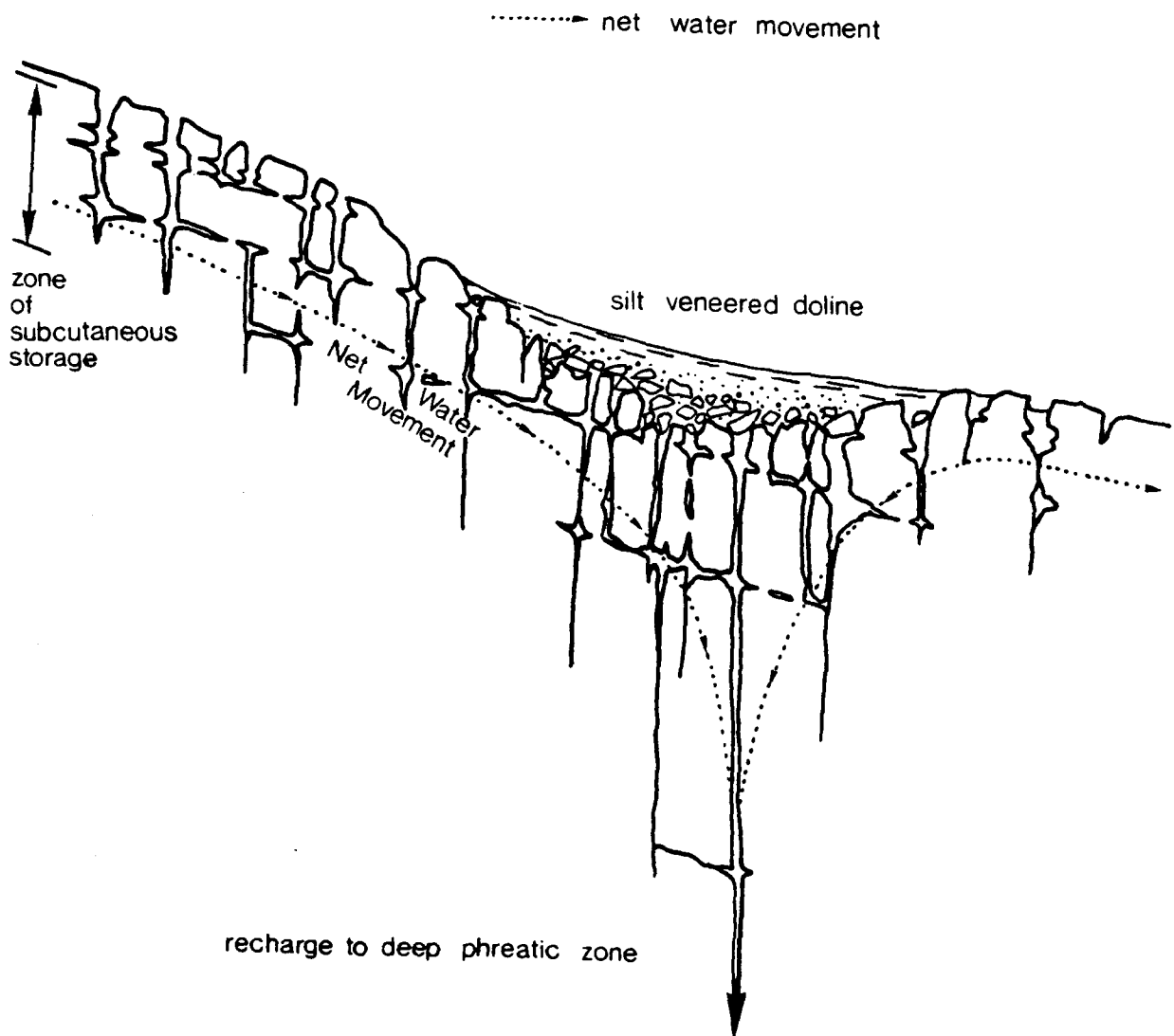
atmospheric pCO_2 from reaching equilibrium. Less obviously, the semi-arid conditions tend to generate thin clayey soils of low organic content which, compared to more mature soils, generate lower, albeit still substantial, CO_2 concentrations in solution. Overall the recharge at equilibrium with atmospheric CO_2 should yield only about 3 $mg.l^{-1}$ of dissolved CO_2 (calculated upon data from Roques, 1962 and Trombe, 1952) which results in a similar concentration of Ca^{2+}. Flushes of such composition may indeed occur during rapid deep infiltration, but comparison of such low concentrations with the average spring water chemistries of Table 4.1 shows that other concentrating processes predominate, namely (1) enhanced CO_2 solution with subsequent carbonate dissolution in the high pCO_2 humus-rich fraction of the "subcutaneous" zone, (2) oxidation processes and (3) evaporative concentration both at the surface and by capillary action.

Despite the aridity there is probably sufficient flora in the high altitude areas (Plate 1.1; Mandeville, 1978) to concentrate the near surface pCO_2 by between two and three orders of magnitude (eg. Bogli, 1980) and thus greatly increase the Ca^{2+} and HCO_3^- concentrations by the reactions:

$$CO_2 + H_2O \rightarrow H_2CO_3 \rightarrow H^+ + HCO_3^- \qquad \ldots\ldots (1)$$

concurrent with $CaCO_3 \rightarrow Ca^{2+} + CO_3^{2-}$ $\qquad \ldots\ldots (2)$

which combine to give $CaCO_3 + CO_2 + H_2O \rightarrow Ca^{2+} + 2\ HCO_3^-$ $\qquad \ldots\ldots (3)$

$$\text{dissolved limestone}$$
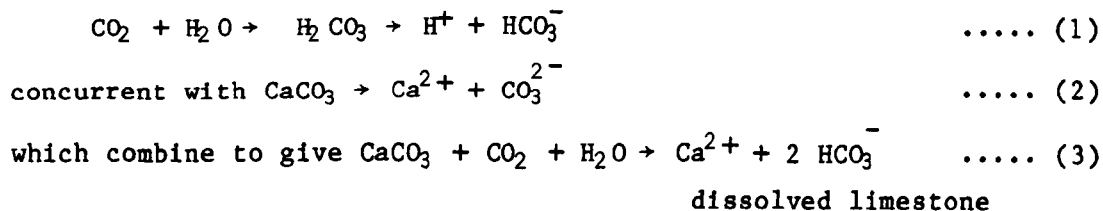
Less simple reactions may be proposed for Ca - Mg carbonates, but neither the aquifer compositions nor the composition of the dissolved salts correspond to pure calcite or dolomite, and complex "equilibrium" conditions result in apparently incongruous carbonate dissolution. This is illustrated by the mean Ca/Mg ratio of spring waters which is:

2.77 in the upper HSG, i.e. almost entirely limestones

2.48 in the intermediate HSG comprising mixed limestones and dolomite and

1.87 in the Lower HSG - dolomites with subordinate limestones.

An assumption of near equilibrium conditions in most spring waters is justified by a random selection of eight limestone spring hydrochemistries from Appendix C which was processed by the BGS "Wateq" computer program[1], and which indicated states of predominantly slight oversaturation with respect to quartz and the common carbonate minerals shown in Table 4.2. Nevertheless it is necessary to qualify the "near equilibrium" by observations of a small number of supersaturated springs which precipitate large quantities of aragonite (eg. Minabak and Misfah, appendix C Nos. 004 and 057 respectively), whilst all limestone springs are likely to be undersaturated with respect to all the carbonate minerals shortly after recharge, both for kinetic reasons, and due to the "mixing effect" of Bogli, 1980[2].

The lower of the Ca/Mg ratios given above is derived from the Saiq and Mahil formations, is significantly greater than unity and is higher than expected for dolomite (Langmuir, 1971) implying that the groundwater chemical compositions are determined primarily by the Saiq limestone rather than the overlying dolomite. This feature is consistent with (1) empirical speleological evidence, both from Oman and elsewhere, of preferred limestone dissolution in mixed limestone-dolomitic formations (eg. Rauch and White, 1970), and (2) with the experimental solubility data of Langmuir (eg. in UNESCO, 1984). The other Ca/Mg ratios of between two and three, are typical of springwaters from a Mesozoic Limestone sequence (Meisler and Becker, 1967) and are indicative of normal diagenetic processes of dissolution/reprecipitation, and especially of the phase transformation: High Mg calcite → Low Mg calcite. Occasional residues of high Mg calcite are found in all the main limestone formations of the HSG, but are more commonly associated with Palaeogene and later limestone formations. Strontium is similarly partitioned into the aqueous phase during diagenesis, as shown in Table 4.3, but its relation to the Ca concentration is strongly influenced by formation conditions (other than temperature) and hence neither the Mg or the Sr concentrations give a clear indication of the extent of primary carbonate dissolution.

---

[1] Courtesy of Dr A Bath of BGS - IoH Wallingford
[2] ie. Due to the non-linear relationship between dissolved CO_2 in equilibrium with dissociated $CaCO_3$ in solution, it is possible to mix two carbonate saturated solutions of differing composition to produce an undersaturated mixed solution.

Table 4.1 Summary of Hydrochemical Variation within the Hajar Super-Group Springs

(Computed from data in Appendix C)

Parameter	mean	std. dev.	skew	kurt	No. of samples	Significant correlations p < 0.001, coef. > 0.4
(A) Upper HSG Limestone Springs						
temp °C	36.9	5.6	0.35	− 0.27	26	Sr,SiO$_2$
Elec. Cond.	653	198	0.24	− 0.94	31	Mg,Na,K,Sr,SiO$_2$,SO$_4$,Cl,F
pH	8.0	0.5	0.61	− 0.34	31	−HCO$_3$
Ca^{2+}	69.1	17.3	0.02	− 0.95	31	
Mg^{2+}	24.9	6.8	− 0.80	0.99	31	EC,SO$_4$
Na$^+$	54.6	34.1	0.63	− 0.04	31	EC,K,Sr,SiO$_2$,SO$_4$,Cl,F
K$^+$	3.3	1.4	0.74	0.15	31	EC,Sr,Cl,F,I
Sr^{2+}	0.99	0.40	0.19	− 0.89	31	EC,Na,K,SiO$_2$,Cl,F
SiO$_2$	22.9	10.4	0.14	1.38	31	EC,Na,Sr,Cl,F
HCO$_3^-$	211	48.8	− 0.58	− 0.86	31	− pH
SO$_4^{2-}$	101	51.1	0.86	0.26	31	EC,Mg,Na,Cl
Cl$^-$	71.7	40.1	0.40	− 0.86	31	EC,Na,K,Sr,SiO$_2$,SO$_4$
F$^-$	0.52	0.42	2.46	8.14	31	Ec,Na,K,Sr,I
IO$_3^-$	0.021	0.014	− 0.44	1.94	5	EC,Na,K,Sr,I
total I	0.23	0.12	0.27	− 0.72	28	
NO$_3^-$	4.94	3.3	1.38	2.81	31	
(B) Lower HSG Springs; Mostly from Dolomite						
temp °C	26.1	3.9	0.77	2.19	12	K
Elec. Cond.	512	69	0.91	0.70	16	Mg
pH	8.3	0.5	0.03	− 0.41	16	− Ca, −HCO$_3$
Ca^{2+}	54.5	17.6	0.75	− 0.26	16	− pH, HCO$_3$
Mg^{2+}	29.1	6.8	− 0.05	0.44	16	EC, −Na, HCO$_3$
Na$^+$	21.3	7.7	1.15	0.36	16	−Mg
K$^+$	1.7	1.4	3.06	10.8	16	
Sr^{2+}	0.56	0.13	0.53	− 0.74	16	
SiO$_2$	11.1	4.3	− 0.37	4.17	15	
HCO$_3^-$	233	69	0.32	− 0.58	16	−pH, Ca, Mg
SO$_4^{2-}$	44.0	18.9	0.80	0.11	16	
Cl$^-$	35.7	16.2	1.53	2.47	16	
F$^-$	0.17	0.08	1.44	1.81	16	
total I	0.013	0.003	− 0.48	− 0.60	11	
NO$_3$	4.11	2.83	0.79	0.46	16	

Table 4.2 Limestone Spring Saturation Indices Log (IAP/KT)
with respect to the common carbonates and quartz

Saturation Indices

Location	No*	T°C	Aragonite	Calcite	Dolomite	Quartz
Fanjah	89	40	0.671	0.934	1.867	0.409
Al Bir	1	40	0.622	0.885	1.788	0.175
Al Hubi	2	33	0.082	0.342	0.761	0.386
Hayl Minabak	4	44	0.431	0.696	1.362	0.313
Nakhl	20	37	0.063	0.325	0.632	0.403
Hasanat	43	31	0.259	0.518	0.964	0.519
Al Ajal	46	41	− 0.135	0.104	− 0.258	1.410
Ghala	56	44	0.490	0.755	1.508	0.434

*   locates details in Appendix C

Table 4.3   Spring Water/Host Rock Mean Enrichment Factors
with respect to Ca.

Component	Limestones (Wasia/Kamah)	Dolomites (Mahil/Saiq)
Mg	27.9	1.77[1]
Sr	9.6	12.9
SiO_2	6.52	2.72
S[2]	484	256
Cl[3]	701	335

NB. Data based upon 46 HSG dolomites, 42 HSG Limestones, 31 spring
waters from limestone and 16 spring waters from dolomite.

(1) 1.12 if only Mahil, i.e. pure dolomite, is considered.

(2) Assuming SO_4^{2-} is the sole S species in solution.

(3) Lattice-bound Cl; ie. Carbonate analyses do not include
surface-bound Cl^-.

In Spring waters from the HSG there is an average ionic disparity between $(Ca^{2+} + Mg^{2+})$ meq and HCO_3^- meq of 1.51 to 1, which illustrates the importance of additional "non-carbonate" processes in generating the observed hydrochemistries. Excess sulphate is responsible for a large proportion of this chemical imbalance, cf. Table 4.1, and may originate in several different ways. The simplest mechanism of $CaSO_4$ dissolution is probably unimportant since, although ghost relicts after evaporites are common in some parts of the Mahil dolomites, gypsum and anhydrite are almost entirely absent from surface exposures in the HSG (in marked contrast to their abundance in the Palaeogene carbonates). Alternatively the presence of sulphide in the form of pyrite allows oxidation reactions such as:

$$2FeS_2 + 7O_2 + 5H_2O + 8\ CaCO_3 \rightarrow 2\ FeO.OH + 8H^+ + 4SO_4^{2-} \qquad ...(4)$$

which would result in: $2H^+ + CaCO_3 \rightarrow Ca^{2+}\ 2HCO_3^- \qquad ...(5)$

i.e. 4 and 5 combine as (6):

$$2FeS_2 + 7O_2 + 5\ H_2O + 8CaCO_3 \rightarrow 2FeO.OH + 8Ca^{2+} + 8HCO_3 + 4SO_4^{2-} \qquad ...(6)$$

pyrite   limestone geothite   solution
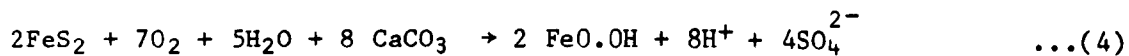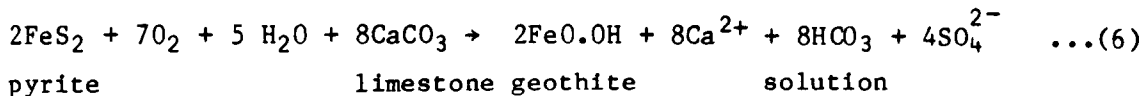
The required sulphide for the above and similar reactions occurs throughout the HSG limestones as finely disseminated pyrite at typical concentrations of 0.05 to 0.1%, or at higher concentrations in the more euxinic black carbonaceous mudstone facies. Indeed, oxidation would probably be concentrated in the latter pyrite-rich horizons, eg. giving rise to the goethite pseudomorphs which are commonly found in the basal Saiq limestones of Jebel Akhdar. In the reaction (6) above, the limiting factor is likely to be the availability of dissolved oxygen as much as the concentration of sulphide. At the elevated subsurface temperatures of the limestone massifs, the oxygen solubility is reduced to only about 6 mg 1^{-1} (Hem, 1970) and is equivalent to about 10 mg 1^{-1} of sulphate or only about 12% of the observed mean SO_4^{2-} concentration.

Furthermore a few limestone groundwaters evolve H_2S (eg. Wadi Mu Aydin borehole-Howsam, pers.comm.1980; falaj Al Qaryah) in which case the total concentration of sulphur species is higher than shown in Appendix C, and the proportion of sulphur derived from pyrite oxidation would be

correspondingly lower. The Wasia limestone formation is the source rock for both of the above $H_2 S$ rich groundwaters, and also happens to be the most "organic rich" of the HSG formations, as indicated by kerogen-rich acid-insoluble residue concentrations of commonly 2 to 3% and occasionally as much as 5%. This association reinforces a hypothesis of probable $H_2 S$ derivation by organic oxidation reactions in which dissolved oxygen is not involved, but in which sulphate is reduced, eg:

$$SO_4^{2-} + 2H^+ + 2CH_2 O \longrightarrow H_2 S + 2CO_2 + 2H_2 O \quad \cdots \quad (7)$$

"nominal organic fraction"

(after Stumm and Morgan, 1970)

with subsequent carbonate dissolution reactions as in (3).

Direct evidence of oxygen depletion in limestone spring waters is sparse but is supported by the composition of evolved gases at Rustaq and Taww, shown in Table 4.4, although a reverse process - i.e. oxygen liberation by thermophyllic algal photosynthesis - may have affected the original oxygen concentration in both cases.

Table 4.4   Evolved Gas Compositions from Limestone Springs

(mol %)

	Rustaq	Taww	(Air)
N_2	92.0	86.0	78.1
O_2	5.8	14.0	21.0
CO_2	2.20	-	0.03
$T^o C$	46	38	-

Very low chloride concentrations in the rock relative to the spring waters, indicated in Table 4.3, illustrates the trivial contribution to the chloride budget provided by carbonate dissolution, and hence the importance of evaporative concentration prior to aquifer recharge. Unfortunately the use of chloride (and Na^+) as a quantitative indication of evaporation is ambiguous (cf. chapter 3) and hampered further by its high variability: $Cl^-_{mean\ 1st\ spring\ water} = 76\ mg.l^{-1}$, $\sigma = 125\ mg.l^{-1}$. The significance of the more conservative ions in solution (mainly Na^+, K^+, Cl^- and SO_4^{2-}) is therefore only marginal insofar as they enhance the total ionic strengths of the limestone groundwaters to between 0.007 and 0.022, thereby increasing the calcite solubility by about 10 to 20%. However, their effect is more than counteracted by reduced calcite solubility under the prevailing high groundwater temperatures.

In addition to chemical considerations, studies of carbonates from other environments have demonstrated a strong correlation between karstic development and fine grain size, and especially the micritic content, irrespective of rock composition (Dreiss, 1984; Rauch and White, 1970). In the case of the HSG this should favour dissolution within the Sahtan porcellanites, and various lime mudstone units of the Wasia and Kahmah formations, but supporting evidence is lacking due to immature karst and inadequate speleological data.

Similarly, given the sparcity of subsurface data it is difficult to assess the extent of "deep" groundwater circulation, i.e. beneath the spring outflow levels. This is an important question from the point of view of water supply since deep karstic development is potentially the main hard-rock storage available for exploitation. The position of Hammam vauclusian spring in the piedmont alluvium of Rustaq is proof that deep groundwater can occur, but other considerations suggest that, elsewhere, it is poorly developed or absent. For example: (1) Deep drilling in many limestone piedmont areas e.g. the southern Akhdar has seldom located significant groundwater flow pathways; (2) Piedmont spring waters are of fairly consistent chemical composition and close to equilibrium with respect to the aquifer composition. Therefore at the outflow end of long

groundwater pathways, the chemical capacity for further (deep)
dissolution is greatly reduced. Alternatively maximum hydrochemical
aggression due to mixing and/or CO_2 influx occurs close to the main
source area, i.e. high in the aquifer; and (3) Over the time scale
involved in karstic processes, continued uplift of the Jebel Akhdar
would tend to "exhume" any deep groundwater pathways. Thus, if present
at all, deep groundwater pathways are probably restricted to
pre-existing fractures in coastal or near coastal carbonate aquifers
which would have been amenable to development during past marine
regression.

4.4 Chemical and Isotopic Indicators of Groundwater Provenance

Combined surface and groundwater flow traverses extensive limestone
exposures in two areas; Wadi Fida (Figure 4.5, Plate 4.6), and Wadi
Dayqah (Figure 4.7, Plate 4.7). In both cases the absence of rock bars
and the unknown saturated thickness of alluvium in the wadi bed prevents
the comparison of total flow measurements in upstream and downstream
sections. However, comparison of chemical (Cl^-) and isotopic results
from successive sampling sites allows changes in water composition to be
correlated, qualitatively, with changes in provenance. For example, if
water enters and leaves the limestone area with little or no change in
composition, then the wadi is either an effluent or laterally confined
groundwater system with no "bank drainage" contribution. On the other
hand, large changes in the chemical or isotopic profile must be caused
either by pollution such as irrigation return, or by influent conditions
(recharge from the limestones, i.e. of different provenance from the
input wadi water). Since intermittent turbulent flow in the wadi bed
facilitates rapid mixing, zones of significant recharge can therefore be
delineated to within intersampling distances. In order to avoid
possible wadi effluent conditions after rainfall, samples from both
wadis were taken towards the end of a recession period (December 1980),
i.e. when recharge to wadi alluvium from limestone storage was most
likely to occur.

The Western Piedmont

Groundwater entering Wadi Fida (point A figure 4.5; and Yanqul
falaj sample 162 appendix C) is derived from a 1300 km^2 combined
alluvial-ophiolite catchment of relatively low relief (less than 1000 m)

111

Figure 4.5

TERTIARY LIMESTONE ISOTOPE SAMPLING SITES
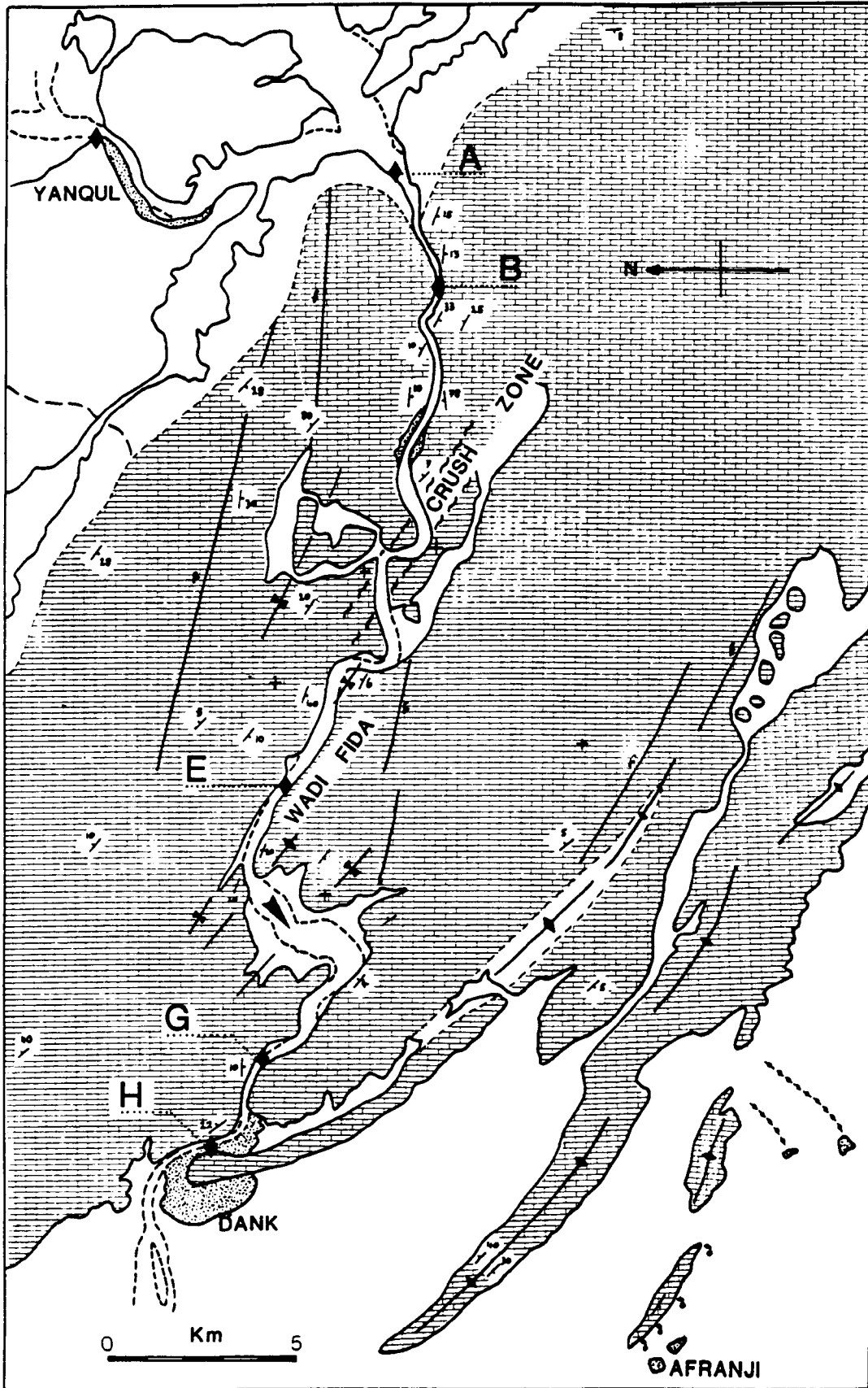
Figure 4.6

Wadi Fida : Isotopic and Chemical Profile
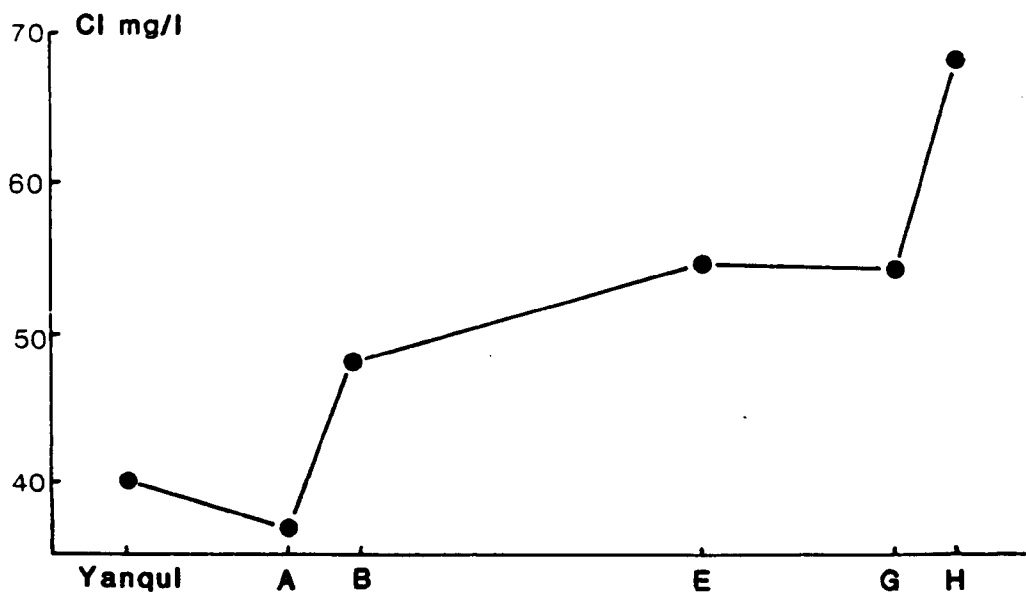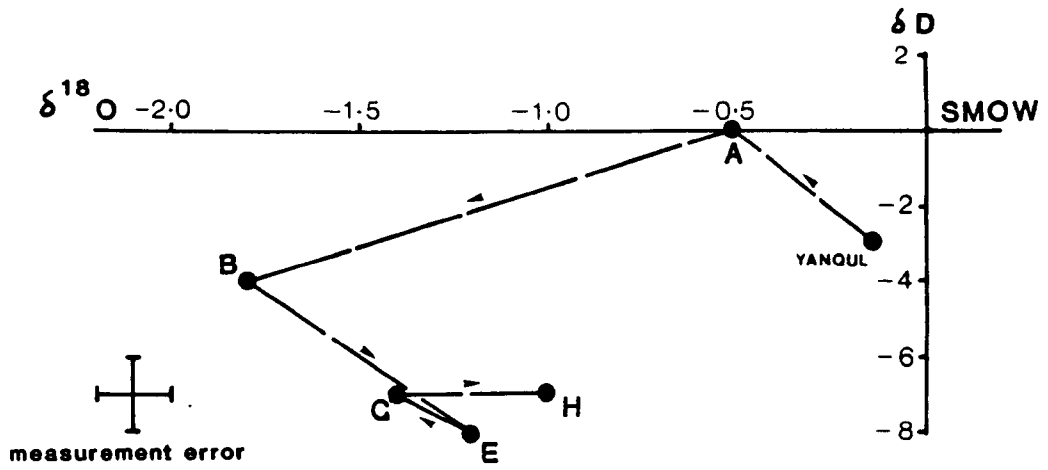
in which the baseflow of the order of several hundred litres/sec is largely brought to the surface between marly limestones of Late Palaeocene and/or Lower Eocene age[1]. In the upstream section, the discrepancy in both Cl^- and isotopic composition between Yanqul and point A (Figures 4.5 and 4.6) shows that a major groundwater input occurs from the east of the limestone as well as from the main fluvial channel of Wadi Yanqul. In the limestone section, large increases in Cl^- from A to B and from G to H coincide with the emergence of surface water, irrigation return, high evaporation rates and widespread transpiration from rushes, oleander, tamarisk etc. in the wadi bed. Otherwise the chloride content shows only a normal gradual increase in salinity with downstream position (points B to G). The isotopic variation of the same samples is less simple. Only the lowermost wadi section, G to H, is consistent with the normal evaporitic trend of large ^{18}O enrichment coupled with slight deuterium enrichment. The isotope shift A to B, the reverse of an evaporitic trend, occurs in the most upstream limestone area where recharge to the wadi is least likely, and is thus difficult to account for. However, the general pattern of deuterium depletion throughout the limestone section is incompatible with that of a single groundwater source flowing from points A to H, and indicates subsurface inflow to the wadi from an isotopically variable but strongly depleted (i.e. isotopically light) source from within the limestone. This is consistent with the known light isotopic composition of large scale rainstorms (cf. section 2.5) which recharge the limestones initially, either by direct infiltration, or by flash flood effluent conditions in the main wadi. The latter is exemplified by the intense storms of February and March 1976 which resulted in an estimated peak discharge at Dank of 1800 cumecs (Gemmell, 1979).

Surface exposures of the Palaeogene limestones revealed only minor karstic solution features, but faulting associated with folding and the crush zone of Figure 4.5 provides numerous potential groundwater pathways for flood recharge. Hence the chance similarity in chloride content between wadi and limestone waters appears to mask the presence of substantial groundwater storage in zones of highly fractured limestone.

---

[1] eg. Gemmell 1979, measured an apparent baseflow of 340 litres/sec. Visual comparison with the upstream surface input suggests a slightly lesser flow but the underflow at each site is indeterminate.

On the downstream side of the limestone hills lies an anomalous "spring line" of minor seepages, both near Ibri (Al Hajar, sample 406; Al Qali, sample 407 appendix C; Figure 4.5) and south of Dank (Afranji, sample 165; Falaj, sample 177, appendix C; Figure 4.5). There are three possible origins: water table seepage through the limestone from the large upstream alluvial catchments, deep circulation and emergence along a piedmont bounding fault, or local limestone dewatering. Although the Afranji area springs are slightly brackish, hydrochemical comparison of these sources with other normal Tertiary limestone groundwaters, Table 4.5, shows no significant anomalies such as might be associated with deep flowpaths and long residence times.

Table 4.5 Summary of Water Compositions from the Tertiary Limestone

I	Ca^{2+}	Mg^{2+}	Na+	K^+	Sr^{2+}	SiO_2	CO^{2-}	HCO_3^-	SO_4^-	Cl^-
134	169	99	628	14.2	3.7		0	295	394	890
165	98	45	190	7.2	2.1	33.3	0	224	235	271
177	82	44	188	7.4	3.0	25.1	0	254	210	272
181	30	49	61	4.4	1.0	26.7	6	261	97	84
218	42	41	117	5.8	1.4		0	276	143	155
385	62	19	320	1.5	2.2	13.2	0	122	65	33
386	67	25	49	2.6	1.8		0	224	93	91
388	47	23	29	1.7	2.8		0	163	78	31
389	65	32	50	1.8	3.5	14.7	0	183	94	69
390	68	16	15	1.6	1.8		0	181	63	36
398	52	24	59	2.8	2.3	16.0	0	173	82	97
401	46	24	26	1.9	1.2	14.0	0	167	51	38
406	27	47	55	3.7	1.0	24.2	0	224	68	80
407	31	48	71	3.7	1.1	24.8	0	236	66	92

[N.B. 'I' locates source details in appendix C]

On the contrary, the tritium values of 25.8 and 16.4 for Al Qali and Afranji respectively (Appendix B) are those of recent meteoric origin. Furthermore, the low spring temperatures are inconsistent with a deep fault

guided flowpath. Both the low spring discharges (invariably less than 5 litres/sec) and the elimination of distant provenance therefore implies dewatering from local hard-rock storage. The springs and seepages are located adjacent to the south-western edge of the limestones where anticlinal folding is most intense and where longitudinal fracturing would optimise recharge. Subsequent to recharge the slow limestone dewatering is probably caused by flow attenuation against the relatively impervious marly outwash sediments which are characteristic of most of the south-western piedmont areas.

Piedmont folding of similar structural style but on a much larger scale (both in amplitude and wavelength) occurs further north in the Buraimi area; eg. Jebel Haffit, Jebel Huwayyah. However, as there are no comparable springs in this area, limestone recharge and storage seem to be insignificant, though whether this results from less severe fracturing, interfolding of marl aquicludes, or some other factor is not known.

Wadi Dayqah

Apart from a small alluvial fan at the coast, groundwater in Wadi Dayqah is laterally bounded within a 42 km gorge through the south-western Sharqiyah massif. This gorge is divided into upper and lower sections by a low relief area at Mazara which is underlain by impervious quartzite. Otherwise the gorge is entirely cut into limestones of both folded para-autochthonous "Hajar Super Group" and relatively undisturbed Tertiary formations (Figures 4.7 and 4.8). Folding in the massif is irregular and more complex than in most other sections of the Hajar limestone, and approximates to an anticlinorium with an overall north-easterly dip. Secondary matrix porosity, due to shrinkage by dolomitisation, is locally well-developed but karstic solution features appear to have developed only along prominent bedding planes and bedding/fracture intersections in the massive limestones.

Surface flow is typically about 250 litres/sec and is almost continuous throughout the Hajar Super Group and quartzite exposure. However, as the alluvium is at least 20 m deep in places, and composed of coarse rounded and generally uncemented gravel, the underflow is probably much greater than the surface flow. In the narrower sections of the upper gorge, "cliff to cliff" surface flow is sometimes less than 10 metres wide, with a steep average wadi gradient of 0.008 as opposed to less than 0.002 in the lower gorge. Consequently the upper streamflow is rapid with a probable throughflow time

Figure 4·7

WADI DAYQAH ISOTOPE SAMPLING SITES

GULF OF OMAN

X
HAYL AL GHAF

ABAYAH

L
N

AL MISFAH

P

MAZARA

W

I

J

H

F

E

B

A

TUL

CULTIVATED AREAS
TERTIARY LIMESTONE
HAJAR LIMESTONE
AMDEH QUARTZITE

0   Km   5
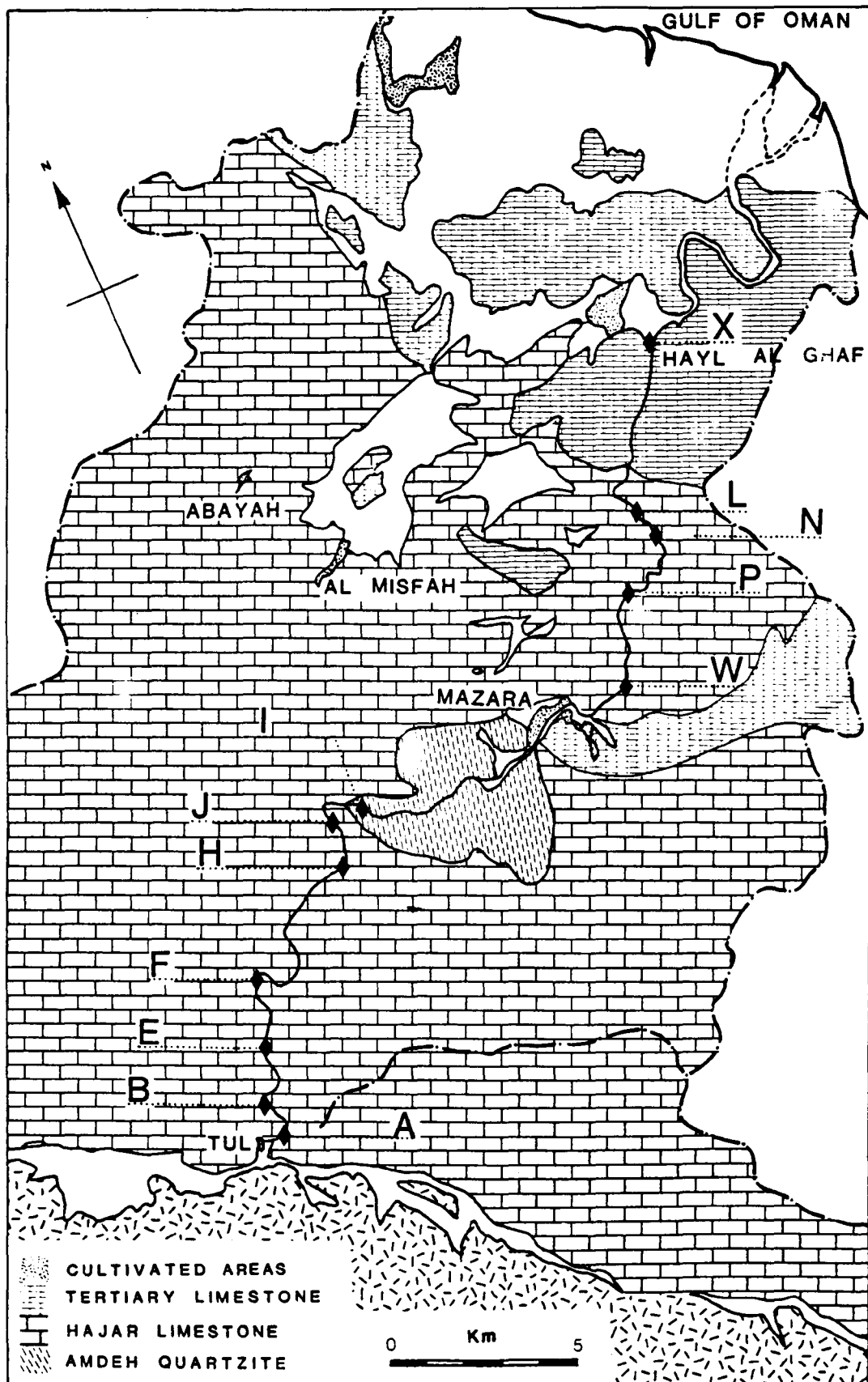
Figure 4·8

WADI DAYQAH
ISOTOPIC (A),HYDROCHEMICAL (B),and GEOLOGICAL SECTION (C)

A

δ D (vertical axis, values 0, 2, 4, 6, 8, 10)

Points: A, P, N, X, F, H, I, W, E, J, L, B

δ ^{18}O (horizontal axis, values 1·0, 1·5, 2·0, 2·5, 3·0, 3·5)

B

Cl mg/l (vertical axis, values 55, 60, 65, 70, 75)

salinity increase at Mazara
due to irrigation return

dilution
by
recharge

A   B   E   F   H   J   I   W   P   N   L   X

Isotopic indications of recharge

C

Hajar
Super
Group

Tertiary

Tertiary

X

Quartzite

SW-NE Section of Wadi Dayqah
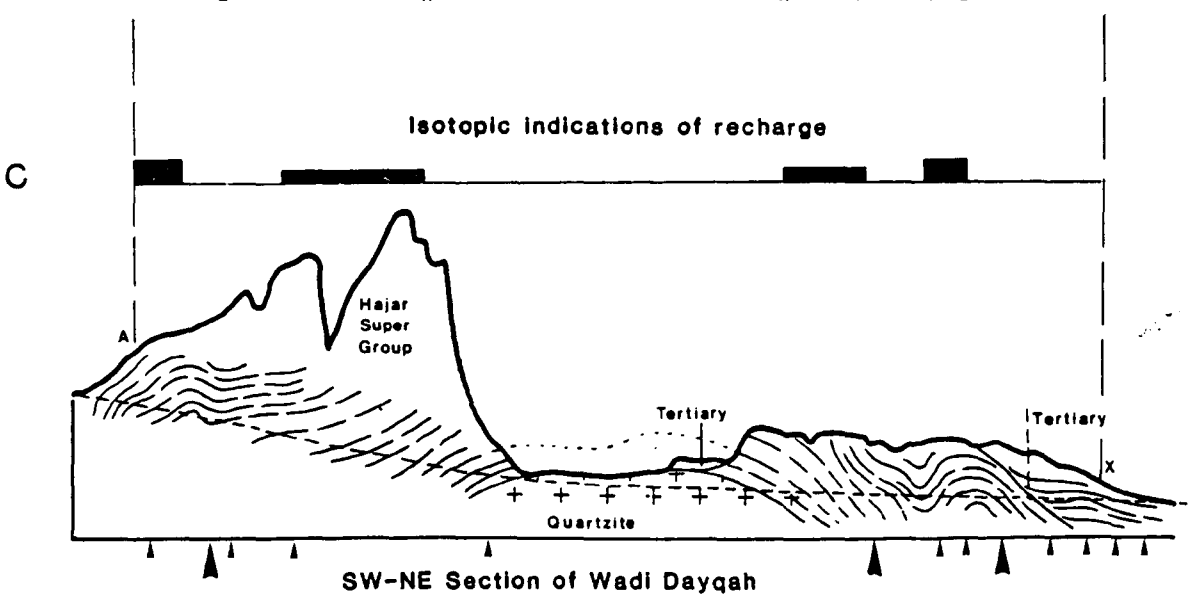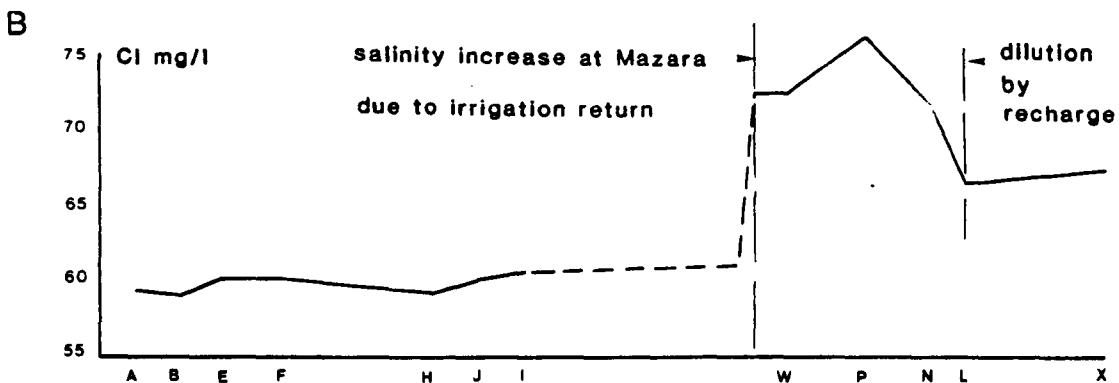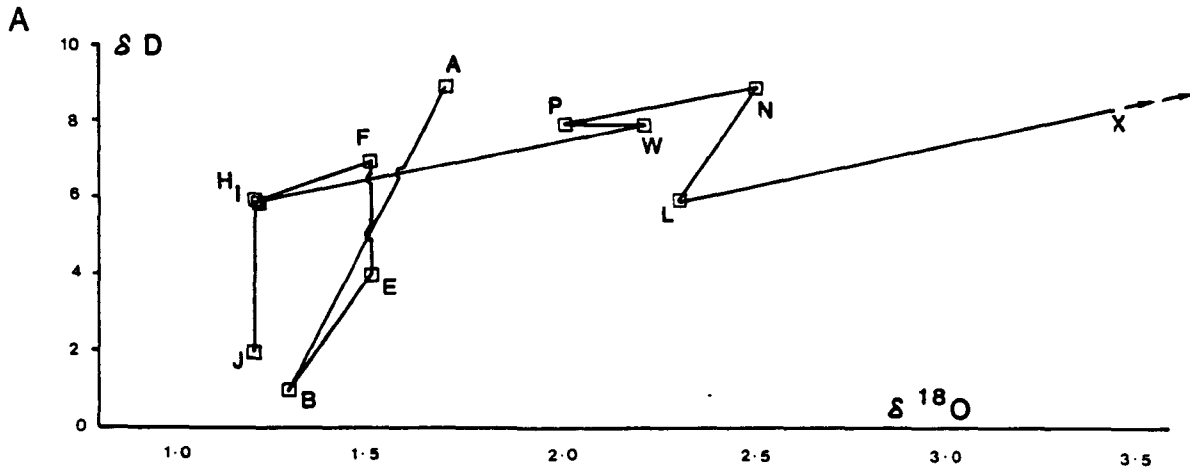
arrows indicate major and minor subkarstic development

horizontal-vertical structure 1:1   relief outline schematic only

of less than a day. North of the Mazara inlier, the relief is less extreme, the gradient is reduced and, in the exposed Tertiary section, surface flow is absent.

The Ca/Mg content of groundwater entering the upper gorge at Tul is 0.40. Comparison of this figure with similar ratios for average ophiolite gravel waters and for average limestone waters, of 0.31 (standard deviation 0.2) and 2.74 (standard deviation 0.98) respectively*, illustrates the former source as the main input to Wadi Dayqah during long recessions.

There is little hydrochemical change in the upper gorge. For example, the Ca/Mg ratio increases only slightly from 0.40 to 0.48 (samples 333 and 334, appendix C) whilst chloride varies even less from 59.5 to 60.7 mg/litre (Figure 4.8), thus suggesting minimal recharge to the wadi from the highest part of the massif.

A substantial contrast in altitude exists between the upper ophiolite catchment, 300 to 1000 metres, and the limestone massif, 1000 to 1900 metres, into which the upper Wadi Dayqah is incised. Consequently the isotope-altitude/temperature relationship (cf. Section 2.5) ensures differential isotopic composition between the two potential groundwater sources, ie. rainfall-infiltration into the high relief limestone will be colder and hence of lighter isotopic composition. As in Wadi Fida, the isotopic profile of the upper wadi, shown in Figure 4.8a, apparently conflicts with a simple model of invariant hydrochemistry. The anomalous isotopic vectors AB to JI do not follow an evaporative trend, and are too large to be explained either by sampling or analytical errors. Such large isotopic variations in conjunction with the small chemical variation can therefore only be reconciled by minor dilution with limestone groundwater of very much lighter isotopic composition than the wadi water. The required isotopic contrast between these two water types is consistent with the results shown in Figure 2.16, Section 2.5.

In the central and lower wadi course the isotopes conform to more normal trends in which the chemical and isotopic data is in obvious accordance. Vectors I to W, P to N and L to X in Figure 4.8a are characteristic of

---

* Derived from Tables 4.1 and 5.2b.

high rates of evaporation, the magnitudes being roughly proportional to the respective lengths of surface flow. Reverse isotopic shifts such as NL, and to a lesser extent possibly WP, must be caused by dilution by limestone water. The chloride data shows only two significant changes corresponding to irrigation return from the village of Mazara, and to dilution of wadi water by dewatering of the Hajar limestones between Mazara and Hayl Al Ghaf, mainly between sampling points N and L; Figures 4.7 and 4.8b. Further westwards, along strike from the downstream Hajar limestone area, limestone spring sources in adjacent catchments are found to be of broadly similar chloride concentrations, eg:

Al Misfah,   sample 267;   31 mg/litre Cl^-

Abayah   ,   sample 269;   36 mg/litre

Siya   ,   sample 446;   32 mg/litre

By assuming that limestone recharge to Wadi Dayqah is likely to be of similar chloride content, eg. 33 mg/litre, the data in Figure 4.8b can be used to compile a chloride mass balance equation from which the extent of inflow is found to be about 30% of the upstream wadi flow. However, this estimate is derived after about 2 years of predominantly dry conditions (with occasional minor recharge events). Therefore, in view of the relatively short recession constant of typical limestone grounwater sources (cf. Section 6.3) a limestone recharge estimate in excess of 50% of the total flow would probably be more appropriate to shorter recession periods.

4.5   Occurrence and Origin of Thermal Springs

Groundwater temperature variation

Normally, groundwater temperature is related to the air temperature of the originating precipitation and is generally approximated, in temperate latitudes, as mean annual air temperature + 2 ± 0.5°C at between 10 and 20 m depth (Collins, 1925), below which the temperature conforms to the local geothermal gradient (Todd, 1959). Whilst this "rule of thumb" is not entirely applicable to the Oman environment, it illustrates the essentially conservative nature of the thermal groundwater régime which results from the insulating effect of the unsaturated zone on the water table. In general therefore, spatial and temporal variations are attenuated with increasing

depth to the water table. The scale and amplitude of the spatial variation
may be judged empirically for an area of normal groundwater temperature on
the Batinah coast where the inverse depth-variation (σ) relationship,
measured in 317 tightly clustered wells in the Central Seeb fan coastal belt,
is summarised in table 4.6.

Table 4.6 Depth-temperature variation during November
for a 10 km^2 coastal area

(Coastal November mean air temperature = 22.9°C,
Mean annual air temp = 26.6°C)

depth to water table	mean groundwater temperature ($^\circ$C)	std. devn.,($^\circ$C)	sample (n)
0-2	27.5	2.16	8
2-4	28.6	1.78	112
4-6	28.6	2.14	113
6-8	29.3	1.76	70
8-10	30.5	0.74	14

The temperature increase with depth in this table is a complex function
of (1) evaporative cooling of irrigation return in the seaward (shallower)
water table, (2) the effects of the winter air temperatures, and (3) complex
flow in a heterogeneous aquifer (cf. section 6.4). Nevertheless, the
underlying trend shows that spatial variation is $\pm$ 1.0°C at depths of
10 m.

With increasing depth, the seasonal variations in temperature consist
of:

(1) an amplitude attenuation expressed as $Px = Po\ e^{-X} \sqrt{\dfrac{\pi}{k_t\ r}}$

where Po   is the amplitude of the ambient air temperature
fluctuation,

    Px   is the amplitude of the groundwater air temperature
fluctuation,

     r   is the length of the fluctuating period,

and k_t is the thermal conductivity of the aquifer. (Ogil'vi, 1932).

Table 4.7 Annual Temperature Variation of Selected Groundwaters (°C)

Alluvial Aflaj measured at source	Sept	Oct	Nov	Dec	Jan	Feb	Mar	Apr	Jun	Jul	Aug	Sep	Ann Range	
Semail SI	33.0	–	33.9	33.3	33.3	32.8	33.7	34.0	–	33.4	33.8	33.2	1.2	
Rustaq Maaza	32.2	31.4	31.7	32.0	31.6	31.8	32.0	31.8	–	32.0	32.0	31.6	0.8	foothills
Izki Melki	30.2	29.5	29.6	28.9	28.2	28.9	29.1	29.5	–	30.6	30.3	30.8	2.6	
Nizwa Dariz	32.0	32.0	32.0	31.5	31.3	32.0	32.8	32.2	–	32.3	32.0	32.3	1.5	
Bisyah	31.5	31.5	31.8	31.4	31.3	31.3	33.7	31.9	–	32.0	31.6	31.4	2.4	
Adam Al Ayn	34.0	34.0	34.0	33.8	33.8	33.7	33.8	34.0	–	33.5	33.6	33.6	0.5	Interior Plain
Adam Malah	33.2	33.2	33.0	33.0	33.0	33.0	33.8	33.2	–	33.4	33.0	33.0	0.8	
Bosher Main	38.5	38.1	37.1	37.3	36.8	36.8	36.5	37.8	38.0	38.0	37.7	37.8	2.0	
Nakhl	38.0	33.5	35.0	34.1	32.8	34.3	35.5	–	37.4	–	–	–	5.2*	Limestone Springs
Rustaq Hamman	45.0	44.8	45.0	44.5	44.8	44.4	45.0	45.8	–	45.3	44.9	44.0	1.8	

NB Many of these fluctuations are influenced more by recharge than by air temperature

*   This is associated with an inverse relationship between falaj discharge and temperature i.e. mixing of intermittent cold water with a base flow of thermal water.

122

and (2), a phase shift between air and groundwater extreme annual
temperatures.

In practice this phase shift is not discernible at depths of less than
about three metres, but is typically about two months at depths of 10-12 m
and up to six months at a depth of 25 metres (Konoplyantser, 1963) which is
consistent with data from alluvial sources in Table 4.7. All of the sources
in this table originate at depths of 10 m or more and typically vary by $<2^\circ$C
throughout the year. Median peak temperatures occur in September though
comparable maxima of up to $+5^\circ$C also occur sporadically throughout the year
following recharge.

Substantially greater annual temperature variations are associated with
perennial surface waters subject to continuous evaporative cooling (eg. δT
$^\circ$C = 14 at Al Khod in Wadi Semail; 11 at Hawqayn in Wadi Hawqayn; and 15 at
Labijah in Wadi Bani Kharus). This in turn produces anomalous temperature
fluctuations in downstream recharge areas. In general however the
temperature data of Appendix C indicates a relatively consistent "normal"
range of between 30 and 33°C.

Thermal springs

One of the striking features of groundwater in the Oman mountains is the
occurrence of numerous low altitude limestone springs which range in
temperature from about 33 to 62°C. At the lower end of this temperature
range a problem arises as to what constitutes a thermal spring. For example,
a shallow well water temperature of 36°C in summer at low altitude in low
albedo serpentinite gravel is quite normal, whilst the same temperature
occurring from emergent limestone spring water at medium altitude could not
be explained without some "extra-insolative" warming process. There is no
generally accepted definition of a thermal spring, though Waring (1965)
considered that "in tropical areas some springs that are only a few degrees
warmer than the (mean annual) air temperature may be considered thermal".
This view is inapplicable in the hot arid conditions of Oman since the
"steady state" groundwater temperature may be approximated as mean annual air
temperature $+ 5.5 \pm 2.5^\circ$C; an expression derived from 150 isolated pumped
well and alluvial falaj temperatures (measured at source) typical of the
foothill and interior areas (cf. Appendix C13):

	mean temperature $^\circ$C	σ $^\circ$C
groundwater	32.3	2.3
air	26.6	1.3

In the present context, thermal springs are therefore regarded as those whose median temperature $>$ mean annual mean annual air temperature + 8°C, which, in terms of the limestone piedmont areas, is effectively equivalent to springs in excess of 35 to 37°C. Other thermal anomalies are associated with fault zones in the ophiolites and are therefore discussed in chapter 5.

Non ophiolite thermal anomalies are shown in relation to the autochthonous limestone in figure 4.9 from which two features are immediately apparent. Firstly, the spring distribution is unrelated either to catchment area or aquifer volume. The great massif of the southern Jebel Akhdar for instance has a single thermal anomaly of only marginally higher than normal temperature (Al Qalah falaj - northern branch) whilst the minor catchments of the Jebel Bosher area have a disproportionately large number of springs over a wide range of temperatures. Secondly, without exception all the springs occur at the outer edge of major anticlinal structures. Furthermore, there is a close correlation between hot spring occurrence and steeply dipping limestone with a history of reactivated tectonic disturbance during the mid-Tertiary (cf. maps 1 and 2). This distribution is not simply physiographic in origin as numerous other springs within the Jebel Akhdar inliers include comparable low altitude examples of exclusively lower than average temperatures, ie. the origin of thermal springs is at least partially controlled by structure.

In addition to spring chambers in the limestone itself, many springs are emergent from the bounding (and now steeply dipping) "basal thrust fault"; a zone of up to 300 m wide composed of sheared serpentinite, Hawasina sediments and metasediments downfaulted against crumpled autochthon, all of which is commonly eroded and concealed beneath a fluvial sedimentary or occasionally travertine/calcrete cover. Irrespective of the final spring chamber lithology, the groundwater pathways have invariably developed within

Figure 4.9

Temperature (°C) and Distribution of Thermal Springs
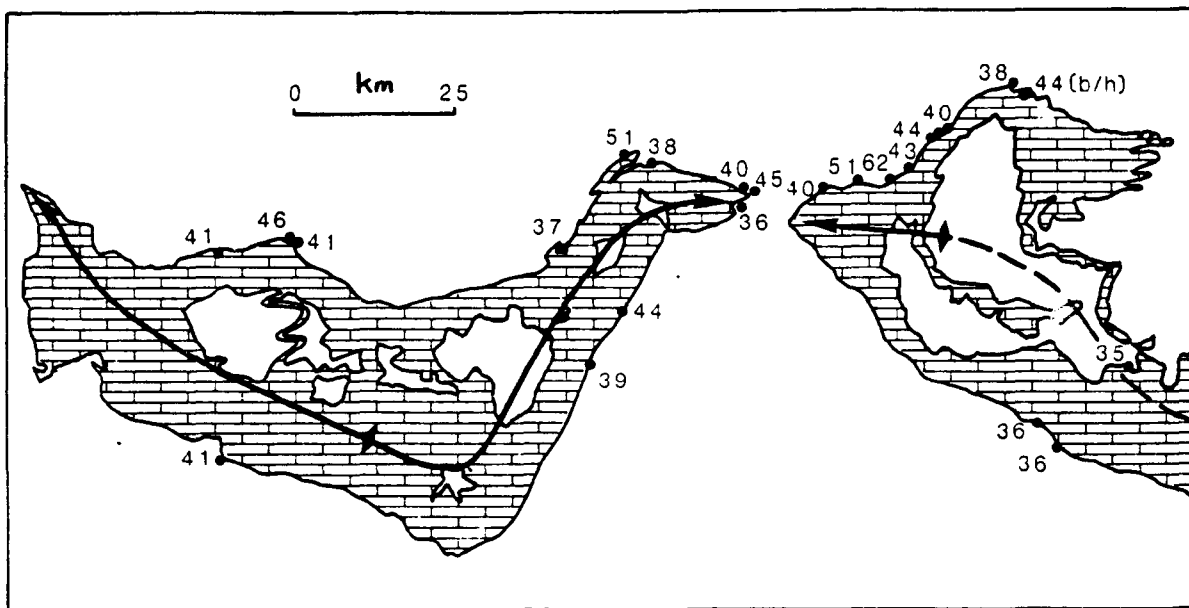
NB Thermal springs also occur at Al Khatt in the S.W.Ruus al Jibal

tectonically disturbed autochthon in which high level irregular or box folding, cataclasis, occasional imbrication and Fe ± Si enrichment are widespread. The thermal groundwater pathways are therefore determined, in part, by reactivation of the lowest nappe thrust zone against the HSG limestone during uplift with consequent shedding of the nappe sequence into marginal monoclinal troughs. However equally important factors in determining spring positions are the fault guided flowpaths within the autochthon itself (cf. section 4.2).

The distribution of hot springs along an obvious fault system raises the possibility of seismicity as the fluid diffusion process. Sibson, Moore and Rankin (1975) discuss such a mechanism in which high level seismic events of moderate to large magnitude (M5 to M7) are held to account for such features as the elevated temperature due to geothermal heating of deep connate water, fault zone mineralisation by high temperature solutions, and spring discharges of the order of 10^{10} litres/year. Superficially this is consistent with the long residence times of many thermal spring-waters as indicated by the absence of tritium (appendix B1), the stable spring discharge of the Bosher spring line, which amounts to about 0.4×10^{10} litres/year, and sporadic fossil evidence of silicification (Stanger, 1985) and iron (hydrothermal?) replacement along the fault zone. However such a model implies very recent or episodic fault activity coupled with an exponentially recessive spring discharge and declining water temperatures, features which conflict with both the seismic and historic record. The former, summarised in figure 4.10 (B.G.S Global Seismology Unit, unpublished data), shows remarkable tectonic quiescence throughout almost the whole of Northern Oman since records began in 1900.

Historical evidence of spring temperature stability and distribution is provided by a few early travellers in the Gulf region such as Miles (1901) who described the hot springs at Nakhl as one main and 20 minor springs with a temperature range of 39 to 4P C which compares with the same number of contemporary springs at between 33 and 3P C. Stiffe (1860) made observations at Bosher and Ghalla of a large spring at 38° C and four small springs of which the hottest was 46° C, the other three ranging from 42 to 4P C. From the site descriptions, both spring discharges and temperatures are similar to those of present day conditions. In particular the temperature of the main spring at Bosher still averages 38° C (Table 4.8) whilst the other springs of the Bosher-Ghallah area currently vary between 40 and 44° C. Finally, the oldest comparison is facilitated by Fraser (1824) who refers to spring

Figure **4.10**

Summary of Seismic Activity in the Region of Oman

Km
0   100   200

EPICENTRE -
MAGNITUDES
< 5   ·
5 - 5·5   ●
5·5 - 6   ●
6 - 7   ●
> 7   ●

Based upon
B.G.S. Data (1900 - 1982 unpublished)
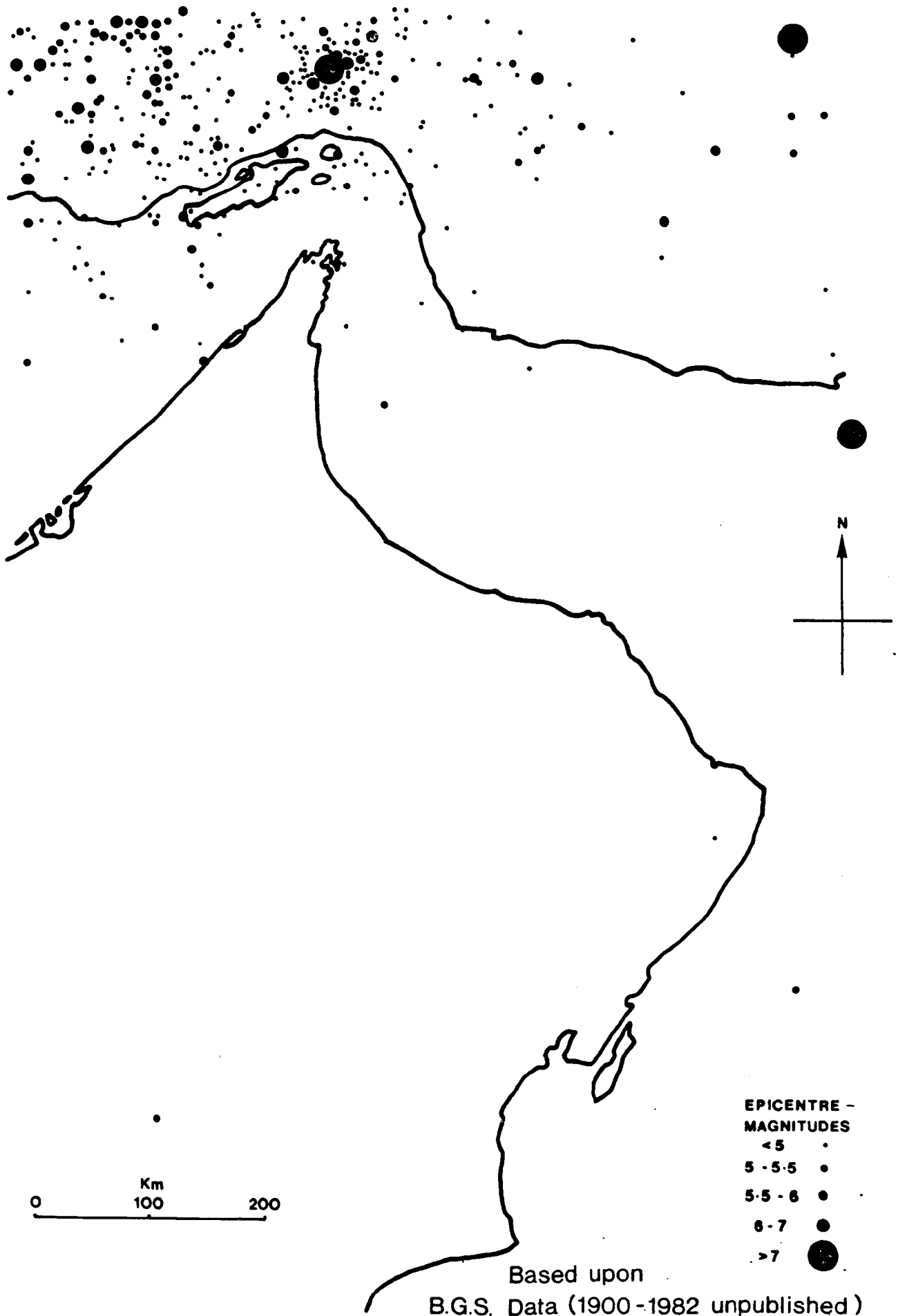
waters at 44°C issuing from red limestone "south of the bay of Muscat". Although the location is imprecise, the reference to red limestone narrows the alternatives to either "Falaj" near Bosher village or, more probably, Sunub whose current temperatures are 40°C and 43°C respectively (Table 4.). Thus within a degree or two ie. within the annual temperature variation and measurement error, the spring temperatures have been stable for over 150 years, and may therefore be taken to indicate permanent equilibrium thermal conditions.

Only two estimates of the thermal gradient are currently available from the Oman mountains. The first is a low value of 1.4°C/100 m from a PDO borehole; "Hamrat ad Duru 1" (P.D.O. Pers.Comm., 1982), which is sited some 40 km south-west of the mountain axis and hence is probably atypical of the thermal spring environment. The second, from a borehole in cemented Neogene sediments of the Eastern Batinah Plain, is 2.3°C/100 m (probably a slightly non-equilibrium value), and is also slightly less than average; i.e. certainly not indicative of an abnormally high heat flow. Furthermore, there is no evidence of residual heat of either magmatic or tectonic origin from the base of the nappe sequence. On the contrary metamorphic grades in the basal thrust zone are generally low to medium temperature facies and of very thin extent. Finally, investigations of Si-Mn-Fe-Ni-As mineralisation associated with the thrust zone are indicative of low temperature paragenesis (Stanger 1985; Stanger and Neal, in preparation). Ultimately, therefore, the heat source appears to be normal upward thermal diffusion from radioactive decay in the lower crust. Consequently, a mechanism for heat concentration is required to account for the thermal springs.

A plausible, albeit speculative, heat flow model is based upon the observation that the largest thermal anomalies lie in locally highly asymmetric structures in which the Hajar Super Group dips steeply beneath a thick mantle sequence cover. This cover has a relatively low bulk thermal conductivity and hence acts as an insulating wedge against which isotherms are refracted through highly conductive "saturated" carbonates (Figure 4.11). Further refractive focussing of the isotherms may also be effected by differential thermal conductivity between the "HSG" and the underlying impervious metasediments.

Figure 4.11

Schematic Effects of Thermal Refraction

HIGHLY CONDUCTIVE HAJAR
SUPER GROUP

LOW
THERMAL
CONDUCTIVITY
MANTLE
SEQUENCE

METASEDIMENTS

HOT
SPRING

INCREASING ISOTHERMS
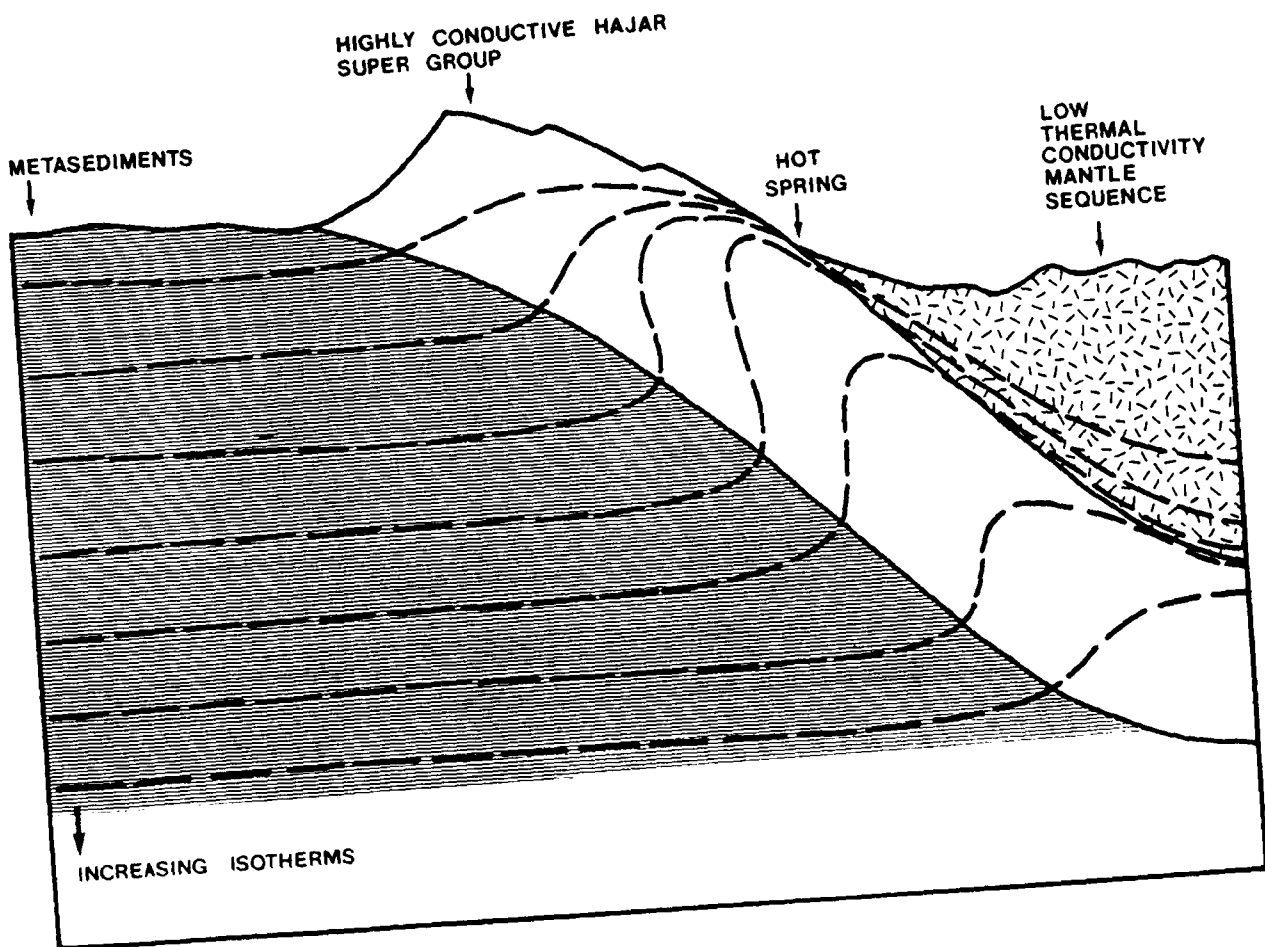
An important feature of this thermal distribution is the very
localised heating of meteoric groundwater circulation close to the
spring outflow points. Some support for this model is supplied by the
detailed time series of spring discharge, salinity and temperatures
given in Gibb et. al. 1976, Appendix 5; Aflaj. These data indicate
that after rainfall, a short term increase in discharge and decrease in
salinity occurs, as is consistent with expected short-circuiting of the
base flow groundwater pathway. However, an equivalent decrease in
temperature due to "cold" recharge does not occur, thereby implying that
groundwater heating occurs close to the spring chamber.

A second consistent line of evidence concerns stable isotopes of
the thermal spring water. Due to the higher altitude and hence colder
recharge in the limestone areas, limestone groundwaters are relatively
depleted in $\delta^{18}O$ and deuterium, but otherwise clearly follow the same
meteoric rainfall trend as other groundwaters in Oman, cf Appendix B1,
and hence appear to be of near surface circulation. The alternative
hypothesis, of deep groundwater circulation into an active hydrothermal
system, would have been expected to produce a substantial $\delta^{18}O$
enrichment by thermally controlled rock-water isotopic exchange, e.g. as
in Lardarello, Italy, Icelandic Geysers, Yellowstone Park, Orakeikorako,
New Zealand etc. (Fritz and Fontes, 1980; Sheppard and Lyon, 1984).
Similarly major and minor element hydrochemistry of the thermal springs
is entirely normal for limestone groundwaters and shows neither evidence
of water-rock interaction at elevated temperatures, nor any good
correlation between major element chemistry and temperature (Table 4.8).

Throughout most areas of spring occurrence, the tritium (^{3}H) values
are about average for recent meteoric groundwater circulation but, as
discussed in section 4.2, the low tritium content of the Bosher spring
line indicates an unusually long groundwater flowpath apparently
eastwards from the Jebel Tayyin massif. In view of this complex
hydrogeological régime and its efficient means of heat scavenging and
redistribution within the aquifer (including the hottest spring of 62°C
at Hamman al Ali), a satisfactory geothermal analysis awaits more
complete data upon the three-dimensional temperature and groundwater
distribution.

Table 4.8

Limestone Hydrochemical-Temperature Relationships

A)   VARIATION OF LIMESTONE SPRING TEMPERATURES WITH MAJOR ELEMENT COMPOSITIONS

No	T	Ca	Mg	Na	K	Sr	SiO	CO	HCO	SO	Cl
484	61	120	29	133	6.9	–	41.0	0.0	216	260	192
57	50	85	29	90	3.8	1.2	38.5	0.0	225	197	110
86	46	57	23	87	5.5	1.7	29.5	0.0	220	160	156
98	44	110	57	555	20.5	1.5	–	0.0	183	244	920
56	44	94	37	99	4.4	1.4	30.8	0.0	242	184	120
4	44	54	20	46	3.5	0.8	23.5	0.0	185	49	77
484	43	89	28	110	5.4	–	28.0	0.0	852	163	162
309	41	77	23	100	4.7	1.4	25.5	0.0	153	93	70
209	41	104	16	70	6.3	1.7	44.3	0.0	247	125	85
87	41	67	26	65	4.3	1.5	26.1	0.0	222	70	100
5	41	75	23	16	3.7	0.6	19.4	0.0	237	92	31
89	40	68	28	49	2.6	1.1	25.9	0.0	251	87	65
90	38	56	27	22	2.3	0.8	17.5	0.0	251	60	48
55	38	84	32	75	4.4	1.4	27.3	0.0	237	146	120
485	38	102	48	525	25.0	–	22.0	0.0	156	180	32
13	37	64	28	16	1.9	0.6	21.9	0.0	254	149	32
266	37	95	40	479	14.4	4.0	22.6	0.0	132	207	594
53	37	42	34	69	3.7	1.1	26.1	0.0	271	85	90
20	37	81	32	57	4.0	1.1	22.7	0.0	253	77	91
14	37	57	29	14	2.1	0.7	18.3	0.0	234	140	35
329	36	42	18	51	1.6	0.7	15.8	0.0	120	85	45
251	36	71	29	146	3.0	1.7	33.4	0.0	200	237	154
102	35	80	26	100	3.3	0.9	28.4	0.0	250	127	119

N.B. 1) 'No' locates source details in appendix C
      2) List includes borehole sample (98) from Wadi Aday

B)   CORRELATIONS (> 0.35) WITH TEMPERATURE FOR 43 HSG SPRINGS

parameter	correlation coefficient	Significance ("p" level)
pH	– 0.405	0.004
EC	0.454	0.001
Ca*	0.360	0.009
Na	0.472	0.001
K	0.531	0.000
Sr	0.707	0.000
SiO_2	0.625	0.000
SO_4	0.573	0.000
Cl	0.389	0.000
F	0.519	0.003
I	0.443	0.003

*   0.480, p = 0.003, n = 23 for "thermal" springs only.

131

4.6   The Musandam Massif

Geology

The most immediately striking feature of the Musandam Peninsula is its high relief (maximum 2087 m in Jebel Harim, Figure 4.16) and intensely dissected physiography in which wadis are fjord-like with cliff heights often exceeding 500 m and sometimes exceeding 1000 m. The massif is superficially comparable to the Jebel Akhdar insofar as it is predominantly composed of a very thick (3000 + metres) grey-weathering carbonate succession, more or less contemporaneous with the Akhdar H.S.G. On the other hand, important differences in structure, base level of erosion and the alluvial-hard rock relationships combine to produce hydrogeological conditions that contrast markedly with other limestone areas of the Oman mountains.

The regional stratigraphy, initially outlined by Hudson et al. 1954, and Hudson, 1960, and subsequently extended by Ricateau and Riché, 1980, is summarised in Figure 4.12. The original base of the sequence is not exposed, but a total thickness of between 3400 and 3700 m has been estimated of which the great majority is pure to argillaceous limestone to dolomite (the latter predominating towards the base of the sequence) with totally occluded primary porosity. The only non-carbonate deposition is found in the Ghalilah formation which includes complete gradations between limestone and lime-mudstone, and between limestone and quartz-sandstone. These tend to occur in cyclic repetition resulting in relatively thin bedded units of low overall competence which, in consequence, are strongly folded. These tight folds, both in the Ghalilah formation and occasionally in thin bedded limestones elsewhere, have a wavelength of the order of one km or less and are superimposed upon a series of much larger open folds in which dip angles seldom exceed 20° , and wavelengths are of the order of 10 km. These major fold axes and the predominant fault lineations share a common NNE-SSW trend and together constitute the main structural features of the peninsula (Figure 4.13). Both regional mapping (Biehler, et al. 1976) and offshore seismic data (Ricateau and Riché, 1980) differentiate between two major sets of predominantly eastward dipping faults. The most prominent of these consists of vertical to steeply dipping normal and reverse faults of relatively minor displacement (tens to hundreds of metres) which are more numerous towards the east.

Figure 4.12   Lithostratigraphic Summary of the Musandam Massif

Age	Formation			thickness (m)	Karst Springs	Lithology
U' CRET. MUTI	SHAMAL			–		Shamal : Radiolarian Chert
						Muti : marl & shale
M. CRET.	WASIA			–		Wasia : marl & limestone
LOWER CRETACEOUS	MUSANDAM SUPER GROUP	Ms 4	I	130		Argillaceous limestone
			H	150	◄	Lime mudstone / wackestone / packstone
			G	320		
U' JURASSIC					◄	Fe – layer
M. JURASSIC		Ms 3	F	370		Lime packstone with corals
			E	280	◄	Monotonous Lime Mudstone
		Ms 2	D	240	●	
LOWER JURASSIC			C		●	Argillaceous Limestone
		Ms 1	B	280	◄	Dolomite
			A			Lime Mudstone / Wackestone
	ELPHINSTONE GROUP	GHALILAH		300		Argillaceous to arenaceous limestone, sandstone and shale
						Bioclastic Limestone
TRIASSIC		MILAHA		100		Argillaceous dolomitic limestone : reefal in S.E.
PERMIAN	RUUS AL JIBAL GROUP	GHAIL		600		Dolomite
		HAGIL		260	◄	Dolomite and Limestone
		BIH		625+	◄	Dolomite
SHAMAL ETC				–		Chert & minor shale

Figure 4·13

Main Structural Features of the Musandam Peninsula

DIP AND STRIKE

THRUST FAULT

FAULT WITH DOWNTHROW

FOLD AXIS

TILT AXIS
(SUBMERGENCE TO
THE NORTH)
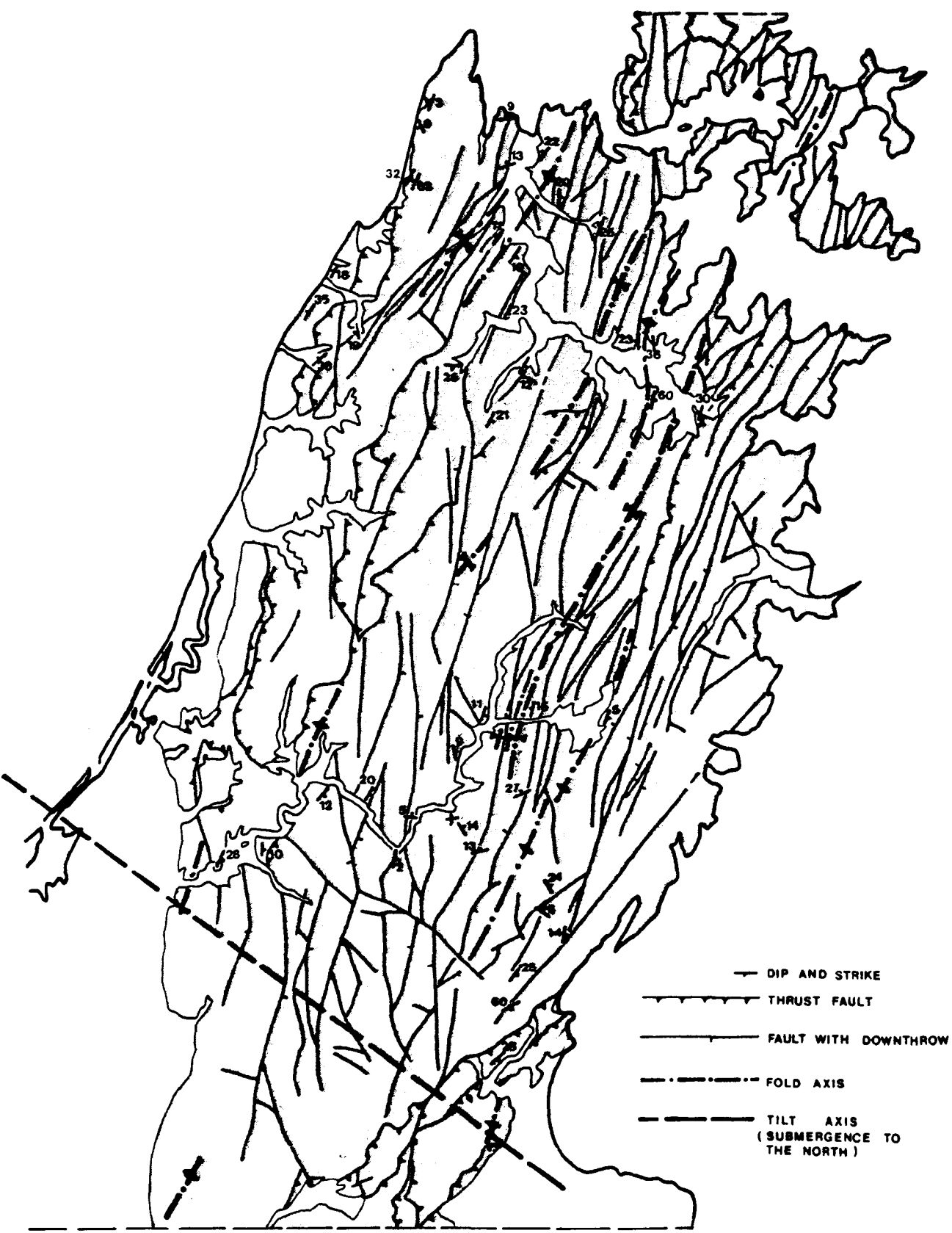
The post-Cretaceous history of Musandam is mainly pieced together from borehole data and seismic evidence from adjacent marine areas. Between the Upper Palaeocene and Lower Miocene, sedimentation was predominantly evaporitic in the shallower restricted conditions to the west, and turbiditic in the subsiding oceanic basin to the east (i.e. the Gulf of Oman), whilst emergence of the limestone massif itself probably produced the peneplanation, vestiges of which are still apparent in the higher areas of Musandam (eg. Plate 4.8). As in most of the Oman mountain area, the Upper Miocene was an epoch of vigorous uplift (Ricateau and Riché, 1980), and was followed by intermittent fluvial erosion to the present during which antecedent drainage patterns of the two major wadi systems, Al Ayn and Bih, have been deeply incised into the limestone massif.

There are no outcrops of undoubted Tertiary sediments in Musandam. The oldest post-Mesozoic unit, the "Al Ghanam Marl", was considered by Vita-Finzi (1973) to be of late Quaternary age. This is a red marl, sporadically distributed in pipe-fill and topographic depressions in the northern and western areas but is of much too limited occurrence to be of any hydrogeological significance. A minor unconformity separates the marl from the only other exposed unit: the ubiquitous "Makhus" formation. This consists of fluvial gravel and conglomerate with subordinate colluvium and aeolian silt in various stages of carbonate cementation. The cemented horizons are highly careous and permeable and tend to form the low relief interfluvial platforms commonly interspersed between the braided main alluvial channels. High seismic reflectance of these "calcrete" markers was used by Fita-Finzi (1973) to extrapolate wadi thalwegs to their present offshore positions, from which it was concluded that the Makhus deposits lie well below the level of the last marine regression (Flandrian). Indeed, at its maximum in the northern peninsula, the combined subsidence and eustatic submergence has totalled over 60 metres during an estimated 10^4 years. On the basis of stable alluvial fans, beach sand positions, etc., the subsidence-emergence hinge-line is estimated to lie approximately between Ras Al Khaimah and Diba (Figure 4.13). North-north-east of this line other subsidence-related features abound. These include the scenically impressive, recently drowned coastline of northern and eastern Musandam, the general absence of tidal notches or wave cut platforms (M.D.C. pers.comm.), and the generally NNE dipping plunge of the major limestone

structures. Furthermore, there is a striking lack of any break in slope between limestone cliff and wadi fill whereas collapse structures and cliff débris, where present at all, are almost entirely restricted to higher relief steeply sloping tributary wadis. Therefore, although minor episodes of uplift have produced small beach sand accumulations in Lower Wadi Al Ayn, the overall geomorphological evidence points overwhelmingly to substantial Quaternary subsidence accompanied by deep alluvial sedimentation in the major wadis.

Neither resistivity soundings nor exploration drilling has yet established the maximum depth of the alluvium. Boreholes in Wadi Al Ayn, some 5 km upstream from Khasab have encountered massive limestone from between 61 and 71 m depth, i.e. about 15 to 25 m below sea level, but these are minimum depth figures and probably relate to the variable "subcrop topography" rather than to the maximum alluvial depth. In Lower Wadi Bih boreholes to below sea level do not penetrate the limestone (Figure 4.14). More surprisingly, a 373 m borehole in the central Rawdah Bowl (Figure 4.15), within 3 km of the upper Bih watershed, also failed to reach bedrock, and since the wellhead altitude is 378 ± 2 m, it is therefore concluded that the alluvial base of Wadi Bih is close to or below sea level throughout its entire course. By implication, since Wadi Al Ayn is further north of the tilt axis, the subsidence should be greater and the alluvial base is likely to be well below sea level throughout its length.

Ground Water Occurrence

Despite the generally high relief of interior Musandam, the incised wadis have behaved as "line sinks", permitting rapid infiltration to a relatively flat, low relief regional piezometric surface. This is illustrated by the few available static water levels from boreholes:

M6-M9	6 m
Bih Wellfield	5 m
Tawi Burayrat	20-25 m
Rawdah Bowl	21 m (located in Figure 4.16)

[Data reduced to mean sea level by differential altimetry except for Lower Wadi Bih where levels were measured optically].

Figure 4·14

Schematic Section of Lower Wadi Bih , Musandam
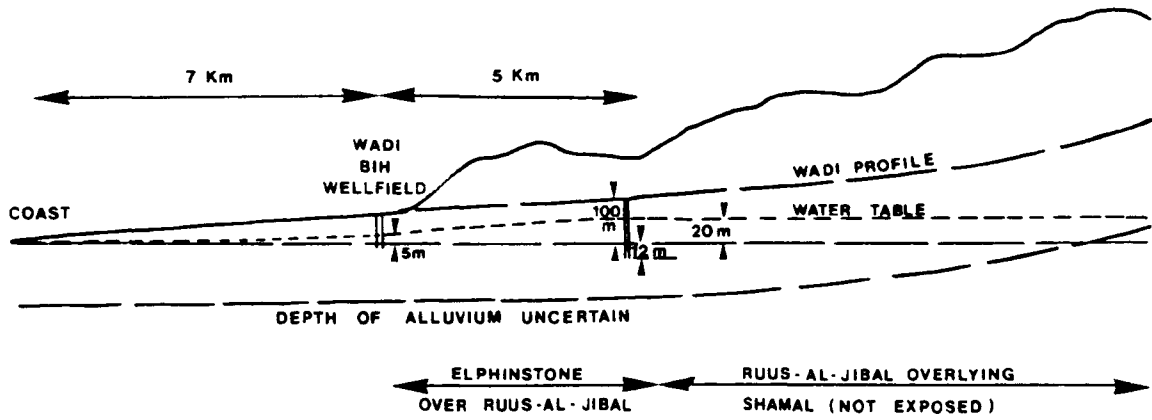
Figure 4·15

Schematic Section of the Rawdah Bowl, Musandam
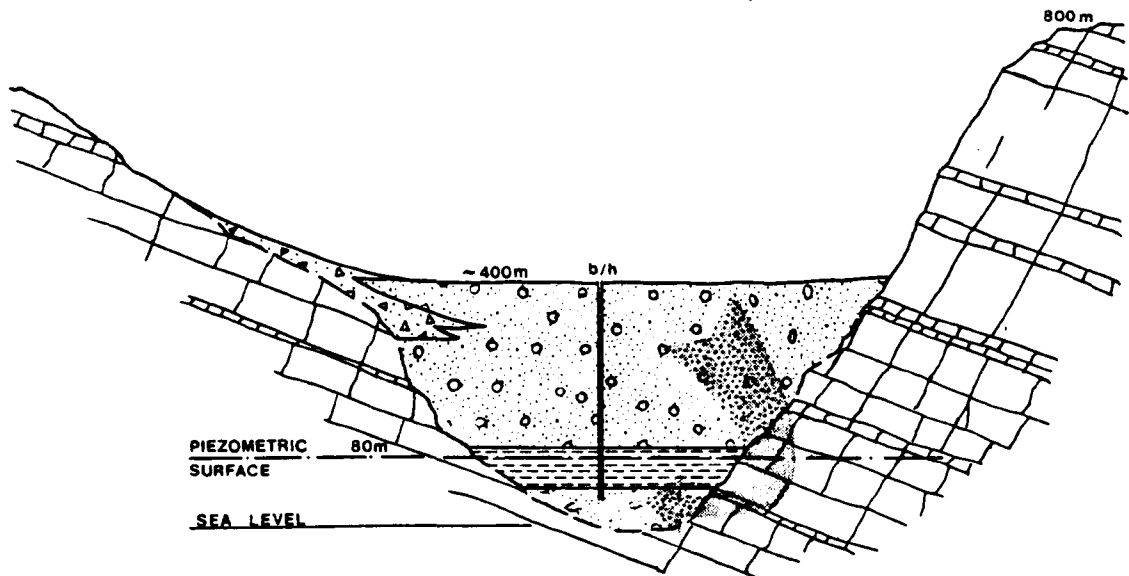
Figure 4.16

The Musandam Limestone Massif – Locations and Catchment Boundaries

Al Ghanam Is.

Qidah

Khasab

Al Jadi

Bukha

Faghna

Grumda

M6-9

Wadi Al Ayn

N

J. Harim

Limah

Ras Al Khaimah

Hagil

Rawdah

Wadi Bih

Burayrat

Al Khatt

Bayah

Diba

0	Km	20

⌁   CATCHMENT   BOUNDARIES

▦   CULTIVATION

☰   SHAMAL AND   OTHER   ALLOCHTHONOUS
    FORMATIONS

    MAKHUS AND   UNDIFFERENTIATED
    QUARTERNARY

●   BOREHOLES

+   MAQAQAH   SPRING

×   KHATT   SPRINGS
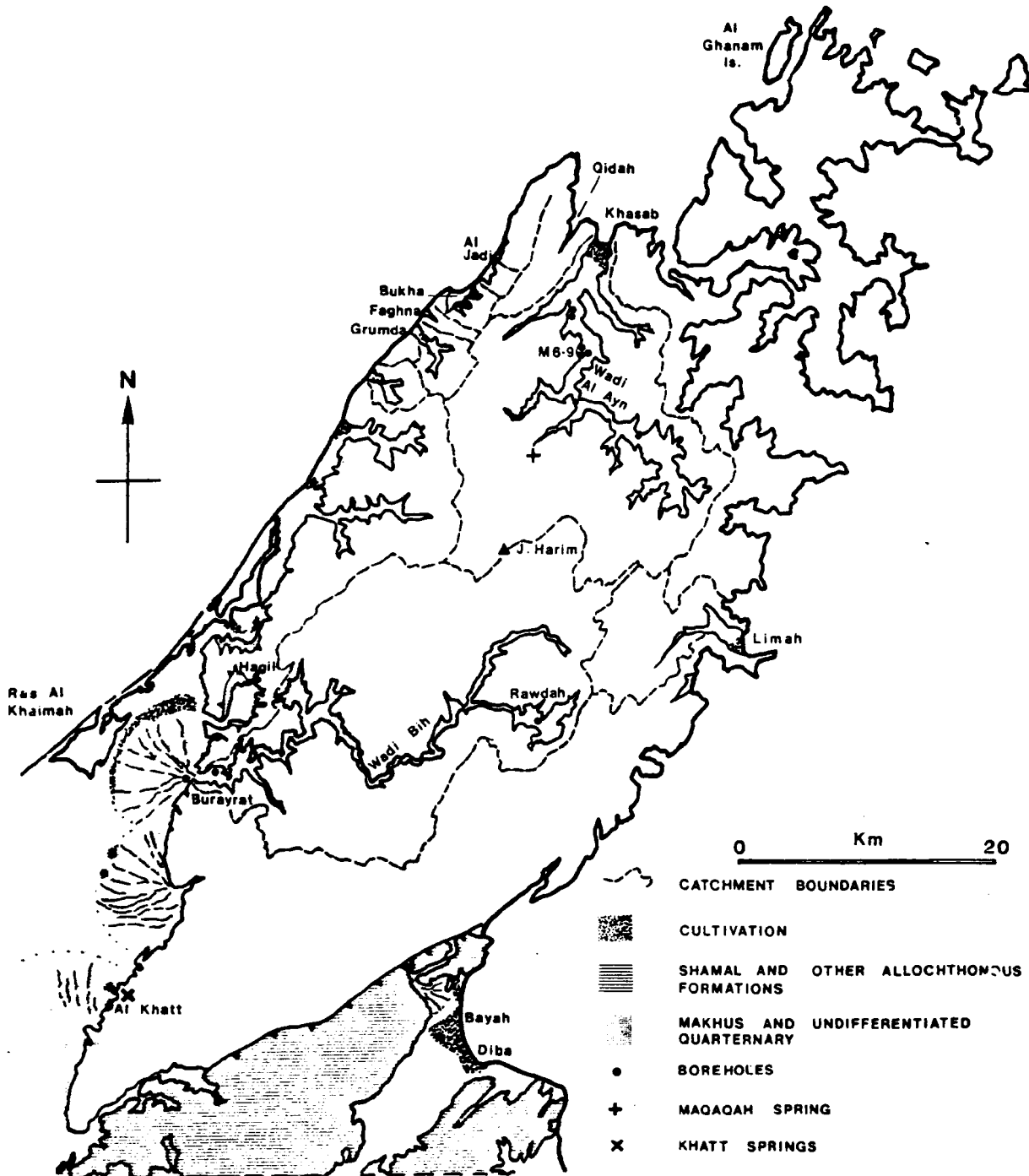
The low piezometric surface is best illustrated at Rawdah where a borehole pierced a confining clay layer* between about 320 and 360 m depth. The underlying (artesian non-overflowing) groundwater was of low salinity and high tritium content (samples 236, 261 Appendix C; Appendix B) and is therefore of recent recharge origin. For such confined conditions to prevail, groundwater flow clearly must have occurred, at least in part, through limestone (Figure 4.15).

The presence of highly transmissive discrete groundwater pathways in otherwise effectively impervious limestone is such that direct comparison between hard-rock and alluvial transmissivity is meaningless. The predominantly impervious nature of the limestone is illustrated by six boreholes penetrating gravel limestone in Wadi Al Ayn which were all dry below the limestone subcrop. Furthermore, a rough calculation of modal drought conditions in Wadi Al Ayn, shows approximate balance between water requirement and supply:

Al Ayn Catchment Area	364 km^2
30 mm modal rainfall with 50% losses	5.5 m^3/a
Khasab irrigation requirement (160 ha at 1 litre/sec ha)	5.0 m^3/a

Under **normal** conditions, groundwater leakage to the sea through limestone, i.e. "short-circuiting" the normal groundwater flow through Wadi Al Ayn and Khasab, is therefore likely to be minimal. On the other hand, after heavy rains, the corresponding groundwater flow at Khasab is much smaller than similar calculations would predict, and must be accounted for by alternative subkarstic leakage from the alluvium between high and low water-table levels, i.e. in the zone in which karstification is most likely to develop (Bogli, 1980). The presence of low salinity fresh water at Qidah and North Al Jadi (Appendix C, Nos. 471, 259), both in small near coastal catchments of low to zero

* This clay is a dark grey kandite type (D.T.A./XRD data) and does not correlate with the Al Ghanam marl. The presence of such a fine grained lithology in an 800 m depression at the head of a gorge is problematic, but presumably derives from restricted estuarine conditions during a period of maximum regression.

139

alluvial storage, further indicates the **locally** highly transmissive
nature of the limestone. This is seldom apparent from surface exposure
though protokarst has developed sporadically in Sultan Salala (low
magnesian calcite), Wadi Shab-Khamsi (high magnesian calcite), and Lower
Wadi Bih-Wadi Shab (dolomite), and is found in all the major
stratigraphic units except the Ghalilah formation (Figure 4.12). There
is therefore little or no petrological control upon rock dissolution
apart from the relative insolubility of the most impure limestones.
Early reconnaissance reports on Musandam have regarded these
argillaceous and siliceous horizons of the Ghalilah and Shamal
formations as potentially giving rise to perched water-table conditions
(Burdon, 1972; Gentle, 1976; "Professional Group - Australia," date
unknown). Whilst this may occasionally be the case, the evidence is
inconclusive and rests upon:

(1) A high water-table in gravels which possibly overlie shamal
chert at the mouth of Wadi Bih (Figure 4.14; Halcrow, 1967), and (2)
slow infiltration in coastal alluvium overlying the Ghalilah formation
at Bukha (Gentle, 1976). Otherwise extensive search throughout the
peninsula failed to relate the "impervious horizons" to spring location,
overlying karstic development, fresh water limestone, or any other
indication of perched groundwater.

**Table 4.9 Hydraulic Gradient in Coarse Piedmont Alluvium
of the Musandam Peninsula**

Location	Hydraulic Gradient (i)	Extent of Saline Intrusion
Bayah	0.0007	minor
Khab Gap	0.0002	N/A
Bukha	0.0002 to 0.0001	severe
Al Jadi north	0.007	minor
Al Jadi south	0.0005	moderate
Fudrah	0.008	severe
Grumdah	0.007	moderate
Tibat	0.005	moderate
Wadi Al Ayn (Khasab)	-	moderate

The only undoubted example of perched groundwater is Maqaqah spring (Figure 4.16 and No. 209, Appendix C). This lies in a cliff face at an altitude of 400 metres, and occurs at the lowest point of a minor thrust plane where it has been deformed into a series of large open folds superimposed on a general dip of 035/20E.

The importance of structure rather than petrology as the dominant control over hard-rock groundwater distribution is shown by several other features such as fissure flow into alluvium at North Al Jadi, and the alignment of faults with groundwater (± spring flow) as at Qidah and Al Khatt. The minor spring line at Al Khatt is, however, atypical in terms of temperature; $39 \pm 2^{\circ}$C, and salinity; 2300 to 2800 μmhos. These springs lie to the south of the "hinge line" and therefore emerge under more normal inland conditions comparable to the thermal spring systems of the Jebel Akhdar.

Water Use

The exceptional infiltration-drainage conditions create problems for the two contrasting styles of agriculture. In the first of these, perennial crops (date groves), and hence the only permanent settlements, are concentrated in wadi mouths and favourable alluvial embayments around the perimeter of the peninsula in order to intercept the near sea level groundwater "leakage points", and are consequently based upon shallow hand-dug well irrigation. These areas tend to lie at the foot of steep to precipitous catchments and are therefore underlain by coarse highly permeable clastic sediments of sand-to-boulder grade with a veneer of either beach sand or aeolian silt. Such conditions are very highly transmissive and cause the post-recharge water-table to recede rapidly to a low gradient. This results in a relatively shallow saline interface conforming to the Ghyben-Harzburg relationship (Ghyben, 1888; Harzberg, 1901). The estimated hydraulic gradients (Table 4.9) therefore tend to reflect the risk of saline intrusion though, as in most of coastal Oman, the introduction of diesel pumped irrigation has already upset the fragile hydrostatic equilibrium and caused serious to ruinous coastal salination in some areas (cf section 6.4 and Appelgren, 1976), especially at Bukha.

In the mountainous interior the depth to water table and the large differential alluvial/hydraulic gradient preclude the construction of wells and aflaj respectively. The only other water source, the perched spring discharge at Maqaqah, is little more than one litre/sec, and is mostly lost by seepage into boulder scree below. Of necessity therefore, the second style of agriculture is "dry farming" in which wheat is grown in stone walled silt enclosures. Though hundreds of these fields are scattered around the mountains, generally in the cooler medium to high altitude plateau areas (Plate 4.8), they are merely speculative ventures by the "Shihuh" (Dostal, 1972). These goat-herding tribesmen plant wheat to germinate in the first (if any) winter rains. Moisture retention is high in the silty soils but at least one more heavy rainfall, about half way through the three month growing period, is necessary if the wheat is to ripen, and since such rainfall is unreliable even in the relatively favourable high altitude winter conditions, the crop failure rate is typically greater than 50%. Successful harvests are therefore regarded merely as a useful supplement to the normal pastoral occupation. The best example of water retention is a small high plateau area on the NW slopes of Jebel Harim where silt overlies a gravel fill that has accumulated behind a landslide and subsided by sedimentary compaction. Runoff into this depression produces the ephemeral lake of Plate 4.9, and subsequent grassy pasture. Ponded (perched) water in similar silty conditions at lower altitude is less common, but is known to occur after heavy rains at the head of the two main wadi systems (Wadis Al Ayn and Bih). Such water retention, however, is exceptional and seldom lasts for more than a week or two.

Attempts to retain sufficient runoff to water goats have been made by the construction of deep covered cisterns of up to 250 m^3 capacity in wadi interfluves, but these are often polluted and do not last from winter to winter. Before recent tanker supply it was therefore necessary for Shihuh living in the interior to travel to the coast to obtain potable water (Burdon, 1973), a tradition which underlines the basic inaccessibility of water resources in the peninsula.

4.7 The Tertiary Limestone : Aquifer or Aquiclude?

Lower Tertiary transgressions produced shallow marine sedimentation over a huge area of the Arabian platform stretching throughout the Gulf

area to Jordan and Iraq in the west, and to Yemen and Dhofar in the south. Alternations of pale crystalline limestones and soft marls from this sequence now form the familiar broken, low relief topography which typifies the Gulf and Negd regions and which form a major, and in many areas, the only aquifer system.

Conventionally the sequence is divided into:

       4 Fars
       3 Dammam
       2 Rus
and 1 Umm er Radhuma.

This stratigraphy is well known from oilwell data (Powers et al., 1966; ARAMCO data) and hence microfaunal correlation throughout the Tertiary province is consistent and relatively straightforward. However the formation nomenclature quoted by some water resources studies is based upon the recognition of lithofacies and consequently incurs both synchronous and diachronous discrepancies in correlation. These errors are corrected in Table 4.10 which also tabulates some of the more important hydrogeological differences and similarities between adjacent areas.

The Fars formation was derived from a lesser transgression and is separated from the preceding formations by a period of mid-Tertiary tectonism in which epeirogenic uplift and tilting ("Gulfwards") of the Arabian Peninsula, and the much more vigorous uplift of the Oman mountains took place. Consequently Fars deposition is more localised and of more terriginous aspect (predominantly calcarenite, calciferous sandstone-conglomerate with a high siliclastic content). By contrast, the Dammam-Rus-Umm er Radhuma series is consistently conformable and shallow marine with a minimum of terriginous material except for the basal transition zone (i.e. just above the Umm or Radhuma or Lower Fars unconformity against the upper Cretaceous). The lithofacies are complex (Table 4.10) but broadly fall into two types:

    (1) mixed limestone-marl or non anhydritic, and
    (2) mixed limestone-marl-evaporite, or anhydritic.

West of Oman, in the southern Gulf littoral, the Tertiary is deposited over a stable platform region where gently dipping halokinetic fold axes

TABLE 4.10   HYDROGEOLOGICAL SUMMARY OF THE EASTERN ARABIAN TERTIARY PROVINCE

			NE. SAUDI ARABIA	QATAR	U.A.E./OMAN BORDER #	OMAN: CAPITAL AREA	OMAN: CENTRAL INTERIOR	DHOFAR
NEOGENE	PLIOCENE	KHARJ	Aeolian sand, halite silt and clay / 28 Lacustrine calcarenite, poor aquifer		Aeolian sand and Sabhka	fluvial gravel aquifers / Dune sands, not an aquifer	Gravels, sand and sabkha. Significant aquifer only in Awaifi area. / Absent	Patchy fluvial calcarenite / 100 (approx)
	MIOCENE	HOFUF	10-30 Marl and lst with sands in upper part. Poor unconfined aquifer.	0-110 Alternating chalk and lst. Unimportant. Basal marl a local aquiclude.	Absent	150 (maximum) Chalky lst to impure coloured marls and calciferous sst/calcarenite. Locally gypsiferous. Impervious aquiclude.	Typically up to 150 but >300 near SE, feathering out to the west. Predominantly clastics with evaporites near the base. T 28 to 16,700.	Upper conglomerate overlying chalky marl. Low yielding, brackish. Little known but probably an aquiclude in most areas. Present only in the coastal plain.
		DAM	60-110 Compact hard lst, chalky to marly. Fissured and karstic upper section. Small but good aquifer.		Up to 1600 Thins rapidly to the south. Poorly exposed. Thick lst with substantial siliclastic fraction, overlain by upper conglomerate. Locally good yields of low salinity.	50? Uncommon reefal facies, very high yielding but sometimes brackish. T 500 to >2000. Bounded by a marl/conglomerate aquiclude.	Upper fars less brackish than lower / basal carbonate	Taqa formation : lst/siltst.
	OLIGOCENE	HADRUKH	25-90 Clean sands beneath marl, siltstone and calcarenite. Excellent aquifer but of limited extent.	Absent				
LOWER TERTIARY OR PALAEOGENE	EOCENE	DAMMAM — Alat, Khobar, Alveolina, Saila, Midra	33-200 Marl Aquitard. Limestone: (locally careous) Moderate to good aquifer. Fissured limestone, porous and dolomitic. Marl in places. Limestone a good aquifer. Shalley aquitard (sometimes absent) overlies 20m of dolomite.	13 Lst and dolomite / 24 Massive dolomite / 9 Simsima chalk / 3 Midra shale. North / South. Absence of shale Basal shale, where permits gypsum present, confines removal in Rus Rus. and hence karst aquifer development.	800+ (UAE) Lst with shalley intervals overlying shale and marl. Moderate yields from upper aquifer further west. Brackish. Sustainable yields seldom >0.5 l.s⁻¹ m⁻²day⁻¹. Dank Shales and siltstone with minor lst in middle section.	up to 1500 Rus/Dammam often undifferentiable. Hard pale crystalline lst succession with dolomite and minor sandy/marly horizons throughout. Slightly gypsiferous marls aquicludes in two thick (>200m) aquicludes in the central Rus and central Dammam. Otherwise the marl fraction decreases upwards. Major evaporitic facies absent. Lst yields are mostly poor to zero but highly variable with locally high yields from fractured sections of the massive Rus and upper Dammam lsts. eg.T typically >5 to 150 but up to 930 in fractured zones.	Absent / 0 to 100 from E to W, largely absent in the east. Subkarstic lst but seldom a significant aquifer except in the Yibal/Lekhwair areas. T: about 5. Potable in S deteriorating to very saline in the N, but large areas of unknown water quality.	50-200 Habshiya formation: Jebel area only. Interbedded crystalline lst, dolomite, coloured marl and chalk. Low vertical permeability and recharge. A few perched springs but not normally an aquifer.
		RUS	20-200 Facies A: Anhydrite and gypsum, <100m, minor lst. An aquiclude. Facies B: Non Anhydritic. Collapsed karstic lst, marl and dolomite. Good to moderate aquifer in hydraulic continuity with Umm er Radhuma.	55 Rus chalk. Positive relief structures: Crystalline lst lst/dolomite. Chalky lst An important aquifer. Negative relief structures: lst/dolomite thick marly dolomite. Mainly anhydritic facies. An aquiclude. Argillaceous lst. Thin basal dolomite.	0 (east) to >100 in west, eg Lekhwair. Hard crystalline and impermeable lst and with lateral attenuation and transition to alternating soft lst and anhydrite to the west. Calciferous shales in the lower section to the south-east, with low yields. Brackish.		0 to 200 thickening to west. Gypsum/Anhydrite with dolomite marl association. T=300 to 1500 but generally subordinate to the UeR aquifer with which it is commonly in hydraulic continuity, especially towards the S. Otherwise SO₄ concentrations high.	200-100 (north) 100-0 (south) Massive gypsum Outcropping. with minor lst Hard crystalline and dolomite. lst with chalk Karstic removal and marl. of gypsum leading to aquifer conditions.
		UPPER UMM-er-RADHUMA	243-700 Lst, up to 10% dolomite. Locally karstic and infilled with argillaceous sediment. South / North Dominantly More argillaceous calcarenite over and evaporitic. dolomite over argillaceous lst. Very poor aquifer. An excellent aquifer. Marl and Shamar shale aquiclude at base.	270-370 Dominantly lst/dolomite with increasing marl content downwards. Upper unit an excellent aquifer of high yield and porosity. Lower horizons variable. Upper horizons in hydraulic continuity with the Rus aquifer where the later is developed.	770 at Suneina (Mid UeR) Not exposed >65 in Dank b/h, upper shaley to lower buff lst. Possibly present in the core of J. Haffit. Aquifer properties unknown.		50-150 absent in the east. Main Tertiary aquifer. Thick lst, dolomite and 250-0 from the calcarenite with Saudi border to sporadic shaley the west. horizons. Outcrops only at Fahud. T>1 to 20,000 due to differential fracturing and dissolution, but typically T=about 600. S=10⁻⁴ to 10⁻⁵. Old groundwater but piezometric surface sensitive to modern recharge in some areas. Frequently brackish. Shamar shale.	300-100 Massive hard lst with increasing marl and shale to the north. Important recharge zone in karstic lst. 350-250 (mid- UeR) Massive hard lst, often with shale horizons typically concentrated 20 to 60m below the upper/middle boundary. Minor marl and dolomite. Exposed in Jebel al Qamar. Subkarstic to karstic, high yielding in uppermost 50 to 100m. (beneath mid-shaley zone). up to 66 (lower UeR) Shamar shale.
	PALAEOCENE	MIDDLE AND LOWER UMM-er-RADHUMA				100? Sporadic reefal, intertidal and supratidal lsts in palaeo-topographic depressions. Lateral transitions to marl. Siliclastic detritus in base. Not normally an aquifer. 0-350 Basal Interitic sst/conglomerate. Heavily cemented. Low yielding. Brackish. Terrigenous non-carbonate formation.		
	CRETACEOUS		Simsima/Juwaiza/Fiqa/Muti More or less indurated calcarenite, sst, lst and shale.			Mainly Cretaceous to Permian nappe sequence onlap to R.S.G. trivial except 'E of Ni Dayqah'.	Cretaceous to Precambrian sediments.	Cretaceous to Pre-Cambrian basement

key lst and including J. Haffit, and the Dank Yanqul areas

(GDC 1949) equate the Dammam with the upper Eocene, and the Rus formation with the middle Eocene

have produced north-south-trending ridges and troughs with a predominance of non anhydritic, and thicker anhydritic sedimentation respectively (Bakiewicz et al., 1982). Comparable sedimentation has also produced thick gypsum deposits in south Oman, north of the Hadramaut arch. Anhydrite aquicludes are best developed in the Rus formation where typically they confine groundwater in the Umm er Radhuma. Where exposed however, the anhydrite is subject to dissolution to leave karstic limestone in hydraulic continuity with both the Damman and Umm er Radhuma formations, i.e. giving rise to optimum aquifer conditions. In the desert foreland areas which border the Oman mountains, both residual evaporite and confined connate conditions tend to give rise to brackish or saline groundwater as in Fahud where the only available groundwater, from the Umm er Radhuma, has an E.C. of 6000 to 11000 µmhos.

Deposition of limestone-marl facies is characteristic of both shallow ridge environments within the platform area, and of old positive relief areas such as the "Hadramaut Arch", the Haushi-Huqf swell, and the Oman mountain arc. In the latter case, the variable post-Mezozoic topography has resulted in relatively patchy deposition of the Umm er Radhuma, followed by more general Lower to middle Eocene sedimentation ranging in total thickness from a few tens of metres to over 2000 metres.

Despite the superficial similarity of limestone-marl facies between northern Oman and elsewhere, several important contrasts actually or potentially affect their respective hydrogeological characteristics due, primarily, to the differing tectonic régimes. Firstly, the stability of the Arabian platform is such that Palaeogene faulting is almost entirely absent, whereas mild to intense fracturing is common throughout the Oman mountains. The consequent karstification, where developed at all, thus tends to occur by large-scale fault plane dissolution in Oman as opposed to evaporitic and relatively localised joint dissolution in the Gulf Littoral. In all cases, karstic features are best developed close to sea level (e.g. Plate 4.10) or in near coastal areas of relatively recent uplift where "water-table" fluctuations in meteoric circulation permit, (e.g. Plate 4.11, Qatar etc.). Secondly, lateral compression away from the Oman mountain axis, and local movement of the underlying Mesozoic

formations have produced locally severe folding in areas such as the western piedmont (Buraimi to Yanqul), the Capital area, and Wadi Bani Khalid in the Sharqiyah. Where the lithology consists of alternating limestones and marls (e.g. Buraimi and Rusayl) this folding has had the effect of blocking potential groundwater pathways by marl aquicludes, thus inhibiting any original hydrogeological potential. On the other hand, folding in purely carbonate sequences produces fracturing which appears to have enhanced subsequent groundwater flow, e.g. the Bosher area. Thirdly, early uplift and subaerial exposure of the Palaeogene limestones during the upper Eocene and Miocene regressions has resulted in recrystallisation to a harder, diagenetically more mature limestone than most contemporary carbonates of the desert interior, though the significance of this to the subsequent dissolution history has not been analysed in detail.

The Piedmont Limestones

Early Tertiary limestones commonly delineate the mountain front along both sides of the mountain axis. On the Batinah side, the limestones form a discontinuous arcuate "mid-plain" scarp of low relief interfluvial outcrops with planar dips to seaward of between 5 and $23°$. The Batinah alluvial drainage is orthogonal to this feature and crosses it in a series of nick points (Plate 4.12, Figure 4.17) where groundwater becomes laterally constricted and channeled into near surface flow, thereby enabling the construction of falaj water supplies for villages such as Jammah and Wadi Bani Rabiah. Further seaward, on the Batinah, the surface gradient and substantial depth to groundwater precludes this method of groundwater supply (Figure 4.17). One of the most prominent features of the Batinah groundwater distribution, also shown in figure 4.17, is the steep northward dip of the water-table contours away from the Tertiary limestone outcrop. In view of the nick points mentioned above, the most plausible explanation is that the Tertiary limestone behaves as an hydraulic barrier to groundwater draining from the piedmont zone, and is succeeded by relatively much more transmissive alluvium; Figure 4.18a. However, the depth-to-water-table data is, on its own, insufficiently precise to differentiate between an alternative hypothesis proposed for the Lansab and Rusayl catchments (Jones, 1978) in which the Tertiary limestone is itself the highly transmissive groundwater sink (Figure 4.18b). The former model is best illustrated by the Dhahirah on the western flank of the mountains where alluvial accumulation is relatively thin and the Palaeogene strata better exposed. Here the Tertiary formation is more or less contemporaneous with the Batinah limestone, of comparable macro and micro texture, and for the most part has a mirror image structure,

146

Figure 4·17   The Palaeogene Barrier of the Batinah Plain, and its effect upon Groundwater and Village Distribution

Jz DAYMANIYAT

SOHAR

SEEB

Km
0   10   20

N

▼ Deep Boreholes
   Other Boreholes
● Mid-Plain Villages
▲ Dip

   Palaeogene Limestone

   Mountain Front

   Depth to Piezometric Surface (after Gibb 1976 ; Iliaco 1975)

Jz SUWADI

BARKA

AL KHABURAH

AS SUWAIQ

no   groundwater   data

● AL QUSAYR

FALAJ AL HARTH

● KHASAF
   15

FALAJ BANI RABIAH   18

   12 MUSHAYQ

See map 2
for Seeb-Muscat
geological details

18
HAMMAH 23

18

BASE (SOUTHERN LIMIT) OF PALAEOGENE CARBONATES

Figure 4·18

Schematic Section to show Groundwater Flow in the Piedmont Palaeogene
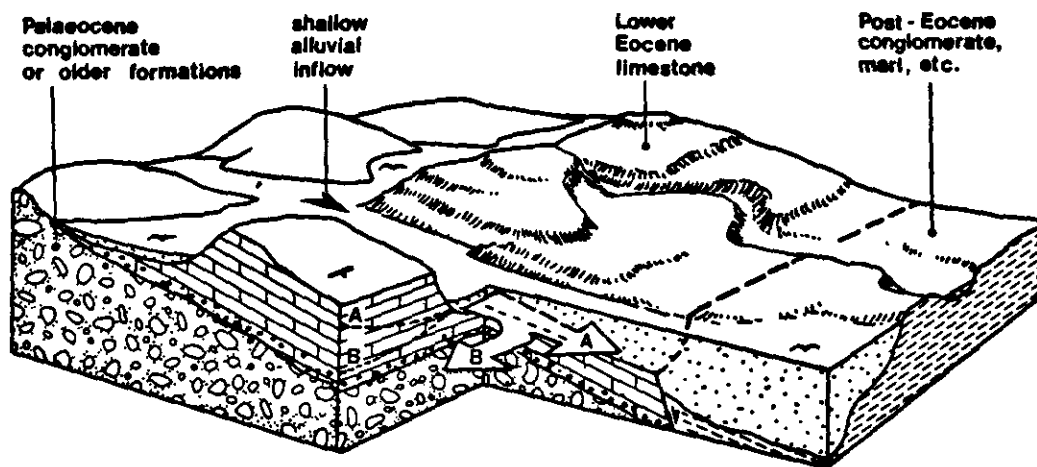
A: Flow assuming alluvial transmissivity >> limestone transmissivity

B: Flow assuming alluvial transmissivity << limestone transmissivity

Figure 4:20

West-East Tertiary Section East of Buraimi

The alternative interpretations are dependant upon the age (A Eocene, or B Palaeocene) of the conglomerate in borehole G (BUEH 4)

148

Figure 4.19

Ibri-Sulayf Gaps: Salinity (μmhos/cm) and Main Groundwater Flow (arrowed)
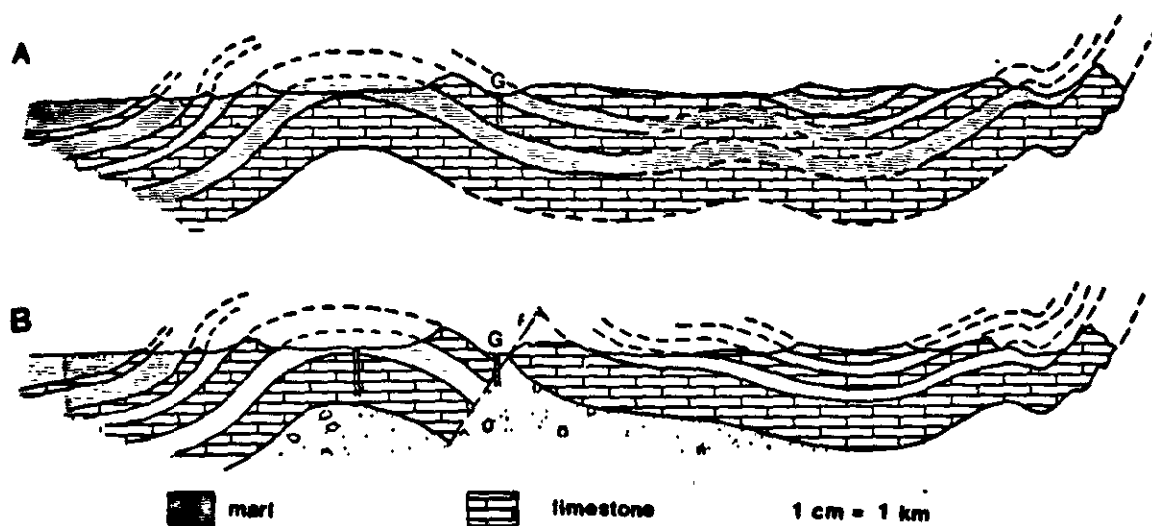
i.e. low angle planar tilt to south or westwards. Two major alluvial breaches in this otherwise unbroken 75 km limestone scarp coincide with the major falaj and agricultural settlements of Ibri and Sulayf. Letts, in Bowen-Jones (1978), produced a very detailed survey of the numerous hand-dug wells and aflaj of these areas in which total yields, specific capacities, water levels and salinities were analysed. These results show groundwater flow to be concentrated only in or adjacent to the currently active fluvial channels both upstream and downstream of the limestone gaps (e.g. Figure 4.19) with higher salinity embayments on either side of the downstream alluvium. Had the limestone behaved as a highly transmissive sink, fresh groundwater would have been channelled laterally to produce subsequent emergence along a much broader downstream front.

North-west of Sulayf, the Tertiary carbonates display a transition in tectonic style from simple tilting to that of more intense fracturing and multiple folding in which anticlinal cores are frequently composed of impervious marl and siliceous sediments of the Haliw (upper Hawasina) formation. Only in Wadi Fida is there sufficient continuous carbonate exposure to constitute a significant aquifer, (cf. section 4.4).

The Buraimi Area

North of Wadi Fida, where the Tertiary carbonate exposure is more sporadic, the expanding water demands of Buraimi and Al Ayn have prompted a more detailed study of both the limestone and alluvium.

Examination of the limestones across an east-west traverse, Figure 4.20, reveals a rich microfauna including **Nummulites sps., Discocyclina, Operculina and Bryozoan and Algal débris**, which confirms a Lower Eocene ± Upper Palaeocene correlation with the more southerly limestones, rather than with the Maastrichtian (Juweiza/Simsima formations), assumed by some previous hydrogeological investigators. This error is probably due to an unusually high fraction of "Semail" clastic material found in the basal limestones, and which is also a characteristic of the Juweiza type section (Glennie et al., 1974).

Of the many borehole tests north-east of Buraimi (PAWR-GDC, 1980-82 unpublished), most penetrate both saturated alluvium and limestone, and thus present some difficulties of differentiation between the respective

Figure 4.21

Depth–Salinity Variation in BUEH5 (well D Figure 4.22)

E.C.   μmhos/cm
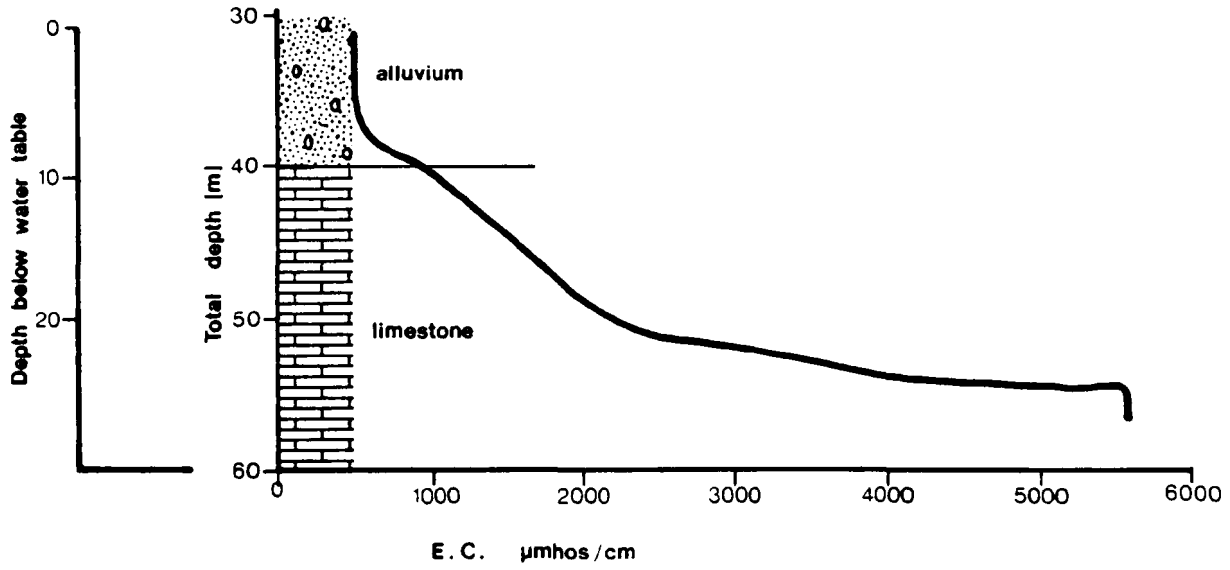
characteristics. Identification of the productive zone(s) is largely achieved by comparing the test water salinities with those of fresh water from the alluvium and relatively brackish water from the underlying "hard-rock" formations, shown in Figure 4.21 and Table 4.11. By assuming that all the yields are from the limestones, any estimates of transmissivity are therefore overestimates, but as the yields are consistently low the correspondingly low transmissivity values serve to emphasise the poor aquifer properties of the underlying Tertiary formation. The only well in the area to penetrate exclusively Palaeogene formations is BU 13 (M on Figure 4.22). This penetrated 30 metres of mixed limestone and marl, followed by 45 metres of pure limestone. Of this, only 20 metres were saturated and the yield was 0.1 litre/sec.

North of Jebel Huwayyah six boreholes (A to F, figure 4.22) penetrating between 10 and 110 metres of the lowermost Tertiary; i.e. conglomeritic limestone to marl, were all incapable of sustaining an airlift yield of greater than 0.5 l/sec, almost all of which was derived from the overlying alluvium. Recovery tests all indicated transmissivities of less than one m^2/day. At a higher horizon borehole G drilled through about 20 m of subkarstic limestone before penetrating a further 20 m into conglomerate of possible Palaeocene age. Borehole H, further north, encountered 14 m of marly mudstone beneath 18 m of alluvium. Both holes were almost dry with very slow recovery rates (transmissivity < 1 m^2/d). Likewise in Wadi Mahda, boreholes I to L (figure 4.22), were all low yielding. In borehole I for example, 90 m of green-yellow and grey fractured limestone had an airlift yield of only 3.7 l/s with 15 m of drawdown, most of which was derived from the lowermost 4 m of saturated alluvium. The saturated section of borehole J was entirely within 50 m of multi-coloured limestone and mudstone, and yielded 4.2 l/s with 10.7 m of drawdown. However, the producing section was probably all in the uppermost 10% of the limestone, in a sandy facies, giving a transmissivity of 20 m^2/d (mean of Jacob early and late time data, and Theis recovery). Of the two limestone storativity estimates, 0.5% is more plausible than that of 7%.

The low borehole yields are consistent with an almost total absence of karstification in the exposed limestones and dolomites. Potentially more extensive carbonate solution may occur at or below the water table, but in view of the groundwater flow pattern implied by the area piezometric surface

Table 4.11

Examples of formation - salinity contrasts from the Buraini area

(after GDC, 1982)

Well (Figure 4.21)	E.C. alluvium	limestone	freshwater thickness (m)
A	7200	16,900	-
B	-	19,500	-
C	1020	12,300	8
D	500	5,640	6
E	920	3,100	5
G	-	10,600	-
H	1450	2,200	19
I	430	2,080	3 + mixed zone
J	520	5,000	15 + mixed zone

Figure 4·22

BURAIMI AREA: PIEZOMETRIC SURFACE

NORTH and EAST. Sept 1982. AFTER G.D.C.
SOUTH · WEST. 1968. AFTER GIBB 1969

Km
0   5

.... AFLAJ
≡ TERTIARY LST.
PRE — TERTIARY

290   300   320   330   MAHDAH

WADI
KAHAL   K

280   F●   380

E●

D●   H

260

C●   G
B●

A

240   MASUDI   HILLI   J HUWAYYAH

280   BURAIMI

JIMI   300   320   340   400
HAMASA
380
MUWAYQII   360
MUTARADH   AL AYN   M

WADI SHIK

N
380

320

J. HAFFIT
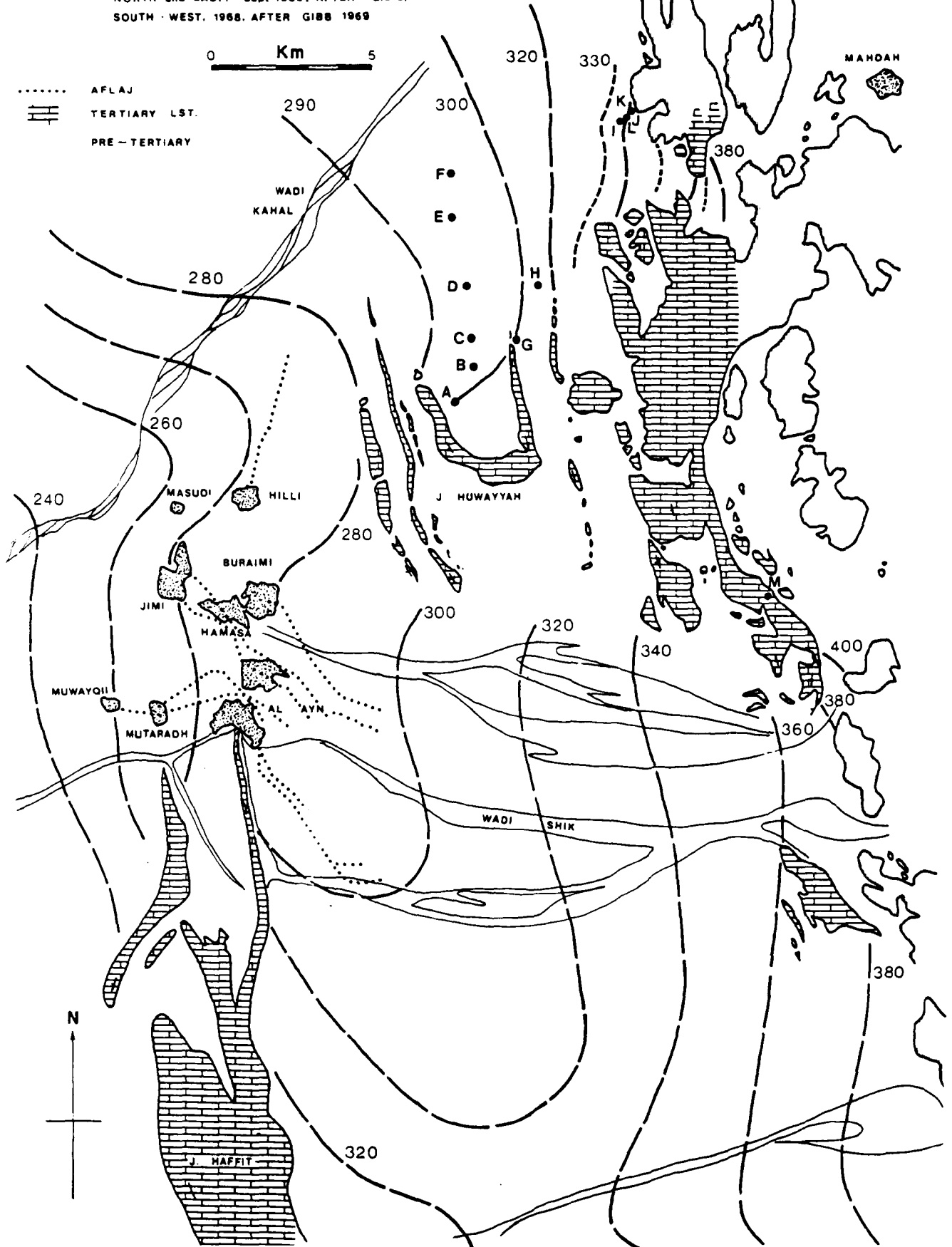
NB: Static water levels in the Mahda gap in 1980 were about 4m higher than in 1982

154

(figure 4.22), significant groundwater pathways in the limestone do not seem to occur. On the contrary, the contours indicate a predominance of alluvial groundwater flow along a broad front, both from Wadi Shik and from Wadis Kahal-Mahdah, whilst a steepening of the hydraulic gradient at limestone nick points again points to the "banking up" of groundwater upstream of the Tertiary limestone. Depressions in the piezometric surface to the north-north-east and south-south-east of Buraimi and Al Ayn are both caused by artifically accelerated line sink drainage into the falaj systems.

Boreholes K and L, Figure 4.22, are reported to have penetrated marls and limestones of the Lower Fars formation beneath shallow saturated alluvium. The total yield, of only 1.5 l/s (PAWR) was mainly from the alluvium, implying trivial groundwater potential in the Fars formation. However, poorly exposed dolomites some 12 km north-north-west of Hili, i.e. west of the mountain front, also probably belong to the Lower Fars, and are reported to give locally good yields. These transmissivity estimates vary from 200 to 650 m^2/d, with an estimated storativity of 3% (Gibb-Huntings, 1970).

The Rusayl-Lansab Area

South of a line between Al Khod and Medinat Qaboos, Palaeogene formations outcrop continuously across an area of over 140 km^2 in the form of heavily incised northward dipping limestone scarps with crest altitudes of up to 390 m. From east to west progressively larger catchments drain across this predominantly limestone succession. Apart from a few minor catchments north-east of Bosher, these are wadis Lansab, Rusayl and Semail. Due to the close proximity of the Capital, the alluvial outwash from these wadis has been developed (and overdeveloped) as an important, (and prior to desalination, the only) source of urban water supplies. A lesser but still substantial number of boreholes has been drilled either into limestone beneath an alluvial cover of variable thickness, or less often, have penetrated directly into the limestone. The hydraulic properties of the Palaeogene formations are thus better known in the Lansab-Rusayl area, than elsewhere. However, apart from the work of Jones (in Scott-Wilson-Kirkpatrick, 1977 a and b; and Jones, 1978) hydrogeological interest has been largely centred upon the alluvium of the lower wadi courses, and no other attempts have been made to evaluate the Tertiary as a separate aquifer system.

155

The major lithostratigraphic units are:

(5) Miocene, impervious carbonate aquiclude

(4) Oligocene, limestone reef

(3) Middle Eocene, massive limestone aquifer ($\equiv$ Dammam)

(2) Lower Eocene to Upper Palaeocene, limestone-marl alternations
     equivalent to the Rus and Umm er Radhuma

(1) "Palaeocene Conglomerate".

The precise age of the basal conglomerate is uncertain, being
post-Maastrichtian and pre-uppermost Palaeocene. Although it is an entirely
non-carbonate formation and locally unconformable against the overlying
Palaeocene/Eocene carbonates, it is nevertheless stratigraphically and
structurally appropiate to consider this "conglomerate" as an integral part
of the Palaeogene series of aquifers. The formation varies greatly both in
thickness: absent to several hundred metres, and in composition: from
coarse quartzite/chert cobbles in a hard iron rich lateritic heavily cemented
matrix, to soft friable ferruginous marl. The latter resembles red clay in
drilling returns and is often gypsiferous. As a result, associated
groundwater is typically brackish with moderate to high SO_4^{2-} concentrations
The only borehole to penetrate exclusively Palaeogene conglomerate, in the
south-eastern Lansab catchment, yielded insufficient water to test and was
slightly brackish, with an E.C. in excess of 2500 µmhos. Both porosity and
transmissivity in the Palaeocene conglomerate is small, and of significance
only in the central Lansab area ("Lansab old field, Figure 4.23; map 2)
where a substantial high altitude catchment, Jebel Bosher, drains towards the
Tertiary limestone scarp in a series of braided fluvial channels. Here the
Palaeocene conglomerate is sporadically draped by more recent conglomerate
terraces and uncemented gravels, in which groundwater flow is restricted to
narrow discrete channels, to form a complex composite aquifer. Of the 28
boreholes in this area, many were failures whilst, of the remainder, tests
gave typical transmissivity values of 5 to 30 m^2/day with a short term
storativity of 0.6% (Jones, 1978). Association of the higher transmissivity
estimates with aquifer stage, i.e. with a greater thickness of saturated
upper gravels, emphasises the relatively poor aquifer properties of the
Palaeocene.

The succeeding shallow marine sedimentation forms a continuous,

apparently conformable sequence throughout the upper Palaeocene to Middle Eocene (units 2 and 3 above). The lowest horizons are of discontinuous Palaeocene succeeded by continuous Lower Eocene consisting of limestones and lime cemented quartz sandstone/conglomerates with upward development of both thick bedded estuarine and patchy reef facies. These are succeeded by alternations of thick orange marl (sometimes gypsiferous) and thinner dm. to m. bedded pale cream limestones, i.e. the soft and hard alternations which form the south facing scarps of the succession. Occasional calciferous sandstone, ironstones and mudstones are of relatively minor occurrence. Progressively deeper water deposition into the middle Eocene results in a passage to monotonous dm. to m. bedded limestones of more uniform facies containing a more abundant nummulitic fauna towards the top. The Palaeocene-Lower Eocene, and Lower-Middle Eocene boundaries are difficult to identify on micropalaeontological grounds, and no criteria could be identified for their differentiation in the field. The boundaries shown on map 2 are therefore only approximate. The thickness reaches a maximum of 1500 m in Wadi Rusayl and is attenuated to both east (Azaiba) and west (Al Khod), i.e. to about 750 and 1000 m respectively.

Apart from a regional northerly dip of about 7° away from the mountain axis, the Palaeogene succession has been subjected in several areas to locally severe mid-Tertiary deformation. This is most marked at Al Khod where both easterly and southerly increase in dip terminates as near vertical to overturned limestone. Erosion of the accompanying fractures accounts for a breach in the limestone scarp at this point by Wadi Semail. The barrier effect of steeply dipping marly limestones probably precludes significant underflow past Al Khod, though this point, one of the key imponderables in water balance studies of the lower Wadi Semail, is unproven. In the Lansab catchment, the two most important folds, the Ghubrah monocline and Misfah syncline, are both north-south trending. The former is coaxial with and probably caused by a normal fault in the underlying Hajar Super Group but the origin of the latter is unclear. Neither fold bears any obvious relation to the dominant fracture pattern though erosion of the intervening anticlinal area (Lansab old field) may have been fault guided. Two sets of fracture lineations are clearly defined (Figure 4.23 and Map 2). The dominant lineation east-west to NE-SW, sub-parallels the mountain

157

piedmont (i.e. Jebels Tayyin-Bosher) and is apparently caused by compression due to detachment and possibly minor displacement of Jebel Bosher (i.e. par-autochthonous Hajar Super Group). The second, WNW-ESE, fault lineation deep-seated fracture swarm which penetrates both the allochthon and autochthon to at least as deep as the Permian/Pre-Permian unconformity.

The presence of the Bosher spring line indicates the impervious nature of the nappe units beneath the Tertiary succession, and thus suggests complete hydraulic discontinuity between the Hajar and Tertiary limestones along such faults. Near surface lateral flow along both sets of faults is however quite possible as depressions and limestone breaches such as Wadi Lansab have developed by fault guided erosion.

Holokarstic features are entirely absent from the Palaeogene carbonates. The rubbly careous weathering texture of most surface exposures (eg. Plate 4.11) gives a spurious impression of widespread subkarstic solution opening but is associated with both a high incidence of dry and low yielding wells, and a high overall runoff/rainfall ratio. Significant solution opening is therefore not amenable to surface assessment. On the other hand, loss of circulation in drilling records shows that localised fissure solution at or close to the water-table is sometimes well developed.

Most of the transmissivity estimates are from boreholes in or close to fractures near the top of the succession, i.e. Mid Eocene limestone, and typically vary from 5 to 200 m^2/day. Figure 4.23 illustrates the test values at Muaskar Al Murtafa'a, Lansab and Qurm together with the distribution of dry or nearly dry boreholes. Some of the values from Lansab New Field may be overestimated due to higher yielding contributions from the overlying alluvium. In Figure 4.23 it is important to differentiate between the very high transmissivity values of the Oligocene reef and the rather poor to indifferent transmissivities of the adjacent Eocene limestone. Previously, the lack of this distinction has contributed to unrealistically optimistic estimates of transmissivity throughout the Palaeogene succession. A second factor which has been held to indicate high limestone transmissivities, is the very steep hydraulic gradient which developes in the "Tertiary neck" of Wadi Lansab during recession; Figure 4.24. As discussed earlier, this is open to two interpretations i.e. highly transmissive lateral flow in the limestones, or highly transmissive alluvial drainage away from relatively impermeable limestone. The latter is the preferred model for several reasons:

Figure 4·23

Lansab-Rusayl Tertiary Carbonates: Structure and Transmissivities

N

Gulf of Oman

Qurm

Rusayl Fan

●C

70-1500

D●

125 ■

high
■25
4000
●
B
■20-50
500-
25000
■90-500
4000 ■
80
10-400

●A

Lansab
New
Field

■90

Lansab Old Field

Ghubrah
Monocline

KEY

● Brackish low yielding
boreholes in Miocene
marl

■ Medium to high yielding wells

⊙ Dry or very low yielding boreholes

Miocene marl

Major fractures

Reef limestones

Mesozoic limestones of J.Boeher

Palaeocene-Eocene limestone

Misfah Syncline

0   Km   5

159

Figure 4·24

Lansab Old Wellfield : Piezometric Surface (m.a.m.s.l.)
Modified after Jones 1978

a) in recession July 1975

~ Main groundwater inflow

Palaeocene conglomerate

b) after recharge Dec.1977 to Jan 1978

Eocene limestone

Semail cumulates

160
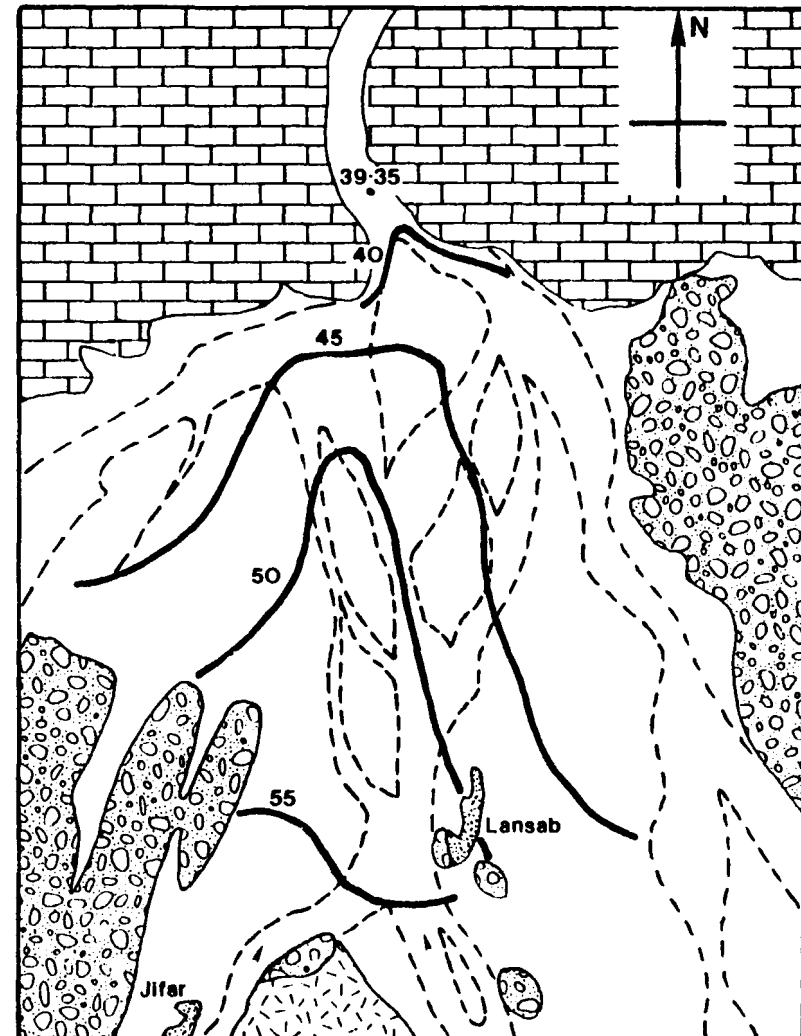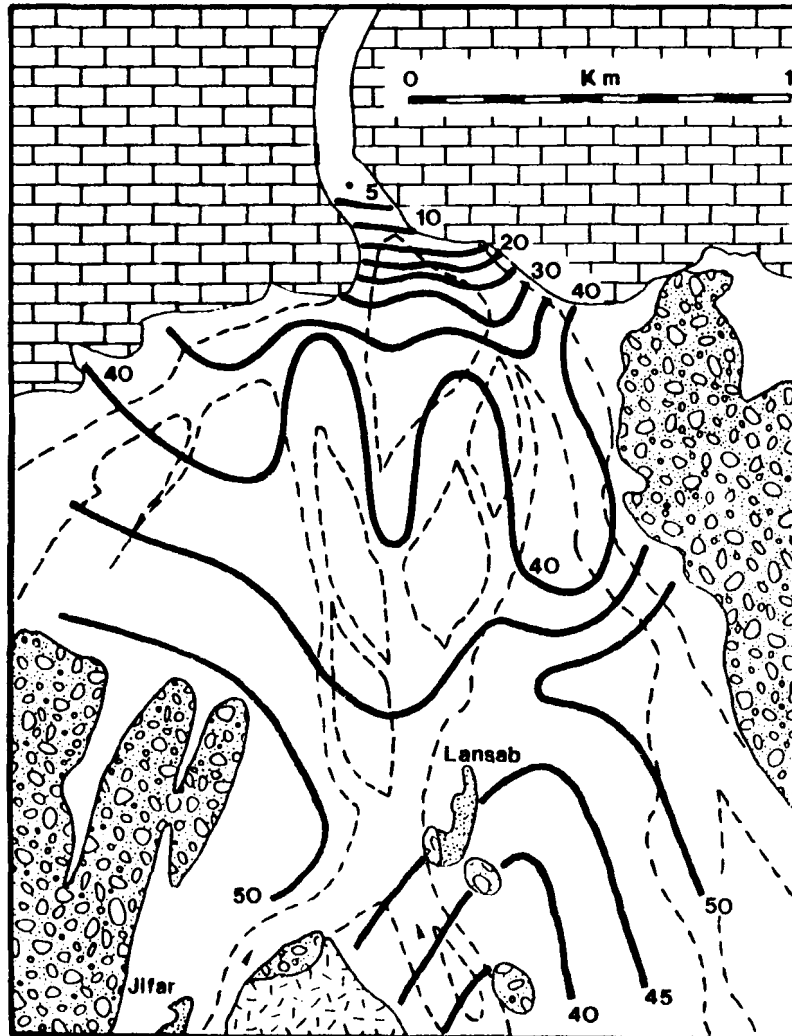
Figure 4.25

Reef limestone S.W.L. Variations

(1) Excavations, for aggregate, in the Lansab gorge has exposed a minimum of 10 metres in an unknown thickness of coarse "clean" rounded gravel whose transmissivity is likely to be at least comparable to, and probably greatly in excess of, the limestone, thus creating a north-south "line sink".

(2) The limestone water is of lower tritium content than the alluvium; 7 T.U. from Muaskar Al Murtafa'a, as opposed to 17 T.U. from the alluvium of "Lansab New Field". This indicates a greater proportion of older water in storage and consequently a relatively inactive groundwater system with a smaller proportion of recent flood recharge.

(3) The higher salinity of limestone groundwater implies a long residence time and/or a small water-rock ratio, which is inconsistent with a model of active short-term recharge and drainage. Alternatively, since large scale groundwater leakage into the limestone would tend to dilute the existing water in storage, the salt mass balance would require a huge volume of brackish water to maintain the observed salinities. Although no estimates of limestone storativity are available, there is no evidence for the implied large scale storage of brackish water.

(4) The fracture pattern in Wadi Lansab is mainly sub-parallel to the alluvial channel and thus, apart from local "bank storage", is unfavourable to continuous lateral groundwater flow.

(5) The piezometric surface is similar in form to the previously cited examples (Batinah, Ibri, Wadi Shik, Mahda) where the downstream hydrochemical and piezometric contours conform to a narrow alluvial rather than a broad limestone drainage system.

Oligocene sedimentation is poorly developed or absent except for a reef between Al Khod and Seeb Airport. This is fault-bounded to the south by the middle Eocene limestone and is largely concealed beneath limestone sand and marls of probable Miocene age. The main exposure, north-west of Muaskar Al Murtafa'a, consists of a geometrically complex frame of hermatypic corals, algae and bryozoa with intersticial bioclastic lime-mudstone to packstone infillings. The reef substrate is not exposed. A rich fauna of corals, echinoids, large foraminifera (eg. **Halkyardia Maxima**) and lamellibranchs suggest an age of Middle and possibly lower Oligocene. The main reef facies

consist of red, pink and white coralline limestone, creamy yellow dolomite and a patchy caprock of black ironstone, both in place and in collapse structures. East of Muaskar Al Murtafa'a the reef is not exposed, whilst further west, between Wadis Semail and Rusayl, the lithology changes to a more uniform heavily cemented slope facies. Still further west, the reef terminates before reaching Wadi Semail itself. Intertidal and subaerial exposure of the main reef is probably responsible for the ironstone formation, widespread dolomitisation and the karstic collapse and solution features which are common north-west of Muaskar Al Murtafa'a. Very high porosity and permeability at deeper levels is more evident from the total circulation loss experienced during the construction of two boreholes through the forereef (northern) slope. In a few aquifer tests, the drawdown-time variation was insufficient to permit adequate transmissivity estimation, (Jones, 1978). Otherwise, the transmissivities, measured over a two km wide area, varied between extreme values of 20 m^2/day and 25000 m^2/day, with typical values in the range 500 to 4000 m^2/day; Figure 4.23. This reflects the heterogeneity of reef lithofacies and contrasts with the low transmissivity of 25 m^2/day for the slope facies near Wadi Rusayl. Full advantage is taken of this high yielding formation by an estimated wellfield abstraction of about 1.25 x $10^6 m^3$/yr (1980 projection from 1975-76 data) with the corresponding piezometric response shown in hydrographs W39/40; Figure 25. Some storm water recharge occurs during the winter months whilst a substantial fraction of the abstraction is perennially recharged by recycling sewage effluent from the adjacent urban supplies. Thus, in the absence of any long term piezometric decline, (figure 4.25), the reef recharge-abstraction appears to be in approximate balance.

The aquifer geometry, and hence the groundwater storage, is unknown but both the small decline in static water level between flood recharge events and the low tritium concentration of 0 to 5 T.V. (and hence minimal dilution of old groundwater with more recent high tritium flood water), indicates a large groundwater reserve.

Two potential threats to water quality threaten the reef's long term viability as an important aquifer; i.e. saline intrusion and effluent recharge. The former problem is caused by depression of the well field water table to below sea level, thus reversing the hydraulic gradient between the reef and the sea (about 5 km away) and inducing landward groundwater flow.

Serious sea water intrusion has occurred in the Mawallah wellfield only four km to the north (cf. section 6.4) but has so far been blocked at Muaskar Al Murtafa'a by the presence of low transmissivity marl between the reef and the sea. However, as no deep boreholes are available to monitor the saline interface in this area, the long-term risk is indeterminate. Effluent from the Muaskar al Murtafa'a water supply constitutes the second source of salination, mainly the gradual build-up of chloride and nitrate in the aquifer, and accounts for the local salinity anomaly of sample 134, Table 4.5; Appendix C.

In view of the importance of the reef aquifer, a gravity survey was undertaken to examine the extent of the reef beneath the marl/alluvial cover. This survey used high precision methods with a La Coste and Romberg gravity meter. Inter-measurement distances were typically about half a kilometre; closer in the vicinity of the reef outcrop and other areas of variable relief, and more widely spaced in the flat alluvium of the Rusayl fan. Elevation control was by optical levelling using closed loops tied in to U.S. Navy geodetic doppler master station 7911001 at Seeb, and Seeb International Gravity Station (Evans and Shelton, 1971). By this means elevations were reduced to a precision of ± 0.01 m. Latitude and longitude were calculated from the U.B.M. grid zone 40 co-ordinates to a precision of ± 10 m. The Eocene dip slope to the south of the Rusayl survey area is heavily dissected by a high density of consequent drainage channels and was thus not amenable to two-dimensional terrain correction modelling. The terrain corrections were therefore derived from 1:10,000 scale contour maps with 10 m contour intervals using the Hammer compartment method, zones C to I, (Hammer, 1939), and an assumed mean Palaeogene limestone density of 2.49. The reduced data is summarised in Table 4.12, the survey area is shown in Figure 4.26, and the simple Bouguer anomalies and sections are shown in Figures 4.27 and 4.28. The two Bouguer profiles contrast markedly due to the high reef density relative to the alluvial sediments of the Rusayl outwash fan (western traverse), and the low reef density relative to the coastal marls in the eastern traverse. In both cases however, the simple Bouguer anomalies attributable to the reef are small; only about 1.5 mgal. Variable density and subcrop geometry of the reef is ambiguous with respect to the formation thickness, but in both traverses, significant lateral extension of the reef beneath later formations clearly does not occur, i.e. the aquifer is not much larger than it would appear from the limited surface exposures.

Table 4.12 Rusayl Fan Gravity data (mgal)

Station ID	Lat	Long	elev(m)	RD*	tide corr	terr corr	GLT	GOB	FAA	SBA
1	23.560	58.203	73.87	− 22.556	0.12	0.07	978857.22	978909.27	74.847	66.581
2	23.564	58.203	69.00	− 20.147	0.12	0.08	978857.53	978911.53	75.453	67.732
3	23.567	58.204	53.26	− 16.150	0.12	0.13	978857.71	978915.74	74.470	68.510
4	23.567	58.225	45.39	− 14.910	0.07	0.07	978857.74	978916.87	73.140	68.061
5	23.572	58.225	40.54	− 12.543	0.07	0.03	978858.04	978919.20	73.672	69.135
6	23.576	58.225	36.82	− 11.713	0.07	0.02	978858.32	978920.02	73.057	68.937
7	23.581	58.225	33.67	− 10.337	0.07	0.01	978858.62	978921.38	73.152	69.384
8	23.583	58.224	33.42	− 8.849	0.08	0.01	978858.74	978921.88	73.453	69.713
9	23.584	58.223	28.27	− 8.704	0.08	0.01	978858.86	978923.03	72.895	69.731
10	23.589	58.220	27.43	− 8.734	0.08	0.01	978859.15	978923.00	72.311	69.242
11	23.593	58.219	27.00	− 9.137	0.08	0	978859.45	978922.58	71.465	68.444
12	23.598	58.218	33.20	− 10.703	0.08	0	978859.76	978921.02	71.507	67.792
13	23.605	58.215	20.86	− 7.651	0.08	0	978860.21	978924.07	70.296	67.962
14	23.614	58.213	21.30	− 6.792	0.08	0	978860.80	978924.93	70.703	68.319
15	23.623	58.210	19.35	− 6.025	0.08	0	978861.43	978925.69	70.238	68.073
16	23.638	58.204	15.96	− 5.718	0.08	0	978862.39	978926.00	68.538	66.572
17	23.565	58.261	51.87	− 16.682	0	0.10	978857.56	978915.06	73.508	67.704
18	23.570	58.260	34.72	− 13.044	0.01	0.05	978857.88	978918.66	71.491	67.605
19	23.574	58.260	30.24	− 10.498	0.01	0.02	978858.18	978921.17	72.319	68.935
20	23.578	58.260	25.60	− 8.455	0.02	0.01	978858.45	978923.21	72.668	69.803
21	23.582	58.261	21.68	− 7.280	0.02	0.01	978858.70	978924.39	72.382	69.956
22	23.586	58.261	18.76	− 3.829	0.03	0.01	978858.98	978927.85	74.661	72.562
23	23.596	58.262	11.40	− 0.842	0.04	0	978859.62	978930.84	74.372	73.456
24	23.603	58.262	5.88	+ 1.255	0.04	0	978860.05	978932.93	74.695	74.037
25		58.262		+ 2.224	0.05	0				
26	23.628	58.262	2.00	+ 3.858	0.08	0	978861.76	978935.58	74.435	74.211

* Drift corrected gravity value relative to Seeb

Figure 4·26

Rusayl—Seeb Reef Area : Gravity Survey Points

Semail fan

to Seeb

Gulf of Oman

•16

•26

15 •

•25

•14

•24

•13

Older conglomerate terrace

Wadi Rusayl

•12

x

•23

•11

Miocene
lst. & marl

7 •10

•22

•9

REEF •8

21 to Muscat

•7

•20

•6

•19

•5

•18

3

• 4

17

2

Eocene limestone

1

| 0 | Km | 5 |
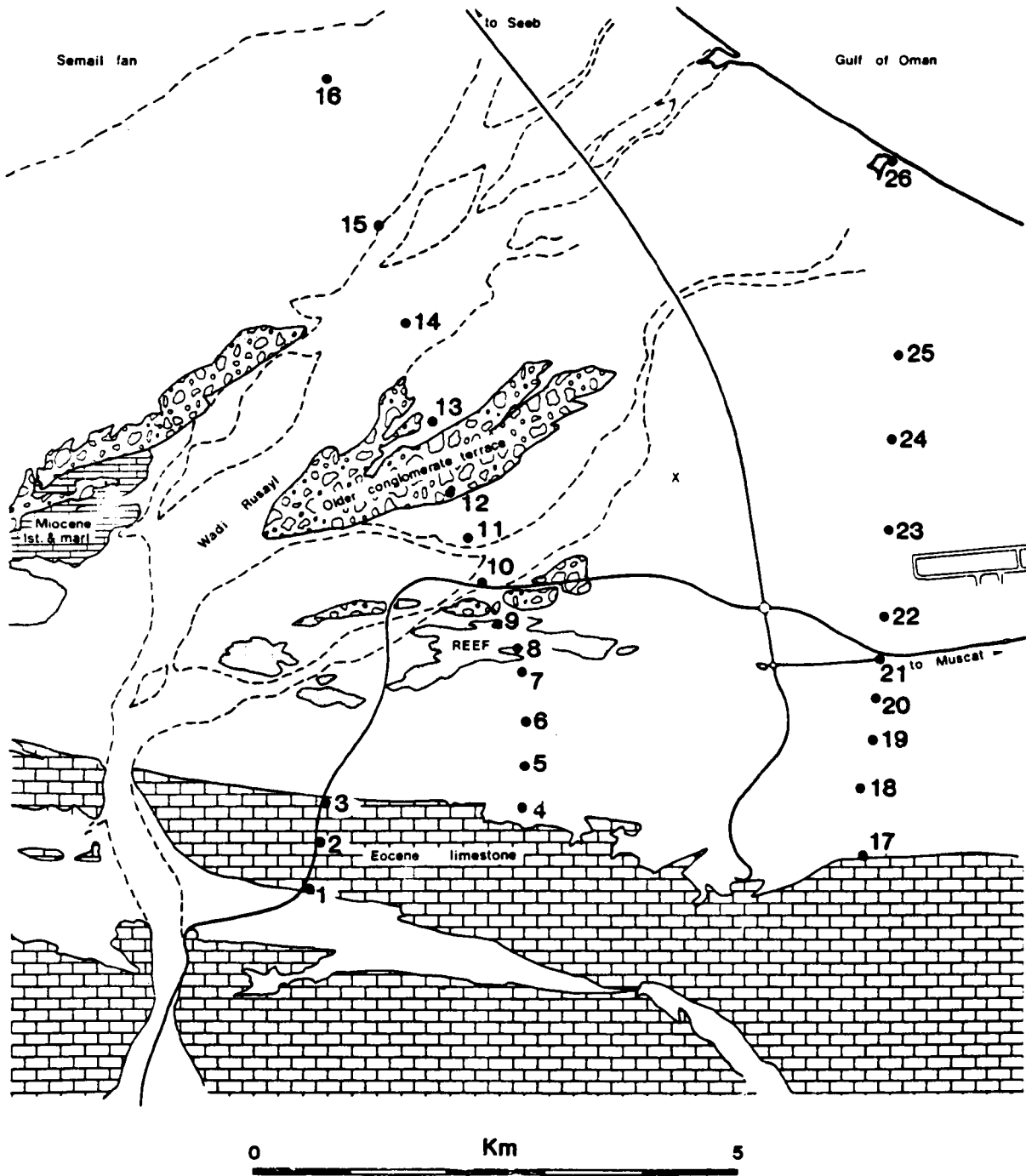
Figure   4·27

Simple Bouguer Anomalies–Eatern Reef Traverse
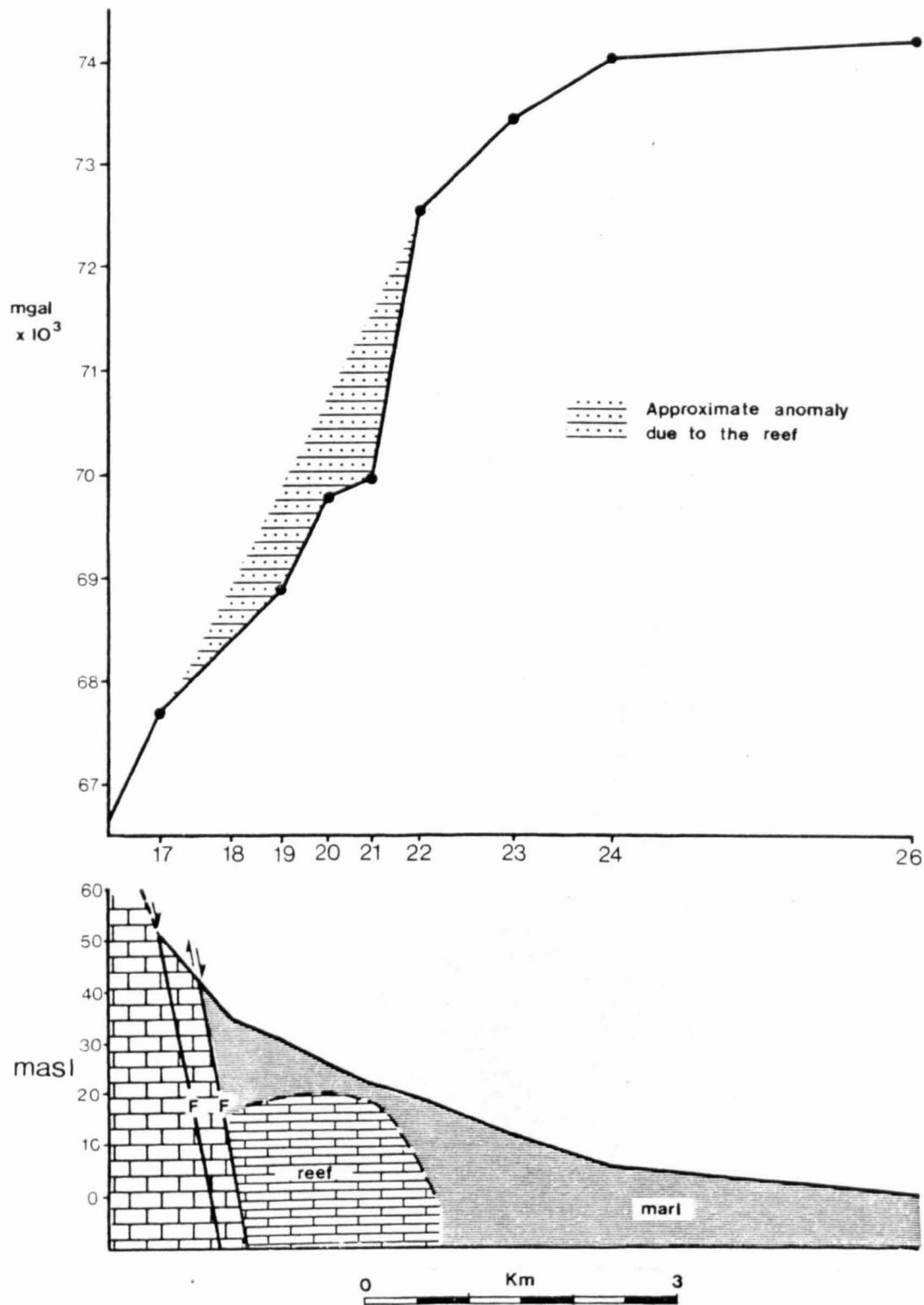
Figure   4·28

Simple Bouguer Anomalies–Western Reef Traverse

Approximate anomaly
due to the reef

mgal
x 10³

Station Number

Borehole along strike from gravity station 12 (X, figure 4·26)
penetrates limestone from −2 m to the bottom at −82 m

masl

Km

Post − Miocene conglomerate etc.   marl

Oligocene Reef   Eocene limestone
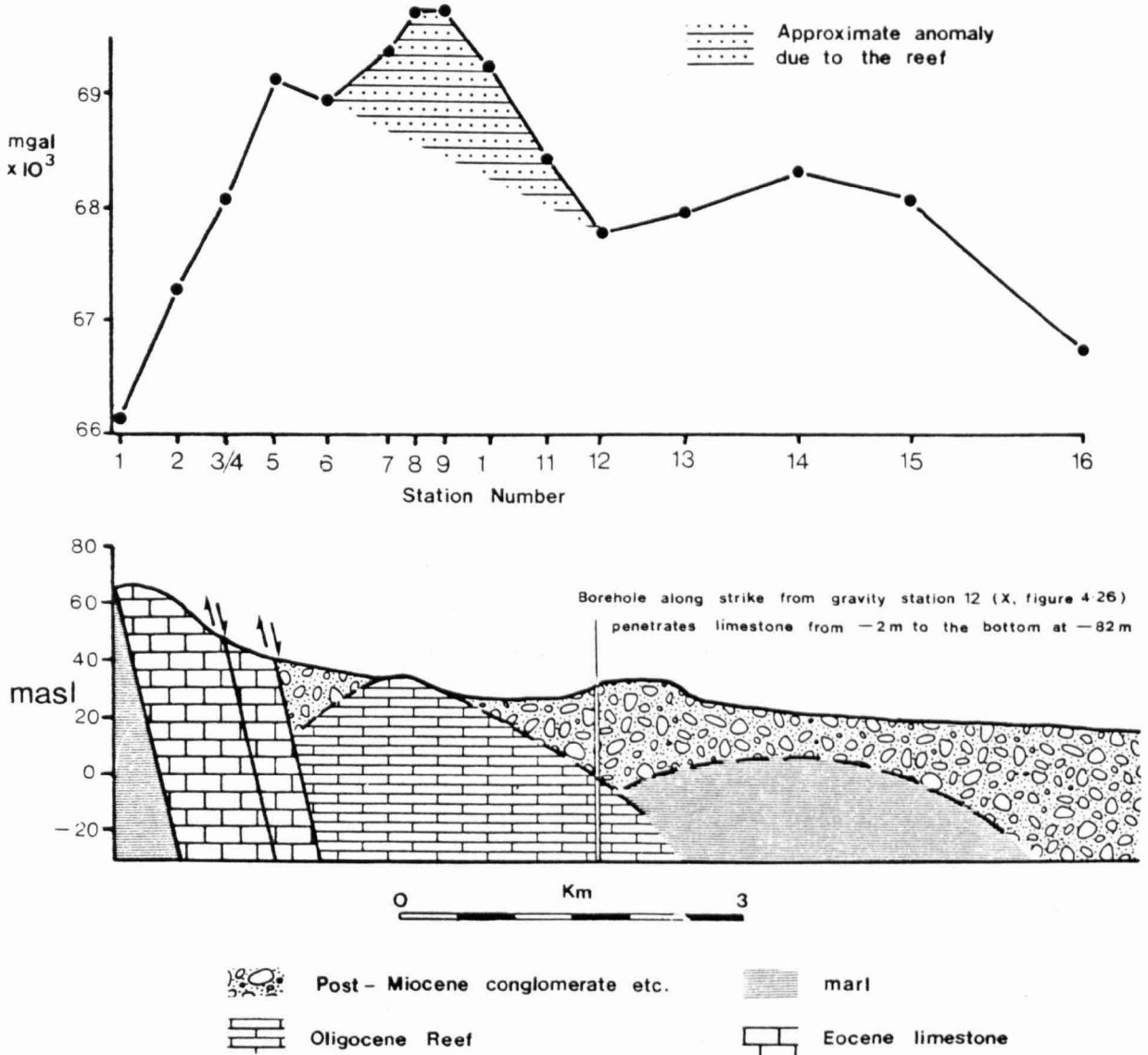
No other comparable reef aquifers are exposed in the Tertiary of Oman. If others exist beneath later sediments they are likely either to be in saline coastal positions further east, or to contribute to the overall storage of the Batinah further west.

The Miocene sediments are mainly regressive impure lime mudstones, marls, dolomites or calc-arenites with a sparse fauna and a high proportion of derived clastic material of Palaeogene, Hawasina and Semail origin. The formation is typically exposed as a drape around the Oligocene reef, and as low relief poorly exposed ground in the Rusayl fan-Qurm interfluves. Borehole data (e.g. A, Figure 4.23) suggests a maximum depth of about 150 m, overlying Middle Eocene limestone. In the Semail fan, probably contemporaneous carbonate sediments of different facies form the substrate to the oldest terrace conglomerates into which the main fluvial channels have incised. These are chalky, structureless masses, locally forming wackestones with rounded cobbles of basic rock: an unusual lithology which appears to originate as a lime-mudflow. In the few exposures where bedding is discerible, these sediments are horizontal. Faulting, jointing and matrix porosity are all absent. The few wells which penetrate the marl, near Seeb airport eg. A, B, C and D, are all very low yielding and brackish to saline.

The Sharqiyah Massif
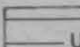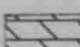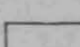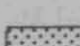
South-east of the Sayh Hatat inlier the main mountain axis parallels the coast as far as the eastern termination of the Hajar mountains at Ras Al Hadd. The great majority of this area is continuous carbonate exposure (Figure 4.29, Plate 4.7) and, between Sur and Wadi Mijlas, constitutes a substantial aquifer. The high part of the massif, up to about 2000 m, must also be the source area for a large proportion of the surface runoff into the Wadi Al Batha Plain, i.e. the main alluvial basin of the Sharqiyah (cf. section 6.2), although measured rainfall-runoff relationships for this area have not yet been measured.

The culmination of the massif is coincident with a high south-west facing scarp from which, with the exception of Wadi Bani Khalid, both relief and structure have a general dip to seawards. Surface drainage is approximately radially disposed around the culmination (Figure 4.29) and has incised into the limestones along a dominantly antecedent rather than a

Figure 4.29   The Sharqiyah Tertiary Massif : Locations and Main Structural Features
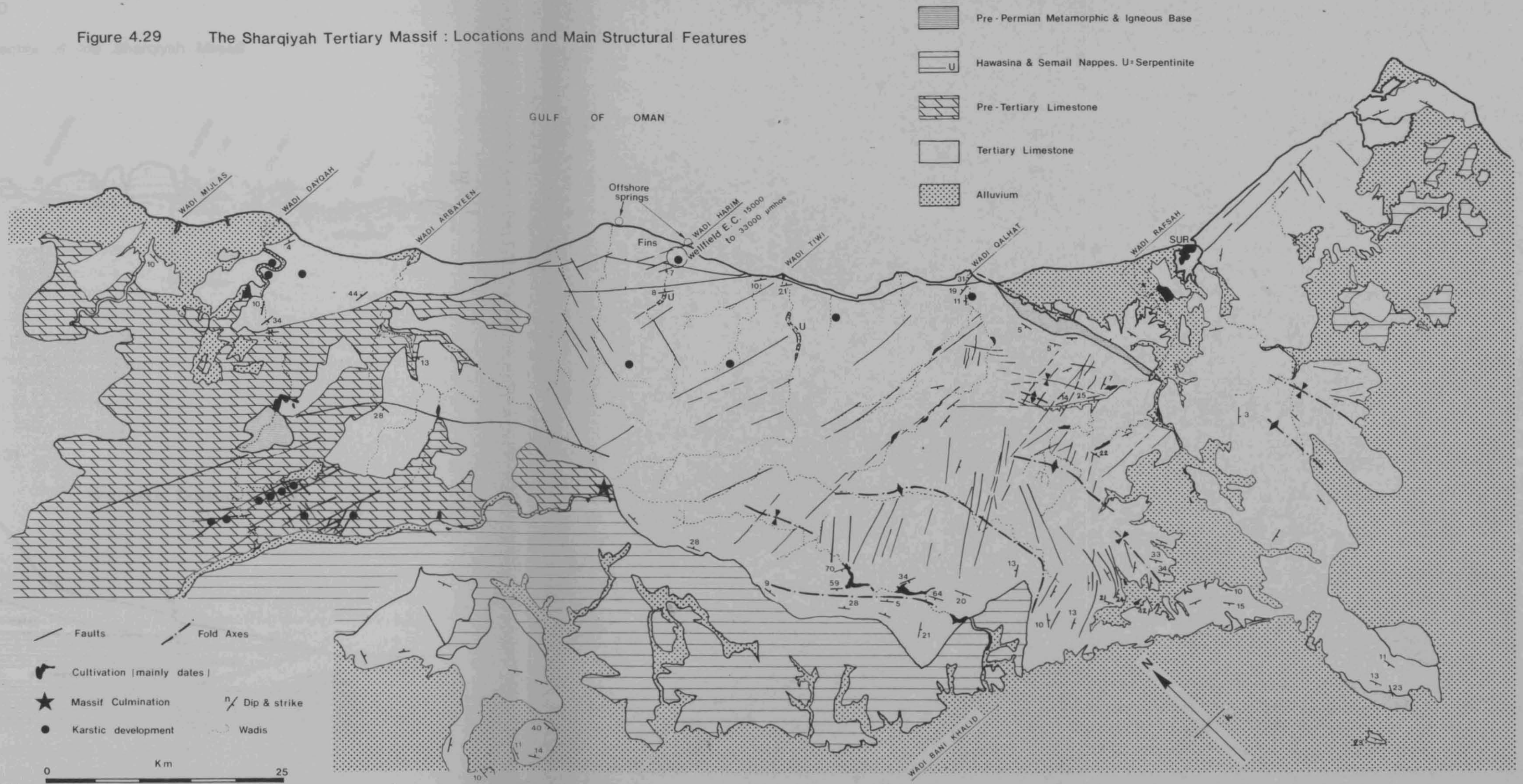
Pre - Permian Metamorphic & Igneous Base

Hawasina & Semail Nappes. U = Serpentinite

Pre - Tertiary Limestone

Tertiary Limestone

Alluvium

GULF   OF   OMAN

WADI MIJLAS

WADI DAYQAH

WADI ARBAYEEN

Offshore
springs

WADI HARIM

Wellfield E.C. 15000
to 33000 μmhos

WADI TIWI

WADI QALHAT

WADI RAFSAH

SUR

Fins

U

U

U

WADI BANI KHALID
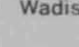
Faults

Fold Axes

Cultivation (mainly dates)

Massif Culmination

Dip & strike

Karstic development

Wadis

N

Km

0   25

Figure 4·30

Structural Section of the Sharqiyah Massif
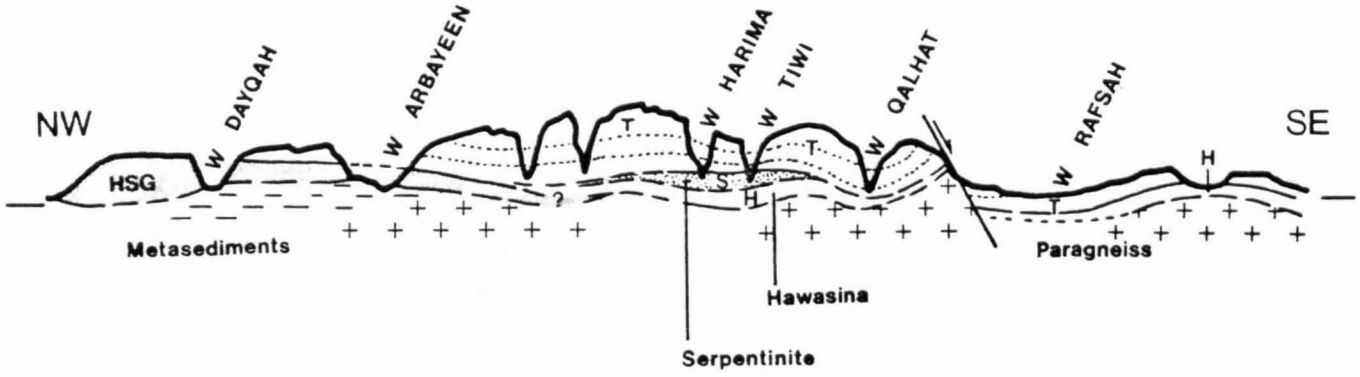
Figure 4·31

Sharqiyah Coastal Section
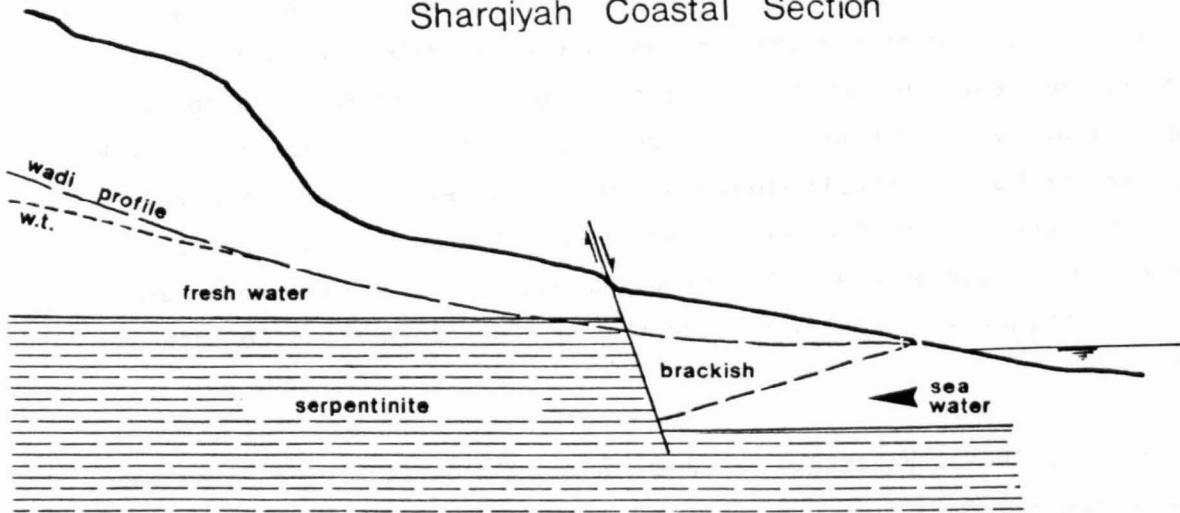
fracture pattern to produce some of the deepest and most scenically impressive gorges in Oman.

Although all the coast and the south-eastern perimeter of the massif (Wadi Rafsah) are entirely Tertiary in age, there are enough sporadic outcrops of Pre-Tertiary rocks as inliers and edge exposures to deduce an essentially impervious base to the Tertiary sequence. Examining the underlying formations from north-west to south-east, the Amdeh quartzite of the Sayh Hatat and Dayqah (Mazara) inliers give way to more varied lithologies including quartzite, shale and weathered arkose in the Wadi Arbayeen inlier. The granitic basement source material for the arkose is obscured for a further 60 km beneath the maximum development of Tertiary limestone (up to 2500 m, Glennie et al., 1974) where the underlying rocks are serpentinites of the Semail nappe. The latter occur extensively beneath the south-western scarp at an altitude of 250 m or more and also as small inliers close to sea level in the lowest exposures of Wadis Tiwi and Harima, thus implying a north-easterly dip to the aquifer base. The only true crystalline basement both beneath the Tertiary limestone, and indeed, the whole mountain arc, is exposed at the eastern end of the massif. Glennie et al. differentiated these rocks into two units; the "Qalhat metamorphics", (meta-volcanics) and "Jebel Ja-Alan granitic basement", but the identification of syenite and granite in place, and of muscovite schist, slate and phyllite in the basal Tertiary lime-mudstone-conglomerate of the Ma'Ayah pass, and of granitic gneiss and hybrid acid-ultramafic rocks near Qalhat (in addition to the basic porphyry described by Glennie) strongly suggests that the two formations belong to a single crystalline complex in which differing descriptions merely reflect a greater preponderance of basic rocks in the more northerly outcrops. A thin layer (< 10 m) of ferruginous brecciated chert overlying the Qalhat crystalline series in probably an attenuated remnant of the much thicker Hawasina (Halfa formation) series which is extensively exposed beneath the Tertiary formations to both east and west.

The structural relations between the two major limestone formations, the nappe units and the crystalline base are illustrated in Figure 4.30. The thick Tertiary sequence conceals the eastern termination of the Hajar Super Group but, at least locally, the massif may be divided into a compound aquifer in which the Hajar Super Group is separated from the Tertiary limestone by Hawasina shales and cherts. The significance of a separate

172

lower aquifer is, however, unimportant since the Hajar Super Group is attenuated south-eastwards and thus pinches out at an unknown but considerable depth beneath the active Tertiary groundwater system. South-eastward decrease in importance of the Hajar Super Group is illustrated in Wadi Arbayeen where surface flow appears close to the Tertiary-Mesozoic limestone contact rather than the Mesozoic-Pre-Permian contact, and suggests relatively low transmissivity of the lower limestone unit.

The basal Tertiary is of upper Palaeocene age both at Qalhat in the south-east, where it consists of "normal" shallow marine limestone and dolomite facies, and in the Quryat area to the north. In the latter case it is thinner and of more complex aspect including a basal terriginous unit of variegated clay to conglomerate grade, overlain by about 140 m of bioclastic partly dolomitised limestone, and capped by a complex of cliff slump débris in a regressive shallow limestone matrix (Montenat et al., 1977). Between these two areas, the intervening basal Tertiary sequence is incompletely known but appears to consist of discontinuous Palaeocene marl-limestone deposition in palaeotopographic depressions comparable to those of the Capital area. The major transgressions of the Lower and Middle Eocene age have resulted in much more consistent and widespread carbonate sedimentation to the extent that most of the 2000 + m thickness of the central massif consists of monotonous modular to massive shallow marine, partly dolomitised limestone. Towards the edges of the depositional basin this sequence becomes greatly attenuated and more varied as seen in Wadi Rafsah where much of the sequence is represented by argillaceous limestones and black shales, and in the various synclinal residuals to the south-west of the massif (figure 4.29) where the Lower to Middle Eocene (the only Tertiary rocks present) totals less than 100 m. The latter consists of ferruginous dolomitic marl overlain by calciferous quartz sandstone and a caprock of haematite cemented radiolarite grit. The aquifer potential of these marginal facies is minimal.

The two limestone units at the north-western end of the massif (cf. section 4.4) are of strikingly different character: namely old diagenetically mature, tightly folded and thoroughly recrystallised dark grey mesozoic limestones of the Hajar Super Group are overlain by the relatively soft pale-weathering and gently tilted marls and limestones of Palaeogene age. Coincidentally, a feature of the Eocene limestones at the other (southeastern) end of the massif is that, although the above **stratigraphic**

distinction does not apply, the bimodal facies distribution persists, i.e. the Lower Eocene limestone is dark grey or black and, in the field, and would be undifferentiable from Mesozoic limestones such as the Kamah or Wasia formation except for the presence of nummulites.

The absence of upper Eocene sediments and progressively more intense folding towards the south-east results in a major unconformity between the Middle Eocene and subsequent carbonate sediments. The latter are derived from a third but lesser transgression during the Oligocene, which has overstepped the radically altered Upper Eocene topography to produce sporadic deposition of relatively thin shallow-marine carbonates of not more than 200 to 300 m thickness. Within the south-eastern massif these take the form of low relief inliers, but east of Wadi Rafsah, previously high relief of the Huqf-Ja-Alan arch, (in which Eocene deposition was reduced or, in places, even absent), was subject to widespread Oligo-Miocene (Aquitainian) sedimentation which now covers the more or less flat-bedded terraces south of Sur. This second period of sedimentation incorporates a larger proportion of terriginous material and is generally of more variable lithology, such as the interdigitated large foraminiferal limestones and sandy marls of the Quryat area (Montenet et al., 1977), the pelagic chalk of the Dibab coastal strip, the back-reef and reefal limestones between Sur and Qalhat, the alternating black shales and orange-brown limestones of the Abat and Wadi Bani Khalid inliers, and the extensive terraces of coloured sandy marl and yellow dolomitic limestones south and east of Sur, Figure 4.29. All of these are low-relief areas of relatively undisturbed, soft friable immature sediments with horizontal or low angle dip, and are therefore easily differentiable from the early Tertiary rocks.

Where groundwater exists within the massif, its presence is indicated in the lower sections of the major wadis where outcrop or shallow subcrop of the impervious base forces the groundwater to the surface (eg. the wadis indicated in Figure 4.29). On this evidence only the early Tertiary rocks of the central massif appear to constitute a significant aquifer. The apparent hydrological distinction between an early Tertiary aquifer and a mid-Tertiary aquiclude has several causes. Firstly the mid-Tertiary sequence, though widespread east and south of Sur, is of low relief and therefore receives insufficient rainfall for

significant karstic dissolution to have occurred. Secondly, only the harder, more lithified and more competent early Tertiary rocks have been subjected to the upper Eocene period of deformation. Consequent opening-up of fractured groundwater pathways within the limestones has led to more advanced, and occasionally cavernous, karstic development (Figure 4.29)which has been further enhanced both by the greater age of the early Tertiary sequence (i.e. longer subjection to meteoric solution) and by the "purer" limestone sedimentation of the offshore pelagic environment. By contrast, none of the near-shore or coastal Tertiary sedimentation of either calc-arenite or calc-argillite facies displays any solution features. On the contrary, the marls of the Wadi Rafsah area are commonly gypsiferous, and testify to the lack of meteoric leaching.

The structural control upon groundwater flow is most obvious in the central massif area where large scale east-west and north-south trending faults, at 45° to the main anticlinal axis form a prominent conjugate shear system coincident with the appearance of ground/surface water in Wadis Qalhat, Tiwi and Harima. Further south-east the simple low angle anticlinal structure diverges into more complex multiple fold axes in which faults are more numerous and predominantly transverse (Figure 4.29). The relatively high incidence of springs in this area is mostly traceable to fault lineations, but no clear structural pattern to the groundwater distribution is evident.

The largest groundwater discharge of the massif is the southward draining catchment of Wadi Bani Khalid where a roughly estimated total surface discharge (spring baseflow) of between 7 and 10 x 10^6 m^3/year is derived from transverse fault line drainage from the main, high relief, anticlinal axis.

In all the wadis draining to seaward, fresh groundwater, if present at all, is invariably found several kilometres inland, and hence landwards of a series of large faults parallel or subparallel to the coast, Figure 4.29. Seawards from the fault zone, the high salinity, (EC between 15000 and 33000 μmhos) in Harima wellfield, the lack of any coastal vegetation, and extensive karstification near sea level (i.e. very high gross transmissivity) all point to a groundwater system in which saline intrusion predominates over minimal fresh-water flow to

seaward, as shown in Figure 4.31. Leakage of fresh water to sea is known from two offshore springs (Figure 4.29) and is thus associated with discrete confined karstic flowpaths in hydraulic continuity across the coastal fault zone. However, as none of the major wadis appears to have sufficient groundwater excess to maintain a stable saline interface at the coast, large subsurface baseflow losses to sea seem to be improbable. Between the centre of the massif and the coast several examples of closed drainage and very large endokarstic features are known. These are some of the best developed karstic features in Oman, and are likely to promote very rapid infiltration and recession, in keeping with the exceptionally dry and barren limestone surface features.

4.8 The Minor Limestone Aquifers

The "Exotic" Limestones

The "Exotic Blocks" (Tschopp, 1967) or "Oman Exotics" (Glennie et al., 1974) are limestone klippen ranging in size from large (house sized) boulders up to the 360 km^2 mountain group of Jebels Khawr-Ghul (e.g. Map 1). Though distributed widely from Wadi Hatta in the north to the Wahiba sands in the east, the "Exotics" constitute a distinctive facies, easily recognised by the morphology of ubiquitously high-relief precipitous slopes displaying deeply etched wall karren, and by the pale grey-cream high albedo surface which gives rise to the common local name "Jebel Abyad", i.e. "white mountain".

Two generations of Exotics were identified by Glennie. The first, containing a Permian fauna of rugose corals and fusulinid foraminifera, typically consists of brecciated reefal bioherms. It is seldom greater than 100 m thick and tends to form the smaller Exotic outcrops. The second generation, recognised by a Triassic fauna of **Involutinaa** foraminifera, **Spiriferina,** Megalodontid lamellibranchs, Goniatites and rare Crinoids, has accumulated to a much greater thickness, up to 900 m, in the south-western Jebel Akhdar area where the formation is fragmented into the Jebels Khawr-Ghul, Misfah and Misht. The Triassic Exotics are more varied than the Permian and include both extensive fore-reef and back-reef/lagoonal facies, thus providing the faunal and petrographic variety described by Glennie (1974) and Graham (1980). In addition to the reefal characteristics, much of the thick Triassic sequence consists of monotonous massive to finely laminated unfossiliferous marbles originating as lime mudstones, packstones and, rarely, stromatolites, with occasional decimetre-bedded radiolarites in

the highest horizons (eg. Dann, Jebel Khawr). Overall the Exotic limestones may be summarised as shallow marine limestones of reefal and associated affinities deposited under moderate to high energy conditions and succeeded by later thick lime mudstones deposited under lower energy conditions on a subsiding substrate.

Despite the high initial porosity of most reefal structures, the petrofabric evidence presented by Graham (1980), field observations, the low mean Sr content (205 ± 90 as opposed to 460 ± 460 for the Hajar Super Group limestones) and almost exclusively low Mg calcite mineralogy, all indicates thorough lithification of an originally open system resulting in the occlusion of all primary porosity by pervasive sparry cement.

The tectonic position of the Exotics at the top of the Hawasina Series is demonstrated by common megabreccias and olistostromes at the basal contact with the "Haybi Volcanics" (Searle, 1980), the latter itself forming one of the higher nappe units. Though seldom fully exposed, this basal complex is up to about 100 m thick and tends to prevent hydraulic continuity with underlying limestones. In Jebels Misfah and Akhdar for example, the limestones are clearly separated by Hawasina sediments, whilst further south in Jebel Khawr, Masil spring consists of "Exotic" groundwater perched over a thick sequence of cherts and vesicular basalts.

Significant groundwater occurrence is only known from the largest Exotic, ie. Jebel Khawr-Ghul. Here, deformation during tectonic emplacement has resulted in locally severe folding (eg. figure 4.32), thereby creating secondary porosity and initiating erosion/solution along cross and tension faults. The structural importance to groundwater flow is demonstrated by the five existing springs which are all clearly aligned with the low relief intercepts of such faults (Map 1). As in the Hajar Super Group, karstic development is immature, and mainly consists of uncommon pipes and exit holes developed in widely spaced joints of the southern and western edges of the massif. Only one borehole has been drilled in the exotic limestones, at Al Ala, which gave a yield of only 2 l/s and a specific capacity of only 8.6 m^2/day (P.A.W.R. data). Unfortunately, although penetrating to a depth of 215

~etres, this borehole is aligned with the core of the Misfah syncline where
closure of any secondary porosity is likely to be greatest and hence where
karstic development is least likely to occur.

Nevertheless, the extent of village agriculture in the shallow piedmont
areas adjacent to Jebel Khawr is greater than the low alluvial storage
potential should allow, and implies groundwater transfer from the limestone
to alluvium of the order of 50 l/s in the east (Wadi Sayfam) and 100 l/s in
the north-west (Wadi Al Ayn). Spring discharges, by contrast, normally total
a trivial 10 to 20 l/s but are notable for two reasons. Firstly, the spring
waters are the "purest" found in Oman, with exceptionally low Na^+, Cl^- and
SO_4^{2-} concentrations, (Table 4.13). To some extent this may be due to the
relatively low groundwater temperatures and purity of the limestone, but is
also affected by a combination of the steep slopes and groundwater pathways
resulting in rapid runoff/infiltration, and short period recession. The
latter is demonstrated by Dann spring which diminishes from an estimated 50
l/s to zero discharge in only six months, thus indicating a low storage
groundwater system with short surface and aquifer residence times. Secondly,
Ma'Awal spring has the property of "ebb and flow" discharge at approximately
hourly intervals. This feature, locally attributable to a "Djinn holding
back the water", is an example of an intermittent spring, i.e. one in which
the outflow channel is sufficiently narrow, and an aquifer chamber
sufficiently airtight to permit a siphon mechanism to operate (Figure 4.33).
The rarity of this phenomenon may be judged from Bridge (1924), whose
inventory of ebb and flow springs in America and Europe totalled only 15.

The Mayhah Formation

North-west of the Jebel Akhdar, the upper members of the Hajar Super
Group succession, namely Triassic to Cretaceous equivalents of the Sahtan,
Kamah and Wasia groups, reappear as several relatively small
par-autochthonous inliers. Collectively known as the Mayhah formation
(Glennie, 1974), this is a condensed succession of up to about 600 m of
argillaceous lime mudstones, oolites, turbidites and conglomerates with
subordinate cherts and shales. Apart from a tendency towards more widespread
silification, the dark grey weathering, dominantly carbonate lithologies are
superficially similar to its lateral equivalents in the Jebel Akhdar.

178

Table 4.13 The Hydrochemistry of Exotic Limestone Groundwaters

No.[1]	T	Ca	Mg	Na	K	Sr	HCO$_3$	SO$_4$	Cl	F
23	26	69	11	9	2.5	0.3	217	29	17	.05
24	25	53	23	33	2.0	0.5	220	68	25	.19
336	30	55	9	45	1.6	0.3	138	19	17	.05
417	28	31	12	19	2.4	0.4	236	35	25	.07
*	-	45	33	42	3.5	-	268	59	62	-

[1] No refers to spring source details in Appendix C

* "Amqah" quoted by S.A.G.P., 1975; High Mg, Na and Cl attributable to partial surface flow (incurring evaporation), and serpentinite within the source area.

Figure 4.32

NE-SW Sketch Section of the South-Western J. Akhdar Area

J Khawr

EXOTIC
SPRING
LINE

f   f   f   f   f   f   f

J Ghul   J Misfah   J Shams

U

U

H. S. G.

H.D.

H.D.

0   km   10

▨ Exotic limestone   U = Serpentinite
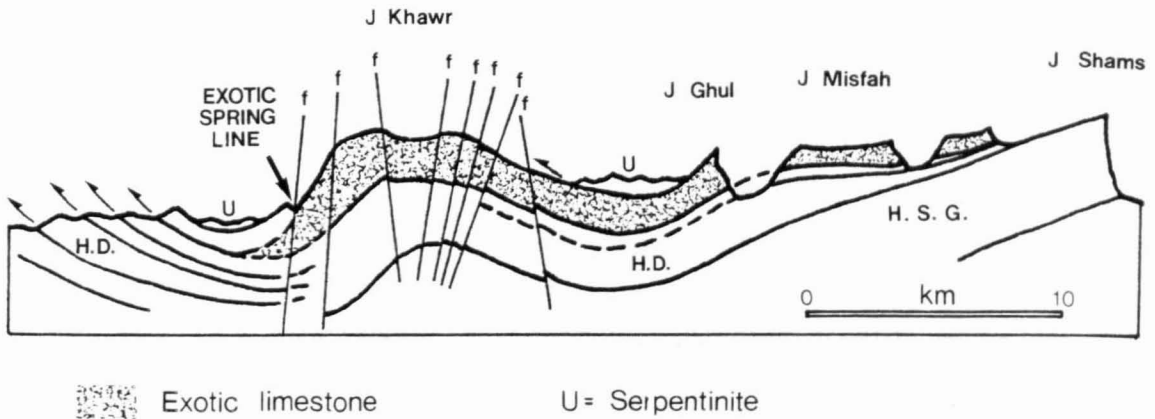
Figure 4.33

Schematic mechanism of an Intermittent
Spring   (after Bogli 1980)

To siphon out volume C requires a
narrow, ie. commpletely water
filled, drain, and an air tight
storage chamber

C
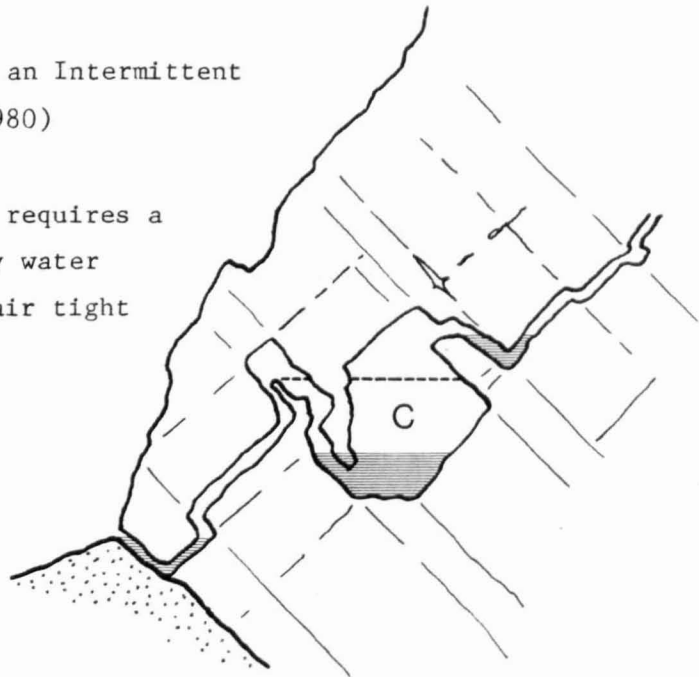
On the other hand, being detached and relatively thin, the Mayhah
formation has been subject to more intense supracrustal deformation and
fracturing during nappe emplacement and uplift, a feature most clearly
displayed in the massive irregular box folds of Jebel Sumeini.

Bowen-Jones (1978) reported hot (about 39 C?) springs, with E.C.s of
greater than 1000 μmhos, from the Mayhah formation at "the foot of Jebel
Rais" in the Indhid valley about 15 km north of Miskin, but these could not
be located in the present study. Judging from the absence of substantial
agriculture in this area, their total discharge is probably negligible. The
only usable groundwater occurrence is on the northern side of Jebel Ghashnah
(Ajran village) where a minor spring-line discharges a total of about 20
l/s. The water chemistry (samples 361, 366, appendix C) is consistent with
normal limestone springs with a moderately long residence time, i.e. a high
Cl^- content, 130 mg/l, for the relatively low temperatures of 31 to 39 C, and
is notable only for its unusually high fluoride content of 0.82 mg/l.
Several factors suggest that further groundwater storage in the Mayhah
formation is insignificant. Firstly the low temperatures and hydrochemistry
are both inconsistent with deep groundwater circulation. Secondly, the
aquifer is overlain by and locally overthrust onto impermeable Hawasina
sediments, thus limiting the potential aquifer volume, and thirdly, despite
locally intense fracturing the Ajran spring yield is small in relation to the
total outcrop volume of Jebel Ghashna.

In Jebel Sumeini there is no groundwater yield from either the Mayhah
formation, nor the overthrust Maqam limestone (a lateral equivalent of the
Akhdar Group).

The Hawasina Nappes

Over a quarter of the Oman mountain arc either consists of, or is
underlain at shallow depth, by the Hawasina nappe sequence. The lithological
variety covers the complete spectrum of carbonate and siliceous oceanic
sediments, but is typically cm. to dm.-bedded fine-grained radiolarites and
more or less silicified shallow to deep-water limestones. Linked primary
porosity is totally absent. Supracrustal isoclinal, box and irregular
folding is ubiquitious, complex and, in the absence of marker horizons, often
structurally indeterminate.

Despite the very large outcrop area and locally intense fracturing, no large springs are known to originate from the Hawasina. The Al Ajal springs (samples 44 and 45, Appendix C) though emergent through Hawasina cherty-limestones have chemical and thermal characteristics which point to a non-local source within either the Muti or Akhdar Group limestones of the upper drainage basin. Indeed the " banking up" of groundwater at alluvial gaps through the Hawasina foothills (e.g. Wadi Bahla, in Stanger, 1987; Wadi Al Kabir, in Letts, 1978) testifies to the effectively impermeable nature of most Hawasina sediments. This is borne out by the few existing borehole tests in Hawasina sediments, such as that of BUEH13 in the Mahda gap where 25 m of limestone mudstone and chert alternations of the Dhera formation produced only a trivial yield (GDC data). Although the Hawasina itself normally behaves as an aquiclude, occasional seepages both from hard rock and its derived alluvium (coarse angular loosely cemented breccia and conglomerate) are the sources of innumerable water-holes, ephemeral surface flows and shallow bailed wells upon which many Bedu depend e.g. the small springs from vertically bedded Wahrah formations east of Araqi and Daris. These sources are recharged by infrequent low altitude rainfall with high evaporation losses and tend to have very long residence times resulting in high chloride and high to very high sulphate compositions, often far in excess of the recommended limits for drinking water (W.H.O., 1971; U.S. DHEW, 1962), in which the E.C. typically ranges from 2000 to 8000 μmhos cm^{-1}. Groundwater in Hawasina drift is generally laterally confined and of shallow depth, and thus seldom justifies pump-set development.

CHAPTER 5

THE OPHIOLITES

5.1 Groundwater and the Ophiolite Environment

Some 30,000 km^2, or about 48% of the Oman mountain area, consists of the Semail Nappe. This, the largest and probably the best exposed and preserved of all ophiolite complexes, has fortuitously undergone minimal deformation relative to most other contemporaneous "alpine" ophiolites scattered throughout the Tethyan orogenic belt. The structural integrity of the nappe as, initially, a single allochthonous sheet up to 15 km thick, has largely been maintained although mid-Tertiary transverse faulting, uplift, erosion and local repetition has since broken up the nappe into about 15 detached blocks.

The ophiolite geomorphology is distinctive and is characteristic of most of the foothill areas. It consists, in the ultramafic rocks, of sharp-peaked sierra of relatively low relief with dark weathering friable surfaces, and of more rounded medium relief hills in the basic rocks. The entire terrain is dissected by innumerable structurally controlled secondary wadis draining into major fault guided or "superimposed" primary wadi systems. Drainage density in the ultramafic areas is substantially greater than in the basic areas. Steep hill slopes, typical of the arid climatic régime, are accentuated in some areas, notably in the north, by continued vigorous uplift resulting in incised precipitous wadi courses. With the exception of occasional remnants of cemented terraces, flat ground within the ophiolite areas is virtually absent.

A marked contrast in geological and hydrogeological properties exists between the upper Semail nappe, the "Crustal Sequence", and the lower nappe or "Mantle Sequence". The former suite is highly variable, both texturally and petrologically, and is dominated by gabbros and basalts with subordinate troctolites, pyroxenites, trondhjemites, diorites and a wide variety of minor acid to ultrabasic variants (e.g. Glennie et al. 1974; Browning, 1982). The structural relationships between the various lithologies are complex, approximating to a

183

pseudo-stratigraphy pierced by several intrusive episodes, but may nevertheless be considered together insofar as their crystalline texture is monotonously impervious, i.e. the crustal sequence as a whole behaves an an aquiclude. The mantle sequence, however, differs markedly from most other crystalline lithologies due to the development of widespread groundwater flow. This is caused by intense fracturing, structural incompetence and thermodynamic instability with respect to normal groundwater recharge compositions. It is therefore more appropriate to think of the mantle sequence as an aquifuge in which fracture flow of low transmissivity is ubiquitous, at least in the near surface environment (i.e. < tens to hundreds of metres depth).

Three groundwater chemical types occur within the ophiolite; cf. Figure 5.1. Two of these, discussed in detail in section 5.3, have a relatively narrow compositional range derived by mutually exclusive water-rock reaction processes, whilst the third and much less common category associated with the crustal sequence, covers a wide range of composition.

5.2 The Crustal Sequence

Few wells and boreholes have been constructed in the basic rocks and most of these have been unsuccessful. For example, of four coastal boreholes penetrating 20 m.b.m.s.l. in basalt beneath shallow sandstone on Masirah Island*, two were completely dry whilst the other two yielded insufficient water to test. Similarly, hand dug wells excavated in massive jointed gabbro adjacent to alluvium in Wadi Bani Kharus produced only trivial yields. Without exception, the "basic rock" sources, given in Table 5.1, have weathered zone source areas, i.e. from a near surface "aquifer" of highly fractured 'in situ' breccia or locally derived gravel. High porosity and permeability in such sources sometimes produces deceptively optimistic results during short period aquifer tests, i.e. high yield with low drawdown. An example from the Birkat al Mawz outwash plain, where 2-5 metres of conglomerate overlies weathered

---

*   Arguably a dextrally displaced fragment of the Semail Nappe (Glennie et al., 1974; Moseley and Abbots, 1979), but indistinguishable from lower basalts of the mainland extrusives.

Figure 5.1

Ophiolite groundwater : Hydrochemical types

+ OH⁻ + CO₃²⁻ + HCO₃⁻
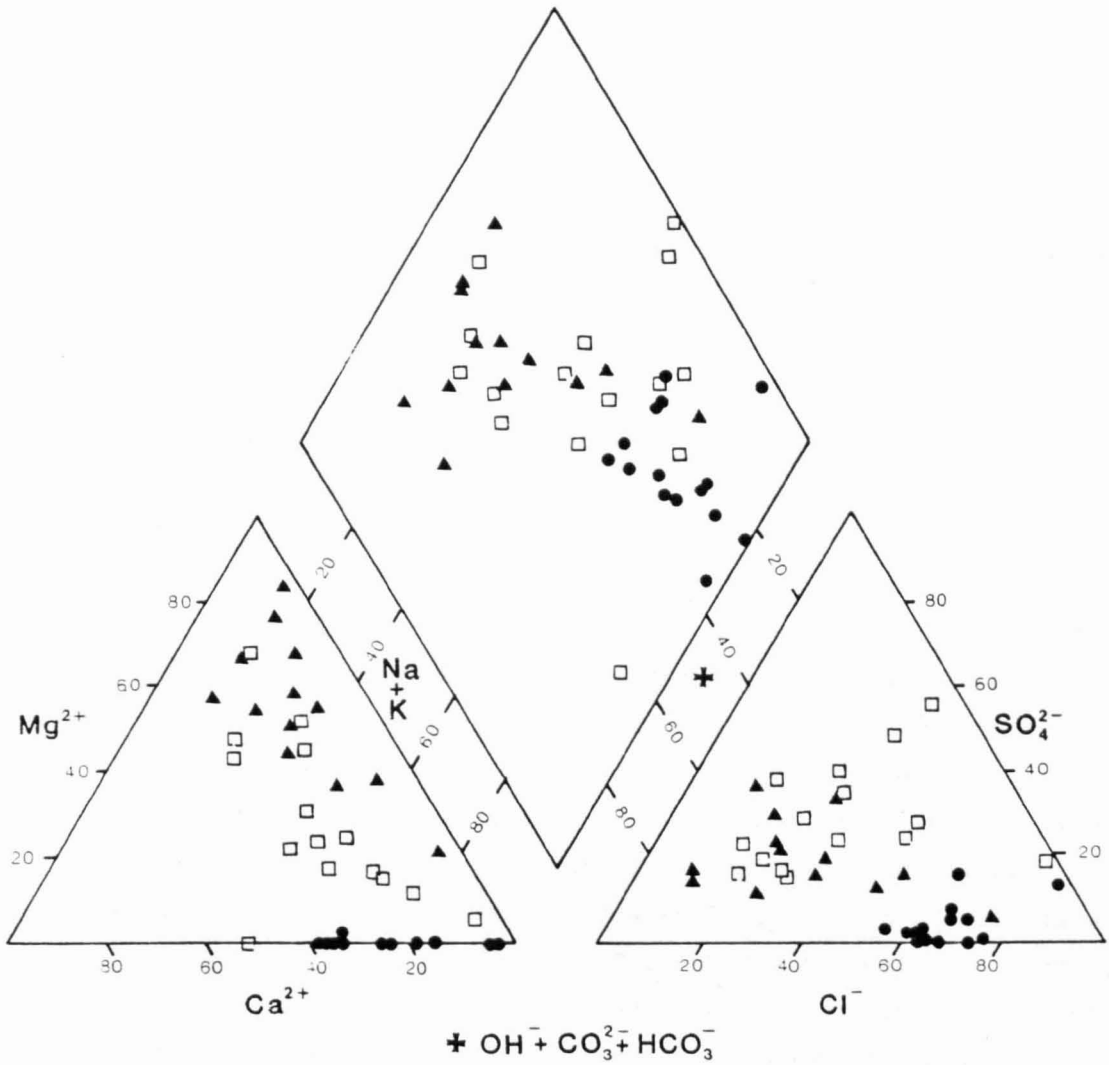
▲ Mantle sequence surface waters
● Mantle sequence alkaline springs
□ Crustal sequence ground waters

gabbro (grid: 6615,25324), produced a rapid and abrupt increase in drawdown coupled with a major loss in yield after 24 hours of pumping, caused by the cone of depression extending rapidly to the lateral confines of the aquifer. A complete gradation exists from fractured fresh gabbro to derived and weathered alluvium. The latter occasionally reaches sufficient volume to supply permanent well or falaj supplies with low storage/high transmissivity characteristics, but such perennial groundwater supplies seldom exceed 2 to 3 litres/sec.

The large hydrochemical range of crustal sequence groundwaters, Figure 5.1, is determined by such factors as residence time, near-surface evaporation and equilibration with aeolian carbonate, rather than by the intrinsic rock chemistry. Two examples of springs emergent from prominent faults in gabbro are known (210, Table 5.1, and 312, Table 5.8, Appendix C), both of which have high Ca/Mg and low $(CO_3 + HCO_3)$ contents indicating an origin in underlying ultramafic rock, but otherwise there are few unique indicators of groundwater provenance. The economic potential of the basalts and associated metalliferous sediments as host rocks to sulphide concentrations has attracted considerable interest (Fleet and Robertson, 1980; Carney and Welland, 1974; Smewing et al., 1977; Alabaster, 1982). The sulphides may lead to highly acidic-sulphate rich groundwaters, as found in the 'Sohar' copper mine. Such anomalies, however, are confined to localised connate conditions and do not affect the hydrochemistry of normal meteoric waters. More generally, the higher sulphate concentrations (Table 5.1) roughly correlate with the corresponding chloride concentrations and are therefore attributable to evaporation rather than to primary solution. A few Cu-Pb-Zn traces are noted (appendix C15) but in view of the ubiquitously alkaline state of groundwater throughout the mountain region, in which the solubility of most transition metal species is depressed (Stumm and Morgan, 1970; Garrels and Chryst, 1965), they are disregarded as significant geochemical indicators.

5.3 Groundwater in the Mantle Sequence

About 60% of the exposed ophiolites are "mantle sequence" rocks whose primary composition consists exclusively of the ultramafic

186

Table 5.1

GROUNDWATER COMPOSITIONS FROM THE CRUSTAL SEQUENCE

No.	pH	E.C.	Ca	Mg	Na	K	Sr	CO	HCO	SO4	Cl	NO3
127	7.8	1665	83	59	347	5.4	1.6	0	290	363	310	15.1
126	8.4	545	36	25	110	4.1	0.3	12	218	167	50	17.7
190	8.0	545	43	35	31	2.6	0.4	0	268	79	47	4.4
194	7.5	1410	134	57	184	2.6	1.6	0	368	374	193	8.4
195	8.4	460	19	42	16	2.4	0.2	5	171	95	63	0.4
210*	8.9	5000	626	.2	669	3.7	2.0	10	16	527	1620	2.7
239	7.4	3040	128	157	425	6.8	2.1	0	408	526	710	19.0
248	8.3	629	31	40	73	2.3	0.5	0	283	77	40	16.6
264	8.9	2320	63	16	105	3.5	0.8	3	183	622	68	9.9
272	8.1	4410	284	173	720	1.3	4.2	0	254	1594	810	23
273	8.7	2860	109	51	580	0.9	1.4	0	356	815	430	20
274	8.9	1710	73	36	285	4.1	1.2	0	271	279	360	19
330	8.5	963	32	65	78	1.3	0.6	0	346	68	106	3.8
338	8.2	1905	52	28	353	1.6	0.9	0	335	247	370	12.5
339	8.8	826	8	5	178	1.3	0.1	5	307	65	54	12.2
406	8.0	3570	243	115	500	1.9	2.7	0	216	814	360	9.5

N.B. No. Locates source details in appendix C.

* "Al Ain Al Ghumar" is an example of upward seepage from
   underlying ultramafic rock, and is atypical of the
   crustal sequence environment.

minerals: olivine (Fo > 87%) > orthopyroxene (enstatite) > clinopyroxene ± accessory chromite. The great majority of the mantle sequence is partially serpentinised harzburgite with minor dunite and occasional lherzolite which, below the petrologic Moho, may be regarded as originally upper mantle material depleted by metasomatism of all the more mobile elements to leave a geochemically barren refractory residue. The variation of both primary modal and mineral compositions (Brown, 1982; and Figure 5.2) shows no consistent variation with depth, and since the scale of petrologic variation is trivial (normally less than 10 m) compared to the length of groundwater pathways, the mantle sequence compositon may be regarded as effectively homogeneous.

The simple nature of the magnesium silicate geochemistry is reflected by the predominant hydrochemical characteristics of surface and near surface groundwaters such as the high Mg/Ca ratio which develops, even in those wadis with an upstream limestone catchment, ie. with an upstream input of predominantly $Ca^{2+} - 2HCO_3^-$ type (Table 5.2), and by the consistent Mg^{2+} concentrations of about 40 mg/litre, suggestive of approximate water-rock equilibrium conditions. $Mg^{2+}-2HCO_3^-$ type water is generally present as shallow groundwater in the ultramafic wadi gravels and is also common as ephemeral or even perennial surface flow, especially at rock bars, shallow bedrock, or over heavily cemented sections of alluvium (calcrete), where the water table banks up behind hydraulic barriers. In many wadi sections this leads to frequent alternations between surface and groundwater flow.

Village agriculture is primarily dependent upon this "surface" resource, although its position within a wadi course is usually determined, albeit indirectly, by springs of entirely different hydrochemical character. These exceptionally alkaline* springs have a pH of between 11 and 12, due to high $Ca^{2+}-OH^-$ concentrations but, paradoxically in view of the magnesium silicate host rock compositions, have low silica and almost zero Mg^{2+} concentrations (Tables 5.3 and 5.4). Upon emergence and mixing with $Mg^{2+}-2HCO_3^-$ type waters, the hydroxide component of such spring waters precipitates carbonate almost

---

* N.B. Although almost all water in Oman has a pH of > 7, "alkaline" in the context of this chapter refers to extreme alkalinity in which hydroxide predominates.

188

Figure 5.2

Mantle sequence : Mineral and modal compositions
modified after Brown 1982
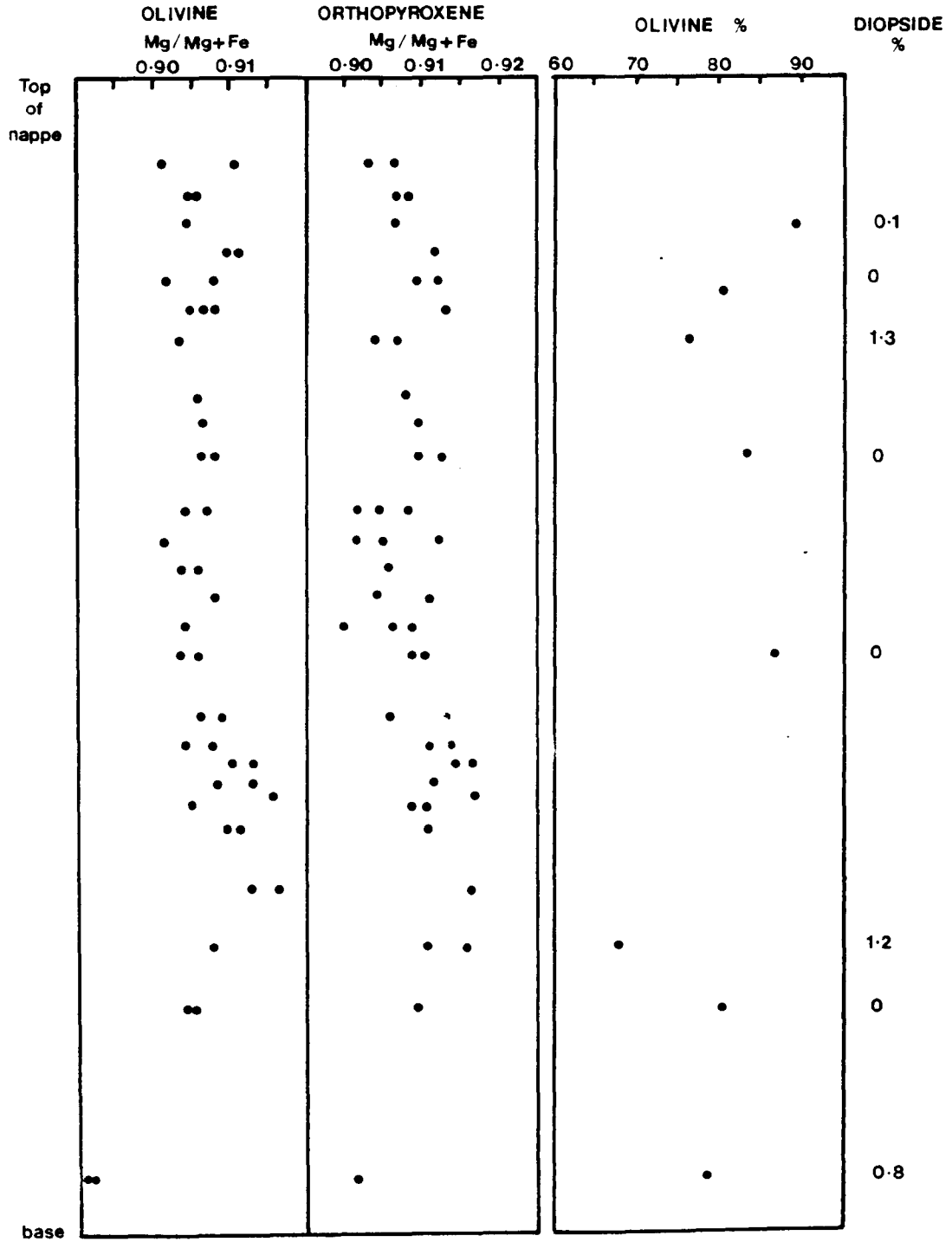
Table 5.2   Examples of Mantle Sequence Wadi Water Compositions

(a)   Wadis with upper catchments in Limestone.

No	pH	EC	Ca	Mg	Na	K	Sr	CO_3	HCO_3	SO_4	NO_3	Cl	SiO_2
22	8.7	445	32	40	50	4	.4	12.0	188	145	6.6	42	
91	8.3	522	24	36	47	5	.2	10	176	46	6	80	
137	8.4	485	29	46	38	4	.2	4	220	59	9	45	19
291	9.0	392	16	36	21	2	.3	0	183	23	5	32	28
314	9.2	409	27	35	15	2	.3	0	171	28	13	27	20

(b)   Wadis with catchments wholly in ultramafic areas

No	pH	EC	Ca	Mg	Na	K	Sr	CO_3	HCO_3	SO_4	NO_3	Cl	SiO_2
21	8.0	305	20	42	12	4	.3	0	166	90	4.4	25	
37	10.4	306	7	37	11	1	.2	16	98	30	9.5	11	16
38	8.1	336	34	40	17	2	.2	0	150	25	13.0	30	18
41	8.5	450	4	59	15	5	.4	0	88	71	7	45	4
75	9.6	605	4	17	110	6	.0	26	21	16	1	181	12
92	8.6	747	24	71	83	5	.2	22	231	84	1	120	18
99	8.1	305	11	31	20	2	.3	0	130	32	4	25	
106	8.3	319	18	34	15	2	.2	8	139	11	3	25	9
130	8.5	385	9	40	93	2	.2	10	134	39	5	50	17
160	9.3	480	3	55	28	2	.3	29	268	140	5	65	
246	8.3	415	9	51	16	1	.2	7	193	32	6	45	
278	9.8	471	12	50	17	2	.3	14	167	30	10	33	22
289	8.6	440	17	40	22	2	.2	7	170	24	10	38	27
290	8.4	451	6	26	25	3	.0	6	101	21	16	66	20
343	9.8	710	8	44	60	3	.3	0	187	35	3	93	20
376	9.0	531	16	40	38	2	.2	6	165	33	2	59	14
396	8.7	385	11	34	11	1	.3	0	167	31	9	31	11

Table 5.3

ALKALINE SPRING COMPOSITIONS FROM THE BASAL
THRUST ZONE OF THE SEMAIL NAPPE

I	ph	Ca	Mg	Na	K	OH	SO_4	NO_3	Cl
62	11.6	61	0.026	230	12.3	77	8	0.4	317
63	11.7	54	0.021	250	13.0	76	0	0.2	340
64	11.6	38	0.352	251	15.6	59	8	0.4	349
65	11.8	23	0.008	331	15.6	85	45	2.2	411
66	11.6	23	0.010	260	14.4	78	30	0.0	394
74	11.0	50	2.200	115	6.50	31	23	0.7	160
116	11.4	79	0.100	174	7.60	57	21	0.9	255
205	11.8	52	0.050	317	11.8	105	11	2.9	415
206	11.9	55	0.023	273	13.3	115	4	5.6	385
207	11.9	91	0.033	287	13.4	104	32	4.5	380
208	11.9	89	0.054	245	13.8	104	13	5.1	365
286	11.4	59	2.600	254	10.7	76	7	2.8	224
287	11.5	62	0.051	184	8.70	42	6	0.5	256
288	11.4	55	0.037	191	8.80	68	6	0.7	280
369	11.2	71	0.290	133	7.40	45	7	2.3	212
370	11.2	76	0.015	136	6.80	53	12	1.9	221
422	11.8	66	0.026	66	6.00	39	17	6.0	178
MEAN:		59	0.347	217	10	71	15	2	302

Ca/Sr ratio = 276.5   Na/K ratio = 20.3
Na/Cl ratio = 0.7   Ca/K ratio = 0.8

(N.B. 'I' locates source details in appendix C)

Table 5.4

CUMULATE ZONE ALKALINE SPRING COMPOSITIONS

I	ph	Ca	Mg	Na	K	OH	SO_4	NO_3	Cl
48	11.2	29	0.400	173	15.3	40	23	2.0	225
59	11.2	112	0.017	251	7.50	65	37	2.2	430
67	11.6	14	0.100	348	11.2	74	3	1.6	276
70	11.3	117	0.006	243	8.40	64	143	1.1	436
72	11.3	70	0.009	233	14.0	83	19	1.2	320
76	11.2	86	0.177	162	7.60	71	12	1.4	274
78	11.5	78	0.020	144	4.70	59	12	0.0	165
80	11.2	92	0.500	209	8.80	66	9	2.3	227
93	11.4	84	0.380	354	9.30	72	4	0.9	289
105	11.2	64	0.217	78	4.70	34	9	0.8	139
138	11.2	27	0.110	194	11.5	39	7	0.5	236
139	11.0	25	0.150	204	10.6	35	21	0.6	223
203	11.8	45	0.089	309	16.6·	102	30	6.2	370
230	11.7	83	0.062	559	23.0	65	42	5.3	785
231	11.0	4	4.500	841	31.0	14	25	4.1	950
233	11.6	63	0.078	270	12.0	58	2	8.8	380
237	11.7	56	0.111	567	30.3	63	71	0.7	750
238	11.7	72	0.131	565	23.0	83	88	2.0	735
243	11.1	84	0.145	104	7.80	17	45	0.4	211
271	11.4	48	0.266	273	12.1	56	16	0.6	352
279	11.1	53	0.032	165	6.90	59	9	1.3	203
294	11.5	85	0.035	262	6.50	95	7	4.4	446
312	11.4	66	0.002	367	8.90	34	63	2.1	453
342	11.3	45	0.001	207	5.50	38	32·	3.5	324
354	11.3	33	0.100	163	8.80	65	7	2.0	205
364	11.5	61	0.034	174	9.90	55	7	0.8	251
365	11.5	57	0.026	175	9.10	70	7	3.9	229
372	11.5	57	0.420	254	12.9	80	15	3.7	317
373	11.1	50	2.020	204	6.10	45	20	3.5	269
375	11.3	29	0.015	120	4.50	42	15	3.2	151
393	11.2	58	0.004	149	6.10	60	18	1.3	213
394	11.0	4	0.036	306	12.5	28	16	0.4	330
408	11.4	59	0.004	138	6.10	62	3	5.7	174
454	11.6	54	0.071	407	12.7	93	47	5.5	341
456	11.4	43	2.200	100	4.90	62	10	4.4	121
MEAN:		57	0.353	265	11	58	25	2	337

Ca/Sr ratio = 175.1   Na/K ratio = 23.2
Na/Cl ratio =   0.8   Ca/OH ratio = 1.0

(N.B. 'I' locates source details in appendix C)

192

instantaneously (Plate 5.1) by such reactions as:

$$Ca^{2+} + 2OH^- + Mg_2^{2+} + 2HCO_3^- \rightarrow CaCO_3 + 2H_2O + Mg_2^{2+} + CO_3^{2-} \quad (1)$$
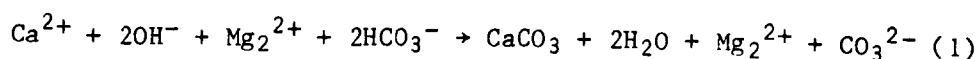
In this reaction the common ion effect retains the magnesium in "Mg^{2+}-$2HCO_3^-$" dominated solution, and the CO^2 solubility increases with the pH. Consequently as alkaline water emerges by upward seepage from the ultramafic rock, the saturated wadi gravels become impervious due to carbonate cementation, thereby forcing the main flow of alluvial groundwater to the surface. Alternatively, emergence of alkaline water from exposed subaerial fractures in the ultramafic rock facilitates direct reaction with atmospheric CO_2:

$$Ca^{2+} + 2OH^- + CO_2 \rightarrow CaCO_3 + H_2O \qquad\qquad (2)$$
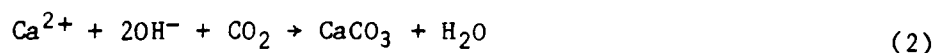
Thus alkaline spring occurrence is closely associated with travertine and calcrete/conglomerate terraces and/or wadi beds (Plate 5.1). Furthermore the "self sealing" tendency of individual spring pathways results in both lateral and vertical spring migrations, often to successively higher outflow points. In this way, flat sedimentary terraces frequently occur close to emergent wadi water, thereby creating the conditions necessary for village settlement. Less usefully, the propensity of hydroxide solutions to precipitate carbonates upon aeration has the unfortunate consequence that pump impeller housings and borehole screens in such waters rapidly become occluded and useless.

Although the low relief intercepts of mantle sequence groundwater pathways commonly coincide with bicarbonate type wadi water, there are many examples of either isolated alkaline springs, or of alkaline e.g. springs emergent up to 50 m above the associated wadi waters (eg. Murayrat, Wihi al Murr, Jalah; and Wadi Jizzi, Jill alkaline spring line respectively, cf. appendix C), i.e. independent of local wadi water recharge. Indeed, the occurrence of alkaline groundwater in all known wells and boreholes within massive ultramafic rock (Wadi Kabir, Izki, Ibra, Nizwa, Semail Firq, Taymissah, Dahir and many isolated hand-dug wells) all testified to its almost universal presence in the ultramafic saturated zone. Notwithstanding this widespread groundwater

distribution, its occurrence as springs shows a clear correspondence with major structural features of the mantle sequence, and in particular with the ophiolite basal thrust zone and crustal-mantle sequence boundaries (Figure 5.3). The basal sheared zone is the most prominently fractured feature of the Semail Nappe. It is typically composed of up to about 800 m of complex, locally imbricated or brecciated serpentinite in which foliation is parallel or sub-parallel to the basal thrust. The lower boundary, i.e. the thrust plane itself, is marked by a thin, generally less than one metre, cataclastic, sometimes mylonitic reworked serpentinite schist, whilst the upper boundary is an ill defined upward passage into less severely sheared harzburgite. Despite its homogeneous geochemistry, varied and alternating degrees of foliation and serpentinisation tends to create a pseudo-layered appearance which has been mapped as a separate "banded unit" by Glennie, 1974; and Searle, 1980. The potential for groundwater seepage through such an intensely sheared unit is great on both meso- and macro-scales.

Near the top of the ultramafic sequence, a transition from harzburgite to rocks of essentially magmatic origin is marked by the sporadic distribution of chromite segregations, dominant dunite, a great increase in clinopyroxene content (i.e. Lherzolite), and a layered macrotexture. Higher in the sequence there is progressive olivine depletion and plagioclase enrichment. Thus a marked contrast in structural competence arises between gabbro and underlying serpentinite/harzburgite which, during tectonism, has resulted in increased shearing and local dislocation. Though insufficient to disrupt the overall unity of the nappe structure, these features have been sufficient to produce an important groundwater pathway within the nappe. In addition to the apparently higher transmissivity, the common occurrence of alkaline spring waters at or close to the crustal-mantle boundary is also enhanced by the hydraulic barrier effect of the crustal sequence which tends to outcrop downstream and orthogonal to the surface drainage pattern (Figure 5.3). Apart from these two settings, most of the remaining alkaline springs are closely associated with further complications of the lower nappe macro-structure such as local convergence of the basal thrust and cumulate zones, with

194

Figure 5·3

Simplified map of the Semail Nappe showing alkaline
ground water occurrence in relation
to the mantle sequence

LOCATION MAP

IRAN

ARABIAN
GULF

GULF
OF
OMAN

U.A.E

SAUDI
ARABIA

OMAN

N

● alkaline spring occurrence

⚡ alkaline water in wells and boreholes

mantle sequence,mainly harzburgite

crustal sequence-mafic,ultramafic cumulates,gabbros,dolerites,
basalts etc,.

0   Km   50

FUJAIRAH

WADI FAYD

ABAL

HAYL

B'LAD

AL QUFAYS

RAYL

DAHIR

HUWAYL
QUFAYS

HAYL

RUSTAQ

MUSAYFIYAH

HAWQAYN

SLAYAH

AL KHOD

MUSCAT

KARKU

SEMAIL
TAWIYAH

FALAJ

NIDAB

MAZERA
MAGHUTH

KHAFIFAH

SAYYAH

JALAH

BAHLA

JILL

MAZARA

SAMAD

IBRA

Ophiolite outline after Glennie et. al

consequent thinning and folding at the leading edge (Jebel Awq, Bahla, Ibra), and major faults, at least some of which appear to be relics of original transform faults (Smewing, 1982). The spring-structural association is particularly striking where the mantle sequence terminates at marginal faults against alluvium of lower relief. Here spring development is unrestricted by either flash flood erosion or hard-rock confinement, and consequently develops linear travertine terraces up to several kilometres in length (e.g. Jill, Mazara, Rustaq and Al Uthrat spring lines).

5.4 Low Temperature Serpentinisation

In considering the origin of $Ca^{2+}-2OH^-$ type groundwaters, it is necessary to differentiate between two superficially similar processes; "medium temperature alteration" and "low temperature precipitation" serpentinisation. The first process, which has produced the most extensive and obvious results, was one of partial hydration (i.e. serpentinisation) of the entire mantle sequence. With the exception of wholly serpentinised fracture planes, the field and petrographic evidence indicates more or less uniform and pervasive hydration, i.e. unrelated to either the water table or proximity of the weathered zone, in which alteration of the anhydrous mafic phases is clearly pre- or syn-tectonic, and is contemporaneous with nappe generation, detachment and transport in the marine environment (Glennie, 1974; Brown, 1982). Similar observations in other alpine ultramafic environments, in conjunction with experimental evidence for the system $MgO-SiO_2-H_2O$ (Bowen and Tuttle, 1949) have impressed early workers with the "hydrothermal" or even "metasomatic" character of such serpentinisation processes. In particular the reaction:

$$6\ Mg_2SiO_4 + Mg_3Si_4\ O_{10}(OH)_2 + 9H_2O \rightarrow 5\ Mg_3Si_2O_5(OH)_2 \qquad (3)$$

forsterite   talc   serpentine
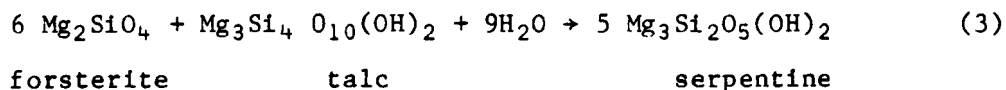
(Chernosky, 1973)

fixes the upper temperature limit of serpentine formation at 500° C. Various models have been proposed for "normal" serpentinisation at slightly lower temperatures, such as the brucite precipitation/constant bulk-rock composition reaction;

$$2 \, Mg_2SiO_4 \; + \; 3H_2O \; \rightarrow \; Mg_3Si_2O_5(OH)_4 + \; Mg(OH)_2 \qquad (4)$$

forsterite   serpentine   brucite

(Johannes, 1968),
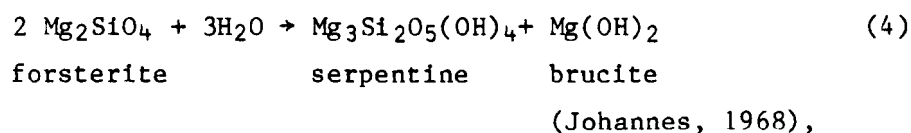
the constant volume reaction;

$$5 \, Mg_2SiO_4 \; + \; 4H_2O \; \rightarrow \; 2Mg_3Si_2O_5(OH)_4 \; + \; 4MgO \; + \; SiO_2 \qquad (5)$$

forsterite   serpentine   removed

(Turner and Verhoogen, 1960; Hostetler et al., 1966),
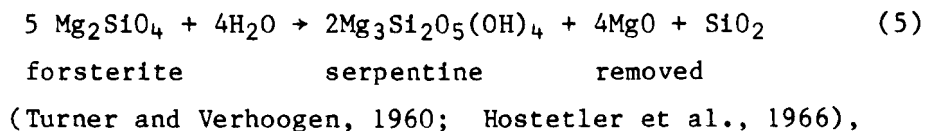
and a "compromise reaction" requiring an external source of silica;

$$3 \, Mg_2SiO_4 \; + \; 4H_2O \; + \; SiO_2 \; \rightarrow \; 2 \, Mg_3Si_2O_5(OH)_4 \qquad (6)$$

forsterite   serpentine

(Coleman, 1971).
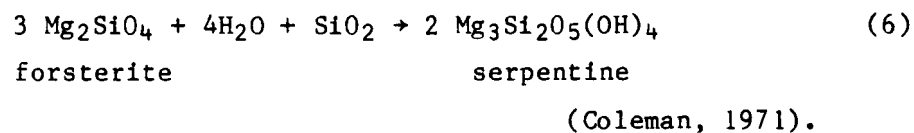
Calculations involving forsterite and brucite show that such reactions may take place between $400^\circ C$ (4 Kbars), and $180^\circ C$ at atmospheric pressure (Bowen and Tuttle, 1949; Powell, 1978), but these concern only the principal end-member component, forsterite, thereby creating problems of MgO/SiO_2 redistribution. To some extent this is obviated by incorporating the pyroxene component (if present in the primary assemblage) in the reaction;

$$Mg_2SiO_4 \; + \; MgSiO_3 \; + \; 2H_2O \; \rightarrow \; Mg_3Si_2O_5(OH)_4 \qquad (7)$$

forsterite enstatite   serpentine

(Coleman, 1971)
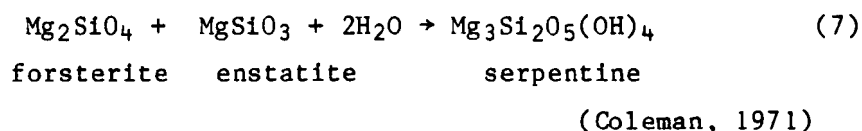
However, these are all "in situ" alteration reactions and are not necessarily applicable to the low pressure - temperature conditions of meteoric circulation. More recently therefore, attention has been focussed upon the isotopic and hydrochemical evidence for low temperature serpentinisation (Barnes, La-Marche and Himmelberg, 1967; Barnes and O'Neil, 1969; Barnes, Rapp, O'Neil, Sheppard and Gude, 1972; Wenner and Taylor, 1974; and Barnes, O'Neil and Trescases, 1978). In this process the serpentinising fluid pathways may be regarded as a chemically open system in which the input consists of essentially $Mg^{2+}-2HCO_3^-$ type surface water, and the output consists of the $Ca^{2+}-2OH^-$ type spring waters. The major ions Na^+, K^+, SO_4^{2-}, Cl^- and NO_3^- are only indirectly affected by the serpentinisation reactions

and are therefore considered separately. The partial reactions may be expressed for each end-member phase as:

olivine dissolution

$$3\ H_2O\ +\ 2Mg_2SiO_4\ \rightarrow\ Mg_3Si_2O_5(OH)_4\ +\ Mg^{2+}\ +\ 2OH^- \tag{8}$$
$$\text{forsterite} \qquad\qquad \text{serpentine}$$

$$2\ H_2O\ +\ Fe_2\ SiO_4\ \rightarrow\ 2Fe(OH)_2\ +\ SiO_2 \tag{9}$$
$$\text{fayalite}$$

pyroxene dissolution

$$2H_2O\ +\ 3MgSiO_3\ \rightarrow\ Mg_3Si_2O_5(OH)_4\ +\ SiO_2 \tag{10}$$

$$H_2O\ +\ FeSiO_3\ \rightarrow\ Fe(OH)_2\ +\ SiO_2 \tag{11}$$

$$H_2O\ +\ CaSiO_3\ \rightarrow\ Ca^{2+}\ +\ 2OH\ +\ SiO_2 \tag{12}$$

The precipitation reactions are

$$3(Mg^{2+}\ +\ 2OH^-)\ +\ 2SiO_2\ \rightarrow\ Mg_3Si_2O_5(OH)_4\ +\ H_2O \tag{13}$$

with the additional reactions, involving the input components, of:

$$Mg^{2+}\ +\ HCO_3^-\ +\ OH^-\ \rightarrow\ MgCO_3\ +\ H_2O \tag{14}$$

$$Ca^{2+}\ +\ HCO_3^-\ +\ OH^-\ \rightarrow\ CaCO_3\ +\ H_2O \tag{15}$$

In the absence of petrologic and kinetic details, the total reaction equation is indeterminate. Nevertheless several conclusions may be drawn from these equations. Since the fluid output is almost totally devoid of SiO_2 and Mg (Tables 5.3 and 5.4) irrespective of the Mg input, these components are conserved within the system. The reaction of equation (13) therefore involves a balance between Mg, from equation (8) and the input water, and silica derived from equations (9) to (12). Hence serpentine precipitation appears to be buffered by differential olivine-pyroxene dissolution, cf. Section 5.6.

In view of the equimolar $Mg^{2+}/2OH^-$ ratio in equations (8) and (13), "output" hydroxide can be generated only by equation (12) or by alternative iron end-member hydration reactions (i.e. variations in equations (9) and (11)). The latter possibility is difficult to assess directly due to the poorly crystallised, fine grained and finely disseminated nature of the residual iron minerals. However, as the average molar Ca/OH ratio is close to unity, at 1.04, as predicted by equation (12), clinopyroxene[1] dissolution seems to be the only significant process involved in generating the hydroxide signature of the "output" water. Conversely, the $Ca^{2+}-2OH^-$ output of spring water must represent a minimum degree of serpentinisation. Indeed as Ca is only present in the rock to an extent of 0.69% CaO (σ = 0.4%, 23 analyses, excluding two diopside rich anomalies of about 7.1% CaO), it is probable that the great majority of low temperature serpentinisation involves just olivine and enstatite to leave minimal trace of Ca^{2+}, Mg^{2+} or OH^- in the output spring water. Furthermore, any original bicarbonate (or carbonate) in the input water would be precipitated due to reactions (14) and (15) giving rise to carbonates ranging in composition from aragonite to dolomite, thereby accounting for the exclusively Ca-OH-Na-Cl spring chemistries, irrespective of the input water compositions.

The field criteria for recognition of low temperature serpentine are: (1) the lack of any perceptible fibrous or crystalline structure, (2) the absence of iron phases or other inclusions resulting in typically pale colours varying from waxy yellow, cream or green to silver or, rarely, translucent white, and (3) relative softness of the mineral. Some specimens , in fact, closely resemble talc in appearance, hardness and "soapy feel" and therefore require chemical or X-ray diffraction analysis for correct identification.

A slight but consistent chemical contrast between high and low temperature serpentine is summarised in Table 5.5 in which the original analyses have been recalculated to "subtract" the chromite present in alteration serpentine. The contrasting compositions are arguably affected by finely disseminated Fe and Mn hydration products in the

---

[1] Strictly, the CaO content of the mantle sequence is about equally divided between diopside (about 1% of the rock, with a CaO content of 20%) and enstatite (about 20% of the rock, with a CaO content of 1%). For simplicity of discussion, "clinopyroxene" is regarded as synonymous with "Ca-pyroxene" irrespective of whether the latter exists as diopside or as solid solution within the enstatite.

alteration serpentine, but it is difficult to account for the low NiO and Al_2O_3 concentrations in precipitation serpentine other than by their relative insolubility (Pourbaix, 1963; Barnes and O'Neil, 1969; Barnes et al., 1972) and hence exclusion from, alkaline groundwaters.

In thin section the low temperature serpentine is identified as late stage (cross-cutting), unstrained, colourless and generally inclusion free veins. Open space deposition of larger compound veins of serpentine and carbonate are uncommon but diagnostic features. One such example from the Dibba ultramafic area (Sample 7, Table 5.5) displayed a unique petrofabric of cream coloured translucent botryoidal serpentine with orthorhombic extinction crosses, within net veined dolomite. This sample was also atypical in having an unusually high Si/Mg ratio and may therefore be unrepresentative of normal low temperature serpentines.

X-ray diffraction proved less useful in discriminating between serpentines of high and low temperature origin. Only the rare orthorhombic form is readily differentiable due to its low crystallinity which gives rise to broadened peaks. Otherwise serpentines of varying habit (vein or matrix) and texture appear to be complex mixtures of the various polymorphs described elsewhere (eg. Whittaker and Zussman, 1956; Wicks, 1969). All produce identical main peak reflections; 002, 020 and 004. The most variable and hence diagnostic parts of the spectra, from $d = 2.15$ to $d = 3.60$, are shown in figure 5.4, but apart from a tendency for low temperature serpentines to crystallise as chrysotile rather than lizardite, there is no clear correspondence between origin and diffraction pattern.

Alkaline Groundwater Provenance

Although the extent of the serpentinising fluid pathways is not amenable to direct observation, several features are incompatible with a purely local springwater origin. For example, the differential head between some springs and adjacent spring waters, the common lack of any significant catchment area in the spring vicinity, and the slow rate of recession of many springs observed over two to three years, can only be explained by a long groundwater pathway and consequently a large storage capacity. Moreover, seven of the nine tritium measurements of alkaline springs were sufficiently low to confirm their origin as pre-nuclear bomb test recharge, (appendix B). This indicates a minimum base flow

Table 5.5 Chemical variation between the two Serpentine facies

Samples 1-6 by X-Ray fluorescence, 7 by electron microprobe

| Sample | Alteration Serpentine* | | | Precipitation Serpentine | | | |
	1	2	3	4	5	6	7
SiO_2	38.50	36.80	39.35	40.92	41.96	42.49	48.29
Al_2O_3	0.77	3.39	1.05	0.0	0.01	0.0	0.28
Fe_2O_3	8.26	11.59	8.84	6.02	1.34	1.57	0.05
MgO	38.22	34.15	37.04	40.11	41.21	41.52	35.08
CaO	0.0	0.35	0.16	0.32	0.19	0.12	-
MnO	0.13	0.17	0.12	0.05	0.02	0.01	0.05
Na_2O	0.76	0.0	0.0	0.03	0.83	0.0	0.0
P_2O_5	0.04	0.0	0.05	0.0	0.04	0.0	0.0
Cr_2O_3	0.0	0.0	0.0	0.6	0.0	0.7	0.05
NiO	0.29	0.20	0.34	0.05	0.10	0.07	0.05
S	0.0	0.04	0.0	0.0	0.01	0.0	0.12
L.O.I	13.34	13.30	12.99	13.97	13.88	14.49	13.60
Σ	100	100	100	101.56	99.62	100.32	97.09
	(100.82)	(99-82)	(99.77)				

* As analysed the Cr_2O_3 content varies from 0.37 to 0.48% (5 analyses) due to inclusions of aluminous magnesiochromite. In order to compare pure serpentine chemistries, the chromite phase has been "subtracted" using the ratios "Cr_2O_3 49.3, FeO 14.5, MgO 13.9, Al_2O_3 16.2, (Peters and Kramers) and the resulting compositions recalculated to 100%. K_2O and BaO concentrations are both less than 0.1%.

1   Dark green serpentinised harzburgite from the base of the Semail nappe.

2 and 3 Black serpentinised harzburgite from near the top of the mantle sequence.

4   Soft silvery coating on transparent precipitated tabular brucite. From the base of the Semail nappe.

5   Yellow "soapy" precipitated serpentine from the mid-ultramafic unit.

6   Pale green "waxy" serpentine from the upper ultramafic unit.

7   Translucent cream botryoidal orthorhombic serpentine from vein in Dibba ultramafics.

Apart from the accessory chromite, the monominerallic serpentine composition of all samples was confirmed by X-ray diffraction.

201

Figure 5.4

X–Ray diffraction spectra of mantle sequence serpentines
(d 2.25 to 3.60)
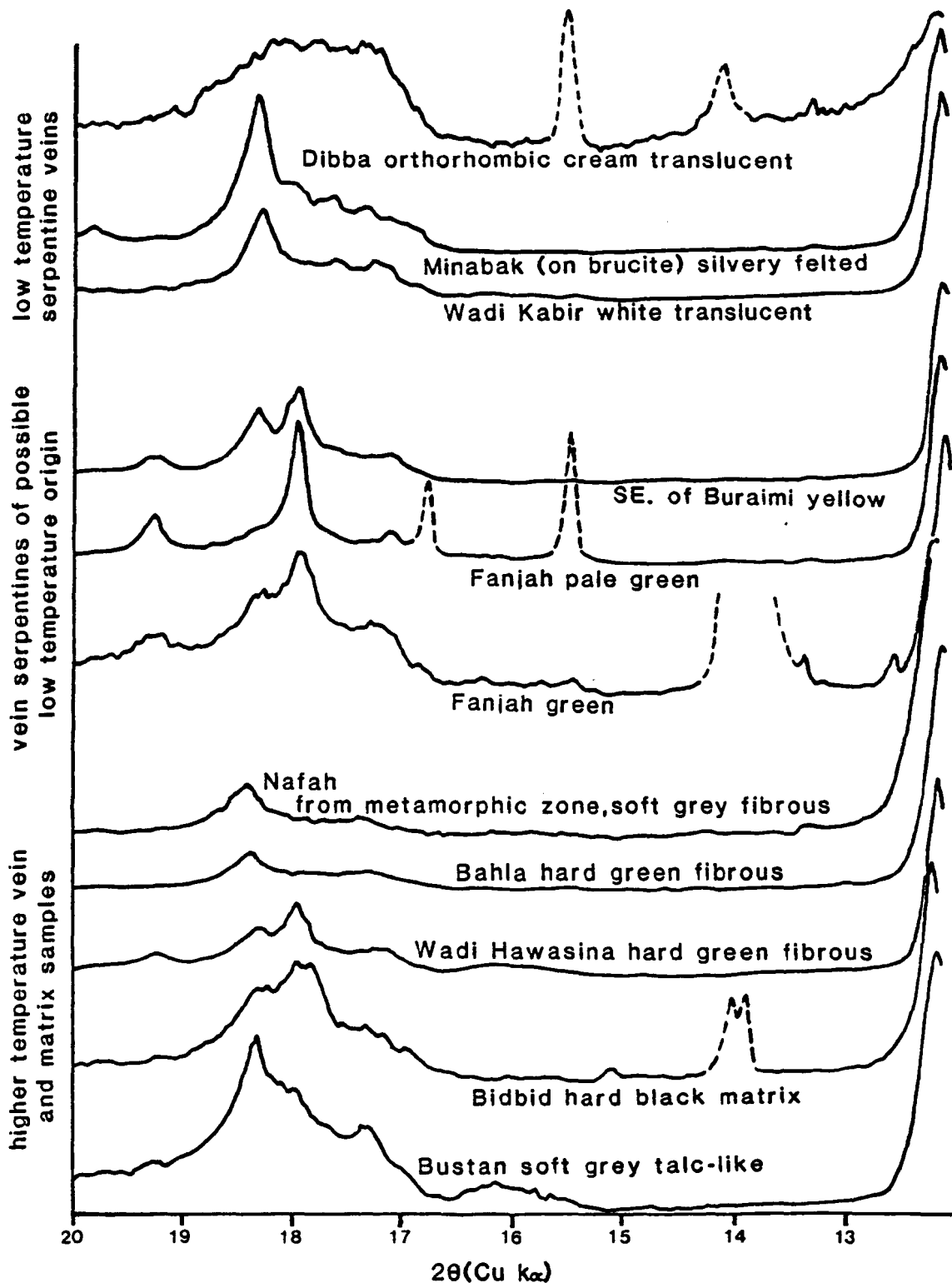
all specimens produced major peak reflections – 002 ,020 and 004
with normal spacing and intensity.
Spurious peaks,mainly due to dolomite,are indicated by broken lines

residence time of 25 years, which again points to a long groundwater pathway. The two larger tritium values (Wadis Bahla and Hawqayn), are both from sites where large alluvial grou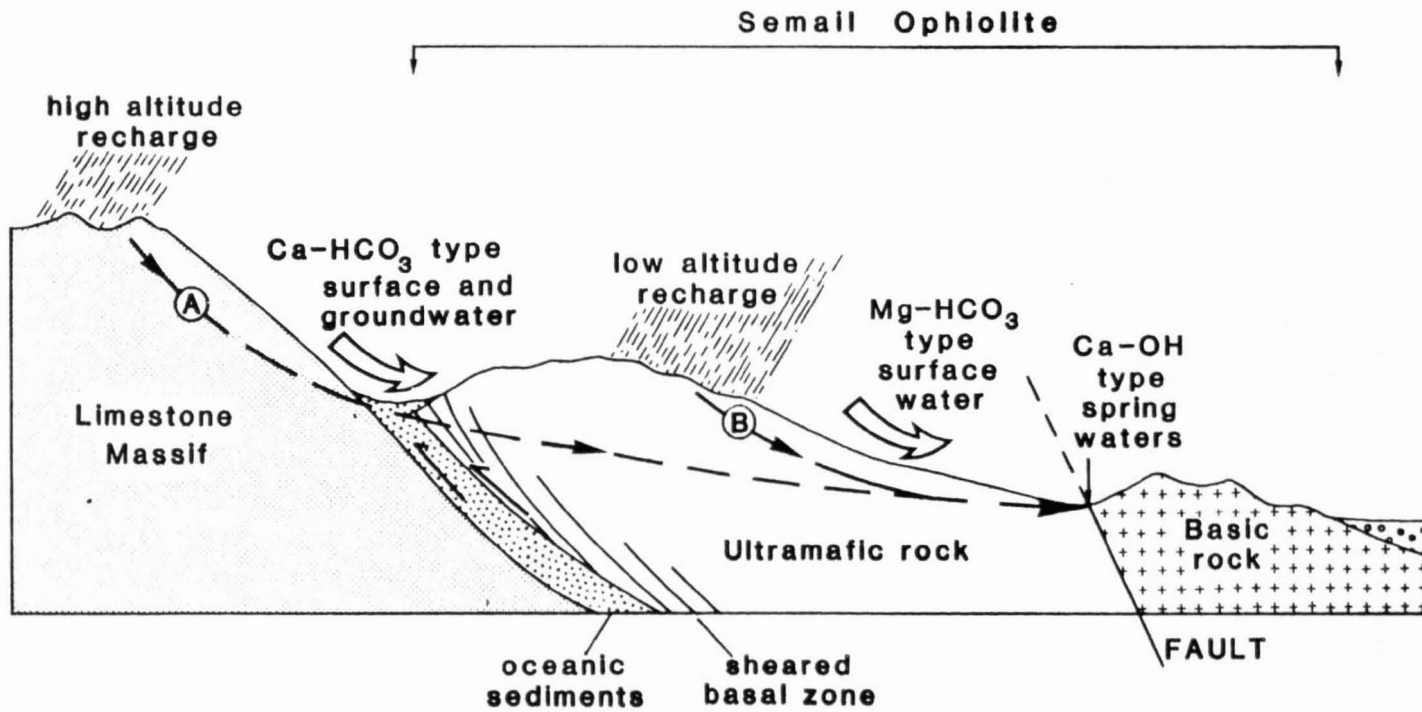ndwater or surface flow is likely to recharge short, relatively local flowpaths in the upstream ultramafic rock. Indeed, the more recent low tritium and older but higher tritium values from Bahla provide proof of groundwater pathways with both long and short residence times contributing to single spring discharges.

Two potential source areas, shown schematically in Figure 5.5 as 'A' and 'B' could account for the extensive flowpaths. In order to test these alternatives the $\delta^{18}O/\delta^2H$ isotopic composition of ten paired samples of adjacent spring and wadi waters were analysed. Spring waters originating through pathway A would be of distant, often high altitude, recharge having an isotopic composition unrelated to the relatively local recharge of wadi waters. On the other hand, in pathway B, each pair of wadi and spring waters have a common recharge area and should therefore show a consistent isotopic relationship. Despite the disparity of residence times between surface and spring waters, the strong δ^2H depletion of every paired sample, shown in figure 5.6, therefore shows the second alternative to be correct, i.e. deep groundwater flow originating from beyond the mantle sequence can be discounted.

Regarding the depth of ultramafic groundwater circulation, the only indication is that of spring temperature. This varies from 21° to 40.5° C as compared to the normal groundwater temperature in Oman (at comparable altitude) of 30 to 33° C. The lower spring temperatures correspond to small discharge springs and seepages where evaporative cooling is intense. Otherwise comparison between alkaline spring waters with surface stream waters, where they occur in close proximity, shows the former to be almost invariably warmer by an average of 4.3° C. In some cases it is possible that this differential water temperature is also due to evaporative cooling, but many springs have temperatures exceeding 36° C which, together with differential water temperatures of up to 15° C, clearly indicates geothermal warming. Therefore if a geothermal gradient of 1° C/30 m and isotropic thermal conditions are assumed, the data (appendix C) suggests that alkaline groundwater circulation varies from near the surface to approximately 300 m in depth.

Figure 5.5

Typical geological section to show potential groundwater pathways through the ultramafic rock

Semail Ophiolite

high altitude recharge

Ca-HCO$_3$ type surface and groundwater

low altitude recharge

Mg-HCO$_3$ type surface water

Ca-OH type spring waters

Limestone Massif

Ⓐ

Ⓑ

Ultramafic rock

Basic rock

oceanic sediments

sheared basal zone

FAULT

Length of section about 30 Kilometers

Figure 5.6

Isotopic Composition of Alkaline Springs

and Associated Wadi Waters
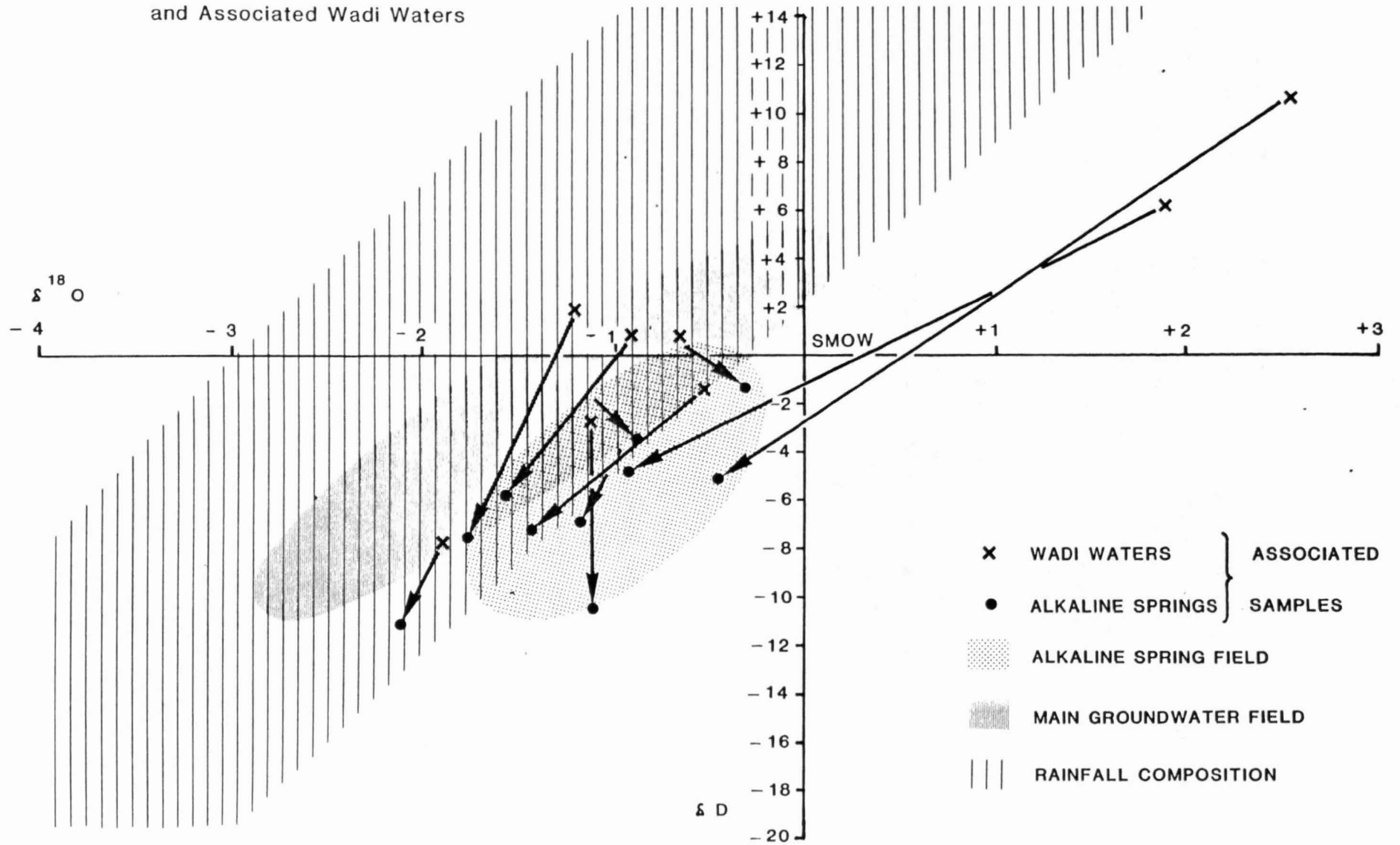
5.5 By-Products of Low Temperature Serpentinisation

Carbonates and Hydroxides

The most obvious consequence of meteoric serpentinisation is the exceptionally high pH which, as already shown, results in widespread carbonate precipitation. Three carbonation processes are involved: (1) air-water reaction, (2) water mixing reaction, and (3) water-hydroxide (solid) alteration, the latter being strictly a post serpentinisation process.

The direct atmospheric CO_2 reaction, equation (2), produces either aragonite or low magnesium calcite, and occurs in several habits such as thin (~ 1 mm) surface films on the surface of non turbulent spring chambers, and small white "cauliflower shaped" concretions along rock surface/joint intersections (Plate 5.2). In an example from Jebel Awq (EA 5430, 5230) alkaline groundwater seepage was sufficiently small to be entirely lost by rapid evaporation. Consequently carbonation was incomplete, the Ca^{2+} and OH^- activities were raised above the $Ca(OH)_2$ saturation level, and portlandite, $Ca(OH)_2$, was precipitated as a microcrystalline intergrowth with calcite (Neal and Stanger, 1984). More commonly, isolated spring flows are larger and more turbulent, thereby inducing vigorous aeration, CO_2 mixing and consequently travertine "drape" formation (Plate 5.3). In some areas the need to reduce the spring alkalinity for irrigation has led to artificial utilisation of the same effect. This is traditionally achieved by channelling the spring water into large shallow tanks for maximum atmospheric CO_2 absorption, (Plate 5.4). Utilisation of this effect merely requires periodic removal of the lime mud precipitate.

The mixing process, reaction (1), takes place both at the surface (Plate 5.1) and within the ultramafic rock. The almost instant surface precipitation produces granular aragonite whereas precipitates in the groundwater environment may be euhedral aragonite or calcite. Groundwater mixing is an irregular episodic process during which Ca - OH type groundwater, generated by water-rock reaction under "quiescent" aquifer conditions, is diluted with a relatively smaller volume of

Mg-HCO$_3$ type water by flash flood recharge. Subsequently, during drought and recession, the diluted upper groundwater system regains chemical equilibrium with the host rock and reverts to normal alkaline conditions. Fluctuations in the piezometric surface therefore coincide with periods of hydrochemical mixing and potential carbonate precipitation, thus accounting for the abundant veins and open-space crystal aggregates of white to pale green pseudo-hexagonal calcite, typically found in the lower levels of ultramafic well excavations. During the course of eight field visits to an alkaline spring at Karku (FA 6069, 5831) detailed examination of a gelatinous sediment in the base of the spring chamber yielded calcite of a granular texture. This was of entirely different texture from the surface calcite layer which sealed the spring chamber from atmospheric CO$_2$ contact, and was apparently flushed out of the ultramafic rock as an unlithified precipitate by the circulating groundwater. Isotopic analysis of the differing carbonate habits (Table 5.6) illustrates the close similarity between isotopically "heavy" carbonates from the spring sediment and mixed wadi water environments as opposed to the "light" surface carbonate layer, and suggests a common "mixed water" origin of the former. This conclusion is consistent with that of O'Neil and Barnes (1971) whose detailed study of carbonates from American ultramafic environments explained the anomalously lighter isotopes of the air-water reaction by simple kinetic considerations of $C^{12}O_2/C^{13}O_2$ diffusion. Moreover, the same work demonstrated that all the carbonates studied, including veins, travertines, scums, sludges and conglomerate cements were of near surface/low temperature origin, i.e. < 50°C, in contradiction to the previously supposed hydrothermal origin of some carbonates. Less commonly, and on different occasions, the Karku spring sediment included both X-ray amorphous Ca(OH)$_2$ and brucite, Mg (OH)$_2$, gels. The former, though rare, may be readily explained as the flushing out of spring water which is locally supersaturated with respect to Ca(OH)$_2$ due to low temperature diopside serpentinisation with a high rock/water ratio. The presence of Mg(OH)$_2$ requires a more complex explanation. The virtual absence of silica and magnesium in all the alkaline spring waters implies that during serpentine precipitation the partial reactions (8) to (13) constitute a buffered system in which the relative amounts of olivine and pyroxene dissolution are stoichiometrically controlled by the precipitation reaction (13).

Table 5.6 Isotopic Composition of Precipitated Carbonates
(after Neal and Stanger, 1984)

	$\delta^{13}C$	$\delta^{18}O$
Surface crust	- 23.4	13.8
Granular precipitate	- 13.5	25.3
Vein dolomite	- 7.8	30.6
Vein calcites	(- 7.1	26.4
	(- 9.2	28.1
	(- 15.8	27.7

Table 5.7 Analysis of Brucite from Ultramafic Environments
1: "Precipitated", 2 and 3 "Alteration" Types.

	1	2	3	Stoichiometric $Mg(OH)_2$
MgO	68.42	60.38	59.45	69.10
Na_2O	0.34	-	-	0.00
BaO	0.11	-	-	0.00
FeO	0.00	8.74	11.20	0.00
H_2O	30.98	30.88	29.35	30.88
Σ	99.85	(100.00)	(100.00)	100.00

Anal. 1. "Mixed Water Type" brucite. Water clear, coarsely crystalline aggregates from serpentinite/metasedimentary mélange, Minabak, Oman. Al_2O_3, MnO, K_2O, P_2O_5, S, CaO and NiO were all less than the detection limit of 0.01 wt % (by energy dispersive X-ray fluorescence).

Anal 2. "Alteration" brucite. Based on Shtynberg and Chaschuklin (1969) data. FeO component calculated as the mean of 14 brucite samples (σ = 3.4 wt %) from the Urals.

Anal 3. Based on Hostetler et.al (1966) data. FeO component calculated as the mean of 5 brucite samples (σ = 2.3 wt %) from New Zealand and Western U.S.A.

Excess Mg^{2+} in solution, reaction (8) is therefore only possible in the absence of, or after the 100% serpentinisation of pyroxene. On the other hand, excess hydroxide is only available from the dissolution of clinopyroxene, reaction (12) i.e. where groundwater is actively serpentinising co-existent olivine and pyroxene, it is not possible to produce an excess of both Mg^{2+} and OH^- (+ Ca^{2+}) in solution; cf. section 5.6. This leaves two alternative processes. The first is reaction (8) which, if taken to completion;

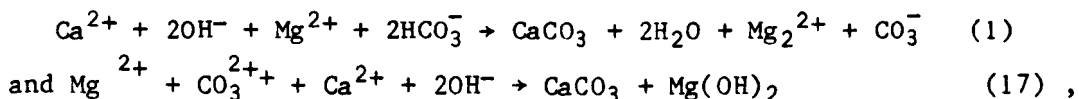$$3H_2O + 2Mg_2SiO_4 \rightarrow Mg_3Si_2O_5(OH)_4 + Mg(OH)_2 \qquad (16)$$
$$\text{forsterite} \qquad\qquad \text{serpentine} \qquad \text{brucite}$$
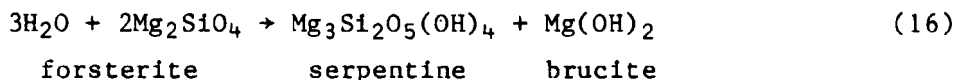
constitutes the conventional higher temperature or "alteration" reaction of Johannes, 1968; Moody, 1976; etc. In this mode of occurrence, brucite is difficult to distinguish optically due to its similarity to, and close association with the more abundant serpentine. Its recognition in the past has therefore mainly relied upon differential thermal analysis, wet chemical methods, or X-ray diffraction. The latter method was used in a detailed search of 15 partially to completely hydrated serpentinite samples from the Oman mantle sequence, of which two samples were found to contain small amounts (probably < 5%) of brucite. In each of these cases orthopyroxene was either very sparsely distributed or absent in keeping with most, if not all, other reported occurrences of brucite of ultramafic association (Shteinburg, 1960; Sakamoto, 1959; Eckhardt, 1956; Van Bilson, 1960; and Hostetler et al, 1966). In particular Hostetler et al have reported an empirical inverse relationship between orthopyroxene content and the presence of brucite. It therefore appears that the inhibition of brucite formation by silica release (pyroxene breakdown) is as important in the alteration as in the precipitation process.

In its simplest form, brucite precipitation is the product of the reactions:

$$Ca^{2+} + 2OH^- + Mg^{2+} + 2HCO_3^- \rightarrow CaCO_3 + 2H_2O + Mg_2^{2+} + CO_3^- \qquad (1)$$
$$\text{and } Mg^{2+} + CO_3^{2+} + Ca^{2+} + 2OH^- \rightarrow CaCO_3 + Mg(OH)_2 \qquad (17) ,$$

and indeed, coprecipitation of brucite gel with isotopically heavy granular carbonate is precisely as observed in the alkaline spring chamber at Karku. For equation (17) to proceed requires a molar excess of OH^- over HCO_3^- , i.e. for the alkaline spring water components to exceed the surface water components. This condition is seldom encountered in the surface environment, hence the much more abundant bicarbonate water normally maintains the "mixed water" pH below the brucite saturation level, and accounts for the scarcity of brucite gel. Further support for the above mixing model comes from an assessment of hydrogeological relationships at the mantle sequence/autochthonous limestone thrust contact at Minabak, (EA 933,935). Here, intense uplift and erosion has exposed a heavily sheared interface between groundwater pathways of predominantly hydroxide and bicarbonate type respectively. Detailed examination of vein material from the basal serpentinite at this site revealed soft pale silvery serpentine (Analysis No.4, Table 5.5), coating thick euhedral clusters of water clear brucite (Analysis No.1, Table 5.7), both of which are obviously late stage precipitates. The chemical composition of such brucite provides another criterion for identifying low temperature serpentinisation. Published analyses of fine grained brucite intimately intergrown with serpentine has previously included an $Fe(OH)_2$ component of about 12% (eg. Analyses 2 and 3, Table 5.7) due to hydration of the fayalite end-member, and consequent variations on reaction (9). This, however, cannot occur during mixed water precipitation due to the insolubility of iron oxide/hydroxide minerals under high pH conditions, whereas the Minabak brucite precipitated from mobile alkaline solution and is of exceptional purity (Analysis 1, Table 5.7).

The petrographic relationship between precipitated serpentine and brucite is one of successive rather than co-precipitation, and is probably influenced by the sensitivity of the two alternative reactions to intermittent fluctuations in pH, silica introduced from the bicarbonate type water, silica released by differing olivine-pyroxene ratios along the ultramafic groundwater pathway and above all, by the kinetics of precipitation. The description of a brucite-"protoserpentine" gel from a similar alkaline groundwater environment in California (Luce, 1971) could therefore be explained by the flushing out of such varied reaction products by partially mixed but $Ca^{2+}-2OH^-$ dominated groundwater types.
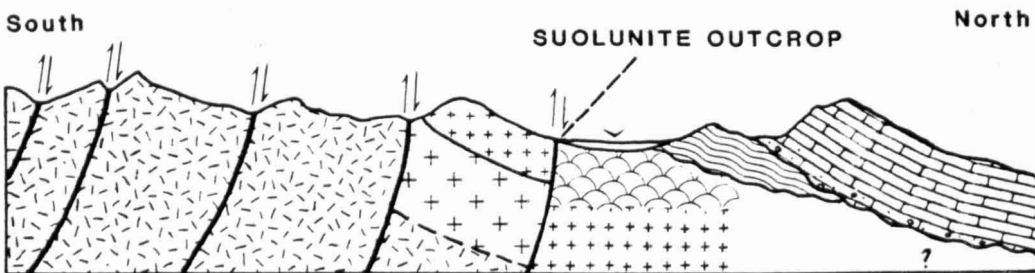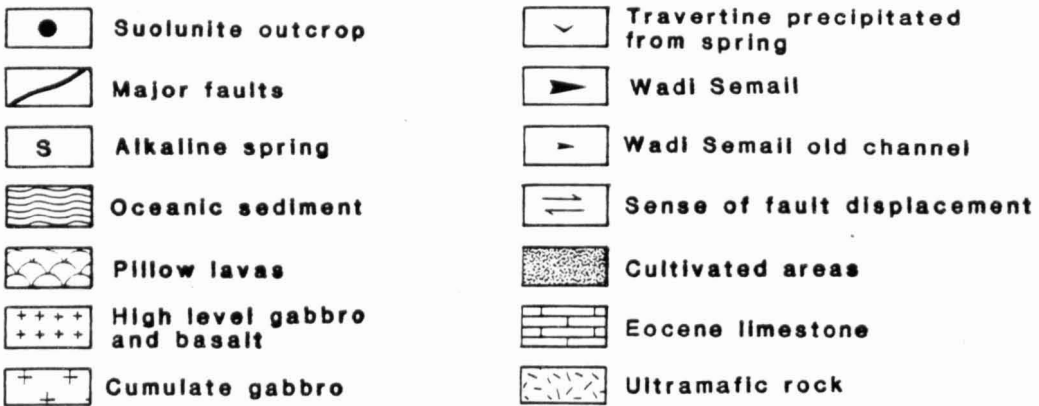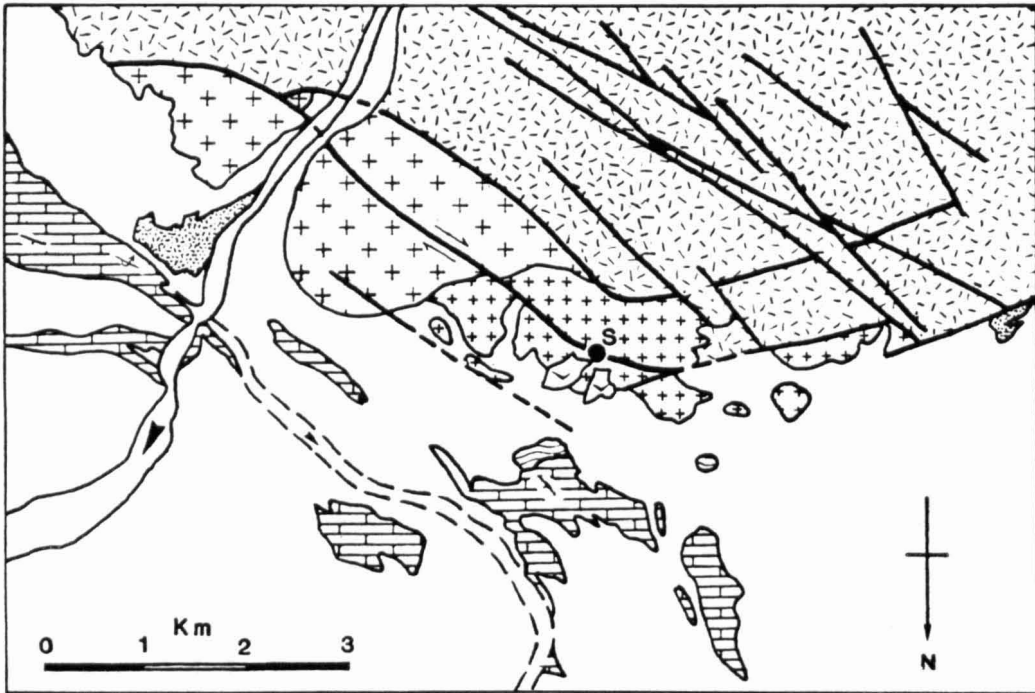
Evidence for reaction between $Ca^{2+}-2OH^-$ type groundwaters and basic rock is uncommon, but a particularly clear example occurs west of Al Khod (FB 083, 081). Here the northern edge of the ophiolite is strongly faulted in such a way as to provide a groundwater pathway at a sharp ultramafic-basic rock interface, Figure 5.7. The reaction product is suolunite $[Ca_2Si_2O_5(OH)_2.H_2O]$, Table 5.8, a rare mineral previously reported only from two other semi-arid ultramafic environments in Yugoslavia (Stojanovic et al., 1974), and Mongolia (Huang, 1965). This product occurs as an open space precipitate coincident with an alkaline spring (No. 312, Appendix C) within a prominent narrow fault zone, some three to four metres proud of the host rock. It takes the form of stellate concretionary aggregates in which successive cycles of precipitation have produced alternate fine equigranular and coarse bladed crystals in concentric layers (Stanger and Neal, 1984). Apart from a thick weathered layer of calcite, and up to three per cent of carbonate inclusions in some specimens, such masses are essentially monomineralic. Since the spring waters typically contain less than 1.0 mg l^{-1} of silica, an independent silica source is required for suolunite generation of which the most likely source is plagioclase:

$$Ca^{2+} + 2OH^- + CaAl_2Si_2O_8 + 4H_2O \rightarrow Ca_2Si_2O_5(OH)_2 . H_2O + 2Al(OH)_3 \quad (18)$$
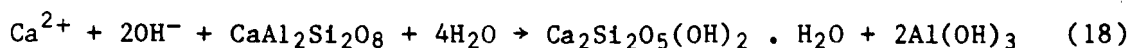
In this reaction suolunite is a precipitate from mobile aqueous phases whilst the $Al(OH)_3$ component either combines with residual plagioclase to produce various calcium aluminosilicates (or in the case of the Na - albite end member fraction; analcime) or dissolves in the highly alkaline conditions to give $Al(OH)_4^-$ ions which are flushed from the system. Evidence in support of the former process is found in the widespread alteration products of plagioclase found in joints and faults throughout the basic rocks of the area. This "rodingite" assemblage consists of hydrogrossular $[Ca_3Al_2(OH)_{12}]$, prehnite $[Ca_2Al_2Si_3O_{10}(OH)_2]$, and zoisite $[Ca_2Al_3Si_3O_{12}(OH)]$, all of which are relatively basic and retain the immobile Al fraction of the original plagioclase. Field evidence both from Oman and from other rodingite

Figure 5.7

Environment of suolunite occurrence

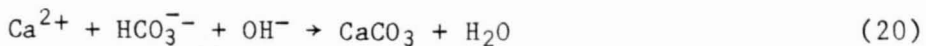|			
●	Suolunite outcrop	⌄	Travertine precipitated from spring
	Major faults	►	Wadi Semail
S	Alkaline spring	‑	Wadi Semail old channel
	Oceanic sediment	⇄	Sense of fault displacement
	Pillow lavas		Cultivated areas
+ + + +	High level gabbro and basalt		Eocene limestone
+ +	Cumulate gabbro		Ultramafic rock

SECTION THROUGH SUOLUNITE OUTCROP

locations (Glennie et al., 1974; Honnorez and Kirst, 1975; Lauder, 1965; Bell et al., 1911; and Coleman, 1967) invariably indicate contemporaneous serpentinisation of diopside rich ultramafic rocks (ie. Ca^{2+} and $2OH^-$ generation). Meanwhile under the predominant alkaline conditions silica, derived from plagioclase dissolution, undergoes significant H_4SiO_4 dissociation resulting in high silica solubility (Hem, 1970; Siever, 1957), and is therefore available for direct reactions with Ca^{2+} and OH^-. Alternative aqueous silica sources, dissolved in ephemeral runoff or surface water channelled along the fault, is discounted as such water is invariably characterised by Mg^{2+} and HCO_3^- ions, Table 5.9. Upon mixing with $Ca^{2+} - OH^-$ type water, both these components would undergo alternative reactions to precipitate serpentine and carbonate, thereby precluding suolunite formation:

$$6OH^- + 2\ Si(OH)_4 + 3\ Mg^{2+} \rightarrow Mg_3Si_2O_5(OH)_4 + 5H_2O \qquad (19)$$

and

$$Ca^{2+} + HCO_3^- + OH^- \rightarrow CaCO_3 + H_2O \qquad (20)$$
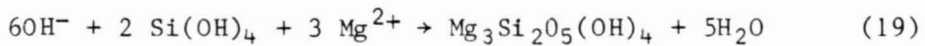
The abundance of either HCO_3^- or Mg^{2+} ions in most natural surface waters at the ultramafic/basic boundary zone therefore accounts for suolunite rarity.

Redox processes

Comparison between the hydrochemistry of mantle sequence surface and spring waters reveals strongly contrasting oxidation states in many components; Table 5.10. Superficially the most striking of these is the almost total reduction of iodate to iodide. However total iodine in spring waters undergoes an almost three-fold enrichment relative to surface water and must therefore be influenced by the solution of pre-existing iodine salts in the ultramafic rock. The extent of reduction is therefore better indicated by the more conservative nitrogen system. Although other nitrogen species were not determined, nitrate, influenced only by redox processes, shows a marked reduction to nitrite, the mass balance discrepancy between the two species presumably being balanced by still further reduction to NH_3.

Table 5.8

X-Ray Fluorescence Analysis of Suolunite

Norm	wt%, Measured	Stoichiometric $Ca_2 Si_2 O_5 (OH)_2 H_2 O$
SiO_2	41.91	44.78
CaO	44.66	41.79
MgO	0.29	0.0
$Al_2 O_3$	0.72	0.0
$Na_2 O$	0.39	0.0
L.O.I. ($H_2 O + CO_2$)	14.14	13.43
Σ	102.11	100.00

$Fe_2 O_3$, TiO_2 and $K_2 O$ all < 0.001%

Traces (ppm)

Rb	1	Pb	6	Nb	2
Sr	31	Ni	4	Ga	0
Y	0	Cu	5	Th	1
Zr	12	Zn	6		

N.B.   The low silica, high CaO content is attributable to minor substitution of Al in Si positions and slight weathering to form $CaCO_3$. Loss of CO_2 accounts for the high L.O.I.

Table 5.9

Water Chemistry from the Suolunite Area
    concentrations in mg 1^{-1}

Sample Nos*	1			2	3
pH	8.2	–	8.8	8.4	11.4
Ca	14.0	–	23.0	14.0	66.2
Mg	63	–	128	41.3	0.002
Na	120	–	280	20.5	367
K	4.0	–	8.0	1.6	8.9
SiO_2	22.0	–	30.0	21.0	4.6
OH		0		0	34
HCO_3	107	–	438	176	0
SO_4	110	–	252	55	63
NO_3	0.5	–	2.0	5.0	2.4
Cl	180	–	495	30.0	453
T($^{\circ}$ C)	21	–	36	28	37

* 1: Perennial surface flow from Wadi Semail, sampled where it crosses the suolunite fault. Figures give the range from biweekly sampling over 15 months.

2: Ephemeral surface flow or shallow (alluvial) groundwater from the ultramafic areas.

3: Alkaline spring water from close to the suolunite outcrop. (No.312, Appendix C).

215

Table 5.10

Oxidised-Reduced Species in Surface and Spring Waters from the Ultramafic Environment

| | Surface waters | | | Spring waters | | |
	mean	σ	range	mean	σ	range
Iodate	15.8	6.8	4/33	1.8	3.4	0/18
Iodide	2.6	–	0/14	49.1	–	17/21
Σ Iodine	18.4	8.8	5/39	50.9	22	17/127
Nitrate	5.8	3.8	1/13	2.9	2.6	0/9
Nitrite	< 0.03	–	< 0.03	.25	.27	0/08
Sulphate	59.2	31.1	11/17	13.6	9.9	2.5/32
Sulphide	0	–	–	3	–	0-8

Iodine species in μg/l. All other values in mg/l.
Iodine species data is based on 55 alkaline springs and 30
surface waters. Nitrate, Nitrite and Sulphate data is from
16 paired spring-surface water sites. Sulphide values are
semi-quantitative only, (cf. Appendix C for full details).

In the absence of sulphate reducing bacteria and evaporative precipitation, neither of which is likely to obtain in the groundwater system, sulphate normally exhibits conservatism in solution. Hence the longer to very much longer residence time of the spring waters relative to surface waters would normally result in higher sulphate concentrations in the former. Therefore, in view of the rather high relative electron activities necessary to reduce SO_4^{2-} (Stumm and Morgan, 1970), its four-fold depletion in spring waters is also evidence of exceptionally reducing conditions. This is also conclusively shown by redox values (Eh) of typically -165mV, and lowest value of -630 mV (Figure 5.8; Appendix C6) which may be taken to indicate generally negative Eh throughout the ultramafic environment. Indeed since (1) slight atmospheric oxygen diffusion probably occurs at the spring chambers, and (2) the springs are the product of average geochemical conditions within the groundwater pathways, even more negative Eh is probably of widespread local occurrence.

The most profound evidence of reduction is that of the spring water itself as shown by the discovery of evolved hydrogen rich gases in many springs. These gases were observed as occasional bubbles on irregular streams in only a dozen of the alkaline springs, but the presence of soft white carbonate mud in the bottom of most spring chambers led to the fortuitous widespread preservation of conical depressions caused by gas flow, and the conclusion that persistent gas release has occurred at some stage in all the alkaline springs investigated.

Measurable gas flows vary from barely detectable to about 10 ml/s, but more substantial flows, of the order of 10 l/s, occurred from an inaccessible rock crevice at B'lad and from an 80 m borehole at Nizwa (Figure 5.9). The gases, sampled by water displacement at various alkaline springs, had compositions varying from that of almost pure hydrogen; 99% at Huwayl Qufays, to almost pure nitrogen; 96% at Murayrat, and an approximation to air at Wadi Zabin:
76.9, 78.1% N_2 20.5, 20.9% O_2 0.9, 0.93% (atmospheric composition, underlined from Weast et al., 1981-2). In addition small quantities of methane, < 4.5%, together with trace amounts of higher saturated hydrocarbons < 120 vpm, occurred with the hydrogen-rich gas

Figure 5.8

pH-Eh Range of Alkaline spring Waters
after Hem 1970

pH
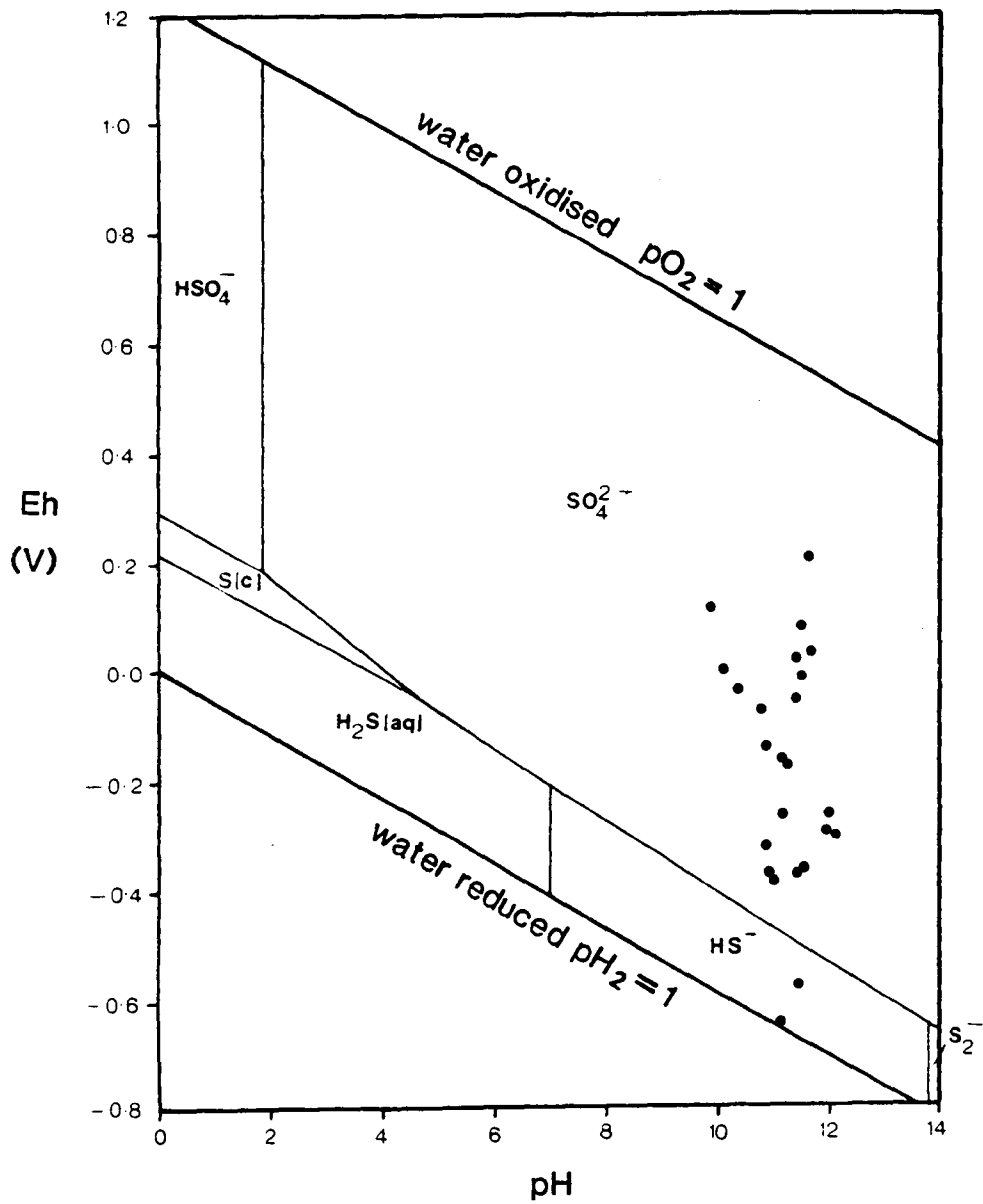
Sulphur species,at 1 atmosphere,25 C and 96mg/l
total S as SO_4^{2-} superimposed

Figure 5.9

Location of Gas Sources in the Semail Nappe
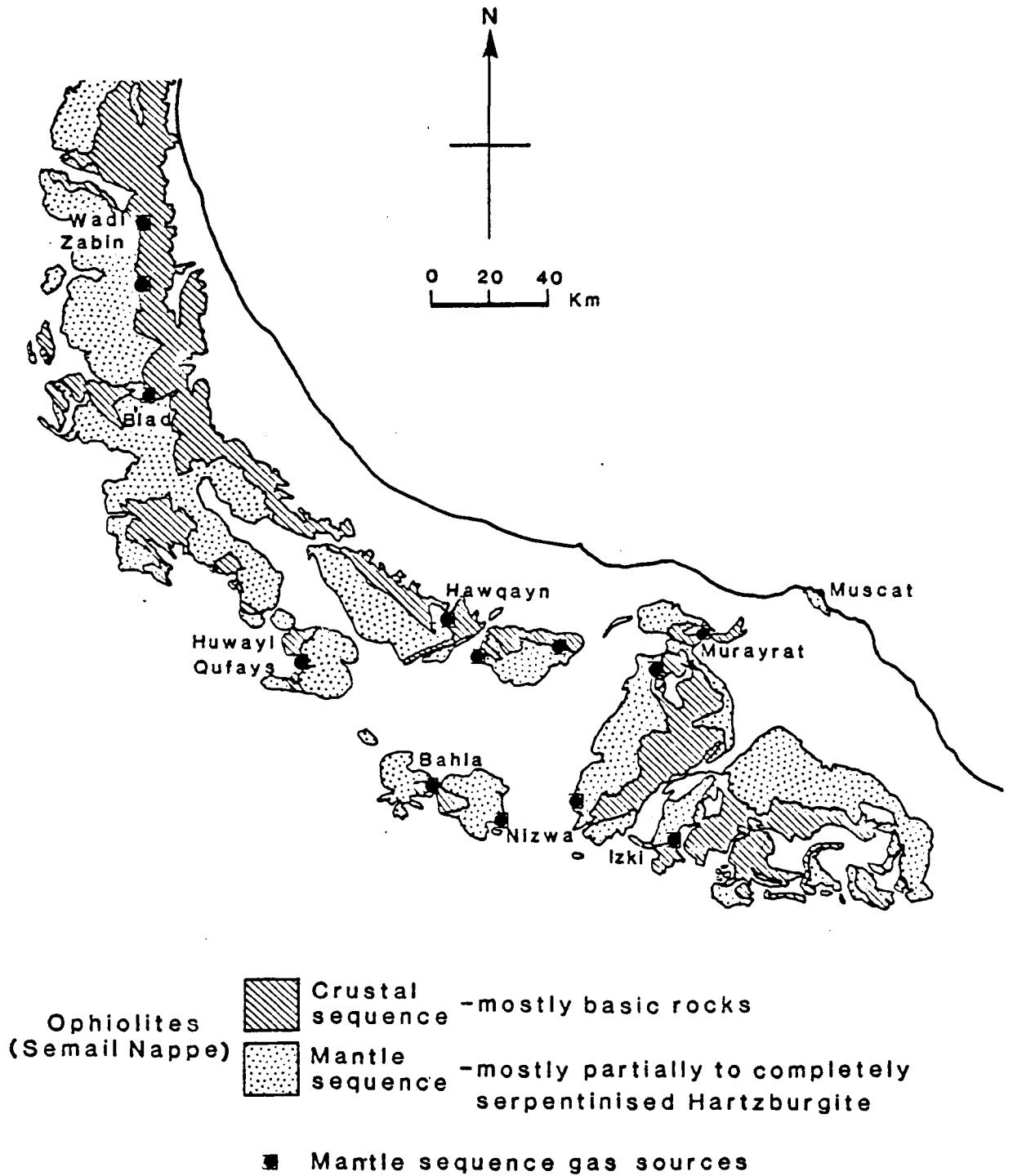
Table 5.11   Compositions of natural gases from Oman
              (after Neal and Stanger, 1984b)

Location		H_2 %	N_2 %	O_2+Ar %	CH_4 %	CO %
Bahla	(1)	82	15	2	2	0
	(2)	55	38	7	2	0
	(3)	43	43	13	0.9	0
	(4)	97	2	0.1	1	0
	(5)	53	38		2.2	0
Hawqayn	(1)	39	50	10	1.1	0
	(2)	48	40	8	4.3	0
	(3)	47	38	8	4.3	0
Wadi Zabin	(1)	2	76	21	0.2	0
	(2)	1	77	21	0.2	0
Murayrat	(1)	0.1	96	4	0	0.1
	(2)	0	78	22	0	0
Nizwa		95	1	0	4.0	0
Huwayl Qufays		99	1	0	0	0
B'lad		22	76	1	0	0
Air		0	78.1	21.8	0	0

Location		Ethane	Propane	iso Butane VPM	n- Butane VPM	Total Hydrocarbons VPM
Bahla	(2)	63	17	2	11	114
	(3)	70	15	2	10	112
	(4)	78	18	2	12	110
Hawqayn	(2)	5	1	1	1	8
	(3)	5	1	1	1	8

whilst trace amounts of CO, 0.1%, occurred with the most nitrogen-rich gas; Table 5.11. Although contaminated by entrained air at the wellhead, "Draeger" chromatography tests of the Nizwa borehole indicated a hydrogen content of < 5% and hydrocarbons (probably methane) at about 0.5%.

The isotopic content ($\delta^2 H$ $^0/_{00}$ with respect to SMOW) of the hydrogen was - 697, - 699, - 699 and - 714 for Nizwa, Bahla, Huwayl Qafays and B'lad respectively (Figure 5.9). These values are amongst the most deuterium depleted so far reported and, in relation to the $\delta^2 H$ range of + 10 $^0/_{00}$ to - 10 $^0/_{00}$ SMOW from 30 alkaline springs, corresponds to an equilibrium fractionation temperature of between 20 and $50^0 C$ (Neal and Stanger, 1984b; Bottinga, 1969; Friedman and O'Neil, 1977) i.e. an estimate which brackets the mean alkaline groundwater temperature of about $32^0 C$, and thereby implies contemporaneous reduction and low-temperature serpentinisation.

The driving mechanism behind all these redox reactions is the progressive oxidation of the iron minerals formed by dissolution of the fayalite and "ferrosilite" end-member fractions of the primary mineral assemblage. These typically have an FeII : MgII molar ratio of about 1:10 (Figure 5.2). The iron phases generated by serpentinisation are variable brown coloured, fine grained, amorphous and often finely disseminated making positive mineral identification difficult, but the microscopic characteristics are closer to goethite ($\alpha Fe0.OH$) and lepidocrocite ($\gamma-Fe0.OH$) than to haematite ($\alpha-Fe_2O_3$), whereas the lack of any relationship between degree of serpentinisation and magnetic susceptibility excludes magnetite (Fe_3O_4) as the dominant iron-rich phase.

Both the gas composition and hydrological conditions within the ultramafic rock point to an essentially two stage oxidation process. The first stage is initiated by groundwater recharge in which both dissolved and entrained air from the atmosphere and phreatic zone is introduced into the upper saturated zone of the ultramafic aquifer. With continued serpentinisation, $Fe(OH)_2$ is released (reaction 11) and reacts with the dissolved and free oxygen by such reactions as:

$$2Fe(OH)_2 + \tfrac{1}{2} O_2 \rightarrow Fe_2O_3 + 2H_2O \qquad\qquad (29)$$

$$3Fe(OH)_2 + \tfrac{1}{2} O_2 \rightarrow Fe_3O_4 + 3H_2O \qquad\qquad (30)$$

$$2Fe(OH)_2 + \tfrac{1}{2} O_2 \rightarrow 2\,FeO.OH + H_2O \qquad\qquad (31)$$
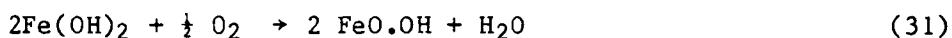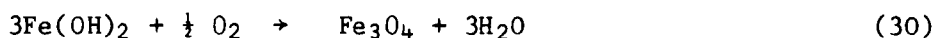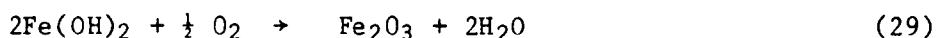
Hence the observed excess of nitrogen produces the gas composition trend shown on the left hand edge of Figure 5.10.

The most oxidising of these reactions, (29), produced haematite mixed with a copper bloom and elemental sulphur, and was observed in ultramafic joints at a single anomalous ophiolite spring (Wadi Bani Kharus, grid 56820, 259080). At this site perennial "upstream" surface water recharge occurs by coincidence of both surface and groundwater flow along a major fault line, thereby maintaining a relatively high groundwater oxygen content. Elsewhere, groundwaters were depleted of available oxygen and evolved under the more anoxic conditions of reactions 30 and 31.

Given this combination of decreasing redox potential and increasing pH, the water and ferrous hydroxide would be in equilibrium but would progressively approach the limit of water stability, about -650 and -715 mV for pH^s of 11 and 12 respectively (Figure 5.8). Ultimately, total oxygen depletion would result in the second stage; that of water decomposition by further ferrous iron oxidation reactions such as:

$$2Fe(OH)_2 \rightarrow Fe_2O_3 + H_2O + H_2 \qquad\qquad (32)$$
$$\text{haematite}$$

$$3Fe(OH)_2 \rightarrow Fe_3O_4 + 2H_2O + H_2 \qquad\qquad (33)$$
$$\text{magnetite}$$
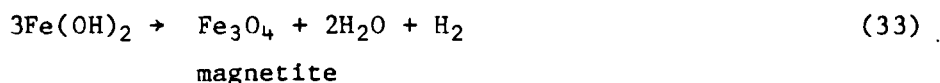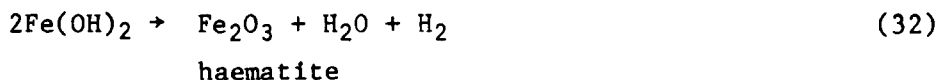
The lack of any consistent end product suggests that the oxidation process often fails to reach completion. Also the process is complicated·by the non-equilibrium co-existence of the three main component gases, Figure 5.9, which implies that different stages of the "cycle" may be degassing simultaneously at any spring site, as would be expected from variations in residence time, differential rates of fluid flow and varying groundwater pathways.

Figure 5.10

Evolved Gas Compositions
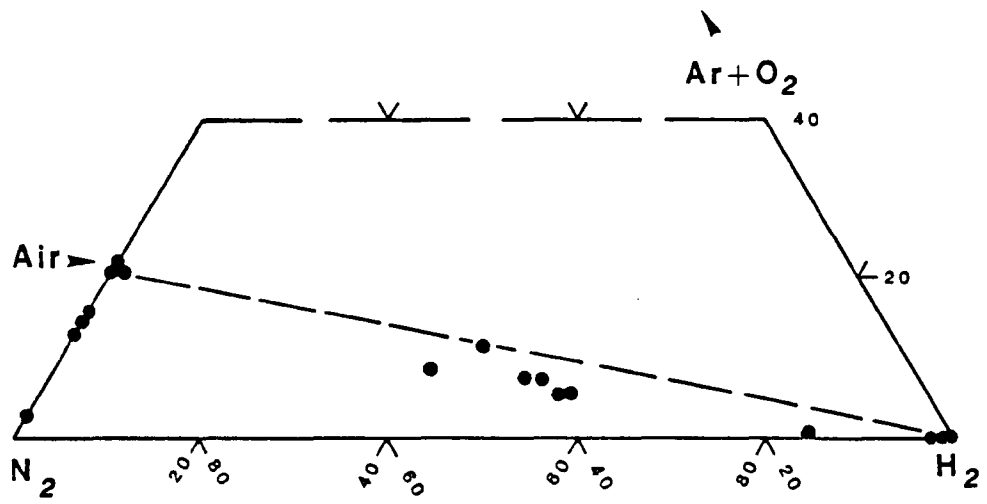
The "de facto" mass balance deficit of the sulphur species, Table 5.10 must indicate a sulphur "sink" within the ultramafic rock but, so far, this has not been identified. The nature of this sink is probably sulphide in the form of finely disseminated or otherwise concealed pyrite since, (1) HS^- as the alternative species is too dilute to account for the SO_4^- depletion, (2) thermodynamic modelling precludes the existence of elemental sulphur under high pH conditions (Stumm and Morgan, 1970), and (3) iron minerals are the only substantial reactive products of serpentinisation.

It is suggested that the conversion of sulphate to sulphide occurs in the initial sections of the groundwater pathways where active serpentinisation creates a negative Eh gradient. Although there is no available data on trace reduced phases in the Semail "harzburgite", detailed analysis in other alpine ultramafic rocks has demonstrated the widespread and possibly universal association between partly to completely serpentinised ultramafic rocks (never the fresh peridotites), and reduced species such as native metals, intermetallic compounds and sulphides low in sulphur (Ramdohr, 1967, 1969; Deutsh et al., 1977; De Quervain, 1945, 1963; Chamberlain et al. 1965; and Chamberlain 1966). Such products and especially those of the less reactive metals (Ni, Co, Cu, Pb, Zn, Ag) would, if present as sulphides, be produced by reactions of the form:

$$NiFeS_2 + 2H_2 + 2OH^- \rightarrow NiFe + 2H_2O + 2HS^- \tag{34}$$
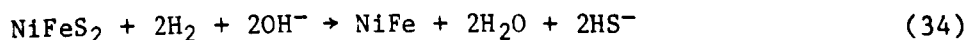
Many similar reactions could be proposed for the other common trace minerals such as native nickel, awaruite (Ni_3Fe), wairauite (CoFe), heazlewoodite (Ni_3S_2), millerite (NiS) etc. Both input and output mechanisms for the potential precipitation of sulphide from groundwater therefore arise. Firstly, the reduction of sulphate to sulphide as groundwater enters an environment of active serpentinisation, and secondly, dissolved hydrogen in groundwater flow from a serpentinising to non-serpentinising environment would precipitate any complexed sulphur species. The latter process was proposed by Coveney (1972) to account for gold deposits in Californian serpentinite;

$$2AuS^- + H_2 \rightarrow 2Au^o + 2HS^- \tag{35}$$

in which at least 80% of the ore bodies were situated next to or no greater than 30 metres from the serpentine wall rocks. Thus, whilst recognising that most extensive "high level" sulphides are of undoubted hydrothermal origin (Alabaster, 1982), these low temperature mechanisms also seem to play a part in the redistribution of minor sulphides, mainly pyrite, at the basic/ultramafic fault bounded interface and in wholly serpentinised mantle sequence rocks (Coleman et.al., 1979; Carney and Welland, 1974 respectively).

The Salt Balance

The remaining unusual feature of alkaline spring waters is their high salt contents. Under the prevailing high pH-low Eh conditions within the ultramafic rock, even the most conservative of the major ions in solution, i.e. chloride, may behave abnormally by tending to precipitate as $Fe_2(OH)_3Cl$ (Kohls and Rodda, 1967; Rucklidge and Patterson, 1977). However as the (Na+K)/Cl ratio is consistently less than unity, Tables 5.3 and 5.4, substantial chloride loss from solution is minimal and may therefore be ignored in a first approximation of the chloride mass balance.

Given the amount weighted mean chloride concentration for rainfall of about 8 p.p.m., the data for surface water, Table 5.12, implies evaporative concentration by an average of 89%. This estimate, though high, is consistent with the low rainfall over the ophiolites and the high surface temperature (Section 2.2) as well as with previous physical measurements (Gibb et.al., 1976). Furthermore the evaporation produces a marked shift in mean isotopic composition between rainfall/runoff and surface waters of about $\Delta\delta D = 10$ $^0/_{00}$ and $\Delta\delta^{18}O = 3$ $^0/_{00}$. The same cannot be said for the spring waters, which exhibit a further four-fold enrichment in chloride without any increase in heavy isotope concentration, Figure 5.11. This corresponds to the lack of any soil cover and consequently with minimal near surface retention during mantle sequence recharge, which prevents further significant groundwater evaporation. Alternatively, most of the chloride in spring water must be leached from the "aquifer". Notwithstanding the poor overall correlation (0.52) between degree of

Table 5.12 Chloride concentrations from the mantle
sequence environment, $(mg.l^{-1})$

Source	Cl^-	σ	n	F*
Amount weighted rainfall	8			-
surface waters, Mg - HCO_3 type	78.2	58.4	71	9.8
high pH springs, basal zone	302	84	17	38
high pH springs, cumulate zone	319	168	37	40
Springs and wells from the Nizwa - Mu Aydin catchment, i.e. from all levels of the mantle sequence	281	183	55	35

* enrichment factor with respect to rainfall

Figure 5.11

Isotopic Composition of Different Groundwater Types

$\delta^{18}O$

δD

SMOW

Mean Rainfall

● limestone spring and piedmont alluvium
○ normal groundwaters from coastal and foothill areas
▲ ophiolite gravel waters

227
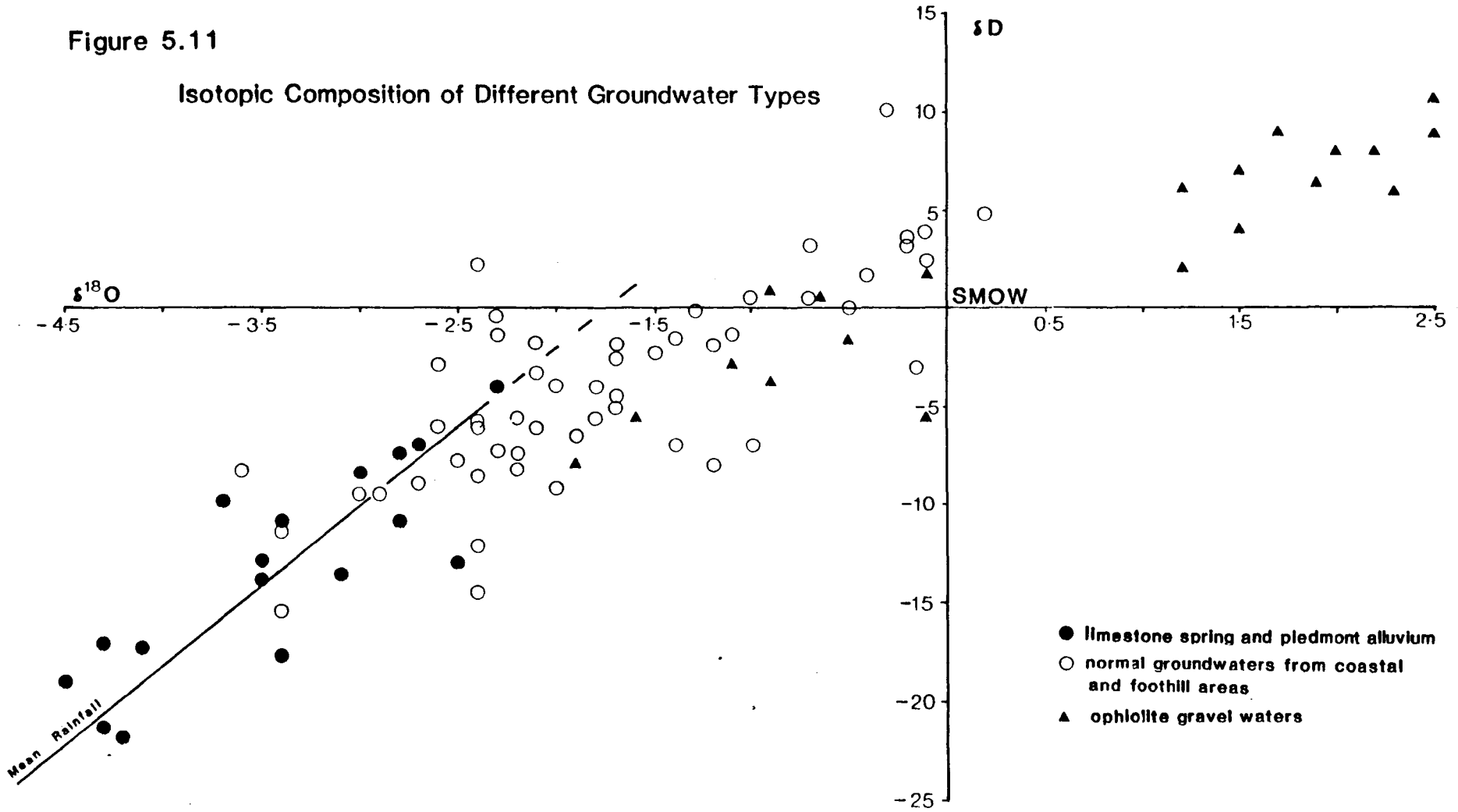
serpentinisation and chloride content in the Semail ultramafics, there is a clear contrast in chloride concentration between fresh and serpentinised peridotite. Analagous data reported from other ultramafic rocks indicates a typical chloride contrast of 88 to 400 or more ppm (Rucklidge and Patterson, 1977; Earley, 1958; Kuroda and Sandell, 1953) which suggests that marine chloride introduced during early serpentinisation was adsorbed onto positively charged crystal surfaces (Miura et al., 1979) and is thus available for later release to solution during a subsequent phase of low-temperature rock dissolution, i.e. the spring chloride anomalies seen in Oman must therefore be a legacy of residual sea salts fortuitously preserved by slow meteoric circulation with a high rock/water ratio. In exceptional cases relatively short low flow groundwater pathways in the main harzburgite rock mass may be completely devoid of diopside and hence of Ca^{2+} and OH^-, in which case evaporative encrustations of halite around the outflow seepages are the sole indications of groundwater serpentinisation (Plate 5.5).

Numerous features testify to the transient nature of low temperature serpentinisation processes. The non-equilibrium gas assemblage, irregularity of hydrogen discharge from some springs, intermittent hydroxide precipitation in spring chambers, the presence of "mixed water" products in the upper aquifer, and hydrochemical variation within individual springs, Table 5.13, all serve to illustrate the irregularity of the process both in intensity and periodicity according to the prevailing hydrogeological conditions. Indeed many of the above ph-redox processes were temporarily curtailed immediately after major rainstorms due to short-circuiting of the groundwater pathways by $Mg^{2+} - 2HCO_3^-$ type water. In this respect, the semi-arid ultramafic environment with its characteristically infrequent, low CO_2 recharge, lack of soil and well defined input-output hydrochemistry, provides a window upon processes which, in other environments, would be either cryptic or inactive.

5.6 Post-Serpentinisation Reactions

The Semail nappe differs from most other ultramafic terrains by its lack of widespread post-serpentinisation chemical degradation

Table 5.13

KARKU ALKALINE SPRING : VARIATIONS WITH TIME

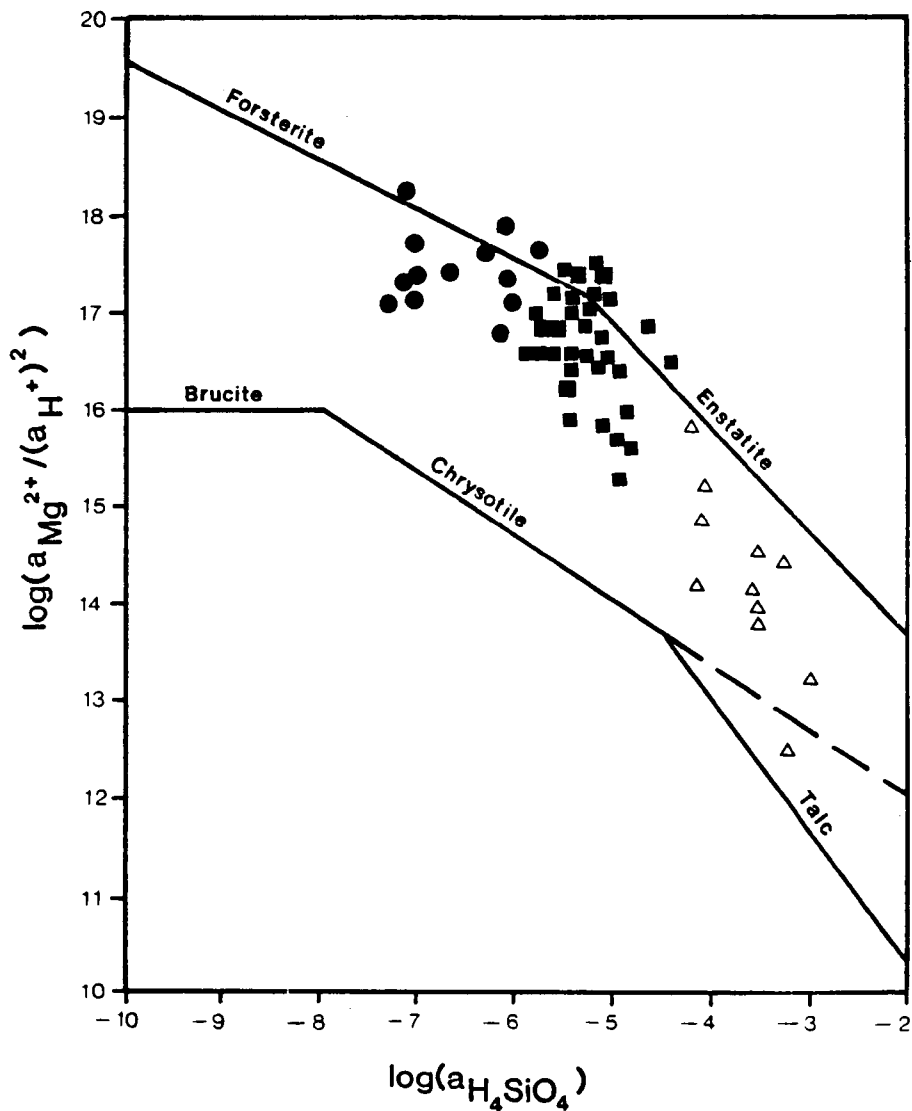| No.*	T°C	Date	pH	Ca	Mg	Na	K	Sr	OH	CO_3	HCO_3	SO4	NO3	Cl	SiO2
68	34	9.79	10.4	33	.05	333	17.8	.14	0	80	19		0.8	298	122
133	30	11.79	9.9	5	12.00	416	10.8	.04	0	5	118	142	1.5	346	0.4
203	32	02.80	11.8	45	.09	310	16.6	.29	102	0	0	30	6.2	370	27.4
233	31	04.80	11.6	67	.08	260	12.0	.25	59	0	0	2	8.8	380	1.0
271	36	06.80	11.4	48	.27	273	12.1	.32	56	0	0	16	0.6	352	1.2
376	36	09 80	11.5	58	.42	254	12.9	.30	81	0	0	15	3.7	317	0.7
394	31	10.80	11.0	4	.04	307	12.5	.13	29	0	0	16	0.4	330	0.7
454	34	11.80	11.6	54	.07	407	12.7	.28	94	0	0	47	5.5	341	0.8

*cf appendix C.

processes. For example lateritic weathering profiles of the form; saprolite-smectite-goethite-haemetite, or serpentine-limonite-goethite/quartz which commonly develops over ultramafic rocks in wetter environments (Maksimovic, 1981; Golightly, 1978, 1981; Nahon et al., 1982) are absent from Oman, whilst the silica-carbonate-goethite "end products" have only developed under relatively restricted local and atypical conditions (Stanger, 1985). The reasons for such limited serpentinite alteration are governed by the stability relations between aqueous solutions and the hydrous-anhydrous mineral assemblage, depicted in Figure 5.12. In order to establish a more general view of phase saturation levels, this figure is supplemented by the calculated[1] reaction states of selected appendix C water chemistries both from within and adjacent to the mantle sequence (Table 5.14). As Nesbitt and Bricker (1978) have pointed out, there is no contact between the anhydrous and hydrous phase saturation boundaries of Figure 5.12, and consequently no possible thermodynamic equilibrium with the co-existing fluid. The cluster of spring waters around the anhydrous saturation boundary therefore indicates a "kinetic equilibrium" state in which forsterite and enstatite dissolution is much more rapid than brucite/chrysotile (serpentine) precipitation, i.e. reaction kinetics are controlled by the precipitating rather than by the dissolving minerals. Examination of Table 5.14 shows that the ultramafic groundwater is grossly oversaturated with respect to chrysotile but only slightly oversaturated with respect to brucite; i.e. a saturation contrast of 9 orders of magnitude. Therefore, although both minerals may theoretically precipitate, the very much faster precipitation of chrysotile results in its almost total preponderance as the sole hydrous product. This in turn has an important consequence on the dissolution of the hydrous phases, as co-existing olivine and pyroxene will dissolve in such a way as to maintain the Mg-Si stoichiometric proportion of chrysotile, thus explaining both the buffered system deduced empirically in section 5.4 and the cluster of spring water points around the forsterite-enstatite saturation line intersection on Figure 5.12

[1] Calculated using the Institute of Hydrology "Wateq" program (Truesdell and Jones, 1974).

Figure 5.12

Rock–Water Phase Diagram for the system $MgO-SiO_2-H_2O$
after Nesbitt and Bricker, 1978
Saturation boundaries at 25 C / 1bar total pressure and $a_{H_2O} = 1 \cdot 0$

y-axis: $\log(a_{Mg^{2+}}/(a_{H^+})^2)$

x-axis: $\log(a_{H_4SiO_4})$

Labels in plot: Forsterite, Brucite, Chrysotile, Enstatite, Talc

bicarbonate surface waters △

alkaline spring waters { ■ buffered by codissolution of Fo and En.
● formed by excess Fo dissolution

In any groundwater pathway in which the water/peridotite rock ratio is sufficiently small for kinetic equilibrium (and hence serpentinisation) to be approximated, a strict order of events may therefore be defined:
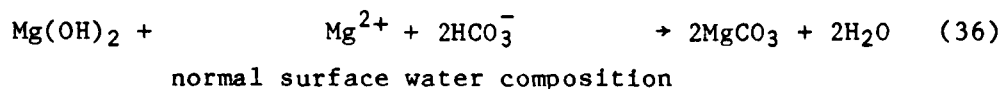
(A)   Olivine-pyroxene dissolution to give serpentine (and $Ca^{2+}-OH^-$ if clinopyroxene or the minor CaO fraction of orthopyroxene is present).

(B)   With either the absence of, or exhaustion of the available pyroxene, the remaining olivine will continue to produce serpentine and brucite, e.g. the spring waters plotting to the left of the forsterite - enstatite intersection point of figure 5.12.

(C)   Only when all the anhydrous phases are exhausted can the alkalinity, or $"log(a_{Mg}^{2+}/a_H^+)^2)"$ fall sufficiently for hydrous phase dissolution to proceed.

In order to establish the extent of total serpentinisation, and hence the likely areas in which process "C" might occur, the eastern Jebel Akhdar (Semail "sensuo stricto") region was mapped by Landsat multispectral image discrimination. To achieve this, areas of totally serpentinised and partially serpentinised ultramafic rock, identified during detailed ground reconnaissance, were defined as "training areas" in a Dipix LCT-11 image analysis system, and used to differentiate the entire image on the basis of destriped bands 4 to 7 maximum likelihood classification. The post-classification thematic image was geometrically corrected and then filtered to give the result shown in Plate 5.6. The final result is based upon indirect evidence of serpentinisation such as the extent of ex-solution of Fe^{III} minerals in weathered surfaces (desert varnish), differential slope reflectance etc., (Rothery, 1982, 1983) and incurs certain errors such as the inability to differentiate between ultramafic outcrop and drift, spurious data from areas in shadow, and misclassification within some crustal sequence areas. Nevertheless the areas of more or less total serpentinisation, at the base of the nappe and within major fault zones, are clearly discernible and correspond to about 5% of the exposed mantle sequence area (i.e. not including the ultramafic alluvium). The same heavily to totally serpentinised areas correspond closely to the occurrence of magnesite, and suggest a correlation with areas in which process "B", above, has taken place.

High Magnesian Carbonates

Magnesite is by far the most common carbonate mineral in the mantle sequence and accounts for about 80% of all the carbonate veins deposited, the remainder being mostly dolomite. Typically it occurs in mm to metre thick veins, is invariably pure white (approximately iron free), and is very fine grained, almost porcellanitic, massive to concretionary in texture leaving little or no petrographic evidence of formation conditions. The problem of magnesite vein origin is obscured by the current lack of any reliable method for the isotopic analysis of magnesite (O'Neil and Barnes, 1971) and by the absence of any known examples of its present day precipitation. On the contrary, though generally undeformed, many magnesite veins are slickensided (Plate 5.7) suggesting a relatively early post-nappe emplacement genesis.

Evidence from other ultramafic areas support an inverse correlation between brucite at depth and surface exposures of magnesite. Hostetler et al., 1966, for example found brucite to be typically unstable along the sheared borders and fracture zones of ultramafic masses, and regarded it as the "prime candidate" as the precursor of magnesite. Indeed a significant feature of magnesite occurrence in Oman, Greece (Dabitzias, 1980) and Australasia (Hostetler et al. 1966) is its close association with dunite but complete absence from pyroxene rich rocks such as websterite, i.e. Magnesite occurrence is restricted to rocks which hydrate to produce serpentine and brucite, e.g. equation (4). In less arid areas, brucite alters to the minerals: hydromagnesite $[Mg_4(CO_3)_3(OH)_2.3H_2O]$, artinite $[Mg_2(CO_3)(OH)_2.3H_2O]$, pyroaurite $[Mg_6Fe_2(CO_2)(OH)_{16}.4H_2O]$, or coalingite $[Mg_{10}Fe_2CO_3(OH)_{24}.2H_2O]$, none of which have been found in the Oman surface environment. Since subaerial weathering does not satisfactorily explain magnesite formation, the most plausible mechanism for its precipitation therefore seems to be following brucite solution within the groundwater environment by the reaction:

$$Mg(OH)_2 + \qquad Mg^{2+} + 2HCO_3^- \qquad \rightarrow 2MgCO_3 + 2H_2O \qquad (36)$$
$$\text{normal surface water composition}$$

This reaction is promoted by the solubility of brucite in most HCO_3^- type groundwaters, (Table 5.14), and is consistent with the field evidence in several ways. Firstly, the requirement of moderate pH waters in the above reaction implies complete serpentinisation in the

233

Table 5.14 Typical Saturation Indices with respect to Brucite
and Carbonates (HCO_3^- type waters)

mineral	pH	ultramafic gravel			alkaline springs		
		8.5	8.8	8.4	11.2	11.4	11.8
brucite		− 2.5	− 2.0	− 4.2	0.75	0.27	1.24
magnesite		0.82	1.27	− 0.33	−	−	−
huntite		− 0.51	1.74	− 2.86	−	−	−
dolomite		0.77	2.11	0.71	indeterminate		
calcite		− 0.34	0.55	0.75	−	−	−
aragonite		− 0.60	0.29	0.49	−	−	−

Table 5.15   The Chemical Composition of Huntite

	wt %
CO_2	49.73
CaO	7.76
MgO	42.37
SrO	0.76
Fe_2O_3	0.02
SiO_2	0.08
SO_3	0
	100.73

H_2O, Al_2O_3 and P_2O_5 = 0.00

traces (ppm) : Mn 0, Zn 5, Zr 46
Cu 17, Pb 19, Y 0

vicinity of the groundwater pathways (though not necessarily complete serpentinisation of the interfractured matrix) and consequently the cessation of brucite precipitation and highly alkaline conditions. Secondly, the greater proportion of primary dunite in the basal zone and "sea water" hydration during emplacement would have been conducive to the precipitation of brucite by reaction (4). Thirdly, reactivation of groundwater pathways in the basal zone by early Tertiary uplift would have facilitated the conversion of pre-existing brucite to magnesite at an early age, thus contributing to the modern scarcity of brucite in the ultramafic rock, and accounting for slickenside formation in the magnesite veins.

A single example of more recent carbonate precipitation under post-serpentinisation conditions was found in Muttrah; UTM grid zone 40, 6583, 26119, where magnesian huntite (with an Mg/Ca ratio of up to 4 as opposed to normal huntite, $Mg_3Ca(CO_3)_4$), an uncommon metastable phase (Stanger and Neal, 1984), and magnesite occurred in serpentinised fractures in the base of the Semail nappe. As in most examples from other environments (e.g. Baron et al., 1957; Faust, 1953; Carpenter, 1961; Veen and Arndt, 1973; Damodaran and Somasekar, 1975) the huntite occurs as soft, pure white, powdery mono-mineralic masses ranging in diameter from mms to several cms. They are mostly spherical, but a few larger masses form "augen" or are irregular in shape. The associated magnesite occurs both as cm. sized discrete cauliflower shaped nodules and as coatings separating the huntite from the serpentine matrix. In the latter case the magnesite is porcellanous in section with a pseudo-oolitic surface both on the inner and outer contacts (i.e. against both huntite and serpentine), as shown in Figure 5.13.

Although it is difficult to envisage the deformation of serpentine by such a soft porous mineral as huntite, several features suggest that it originates as a late stage primary precipitate within the fractured zones. Firstly, the low chloride content and absence of a tectonic fabric in contrast to the host rock, indicates precipitation in relatively recent fresh water rather than early marine conditions. Secondly huntite, with its rhombohedral calcite type lattice (Lippman, 1973), should show a strong Sr depletion upon recrystallisation such as

Figure 5.13

Huntite macrotexture (X1) from a serpentinised shear zone

Legend:
Green Serpentine — strongly foliated
Brown Serpentine
H : Huntite   M : Magnesite
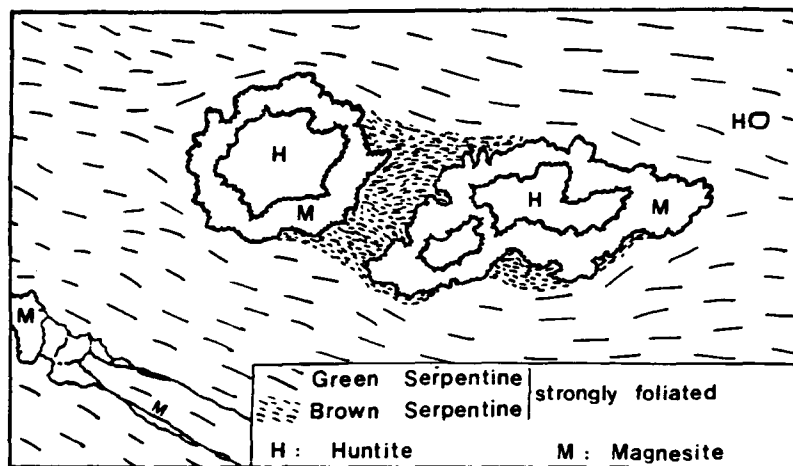
that shown by the transitions: aragonite → calcite (Kinsman, 1969), or calcite↔ dolomite (Al Hashimi, 1976), whereas the observed high Sr content (Table 5.15) is more characteristic of primary carbonate minerals. Thirdly, in common with huntite from other environments, the texture is friable, unlithified and shows no petrofabric evidence of recrystallisation.

The exposed Mg^- huntite was completely dry, but shallow groundwaters and surface waters from almost identical geochemical environments (Table 5.2b) gave a $\left[m_{Mg}{}^{2+}/m_{Ca}{}^{2+}\right]$ variation of: mean 8.3, standard deviation (σ_{n-1}) 7.5, and range 1.9 to 30.2. This compositional range is remarkably similar to the values predicted by Kinsman (1967) for huntite precipitation from carbonate-evaporites. The mantle sequence surface waters vary from slightly undersaturated to slightly oversaturated with respect to most carbonate minerals, and are consistently oversaturated only with respect to dolomite (Table 5.14) which, though common elsewhere in the ultramafic rock, is not associated with the Mg-huntite. Precipitation of Mg-huntite rather than dolomite and magnesite was illustrated by Carpenter (in Schmidt, 1962), and is shown in Figure 5.14 with the $Mg^{2+} - 2HCO_3^-$ groundwater field superimposed. For magnesite (and Mg-huntite) to precipitate, further Mg^{2+} concentration and a supply of OH^- ions is required. Both the composition and paragenesis of the carbonate phases are therefore explained by progressive brucite dissolution, i.e. (1) An initial $Mg^{2+}-2HCO_3^-$ pore fluid with a $m_{Mg}{}^{2+}/m_{Ca}{}^{2+}$ ratio of about 10 is introduced to a serpentine-brucite fracture system: (2) The rock-water system effectively closes, either due to carbonate cementation or to lack of recharge and throughflow under the arid climatic conditions: and (3) Continued release of Mg^{2+} (from brucite) and precipitation of Mg^{2+} and Ca^{2+} (as huntite) progressively elevates the fluid Mg/Ca ratio resulting in Mg-huntite precipitation and finally, as the $m_{Mg}{}^{2+}/m_{Ca}{}^{2+}$ ratio exceeds about 1200, magnesite precipitation.

Despite the sparse and inconspicuous distribution of brucite in the ultramafic weathering zone, its high solubility and dissolution in surface or near-surface waters by the reaction:

$$Mg(OH)_2 + 2\ CO_2 \rightarrow Mg^{2+} + 2HCO_3^- \qquad\qquad (37)$$

(brucite) (atmosphere)
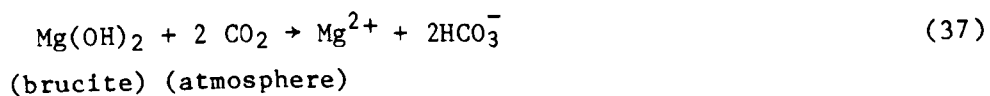
probably accounts for the apparent disparity in Mg/Si molar ratio
between serpentinite and surface waters, i.e.

rock:-   mean 1.44 , st.dev. σ_{n-1} 0.44, range 1.41 to 1.48, no.4
water:-   mean 6.0   , st.dev. σ_{n-1} 2.1, range 3.2 to 9.7 , no.12

The alternative: incongruous dissolution of serpentine, would imply a
silica sink within the weathering zone, but although rare siliceous
phases, such as sepiolite, have occasionally been found, no
volumetrically significant silica sink could be identified.

Figure 5.14

Equilibrium relations of stable (solid lines) and metastable (broken lines) phases,after Carpenter,1962

normal groundwater field shaded
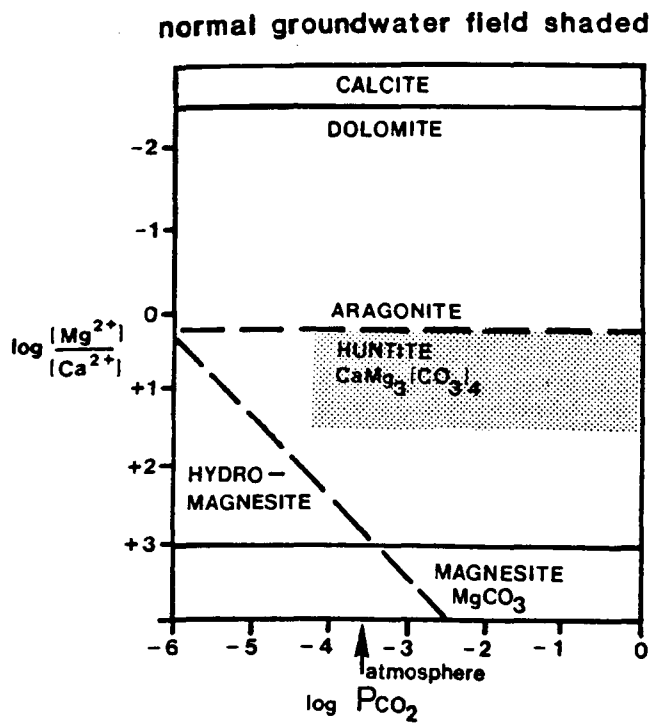
CHAPTER 6

THE ALLUVIAL BASINS

6.1   The Sedimentary Régimes

The primary importance of alluvial groundwater is obvious from the distribution of agriculture both adjacent to and within the mountain zone. In the case of the Batinah plain flash floods debouch onto, and infiltrate, a broad expanse of unbroken flat lying alluvium whose surface extent and downstream (though not lateral) boundaries are well defined, whereas in the mountain and interior regions the alluvium varies from minor wadi beds and small fluvial embayments to basins hundreds of km^2 in extent, and from thin weathered surfaces to deep alluvial trenches. In the latter region, the depth of alluvium, the extent of subsurface water transfer from hard rock to alluvium, and the hydraulic continuity (or discontinuity) between interconnected alluvial areas, are often difficult to determine. Furthermore in the mountain and foothill areas, groundwater storage and flow throughout the basin is generally subject to important human influences of abstraction, consumptive use and irrigation return, thereby creating complex hydrological systems in which water use is interdependent with both water quality and quantity. This contrast between "Batinah" and "Interior" sediments reflects a profound difference in the underlying crustal tectonics between the two regions.

In the interior the alluvium has accumulated as basins in and around the leading edges of the nappe sequence, which in turn rests upon relatively stable continental crust. The age of deposition varies from late Neogene to Quaternary and Recent Periods, during which time the effective base level of erosion, i.e. the dominant control upon clastic sedimentation, appears to have fluctuated through several hundred metres including a rise of at least 300 m to its present high level. This is primarily a diastrophic change and is indicated by: (1) A discontinuous tongue of sabkha and low relief between Umm as Samim to the Arabian Gulf and Masirah Littorals (Patterson and Kinsman, 1977; Figure 1.1) suggestive of previously continuous marine conditions along the interior

desert foreland and (2) the presence of dispersed undated but "recent looking" shallow marine faunas of Ostrea sp. at Jebel Sunaina at 400 m altitude (Letts, 1979), and Cardium sp. near Jebel Madar at 300 m altitude. The latter site being 125 km inland and apparently unrelated to the mountain axial uplift, constitutes the more significant evidence. Contrary to this trend, a brief eustatic depression of sea level in the Arabian Gulf, presumably correlating with the Wurm glacial maximum of about 2×10^4 b.p., is estimated to have been as much as – 120 m (Kassler, 1973). There is no geomorphological evidence to support a significant erosional response specifically related to this stage in the interior foreland, but there is abundant evidence to suggest a current erosional maximum, at least in the foothill areas. This includes the preponderance of only shallow alluvium (typically less than a few tens of metres thick), occasional inliers of heavily cemented terraces, and remnants of fluvial sediments on hard-rock up to 30 m above the present alluvial surface. Consequently the previous sedimentary record of the interior, possibly involving several cycles of Neogene deposition and erosion, is largely lost.

By contrast, the Batinah plain is a subsiding continental margin in which prograde clastic sedimentation appears to have occurred more or less continuously since the mid-Tertiary period. The effective inland edge of the plain may be regarded as the "hinge line" between subsidence to seaward, and uplift along the mountain axis, and is approximately delineated by the discontinuous outcrops of Palaeogene limestone (cf. section 4.7, Figure 6.1). The base of the Neogene is marked by a sharp but conformable facies change from shallow marine Palaeogene carbonates to terriginous conglomerate (eg. Plate 6.1); a distinctive contact, which also forms a seismic reflecting surface and which is traceable with increasing depth of alluvium to seaward. A seismic profile of the Batinah at Khaburah shows that the limestone dips to seaward at a constant $15°$ angle, thus giving a depth of 3.75 km with a two way reflection time of 2.6 s at the deepest (coastal) section; i.e. implying a mean alluvial seismic velocity of 2.88 km s^{-1}. This is consistent with the normal range of 1.5 to 3.7 km s^{-1} for consolidated and/or cemented clastic rocks quoted by Griffiths and King (1965). Further south-east where the Batinah plain broadens out at Wadi Bani Umr (just west of Wadi Bani Kharus), the near coastal sediments reach their

Figure 6·1

Distribution of Agriculture and Main Fluvial Channels
in the Batinah Plain
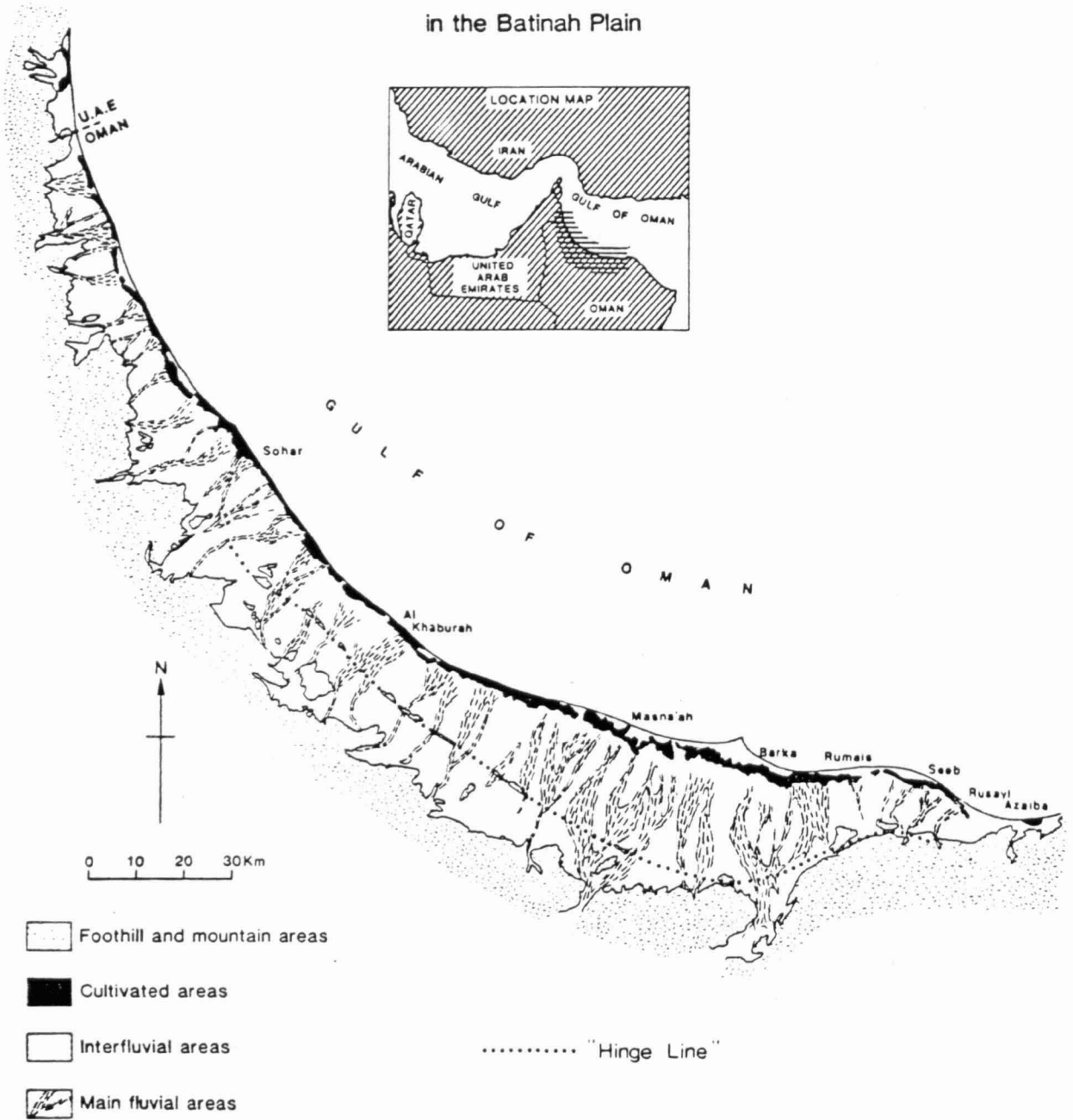
maximum thickness with a two-way reflection time of 3.8 s. Assuming similar seismic velocity of the alluvium, this corresponds to a total alluvial thickness of about 5.5 km. Even allowing for uncertainty and inhomogeneity in the acoustic properties, there is therefore no doubt of the great seaward thickness of the alluvial wedge beneath the Batinah. This wedge pattern is complicated by two features. Firstly the offshore re-emergence of Palaeogene limestone in the Suwadi, Daymaniyat and Fahal islands (Figure 6.1) clearly constitutes a northward termination of the Eastern Batinah sedimentary basin. The nature of this boundary is unclear, but structural and limited seismic data suggest the presence of an offshore steeply faulted monocline with a large throw to the south. Secondly, there is no correspondence between present-day major wadi systems, and simple Bouguer anomalies beneath the Batinah (cf. Shelton, 1984). Rather, the gravity anomalies, of up to 150 mgals, appear to be related to highly variable Pre-Neogene subcrop relief. As these sedimentary boundaries are well beyond and beneath the zone of significant groundwater flow, the aquifer boundaries are effectively the coast itself, and the "saline interface", discussed in section 6.4.

6.2 Interior Groundwater Systems

Few wadi gauging results are available from the interior basins, and since attempts to compile a comprehensive water balance must be integrated with the hard-rock hydrology, quantitative hydrology is therefore discussed more fully in chapter 7. The following descriptions of alluvial basins are therefore largely qualitative. The three main examples, selected to span the range of contrasting geomorphology, also reflect the varying approaches to analysis and levels of knowledge of different areas. With the exception of Wadis Dayqah, Nizwa and Mu Aydin most of the remaining interior basins have received little or no systematic hydrological research.

(1) Wadi Bahla

In draining southwards from the highest scarp of the Jebel Akhdar, Wadi Bahla changes in character, both lithologically and geomorphologically, from a high altitude "source area" to: an upper

243

limestone/ophiolite-bounded piedmont basin, a central
ophiolite/Hawasina-bounded alluvial basin, a lower "outwash" basin, and
finally an area of ephemeral flow terminating in the interior desert, as
shown in Figure 6.2. Insofar as some or all of these environmental
types have counterparts in other interior catchments, Wadi Bahla is, in
many respects, a typical groundwater system. A normal density of
agriculture for example is dispersed over a broad 60 km zone, being
limited in the north, i.e. the mountain piedmont, by the constraints of
soil availability and rapid falaj recession rates, and in the south by
increasing groundwater salinity (Stanger, 1985). In particular the
narrow flood channel is constricted in several places by hardrock "nodal
points", thereby facilitating relatively easy falaj abstraction and
thus development of the important agricultural centres of Bahla and
Bisyah. The foothill configuration has also caused the confluence of
Wadi Bahla with its major tributary, Wadi Sayfam, the latter being a
large and important wadi system in its own right (710 km^2 as opposed to
1120 km^2 in Wadi Bahla upstream of Bisyah). The sedimentary history of
the interfluvial area between these wadi systems is the controlling
influence upon groundwater distribution in the central alluvial basin.
A less obvious feature of the nodal points is their "hard rock
thresholds", or local base levels of erosion, which have given rise to a
stepped wadi profile in which neither excessive incision nor deposition
has predominated. Consequently the local stratigraphy is relatively
well preserved and serves as a model for other interior alluvial
systems. Seven sedimentary units are differentiated although the arid
continental conditions prevalent throughout the Neogene and Quaternary
periods have left no dateable fossils or features prior to the first
archaeological remains. Nowhere do these units all exist together, and,
in many places, only two or three units may be seen or deduced to
exist. The section shown in Figure 6.3 is therefore a schematic
composite approximating to North Bisyah where the stratigraphy is best
exposed.

Figure 6.2   The Sayfam - Bahla Catchment :   Main Physiographic
              Features

JEBEL
AKHDAR

THE WATERSHED
APPROXIMATES

AL HAMRA

GHAFAT   BAHLA

WADI
SAYFAM

WADI BAHLA

BISYAH

N

▲ MAIN HOLOKARST SYSTEMS

H.S.G. & EXOTIC LIMESTONES

HAWASINA

+ OPHIOLITES

..... APPROXIMATE LIMIT OF SEMAIL SUBCROP

PRINCIPAL WATERSHEDS

0   Km   10
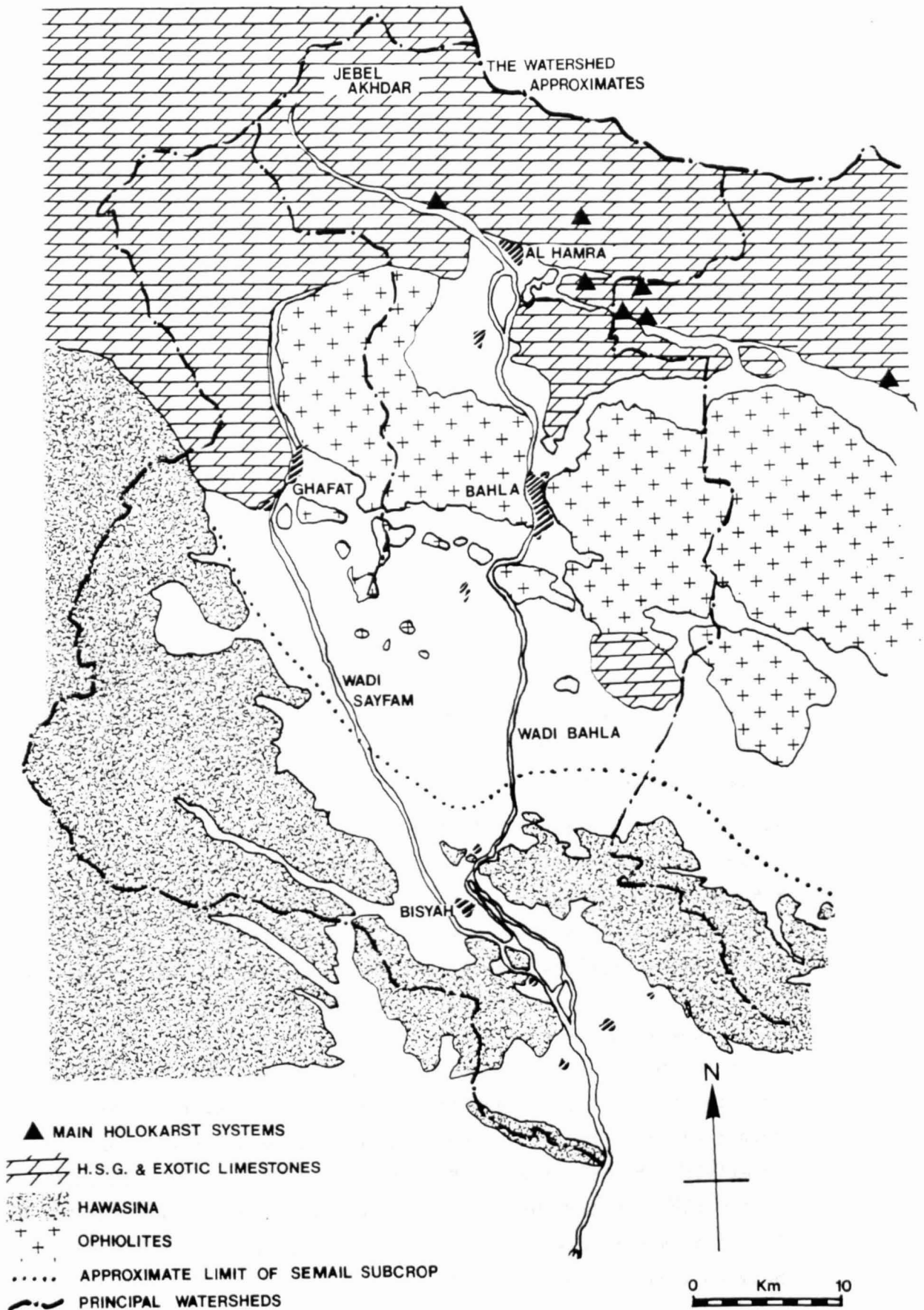
Figure 6.3

Schematic Composite Section of Sediments in Wadi Bahla

"Impervious" bedrock   1: Scree   **2,3,5**: Conglomerate
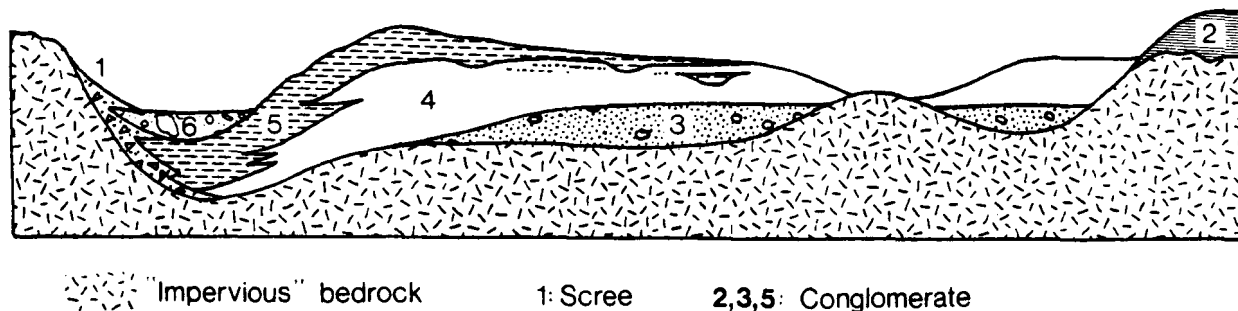
The units are:

1. In situ weathered detritus and medium to coarse angular screes
which drape the lower hardrock hills and partially underly the
surrounding alluvium. Around Bahla this takes the form of friable
irregularly shaped gravel and cobbles whilst, around the Hawasina
hills, cm up to dm or even m thick flaggy limestone and chert
fragments produce a highly heterogeneous colluvium interdigitated
from the oldest to the youngest sediments. Pockets of very high
porosity occur but are of trivial hydrological significance.

2. The oldest horizontally bedded sediments are remnants of an
older cycle of sedimentation. They consist of well cemented
conglomerate terraces whose sand abrasion planed surfaces stand
some 10 metres above the modern flood plain level. The limestone
particles exhibit dew etching whilst chert and igneous pebbles have
well developed desert varnish: both characteristic of an old
stable desert surface (Plate 6.2). The terraces form sub-linear
features which outcrop over less than 5% of the alluvial area.
Even this extent of preservation is fortuitous, owing to the
relatively high relief and resistance to fluvial erosion of the
underlying "radiolarites". Nevertheless erosion into this unit has
profoundly affected subsequent sedimentation and groundwater by
imparting a northeast to southwest trending "grain" to the area
between Wadis Sayfam and Bahla.

246

3. A considerable erosional hiatus, in which up to 20 metres of sediment was lost, left a thin (0 to 5 m) but complex veneer of locally weathered material over exposed ophiolites throughout most of the Bahla/Sayfam interfluvial plain. This consists of very fine grained white to red mudstone with a high proportion of oxidised (reworked?) umber and, less commonly, green weathered basic rocks; the former having uniformly poor hydraulic properties whereas the latter is the productive horizon for several poor to indifferently yielding pumped wells. This base of the present sedimentary cycle was succeeded by about 5 metres of porous fluvial conglomerate, weakly cemented with silty lime and containing occasional sand layers. The unit is not normally seen at the surface but underlies most of the sediments of the central Bahla basin at a depth of between 10 and 15 metres. It is the principal aquifer and is therefore best observed in spoil heaps that surround the many wells of the area. Deposition of this unit has involved the multistage migration of Wadi Bahla to the west of its present course, and lesser eastward migration of Wadi Sayfam.

4. Unit 3 was followed by slow undisturbed accumulation of aeolian silt consisting of about 25% carbonate, and the remainder of clayey silicates (SiO_2 about 30-40%*). Over 10 metres of this very fine grained loess-like sediment have accumulated over large areas in the form of massive to dm bedded, poorly defined undulating laminae, but apart from thin transitional gravel horizons at the upper and lower margins, the unit is entirely devoid of primary fluvial structures. The silt is superficially similar to the reworked finer fraction of fluvial sediments which are widespread in near coastal parts of the Batinah plain, but differ in having a better sorted and more uniform particle size distribution. Furthermore, at North Bahla where no alternative wadi channel exists and where the silt is laterally overlain by high energy sediments (e.g. as in Plate 6.3), it is inconceivable that such extensive fine grained sediments could have been produced by fluvial deposition. In the absence of fluvial activity is is therefore concluded that indications of an apparently high water

---

* The total SiO_2 is only approximate due to unusual X-ray mass absorption characteristics of the carbonate/silicate mix.

table, such as occasional lithified "calcrete" horizons, sporadic
traces of gypsum, fresh water snails and fossil root porosity, are
diagenetic products of subsequent, less arid conditions. Calcrete
horizons are probably responsible for the semi-unconfined rather
than the unconfined conditions reported from some of the tests in
the underlying (unit 3) conglomerates a few km east of Wadi Sayfam
(GDC, 1982 data). The silt is normally unlithified and erodes
easily by deep gullying adjacent to the modern wadi systems, and is
thus best preserved and most easily utilised for agriculture in the
interfluvial areas.

5.   The return to normal fluvial conditions is marked by an upward
passage into weakly cemented gravels. These vary in thickness from
0 to >5 metres near Bisyah, and commonly form the banks of the
active wadi channels. With increasing distance from the wadis the
gravels occur both as attenuated thin veneers apparently of sheet
flood origin, and as scoured gravel-filled distributary channels
incised into the aeolian silt surface. It is probably significant
that the return to a wetter environment, associated with the
aeolian-fluvial transition, coincides with the earliest
archaeological settlements found in Oman, which are thought to have
an age of about 5000 b.p. (Orchard, 1985). However, alternative
evidence, based on more general grounds, of late Pleistocene
tropical aridity between 30,000 and 15,000 b.p. (Williams, 1975),
suggests that the aeolian to fluvial transition may be an older
disconformity in the form of an old stable or deflation surface.

6.   Gravels of the modern wadi courses are predominantly
uncemented, with occasional caliche horizons and irregularly
distributed pebble to clay grade horizons (Plate 6.4). Larger
particle sizes range from large boulders at the limestone piedmont
to sand/fine gravel in the outwash plain some 80 km further south,
throughout which very high porosity and permeability is
ubiquitous. Rapid infiltration into the modern sediments during
flash floods therefore results in maximum recharge and very
shortlived surface flows (eg. seldom >2 days) throughout the wadi,
except at Bahla, where the shallow alluvium may force groundwater
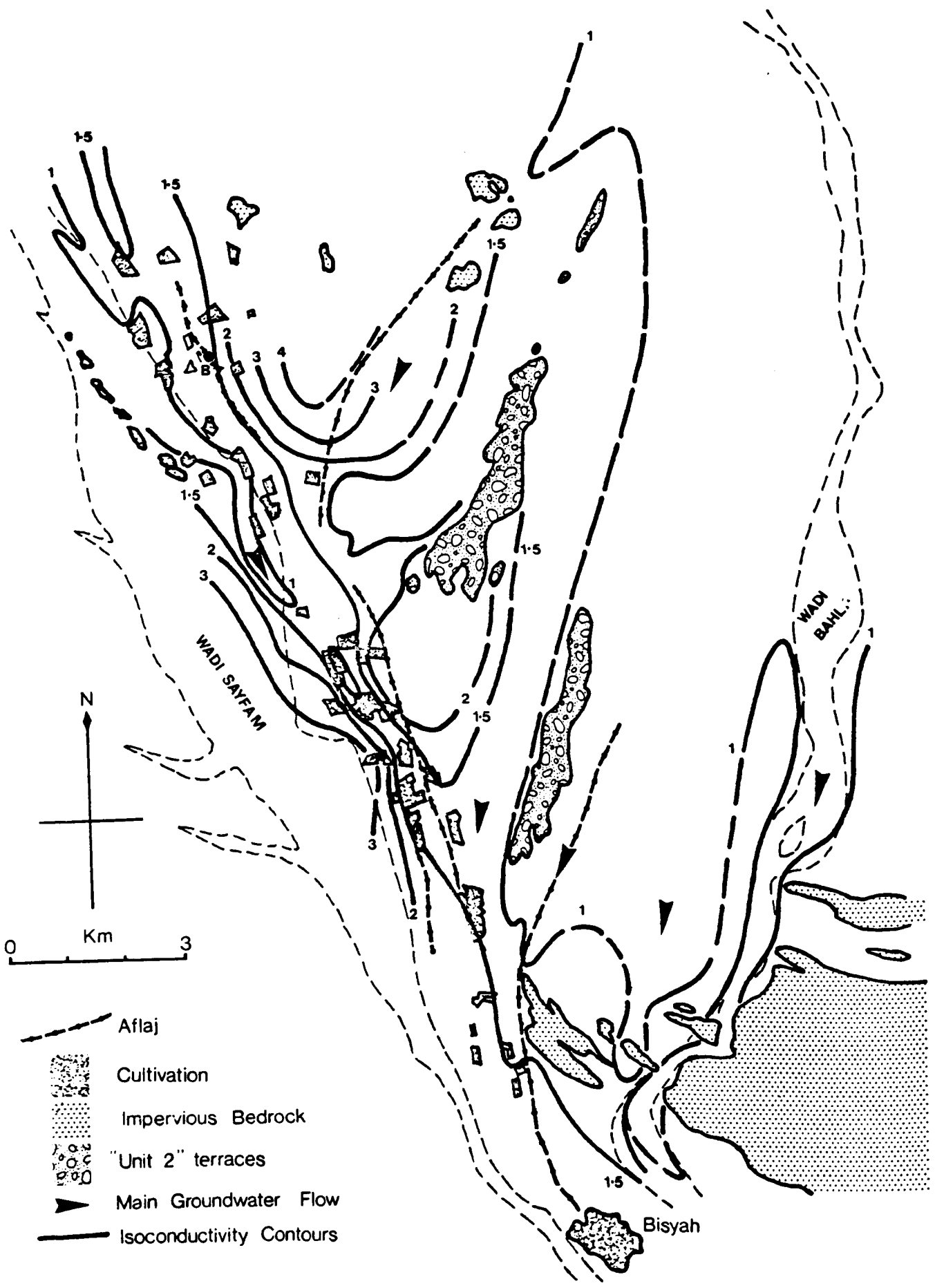to the surface for weeks or even months at a time.

7.   Fine grained dune sand, partly contemporaneous with the modern
fluvial sediments is sporadically distributed but hydrologically
unimportant in the Bahla catchment.

An exception to the above sedimentary scheme is the line of deeply
incised fanglomerates which form high, vertical sided boulder terraces
adjacent to the limestone piedmont and especially radiating from the
major limestone gorges, eg. Plate 6.5. Geomorphologically, they are
equivalent to unit 5, above, but their extent and high degree of
cementation suggest a much older origin. Their bank storage and
probable role in transferring groundwater from limestone to alluvium is
potentially of considerable importance. Similarly, although there is a
shortage of both drilling and geophysical data from the piedmont area,
two borehole logs from "Bahla-WSI-44" and "North Bahla-WSI-47" (the
exact site being uncertain), indicate >70 m of "marl" and 50 m of
gravel respectively (Scott Wilson Kirk-Patrick, 1972). The former,
clearly referring to clayey loess of unit 6, is a surprising thickness
and represents three to four times the maximum observable thickness in
the vicinity of Wadi Bahla. These thicknesses, if correct, therefore
indicate a substantial northward thickening of· the sedimentary aquifers
and consequently, potentially large groundwater storage.

Previously described sedimentary events of the southern interior
(Stevens 1969, 1978) and the western piedmont (Halcrow, 1969) describe,
in general terms, the local conditions of gypsum and caliche formation,
but do not permit the correlation of sedimentary facies with the above
scheme.

East of Al Hamra in the northern (piedmont) basin, some 25 $1.s^{-1}$
groundwater is derived by baseflow transfer from limestone to alluvium,
i.e. from "buried springs". Otherwise primary water supplies with a
total flow varying from about 85 to 620 1.s (1974/75 data), is derived
from aflaj which tap the obvious alluvial aquifers adjacent to, or even
in, the modern wadi channels, e.g. the aflaj of Al Hamra, Bilad Sayt and
Bahla. Further south, downstream of Jabrin (Figure 6.4) the groundwater
distribution of the central Bahla basin becomes more complex. The main
wadi channels of Bahla and Sayfam still contain abundant evidence of
modern recharge, such as trash marks and dense phreatophytic growth
along the banks, but the irregularly disposed agriculture throughout the

249

Figure 6.4 Central Wadi Bahla : E.C.(mmhos) and Groundwater Flow

Legend:

Aflaj

Cultivation

Impervious Bedrock

"Unit 2" terraces

Main Groundwater Flow

Isoconductivity Contours

WADI SAYFAM

WADI BAHL.

Bisyah

N

Km

0 — 3

interfluvial areas strongly suggests the presence of lateral groundwater flowpaths beneath the apparently uniform sedimentary cover. The presence of over 100 hand-dug wells throughout the area permits the approximate delineation of these groundwater pathways since: (1) the salinity of groundwater is closely related to residence time and hence to the throughflow of relatively recent groundwater recharge. i.e. low electrical conductivities tend to plot along the active flowpaths, and (2) the time lag of the water table response behind flood events in the major wadis gives a semi-quantitative measure of the proximity of zones of groundwater recharge. The latter, though only assessed from verbal reports at individual wells, is justified by well hydrograph records from previous consultants (Gibb, 1976) which demonstrate an inverse relationship between the rate of water-table decline, and distance from the Wadi Bahla. In addition, more recent resistivity work (GDC unpublished data) using constant separation traverses, has demonstrated the presence of at least one buried groundwater channel of less than 500 m width and possibly as narrow as 100 m, which follows an old "unit 2" terrace lineation. This and other groundwater pathways, illustrated in Figure 6.4, either follow the same south-westerly trend including the source of Bisyah falaj, or subparallels the main Wadi Sayfam channel. The prominent scatter of farms over what appears to be the old channel of Wadi Sayfam, is based around about 50 wide bore dug wells, some of which have the unusual feature of adits along productive joints of the "unit 3" aquifer. A recovery water level test on a typical well (without adits - B on Figure 6.4) gave a transmissivity value of about 200 m^2/day which compares with recent pumped borehole tests in the same vicinity yielding transmissivity values of between 2 and 200 m^2/day with typical values of 75 m^2/day in most producing wells. The lowest values correspond with the thin sediments of the northern interfluvial area - the "Lajrid plain" - where farms have not been developed. Corresponding high salinity in this interfluvial area is mainly attributable to the high subcrop relief and hence absence of recharge channels, and long residence times. Additional salinity may also arise by strongly evaporated ephemeral surface flow from falaj Lajrid (E.C. = 900 μmhos) which itself originates as irrigation return from Jabrin. South of Bisyah, the pattern of salinity remains complex though with the relatively sparse distribution of wells it is less easy to attribute the rising salinity to specific causes.

To illustrate more fully the overall changing groundwater chemistry throughout a catchment, three hydrochemical profiles are presented in Table 6.1 and Figure 6.5. The first two, wadis Bahla and Nizwa are adjacent wadi systems, both draining the high altitude limestone "source area" of Jebel Akhdar, and presenting similar geological and geomorphological characteristics. As in Wadi Bahla the interfluvial sediments of the Nizwa basins are thin, consisting of 5 to 15 metres of dry coarse alluvium overlying widely spaced buried groundwater channels. Differences in sedimentology between the two basins appear to be minor and consist of: (1) a greater area of old conglomerate terraces in the southern central basin, (2) a suggestion, from the limited borehole records, of a rather higher clay fraction in the northern central Nizwa basin, and (3) a tendency for " buried groundwater channels" to drain towards the main wadi from tributary channels, rather than away from it, as was the case in Wadi Bahla, (Howsam, pers. comm. 1980; and Figure 6.6 reinterpreted CGG, 1975 and PAWR apparent resistivity data from the central Wadi Nizwa basin). In practice, the eventual wadi convergence, and hence mixing of ground-water, further south in both catchments results in similar overall hydrochemical trends. The Wadi Sâmad catchment further east, Figure 6.7, differs markedly in having a much lower altitude hardrock catchment entirely composed of ophiolites. All three profiles are of similar length. The predominant feature in both the "limestone" wadis is the rapid increase in salinity after about 50 km, rising to excessively high levels after about 70 km. This effect is equally well illustrated by the E.C., sulphate and chloride levels shown in Figure 6.5, and correlates with the decreased groundwater velocity/increased residence time which in turn is caused by progressively fine grained sediments and decreasing hydraulic gradient (i). By assuming typical permeability values (k), the downstream groundwater velocity (k.i) may be shown to be of the order of metres or tens of metres/day. In the case of Wadi Samad, the rate of salinity increase is substantially less, and possibly relates to the much lower Ca^{2+} concentration, less alluvial cementation and consequently faster throughflow of groundwater. However, the age of the groundwater is not just a function of the time taken to percolate from the upper catchment, but relates more to the frequency of extreme flood events which significantly reach and recharge the far downstream areas. The latter process is exemplified by groundwater sampled close

Table 6.1 Chemical Profiles of Interior Wadi Systems

Sample Nos. refer to Appendix C site details. Nos. in brackets refer to data from Gibb, 1976, vol 6. Distances are measured from the highest piedmont boundaries. Ionic ratios are of equivalents.

(A) Wadi Bahla

No.	296	(121)	(186)	143	302	305	306	10	
Distance, Km	0	8	14	25	48	56	62	70	
EC	373	560	550	712	920	1600	2340	4500	
Cl^-	22	48	47	103	130	269	427	1115	
F^-	.33	.30	.35	.18	.23	.22	.29	.61	
NO_3^-	7.4	6.0	7.0	6.3	9.1	11.2	10.0	4.4	
SO_4^{2-}	38	62	44	72	123	248	358	834	
Ca/Mg	2.31	1.62	1.41	.39	.54	.40	.35	.79	
Ca/Sr	158	-	-	77	68	44	33	136	

(B) Wadi Nizwa

No.	54	(113)	58	191	223	321	7	8	319
Distance, Km	0	12	21	28	38	48	62	72	78
EC	473	380	800	925	809	1454	1575	2740	1741
Cl^-	38	31	75	137	110	240	280	580	278
F^-	.29	.20	.14	.18	.22	.19	.39	.29	.27
NO_3^-	2.1	8.0	10.4	4.0	4.6	12.2	11.0	15.5	9.8
SO_4^{2-}	53	32	84	99	95	133	239	789	337
Ca/Mg	1.54	1.33	.24	.33	.34	.46	.46	.40	.52
Ca/Sr	168	-	73	85	114	65	70	66	54

(C) Wadi Samad

No.	352	353	349*	348	350	356	355	351
Distance, Km	12	19	25	35	47	52	60	77
EC	533	736	449	838	1054	1066	1366	1541
Cl^-	38	58	57	70	137	94	159	204
F^-	.09	.08	.05	.06	.10	.07	.09	.18
NO_3^-	8.9	8.3	5.4	7.2	7.8	7.2	7.7	11.3
SO_4^{2-}	36	44	20	60	111	97	125	219
Ca/Mg	.36	.29	.23	.26	.33	.32	.27	.39
Ca/Sr	95	130	95	119	57	62	53	51

* tributary wadi

Figure 6.5   Hydrochemical Profiles of Contrasting Wadi Systems   (in mg.l^{-1})
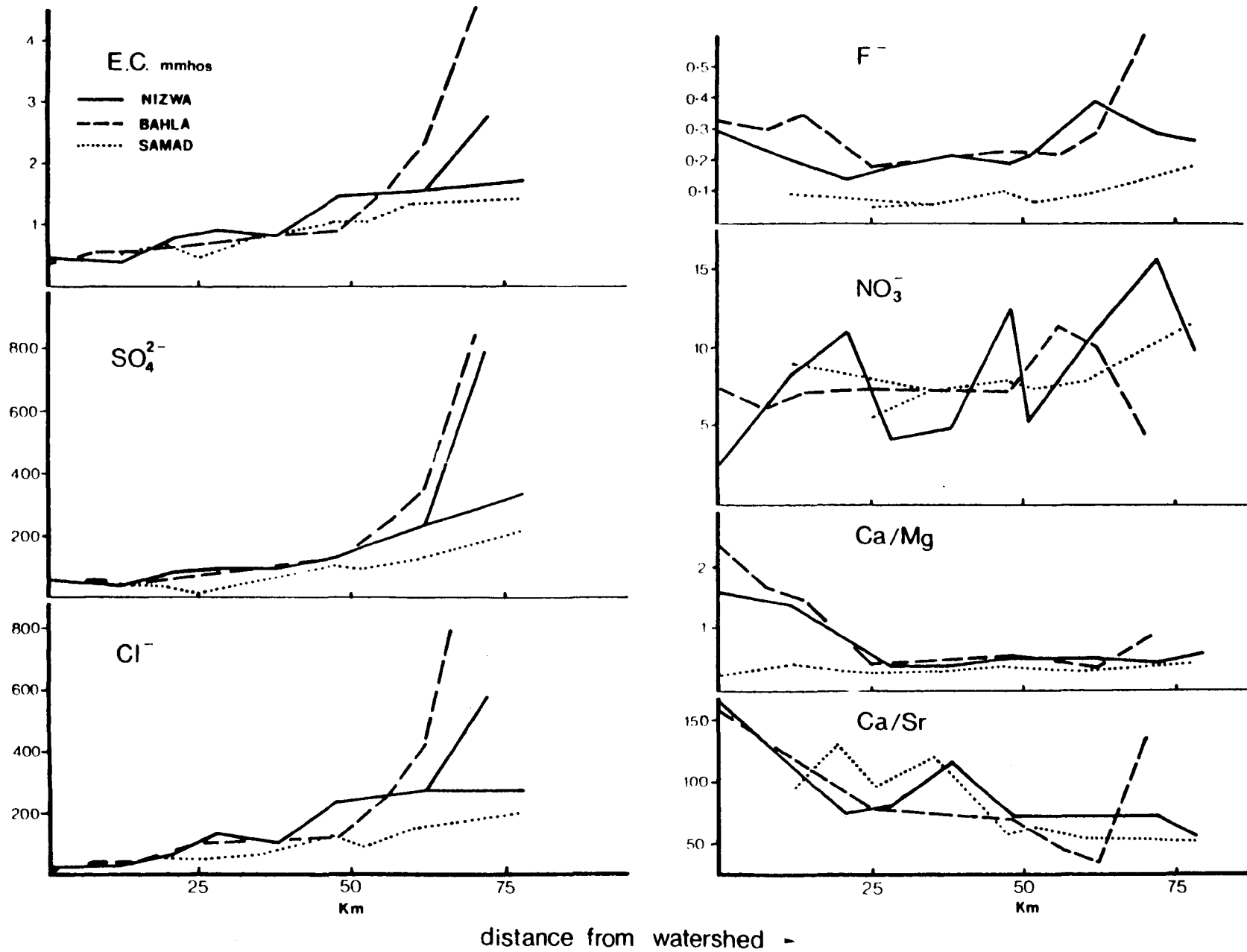
254

distance from watershed ►

Figure 6·6   Apparent Resistivity and Groundwater Flow in the
             Nizwa - Mu Aydin Catchment
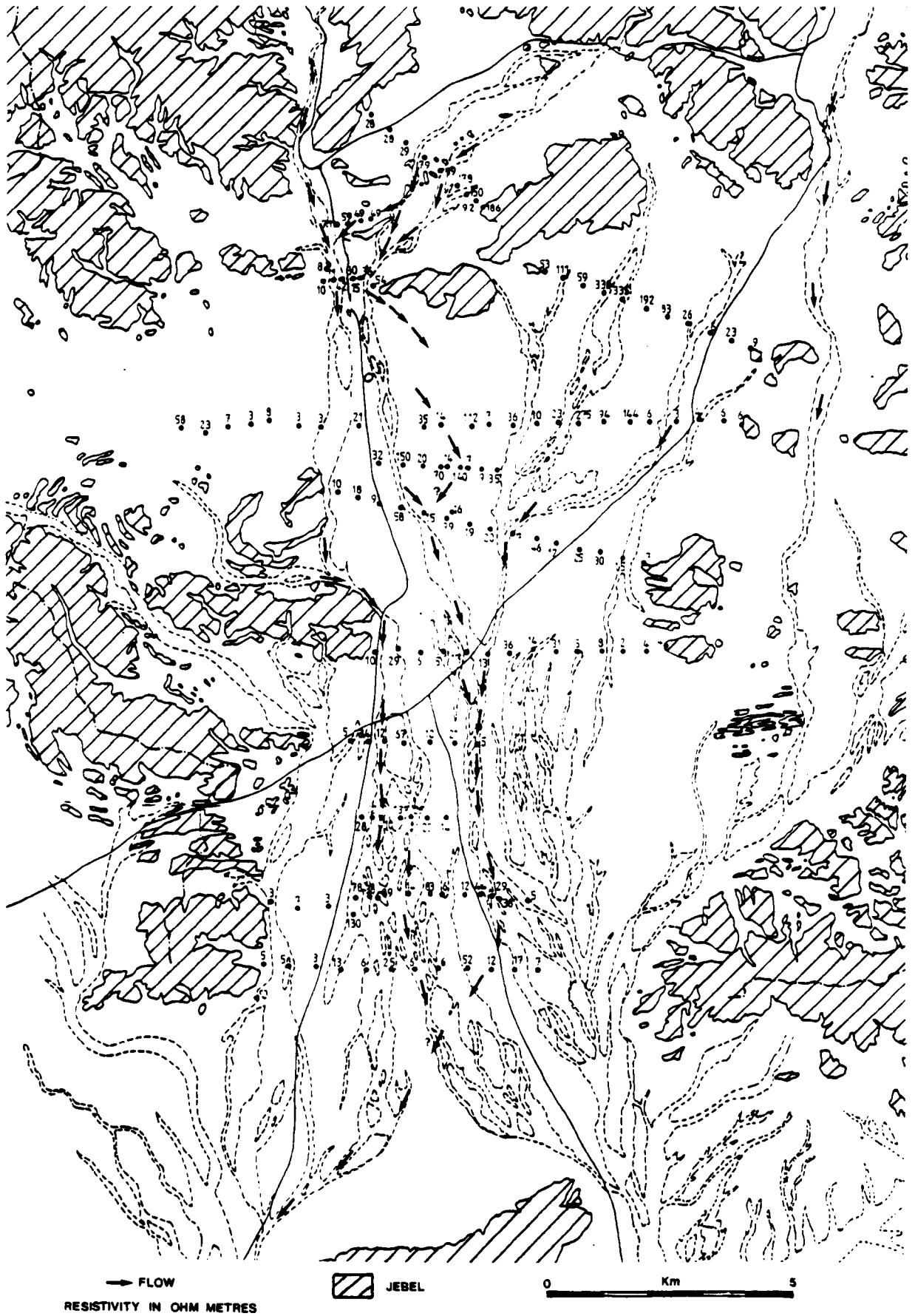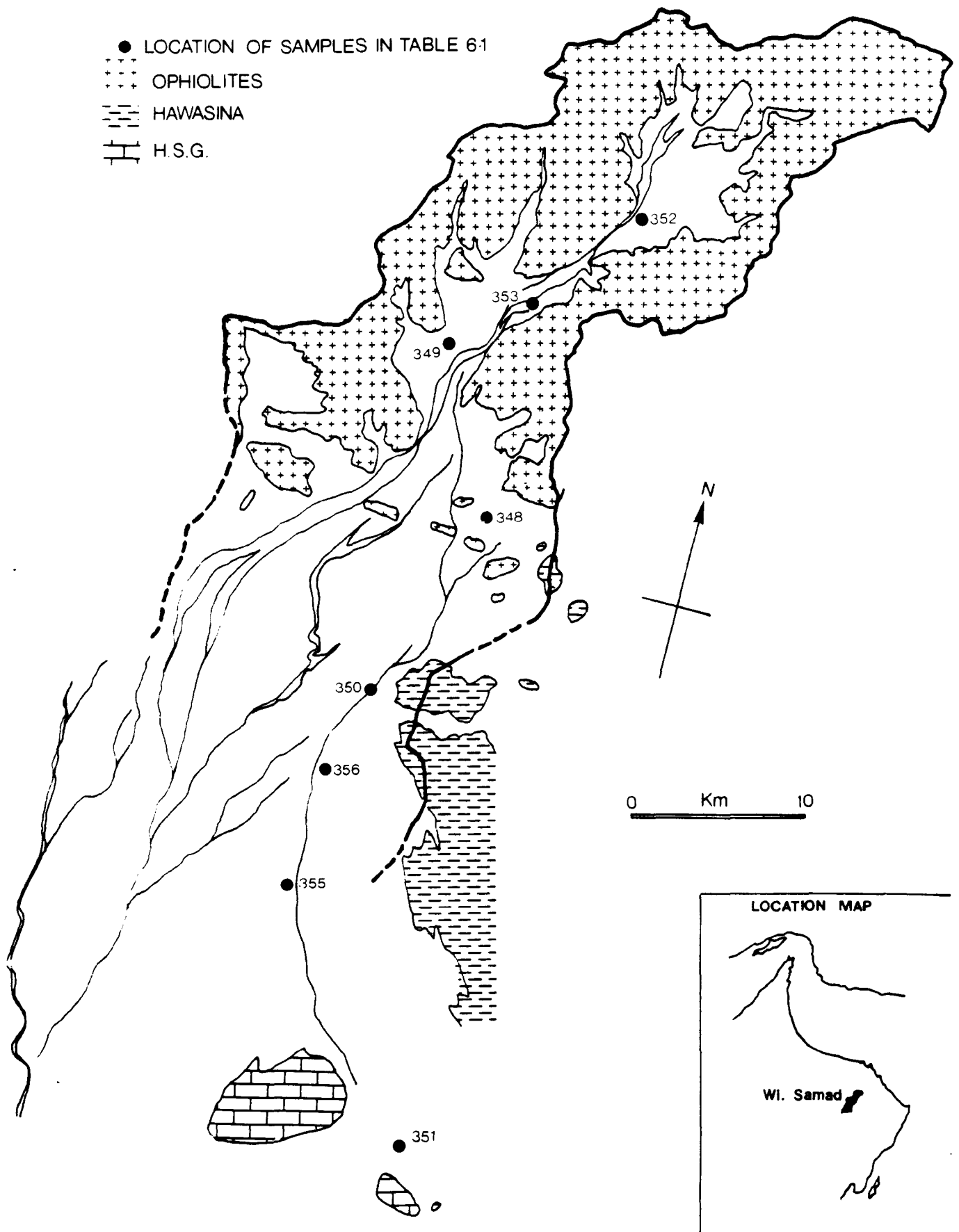
MODIFIED AFTER: ATKINS/P.A.W.R.,1986 & C.G.G. 1975 DATA

→ FLOW   ▨ JEBEL   0 _____ Km _____ 5

RESISTIVITY IN OHM METRES

Figure 6·7   The Wadi Samad Catchment

LEGEND:
● LOCATION OF SAMPLES IN TABLE 6·1
OPHIOLITES
HAWASINA
H.S.G.

to the Bahla/Nizwa watershed in Wadi Taymissah. Here the water cannot have percolated far from its source area, yet had a zero tritium concentration (cf. Appendix B2), indicating a long residence period and clearly infrequent recharge.

Fluoride (F^-) and less conservative ions such as NO_3^- and Ca/Sr show a much more complex behaviour and are generally difficult to correlate with geological parameters. Nevertheless the nitrate results from Wadi Nizwa, Figure 6.5, appear to show that the high concentration around Nizwa town, caused by urban and agricultural pollution, are not maintained far downstream. i.e. Whatever causes the subsequent nitrate variation, groundwater in the downstream areas is either of relatively local storage or derived from tributary wadis and hence owes little if anything to upstream irrigation return.

The calcium/magnesium ratio for the limestone and ophiolite catchments are markedly different, especially in the uppermost 25 km. This obvious correlation with the bulk rock chemistry of the hard-rock source area therefore appears to provide a criterion for differentiating the alluvial groundwater provenance, even in some of the more 'downstream' aquifer systems.

All of the main wadis may be regarded as tongues of relatively fresh groundwater which advance and retreat away from the mountains according to the state of flood and recession. Electrical conductivity monitoring of the major aflaj in Wadis Bahla and Nizwa shows that significant variations in salinity, e.g. ± 12% to ± 21%, are restricted to the piedmont alluvial areas such as Bahla and Nizwa towns, whereas further downstream the salinity is much more consistent: e.g. Bisyah ± 7% over 20 non-consecutive months (a figure close to the accuracy of measurement), and is presumably influenced only by the largest of flood recharge events.

The effect of residence time in increasing salinity results in progressively larger wadi-interfluve salinity contrasts with increasing distance from the piedmont, local variations of 200 to 300% being commonplace. Additional salinity is also caused by: evaporation and transpiration from surface water or high water tables, the dissolution of gypsiferious sediments as at Fulayj south of Bisyah, and alkaline

springs; the latter accounting for most of the anomalies in the upper basins. On the other hand, many tributary wadis, and especially those consisting exclusively of ophiolite gravels, are of lower salinity (typically 400 to 550 μmhos). The most notable negative anomaly is at Adam ('A' on Figure 6.5 and sample 319, Table 6.1) which, despite its 80 km distance from the piedmont, has a main falaj salinity of only 1740 μmhos (as compared to adjacent pumped well salinities of 3700 to 10200 μmhos). Since the catchment boundaries in this instance are ill-defined it is not clear whether any groundwater from wadis Bahla or Nizwa reach Adam, but relatively local recharge directly into the alluvial plain north of Adam seems to be the most plausible explanation.
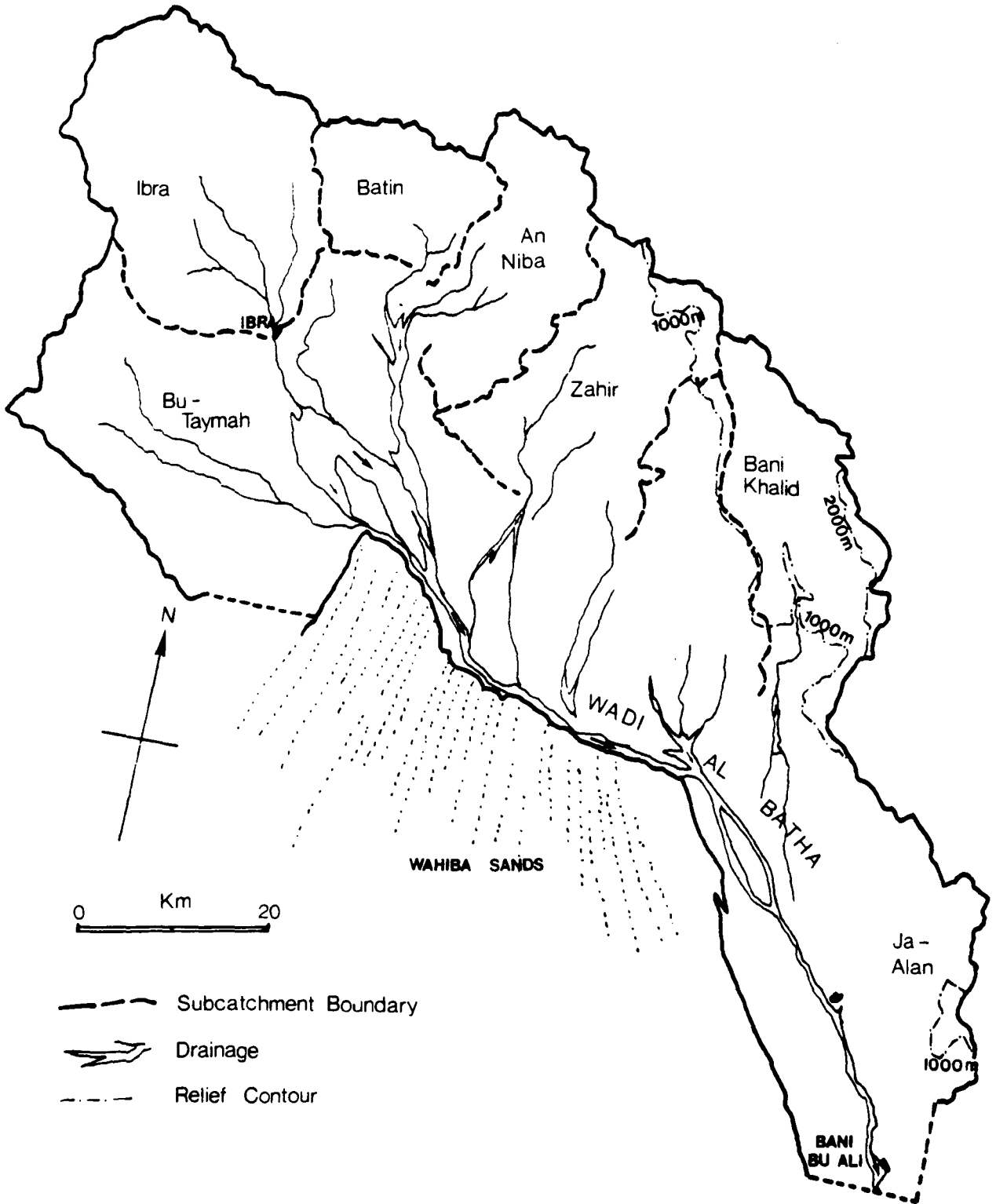
(2) Wadi Al Batha

Wadi Al Batha is the easternmost and, with an area of 5200 km^2, by far the largest of the interior wadis (measured to the furthest downstream village of Bilad Bani Bu Ali; Figure 6.8). Its complex wadi system is deflected eastwards, initially by the Hawasina foothills and subsequently by the Wahiba sand sea, resulting in a unique drainage pattern which runs broadly parallel to the mountain axis for a distance of about 140 km. Unlike the interior wadis of the Jebel Akhdar, Wadi Al Batha reaches the eastern seaboard some 35 km beyond Bilad Bani Bu Ali, although groundwater is too saline in this area to warrant much investigation.

All of the high relief source areas lie to the north of the main wadi and drain into it from a series of en échelon subcatchments with typical areas of about 500 km^2. Of these, the westernmost "Ibra" and northeastern "Wadi Bani Khalid" subcatchments are both the highest relief (up to 1280 and 2200 m respectively) and best defined of the hard rock watersheds. The four intervening subcatchments are individually smaller, less well defined and of slightly lower relief (generally < 1000 m), but together constitute the largest medium to high altitude source area. Wadi morphology and the uniformly low altitude of the largest subcatchment, Bu Taymah, suggest that its contribution to the Al Batha groundwater system is relatively minor.

In view of the complete absence of flood gauging, investigations have concentrated upon assessing the geometry and relative importance of

Figure 6·8   **THE AL BATHA CATCHMENT**

Ibra

Batin

An Niba

IBRA

Bu - Taymah

Zahir

1000m

Bani Khalid

2000m

1000m

N

WADI AL BATHA

WAHIBA SANDS

Ja - Alan

1000m

Km
0   20

BANI BU ALI

——— Subcatchment Boundary

——— Drainage

—·—·— Relief Contour

the groundwater flow from the various subcatchments and establishing the major storage locations within the Al Batha alluvium. However, the conclusions reached by previous consultants upon the basis of isotopic and hydrochemical evidence are called into question, and require partial reinterpretation in the light of the rainfall-groundwater isotopic relationships established in section 2.5, and hydrochemistry from Appendix C. Five representative stations along the main wadi course (Figure 6.9) have the isotopic values shown in Table 6.2 which have been plotted on Figure 6.10. The original arguments (Renardet et al., 1975) used the stable isotope data as follows:

(a) Since the observed composition of groundwater (Figure 6.10) cannot have been derived from the observed winter rainfall composition, the predominant groundwater recharge must have been from monsoon (summer) rainfall.

(b) Groundwater isotope variation is due to either evaporation or rainfall isotopic equilibrium at varying temperatures.

(c) The scatter of groundwater isotopes close to both the world and regional rainfall 'lines'; $\delta D = 8\delta^{18}O + 10$, $\delta D = ^{18}O + 14$, precludes significant evaporation.

Therefore

(d) the variation is solely a function of temperature, and since the monsoon is a consistent regional rather than local phenomenon, the variation is, in effect, solely a function of altitude.

(e) Assuming a typical isotopic/thermal gradient, the mean altitudes of recharge are:

Ibra Alayat	400 to 500 m
Al Kamil to Tawi Sultan	1000 to 1100 m
Bilad Bani Bu Ali	700 to 1000 m

Figure 6.9   Isotope Sampling Sites in Wadi Al Batha

LOCATION MAP

AL BATHA

IBRA

AL MINTIRIB

TAWI
SULTAN

N

WAHIBA   SANDS

AL KAMIL

Jebel

Scale (Km)

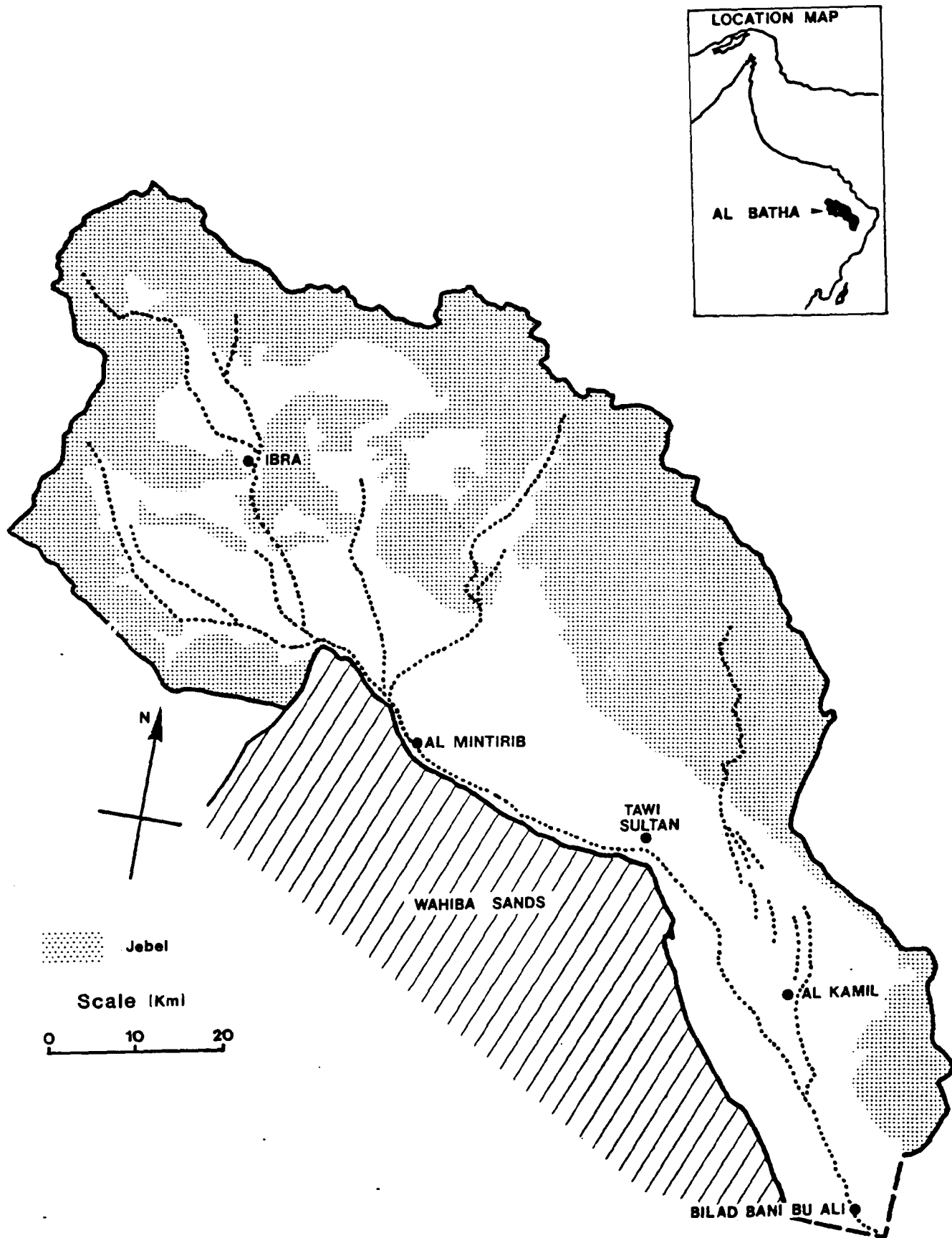0   10   20

BILAD BANI BU ALI

TABLE 6.2   Wadi Al Batha: Isotopic Compositions, After Renardet et al. 1974.

(Mean Values from aflaj except at Tawi Sultan where active groundwater flow would be expected).

|	$\delta^{18}O$	δD	Tritium
Ibra Alayat	− 1.13	− 0.42	12.8
Al Mintirib	− 1.78	− 3.85	6.8
Tawi Sultan	− 2.49	− 7.9	2
Al Kamil	− 2.40	− 8.4	2
Bilad Bani Bu Ali	− 2.0	− 9.2	7.9

TABLE 6.3   Salinity Variation along Wadi Al Batha

(measured from active aflaj)

Site	Distance from upstream piedmont	E.C. μmhos	Appendix Sample N
Musayb, 3 km upstream from Ibra	22	522	245
Hawiyah	81	587	433
Al Kamil	130	616	392
Bilad Bani Bu Ali	145	732	436

Figure 6·10   Groundwater Isotopic Compositions in Wadi Al Batha

Groundwater Data from Rénardét et al 1975
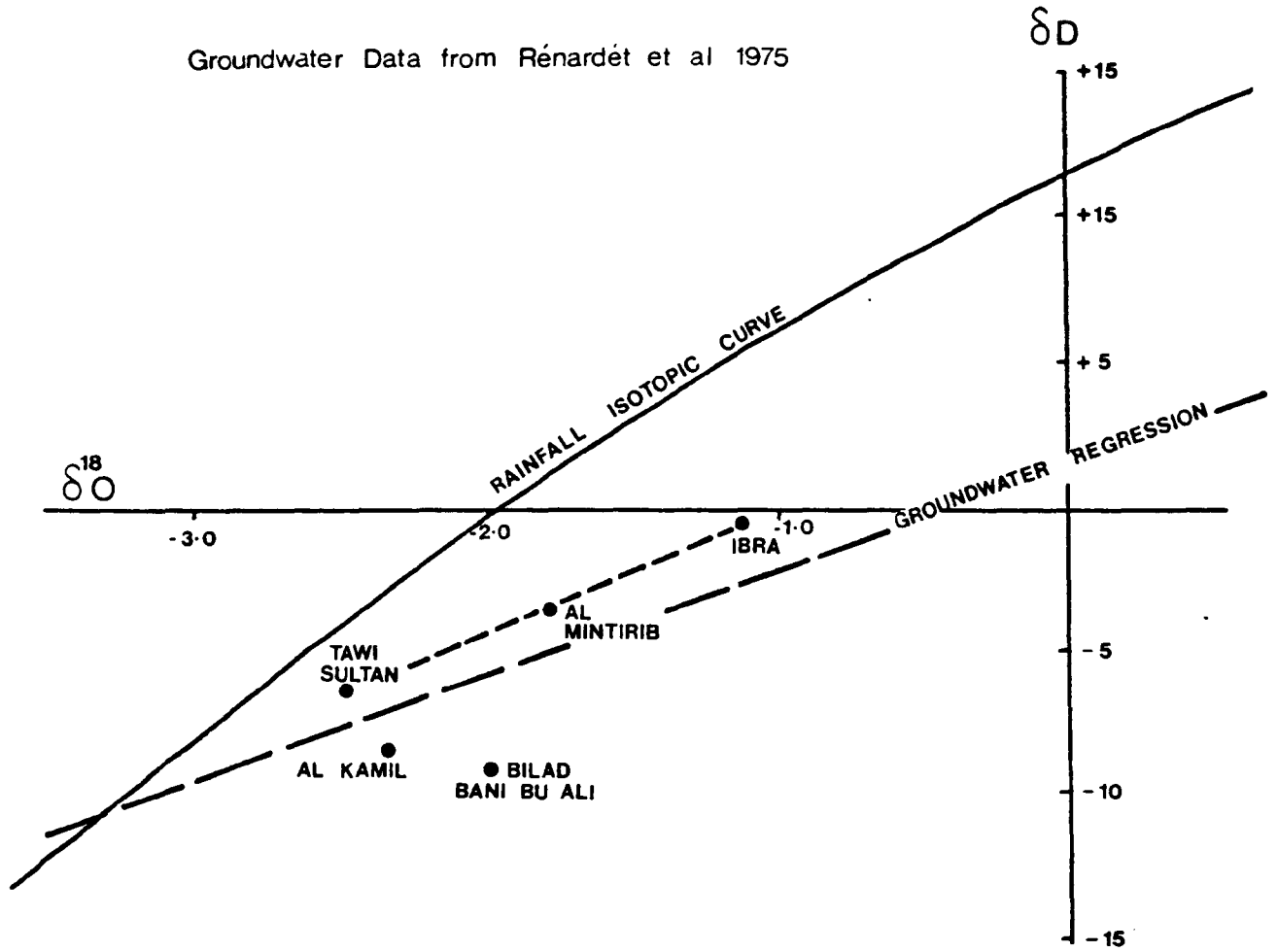
This reasoning, together with the tritium age implications led to the following conclusions:

(i) Since the groundwater isotopes fall into two distinct groups: Ibra to Tawi Sultan (upstream), and Kamil to Bilad Bani Bu Ali (downstream), there is no mixing of the two and therefore groundwater from the upstream basins flows southwards into the sands, rather than eastwards along the line of the wadi.

(ii) High tritium upstream of Ibra points to relatively recent recharge and hence to limited alluvial storage in the Ibra subcatchment.

(iii) The intermediate tritium and stable isotope values at Al Mintirib derives from approximately equal proportions of local recharge and old water from high altitude.

(iv) the isotopic compositions and especially the high tritium value from Bilad Bani Bu Ali cannot evolve from those of Al Kamil and therefore indicate the presence of a hydrological barrier between the two villages.

Whilst some of these points are indubitably correct, e.g. (ii) above, others either carry the arguments too far or are based upon false premise. In particular assumptions " a to d" fail to take account of the recharge variation with time, (a form of the "rainout" variable of Dansgaard, 1964), or implicitly attribute a quantitative precision to isotopic provenance which cannot be substantiated (assumption 'e' above).

An alternative model here proposes that the rainfall, and hence isotopic variation of recharge, is indirectly a function of time insofar as very infrequent but major recharge is isotopically much lighter than normal rainfall events, as depicted in Figure 6.11. i.e. the older the water, the greater the probability of it containing a high proportion of isotopically light recharge. Furthermore, groundwater age rather than source altitude is the dominant control upon groundwater composition, (cf. the altitude variation of individual storm isotopes in figure 2.18). No other explanation accounts satisfactorily for the apparent

Figure 6.11 Schematic Interrelationship Between Recharge Frequency, Intensity ,Groundwater Age and Isotopic Composition
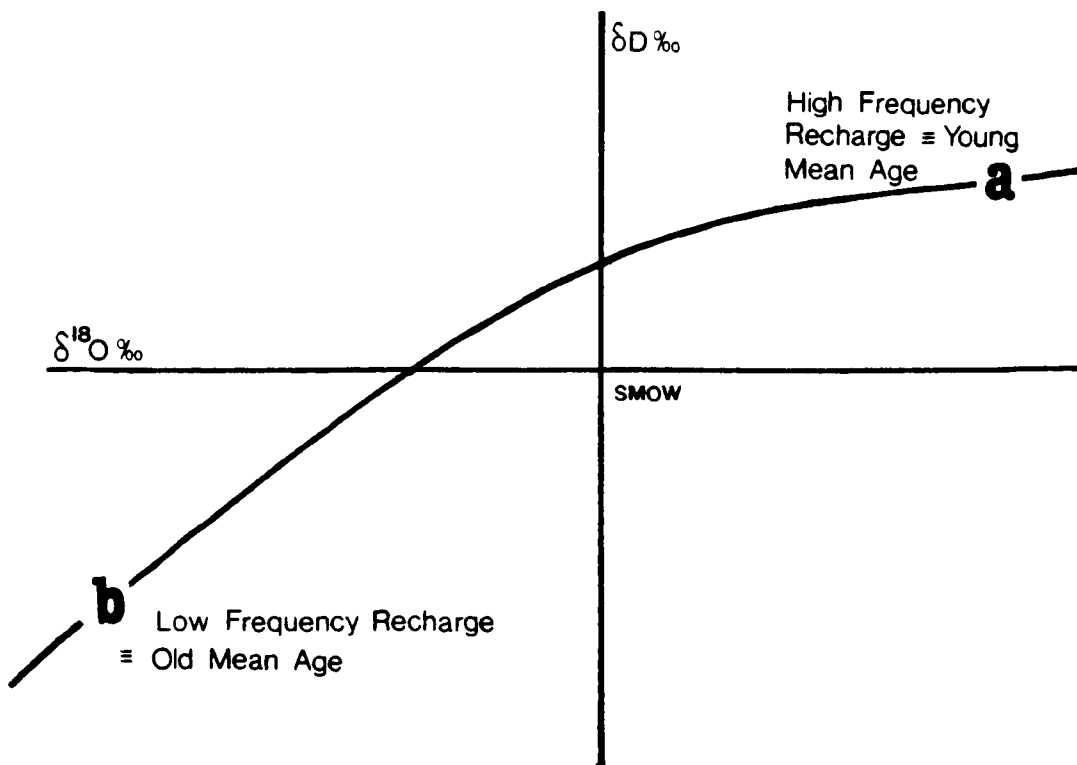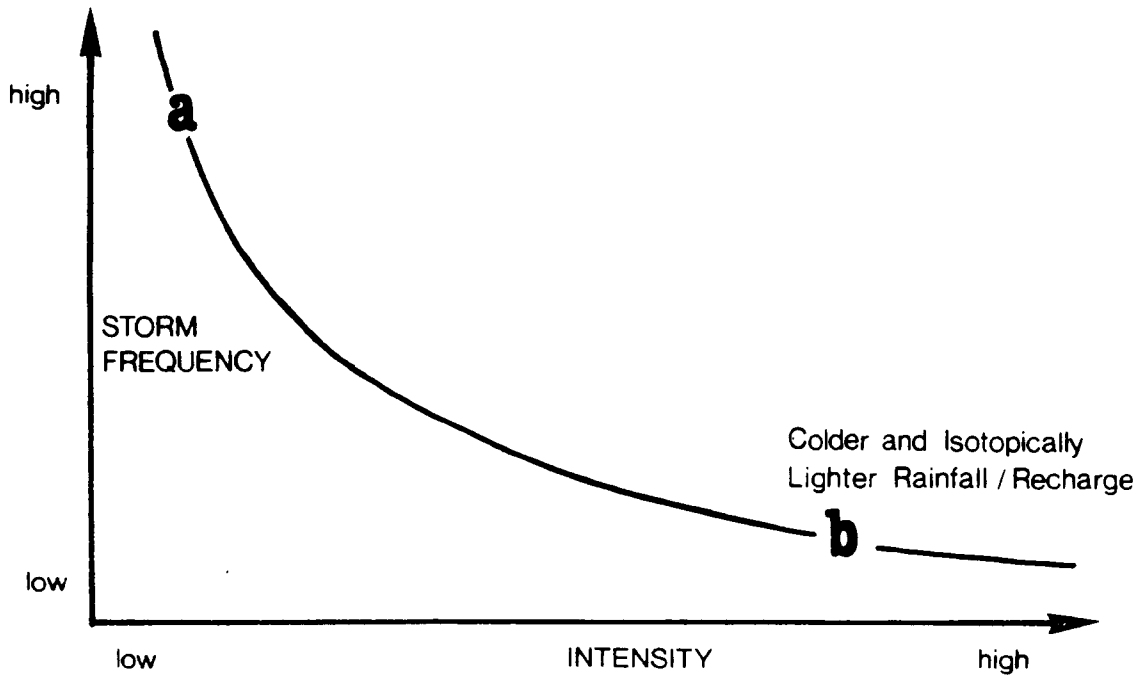
groundwater-rainfall mismatch observed throughout Oman and the Middle East. Considering the Ibra to Tawi Sultan section of Wadi Al Batha, it therefore follows that both the stable isotope and tritium trends simply indicate downstream position with increasing mean age and, by implication, probably increasing alluvial storage. The trend is also of similar slope to the normal groundwater regression line, Figure 6.10, and hence suggests that significant evaporation has occurred during recharge.

Whereas the isotopic evidence is consistent with a single linear groundwater system, the hydrochemical evidence for groundwater confluence from the 'intermediate' subcatchments is less clear cut, irrespective of whether falaj or well salinity is taken as truly representative of groundwater conditions. In the former case, falaj salinities representing averaged groundwaters of the active fluvial channels upstream of individual villages, and summarised in Table 6.3, show a uniform but exceptionally small increase with downstream position. Though not conclusive, such a low salinity gradient is probably anomalous in a linear groundwater flow path because a low hydraulic gradient (conforming closely to the surface gradient) should lead to slower groundwater flow, a longer residence time and hence a higher salinity gradient. For example the mean lower basin gradient of 0.0025 in Wadi Al Batha is less than that of Wadi Bahla (0.004) and should therefore be associated with a higher salinity gradient, whereas the reverse is the case (cf Tables 6.3, Al Batha, with 6.1, Bahla). Furthermore the gradient/flood velocity/particle size relationships, and hence gross permeability of the fluvial sediments, tend to reinforce rather than counter the argument. The low salinity gradient of Wadi Al Batha therefore implies some fresh groundwater mixing from the intermediate catchments. Similarly, examination of the E.C. contours based on well data (Figure 6.12a) appears to imply relatively fresh groundwater confluence from the Zahir and Bani Khalid subcatchments. Unfortunately such a "face value" interpretation cannot be unreservedly accepted as other complicating factors relating to post-recharge processes must be taken into account. For example wells are generally sunk in interfluvial areas at varying distances from the recharge zones and thus have widely varying groundwater ages. As shown above, this results in local salinity gradients substantially greater than those of the main wadi (cf. Figure 6.12a and b, especially between Al Kamil and

Figure 6·12   Salinity as E.C. (mmhos) in Lower Wadi al Batha
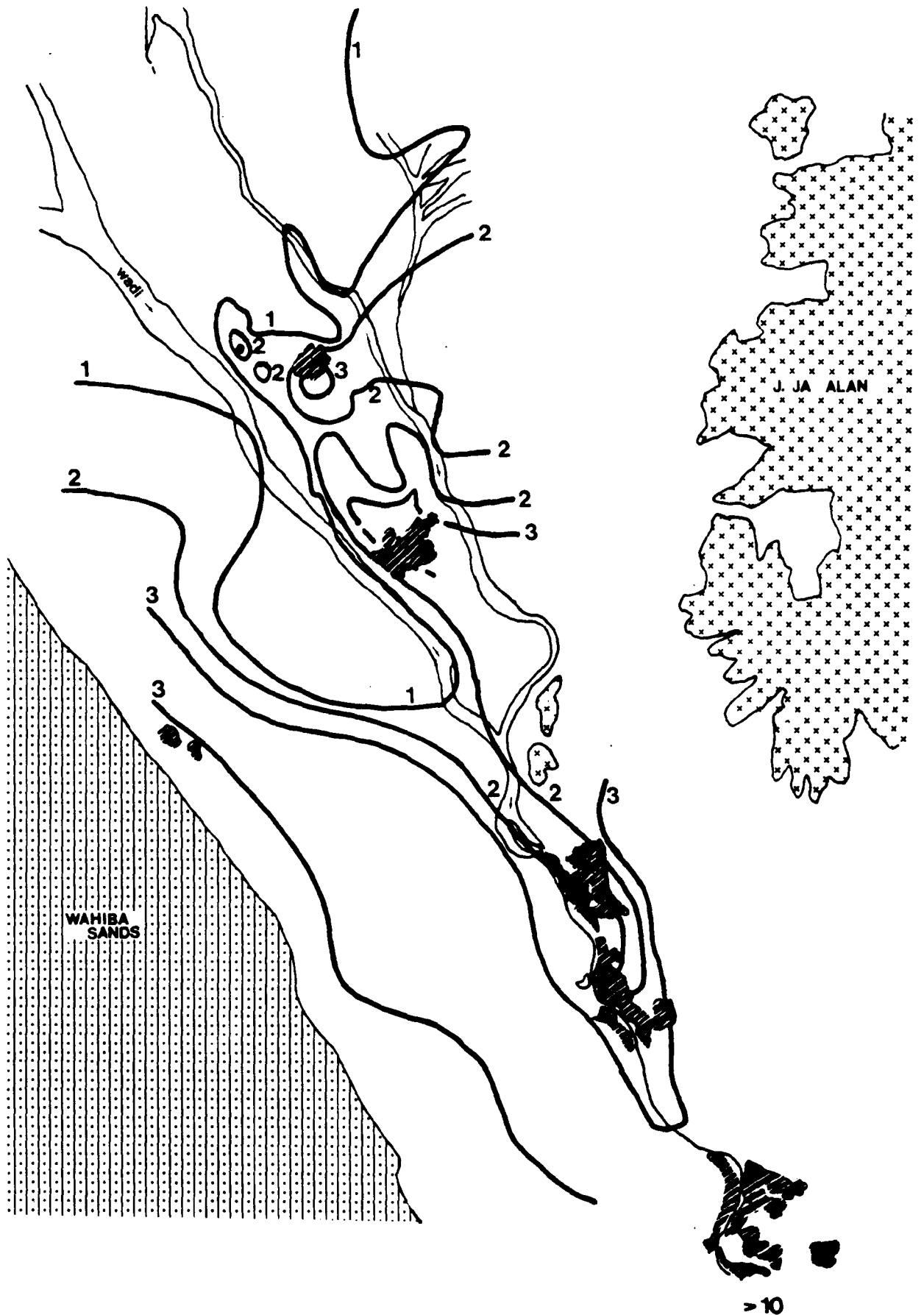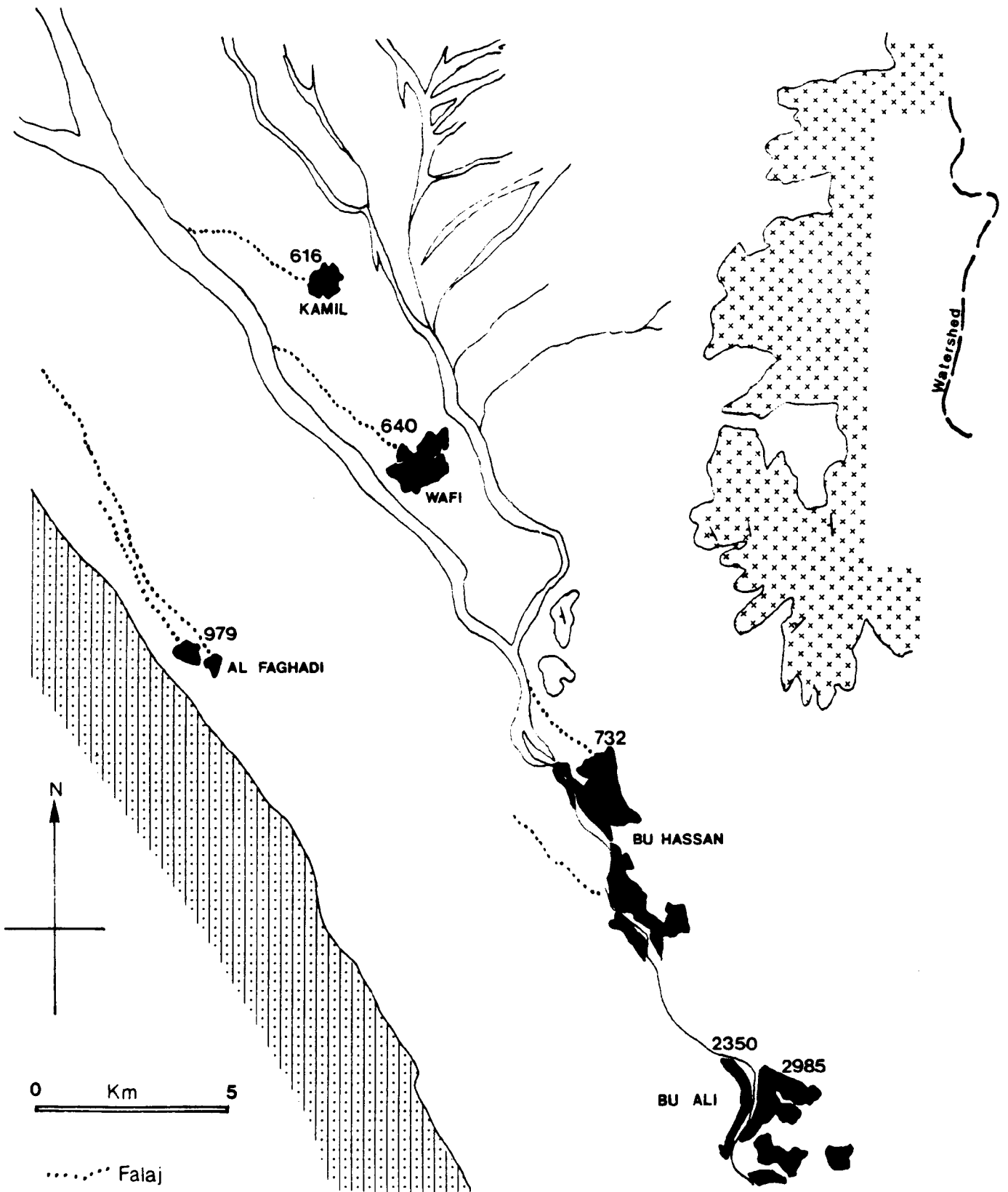A) Well Data

Figure 6·12 B) Falaj Salinity as E.C. (μmhos) in Lower Wadi al Batha

616
KAMIL

640
WAFI

Watershed

979
AL FAGHADI

N

0   Km   5

732
BU HASSAN

2350
2985
BU ALI

········ Falaj

Bilad Bani Bu Ali). Thus the low salinity of Tawi Sultan just upstream of Figure 12 may be attributable to either fresh groundwater confluence from the north, or the unusual position of the well within an active fluvial channel. Many of the high salinity contours in Figure 6.12 are local products of irrigation return and, where groundwater flow is substantial, have only trivial effects upon the downstream groundwater salinity. Only in Wadi Bani Khalid is there clear evidence of large scale groundwater confluence with Wadi Al Batha. At Al Kamil the much reduced deuterium concentration relative to Tawi Sultan, Figure 6.10, is indicative of entirely different provenance and, in view of the much higher relief of the Bani Khalid subcatchment, probably reflects the modifying effect of mean rainfall altitude. Some baseflow from the hardrock piedmont into the Bani Khalid outwash fan appears to be perennial; the available observations being 214 $1.s^{-1}$ in Feb. 1975 (Renardet), 20 $1.s^{-1}$ in March 1979 (Gemmell) equivalent to 0.63 m^3 x 10^6/year, and "very low" (GDC, 1982). The first measurement appears to have been made a few days after heavy rain (eg. 51.4 mm at Sur, cf. Appendix A) and is therefore atypical, but overall a modest baseflow, probably less than 1 m^3 x 10^6/year, and flood infiltration appears to recharge the Lower Wadi Al Batha.

A high tritium concentration in the most downstream area of Bilad Bani Bu Ali is the most problematic of all the isotope results. It is difficult to see how this could be other than of local and recent recharge from the adjacent Ja-Alan massif and hence of only short term significance. Moreover the variable ages and mix proportions of local recharge and groundwater flow from wadis Bani Khalid and Al Batha account for the complex stable isotopic relationships of the Kamil Bu Ali area. There is thus neither isotopic or geological evidence to support the hypothesis of a hydrological barrier in the Lower Al Batha plain.

The greatest imponderable in the Wadi Al Batha water balance is whether large scale groundwater leakage occurs into the Wahiba sands. Upstream of Al Kamil the wadi runs either adjacent to or very close to the sands for over 30 km throughout which the drainage morphology gives the impression of easterly deviation away from a regional south-easterly trend. Some groundwater flow towards the sands in the vicinity of

Hawiyah must occur both to permit gravity feed of the falaj supply from the main wadi into the interdune area of the village, and to prevent progressive salinization of the irrigated areas. Verbal accounts of drilling in interdune depressions (exact locations unknown) also record the presence of fresh water, but the most conclusive evidence is the widespread concentration of phreatophyte growth in the far eastern and southern "Ramlat Wahiba" area where the dunes thin out against the flat coastal plain. This has not been investigated but is clearly visible on ERTS satellite imagery of the area.
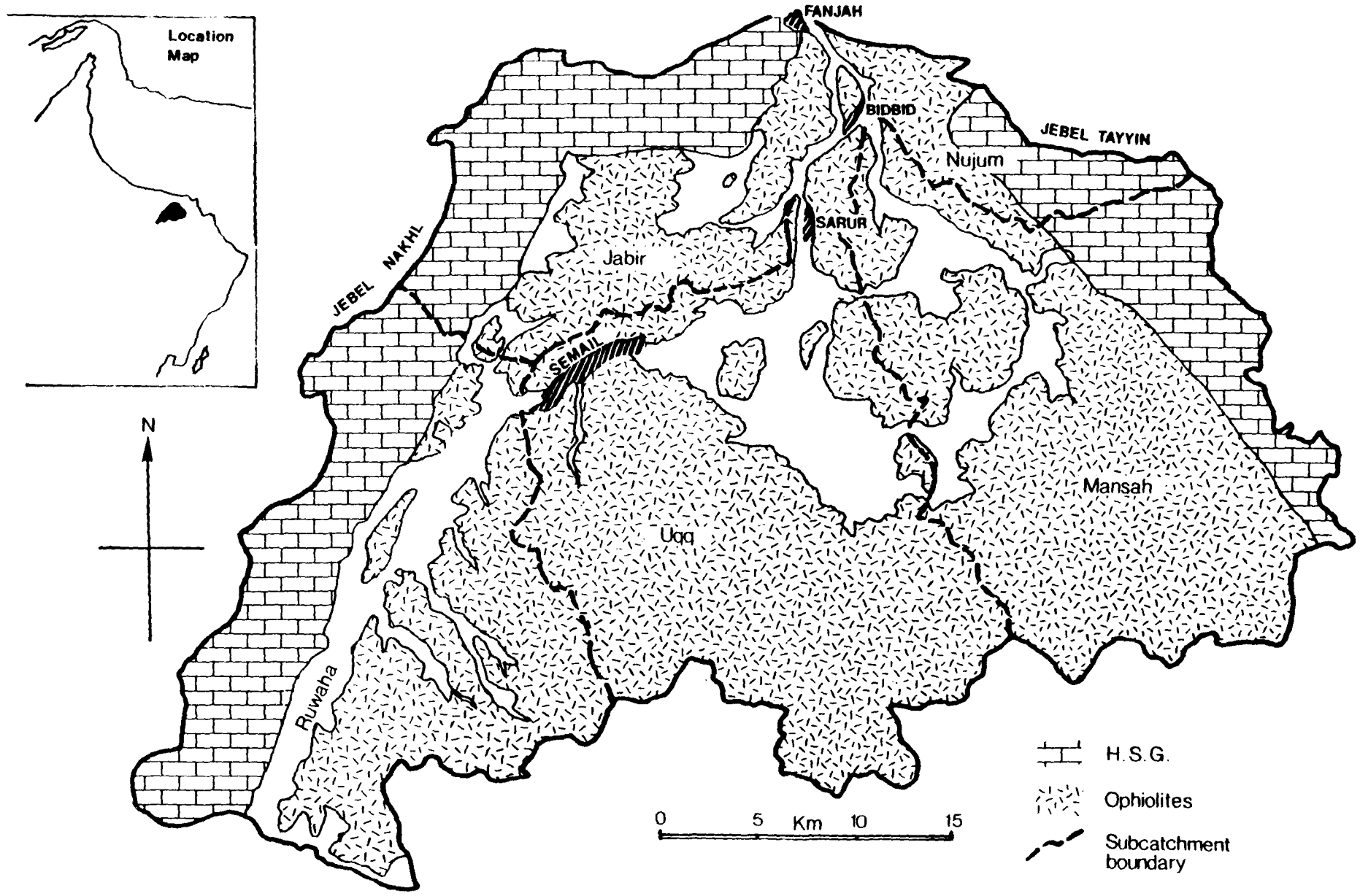
The sub-dune formations, consisting of impervious Hawasina sediments in the west and unexposed but presumably clastic sediments of the Mio-Pliocene desert platform further east, reveals no indication of possible groundwater pathways. Unlike the better known dune sands of the "Liwa" area (in the UAE some 200 km west of Ibri, cf Wilkinson, 1977) there are no date palms or other indications of a shallow/perched water table, so any groundwater channel is likely to be incised into the "desert platform" and thus buried well below the interdune deflation surface. Nevertheless, good falaj supplies adjacent to the sands at Falaj Mashaikh appear to originate as much from groundwater transfer beneath the sands as from the visible wadi channel, and thus supports the hypothesis, albeit unquantified, of southeasterly sub-dune groundwater flow.

(3) Wadi Semail

It is not uncommon for "interior" catchments to drain to seaward across the mountain axis, thereby contributing to sedimentation and groundwater recharge of the coastal plain. The most important examples are wadis Semail, Ahin, Jizzi and Hatta, of which Wadi Semail is distinctive in having a large low relief interior catchment (1635 km^2 to Al Khod, Figure 6.13) separated from a relatively small outwash fan by the high limestone ranges of Jebels Nakhl and Tayyin. Upstream from the "Seeb Fan", the catchment also bears geological and physiographic similarities to Wadi Dayqah (cf. Section 4.4) including an unusually large "hardrock" fraction of the catchment area (84% of the total), but differs in having a hypsometric profile which is strongly skewed towards medium altitude relief, characteristic of the ophiolite hills. Apart

Figure 6-13   The Wādi Semail Catchment

Location Map

N

FANJAH

BIDBID

JEBEL TAYYIN

Nujum

SARUR

JEBEL NAKHL

Jabir

SEMAIL

Mansah

Uqq

Ruwaha

H.S.G.

Ophiolites

Subcatchment boundary

0   5   Km   10   15

from the very steep gorges of Jebel Nakhl, the wadi course has a high mean gradient of 0.008, resulting in rapid flood runoff and active cutback at the southern watershed (e.g. Wadis Bani Ruwaha and Al Uqq). However, breakthrough of the main wadi across the limestone anticline occurs at the structural depression of Fanjah (Figure 6.13) and is more suggestive of an antecedent mode of fluvial erosion.

Hydrologically the Semail catchment naturally falls into the southern, central, and lower or Seeb fan divisions. In the south the most upstream areas (though not always the highest) consist of three sub-catchments; Wadi Bani Ruwaha, Wadi Al Uqq and Wadi Mansah. These "source areas", together with a few smaller and unimportant wadis, all drain into the central catchment where over a distance of 46 km Wadi Semail has incised into and is almost continuously confined by an impervious hardrock complex. The confluence of groundwater into such a relatively narrow channel between western Semail village and Al Khod has permitted the construction of 35 medium to large aflaj which irrigate a corresponding belt of agriculture. In their upstream courses, many of the aflaj are leaky and tap the upstream alluvium with varying degrees of efficiency. Furthermore, their alignments are often en échelon, with lower aflaj recycling irrigation return from aflaj further upstream. Thus with the single exception of a rock bar in central Semail village, it is impossible to measure the total wadi flow directly. The apparent aflaj yield in the central Semail area totals about 2.3 cumecs (winter 1974/75 data from Gibb 1976, equivalent to 72 m ^{3}x10^6/yr) which, with small additional well yields totalling less than 0.2 cumecs, accounts for more than half of the catchment yield, and supports one of the most important agricultural areas of the interior mountains.

The proportion of perennial to annual crops in the central Semail basin exceeds that of the southern catchments, such as Bahla and Nizwa, by about 25% and tends to result in a large seasonal excess of unused or recycled groundwater in the downstream areas. This seasonal flow is illustrated both by the falaj flow at Hassas (the easternmost of the Semail aflaj) which varies from 81 l.s^{-1} in winter to 13 l.s^{-1} in summer, and by the falaj flow at Al Khod; Figure 6.13. The latter falaj abstracts a variable portion of the residual catchment groundwater as it leaves the central piedmont region and is therefore affected as

272

much by upstream abstraction as by the general state of recession. Further downstream the baseflow from Wadi Semail produces ephemeral surface flow which visibly recharges into the "Seeb fan" or "Lower Semail" for months or even years into recession, and which has long been recognised as an important groundwater source by virtue of its proximity to the capital area. The lower alluvial section of the wadi is also contiguous with the eastern Batinah plain and is therefore considered separately in section 6.4.

All three main Semail sub-catchments contain important and well defined alluvial sources in their downstream areas (Figure 6.13). A fourth sub-catchment, Wadi Bani Jabir, also contains some 25 km^2 of alluvium but does not appear to contribute baseflow to the overall Wadi Semail system. Apart from a few scattered and eroded remnants of cemented limestone fanglomerates at the base of Jebel Nakhl, all of the sediments contain numerous Hawasina and/or ophiolite outcrops suggestive of a normally shallow alluvial depth such as a few tens of metres, although no drilling or geophysical data is available to confirm this impression. An obvious lithological contrast occurs between the sediments in: (1) Western Wadi Bani Ruwaha, and (2) the eastern Ruwaha area, Wadi Al Uqq and southwestern Wadi Mansah. The former dominates the main fluvial channel and is derived as outwash from Jebel Nakhl, consisting of medium gravel to coarse limestone boulder gravel/conglomerate with locally very high porosity. The latter consists of uniformly fine ultramafic sand and gravel which also occurs as narrow tongues of alluvium extending far into the upstream foothills, and sometimes almost to the watershed. Except for the few areas where alkaline springs precipitate travertine, these gravels are almost entirely uncemented, and provide small groundwater supplies for numerous small foothill villages. By contrast, the only substantial foothill villages are those based upon much larger spring sources emergent from the foot of Jebel Nakhl. At the eastern Semail catchment boundary, the corresponding limestones are generally lower (Figure 6.13), of much lesser dip and gradient, and probably have a northward dipping mean hydraulic gradient (i.e. towards the Bosher spring line and hence away from the Semail catchment). These physical features, the water isotopes and the hydrochemistry of Wadi Mansah all consistently indicate minimal groundwater contribution from the eastern limestone massif.

Despite the diverse primary water sources and complex "consumptive use" losses, the drainage of discrete sub-basins into a single laterally confined channel has facilitated the compilation of a recession water balance summary. This is based upon a detailed survey of: cropped area, water use, hydrochemistry and water isotopes (Gibb, 1976) and consists of a quantitative assessment of the various ground and surface water components contributing to baseflow rather than to the mean catchment yield including runoff. Such a balance therefore indicates the relative importance of the various potential groundwater storage areas. As no direct measurements of groundwater flow from the alluvial sub-basins exist, indirect estimates were compiled around the single known water flux measurement of central Semail village. In the initial balance published by Gibb (1976), both upstream and downstream gains and losses were estimated using tritium mass-balance arguments (based upon an H^3 contrast of about 50 in the ophiolite gravels, and 30 in the limestone gravels) and mean annual transpiration rates. Here, a modified balance for the same period of winter 1974/75, shown in Figure 6.14, is adjusted to take account of both the reduced seasonal transpiration and conservative hydrochemical data. The latter was used in preference to tritium wherever the original calculation involved either assumptions regarding the tritium concentration or potentially large calculation errors. In both compilations the main imponderable in the balance was whether significant underflow accompanied the visible limestone spring sources. This was best tested at Fanjah where both limestone spring and upstream/downstream wadi waters were fully analysed for chemistry but not for tritium. Consumptive use losses of 8.3 $l.s^{-1}$ were calculated and deducted from the observed total spring discharge of 33.6 $l.s^{-1}$ to leave an apparent base flow contribution of 25.2 $l.s^{-1}$. Chloride, the most conservative of the common ions in solution, would normally have been the most appropriate basis for a mass balance, but in such a downstream position the large seasonal chloride variation in the wadi bed (Figure 6.15) and uncertainties regarding salt distribution in the falaj reticulation system, prevented its use. Instead, a consistent local fluoride anomaly in the spring waters (cf. Appendix C Nos 3, 89, 90, 250, 251, 270; and Gibb 1976, 6) was used to calculate the baseflow contribution which was 24 $l.s^{-1}$. Similar calculations involving less conservative parameters such as the Ca/Mg ratio provided a limit of not less than 14 $l.s^{-1}$ with a probable mean of about 25 $l.s^{-1}$. Thus
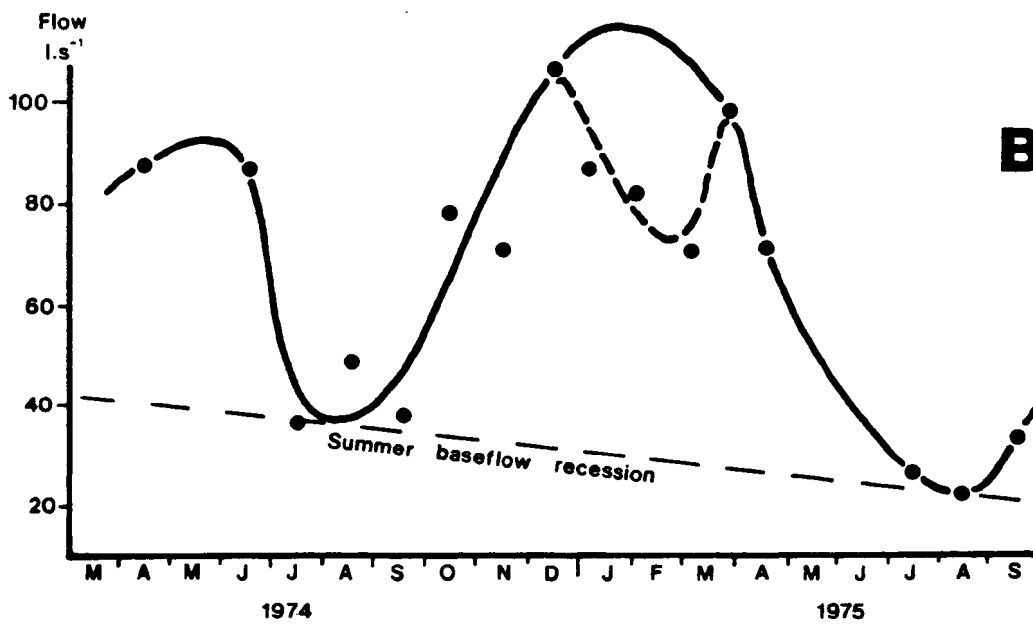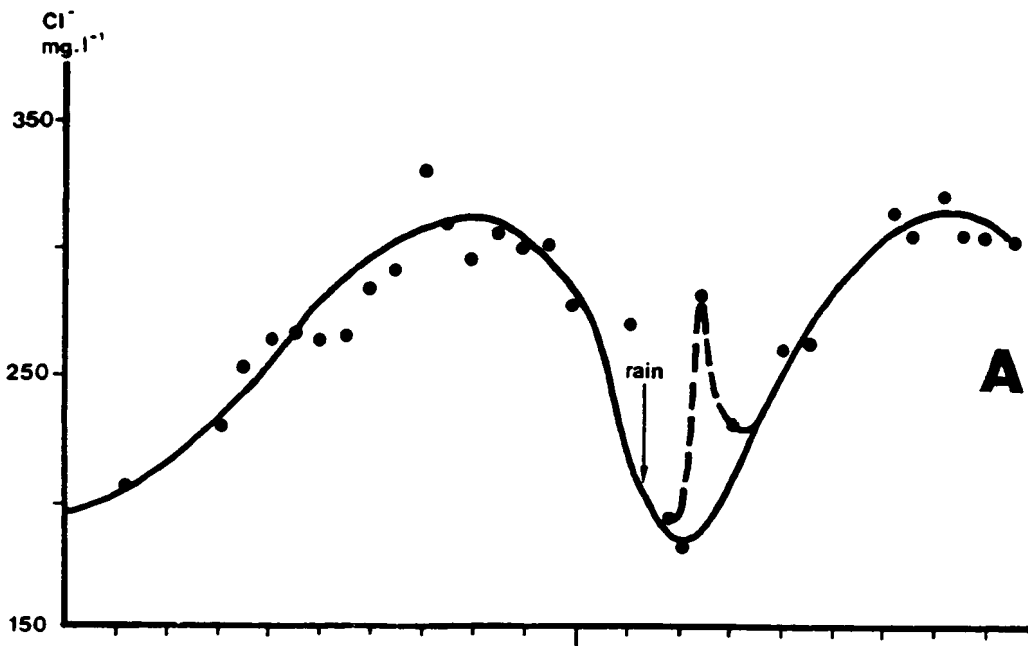
Figure 6.14   UPPER SEMAIL CATCHMENT WATER BALANCE SUMMARY FOR WINTER 1974-75   ($l.s^{-1}$)
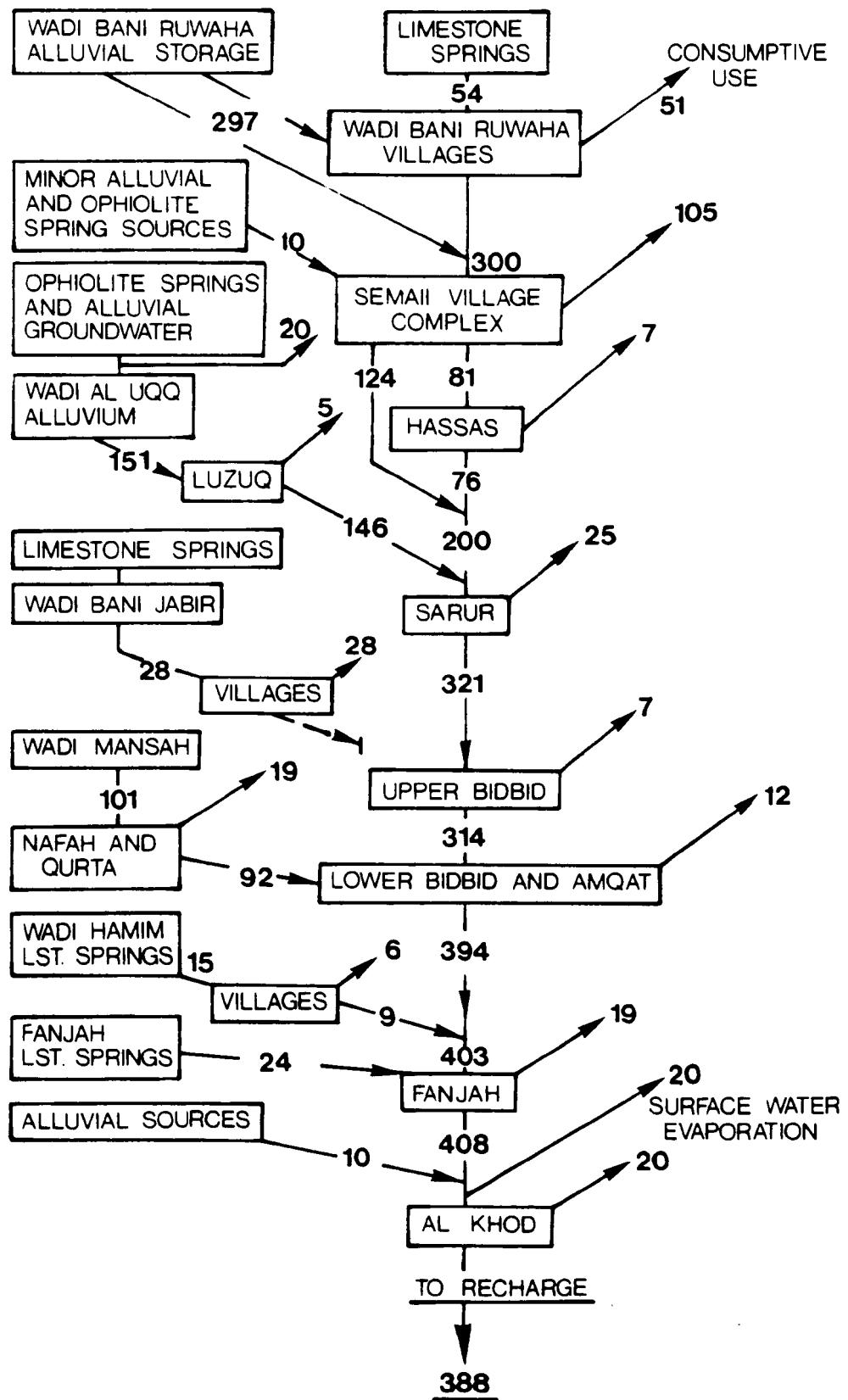
N.B.

Water reaching Al Khod = 29% of total catchment yield
Limestone Springs (111 $l.s^{-1}$) = 15% of total catchment yield
Wadi Bani Ruwahah (351 $l.s^{-1}$) = 48% of total catchment yield

Figure 6.15

Chloride (A) and Falaj Discharge (B) at Al Khod

although the F⁻ analysis was based upon rather imprecise data, the
apparent and calculated baseflows were sufficiently consistent and
similar to indicate that little, if any, unobserved limestone
groundwater flows into Wadi Semail at Fanjah. Given the widespread
presence of impervious Hawasina shales and cherts which either outcrop
or appear to underlie the limestone-alluvial contact at shallow depth,
it therefore seems reasonable to extrapolate the "zero underflow"
conclusion to the rest of the limestone spring areas. Limestone spring
discharges throughout the catchment were therefore taken as the measured
111 $l.s^{-1}$ or only 15% of the total (primary source) catchment yield.
This figure is also in keeping with the contrasting F⁻ content between
spring and alluvial sources in Wadi Bani Ruwaha. Observed alkaline
springs, though more numerous in Semail than in most other studied
catchments, still totalled only about 50 $l.s^{-1}$. Thus the total spring
flow or "hardrock" yield was only about 22% of the overall catchment
yield during winter recession. Examination of Figure 6.14 also provides
estimates of the alluvial contributions from the various sub-basins,
e.g:

Wadi Bani Ruwaha with about 60 km^2 of alluvium ...   ...   297 $l.s^{-1}$

Wadi Al Uqq   with about 75 km^2 of alluvium ...   ...   171 $l.s^{-1}$

Wadi Mansah   with about 50 km^2 of alluvium ...   ...   101 $l.s^{-1}$

As would be expected from the distribution of agriculture, Wadi
Bani Ruwaha proves to be the major baseflow/storage area. To some
extent the main wadi may be regarded as a conduit between the limestone
baseflow and the subcatchment outflow into the Semail aflaj, but as the
spring discharges and village consumptive use (concentrated in the upper
sub-catchment) are closely matched, most of the groundwater storage must
be of alluvial origin. In terms of yield per unit area, an apparent
contrast therefore exists between the high yielding limestone gravels
and lesser yielding ophiolite gravels. It is probable that both greater
aquifer thickness and greater permeability of the limestone gravels
contribute to this contrast but in addition to the lack of aquifer test
data, comparison between the two aquifer lithologies is further impeded
by the question of differential recharge. The main raingauge record in
the catchment is from Semail, Bidbid and Minabak which are all low
altitude stations in the probable rain shadow of Jebel Nakhl, and which
together give a 14 station-year mean of only 62 mm, (1973 to 1980 data,

Appendix A). This is much lower than the equivalent rainfall from other areas, as shown by Horn (1978) who used rainfall data from adjacent catchments to produce a "Thiessen polygon" estimate of 130 mm for the mean catchment rainfall (1974-77 data). Probable rain shadow in the western Semail basins is also implied by comparison with Wadi Al Uqq raingauge data. Although these four raingauge stations are slightly higher than the "rain shadow" gauges (on average 580 m as opposed to 350 m), and of short record length, they give a much higher mean rainfall of not less than 150 mm (combined 8 station-year mean using the 1979-81 data of Appendix A). On the other hand, whilst the alluvial areas of western Semail receive below average precipitation, the western watershed itself, at a mean altitude of nearly 2000 metres, should receive uncommonly high rainfall resulting in greater flood runoff into Wadi Bani Ruwaha than into the other subcatchments. This is consistent with both the recession yield data, given above, and with storm processes in the Semail gap in which high altitude runoff within a few kilometres of totally evaporated rainfall at low altitude have been observed simultaneously.

The catchment recession summary of Figure 6.14 has been recalculated for summer 1975 conditions by increasing the consumptive use figures by 68% (according to the seasonal "Blaney Criddle" crop water requirements of Gibb, 1976), and by assuming that all primary sources recede at similar rates to that observed in the Semail aflaj (41% per year). The resulting water balance, given in Figure 6.16, is less accurate than that compiled for winter conditions but is still sufficient to illustrate several important seasonal features of the catchment:

(1) The summer baseflow (recharge at Al Khod) may be as little as 10% of the winter value. Irrigation leaching therefore becomes more intense throughout the catchment, resulting in the association of higher chloride values with lower falaj flows at Al Khod (Figure 6.15).

(2) during recession the downstream villages may become crucially dependent upon upstream irrigation return for a large proportion of their crop-water requirements.

Figure 6·16 UPPER SEMAIL CATCHMENT WATER BALANCE SUMMARY FOR SUMMER 1975 ($l.s^{-1}$)

(Assuming that primary yields are all reduced by the same proportion as the Semail aflaj i.e. 41% per annum).

LIMESTONE SPRINGS

CONSUMPTIVE USE

WADI BANI RUWAHA ALLUVIAL STORAGE

41

WADI BANI RUWAHA VILLAGES

86

198

230

42

WADI AL UQQ ALLUVIUM

175

SEMAIL VILLAGE COMPLEX

WADI MANSAH

89

11

77

29   13

32

HASSAS

NAFAH AND QURTA

2

120

42

WADI HAMIM LST. SPRINGS

SARUR

12

10   45

12

WADI HAMIM VILLAGES

UPPER BIDBID

FANJAH LST. SPRINGS

2

66

20

LOWER BIDBID AND AMQAT

18

91

32

OPHIOLITE AND OTHER SPRINGS

FANJAH

8

79

35

SURFACE WATER EVAPORATION

17

AL KHOD

NB.

(1) The net piedmont baseflow is only about 20% of the winter value.

(2) The summer consumptive use is 68% higher than in winter

TO RECHARGE

35

and (3) the relative contribution of the various sub-catchments to baseflow at Al Khod is dependent upon seasonality, with a larger ophiolite gravel fraction occurring during the summer.

Some of the best available piedmont surface water measurements, both of floods and surface baseflow, have been measured at Al Khod (P.D.(O) unpublished data; Horn, 1978; Gibb, 1976). Estimates of the total piedmont flow are complicated both by an unknown subsurface baseflow component and by the Al Khod falaj flow which by-passes the gauging point. Nevertheless they provide an important guide to the amount and variation of downstream recharge. The relationship of such flow estimates to upstream processes, however, is fraught with difficulty. For example, the surface baseflow and flood runoff measurements are poorly correlated (correlation coefficient = 0.25) and reflect the attenuating controls of seasonality, antecedent groundwater conditions and local physiographic/rainfall anomalies. Moreover the rain shadow, relief and consumptive use characteristics of the Semail catchment probably create a more variable piedmont baseflow than would occur in most other catchments which drain the limestone massif.

6.3   Water use and Recession

Historically, utilisation of the available water resources has evolved to maximise yields with a high degree of skill and efficiency. This has been achieved by intense social co-operation in order to finance, construct and maintain the necessary and often complex irrigation works known as the "falaj system". Indeed the centrality of the falaj to both village structure and tribal settlement is a ubiquitous feature of virtually all villages and towns in the mountain region, and has been the focus of attention in most social and geographical studies of Oman (eg. Letts and Birks, 1973; Wilkinson 1974, 1977, 1978; Bowen-Jones, 1978; Letts, 1979; and Stanger, 1986 in press). This takes the form of a zonation of domestic and irrigation practice with increasing distance from the falaj portal, (Figure 6.17), and indicates both the priorities given to water use, and the typical villagers' view of the land. In particular, a rough correspondence exists between the area of perennial crops and the minimum observed falaj flow, (Figure 6.18), whereas annual crops are

Figure 6.17 SCHEMATIC ZONATION OF VILLAGE WATER USE IN OMAN

WASHING PLACES,
OFTEN ADJACENT
TO A MOSQUE

FALAJ
PORTAL

FIRST ACCESS
POINT FOR
DRINKING, AND
WATERING
ANIMALS

DOMESTIC AND
GENERAL
VILLAGE USE

PERENNIAL
CROPS,

MAINLY
DATES

FREQUENTLY
CULTIVATED
ANNUAL

CROPS,
MAINLY
ALFALFA

"AWAABI" LAND:
FALLOW OR
OCCASIONALLY
CULTIVATED

ANNUAL
CROPS

VILLAGE
GRAZING

NOMADIC
GRAZING

DISPERSED PHREATOPHYTIC
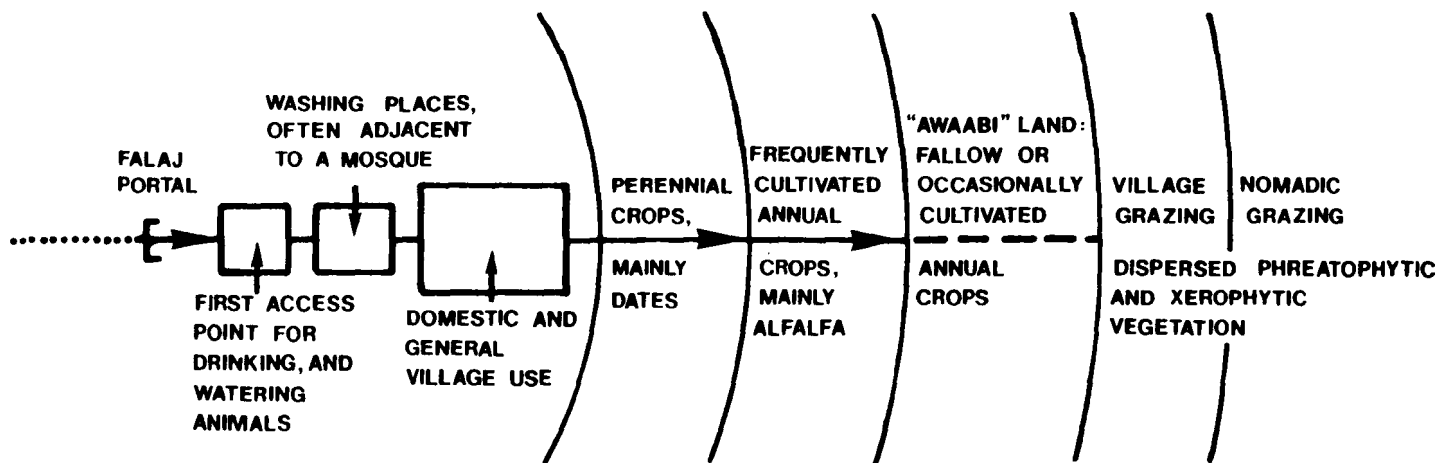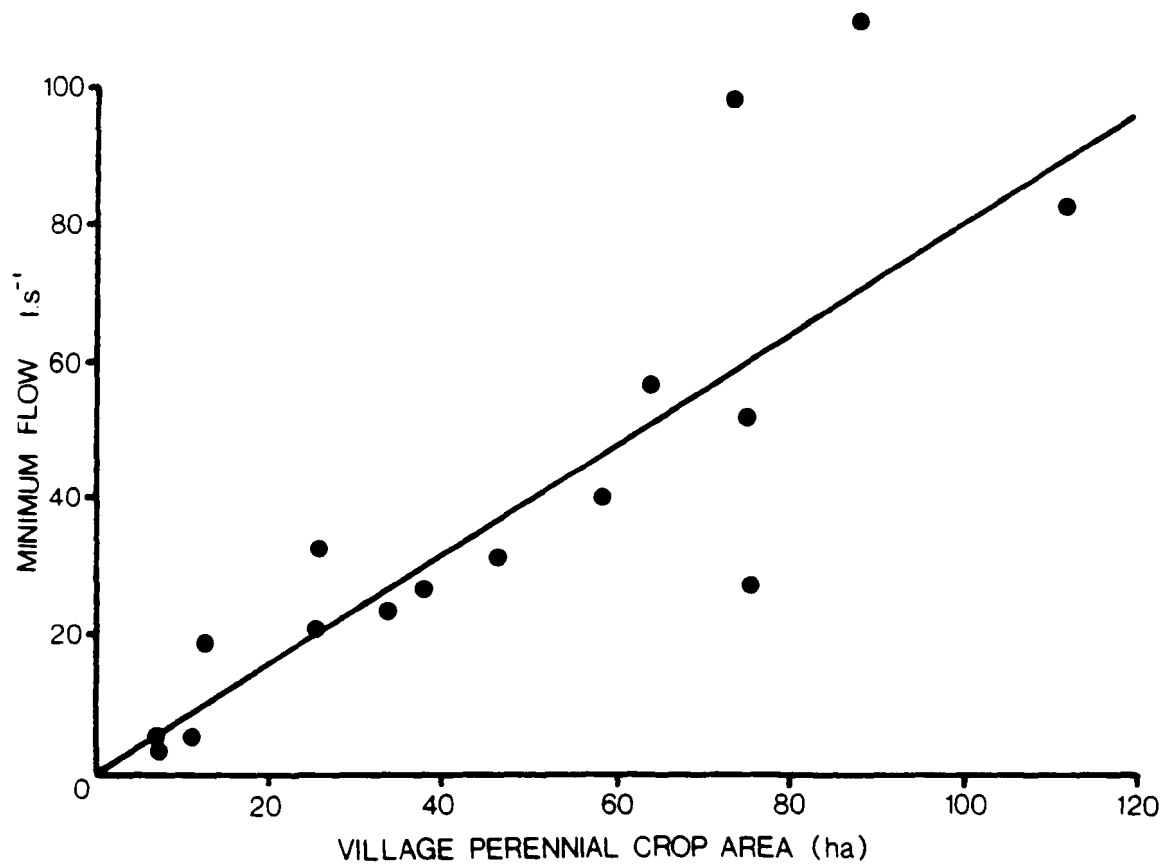AND XEROPHYTIC
VEGETATION

281

Figure 6·18   Perennial Crop Area vs Minimum Falaj Flow

grown on a more opportunistic basis as and when "excess" water is
available. Thus the cropping pattern implicitly reflects the recession
characteristics of the falaj flow. This is illustrated in Figure 6.19,
a hypothetical hydrograph in which a certain minimum flow "q" is assumed
to be available for perennial crops. In fact short periods of drought
"d" may occur without serious repercussions to deep rooted trees
although the yield may be temporarily impaired. Areas a_1 and a_2 are the
"annual crop" water requirements for two consecutive growing seasons
(eg. for fodder, vegetables, cereals, sugar cane etc.). A third growing
season water requirement is shown as having failed. Obviously faster
recessions may be regarded as a measure of drought hazard and eventually
become the limiting factor for crop growth, whereas slow recession
characteristics are better suited to a predominance of perennial crops.
Thus the "quality" of a falaj is judged by its reliability rather than
by its absolute discharge rate. As typical examples of the
crop/recession relationship, falaj hydrographs from Wadi Bahla, shown in
Figure 6.20, may be compared with the following data:

	Al Hamra		Bahla		Bisyah	
	ha	%	ha	%	ha	%
perennial crops	46	42	155	38	54	76
annual crops*	63	58	255	62	17	24

*as measured in spring 1974 (from Gibb, 1976)

Conservative agricultural practice and the rigorous climatic
conditions have resulted in a very limited variety of crops. Between 75
and 100% of the perennially cropped area is devoted to dates (Phoenix
dactylifera) of which about ten different varieties ripen over a five
month period. Limes, mangos, bananas and papayas, together with a few
aromatic shrubs account for almost all the remainder. Of the annual
crops sorghum, green barley, wheat, onions, tomatoes and sugar cane are
all widely grown, but alfalfa ("lucerne" - Medicago sp.), the main
source of animal fodder throughout the region, is pre-eminent.

Figure 6.19 Schematic Falaj Hydrograph to show the Relationship
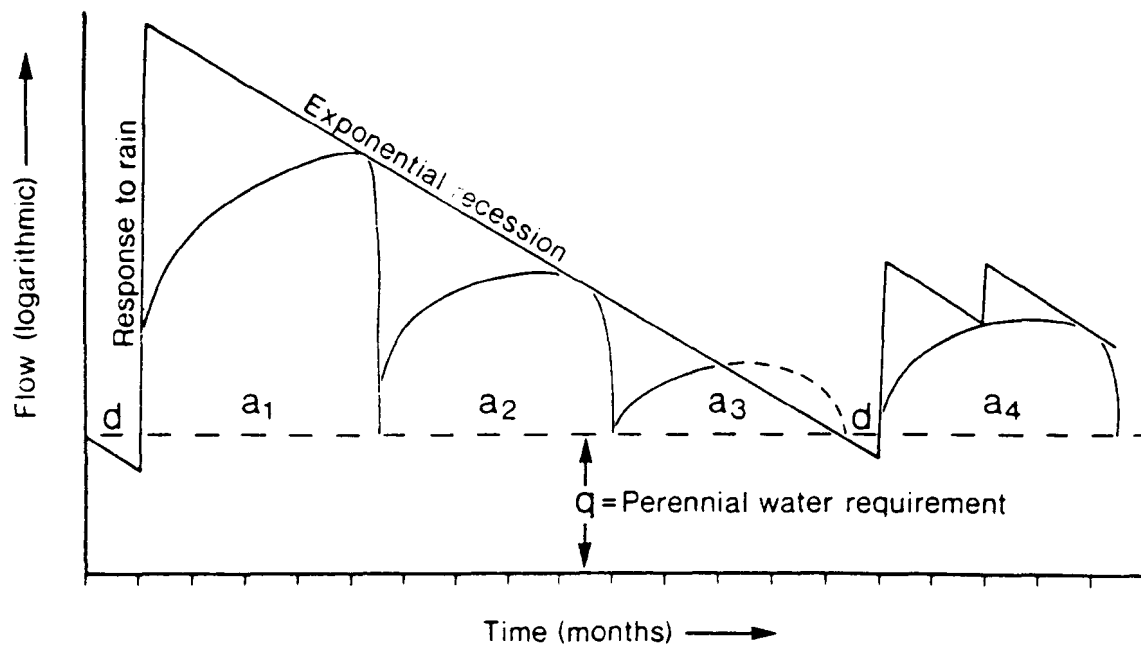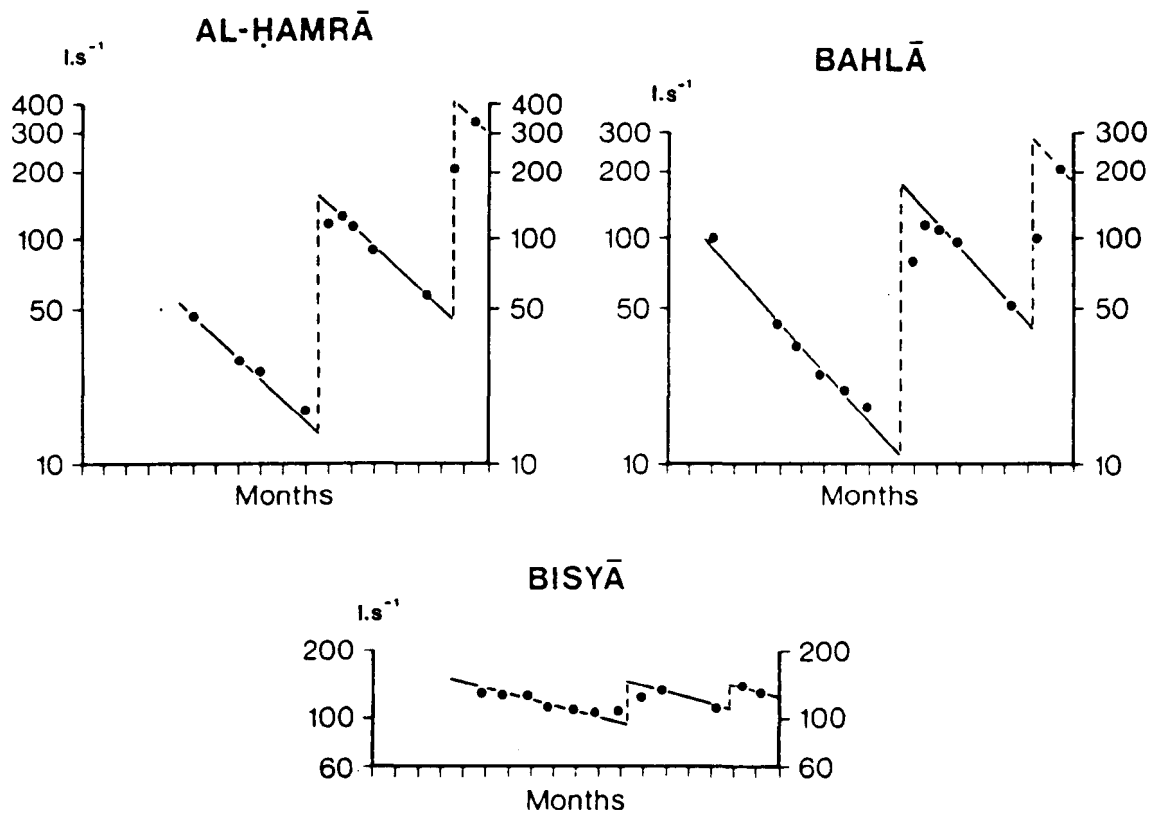
Between Recession and Crop Water Requirements

Figure 6.20   Falaj Hydrographs from Wadi Bahla

Strikingly different farming practices occur locally in two contrasting environments. One of these consists of numerous isolated and almost self-sufficient farms, covering some 350 ha of aeolian silt in Wadi Sayfam, which combines extensive wheat cultivation during "wet winters" with small areas (generally less than 5 ha) of extremely varied crops. The second environment is at Saiq (altitude 2000 m) in the Jebel Akhdar where an almost Alpine climate allows the cultivation of grapes, apricots, pomegranates, figs, walnuts and roses. Neither area however constitutes a significant proportion of the total agriculture.

A slight conflict of priority arises over date palm planting density, typically between 200 and 250 date palms per hectare. Close planting, the most common practice, reduces crop yields but minimises evaporation and irrigation losses, whereas more open spacing produces optimum yields from individual date palms, and permits grassy enclosed grazing or more intensive intercropping. In practice, although alfalfa has a larger consumptive use, its cultivation frequency is such that the average irrigation per unit area of perennial crops is scarcely affected by intercropping. Various consumptive use estimates of the two most important crops (calculated on the assumptions of total ground cover and "infinite" cropped areas) are shown in Table 6.4, and are in close agreement.

Table 6.4 Consumptive Irrigation Rates of Date palms and Alfalfa

	$mm.yr^{-1}$	equivalent $1.s^{-1} ha^{-1}$	Method of estimation	Source
alfalfa	1950	0.618	Penman	Letts, 1979
alfalfa	1750	0.556	Blaney-Criddle	Gibb, 1976
dates	1565	0.496	Blaney-Criddle	Gibb, 1976
dates	1590	0.504	Empirical (Semail village)	Gibb, 1976

However the applied irrigation rate also involves the less precise components of "leachate", channel losses and evaporation. Even though salinization due to poor drainage is rare in Oman, an essential minimum leachate is required to remove salts which accumulate around plant roots as a consequence of transpiration. With increasing dissolved salt

concentration of the irrigation water, the fraction of applied water required to remove accumulated salts also increases. The amount of this leachate is difficult to assess other than in the simplest of linear irrigation systems where estimates of the minimum falaj flow are also known. Such cases, plotted in Figure 6.21, indicate that on average falaj losses and leachate together approximately equal the crop consumptive use, except under brackish conditions when the leachate may be more than double the consumptive use, i.e. under normal conditions the empirically derived minimum irrigation requirement is about 1.0 l s^{-1} ha^{-1}. In addition to the leachate requirements due to brackish water, higher application rates are also required to overcome extreme desiccation due to high exposure and low humidity in the outer village areas, (i.e. annual crops). Letts (1979) estimated that this "oasis fringe" effect increased the consumptive use of alfalfa to as much as 6000 mm yr^{-1} (equivalent to 1.90 l s^{-1} ha^{-1}), and cited an example of alfalfa cultivation on the point of wilting and abandonment despite a high water application rate of 4200 mm yr^{-1} (equivalent to 1.33 l s^{-1} ha^{-1}). Furthermore excess irrigation habitually occurs simply because excess water supply is intermittently available. In view of these considerations an estimate of 3790 mm yr^{-1} (1.2 l s^{-1} ha^{-1}) as the mean crop irrigation rate for the whole of Wadi Al Batha (Renardet, et al. 1975) is probably typical of the entire interior region.

Irrigation efficiency of the overall falaj system is more a function of channel losses and evaporation than of balancing water application rate with the crop water requirements. Both financial constraints and communal farming experience ensure that the latter are closely matched whereas, superficially, the falaj leakage losses are high. For example comparison of discharge and infiltration rates throughout aflaj in the Dhahirah area produced mean losses above the settlement, of 23% (n = 16, range 0 to 70%), and mean losses within the settlement of 27% (n = 9, range 10 to 56%; Bowen-Jones, 1979). Although correct in a local sense such apparently high losses are misleading for several reasons. Firstly, in order to avoid excessive scour and flood damage, most aflaj contain deliberate overspill or excess leakage points in their upper channel so that unusable water (e.g, "e" in Figure 6.19) is returned to downstream alluvial storage. Conversely, during critical drought periods, average falaj leakage and overspill is much less than the 23% given above, and hence falaj

Figure 6.21   Empirical Leachate as a Function of Salinity
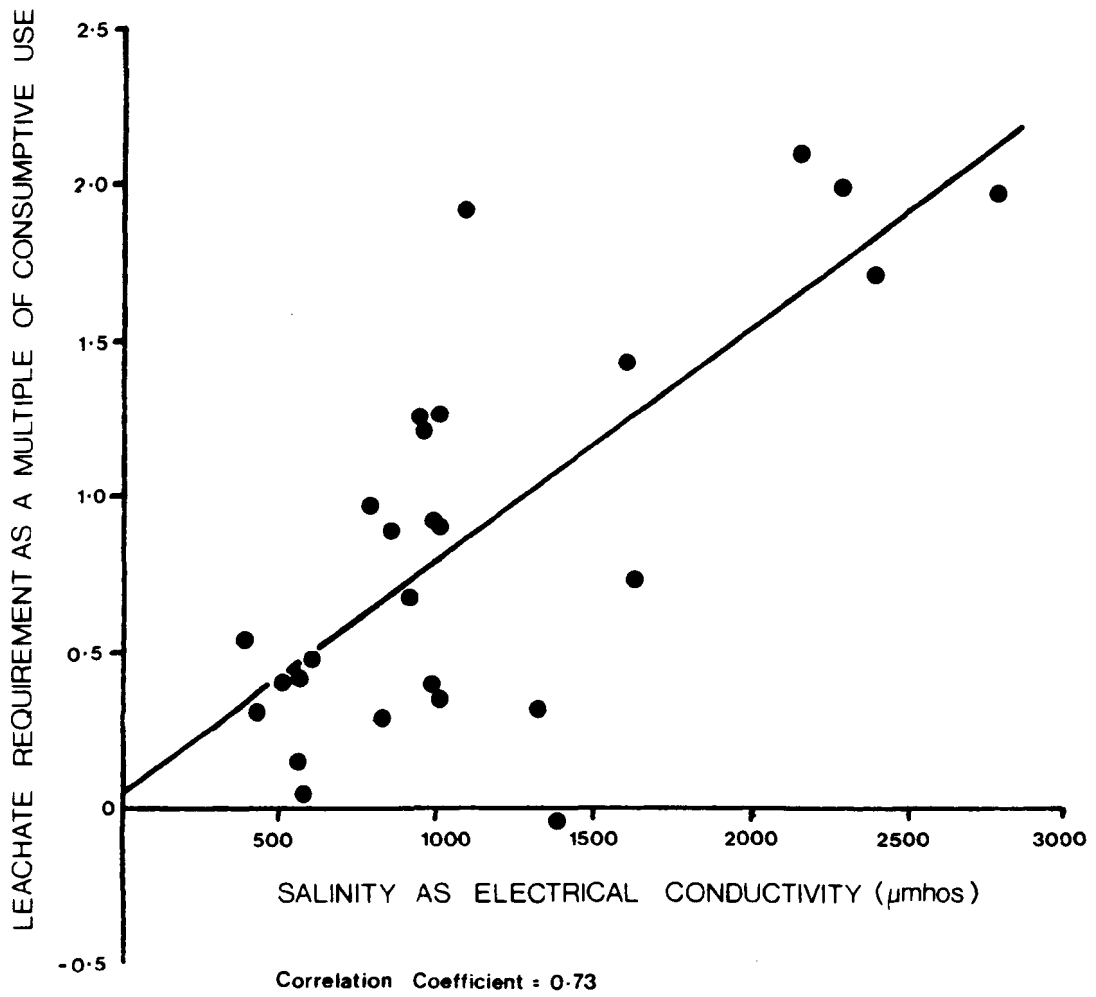
transmission is much more efficient. Secondly, much of the reticulation losses by infiltration are recovered by wells and secondary aflaj in the "downstream" parts of the village. Thus in larger villages such as Nakhl, Semail, (Figure 6.22 a and b), and Rustaq, zones of successively higher salinity correspond to cycles of groundwater recovery and re-application. Thirdly, as discussed in the previous section, excess water in one village almost invariably contributes to the groundwater supply of the next (downstream) village. Consequently real water losses consist almost entirely of evaporation and transpiration.

Most Omanis are, understandably, preoccupied with the "business end" of the falaj. Indeed the term "falaj" is derived from an ancient semitic root-"plg"-meaning "to divide" (Wilkinson, 1977) and refers to the system of village water rights and distribution irrespective of the upstream source. Local interest in the transmission and collection sections of the falaj is therefore largely limited to occasional crises when urgent repair or outright reconstruction is required. This upstream part of the falaj system may be of either "ghail" or "qanat" type.

Ghail aflaj are found in the most mountainous areas, and are constructed as open or "cut and cover" channels according to the type of source. Most point sources, such as the high level limestone springs, are channelled between the spring chambers and villages, often for several kilometres depending upon the availability of flat or terraced cultivable land. In this environment the channel gradients are typically steep and hence potentially severe scour has required a high standard of construction in the form of narrow "djuss" or cement lined channels, aqueducts and so-called "inverted syphons"* which tend to wind high (and often precipitously) above wadi levels to avoid flood damage. Ghail aflaj with larger discharges (e.g. > 10 $1.s^{-1}$) are more commonly sited in wadi beds where surface flow is diverted into unlined or stone lined channels by means of temporary earth and stone dams, as shown in Plate 6.6. These, of course, are vulnerable to flood damage and require rebuilding after all major storms, but have the advantage of simplicity

---

* A misnomer since no syphon mechanism is incorporated.

Figure 6.22   Salinity Increase in Succesive Aflage,   A) Nakhl

E.C. in µmhos

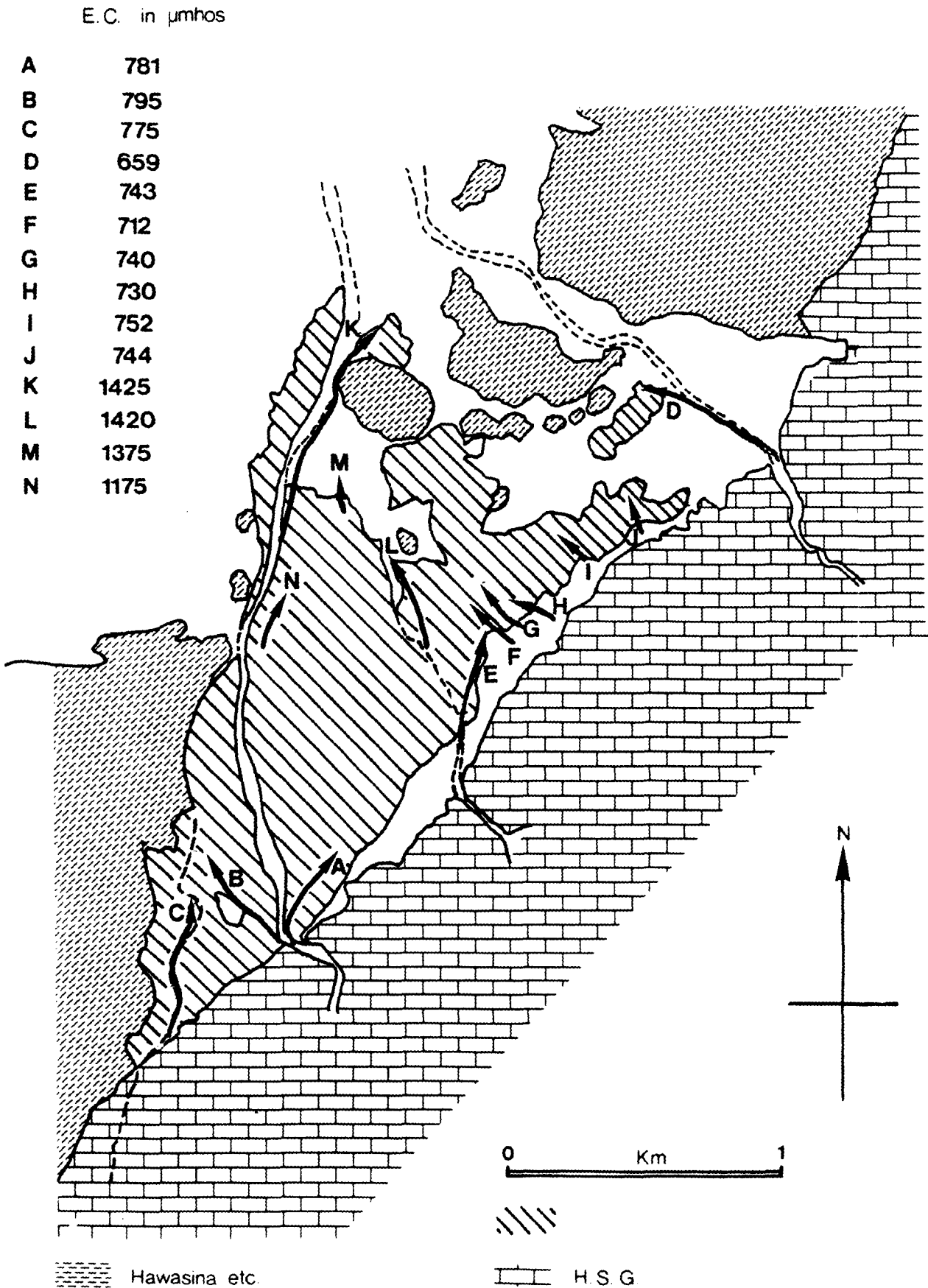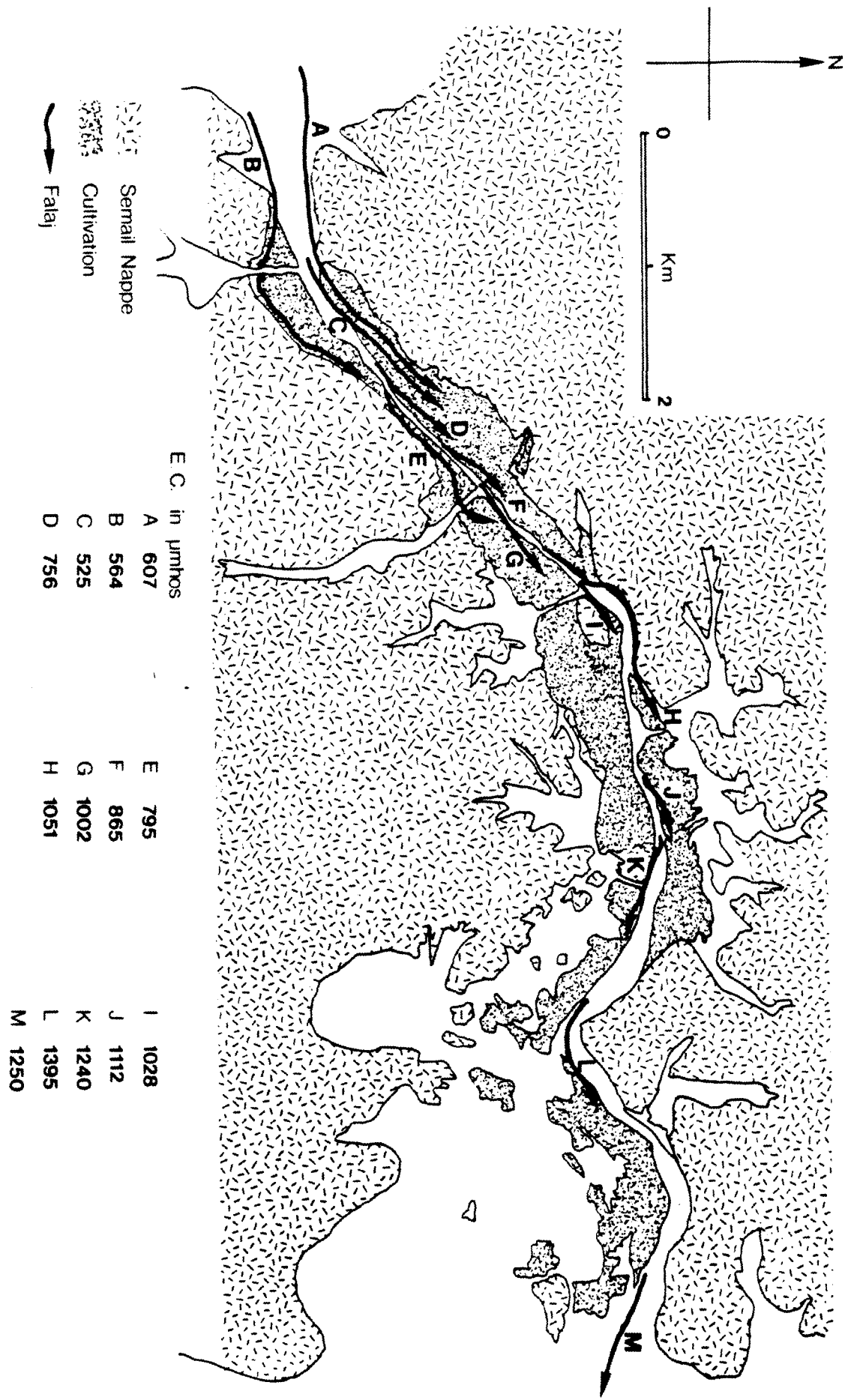|	
A	781
B	795
C	775
D	659
E	743
F	712
G	740
H	730
I	752
J	744
K	1425
L	1420
M	1375
N	1175

0   Km   1

N

Hawasina etc.   H.S.G.

Figure 6-22   Salinity Increase in Succesive Aflage   B) Semail Village

E.C. in μmhos

A 607	E 795	I 1028	
B 564	F 865	J 1112	
C 525	G 1002	K 1240	
D 756	H 1051	L 1395	
		M 1250	

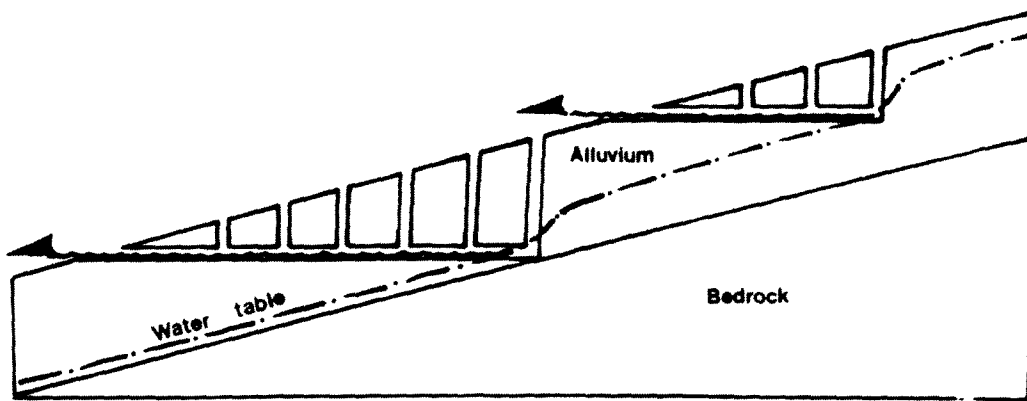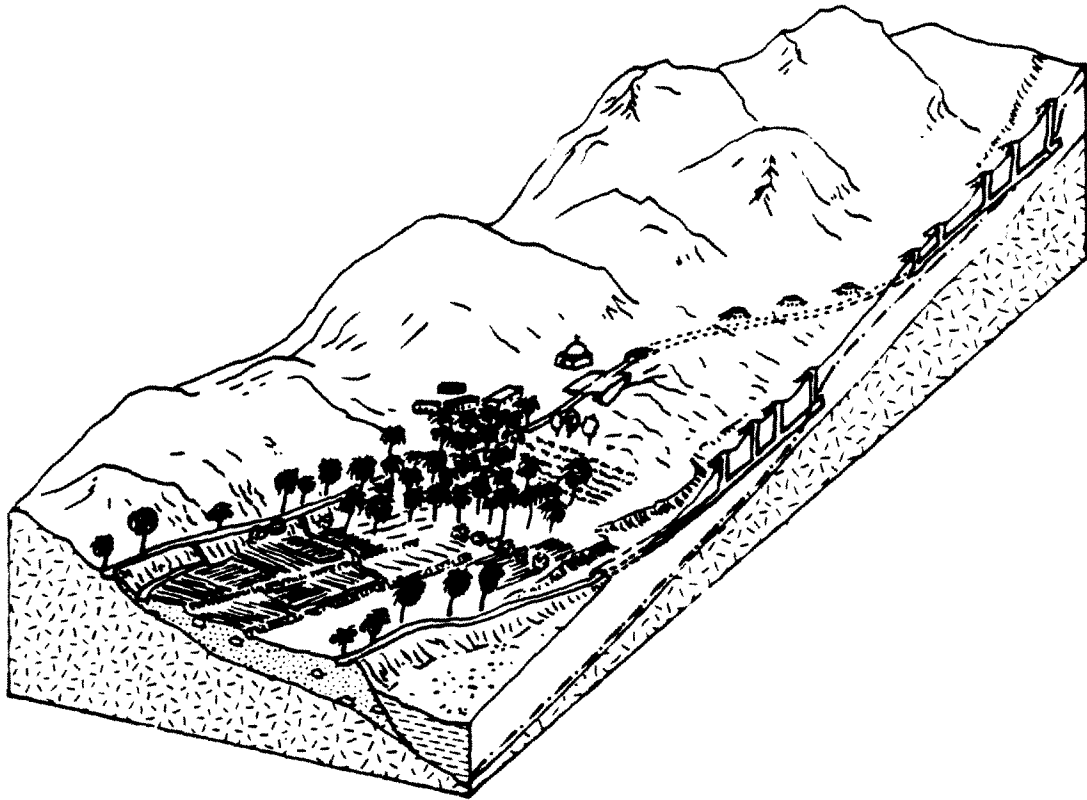Semail Nappe

Cultivation

Falaj

and rapid construction. By contrast, "qanat" aflaj are permanent structures which, historically, have required an enormous investment of resources to construct. They consist of adits, of lower gradient than either the land surface or the local piezometric surface, which are driven upstream in order to intercept either point water sources or, more commonly, the water table. In order to achieve a stable balance between scour and sedimentation the falaj gradient is typically about 0.008 to 0.01 and is thus the most appropriate form of construction for the piedmont and lower foothill areas. Elaborate underground design and methods of adit construction, as described by Letts (1979) and Bowen-Jones (1978), are usually difficult to observe, but the shafts and spoil heaps, produced during both construction and maintenance, form distinctive and prominent linear features in alluvial areas throughout Oman. The most upstream of the shafts is known as the "mother well" (umm), a concept which is apt in cases where point sources (buried springs) are tapped, but which may otherwise be misleading. Most qanat aflaj are built to intersect either surface or buried wadi channels where transmissivities, and hence yields, are highest, e.g. those shown in Figure 6.23. In such cases the hydraulic principle is that of a sub-horizontal "line sink" whose active length may extend for hundreds of metres and thus include several shafts in addition to the mother well. Furthermore the induced drainage caused by falaj construction itself, depresses the local water table to a complex configuration around the mother well which may require either further upstream excavation or the construction of supplementary adits (sa'ad) to enhance the yield during periods of drought. Line sinks directed along the centre of groundwater channels are theoretically the most efficient method of groundwater drainage. In attempting to obtain maximum water recovery the limiting factor is the ability to construct the falaj to the effective base of the highly transmissive alluvium, i.e. to basal cemented conglomerate or impervious bedrock. In some cases this is simply achieved by extending the adit further and deeper into the alluvium. In eastern Rustaq for example, the sub-surface section of falaj Maaza extends for at least six kilometres, with some shafts reputed to be up to 60 m deep. However, the saturated thickness of most large piedmont sources is usually too great to permit such impressive works, in which case it is usual for two or three aflaj to be built in line with successively lower outflow levels (e.g. Figures 6.22 and 6.24). Thus the uppermost falaj(es) depress the water-table

Figure 6.23   Falaj Lineations in Relation to Buried and

Surface Wadi Alluvium : After Letts ; 1979

Existing and Abandoned
Aflaj

Active modern Wadi
Channels

Buried Wadi Channels
deduced upon the basis
of groundwater quality
and well yields

Jebel

Cultivation
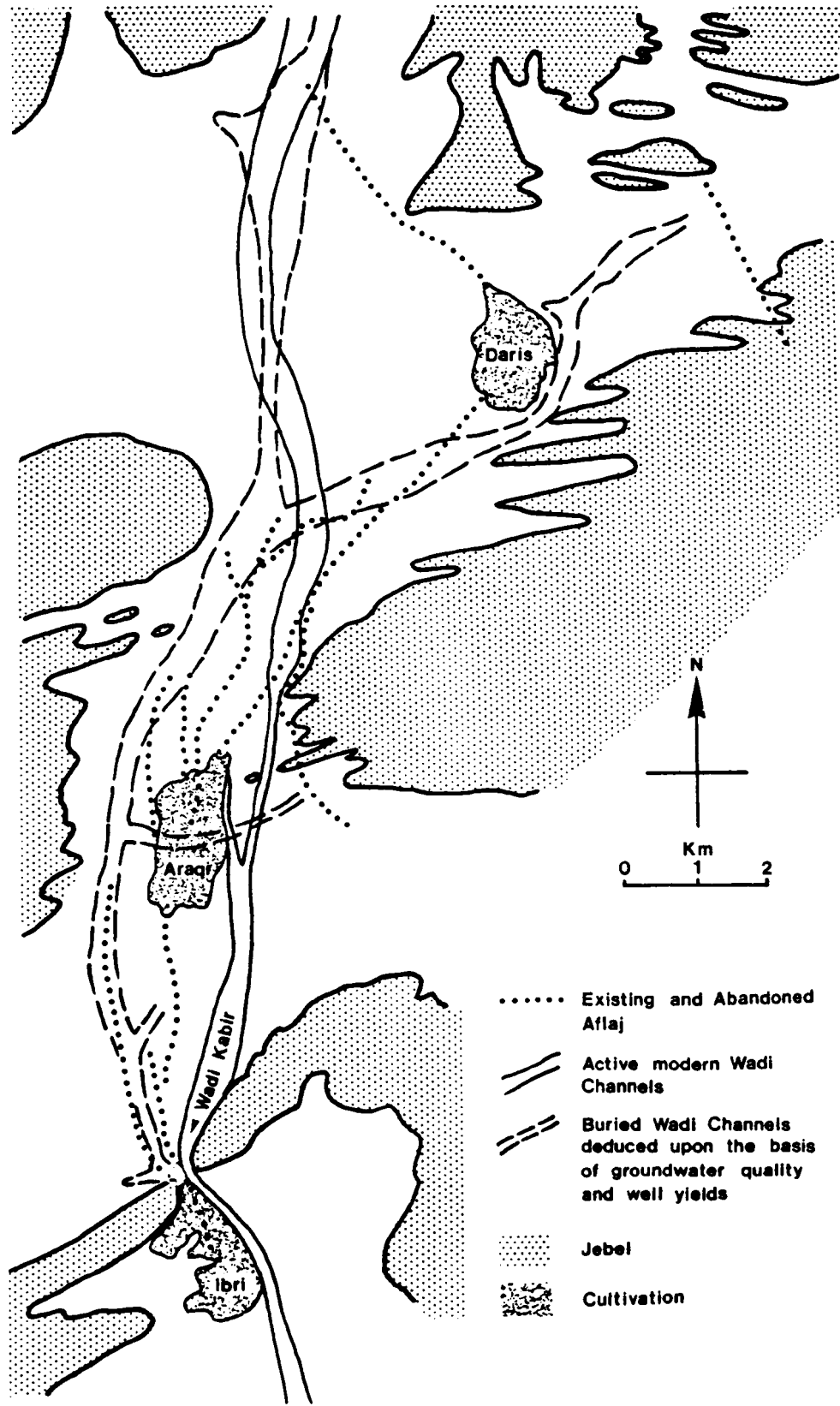
DRAINAGE BY SUCCESSIVE FALAJ ABSTRACTION

sufficiently for the lowermost falaj(es) to be constructed to the base of the high yielding aquifer. The potential effectiveness of this system is not usually apparent, but in the village of Semail an ideal impervious wadi cross section together with falaj gaugings have enabled the total upstream groundwater flow and falaj yields to be estimated, from which it is deduced that 95% of the available groundwater is recovered in the three primary aflaj which tap the wadi upstream of the village.

Given undisturbed recession under consistent channel conditions falaj flows will diminish exponentially according to the relationship:

$$q_T = q_o . \exp\left(-\frac{(t_T - t_o)}{C}\right)$$

where q_o is the initial post-recharge falaj flow at time t_o,
q_T is the reduced falaj flow at time t_T
and C is the recession constant, given by the time required for the flow to recede by a factor of e^{-1}, ie. $q_o/q_T = 0.3679$.

The recession constant is characteristic of each falaj and provides a convenient objective measure of its reliability. Furthermore its relationship to the amount of groundwater in upstream storage is given by the simple expression:

$$S_{(Storage)} = q\ C$$

Thus by integrating q_T over a given period (e.g. one year) the change in upstream storage or "aquifer yield" may be calculated as:

$$\delta S = q \int_{t_o}^{t_T} \exp\left(\frac{t_T - t_o}{C}\right) . dt$$

$$= q_T . C (\exp (3.56 \times 10^6 . C^{-1}) - 1)$$

where C is in seconds, q_T is in $m^3 s^{-1}$ and S is in m^3.

In order to measure the falaj yield of a freely draining aquifer during one year's drought it is therefore only necessary to know the final discharge (q_T) at the end of the year's drought, and the characteristic recession constant, C. The first of these variables is either known from periodic falaj gaugings or, less accurately, may be estimated from the minimum flow/perennial cropped area relationship. Recession constants should be determinate from the slope of falaj hydrographs but, as illustrated in Figure 6.25, practical factors may interfere with the theoretical recession. In addition to inevitable measurement errors incurred by inhomogenous flow and irregular channel geometry, many falaj discharges are significantly affected by as little as one month's root and water-weed growth, by channel collapse, siltation and maintenance, or by variable seepage losses (a function of stage, and hence not proportional to discharge). Generally, larger recession constants are more difficult to obtain since more accurate measurements are required to differentiate small changes in discharge whilst interfering factors are relatively large. For this reason, many aflaj with large upstream alluvial storages such as those of Al Ayn and Buraimi could not be assessed adequately despite accurate gauging for up to three years. Indeed, of 110 hydrographs available[1], only 38 yielded satisfactory recession constants. Furthermore analyses of the various aquifer yields and recession rates over a one year period are not totally objective in that falaj discharges are partially dependent upon antecedent conditions and, in a few cases, had to be estimated from less than a year's observations. Nevertheless the recessions summarised in Table 6.5, provide the best available means of comparison between the main aquifer types. The largest calculated falaj yield, from Birkat Al Mawz, is unrealistically high since, in reality, built in overspill or falaj leakage would greatly reduce the peak discharge. However, the recession constant is consistent with other limestone springs in the table in having low values of approximately 10 to 20 x 10^6 s. The

---

[1] The record lengths vary from about 5 months to 4 years and are taken from a composite data base from: This study; Gibb, 1976; Renardet-Sauti-Ice, 1975; Bowen-Jones, 1978; and unpublished Water Resources Dept. (Sohar) data.

Figure 6.25

Schematic Falaj Hydrograph showing errors and possible departures from the ideal logarithmic recession
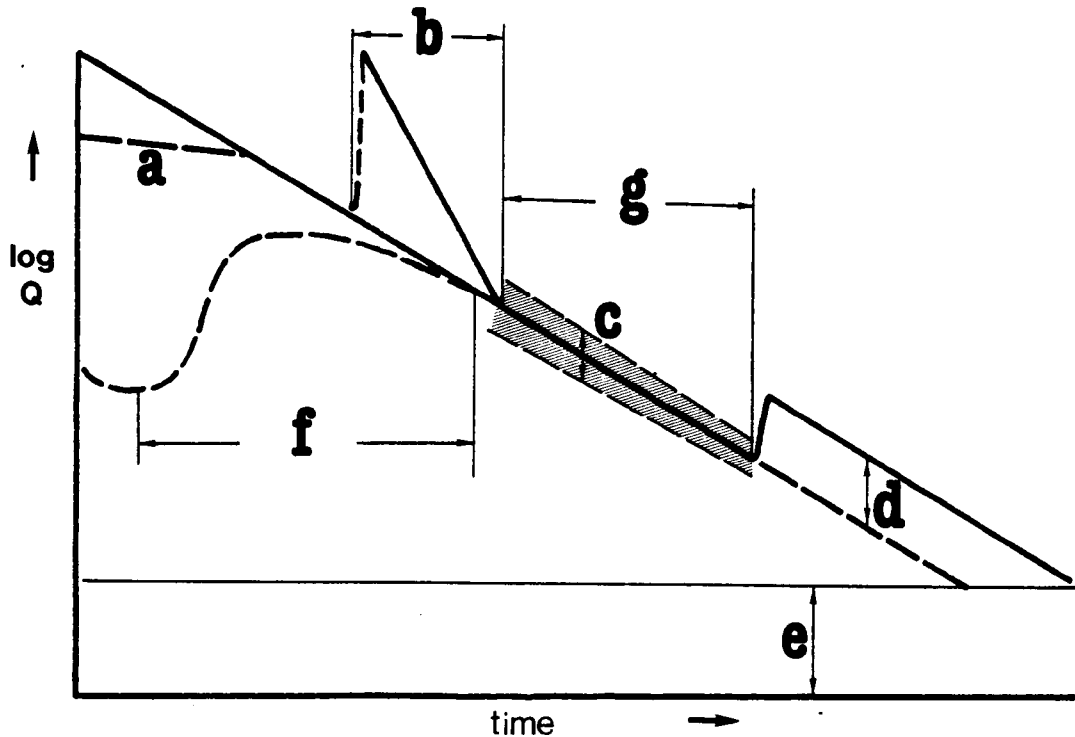
a: High stage leakage consisting of overspill at the start of ghail aflaj, or "built in" seepage losses at the head of qanat aflaj

b: Effect of surface flow or minor groundwater recharge short-circuiting the major flow pathway(s)

c: Measurement error may be only about ± 2% in accurately measured, straight sided rectangular sections with no upstream interference, but is more generally about ± 5% in less ideal situations.

d: Effect of falaj maintenance and especially of silt/weed clearing

e: At low discharges, abnormal hydrodynamic conditions occur (low velocity, increased channel friction etc.) which make accurate measurement impossible.

f: Attenuating effect, upon downstream discharge, of upstream water level recovery after general recharge.

g: Undisturbed recession slope from which active aquifer storage may be calculated.

Table 6.5 Gauged Recession Characteristics Ranked in Order of Yield

Falaj/location	Aquifer and Area of Upstream Alluvium, Km^2	Flow after one years recession $q \ (l.s^{-1})$ T	Mean Annual Flow* $l.s^{-1}$	C Recession Constant $s \times 10^6$	δ Change in Storage** $m^3 \times 10^6$
Birkat Al Mawz,Mi'Aydin	1st spring(?)-piedmont alluvium, 5	40	331	9.4	10.4
Semail aflaj 1 to 3	1st piedmont alluvium, 60	239	314	60.5	9.9
Rustaq falaj Maaza	1st piedmont alluvium, >25	84	278	15.4	8.7
Nakhl f.Thowana	limestone spring —	26.5	185	≃ 10.1	5.8
Nizwa, Wadi Nizwa	1st piedmont alluvium, 72	79	171	22.8	5.4
Ibri f. Mafjur	lower catchment alluvium, >360	134	165	79	5.2
Rustaq f. Hammam	1st spring —	56	141	19.2	4.5
Araqi, Dhahirah	lower catchment alluvium, >330	112	130	≃ 106	4.1
Wadi Jizzi at Mulayyinah	surface baseflow, mixed alluvium,86	51	130	19.2	4.1
Awabi, Wadi Bani Kharus	1st piedmont alluvium, 13	53	125	≃ 20.7	3.9
Al Ahmadi, Wadi Batha	ophiolite gravel 76	92	122	58.4	3.8
Wadi Hawasina	surface flow at Ghuzayn, 13	5	116	≃ 6.7	3.7
Izki, Wadi Halfayn	1st piedmont alluvium, 60	30	100	15.3	3.2
An Niba, Upper Wadi Batha	Tertiary 1st + oph gravel ≃ 52	22	92.6	13.1	2.9
Sulayf f. Shimbu	mixed foothill alluvium, >561	71	83.6	100	2.6
Mudayrib, Wadi Al Batha	ophiolite gravel ≃ 336	63	83.0	· 60.1	2.6
Muslimat, Wadi Ha Awil	1st piedmont alluvium 50	21	82.3	13.7	2.6
Al Hamra, Wadi Bahla	1st piedmont alluvium, 8	17	80.9	12.2	2.6
Bisyah , " "	lower catchment alluvium, 630	55	80.0	44.8	2.5
Ghayzayn, Upper Batinah	mixed foothill alluvium, 13	10	74.8	9.8	2.4
Bahla falaj Maita	mixed foothill alluvium, 90	18	70.2	13.9	2.2
Falaj Rawdah, upper Batinah	mixed foothill alluvium, 24	13	62.8	≃ 12.1	2.0
Falaj Buraimi	mixed foothill alluvium, —	51	60.0	≃ 100	1.9
Sharia, Wadi Samad	ophiolite gravel, 76	18	51.0	17.4	1.6
Thabiti, Wadi Batha	ophiolite gravel, 90	38	47.7	72.6	1.5
Jamah, Mid Batinah	mixed foothill alluvium, >50	41	46.1	140	1.5
Batine, Upper Wadi Batha	ophiolite gravel 87	14	40.5	17.1	1.3
Mahyal, Wadi Mi'Aydin	mixed foothill alluvium 46	21	37.9	29.2	1.2
Hujarimat, Wadi Kabir	mixed foothill alluvium >20	10	36.7	14.3	1.2
Falaj Al Qaba'il, Batinah	lower Batinah alluvium, >41	25	34.8	50.5	1.1
Arqi, Wadi Mijlas	mixed foothill alluvium, 20	7	33.3	12.2	1.0
Tanam, Dhahirah	lower catchment alluvium >35	17	30.0	30.2	0.95
Falaj Al Awhi, Batinah	lower Batinah alluvium >40	18	27.0	41.5	0.85
Falaj Al Harth	upper Batinah alluvium 37	10	21.4	23.1	0.67
Qasf, Hawasina	mid Batinah alluvium ≃ 100	3	14.7	12.0	0.46
Injayd, Wadi Kabir	ophiolite gravel 13	7	14.6	23.9	0.46
Saal, Wadi Rusayl	1st spring —	6	13.1	≃ 20.1	0.41
Khadil, Wadi Al Aridh	ophiolite gravel, 12	10	12.5	74.5	0.39

*Assuming continuous exponential recession for one year to the reduced flow of q_T
** ie: Active Groundwater Depletion over the year prior to q_T

traditional notion of Oman's "unfailing springs" therefore appears to be due to frequent high mountain recharge rather than to the intrinsic aquifer reliability. Of the alluvial sources, the Table shows an important trend from limestone piedmont alluvium at the high yielding end, to "mixed foothill alluvium" and "ophiolite gravel" aquifers of middle to low yielding type, and "Lower Batinah alluvium" amongst the lowest yielding aquifers. This suggests a correlation between aquifer yields and particle size of the alluvium in which the greatest active storage volumes occur in the coarse piedmont boulder gravels close to the limestone massifs of Jebels Akhdar and Nakhl. Correlations between the surface extent of alluvium and the recession constants are weak (correlation coefficients of about 0.4 for limestone piedmont areas and about 0.5 for "mixed foothill alluvial" areas) and underline the relative importance of other aquifer parameters such as the degree of cementation and the saturated aquifer thickness. Probably the most significant conclusion to be drawn from Table 6.5 is that, contrary to many contemporary views, most active groundwater storage and virtually all of the long term reliable baseflow around the Jebel Akhdar lie within the alluvial rather than the limestone sources. Thus the hydrochemically based conclusions of the Semail catchment model, and the more general falaj recession findings are in accord.

6.4   The Coastal Aquifers

In supporting nearly half of Oman's agriculture, the Batinah Plain is by far the most important aquifer of the region. The plain forms a continuous alluvial arc of about 270 km from the U.A.E. in the north to Rusayl in the east, throughout which a cultivated coastal belt is almost continuous, Figure 6.1. At both the north-western and south-eastern ends the plain narrows to a width of 10 to 15 km and consists of adjacent but differentiable alluvial fans. More typically, however, the plain is broader (25 to 30 km wide), with coalescence of distributaries in the lower reaches of adjacent fluvial systems, which render the lateral catchment boundaries indistinct. Wadis Far and Ma Awil, the two major wadis draining the Jebel Akhdar, extend the alluvial boundary further inland for some 30 km into the foothill areas. The former includes a deeply incised alluvial channel of greater than 70 m depth, whereas Wadi Ma-Awil is more typical of the piedmont areas (i.e. south of the "hinge line") in consisting of relatively shallow alluvium[1] with a maximum known thickness of less than 40 m.

---

[1]   Shelton and Stanger unpublished field and gravity data

The piedmont interfluves predominantly consist of coarse and heavily cemented boulder fanglomerates, similar in appearance to "unit 1" sediments of the interior stratigraphy. In their most upstream occurrence, they are slightly to deeply incised and form two or occasionally three well defined high terraces. With increasing distance from the piedmont the particle size and relief diminishes, the terrace levels merge, and, within about 15 km from the coast, the lithology degrades to a superficially monotonous complex of fine gravels and sandy silts. Major drainage systems tend to emerge from Tertiary limestone or Semail construction points along the hinge line, initially as a few well defined wadi channels, but as the surface gradient decreases from about 0.008 to about 0.003 near the coast, overspill channels tend to fan out into innumerable anastomosing distributaries. In traversing the plain flash floods deposit medium to fine gravels as far as the coast, but outside the main channels most of the Lower Batinah is characterised by fine grained carbonate silt, up to about 10 m thick, overlying a sedimentary complex ranging in particle size from clay to medium gravel.

None of the active wadi channels can be regarded as indefinitely stable. In addition to shifting channels caused by sporadic changes in the balance between erosion and deposition, cut-back and wadi capture occur in both the nodal and piedmont areas (e.g. Wadi Semail, Figure 6.26 and Wadi Mistal[1], Figure 6.27 respectively). Aeolian and coastal processes also contribute to the heterogeneity of the sedimentary sequence. For example, the last stage of each flood deposits a veneer of calciferous silt and clay which desiccates and is remobilised during wind erosion. Aeolian deflation of the lower interfluves is also widespread, and sporadic remnants of north-south aligned seif dunes are present at the piedmont margin. Amongst the coastal features, low stable storm dunes and flat silty areas are intersected by both present and past fluvial channels. The existing channels frequently terminate as lagoons separated from the sea by shingle spits formed as storm beaches and modified by vigorous westward longshore drift, whereas old dried-up channels create saline creeks and localised sabkhas, often with evaporites and black authigenic clays.

---

[1] Wadi Mistal has evolved into an unusual configuration in which surface flow from the Ghubrah bowl breaks through the ophiolites to merge with the main Wadi Bani Kharus flood channel whilst groundwater underflow still appears to leak through the former alluvial fan into the Ma-Awil catchment.
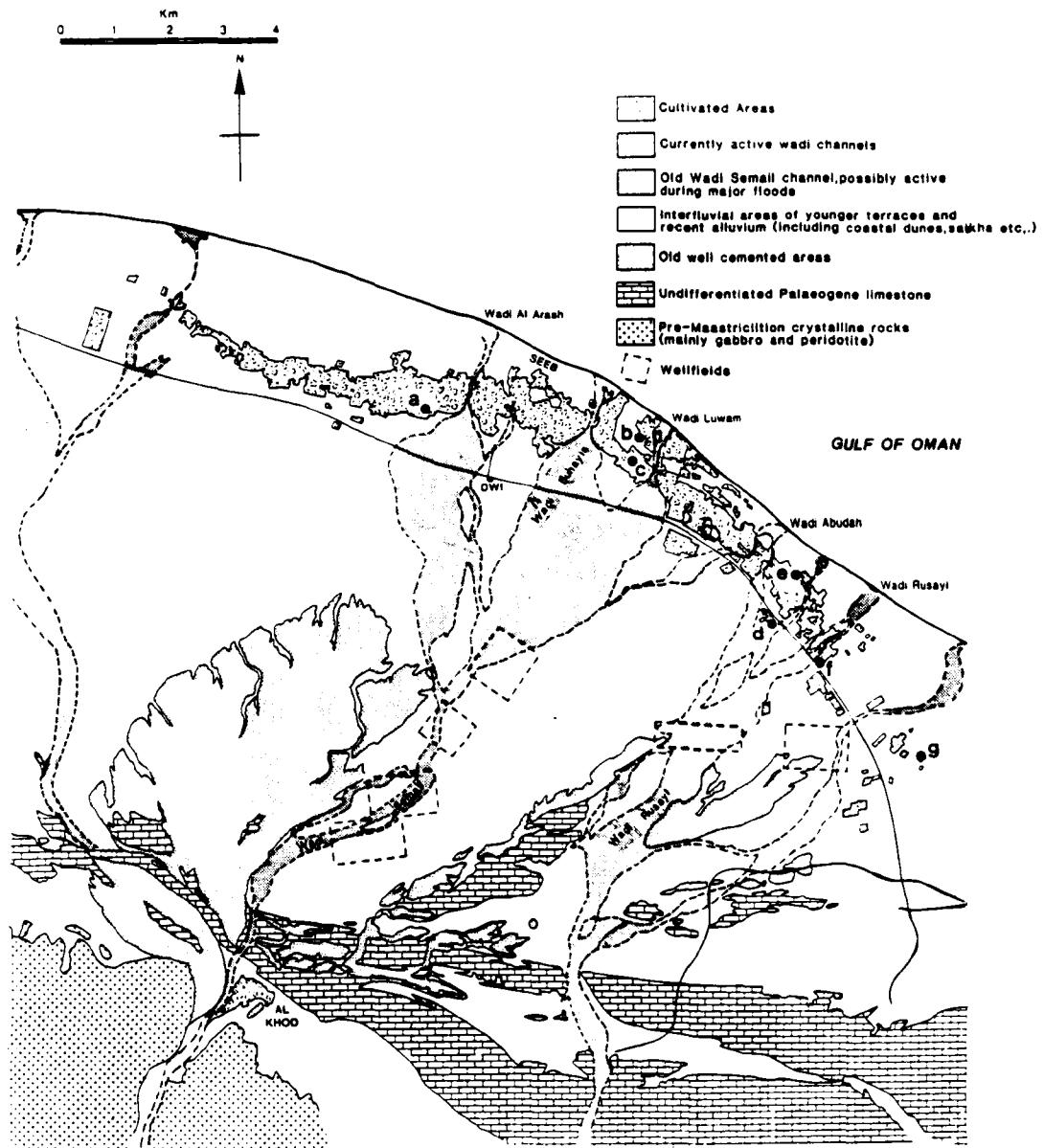
Figure 6.26

The Seeb-Rusayl Alluvial Fan

Km
0 1 2 3 4

N

Cultivated Areas

Currently active wadi channels

Old Wadi Semail channel, possibly active
during major floods

Interfluvial areas of younger terraces and
recent alluvium (including coastal dunes, sakha etc,.)

Old well cemented areas

Undifferentiated Palaeogene limestone

Pre-Maastricitian crystalline rocks
(mainly gabbro and peridotite)

Wellfields

Wadi Al Arash

SEEB

Wadi Luwam

GULF OF OMAN

Wadi Abudah

Wadi Rusayl

AL
KHOD

Figure 6·27   Wadi Capture in the Upper Mistal - Kharus Catchment

H.S.G   Exotic limestone   Semail nappe

● Wadi Capture Point Indicating Present (⤧) and Older (⤤) Channels
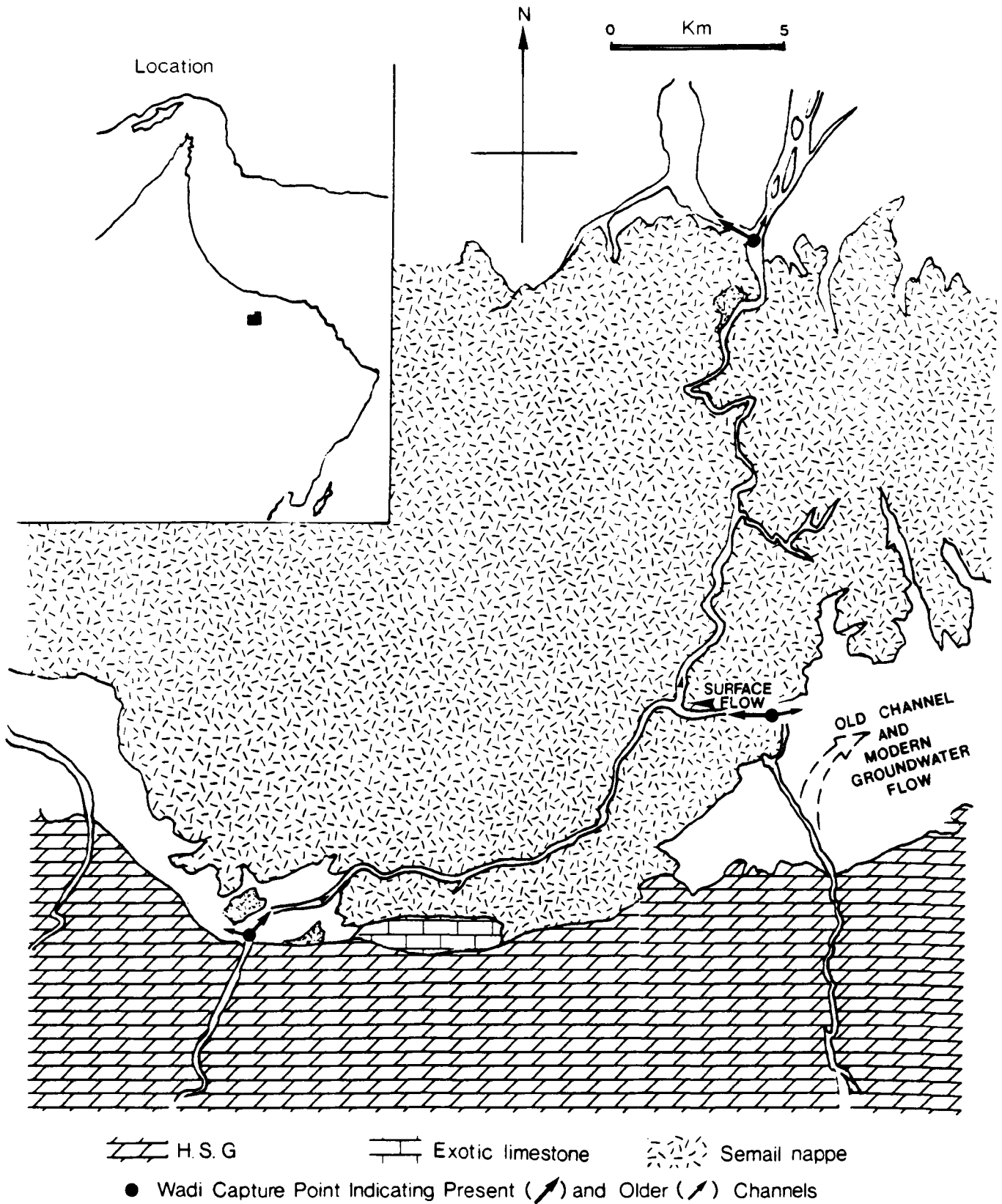
Despite the importance of the Batinah plain to traditional agriculture, almost no subsurface geological data has become available since the initial hydrogeological surveys of 1973 to 1975. These consultants' reports give details of the central and eastern Batinah in which exploration borehole coverage averaged one well per 35 km^2 (twice that density in the Seeb Fan), whereas in the western Batinah inland from the coastal strip, there is no borehole data available. Consequently only the most general conclusions may be drawn concerning the nature and extent of the subsurface facies variations.

Gibb (1976) proposed a zonation comprising:

3 Upper gravels

2 Clayey gravels

and 1 Cemented gravels, possibly correlating with old cemented terraces.

The upper gravels include the most productive aquifer material, and consist of clean subrounded uncemented and well sorted alluvium ranging in size from medium gravel to coarse sand. They occur in modern outwash fans and develop their maximum thickness at a distance of between 10 and 20 km from the hinge line, i.e. at the coast in the Seeb Fan (up to 100 m in depth) as opposed to about 10 km inland in the central Batinah areas (up to 70 m in depth). In parts of the Seeb Fan the underlying "clayey gravels" consist of sparse gravelly horizons dispersed in up to 20 m of thick brown clay which in turn overlies distinctive white marl or moderately lime-cemented gravel. Elsewhere the distinction between zones one and two is commonly less clear or completely absent. Hence a large proportion of boreholes which penetrate the upper gravels reveal an abrupt change to partially cemented gravel followed by a subsequent gradation to completely cemented gravel in which the cementing medium is an apparently random variation between brown clay, white, grey or red marl, or white micritic carbonate. The Gibb report further argued that this cementation was a product of ultramafic rock or serpentinite decomposition resulting in replacement by carbonate minerals, but whilst primary ultramafic phases undoubtedly decompose in the alluvium, the high pCO_2-reducing conditions required for silica-carbonate-goethite replacement of serpentinite (Stanger[1], 1985) are not widespread in the

---

[1] Alluvial groundwaters in Oman are almost invariably slightly oversaturated with respect to the common carbonate minerals, strongly oversaturated with respect to serpentine, and slightly undersaturated with respect to olivine and enstatite.

Batinah groundwater environment. Rather most of the cementation is readily accounted for by the normal diagenetic processes of carbonate dissolution and reprecipitation (e.g. Bathurst, 1975) and by both authigenic and derived clay[2] deposition.

Base flow recharge to the Batinah plain is initially concentrated in relatively shallow highly transmissive piedmont channels in which both the surface and hydraulic gradients are typically about 0.009. Further into the plain the hydraulic gradient steepens to about 0.012 in response to the increased alluvial depth of the mid-Batinah, just north of the "hinge line" (cf. section 4.7). Here the mid-plain groundwater flow is dispersed over a broader front and mainly occurs within the less transmissive clayey and cemented lower gravels, resulting in a maximum depth to the piezometric surface of between 45 and 65 m. Further seaward, the hydraulic gradient shallows to an average of about 0.0006 and sometimes to as little as 0.0004 whilst the surface gradient continues more consistently at about 0.005. The depth to water table therefore declines to seaward, with the water table itself intersecting higher levels of alluvium to give saturated thicknesses of up to 35 m in the upper gravels. Aquifer differences between the high yielding upper gravels, and the lower sediments are indicated by the transmissivity (T) and permeability (K) values determined by Gibb (1976) using step drawdown well tests and specific capacity data adjusted for well losses:

	mean $T, m^2/day$ (test solutions)	mean $T, m^2/day$ (S.C. data)	k, m/day
Upper gravels	550	525	$32 \pm 23(1\sigma)$, n=38
clayey and cemented gravels	223	75	$6.5 \pm 6.9(1\sigma)$, n=32

---

[2] This clay does not contain any relict chromite or goethite and therefore does not seem to be a product of in situ ultramafic rock decomposition.

These permeabilities and gradients imply mean groundwater velocities[1] of the order of, at most, tens of metres per year, and hence a total Batinah transit time of several centuries. An alternative indication of alluvial residence time is provided by comparison of tritium isotopes from near coastal wells and boreholes. In the Seeb fan the relatively steep hydraulic gradient, short flowpath and extensive upper gravels of high transmissivity combine to produce a fast throughflow and hence relatively recent recharge, as shown by tritium concentrations of 24.6 and 4.9 T.U[s]. (Appendix B2). This contrasts with near coastal groundwater derived from potentially longer flowpaths in the central Batinah plain, which are of zero tritium concentration and hence older than about 30 years. These two contrasting areas also exhibit differential stable isotopic compositions, such as:

$\delta^{18}O$ from Seeb fan coastal wells; - 1.63, - 0.73, - 1.39, - 1.34 and $\delta^{18}O$ from Wadis Far to Ma-Awil coastal wells; - 3.27, - 2.44, - 2.88, - 3.60, - 3.15, and therefore constitute another case in which the older the groundwater, the greater the probability of it containing a high proportion of isotopically light water derived from extreme storm recharge events.

The apparent discrepancy in base flow transit time (i.e. centuries according to aquifer parameters vs decades according to isotopic composition) is obviated in the light of the recharge distribution. Concentration of recharge around the active flood channels is demonstrated by water level fluctuations such as those of Figure 6.28. Following rainfall, hydrographs from boreholes in the cemented interfluves indicate little or no water level recovery, whereas those situated in or close to the active flood channels respond rapidly. Piedmont baseflow is therefore supplemented by substantial but intermittent flood recharge across the whole width of the plain which leads to infiltration into the higher permeability zones, and partial short-circuiting of the deeper groundwater flowpaths. Dispersed flood recharge also accounts for both the low salinity of shallow groundwater as it approaches the coastal zone, and the lack of a well defined salinity gradient across the Batinah plain (unlike the interior wadis).

---

[1] since $v = ki$

Figure 6·28   **Selected Borehole Hydrographs from the Batinah Plain**

depth to water table [m]
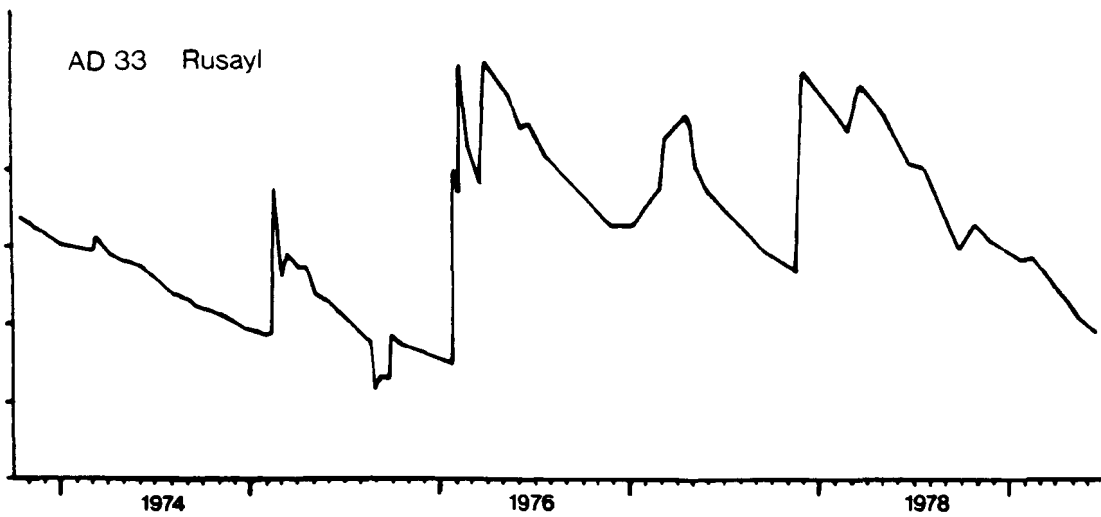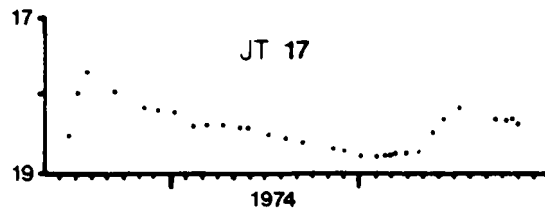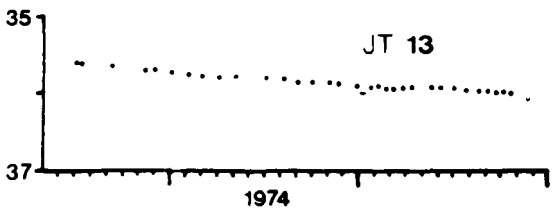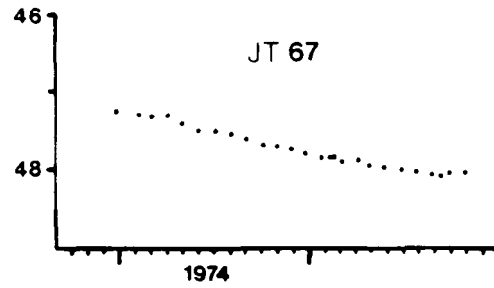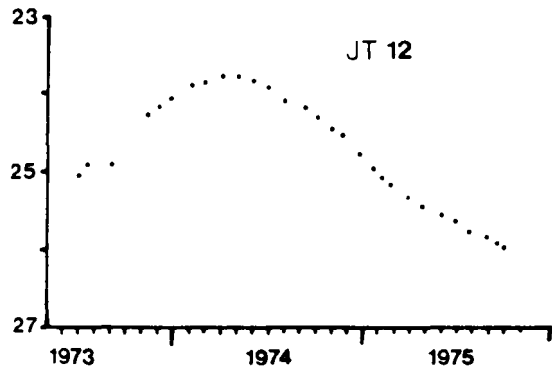
Indeed, despite the medium to long baseflow residence times well salinities (as electrical conductivity) in excess of 1000 μmhos are uncommon upstream of the coastal agricultural belt. Further inland groundwater conductivities typically span the range of 450 to 750 μmhos (cf., for example, analyses 110, 112, 113, 135, 185, 186, 197 and 362, Appendix C) but occasionally, pockets of recent infiltration may be as low as 300 μmhos. The latter figure is comparable to the original flood salinity. For example, the declining flood flow across the coastal road in Wadi Bani Kharus in February 1975, which probably approximates to average flood recharge composition, had a conductivity of 225 μmhos.

Modelling of the groundwater alluvial system is hampered by inadequately quantified baseflow and flood recharge and by the sparsity of geological data. In particular it is probable that buried highly transmissive channels both promote and redistribute a large proportion of the total groundwater flow at depth. The existing borehole density is insufficient to identify such channels but they may be assumed to exist since (1) their presence has been proven in the southern basins despite the stabilising effect of hard rock distribution upon wadi channels, whereas the laterally unrestricted and subsiding sedimentary environment of the Batinah is more conducive to the deposition of buried channels, and (2) both the pattern of salinity and the water table response to recharge (e.g. between December 1973 and December 1974 in Gibb, 1976) are often unrelated to the surface drainage pattern, and therefore imply subsurface redistribution of groundwater by preferred channels.

Heterogeneity in the alluvial system is further emphasised by the piezometric response to barometric loading, which shows that more than half of the non-coastal boreholes are in a semi-confined aquifer. The nature of the semi-confining "layer" is unclear since the distribution of water-table or semi-confining conditions does not correlate with any of the known alluvial features such as total thickness or saturated thickness of the upper gravels. The most likely origin seems to be the deposition of clay laminae and cemented horizons which, though of limited individual extent, are cumulatively sufficient to impart a marked anistropy to the upper aquifer.
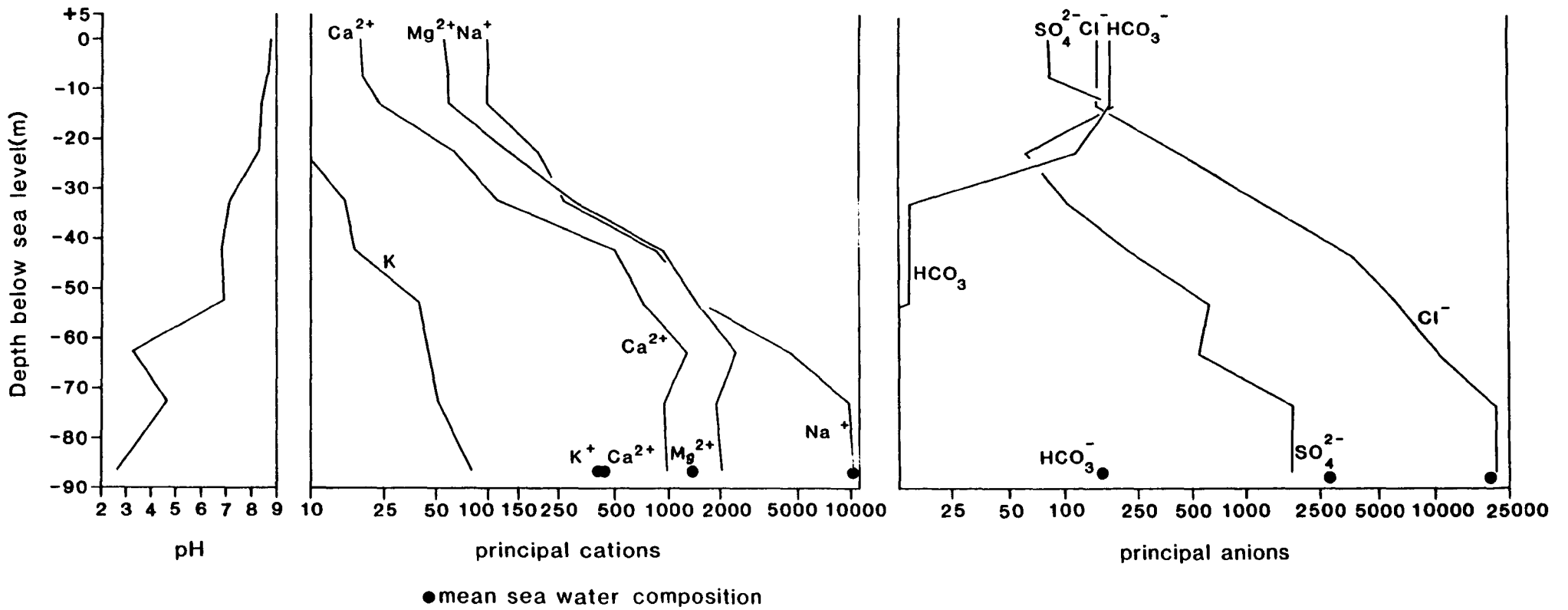
Near the coast the alluvial surface consists of cultivable silty
carbonate soil whilst the depth to water table progressively decreases
to seaward, eventually becoming within reach of hand-dug wells,
generally less than 10 m deep. This has permitted the establishment of
a permanent coastal strip of agriculture by the construction of several
thousand dug wells and, more recently, boreholes from which a more
detailed assessment of hydrogeological conditions is obtainable. The
most important parameter, and the effective seaward boundary of the
aquifer, is the position of the saline interface, approximated by the
50,000 μmhos electrical conductivity contour depicted in Figure 6.29.
This is only encountered in the deeper exploration boreholes (located in
Figure 4.17) at depths which normally vary between − 50 and − 105 m,
although two exploration boreholes south-east of Sohar, which were
expected to intercept the salt water interface at about − 100 m, did not
reach the interface even at depths of − 228 and − 242 m (Fellon, 1978).

Hydrostatic equilibrium between the fresh water wedge and
underlying denser, more saline water should result in a constant ratio
between the thicknesses of fresh water above and below sea level. This
ratio is theoretically 1:40 for a sharp fresh water/sea water interface
but a more realistic model which allows for a zone of diffusion (i.e. a
brackish zone rather than a sharp interface) increases the ratio to
about 1:50. In reality, the ratio is found to vary between 1:48 and
1:62 with larger ratios being attributable to hydrodynamic effects.

A chemical investigation of the zone of diffusion from borehole DWI
in the Seeb area is summarised in Figure 6.30 and displays an
extraordinarily steep pH gradient which cannot be explained by natural
groundwater processes. It is therefore assumed that some form of
electrolytic action between the steel casing and slow moving groundwater
has destroyed the original non-conservative ionic composition and
especially the carbonate species. Nevertheless the Cl^-, SO_4^{2-}, Na^+ and
K^+ ions are probably typical of real aquifer conditions, with Na^+ and
Cl^- indicating a normal sea water concentration below − 75 m. At the
same depth the K^+ concentration is much less than that of normal sea
water and suggests probable ion exchange in the deeper clays. Above the
high salinity zone all the principle cationic trends and Cl^- indicate
natural diffusive mixing between fresh water and approximate sea water
composition over a thickness of about 60 m beneath a 15 m thick fresh
water zone.

Figure 6.29

Schematic Section of the Batinah Coastal Area
(Electrical Conductivity Contours in μS)

Zone of traditional date cultivation

New cultivation

irrigated

non-irrigated

Evaporation from shallow water table

sea

d

sea level

water table

Fresh water

40d

2000

5000

10,000

20,000

50,000

>50,000

Groundwater of Modified Sea-water Composition

Figure 6·30

Chemical Variation in Borehole DW1
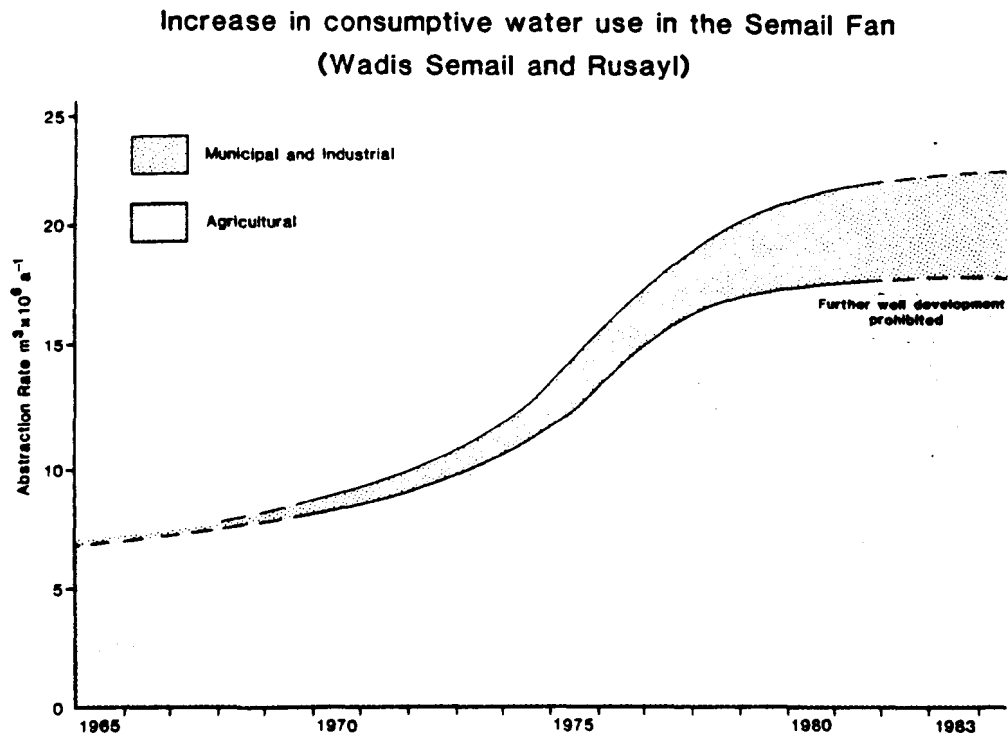

●mean sea water composition

Destabilisation of the saline front in response to increases in consumptive use in the Seeb-Rusayl area, (summarised in Figure 6.31), began to take effect around 1969, some four years before the initial survey. However, most of the early pumps were installed in the more prosperous and productive areas, largely concentrated in the central part of the Seeb Fan coastal belt, i.e. close to the main active wadi channels where the risk of salinization is least, whereas the high risk areas to east and west did not begin to mechanise until later. During the initial water use survey it was therefore still possible to interview farmers about recent salinization trends, changes in cropping pattern and yields, and the increased amounts of extraction. From their answers the initial E.C. of groundwater throughout the entire Seeb Fan was apparently less than about 2500 μmhos. In the areas most affected (east of Wadi Abudah, Figure 6.26, salinity had risen at an alarming rate. Complaints of groundwater deterioration from fresh (less than 2000 μmhos) to brackish (10,000 to 15,000 μmhos) in as little as 18 months were common, though the average period of deterioration seems to have been three to four years.

The surveys reveal three areas of naturally contrasting characteristics represented by the western, central and eastern thirds of the Semail-Rusayl coastal belt. Figure 6.26 shows that the westernmost of these areas lies in an interfluvial zone where direct recharge is minimal and where sediments tend to be fine grained and well cemented. Observation wells a few kilometres inland have shown that despite occasional heavy rainfall the water levels have continued to fall since 1973, indicating that both the inland groundwater storage and lateral recharge from the active wadi channels are relatively small. This area is therefore the most vulnerable to changes in abstraction and consequently was the first to experience salinization, (Map 3a). The subsequent surveys showed a slight landward migration of the edge of the saline front, probably in response to the construction of farms along the new road and abandonment (i.e. cessation of groundwater abstraction) along the seaward margin. Nevertheless, there has been little significant increase in overall salinity which suggests that a new state of dynamic equilibrium has been reached, (e.g. well "a", Table 6.7).

The central Seeb Fan area, being directly in line with the various Wadi Semail distributaries is well placed to benefit from both local

Figure 6·31

Increase in consumptive water use in the Semail Fan
(Wadis Semail and Rusayl)

Legend:
- Municipal and Industrial
- Agricultural

Y-axis: Abstraction Rate m³ x 10⁶ a⁻¹ (25, 20, 15, 10, 5, 0)
X-axis: 1965, 1970, 1975, 1980, 1983

Further well development prohibited

flood flow recharge and maximum groundwater flow derived from the relatively porous and uncemented upper gravels in the central fan alluvial system. This groundwater abundance gives rise to many obvious characteristics. For example, the presence of a thin fresh water layer close to the surface and the ability to cultivate date palms even within the tidal zone is clearly indicative of active seaward groundwater flow. Indeed, the whole central area is situated close to the sea but continues to cultivate a wide variety of crops and ornamental gardens with a vigour and profusion not seen in either of the adjacent areas to east or west (Plate 6.7). Apart from the artificial recharge mound in the vicinity of Seeb caused by the import of desalinated water for irrigation, there is little significant change in groundwater quality between 1973 and 1982 (cf. wells "b" and "c", Table 6.7). The variable ingress of sea water into the coarse gravel estuaries of Wadis Buhayyis and Luwam (in Figure 6.26) is variable, reversible and mainly indicative of the stage of recession in the active wadi channels, and therefore has little bearing on the state of the saline interface elsewhere.

During the surveys, almost all of the eastern third of the Seeb-Rusayl Fan suffered some increase in salinity, but nowhere was the effect as pronounced as in the easternmost and seaward areas where the impact on agriculture was disastrous (e.g. wells "d", "e", "f" and "g", Table 6.7 and Plate 6.8). In some cases up to 20-fold increases in salinity have transformed highly productive smallholdings to deserted saltbush scrub which provides poor pasture even for goats. Even new farms established some four kilometres from the coast have experienced rapid salinization. The eastern area and its hinterland is largely underlain by interfluvial conglomerates of low storage and transmissivity, but differs from the western Seeb Fan in that it receives some groundwater recharge through the relatively coarse alluvium of Wadi Rusayl. Though the catchment area is far smaller than that of Wadi Semail, the groundwater storage of this alluvial system has evidently been sufficient to delay the salinization observed further west. Pumping from municipal wellfields (Figure 6.26) for the Muscat water supply must have intercepted a large part of the groundwater flow to the coast and is known to have depressed the local fresh water-table to below sea level, i.e. reversing the direction of groundwater flow between the wellfields and the sea. Some of these wellfields are now closed but their abstraction must have been a significant factor in the rate of saline invasion, though the ultimate extent of the damage would probably have been the same.

Fresh water is lost from the coastal system by a combination of evaporation from an increasingly shallow water table, consumptive loss through irrigation, and leakage to sea; processes which together maintain an approximate dynamic balance at the saline "interface". This is illustrated in Figure 6.32 by the stable salinity profile of DWI (sited about 1.25 km inland from the nearest abstraction) over a seven year period. On the other hand the effect of initiating or increasing near surface abstraction is to develop cones of depression around the pumped wells which locally reduces the water table and thus induces a state of hydrostatic imbalance beneath the wells. In principle the hydrostatic equilibrium is regained by a rise in the saline interface equivalent to 40 or 50 times the fall in the water table. In reality, however, anistropic permeability and hydrodynamic factors result in both horizontal and vertical movements of the saline front, and in a general broadening of the brackish zone by hydrodynamic dispersion (Bear, 1979). Typically this involves either the horizontal ingress of sea-water along a broad front or, further inland, relatively localised upconing of brackish water, but the precise mechanism of salinization is often difficult to determine. In fine grained aquifers, both mechanisms are insidious and effectively irreversible. Hence seasonal fluctuations in the saline front occur only in the coarse gravel lithologies of lagoons and "estuaries" at the wadi mouths.

The extent of the salinization process is closely related to the historic development of pumped coastal irrigation. Prior to about 1950 the coastal wells were almost all of low yielding animal bailed type ("manjur" or "zagira" type described in Bowen-Jones, 1978, and Letts, 1979) except within about a km from the sea where the fresh water layer is at its shallowest (and thinnest) so that perennial crops, once established, require little or no further irrigation. In the latter case groundwater abstraction was, and often still is, restricted to simple cantilever or hand-bailed wells of even lower yield. Thus overall, the coastal abstraction was not excessive and, due to a long history of trial and error, was approximately in balance with the minimum available groundwater flow. Throughout the 1960S and early 1970S there was a gradual change in agricultural practice marked by a steady increase in pumpset purchases, with the result that by 1974 virtually all of the wells in the coastal belt had been mechanised (Stanger, 1985). Indeed, some gardens had two or even three pumps in

Figure 6·32

Successive Conductivity Profiles Of borehole DW 1
(1978 log after Rousseau)
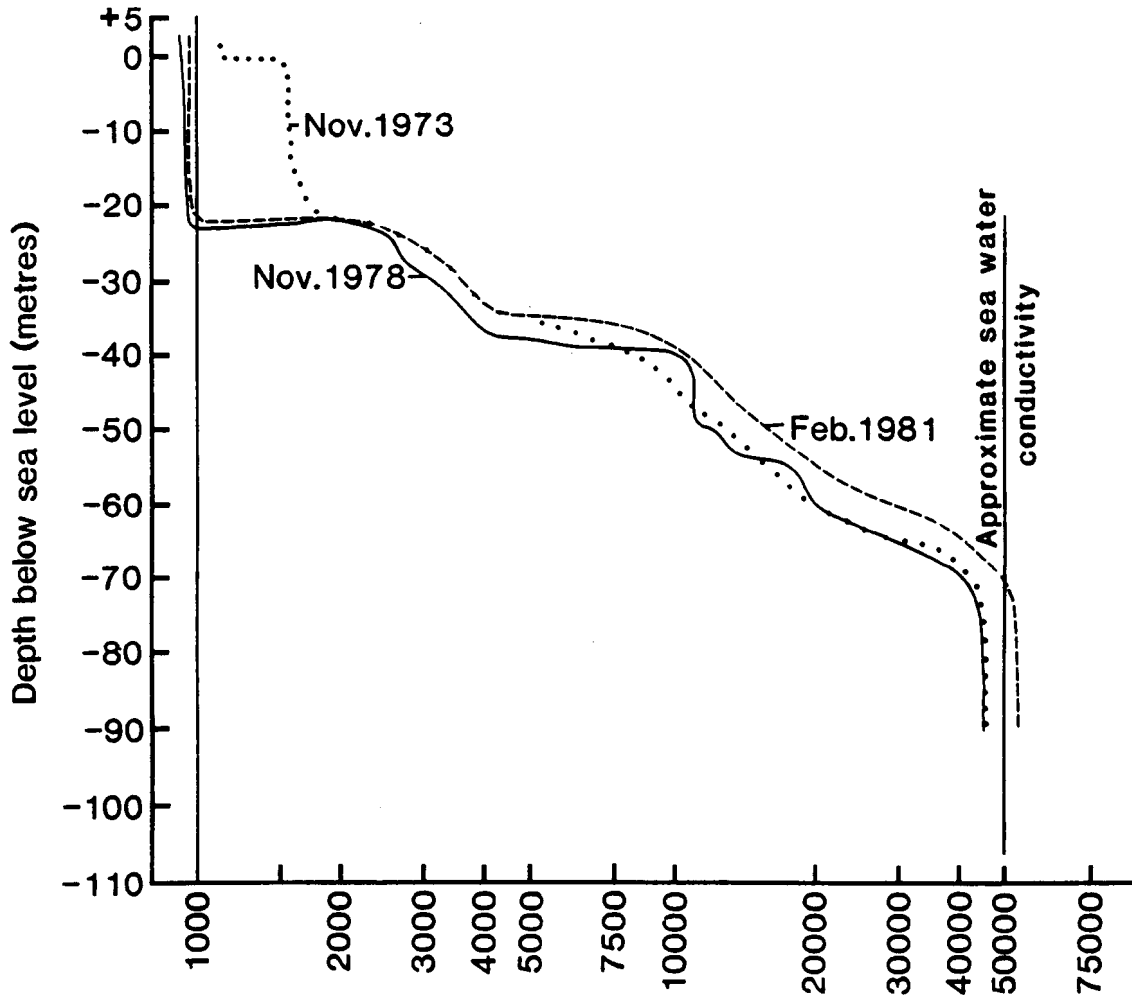
use, both for agriculture and for the increased water demand caused by peripheral urbanisation. Moreover, between 1968 and 1981 a second wave of pump installations, both for hand-dug wells and boreholes, took place inland from the traditional agricultural belt, a process greatly accelerated by the construction of a coastal road between 1973 and 1975. This new development was of markedly differing style, evolving as relatively large scale market gardening farms in response to the expanding demands of the capital area.

Increased abstraction throughout the Batinah coastal zone has occurred on too large a scale to permit comprehensive monitoring of the resultant salinity changes, but successive electrical conductivity (E.C.) surveys of a representative section of the coast over a 9 year period (1973, 1978, 1980-81 and 1981-82) illustrate the form and potential extent of brackish zone and saline front migration. E.C., though subject to differential variation between specific ion concentrations, correlates well with both chloride and total dissolved solids at least up to about 15,000 μmhos (cf. Appendix C4) and was therefore adopted as a convenient parameter to approximate the total salinity. However, total salinity is not the sole criterion for irrigation water suitability. Drainage, crop water application rate and frequency, the leaching requirement under the prevailing climatic conditions, and the sodium adsorbtion ratio are all co-variables (Scofield 1940; Richards, 1954; Todd, 1959; UNESCO, 1961). Therefore, as an aid to the interpretation of the E.C. contours in map 3 an empirical assessment of E.C./irrigation suitability in the Oman coastal area is summarised in Table 6.6.

Initially the Seeb-Rusayl fan (Figure 6.26) was chosen as the survey area for the logistic reasons of ease of access and availability of photographic coverage, and also because of its close proximity and importance to the capital area. Although the hinterland is slightly atypical in respect of the uncommonly thick upper gravels, relatively short flood pathway between piedmont and the sea and possible rain shadow over part of the catchment, various assessments of water resources of the eastern Batinah plain unanimously regard the Seeb area as having an "excess" of recharge over consumptive use (Burdon, 1972; Gibb, 1976; Horn, 1977; Konteatis, 1978; MacDonald et al, 1978). The Seeb coastal zone is thus a conservative example of salinization against which the remaining Batinah may be compared.

TABLE 6.6   Empirical Assessment of Water Quality of Irrigation Water
in the Coastal Areas of Oman

E.C. (μmhos)	
500 to 1500	Water suitable for all crops. Normal domestic water supplies.
1500 to 2500	Water of slightly brackish taste. Sensitive crops such as citrus fruits moderately to severely affected.
2500 to 5000	Very brackish. Bananas and many vegetables severely affected.
5000 to 10,000	Most crops either fail or suffer severe salinization. Above 7000 μmhos alfalfa ceases to be cultivated. Economically viable agriculture becomes difficult to impossible.
greater than 10,000	Date palms will survive but with greatly reduced yields. No other crops survive. Most gardens are abandoned and revert to halophilic scrub
about 50,000	Sea water

TABLE 6.7   Selected Examples of Well Salinity Variation Over
             the Nine Year Survey Period

             (E.C. in μmhos cf. Figure 6.26 for locations)

Well	1973	1978	1980/81	1981/82
a	3000	3700	3800	3850
b	3800	5000	5500	4000
c	2000	2000	2200	2140
d	≃ 1000	≃ 1500	2100	5900
e	2400	≃ 6000	19,300	23,800
f	≃ 800	3000	7860	15,230
g	3130	5100	13,400	18,250

a :   Western area: now virtually stable.

b :   Seaward Central area;   improving slightly in 1981/82 after
        local desalinated recharge.

c :   Landward central area;   stable low salinity.

e f g: Eastern area;   examples of severe salinization.

NB.   Salinity in wells a and b were both much less than 3000 μmhos
        prior to the introduction of pumps.

Superimposed upon the major salinization trends were various perturbations in the E.C. contours. Local positive anomalies were caused by well deepening, well abandonment (frequently accompanied by collapse and subsidence of saline soils), urban pollution and short term increase in extraction. Many such localised salinity anomalies, surrounded by normal groundwater composition, are associated with overpumping, and occur several kilometres inland in which case the mechanism is clearly that of simple upconing of brackish water. Negative anomalies were due to new well development, local ponding and recharge of flood runoff against new road embankments, artificial training of the main Semail channel and water import. In addition, several apparent anomalies, both positive and negative, may have been caused by subjective sampling bias and changes in well access during the four surveys. All the surveys were carried out in the cooler months, between October and early January, to avoid any short term salinity increases associated with higher extraction of water during the summer months. Despite these effects and any variation in the position of the saline interface caused by annual variations in recharge, it became evident that progressive saline invasion was obviously the dominant process.

In general, salinization varying from trivial to total has been experienced in about 90% of the Seeb-Rusayl agricultural belt. In about a third of this area, the increase has been severe (E.C. greater than 5000 μmhos) whilst total crop failure and abandonment has so far occurred in 10 to 15% of the area. It is, therefore, essential to establish whether the saline interface has reached a new state of equilibrium or whether an even larger proportion of the cultivated areas is threatened. Between the surveys of 1980-81 and 1981-2 the E.C. continued to rise significantly in the easternmost area, but a ban on further well development, a decrease in extraction in some of the wellfields and many salinated gardens, and unusually heavy rains in 1982-83, may, at least temporarily, have halted the trend. In some interfluvial areas such as Rumais (some five kilometres west of the Seeb Fan and three kilometres from the sea) and western Seeb there appears to have been a rapid and sometimes severe rise in salinity for two to four years followed by a long period of relatively stable or even slightly improved water quality (Bailey, 1978; cf. Appendix C3 and Figure C1).

Simultaneously, however, the inland water table has fallen steadily without any apparent relationship to either rainfall or groundwater salinity, i.e. a depleting volume of fresh groundwater is subjected to excessive, albeit stabilised, extraction. Thus despite apparent stability of the saline front, the danger still exists of continued saline intrusion into the interfluvial alluvium during future periods of drought.

The extent of changing salinity throughout the rest of the Batinah coastal strip is only known from the Al Khaburah and Wadi Bani Kharus – Ma Awil areas where unrelated salinity surveys have overlapped (e.g. Figures 6.33 and 6.34). The high salinity distribution indicates markedly differing groundwater conditions between the two areas, i.e. a substantial groundwater leakage maintaining a sharp and stable saline interface close to the coast at Al Khaburah, as opposed to the predominantly interfluvial area of Wadi Bani Kharus – Ma Awil where a lesser, more diffused, fresh groundwater flow has permitted the development of a broad saline front up to five km inland. The most noticeable changes have been in the landward edge of cultivation and particularly around the strip of new cultivation along the coastal road, where a patchy increase from less than 1000 to about 2000 μmhos was common.
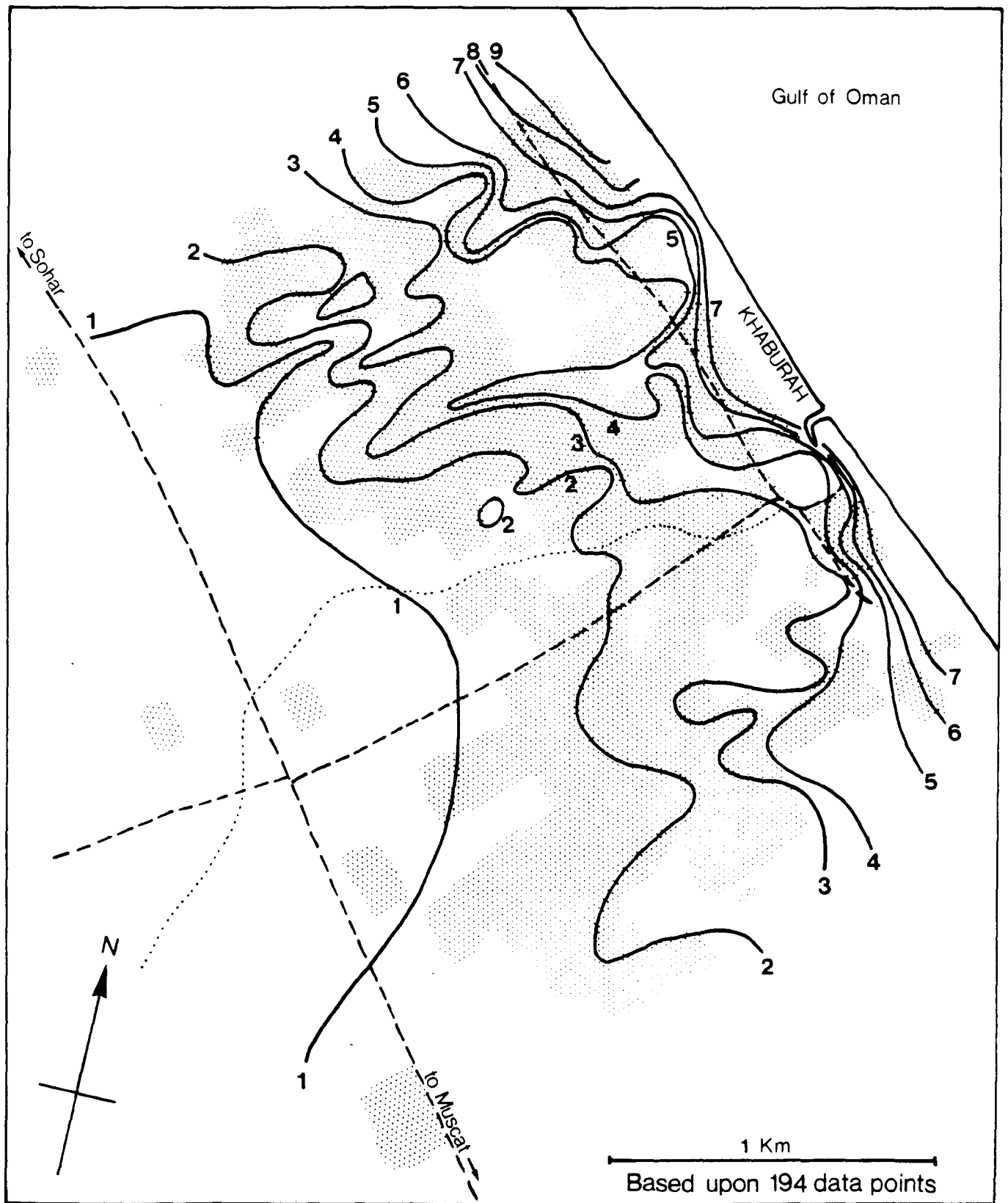
In the Wadi Bani Kharus–Ma Awil area the most variable salinity involved a large landward migration of the 2000 μmhos E.C. contour but in addition there is both a local increase in high salinity intrusion and a widespread encroachment of the medium salinity zone, of between 2500 and 6000 μmhos.

In 1982 commercial water resources studies concluded that an excess groundwater flow to seaward exists in the Al Khaburah area, albeit concentrated some four km north-west of the main town, in the Wadi Jizzi outflow. Nevertheless, many farmers on the inland side of the cultivated strip have experienced an upwelling of brackish water, from approximately 1000 to 3000 μmhos, which has mainly occurred during 1978/79 following widespread pump installation around 1975.

Figure 6·33

E. C. Distribution in the Al Khaburah Area ; After Bowen-Jones, 1978

Field Measurements Undated, but Approximately 1975

Gulf of Oman

KHABURAH

to Sohar

N

to Muscat

1 Km

Based upon 194 data points

Cultivation

Roads

Minor Wadi

E.C. Contours in mmhos

Figure 6·34

E.C. Distribution in the Al Khaburah Area : May/June 1985

Wadi Hawasina
(main channel)
approximately 3Km

Gulf of Oman

KHABURAH

N

1 Km

Based upon 151 data points

Cultivation

Roads

Minor Wadi

E.C. Contour in mmhos

Al Khaburah also illustrates the enhanced contrast between generally deteriorating water quality, and lower salinity even in minor preferred groundwater pathways, irrespective of whether such flow is coincident with buried or surface channels.

Thus, as in the Seeb-Rusayl fan, the response to increased abstraction may be divided into high risk interfluvial areas where prolonged and medium to severe salinisation may occur, and low risk fluvial areas where the groundwater flow may be sufficient to sustain new inland agriculture without (apparently) significant increases in salinity.

Difference in vegetation density between normal and salinated gardens have enabled their distribution to be delineated by multi-spectral satellite image discrimination, as shown in plate 6.9. Apart from small, isolated and newly established gardens in the landward areas which are anomalously indicated as being brackish, almost all of the cultivation is shown to be affected by some degree of salinization. This confirms that the Seeb and Wadi Bani Kharus areas are genuinely typical of the coastal belt and that a consistent pattern of thriving agriculture in major groundwater channels is interspersed between extensive areas of date palms suffering from varying degrees of salinization stress. Although difficult to quantify, the overall area of agriculture severely affected by salinity appears to be comparable to the land area reclaimed by new inland agricultural development.

Apart from the main Batinah plain, coastal environments with much smaller upstream alluvial storage capacity appear to be at particularly high risk of salinization. This is typical of two areas. The first is the narrow coastal zone east of the Seeb Fan where both coastal and inland (wellfield) abstraction has resulted in virtually total salinization (i.e., E.C. greater than 6000 μmhos) of the Azaiba and Rusayl date gardens. The second area is in the recently uplifted alluvial embayments and piedmont colluvium of Musandam (cf. section 4.6). Here the very coarse particle size distribution of the sediments, and steep gradients result in rapid dewatering, shallow hydraulic gradients and consequently a shallow and very unstable saline

interface. Typical results of overpumping are shown in Figures 6.35 and 6.36. In the eastern and drowned northern areas in or adjacent to the Musandam massif, the coastal salinity distributions, though not as severely affected, have nevertheless suffered deterioration similar to that of the Batinah in general, as shown in Figures 6.37, 6.38 and 6.39. In the absence of any large perennial groundwater flow to these coastal sites, it is doubtful whether any agricultural rehabilitation is possible.

Figure 6·35   Coastal Salinity at Bukha and Al Jadi, Musandam

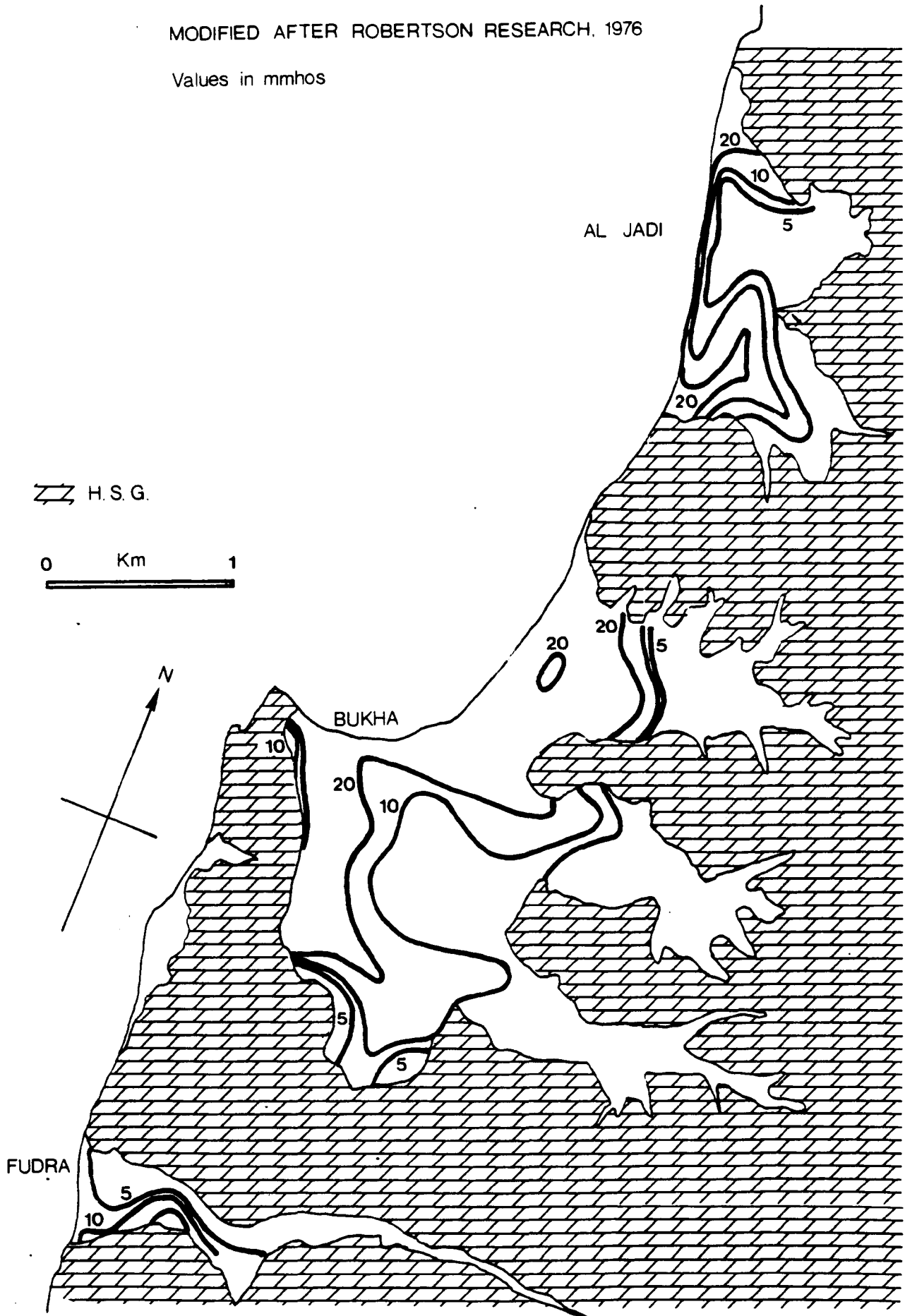MODIFIED AFTER ROBERTSON RESEARCH, 1976

Values in mmhos

Figure 6·36   COASTAL SALINITY AS E.C.(mmhos) IN NORTH-
EASTERN U.A.E.

Modified after Jones and Marrei, 1982

Cultivation

R us al Jibal etc.
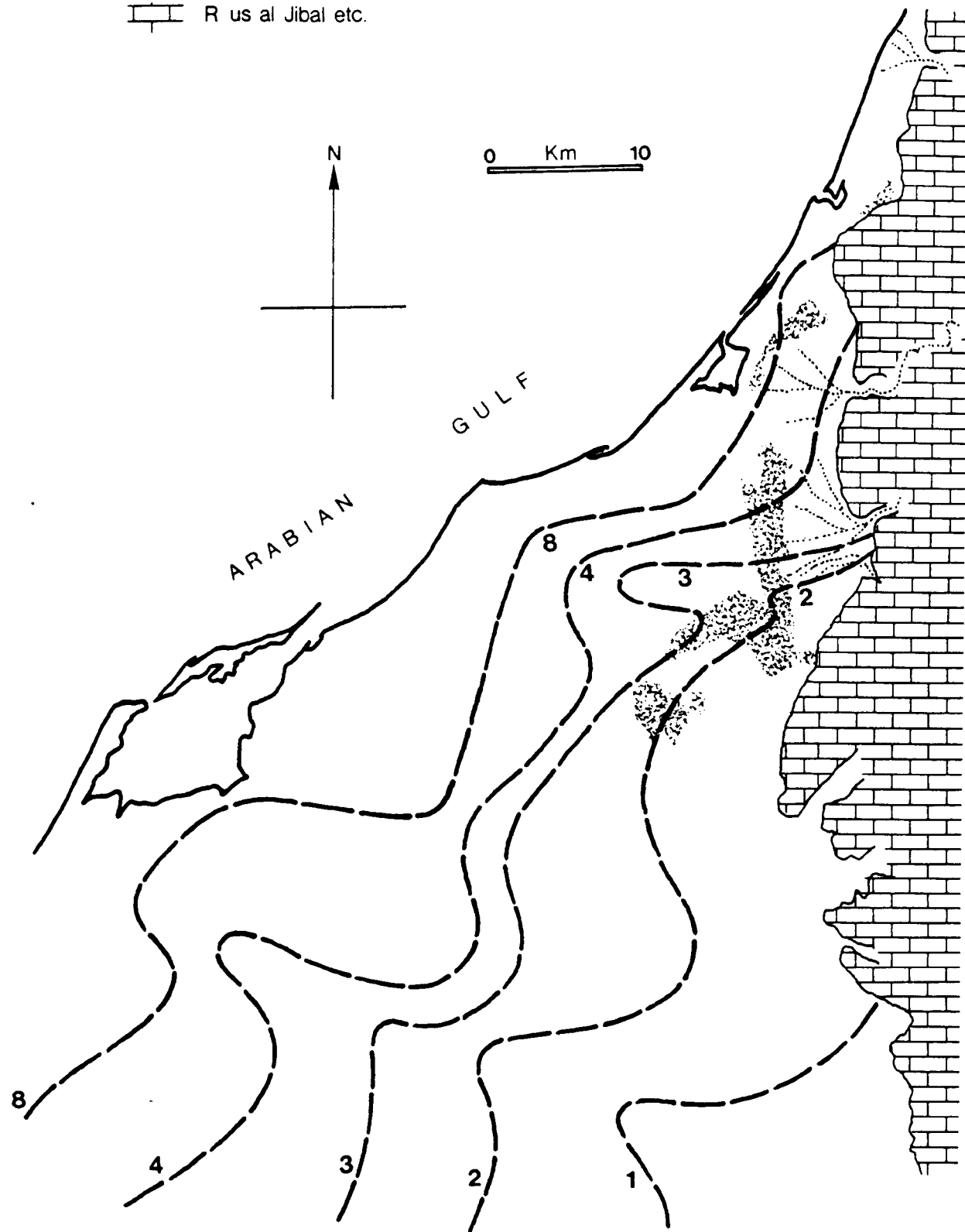
Figure 6·37 Coastal Salinity at Khasab, Musandam

Values in mmhos

Strait of Hormuz

N

7·5

5

4

3

1·5   2

0   Km   2

▨ Cultivation   ⊥ Musandam Limestone
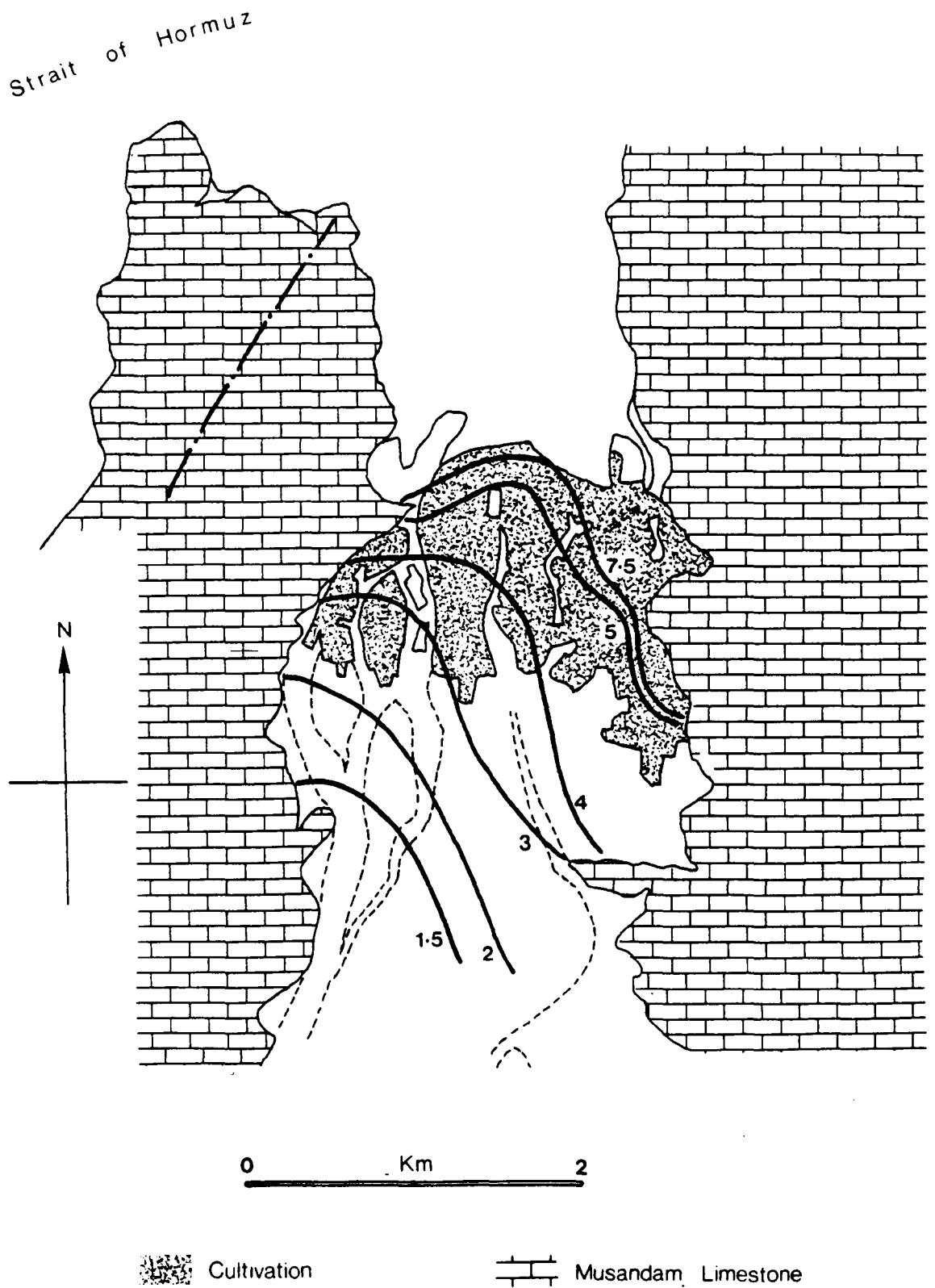
Figure 6·38   Coastal Salinity at Lima, Musandam

Values in mmhos

Gulf
of
Oman

"Bih" Dolomite   Cultivation

N

LOCATION MAP

KHASAB

BUKHA

LIMA
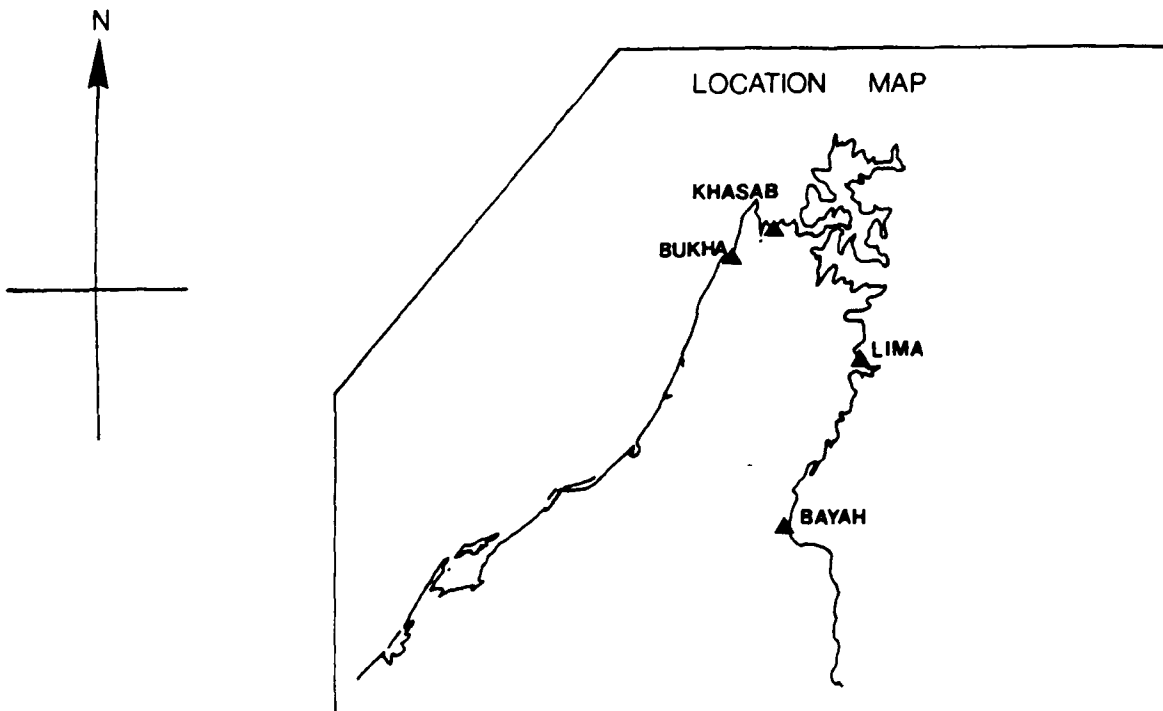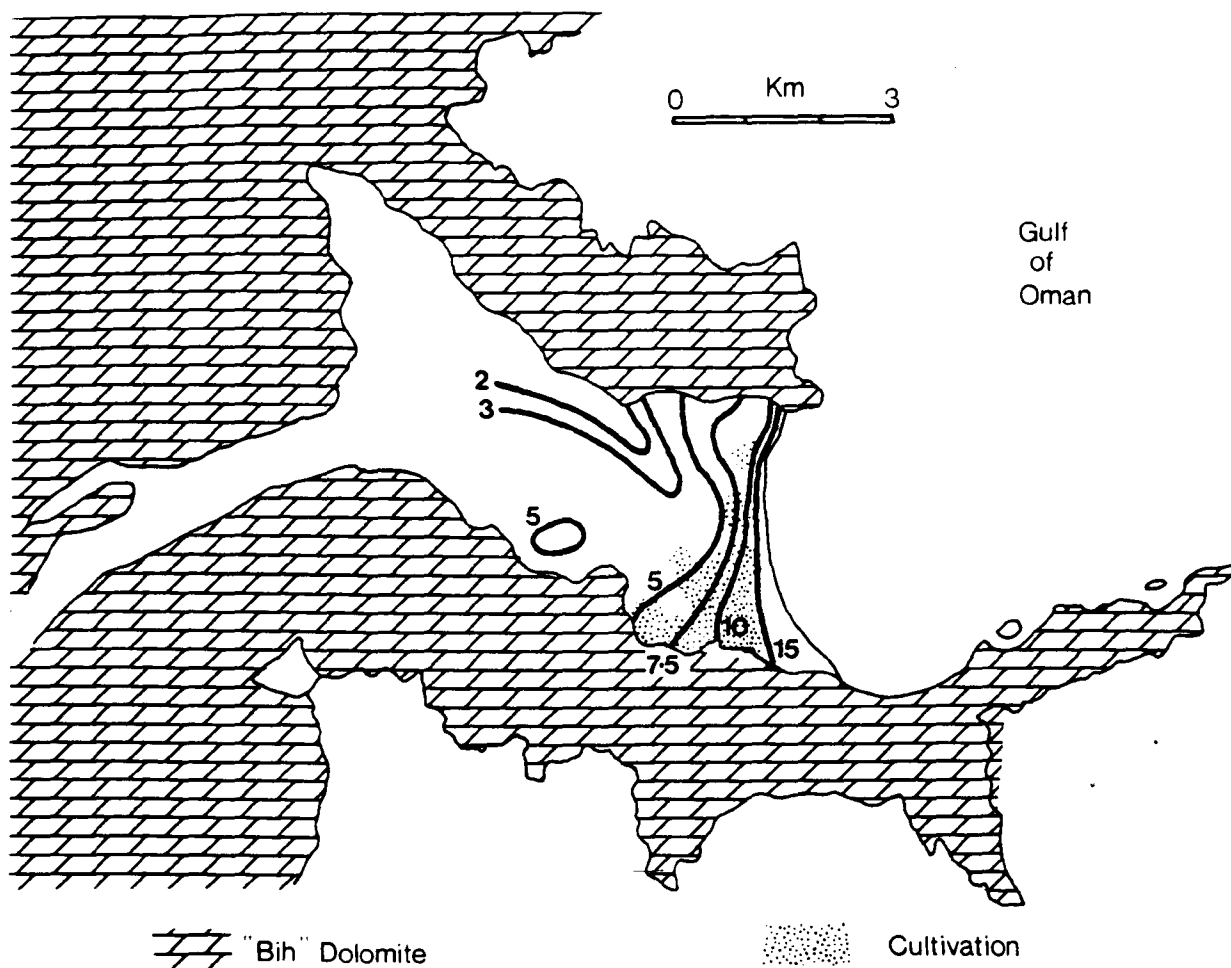
BAYAH

Figure 6·39

BAYAH & DIBBA SALINITY DISTRIBUTION

GULF OF OMAN

N

28
18
62
1
1
64
1
2
3
4
5
2
3
2
5
BAYAH

E.C. contours in millimhos
main groundwater flows arrowed

Spot samples :Jan 1980
▽   562 μmhos
●   1500 μmhos
■   5000μmhos

1975 Survey
modified after Gentle

1967 Survey data
after Halcrow and partners

0   Km   1

3   DIBBA
3 4
4
2
1

▽WAMM
●
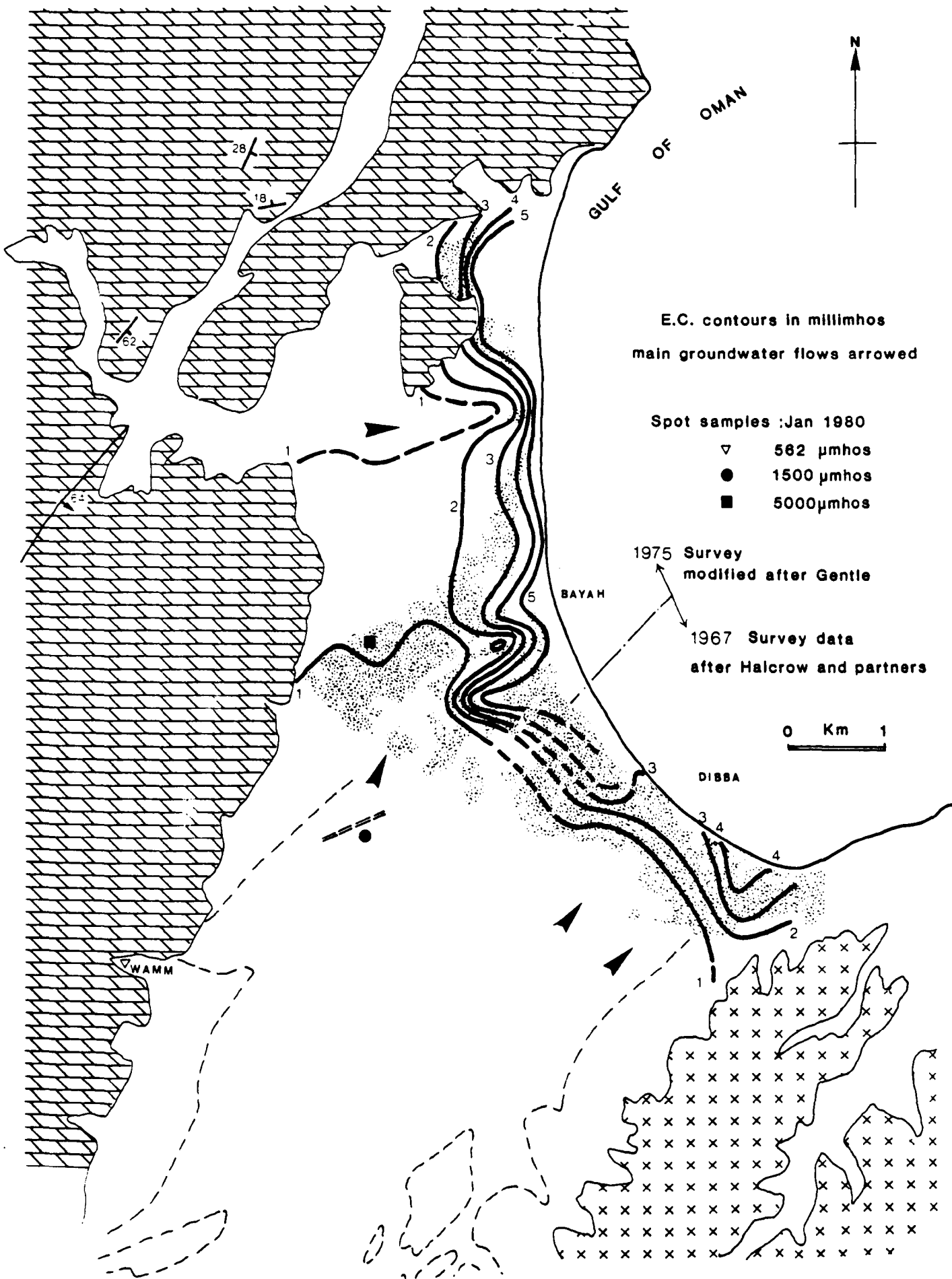
CHAPTER 7

CONCLUDING DISCUSSION

Hydrogeology in Northern Oman is fundamentally different from
almost all the other neighbouring "Gulf" or other Middle Eastern areas.
Elsewhere, the main aquifers tend to be shallow dipping carbonate or
clastic sedimentary aquifers with large storage volumes, very long
residence times and, in recent decades, a gross excess of abstraction
over aquifer recharge, (e.g. Pike, 1983). On the other hand the
previous chapters have shown that the salient features of the Oman
environment are somewhat complex in terms of aquifer types, groundwater
processes and water resources exploitation, and even exhibit many unique
hydrochemical features. In the latter respect large scale hydrochemical
processes in the mantle sequence are only operative because of the arid
conditions, and hence the high rock/water ratio of the fractured
aquifuge, thereby providing an insight into alteration processes which,
in other environments, would be obscured beneath a weathering zone of
oxidising and less alkaline conditions. Perhaps the most important
conclusions regarding this lithology are firstly that all the processes
which have previously been regarded as largely or entirely hydrothermal,
such as serpentinisation, carbonate and hydroxide precipitation, calcium
and sulphide mobility, ultramafic-basic rock reactions etc., either
occur or have analogous processes at low (ambient) temperatures.
Secondly, the discovery of hydrogen generation as a by-product of
serpentinisation is conclusive proof of abiological gas evolution which
may be of significance at greater depth in other environments.

Novel as some of these hydrochemical processes may be, they are
quantitatively trivial in the context of the overall hydrological
system. Throughout the mountain region rainfall and groundwater
storage, in both carbonate and alluvial aquifers, are the limiting
factors which control irrigation and hence agricultural development.
Although the major limestone massifs have by far the largest formation
volumes, their karstic development is generally immature with the result

330

that the most significant storage lies within the piedmont alluvium as opposed to adjacent hard-rock formations. Multifarious evidence for this conclusion is based upon : chemical and isotopic arguments, recession constants, and not least, subjective observations of an enormous infiltration capacity and flood attenuation in Recent coarser alluvium which characterises the piedmont wadis. It is no coincidence that most of the larger provincial towns (e.g. Rustaq, Awabi, Fanjah, Semail, Izki, Nizwa and Bahla) are situated at or close to nodal points in the piedmont drainage systems where remarkably efficient groundwater interception has long utilised the piedmont storage in such a way that the available resources and water use are in equilibrium. The pressing need to expand agricultural output in line with the general growth in economic development, together with the increasing domestic water demand inevitably raises the question of whether the hydrological equilibrium can be maintained. In the interior piedmont and basins, widespread well drilling, digging and deepening have scarcely affected the problems of episodic drought, and have often increased well yields only at the expense of falaj yields. Along much of the coastal belt a much greater increase of abstraction, both in traditional date gardens and in new modern farming enclosures, has induced the alternative problem of rising salinity with correspondingly reduced yields. It is therefore clear that, at least locally, storage deficits are not replenished with sufficient frequency to avoid a long term loss of "equilibrium". It is thus vitally important that the primary objective of hydrogeology : that of modelling the hydrological system to define the maximum sustainable groundwater yield, is achieved.

Whether meaningful groundwater management is possible in the marginal environment of Northern Oman has yet to be demonstrated. Three serious difficulties hinder this aim. Firstly, since the mountain range lies at the extremities of both the Eastern Mediterranean and Monsoonal systems, all the significant rainfall and runoff consists of "extreme events" whose temporal distribution is uncertain. No matter how long the data base, the question of its representativeness must be considered. Secondly, although the hydrological processes are well known, their quantification (especially the rainfall-runof-infiltration and evaporation) is wholly inadequate with the result that hydrological models are heavily reliant upon comparisons and assumptions from

different environments. Thirdly, even assuming that hydrological models are capable of first order accuracy, do they have the precision needed to be of predictive use? For example, although the Wadi Semail/Seeb fan water balance has been estimated to be in long term equilibrium or excess, certain interfluvial areas at the coast have still suffered severe salinisation effects, i.e.: Especially in vulnerable or high risk areas, the water balance should be of a precision which is seldom realised in practice and which requires a very detailed knowledge of the aquifer parameters.

In considering the first difficulty, evidence of past extreme flood events is widespread and ranges from eye-witness accounts and historic records to "trash-mark" evidence of peak flood stages such as date palm logs or fragments on piedmont outwash terraces - (the latter occasionally occurring at astonishingly high levels), to large scale high energy sedimentation or cliff abrasion. This evidence encompasses a wide range of time scales, i.e. from recent decades to at least the late Pleistocene, and has led many researchers to speculate upon possible palaeoclimatic deterioration at least throughout the Holocene epoch, and perhaps continuing to the present. Indeed, a persistent problem of climatic analysis in Oman is the lack of criteria for differentiating between recorded year to year variation, and long term climatic trends (if any). For example, although inter-regional rainfall correlations cannot be demonstrated, regional indices such as the Nile discharge 5000 year "record") and sub-Saharan rainfall (50 year record; Dennett, 1985) show distinct trends spanning millennia and decades respectively, which cast uncertainty over whether the existing rainfall record can ultimately be regarded as "normal".

Unfortunately the regional palaeoclimatic régimes are only poorly understood, being the sum of unsystematic, vague, inferrential and sometimes contradictory conclusions derived from many different disciplines (cf. Brice, 1978; Bintliff and Van Zeist, 1982). Given the sparsity of data it is tempting to correlate features over large distances, e.g. the "unit 4" sediments of Wadi Bahla (and aeolian conditions, cf. section 6.2) appear to correspond to the products of late Holocene desiccation in adjacent regions, such as the cessation of

fluvial sedimentation in the Karkheh basin of Iran (Kirkby, 1977).
However an entirely opposite conclusion may equally be drawn by
comparison with Iranian Lake pollen "spectra" which imply increasing
moisture between 10,000 b.p. and 5500 b.p. (Van Zeist and Bottema,
1977), and sub-pluvial sedimentation in the Rub'al Khali between 9000
and 6000 b.p. (McClure, 1978, and Oates, 1982). Moreover, further
difficulties of interpretation arise firstly from the ambiguity between
climatic and human influences upon sedimentation (e.g. pastoral
overgrazing leading to higher rates of fluvial erosion comparable to
higher rainfall effects) and secondly, more northerly mean seasonal
migration of the ITCZ throughout the early Holocene may have effectively
separated Oman from the Mediterranean climatic province, from which most
of the available palaeoclimatic evidence is derived.

Thus only the most general climatic history of the Gulf area is
discernible. The most protracted climatic deviation occurred during the
Würm glacial maximum in which mean annual seawater temperature was
2 to 3° cooler than at present, whilst air temperatures were probably
some 6 to 7°C lower (Butzer, 1978). Other factors being equal, the
effect of depressed air temperature would be expected to result in
higher rainfall, but a concomitant cold continental high pressure centre
may have effectively blocked the Eastern Mediterranean airflow until
later in the Pleistocene, which would account for the lack of
sedimentary evidence of wet conditions during most of the Würm stage
(cf. Whitney, 1982).

The close of the Pleistocene, Pre-Boreal and Boreal epochs are
represented in south-western Arabia by lake and spring deposits and
fluvially re-deposited aeolian silt indicative of wet periods from about
18000 to 15000 b.p. and from 9000 to 6000 b.p.[1] with an intervening
period of apparently intense aridity (Bintliff, 1982). The climate then
appears to have further ameliorated with the onset of the sub-Boreal
period, between 5500 and 2750 b.p., and may have approximated present
day conditions. At this time, generally cooler Eastern Mediterranean
sea temperatures (Magarity and Kaufman, 1973) and a humid continental

---

[1] or 7000 to 4000 b.p. depending upon equivocal dating criteria.

phase led to high woodland expansion in an arc from Turkey through
Syria, Iran (Bintliff, 1982), and by extension probably to Northern
Oman. Simultaneous agricultural expansion in the near East also closely
coincided with the earliest archaeological remains of Wadi Bahla. About
4000 b.p., a general broadening of the climatic zones produced both a
northward shift of the winter rainfall and a southward retreat of the
ITCZ, with a corresponding decline in monsoon influence (e.g. McGhee,
1979; probably correlating with rotation of the Wahiba dune lineations,
discussed in section 2.2). It is therefore arguable that a
corresponding decline in agriculture throughout much of the region from
Oman to the Eastern Mediterranean may have been due to drier conditions,
but agricultural practice may have been equally important in determining
sedimentation. There is no sedimentary evidence for a significant
change of climate during the second millenium B.C.

An essentially modern climate was established by the Sub-Atlantic
period (2750 b.p. to the present). Marine core studies imply a dry
climate with no unusual extension of the monsoons in the Gulf of Aden
(Olausson and Olsson, 1979), and "moist" conditions with occasional
droughts in the Arabian Gulf (Diester-Haass, 1973), whilst on land the
sedimentary record throughout the entire Gulf region is consistently
represented by fluvial gravels dated from about 400 A.D., i.e. the
"Younger Fill" of Vita-Finzi, 1978; Brooks and Dennell, 1977; Brookes,
1982; and Bescançon, 1980. So far, the best documented climatic
anomalies of the Sub-Atlantic period in Europe (e.g. the "Early Medieval
Warm Era" of 900 to 1200 A.D., and the "Little Ice Age" of 1550 to 1850
A.D.) appear to have no counterpart in either the sedimentary or
archaeological record from Eastern Arabia. However, this probably
arises more from poor resolution than from apparent climatic stability
i.e. the sedimentary record is insensitive to "normal climatic
variations" and may conceal short and perhaps even medium period trends
of rain and drought. Indeed, the "normal climate" is sufficiently
variable that, throughout the Sub-Atlantic period, historic records of
high flood levels, including extreme events such as the great flood of
636-637 A.D. (Le Strange, 1966), can be adequately explained by synoptic
conditions of unusually long return periods without recourse to the
hypothesis of Recent climatic change. On a shorter time scale of up to

about 250 years, provisional dendroclimatic evidence from Juniper and Acacia sections from sensitive sites in the Jebel Akhdar also failed to indicate any significant variation in the long term rainfall.

As a simple illustration of modelling approaches and limitations, the Nizwa-Mu Aydin joint catchment in the south eastern Jebel Akhdar may be assessed in two ways. Firstly, the normal hydrological method compares the irrigated water application (virtually the only "consumptive use") with measured flood runoff records to assess the excess or deficit in current use. This is heavily dependent upon just a few years' records of unknown typicality. The second method utilises the measured chloride concentration of various balance components on the generally valid assumption that groundwater mixing and extended residence times provide a much better guide to long term average losses by evapotranspiration.

> Method 1 (values in $m^3 \times 10^6$ per year)
> The annual piedmont runoff in Wadi Mu Aydin yields;
> mean = 3.8 , median = 0.5, estimated flow for a 1 year return period is 1.0. The extrapolated total hard-rock catchment runoff yields; mean = 12.0, median = 1.6, estimated flow for a 1 year return period is 3.0. Since the mean annual consumptive use is about 17.8 (Atkins, 1986), the implied water deficit is clearly much too large for even approximate equilibrium to occur, and hence agriculture must be sustained by a substantial loss of groundwater storage, i.e. the corollary to infrequent significant recharge deduced in section 2.5. From the recession characteristics given in Table 6.5, and falaj gaugings (P.A.W.R. unpub. and Gibb, 1976), a conservative estimate of the annual change in groundwater storage is about 24.

Thus groundwater in storage, upon which the whole agricultural system depends, is approximately an order of magnitude greater than the mean or median annual runoff. The latter cannot therefore be taken as a meaningful basis for modelling unless a long record (i.e. of decades) is available, and then only if the recession and storage characteristics of the aquifer system are known.

Method 2. Using the rainfall-altitude relationship derived in Section 2.4, the total input to the system is summed from:

interval   2000 m ($\bar{H}$ = 2150 m), rainfall = 334 mm, area = 113 km^2

interval 1400   2000 m ($\bar{H}$ = 1700), rainfall = 300 mm, area = 168 km^2

interval 600-1400 m ($\bar{H}$ = 1000), rainfall = 226 mm, area = 334 km^2

Assuming no significant direct recharge from low altitude rainfall, the total yield is 164 (m^3 x 10^6), with a mean Cl$^-$ concentration of 8.0 mg.l^{-1}. The Cl$^-$ concentration of mountain and piedmont groundwaters (mean of 52 samples) is 36.2 mg l^{-1}, σ = 10.9. Hence the implied infiltration/recharge = 36.2, with an evaporative loss of 78%. The mean annual consumptive use of the catchment is 17.8, which ideally requires an irrigation total of 44.5 although less effective irrigation, allowing a temporary leachate deficit, could be made to balance the mean recharge on the basis of thorough soil leaching during extreme storm events. This conclusion of a slight overall deficit precisely matches the independently derived findings of Atkins, 1986, in which individual users varied from a normal supply in cases of favourable upstream storage, to severe shortage in other "high risk" areas. In terms of the overall water balance, a chemical mass balance approach may therefore be the most accurate, and is certainly easiest in terms of data collection, especially where pre-existing rainfall records are available. Furthermore by comparing rainfall with infiltrated groundwater, no assumptions (and hence implicit errors) are made about the water distribution processes. The disadvantages lie firstly in the uncertainty of the rainfall-altitude distribution, and secondly since recharge composition is averaged over an extensive period it is impossible to assess the effects of annual or other short-period fluctuations.

Conventional or deterministic hydrology should in theory provide a superior basis for quantifying groundwater processes, but as neither a long data-base, nor adequate process studies have been achieved, accurate modelling to the precision required for groundwater management is not yet feasible.

REFERENCES

Alabaster A.,1982, The Interrelationship between Volcanic and Hydrothermal Processes in the Oman Ophiolite. Ph.D. Thesis, Open University. 408pp

Al Hashimi W.,1976, Significance of Strontium Distribution in some Carbonate rocks of the Carboniferous of Northumberland, England. Jour.Sed.Petrol., 46, (2), 369-376.

Alleman F.and Peters T.,1972, The Ophiolite Radiolarite Belt of the North Oman Mountains. Eglogae Geol.Helv. 65, (3), 657-697

Allerup P.and Madsen H.,1980, Accuracy of Point Precipitation Measurements. Nordic Hydrol. 11, 57-70

American Public Health Association / AAWE / WPCF,1975,Standard Methods for the examination of water and wastewater,14th Edn,1193pp,APHA.

Anon, 1976, Handbook of Weather in the Gulf. General Climatic Data. IMCOS Marine Ltd. 101pp.

Anon, 1975, Guide to the use of Ion-Selective Electrodes IS 550/IS 561, Philips, Eindhoven.

Appelgren B.G.,1976, A Summary of Water Resources and Agricultural Development Reports in the Sultanate of Oman. FAO-UNDP unpub.report.

Arakama H.,(Ed),1969,World Survey of climatology, 8, (Northern and Eastern Asia), Elsevier.

Bailey E.H.,1981, Geological map of the Muscat-Ibra Area, Sultanate of Oman. Jour.Geophys.Res., 86, (B4)

Bailey J.M.,1978, Groundwater Quality and Levels at Rumais Agricultural Research Station. Al Mawared al Tabei'eiah, Nov.1978, 26-28.

Bakiewicz W.,Milne D.M.,and Noori M.,1982, Hydrogeology of the Umm er Radhuma Aquifer, Saudi Arabia, with reference to fossil gradients. Quart.Jour.of Engineering Geol., 15, 105-126.

Barnes I.,La Marche V.C.,and Himmelberg G.,1967, Geochemical Evidence of Presnt Day Serpentinisation. Science, 156, 830-832.

Barnes I.,and O'Neil J.R.,1969, The Relationship Between Fluids in some Fresh Alpine Type Ultramafics and Possible Modern Serpentinisation, Western United States. Geol.Soc.Amer.Bull., 80, 1947-1960.

Barnes I.,Rapp J.R.,O'Neil J.R.,Sheppard R.A.,and Gude A.J.,1972, Metamorphic Assemblages and the Direction of flow in Metamorphic Fluids in Four Instances of Serpentinisation. Contr.Miner. and Petrol., 35, 263-276.

Barnes I.,O'Neal J.R.,and Trescases J.J.,1978, Present Day Serpentinisation in New Caledonia, Oman and Jugoslavia. Geochim.et Cosmchim.Acta, 42, 144-145.

Barnes I.,Presser T.S.,Saines N.,Dickson P.,and Koster Van Groos
    A.F.,1982, Geochemistry of highly basic calcium hydroxide groundwater
    in Jordan. Chem.Geol., 35, 147-154.

Baron G.,Caillere S.,Lagrange R.,and Pobeguin T.,1957, Sur la presance de
    huntite danse une grotte de l'Herault (La Clamouse),
    C.R.Acad.Sci.Paris, 245, 92-94.

Barrett E.C.,1975, The Use of Weather Satelite Data in the Evaluation of
    National Water Resources, with special reference to the Sultanate of
    Oman, 41-46.

Barrett E.C.and Martin D.W.,1981, The use of Satelite Data in Rainfall
    Monitoring. Academic Press, 206-215.

Bartholemew I.D.,1983, The Primary Structures and Fabrics of the Upper
    Mantle and Lower Oceanic Crust from Ophiolite Complexes. Open
    University Ph.D. Thesis. 520pp

Bathurst R.G.G.,1975, Carbonate Sediments and their Diagenesis,
    Developments in Sedimentology, 12, Elsevier. 658pp.

Bear J.1979, Hydrodynamics of Groundwater, McGraw-Hill, 567pp.

Bell M.J.,Clarke E.,and Marshall P.,1911, The Geology of the Dun Mountain
    Subdivision. Nelson., New Zealand Geol.Surv.Bull., 12, 1-71.

Bescancon J.,1980, Stratigraphie et Chronologie du Quarternaire
    Continental du Proche Orient. Lyons Symposium on the Pre-History of
    the Middle East.

Biehler J.,Chevalier C.,and Ricateau R., 1976, Geological Map of the
    Musandam Peninsula, Sultanate of Oman, Directorate General of
    Petroleum and minerals, Elf Oman

Bintliff J.L.,1982, Palaeoclimatic Modelling of Environmental Changes in
    the Eastern Mediterranean Region since the last Glaciation. In
    Bintliff and Van Zeist (Eds), 485-527.

Bintliff J.L.,and Van Zeist W.(Eds),1982, Palaoclimates,
    Palaeoenvironments, and Human Communities in the Eastern Mediterranean
    Region in Later Prehistory. BAR International Series 133.

Birks J.S.,and Letts S.E.,1977, Diqal and Muqaydah: Dying Oases in Arabia.
    Tijdschrift voor Econ.en Soc.Geografie, 68, (3), 145-151.

Birmingham University,Dept. of Ancient History and Archaeology,(in press,
    1986?). The Birmingham Archaeological Expedition to Oman: A Report on
    the First and Second Seasons. Jour.Oman.Studies.
            1) Orchard J.C. and Orchard J.J., Archaeological Survey in Wadi
               Bahla (Jawf) and in Wadi la-Mlah (Sharqiyah).
            2) Stanger G., Water Resources, Sedimentation and Early
               Settlement in Wadi Bahla.
            3) Bartlett A.D.H., and Clark A.J., Geophysical Prospecting in
               Wadi Bahla and Wadi La-Mlah
            4) Smith G.R., Gazeteer, together with some Obsevations on the
               Bisyah Area, Wadi Bahla.

Biswas A.K.,1967, Hydrologic Engineering Prior to 600 B.C., Jour. Hydr. Divn.Proc.Amer.Soc.Civil Eng. 93, (MY5), 115-135.

Bleasdale A., and Chan Y.K.,1972, Orographic Influences on the Distribution of Precipitation., cf WHO 1972, 322-323.

Bogli A.,1980, Karst Hydrology and Physical Speliology, Springer-Verlag, 284pp.

Booth B.,1977, The Making of Iran, Geographical Magazine, 243-250.

Bottinga Y.,1969, Calculated Fractionation Factors for Carbon and Hydrogen Isotope Exchange in the system calcite-carbon dioxide-graphite-methane -hydrogen-water vapour. Geochim.et Cosmochim.Acta, 33, 49-64.

Bowen-Jones H.(Ed),1978, University of Durham Research and Development Surveys in Northern Oman. Final Report, Vol 2, Water.

Bowen N.L., and Tuttle O.F.,1949, The System $MgO-SiO_2-H_2O$, Bull.Geol. Soc.Amer., 60, 439-.

Brice W.C.(Ed),1978, The Environmental History of the Near and Middle East Since the Last Ice Age. Academic Press, London, 384pp.

Bridge J.,1924, Ebb and Flow Springs in the Ozarks. School of Mines and Metallurgy, Rolla, 17-26.

British Standards Institution :BS 3680 (1964-1980), Measurement of Liquid Flow in Open Channels.
    Pt 3A Velocity Area Methods
    Pt 3B Guide for the Operation and Establishment of a Gauging Station
    Pt 4A Thin-plate Weirs
    Pt 4B Rectangular Broad Crested Weirs
    Pt 5 Slope Area Methods of Estimation
    Pt 8 Current Meters

Brooks I.A.,and Dennell R.W.,1977, Spatial and Temporal Relations between Geomorphic Elements and Human Occupation in part of Central West Iran. In 10th INQUA Congress, Birmingham.

Brooks I.A.,1982, Geomorphologic Evidence for Climatic Change in Iran during the last 20,000 years. In Bintliff and Van Zeist (Eds), 191-228.

Brown M.A.,1982, Chromite Deposits and their Ultramafic host rocks in the Oman Ophiolite. Open University PhD. thesis, 264pp

Browning P.,1982, The Petrology,Geochemistry and Structure of the Plutonic Rocks of the Oman Ophiolite. Open University PhD Thesis. 404pp

Bruce J.P.,and Clark R.H.,1966, Introduction to Hydrometeorology. Pergamon 319pp

Bryson R.A.,and Hare F.K.,(Eds),1974, World Survey of Climatology, 11, (North America). Elsevier, 420pp.

Burdon D.J.and Papakis N.,1963, Handbook of Karst Hydrogeology with
    special reference to the carbonate aquifers of the Mediterranean
    region. Institute for Geology and Subsurface Research. United Nations
    Special Fund, Athens, Greece. 276pp

Burdon D.J.,1972, Technical Notes on Water Resourses of the Sultanate of
    Oman, FAO Preparatory Assistance Mission, Dec 1972.

Burdon D.J.,1973, Current Problems and Prospects for Agricultural
    Development in the Sultanate of Oman. 6(Water resources) FAO/UNDP
    unpublished report.

Butzer R.W.,1978, The Late Prehistoric Environmental History of the Near
    East. In Brice (Ed) 1978, 5-12.

Carney J.N.,and Welland M.J.P.,1974, Geology and Mineral Resources of the
    Oman Mountains. Inst.Geol.Sciences, London, (Report No 27,
    unpublished)

Carpenter A.B.,1961, Mineral Assemblage Magnesium Calcite—Aragonite—
    Huntite at Crestmore, California. Geol.Soc.Amer.Meet.Abstr. 146

Carpenter A.B., in Schmidtt H.H.(Ed),1962, Equelibrium Diagrams for
    Minerals, Cambridge Mass. The Geological Club of Harvard. 26.

Chamberlain J.A.,McCleod C.R.,Trail R.J.,and Lachana G.R.,1965, Native
    Metals in the Muskox Intrusion. Canad.Jour.Earth Science. 2, 188-215

Chamberlain J.A.,1966, Heazlewoodite and Awaruite in Serpentinites of the
    Eastern township, Quebec. Canad.Miner. 8, 519-522

Chandler T.S.,and Gregory S.,1976, Climate of the British Isles, Longman,
    390pp.

Chernosky J.V.,1973, The Stability of Chrysotile, $Mg_3Si_2O_5(OH)_4$,
    and the free energy of formation of Talc, $Mg_3Si_4(OH)_4$. Geol.Soc.
    Amer.Abstr. (1973 meeting).

Coleman R.G.,1967, Low Temperature Reaction Zones and Alpine Ultramafic
    Rocks of California, Oregon and Washington. U.S.G.S. Bull. 1247, 49.

Coleman R.G.,1971, Petrologic and Geophysical Nature of Serpentinites.
    Bull.Geol.Soc.Amer. 82, 897-918.

Coleman R.G.,Huston C.C.,El-Boushi I.M.,and Bailey E.H.,1979, Occurrence
    of Cu-Bearing Massive Sulphides in the Semail Ophiolite, Sultanate of
    Oman. Unpublished report. (cf.I.A.G.Bull. 2, 179-192, Al Shanti (Ed),
    1979)

Coleman R.G.,1981, Tectonic Setting for Ophiolite Obduction in Oman. Jour.
    Geophys.Res. 86, 2497-2508.

Collins W.D.,1925, Temperatures of water available for industrial use in
    the United States. U.S.G.S. Water Supply Paper.520-F. Washington D.C.
    97-104

Compagnie General de Geophysique,1975, Interim Report. Geophysical
    Investigations of the Manah Area - Unpublished (they were never paid!)

Cook J.M.,and Miles D.L.,1980, Methods for the Chemical Analysis of
    Groundwater. Inst.Geol.Sciences report 80/5, H.M.S.O.

Coveney R.M.,1972, Hydrogen and Serpentinite   Their role in the
    localisation of gold ores at the Oriental mine, Alleghany, Calif.
    A.I.M.E. Meet., San Francisco.

Dabitzias S.G.,1980, Petrology and Genesis of the Vavdos Cryptocrystaline
    Magnesite Deposits, Chalkidiki Peninsula, Northern Greece. Econ. Geol.
    75, 1138-1151.

Damodaran K.T.,and Somasekar B.,1975, Huntite-Magnesite from the altered
    Serpentinites of (the) Nuggihalli schist belt, Karnataka State. In
    Naganna C.(Ed), Studies in Pre-Cambrians, Bangalore Univ., 187-196.

Dansgaard W.,1964, Stable Isotopes in Precipitation, Tellus, 16, 436-468.

Dennett M.,1985, "In Press". Jour.of Climatology.

Denton J.M.,1969, Breeding of the Desert Locust over the southern Arabian
    Peninsula following a cyclone during May 1959. Anti-Locust research
    centre, Occasional report 14/69.

De Quervain F.,1945, Awaruit und Pentlandit im Serpentin von Poschiavo.
    Schweiz.Miner.Pett.Mitt. 25, 305-326

De Quervain F.,1963, Die Erzmineralien des Serpentins von Selva-Quadrado.
    Schweiz.Miner.Pett.Mitt. 43, 295

De Ridder, 1971, Technical Report 4, AGL:SF/IRA 12, U.N.D.P./F.A.O. Rome

Deutsch E.R.,Rao K.V.,Laurent R.,and Seguin M.K.,1977, New Evidence and
    possible origin of native iron in ophiolites of Eastern Canada. Nature
    269, 684-685.

Dewey J.F.,Pitman W.C.,Ryan W.B.F.,and Bonin,1973, Plate Tectonics and the
    Evolution of the Alpine System. Geol.Soc.Amer.Bull., 84, 3137-3180.

Diester-Haass L.,1973, Holocene Climate in the <Arabian> Persian Gulf as
    deduced from grain size and Pteropod distribution. Marine Geol. 14,
    207-223

Dodge E.D.,1985, Ibri M.o.D.borehole 1: Report on lithology and micro-
    palaeontology from 500 to 802m and the possibility of gamma log
    correlation with boreholes in the Salalah area. P.A.W.R. unpublished
    report. 8pp

Dostal W.,1972, The Shihuh of Northern Oman : A contribution to cultural
    ecology. Geog.Jour. 138, (1), 1-7

Dreiss S.J.,1984, Effects of Lithology on Solution Development in
    Carbonate Aquifers. Jour.Hydrol. 70, 295-308

Durfor C.N.,and Becker E.,1964, Public Water Supplies of the 100 largest
    Cities in the U.S.A., U.S.G.S. Water Supply Paper 1812.

Durum W.H.,and Hafferty J.,1961, Occurrence of minor elements in water.
    U.S.G.S. Circular 445.

Early J.W.,1958, On Chlorine in Serpentinised Dunite. Amer. Miner. 43,
    148-156

Eaton F.M.,1935, Boron in soils and irrigation waters and its effect on
    plants, with particular reference to the San Joaquin Valley of
    California. U.S.Dept.of Agric.Tech.Bull. 448.

Eckhardt F.J.,1956, Rontgenographische Untersuchungen am Schweizerit. Nues
    Jahrb.Mineral.Montash, 32-43

Eckstrand D.R.,1975, The Dumont Serpentinite: A Model for Control of
    Nickeliferous Opaque Mineral Assemblages by Alteration Reactions in
    Ultramafic Rocks. Econ.Geol. 70, 183-201

Edmunds W.M.,1975, Water Quality Sampling and Field Chemical Measurements
    for Overseas Hydrogeological Surveys. I.G.S. Hydrogeological Dept.
    report No WD/ST/75/14

English P.W.,1968, The Origin and Spread of Qanats in the Old World. Proc.
    Amer.Phil.Soc. 112, 170-181

Evans R.B.,and Shelton A.W.,1971, The Establishment of a gravity base
    station in Seeb International Airport, Connected to the International
    Gravity Standardisation Net,1971. IGSN71.

Fallon L.E.,1978, Sohar-Saham Agricultural Development Project. Al Mawared
    Al Tabei'eiah. April 1978, 10-14

F.A.O.,1981, The Water Resources of Qatar and their development. 1

Faust G.T.,1953, Huntite $Mg_3Ca(CO_3)_4$, a new mineral. Amer.Miner.,
    38, 4-24

Findlater J.,1977, A Numerical Index to monitor the Afro-Asian Monsoon
    During the Northern Summers. Meteor.Mag. 106, 170-180

Fleet A.J.,and Robertson A.H.F.,1980, Oceanic-Ridge Metalliferous and
    Pelagic Sediments of the Semail Nappe, Oman. Jour.Geol.Soc. 137, (4),
403-422

Fraser J.,1824, Notes made in the course of a voyage from Bombay to
    Bushire <Busheyr> in the Persian <Arabian> Gulf. Geol.Soc.Lond.
    Trans. 1, (2), 409-412

Friedman I.,and O'Neil J.R.,1977, Compilation of Stable Isotope
    Fractionation Factors of Geochemical Interest. Geol.Surv.
    Professional Paper 440-KK, 1-12

Frind E.O.,1982, Seawater Intrusion in Continuous Coastal Aquifer-Aquitard
    Systems. Advances in water research, 5, (2), 89-97

Gadgil S.,Joseph P.V.,and Joshi N.V.,1984, Ocean-atmosphere coupling over monsoon regions. Nature, 312, 141-143

Garrels R.M.,and Chryst C.L.,1965, Solutions, Minerals and Equelibria. Freeman Cooper & Co. 450pp

Gat R.J.,1980, The Isotopes of Hydrogen and Oxygen in Precipitation. In Handbook of Environmental Isotope Geochemistry. Fritz P.,and Fontes J Ch.(Eds). (1) The Terrestrial Environment. Elsevier. 20-47

Gealey W.K.,1977, Ophiolite Obduction and Geologic Evolution of the Oman Mountains and adjacent areas. Geol.Soc.Amer.Bull. 88, 1183-1191

Gentilli J.,(Ed), 1971, World Survey of Climatology, 13, (Australia), Elsevier

Gentle R.I.,1976, Final Report on the Groundwater Resources of Bayah, Bukha, Al Jadi, Fudrah and Ghrumdah, Musandam. Robertson Research International. Unpublished Report for Taylor Woodrow Towell Ltd.

Gemmell B.A.P.,1979, Hydrometeorological Field Instrument Installation, flood observations, General data collection and local staff in-service training. U.N.D.P. Project document 177/001 (unpub.)

Ghyben B.W.,1888, Nota in verband met de voorgenoman putboring nabij Amsterdam. Tidsch.Koninklijk Inst.Ingenieurs.

Gibb Sir A. & Ptnrs.,1969, Abu Dhabi Water Resourses Survey, Interim report (unpub.)

Gibb Sir A. & Ptnrs.,1970, Abu Dhabi Water Resources Survey, Final report (unpub)

Gibb Sir A. & Ptnrs.,1976, Water Resources Survey of Northern Oman (unpub)
    1, Main Report
    2, Appendix A,Rainfall and Meteorology
    3, Appendix B,Surface Water Flow
    4, Appendix C,Geology and Hydrogeology
    5, Appendix D,Survey of Water Use in Villages
    6, Appendix E,Water Chemistry and Isotope Studies

Glennie K.W.,1970, Desert Sedimentary Environments. Developments in Sedimentology, 14, Elsevier 222pp

Glennie K.W.,Pilaar W.F.H.,Boeuf M.G.A.,Reinhardt B.M.,and Hughes Clarke M.H.,1970, Notes to Accompany the Geological Map of the Oman Mountains. Group Research Report RKGR.0008.70

Glennie K.W.,Boeuf M.G.A.,Hughes Clarke M.W.,Moody-Stuart M.,Pilaar and W.F.H.,Reinhardt B.M.,1974, Geology of the Oman Mountains. Verhandelingen van het Koninklijk Nederlands geologisch mijnbouwkundig Genootschap.two vols.

Gole C.V.,Kulkarni G.A.,and Khatavkar G.D.,1972, Study of Orographic Effects on Optimum Number of Raingauges. W.M.O. 1972, 421-431

Goldschmidt V.M.,1954, Geochemistry, Clarendon Press, Oxford. 730pp

Golightly J.P.,1979, Nickeliferous Laterites; A General Description.
   In International Laterite Symposium, New Orleans. Evans D.J.I.,
   Shoemaker R.S.,and Veltman H.(Eds.), 3-23

Golightly J.P.,1981, Nickeliferous Laterite Deposits. Econ.Geol. 75th
   Anniv. vol.,710-735

Graham G.M.,1980, Structure and Sedimentology of the Hawasina Window, Oman
   Mountains. Open University PhD Thesis. 458pp

Grant K.,1982, The July Lower Troposphere over the Middle East. Meteor.
   Mag. 111, 179-182

Griffiths D.H.,and King R.F.,1965, Applied Geophysics for Engineers and
   Geologists. Pergamon 223pp

Griffiths J.F.,(Ed.),1972, World Survey of Climatology, Africa. Elsevier
   10

Groundwater Development Consultants,1980, Umm er Radhuma study. 3,
   Groundwater Resources. Report to the Ministry of Agric. and Water,
   Saudi Arabia. 348pp

Haartz J.C.,Eller P.M.,and Hornung R.W.,1979, Critical Parameters in the
   Barium Perchlorate / Thorin titration of sulphate. Anal.Chem. 51,
   2293-2295

Hammer S.,1939, Terrain Corrections for Gravimeter Stations. Geophysics
   4, 184-194.

Harzberg B.,1901, Die Wasserversorgung einiger Nordseebader. Jour.
   Gasbelenchtung und Wasserersorgung. 44, 815-819, 842-844, Munich

Halcrow Sir W. & Ptners.,1967,Trucial States Council Water Resources
   Survey, Draft Report. 171pp

Halcrow Sir W.& Ptners.,1969, Report on Water Resources of the Trucial
   States.

Hawkins T.R.W.,Hindle D.and Strugnell R,1981, Outlines of the Stratigraphy
   and Structural Framework of Southern Dhofar, Sultanate of Oman.
   Geologie en Mijnbouw, 16, 247-256

Hellwig D.H.R.,1973,Evaporation of Water from Sand. Jour.of Hydrol. 2,3/4
   1) Experimental Set-up and Climatic Influences, 93-108
   2) Diurnal Variations, 109-119
   3) The Loss of Water into the Atmosphere from a Sandy River Bed under
      Arid Climatic Conditions, 305-316
   4) The Influence of the Depth to Water Table and the Particle Size
      Distribution of the Sand, 317-327

Hem J.D.,1970, Study and Interpretation of the Chemical Characteristics of
   Natural Water, 2nd Edn., U.S.G.S. Water Supply Paper 1473

Henriksen A.,and Bergmann-Paulson I.M.,1974, An automatic method for
   determining sulphate in natural soft water and precipitation. Vatten
   30, 187-192

Honnorez J.,and Kirst P.,1975, Petrology of Rodingites from the Equatorial Mid-Atlantic Fracture Zones and their Geotectonic Significance. Contrib.Mineral.Petrol. 49, 233-257

Horn P.M.,Nielsen J.B.,Ali Manthri Issa,and Salaam S.,1977, Climate of the Jebal Akhdar (Saiq), F.A.O.Field Document No 2, OMA 77/001

Horn P.M.,1977a, Rainfall in Oman 1974-1976, F.A.O. Field Document No 3, Water Resources OMA 73/009

Horn P.M.,1977b, Climate of the Batinah 1973-1977, F.A.O. Field Document No 4, Water Resources OMA 77/001

Horn P.M.,1978a, Short Period Rainfall Intensities in Oman. Appendix A to F.A.O. Field Document No 11, OMA 77/001

Horn P.M.,1978b, Rainfall in Oman 1977, F.A.O. Field Document No 6, OMA 77/001

Hostetler P.B.,Coleman R.G.,Mumpton F.A.,and Evans B.W.,1966, Brucite in Alpine Serpentinites. Amer.Miner. 51, 75-98

Huang ,1965, Geological Review (Peking), 23,7

Hudson R.G.S.,Brown R.V.,and Chatton M.,1954, The Structure and Stratigraphy of the Jebel Qamar area,Oman. Geol.Soc.Lond.Proc. 1513

Hudson R.G.S., McGugan A.,and Morton D.M.,1954, The Structure of the Jebel Hagab area,Trucial Oman. Quart.Jour.Geol.Soc. 110, 121-152

Hudson R.G.S.,1960, The Permian and Trias of the Oman Peninsula, Arabia Geol. Mag. 97, 299-308

Ismail I.,1982/3, Annual Reports, Meteorological Dept.,Lefkosa.

Jones C.R.C.,1978, The Water Resources of the Wadi Lansab Catchment, Sultanate of Oman. M.Sc. Dissertation, University College London.

Jones G.P.,and Marrei S.H.,1982, Groundwater Resources in the United Arab Emirates. Middle East Water and Sewage. Jan/Feb 1982,41-51

Johannes W.,1968, Experimental Investigation of the Reaction :Forsterite + H_2O > Serpentine + Brucite. Contrib. Miner.Petrol. 19, 309-315

Kassler P.,1973, The Structure and Geomorphic Evaluation of the Persian Gulf. In "The Persian Gulf: Holocene Carbonate Sedimentation and Diagenesis in a Shallow Epicontinental Sea". Purser B.H.(Ed), Springer-Verlag, 11-32

Katsnelson J.,1963, Comparative Measurements of Evaporation at Lod Airport Bull.Res.Counc.of Israel, 11G, 137-141

Kawabata Y.,1960, On the sufficient number of rainfall stations for small basins. Geophys.Mag.Tokyo 29, 509-512

345

Kaye G.W.C., and Laby T.H.,1973, Tables of Physical and Chemical Constants (14th Edn.). Longman

Kelly B.I.,1985, Evaluating the Potential for Ground-Water Recharge in an Arid Climate: Sultanate of Oman. Bull.Assoc.Eng.Geologists. 22, (3), 281-285

Khurshid Alam F.C.,1972, Distribution of Precipitation in Mountainous Areas of West Pakistan. 290-306 cf. W.M.O. 1972

Kinsman D.J.J.,1967, Huntite from a Carbonate-Evaporite Environment. Amer. Miner. 52, 1332-1340

Kinsman D.J.J.,1969, Interpretation of Sr^{2+} concentrations in carbonate minerals and rocks. Jour.Sed.Petrol. 39, (2), 486-508

Kirkby M.J.,1977, Land and Water Resources of the Deh Luran and Khusistan Plains, Appendix 1. In "Studies in the Archaeological History of the Deh Luran Plain", Hole F.,(Ed). Memoirs Mus.Anthrop. 9, University of Michigan.

Kohls D.W.,and Rodda J.L.,1967, Iowaite, a new hydrous magnesium hydroxide -ferric oxychloride from the Pre-Cambrian of Iowa. Amer.Miner. 52, 1261-1271

Konoplayantsev A.A.,Kovalevsky V.S.,and Semenov S.M.,1963, Natural Regime of Underground Waters. Gosgeoltekhizdat, Moscow

Konteatis C.A.C.,1978, Wadi Semail Aquifer Studies, 3 vols

Krauskopf K.B.,1956, Dissolution and Precipitation of Silica at Low Temperatures. Geochim.et Cosmochim.Acta, 10, 1-26

Kuroda P.K.,and Sandell E.B.,1953, Chlorine in Igneous Rocks. Bull.Geol. Soc.Amer. 64,879-896

Lahann R.W.,and Siebert R.M.,1983, A kinetic model for distribution coefficients and application to Mg-calcites. Geochim.et Cosmochim. Acta. 46, (11), 2229-2238

Langmuir D.,1984, in UNESCO (Ed), Guide to the hydrology of Carbonate Rocks. Studies and reports in Hydrology 41, 69-130

Lauder W.R.,1965, Jour.Geol.Geophysics, 8, 475-504

Lees G.M.,1928a, The Geology and Tectonics of Oman. Quart.Jour.Geol.Soc. 84, (4), 585-670

Lees G.M.,1928b, The Physical Geography of South-Eastern Arabia. Geog. Jour. 71, (5), 441-670

Lessman H.,and Stanescue S.,1972, Some rainfall features in mountainous areas of Columbia and their impact on network design. cf W.M.O. 1972, (1),219-228

LeStrange G,1966, Lands of the Eastern Caliphate. Cass & Co. London

Letts S.E., and Birks J.S.,1973, Attitudes to Falaj Water and their
    Importance. Durham-Oman Research Project, Field Statement No 2.

Letts S.E.,1979, Groundwater and its Present Day Use in Part of Northern
    Oman. Oxford University D.Phil. Thesis. (2 vols)

Levin M.,Gat J.R.,and Issar A.,1978, Precipitation,flood and groundwaters
    of the Negev Highlands: An isotopic study of desert hydrology.
    I.A.E.A. 1-20

Linsley R.K.,Kohler M.A.,and Paulhus J.L.H.,1949, Applied Hydrology,
    McGraw-Hill, New York.

Lippard S.J.,1983, Cretaceous high pressure metamorphism in north-eastern
    Oman and its relation to subduction and ophiolite nappe emplacement.
    Jour.Geol.Soc. 140, 97-104

Lippman F.,1973, Sedimentary Carbonate Minerals. Springer-Verlag. 228pp

Lovelock P.E.R.,Potter T.L.,Walsworth-Bell E.B.,and Weiner W.M.,1981,
    Ordovician rocks in the Oman Mountains: The Amdeh Formation. Geologie
    en Mijnbouw. 16-7746, 487-495

Luce R.W.,1971, Brucite identified as crystallising from a natural cold
    alkaline spring gel. Clay and clay minerals, 19, 335-336

Ma^cDonald Sir M.,et al.,1978, Water Development Programme - Capital Area
    Phase 2, Interim Report, 2 vols.

Magaritz M.,and Kaufman A.,1973, Changes in the Isotopic Composition of
    Eastern Mediterranean Seawater during the Holocene. Nature
    243,461-464

Maksimovic Z.,1981, Types of Fossil Weathering of Ultramafic Rocks in
    south-east Europe. Bulletin T. LXXV de L'Academie Serbe des Sciences
    et des arts. (Natural Sciences No 21)

McClure M.A.,1978, Ar Rub'Al Khali. In Al Sayari S.S.,and Zotl J.G.(Eds)
    Quarternary Period in Saudi Arabia, Vienna, 252-263

McGhee R.,1979, Archaeological Evidence for Climatic Change during the
    past 5000 years. International Conference on Climate and History.
    University of East Anglia

McKenzie and Sclater J.G.,1971, The Evolution of the Indian Ocean since
    the Late Cretaceous. Geophys.Jour.Roy.Astr.Soc. 25, 437-528

Membury D.A.,1983, Low level Wind Profiles during the Gulf Shamal. Weather
    38, (1), 18-24

Meteorological Office,1969, Observers Handbook, H.M.S.O., 242pp

Michard A.,Bouchy J.L.,and Ouezzani-Touhami M.,1984,Obduction Related
    Planar Fabrics in Oman. Jour.Struct.Geol. 6, (1/2), 39-49

Miles D.L.,and Espejo C.,1977, Comparison between ultra-violet
    spectrophotometric procedure and the 2,4-xylenol method for the
    determination of nitrate in groundwaters of low salinity. Analyst 102,
    104-109

Miles S.B.,1901, Across the Green Mountains of Oman. Jour.Roy.Geog.Soc.,
    18, (5), 465-498

Miura, Yasunori,and Rucklidge J.C.,1979, The Structural Occurence of
    Chlorine in Serpentine. Proc.Geol.Assn.Canada/Miner.Assn.Canada.
    Abstr.

Montenat Ch.,Blondeau A.,Bizon G.,Perreau M.,Raju D.S.N.,and Roman J.,1977
    Premier Apercu du Teriaire d'Oman. Bull.Soc.Geol.France. 19, (6),
    1285-1295

Morton D.M.,1959, The Geology of Oman. 5th World Petrol.Cong. (1),
    paper 14, 227-280

Mosely F.,and Abbots I.L.,1979, The Ophiolite Melange of Masirah,Oman.
    Jour.Geol.Soc. 136, (6), 713-724

Murris R.J.,1981, Middle East; Stratigraphic Evolution and Oil Habitat.
    Geologie en Mijnbouw 0016-7746. 467-486

Nahon D.,Paquet H.,and Delvigne J.,1982, Laterite weathering of ultramafic
    rocks, and the concentration of nickel in the western Ivory Coast.
    Econ.Geol. 77, 1159-1175

Neal C.,and Stanger G.,1983, Hydrogen Generation from Mantle Source Rocks
    in Oman. Earth Plan.Sci.Lett. 66, 315-320

Neal C.,and Stanger G.,1984, Calcium and Magnesium Hydroxide Precipitation
    from Alkaline Groundwaters in Oman, and their Significance to the
    Process of Serpentinisation. Miner.Mag. 48, 237-241

Neal C.,and Stanger G.,1985, Past and present serpentinisation of
    ultramafic rocks; An example from the Semail Nappe of Northern Oman.
    NATO advanced workshop on weathering reactions. Drever J.I.(Ed),
    Reidel. 249-275

Nesbitt H.,W.,and Bricker O.P.,1978, Low Temperature Alteration Processes
    affecting ultramafic bodies. Geochim.et Cosmochim.Acta, 42, 403-409

Newberry J.,1966, Preliminary Evaluation of Groundwater Resources, Muscat
    and Muttrah Water Supply. Scott Wilson Kirkpatrick & Ptnrs.

Oates J.,1982, Archaeological Evidence for Settlement Patterns in
    Mesopotamia and Eastern Arabia in Relation to Possible Environmental
    Conditions. in Bintliff and Van-Zeist(Eds.), 359-393

O'Brien A.,H.,and Rodgers K.A.,1973, Xonotlite and Rodingite from Wairere,
    New Zealand. Miner.Mag. 39, 233-240

O'Gilvi A.N.,1932, Thermometry as a method of hydrogeological
    investigation. Gosgeolrazvedizdat, Leningrad

Olausson E.,and Olsson I.V.,1969, Varve Stratigraphy in a Core from the Gulf of Aden. Palaeogeography,Palaeoclimatology and Palaeoecology. <u>6</u>, 87-103

O'Neil J.R.,and Barnes I.,1971, C^{13} and O^{18} compositions in some fresh-water carbonates associated with ultramafic rocks and serpentinites; Western United States. Geochim. et Cosmochim.Acta. <u>35</u>, 687-697

Orchard J.C.,and Orchard J.J., Archaeological Survey in Wadi Bahla (Jawf) and in Wadi la-Mlah (Sharqiyah). Jour.Oman Studies. (in press) cf. Birmingham University, Dept. of Ancient History and Archaeology

Orion ,1970, Grans plot and other schemes. Newslett.Orion Res.Inc., No 2, 49-55

Osborne H.B.,Renard K.G.,and Simaton J.R.,1979, Dense networks to measure convective rainfall in the South-Western United States. Water Resour. Res. <u>15</u>, (6), 1701-1711

Parker D.H.,1985, The Hydrogeology of the Cainozoic Aquifers in the PDO Concession Area, Sultanate of Oman.
1) Text (82pp) and Hydrochemistry
2&3) Water Well Data Summaries

Patterson R.J.,and Kinsman D.J.J.,1977, Marine and Continental Groundwater Sources in a Persian Gulf Coastal Sabkha. Amer.Assn.Pet.Geol. Studies in Geology. <u>4</u>, 381-397

Pedgely D.E.,1969, Cyclones along the Arabian Coast. Weather. <u>24</u>, 456-468

Pedgely D.E.,1970, The Climate of Interior Oman. The Meteor.Mag. <u>99</u>, 29-37

Pencol International Ltd.,1978, Collation,Summary and Analysis of climatological station, water well monitoring and rainfall stations in the Musandam Province. (unpub. report), 3 vols.

Peters Tj.,and Kramers J.D.,1974, Chromite Deposits in the Ophiolite Complex of Northern Oman. Mineral.Deposita (Berl.), <u>9</u>, 253-259

Pilgrim G.,1908, The Geology of the Persian <Arabian> Gulf and adjoining portions of Persia and Arabia. Mem.Geol.Surv.India, <u>34</u>, (4), 1-177

Plummer L.N.,and MacKenzie F.T.,1974, Predicting mineral solubility from rare data: Application to the dissolution of magnesium calcites. Amer.Jour.Sci. <u>274</u>, (1), 61-83

Pourbaix M.,1963, Atlas d'Equilibres Electrochemiques. Ganthiers-Villars, Paris.

Powell R.,1978, Equelibrium Thermodynamics in Petrology. Harper and Row. 284pp

Powers R.W.,Ramirez L.F.,Redmond C.D.,and Elberg E.L.,1966, Geology of the Arabian Peninsula: Sedimentary Geology of Saudi-Arabia. U.S.G.S.Prof Paper 560D, 147pp

Price W.J.,1979, Spectrochemical Analysis by Atomic Absorbtion. Heyden,
    392pp

Racz L.,1979, Palaeocene Carbonate Development of Ras al Hamra, Oman.
    Bull.Cent.Rech.Expl.-Prod. Elf Aquitaine, 3, (2), 767-779

Ramdohr P.,1967, A Widespread Mineral Association connected with
    Serpentinisation. N.Jb.Miner.Abh. 107, (3), 241-265

Ramdohr P.,1969, The Ore Minerals and their Intergrowths. Pergamon.
    New York

Rauch H.W.,and White W.B.,1970, Lithologic Controls on the Development of
    Solution Porosity in Carbonate Aquifers. Water Resour.Res. 6, (4),
    1175-1192
Reid I.,and Frostick L.,1984, Rivers that Rarely Run. Geographical Mag.
    56, (4), 178-183

Renardet-Sauti I.C.E.,1975, Water Resources Survey in North-East Oman;
    Interim Report to the Ministry of Communications. (Unpublished)

Ricateau R.,and Riche P.H.,1980, Geology of the Musandam Peninsula and its
    Surroundings. Jour.Petrol.Geol. 3, (2), 139-152

Richards D.,1975, The effects of reducing raingauge network density on
    goodness of conceptual model fit and prediction. Inst.of Hydrology
    report 28. 25pp

Richards L.A.(Ed),1954, Diagnosis and Improvement of Saline and Alkali
    Soils. Agric.Handbook 60, U.S.Dept.Agric.,Washington D.C. 160pp

Riehl H.,1979, Climate and Weather in the Tropics. Academic Press. 611pp

Riley D.,and Spolton L.,1974, World Weather and Climate. C.U.P. 120pp

Rodda J.C.,1970, On the question of rainfall measurement and
    representativeness. Proc.Int.Assoc.Sci.Hydrol.Symp. 174-186

Roques H.,1962, Considerations theoriques sur la chimie des carbonates.
    Ann.Speliol. 17, 463-467

Rothery D.A.,1982, Evolution of the Wuqbah Block and the application of
    remote sensing in the Oman Ophiolite. Open University PhD.thesis.

Rothery D.A.,1983, Reflectances of ophiolite rocks in the Landsat M.S.S.
    bands: Relevance to lithological mapping by remote sensing. Jour
    Geol.Soc.Lond. 141, 933-939

Rousseau J.P.,and Stanger G.,1978, Groundwater Quality Investigation of
    the South-East Batinah Coastal Plain. Unpublished report for the water
    resources council, Sultanate of Oman.

Roy J.H.L.,Roffey J.,and Gerbier N.E.,1963, Report on Aerial Surveys in
    the Arabian Peninsula. F.A.O./U.N.S.F. Desert Locust Project. Report
    OP/3

Rucklidge J.C.,and Patterson G.C.,1977, The Role of Chlorine in
    Serpentinisation. Contrib.Miner.Petrol. 65, 39-44

Ryden B.E.,1972, On the problem of vertical distribution of precipitation
,especially in areas with great height differences. cf W.M.O.,1972
362-372

Sakamoto C.,1959, Studies on serpentine containing brucite. Kogyo Kagaku
-Zasshi. 62, 1485-1488

Sammis T.W.,and Gay L.W.,1979, Evapotranspiration from an arid zone plant
community. Jour.of Arid Environments. 2, 313-321

Schulze R.E.,1976, On the application of Trend Surfaces of Precipitation
to Mountainous Areas. Water S.A. 2, (3), 110-118

Scofield C.S.,1940, Salt Balance in Irrigated Areas. Jour.Agric.Res. 61,
17-39

Scott Wilson Kirkpatrick & Ptnrs.1972, Report on Water Supply
Investigations in Northern Oman.

Scott Wilson Kirkpatrick,1977a, Monitoring of Groundwater Resources at
M.A.M. Annual Report 1976

Scott Wilson Kirkpatrick,1977b, Groundwater Resources at Wadi Lansab
/Azaiba - A Preliminary Appraisal of the New Field

Scott Wilson Kirkpatrick,1978, Hydrogeological Services Final Report. Two
vols. <M.O.D.Restricted>

Searle M.P.,1980, The Metamorphic Sheet and Underlying Volcanic Rocks
beneath the Semail Ophiolite in the Northern Oman Mountains of Arabia.
Open University PhD thesis. 279pp

Sharon D.,1972, The spotiness of rainfall in a desert area. Jour.Hydrol.
17, 161-175

Shearman D.J.,1977, The Geological Evolution of Southern Iran.
Geographical. 393-410

Shelton A.W.,1983, Open University Oman Ophiolite Project: Memoir Map @
1:250,000 - Simple Bouguer Gravity Anomaly.

Shelton A.W.,1984, Geophysical Studies of the Northern Oman Ophiolite
Open University PhD.thesis. 353pp

Sheppard D.S.,and Lyon G.L.,1984, Geothermal Fluid Chemistry of the
Orakeikarako Field, New Zealand. Jour.Volcanol.Geotherm.Res. 22,
329-349

Shteinberg D.S.,1960, New data concerning the serpentinisation of dunites
and peridotites of the Urals. Inter.Geol.Cong.XXI. Sess.Dokl.Sovet.
Geol.Petrograf.Prov.Izverzh.Metamorph Gonye Porody. Izdalel'stvo Akad.
Nauk S.S.S.R. Moskva 250-260

Shteinberg D.S.,and Chaschuklin I.S.,1969, Composition of Brucite in
Serpentinites and the Procedure for Identifying it. U.S.S.R. Acad.Sci.
Dokl.Earth Sci. 186, 115-118

Sibson R.H.,Moore J.McM.,and Rankin A.H.,1975, Seismic Pumping - a hydrothermal fluid transport mechanism. Jour.Geol.Soc. 131, (6), 653-659

Siever R.,1957, The Silica Budget in the Sedimentary Cycle. Amer.Miner. 42 821-841

Simpson J.,1976, On the possibilities of rain augmentation by cloud seeding in the Persian <Arabian> Gulf area (Qatar and Oman). F.A.O. 34pp

Sleight R.B.,1917, Evaporation from the Surface of Water and River Bed Materials. Jour.Agric.Res. 10, 209-262

Smewing J.D.,Simonian K.O.,El-Boushi I.M.,and Gass I.G.,1977, Mineralised Fault Zone parallel to the Oman Ophiolite Spreading Axis. Geology 5, 534-538

Smewing J.D.,Lippard S.J.,Gass I.G.,Browning P.,and Rothery D.A.,1981, The Geology of the Dibba-Idhn Area (The Dibba Zone),U.A.E. Unpublished report (Open University)

Smith G.R.,1986, Gazeteer,Together with some observations of the Bisyah area, Wadi Bahla. Jour.of Oman Studies, (in press). cf. birmingham University, Dept. of Ancient History and Archaeology.

South D.,1973, The Musandam Expedition 1971-72: III Pre-Quarternary Geology. Geog.Jour. 193, (1), 410-414

Stanger G.and Neal C.,1984, A New Occurrence of Suolunite from Oman. Miner.Mag. 48,143-146

Stanger G.,1985a, Coastal Salinization, a case history from Oman. Agric.Water Management. 9, 269-286

Stanger G.,1985b, Silicified Serpentinite in the Semail Nappe of Oman. Lithos 18, 13-22 880

Stanger G.1986,Water Resources,Sedimentation and Early Settlement in Wadi Bahla. Jour. of Oman Studies 6, (in press). cf Birmingham University Dept. of Ancient History and Archaeology.

Stevens J.H.,1969, Quarternary events and their effect on soil development in an arid environment. Quarternaria 10

Stevens J.H.,1978, Post Pluvial Changes in the Soils of the Arabian Peninsula. in Brice W.C.(Ed.), 263-274

Stewart M.K.,1974, Stable Isotopes in Raindrops: Effects of Evaporation and Isotopic Exchange. Trans.Amer.Geophys.Union 55, (4), 267-

Stiffe A.W.,1860, A visit to the hot springs at Bosher near Muscat, with a route map. Trans.Bombay Geogr.Soc. 15, (6), 123-128

Stojanovic D.,Dordevic D.,and Derkovic B.,1974, Suolunit I Tobermorit U Dijabaznim stenama Kulasa Kod Doboja, Bosna, Jugoslavija <Suolunite and Tobermorite in the Basaltic rocks of Kulashi,near Doboj, Bosnia Yugoslavia>. Bull. du Museum d'Histoire Naturelle, A29

Storr D.,and Ferguson H.L.,1972, The Distribution of Precipitation in
    some Mountainous Canadian Watersheds. cf W.M.O.1972, 243-263

Stumm W.,and Morgan J.J.,1970, Aquatic Chemistry. Wiley Interscience 584pp

Sutcliffe J.V.,and Carpenter T.G.,1967, The Assessment of Runoff from a
    Mountainous and Semi-Arid Area in Western Iran. Proc.General Assembly
    IASH, 383-394

Takahashi K.,and Arakawa H.(Eds.),1981, World Summary of Climatology. 9,
    (Southern and Western Asia) Elsevier 333pp

Takin M.,1972, Iranian Geology and Continental Drift in the Middle East.
    Nature 235, 147-150

Tapponier P.,Mattauer M.,Proust F.,and Cassaigneau C.,1981, Mesozoic
    Ophiolites, Sutures and Large-Scale Tectonic Movements in Afghanistan.
    Earth Planet.Sci.Lett. 52, 355-371

Thesiger W.,1959, Arabian Sands. Longman

Todd D.K.,1959, Ground-Water Hydrology (1st Edn). J.Wiley & Sons 336pp
       /1980,   "   "   "   (2nd Edn).   "   "   535pp

Trombe F.,1952, Traite de Speliol. Payot, Paris

Truesdale V.W.,and Smith C.J.,1975, The Automatic determination of Iodine
    in solution by catalytic spectrophotometry, with particular reference
    to river water. Analyst 100, 111-123

Truesdell A.H.,and Jones B.F.,1974, Wateq, a computer program for
    calculating chemical equelibria of natural waters. Jour.Res.U.S.G.S.
    2, (2), 233-248

Tschopp R.M.,1967, The General Geology of Oman. Proc.7th World Pet.Cong.
    Mexico. 2, 231-241

Turner F.J.,and Verhoogan J.,1960, Igneous and Metamorphic Petrology.
    2nd Edn. M[c]Graw-Hill. New York.

U.N.E.S.C.O.,1961, Salinity problems in the arid zone. Proc.of the Tehran
    syposium. Paris (Arid zone research, XIV)

U.S.Dept.of Health, Education and Welfare,1962, Public Health Service
    Drinking Water Standards. 60pp

U.S.Weather Bureau,1947, Thunderstorm rainfall. Hydrometeorological Report
    5

Van Biljon W.J.,1960, Chemical reactions in the thermal breakdown of the
    serpentine minerals. Neus.Jahrb.Mineral.

Van Zeist W.,and Bottema S.,1977, Palynological Investigations in Western
    Iran. Palaeohistoria 19, 19-85

Veen A.W.L.,and Arndt W.,1973, Huntite and Aragonite nodules in a vertisol
    near Katherine, Northern Teritory, Australia. Nature;Phys Sci. 241,
    (106), 37-40

Vita-Finzi C.,1973, The Musandam Expedition 1971-72: IV Late Quarternary
Subsidence. Geog.Jour. 193, (1), 414-421

Vita-Finzi C.,1978, Recent Alluvial History in the Catchment Area of the
Arabo-Persian Gulf. in Brice W.C.(Ed), 355-362

Waltham A.C.,Brown R.D.,and Middleton T.C.,1985, Karst and Caves in the
Jebel Akhdar,Oman. Trans.Brit.Cave Res.Assoc. 12, in press

Waring G.A.,1965, Thermal Springs of the United States and other countries
of the world - A summary. U.S.G.S. Prof.Paper 492, 383pp

Weast R.C.,and Astle M.J.,(Eds.),1981-82, Handbook of Chemistry and
Physics,62nd Edn. C.R.C. Press Inc.

Wedepohl K.H.(Ed),1978, Handbook of Geochemistry. Springer-Verlag. 4 vols

Wenner D.B.,and Taylor H.P.,1971, Temperatures of serpentinisation of
ultramafic rocks based on O^{18}/O^{16} Fractionation between coexisting
serpentine and magnetite. Contrib.Miner. and Petrol. 32, 165-185

White D.E.,Hem J.D.,and Waring G.A.,1963, Chemical composition of sub-
surface waters. in Data of Geochemistry, 6th Edn.

Whitmore J.S.,1972, The Variation of Mean Annual Rainfall with Altitude
and Locality in South Africa as Determined by Multiple Curvilinear
Regression Analysis. cf W.M.O.,1972, 1, 188-200

Whitney J.W.,1982, Geological Evidence of Late Quarternary Climatic Change
in Western Saudi Arabia. in Bintliff and Van Zeist(Eds.), 231-233

Whittaker E.J.W.,and Zussman J.,1956, The Characterisation of serpentine
minerals by X-ray diffraction. Miner.Mag. 31, 107-126

Wicks F.J.,1969, X-Ray and Optical Studies on Serpentine Minerals. Oxford
University D.Phil. thesis

Wilkinson J.C.,1974, The Organisation of the Falaj Irrigation System in
Oman. School of Geography, University of Oxford Research Paper No 10

Wilkinson J.C.,1977, Water and Tribal Settlement in South-East Arabia.
Oxford Research Studies in Geography. Clarendon Press 276pp

Wilkinson J.C.,1978, Islamic Water Law with special reference to Oasis
Settlement. Jour.Arid Environments. 1, 87-96

Wilkinson J.C.,1980, The Origins of the Aflaj of Oman. Jour.of Oman
Studies. 6, (1),177-194

Williams M.A.J.,1975, Late Pleistocene Tropical Aridity synchronous in
both hemispheres? Nature 253, 617-618

Williams P.W.,1983, The role of the subcutaneous zone in karst hydrology.
Jour.Hydrol. 61, 45-67.(Symposium Issue: Processes in Karst Hydrology)

Wilson H.H.,1969, Late Cretaceous Eugeosynclinal Sedimentation, Gravity
Tectonics , and Ophiolite Emplacement in <the> Oman Mountains,
Southeast Arabia. Amer.Assoc.Petrol.Geol.Bull. 53, (3), 626-671

World Health Organisation,1971, International Standards for Drinking Water 3rd Edn., 52pp

World Meteorological Organisation,1965, Guide to Hydrometeorological Practices, Geneva

World Meteorological Organisation,1972, Distribution of Precipitation in Mountainous Areas. Geilo Symposium, Norway, vol 2, Technical Papers. 587pp.

Yost C.B.,1978, Ground Water System of Jebel Al Qara and its relation to the Occurrence and Quality of groundwater in adjacent Salalah Coastal Plain and Negd. Report to the water resources council by Tetra Tech Int.(unpublished)

Zall D.M.,Fisher D.,and Garner M.Q.,1956, Photometric determination of chlorides in water. Anal.Chem., 28, 1665-1668